ISSN 0021-9673

VOL. 625 NO. 2 NOVEMBER 20, 1992

THIS ISSUE COMPLETES VOL. 625

JOURNAL OF CHROMATOGRAPHY

INCLUDING ELECTROPHORESIS AND OTHER SEPARATION METHODS

ELSEVIER

JOURNAL OF CHROMATOGRAPHY

INCLUDING ELECTROPHORESIS AND OTHER SEPARATION METHODS

Scope. The *Journal of Chromatography* publishes papers on all aspects of **chromatography, electrophoresis** and related methods. Contributions consist mainly of research papers dealing with chromatographic theory, instrumental developments and their applications. The section *Biomedical Applications*, which is under separate editorship, deals with the following aspects: developments in and applications of chromatographic and electrophoretic techniques related to clinical diagnosis or alterations during medical treatment; screening and profiling of body fluids or tissues related to the analysis of active substances and to metabolic disorders; drug level monitoring and pharmacokinetic studies; clinical toxicology; forensic medicine; veterinary medicine; occupational medicine; results from basic medical research with direct consequences in clinical practice. In *Symposium volumes*, which are under separate editorship, proceedings of symposia on chromatography, electrophoresis and related methods are published.

Submission of Papers. The preferred medium of submission is on disk with accompanying manuscript (see *Electronic manuscripts* in the Instructions to Authors, which can be obtained from the publisher, Elsevier Science Publishers B.V., P.O. Box 330, 1000 AH Amsterdam, Netherlands). Manuscripts (in English; *four* copies are required) should be submitted to: Editorial Office of *Journal of Chromatography*, P.O. Box 681, 1000 AR Amsterdam, Netherlands, Telefax (+31-20) 5862 304, or to: The Editor of *Journal of Chromatography, Biomedical Applications*, P.O. Box 681, 1000 AR Amsterdam, Netherlands. Review articles are invited or proposed in writing to the Editors who welcome suggestions for subjects. An outline of the proposed review should first be forwarded to the Editors for preliminary discussion prior to preparation. Submission of an article is understood to imply that the article is original and unpublished and is not being considered for publication elsewhere. For copyright regulations, see below.

Publication. The *Journal of Chromatography* (incl. *Biomedical Applications*) has 40 volumes in 1993. The subscription prices for 1993 are:

J. Chromatogr. (incl. *Cum. Indexes, Vols. 601–650*) + *Biomed. Appl.* (Vols. 612–651):
Dfl. 8520.00 plus Dfl. 1320.00 (p.p.h.) (total *ca.* US$ 5927.75)

J. Chromatogr. (incl. *Cum. Indexes, Vols. 601–650*) only (Vols. 623–651):
Dfl. 7047.00 plus Dfl. 957.00 (p.p.h.) (total *ca.* US$ 4821.75)

Biomed. Appl. only (Vols. 612–622):
Dfl. 2783.00 plus Dfl. 363.00 (p.p.h.) (total *ca.* US$ 1895.25).

Subscription Orders. The Dutch guilder price is definitive. The US$ price is subject to exchange-rate fluctuations and is given as a guide. Subscriptions are accepted on a prepaid basis only, unless different terms have been previously agreed upon. Subscriptions orders can be entered only by calender year (Jan.–Dec.) and should be sent to Elsevier Science Publishers, Journal Department, P.O. Box 211, 1000 AE Amsterdam, Netherlands, Tel. (+31-20) 5803 642, Telefax (+31-20) 5803 598, or to your usual subscription agent. Postage and handling charges include surface delivery except to the following countries where air delivery via SAL (Surface Air Lift) mail is ensured: Argentina, Australia, Brazil, Canada, China, Hong Kong, India, Israel, Japan*, Malaysia, Mexico, New Zealand, Pakistan, Singapore, South Africa, South Korea, Taiwan, Thailand, USA. *For Japan air delivery (SAL) requires 25% additional charge of the normal postage and handling charge. For all other countries airmail rates are available upon request. Claims for missing issues must be made within three months of our publication (mailing) date, otherwise such claims cannot be honoured free of charge. Back volumes of the *Journal of Chromatography* (Vols. 1–611) are available at Dfl. 217.00 (plus postage). Customers in the USA and Canada wishing information on this and other Elsevier journals, please contact Journal Information Center, Elsevier Science Publishing Co. Inc., 655 Avenue of the Americas, New York, NY 10010, USA, Tel. (+1-212) 633 3750, Telefax (+1-212) 633 3764.

Abstracts/Contents Lists published in Analytical Abstracts, Biochemical Abstracts, Biological Abstracts, Chemical Abstracts, Chemical Titles, Chromatography Abstracts, Clinical Chemistry Lookout, Current Awareness in Biological Sciences (CABS), Current Contents/Life Sciences, Current Contents/Physical, Chemical & Earth Sciences, Deep-Sea Research/Part B: Oceanographic Literature Review, Excerpta Medica, Index Medicus, Mass Spectrometry Bulletin, PASCAL-CNRS, Pharmaceutical Abstracts, Referativnyi Zhurnal, Research Alert, Science Citation Index and Trends in Biotechnology.

US Mailing Notice. *Journal of Chromatography* (main section ISSN 0021-9673, *Biomedical Applications* section ISSN 0378-4347) is published (78 issues/year) by Elsevier Science Publishers (Sara Burgerhartstraat 25, P.O. Box 211, 1000 AE Amsterdam, Netherlands). Annual subscription price in the USA US$ 5927.75 (subject to change), including air speed delivery. Application to mail at second class postage rate is pending at Jamaica, NY 11431. **USA POSTMASTERS:** Send address changes to *Journal of Chromatography*, Publications Expediting, Inc., 200 Meacham Avenue, Elmont, NY 11003. Airfreight and mailing in the USA by Publication Expediting.

See inside back cover for Publication Schedule, Information for Authors and information on Advertisements.

0021-9673/92/$05.00

Printed in the Netherlands

CONTENTS

(Abstracts/Contents Lists published in Analytical Abstracts, Biochemical Abstracts, Biological Abstracts, Chemical Abstracts, Chemical Titles, Chromatography Abstracts, Current Awareness In Biological Sciences (CABS), Current Contents/Life Sciences, Current Contents/Physical, Chemical & Earth Sciences, Deep-Sea Research/Part B: Oceanographic Literature Review, Excerpta Medica, Index Medicus, Mass Spectrometry Bulletin, PASCAL-CNRS, Referativnyi Zhurnal, Research Alert and Science Citation Index)

(Continued overleaf)

PREP-93

10th INTERNATIONAL SYMPOSIUM ON PREPARATIVE CHROMATOGRAPHY

CALL FOR PAPERS

Abstract Deadline: December 1, 1992
Send Abstracts to:
Prep-93 Symposium Manager
Barr Enterprises
P.O. Box 279
Walkersville, MD 21793 USA
Abstracts received after December 1, 1992 will be considered for poster presentation.

JUNE 14 – 16, 1993

ARLINGTON, VIRGINIA
USA

CHAIRMAN:
Professor Georges Guiochon
Oak Ridge National Laboratory
and University of Tennessee

SYMPOSIUM MANAGER:
Mrs. Janet Cunningham
Barr Enterprises
P.O. Box 279
Walkersville, MD 21793 USA
Phone: (301) 898-3772
Fax: (301) 898-5596

PREP-93

Journal of Chromatography, 625 (1992) 85
Elsevier Science Publishers B.V., Amsterdam

Publisher's Note

On the occasion of the publication of Volume 500 of the *Journal of Chromatography*, in 1990, a study by the Institute of Scientific Information was commissioned to determine frequently cited papers published in the journal since its inception in 1958. As a result, authors of such frequently cited papers in both the main section and the *Biomedical Applications* section were invited to contribute an article relating the circumstances that led to their research, their views on why their article had such an impact, on what, in retrospect, were the most salient features of their work, and on the present relevance of the that work.

Volume 625, No. 2, presents the first contribution (published under the heading "Chromatography Classic") received in response to this invitation, a paper by J. S. Fritz and G. A. Junk, who look back on their 1974 publication in this journal on the use of macromolecular resins in the analysis of water for trace organic substances. Almost simultaneously, in Volume 582 of the *Biomedical Applications* section, a similar article will appear by O. Magnusson, L. B. Nilsson and D. Westerlund, who put their 1980 article on the determination of dopamine and two of its acidic metabolites by HPLC with electrochemical detection in perspective.

Journal of Chromatography, 625 (1992) 87–90
Elsevier Science Publishers B.V., Amsterdam

CHROM. 24 534

Chromatographic Classic

Use of macroreticular resins in the analysis of water for trace organic contaminants, by G. A. Junk, J. J. Richard, M. D. Grieser, D. Witiak, J. L. Witiak, M. D. Arguello, R. Vick, H. J. Svec, J. S. Fritz and G. V. Calder, *J. Chromatogr.*, 99 (1974) 745–762

J. S. Fritz and G. A. Junk

Ames Laboratory, US Department of Energy and Department of Chemistry, Iowa State University, Ames, IA 50011 (USA)

(First received July 20th, 1992; revised manuscript received July 29th, 1992)

BACKGROUND

The circumstances that lead to the publication of this paper in 1974 are an excellent example of the good things that can happen when scientists of varied backgrounds work together. Calder was then a young physical chemistry professor at Iowa State University who wanted to do some research that was relevant to our modern society. He found that the water supply of Ames, IA, USA had an undesirable taste and odor when water from certain wells was used. The offensive materials had been tentatively identified as phenols and cresols, based on a marginally positive 4-aminoantipyrene color test [1] and the observation that the bad taste and odor increased after chlorination.

Fritz and Willis had been studying the separation of phenols on Rohm & Haas XAD-2, a macroreticular resin of high surface area. Fritz suggested the use of a column filled with this resin for concentrating these suspected phenols from the water with subsequent elution of the adsorbed compounds by a small volume of an organic solvent.

Junk and Svec had been experimenting with the development of the combination of a mass spectrometer and a gas chromatograph. They did not know whether this home-made instrument would solve a real world problem, but decided that in any event they needed to learn more about chromatography in general.

The combined efforts of these three diverse groups resulted in the eventual publication of a method for identification and estimation of neutral organic contaminants in potable water, which was published in 1972 [2]. The concentration step was accomplished by adsorption of the organic contaminants on a column of XAD-2 resin. The major pollutants of the Ames water were soluble coal tar products such as acenaphthylene, alkynaphthalenes, ethyl indenes, indane and indene. Interestingly, the suspected phenols were not found to be present in the water.

Although this and other papers had suggested that the XAD-2 resin might be applicable for extraction of a wide variety of organic solutes, the 1974 paper in the *Journal of Chromatography* was

Correspondence to: Dr. J. S. Fritz, Ames Laboratory, U.S. Department of Energy and Department of Chemistry, Iowa State University, Ames, IA 50011, USA.

0021-9673/92/$05.00

the first comprehensive study on the efficiency of this resin when employed in a standardized analytical scheme. This study established the applicability of using high-surface-area synthetic solids for the accurate determination of organic contaminants present at trace levels in water samples.

SIGNIFICANCE

The test results for a total of 85 different organic compounds were reported in the 1974 paper. Several compounds were studied from each of the following classes: alcohols, aldehydes and ketones, esters, polynuclear aromatics, carboxylic acids, phenols, ethers, halogen compounds, nitrogen compounds, and pesticides. As stated in the report, "The results indicated that the procedure is reliable and accurate, and the porous polymer method can be used with confidence for analysis of natural waters of unknown composition".

So, for the first time a detailed and widely applicable analytical method was available for extraction of organic compounds from aqueous samples. Extremely low concentrations of organic compounds are quantitatively taken up and subsequently eluted by a small volume of an organic solvent. The method was a tremendous improvement over the charcoal adsorption and solvent extraction methods that were previously used.

The porous polymer method also gives in general more complete and predictable recovery of organic compounds than extraction with a liquid solvent. There is only a single-stage equilibration of solutes between aqueous and organic phase in solvent extraction. But there is a multi-stage equilibration in a small resin column and this leads to more complete extraction. It is now realized (in the 1990s) that widespread use of solvent extraction by analytical chemists results in substantial pollution of both air and water. By contrast, solid-phase extractants do not pollute water samples, and only a small volume of organic solvent is needed to elute adsorbed solutes from the mini-column that is used.

It was fortunate that the editors of the *Journal of Chromatography* agreed to publish our manuscript in full and not require arbitrary cuts to save space. As stated in the introduction, "An accurate quantitative estimation of organics in water at parts per million to trillion levels requires great care during all phases of the analysis, from sampling to the final chromatographic separation and measurement. For this reason, the techniques and apparatus used in the proposed standardized analytical procedure will be discussed in considerable detail."

In addition to a detailed description of the various steps in the analytical determination, we were able to provide rather useful information on methods used to prepare aqueous standards of organic test compounds and in proper ways of handling samples prior to analysis. Even the shape of the container used to evaporate the solvent from the eluate was discussed. These discussions may well have been one reason for the frequent citations made by other authors.

In the early 1970s almost nothing was known as to which organic pollutants were actually present in various water supplies. The resin extraction method provided a convenient and easy way to concentrate these unknown compounds to a point where they could be identified and quantified by established analytical techniques. In a few years following publication of our paper in the *Journal of Chromatography* there was a veritable explosion of information regarding the pollutants present in various waters [3–6].

Our 1974 paper again provided an example of the power of using combined gas chromatography and mass spectroscopy as an identification technique for organic compounds in complex analytical samples. Our use of high-surface-area synthetic solids to adsorb very low concentrations of organic compounds from water was successful almost from the very beginning. Injection of a portion of the eluate from the solid into a gas chromatograph gave a number of nice peaks, but we had no idea which compounds these peaks represented. Identification of the gas chromatography peaks from concentrates of actual water samples was only possible because Svec and Junk had available a home-made version of the now familiar gas chromatograph–mass spectrometer.

The porous polymer method was the forerunner of modern solid-phase extraction (SPE). However, practical use of the XAD porous polymer method in the 1970s and 1980s was undoubtedly limited by the lack of high surface area solids available commercially in a purified form of suitable particle size. Many scientists did not wish to grind, sieve and purify their own resin. Additionally, the US Environ-

mental Protection Agency (EPA), which has a strong influence on the acceptable analytical methods relied heavily on solvent extraction and purge-and-trap methods for determining organics in aqueous samples during this time. Current EPA activity is heavily weighted toward SPE procedures.

During the last few years, organic groups chemically bonded to porous silica have become very popular for solid-phase extraction of organic compounds from aqueous samples. These materials are reasonably pure and are widely available at low cost in pre-packed commercially available cartridges.

CURRENT SIGNIFICANCE

Current EPA activity is heavily weighted toward SPE procedures. This may be due in part to the realization that widespread use of solvent extraction by chemists has become a significant source of pollution. Compared to liquid–liquid extraction, SPE has the advantages of using much less solvent, thereby being both safer and less costly, and being free from emulsion formation. SPE methods are easily automated and are compatible with measurement instrumention.

CURRENT RESULTS

During the last few years porous silica with chemically bonded organic groups have become very popular for SPE of organic compounds from aqueous samples. These materials are reasonably pure and are widely available at low cost in pre-packed cartridges. In many cases the recovery of organic test compounds on these silica materials has been reported to be quite good. However, our own results have consistently shown that porous polymeric resins give appreciably higher recoveries for many classes of test compounds.

The silica-based materials and the porous organic resins commonly used in SPE have one major drawback. Because of their hydrophobic nature, poor contact is made between the solid and aqueous phases unless the solid is first treated with an organic "activating" solvent such as methanol. It is likely that this solvent fills up the pores of the extractive solid and promotes better contact with a predominantly aqueous sample. Much of this solvent seems to remain on the solid surfaces although it can be gradually washed off by aqueous solutions. If air inadvertently enters the SPE column, the activating solvent is removed more rapidly and recovery of most organic test compounds is reduced.

A logical answer to this problem is to modify the surface of the solid extract so that it will be more compatible with aqueous samples. Recent work has shown that introduction of a hydrophilic functional group onto the surface of a porous organic resin will make the resin easily wettable by water alone [7]. These resins show higher recoveries for SPE, especially when the test compound is a phenol.

Past results from our laboratory [8] have demonstrated the value of the use of low water volumes and small cartridges. These results have subsequently been verified at other laboratories and our preliminary data [9] show excellent results when using even smaller cartridges containing as little as 10 mg or less of solid phase to extract 10 ml or less of water. These small cartridges are inherently better suited to automation and allow for the use of such small amounts of eluent that the expensive solvent reduction step is unnecessary in most instances.

FUTURE DIRECTIONS

The future for SPE appears to be very bright. There is growing realization that sample preparation, including cleanup and preconcentration, is often the most time-consuming and therefore the most costly step in a chemical analysis. Operations involving SPE can be automated and will often greatly reduce the time needed for analysis.

The trend toward lower water volumes and smaller amounts of solid phase in miniature cartridges certainly will continue. This development will lower the cost due to faster sample processing. Miniature cartridges, properly developed and used, will be better suited to automation which in turn should increase the applications to the determinations of contaminants in biofluids for the purpose of personnel exposures and diagnosis of diseases and possibly their onset. The beneficial replacement of solvent extraction by solid phase extraction procedures for most all routine analyses should finally occur in the near future. This will help to increase the commercial competitiveness which should cause better quality products; the latest count in the August 1991 issue of LC · GC already numbers 63 different suppliers of SPE equipment.

As SPE becomes more efficient and more highly automated, many new applications are almost sure to be found.

REFERENCES

1 F. T. Snell and C. T. Snell, *Colorimetric Methods of Analysis*, Vol. 3, Van Nostrand, New York, 3rd ed., 1953, p. 107.
2 A. K. Burnham, G. V. Calder, J. S. Fritz, J. A. Junk, H. J. Svec and R. Willis, *Anal. Chem.*, 44 (1972) 139.
3 G. A. Junk, J. J. Richard, H. J. Svec and J. S. Fritz, *J. Am. Waterworks Assoc.*, 68 (1976) 218.
4 C. D. Chriswell, R. L. Ericson, G. A. Junk, K. W. Lee, J. S. Fritz and H. J. Svec, *J. Am. Waterworks Assoc.*, 69 (1977) 669.
5 G. A. Junk, C. D. Chriswell, R. C. Chang, L. D. Kissinger, J. J. Richard, J. S. Fritz and H. J. Svec, *Z. Anal. Chem.*, 282 (1976) 331.
6 R. C. Chang and J. S. Fritz, *Talanta*, 25 (1978) 659.
7 J. J. Sun and J. S. Fritz, *J. Chromatogr.*, 590 (1992) 197.
8 G. A. Junk and J. J. Richard, *Anal. Chem.*, 60 (1988) 451.
9 G. A. Junk and J. J. Richard, unpublished results.

Journal of Chromatography, 625 (1992) 91–99
Elsevier Science Publishers B.V., Amsterdam

CHROM. 24 509

New aliphatic boronate ligands for affinity chromatography

Vladimir Adamek*, Xiao-Chuan Liu, Yu An Zhang, Katerina Adamkova and William H. Scouten

Department of Chemistry, Baylor University, Waco, TX 76798-7348 (USA)

(First received May 4th, 1992; revised manuscript received July 14th, 1992)

ABSTRACT

Aliphatic boronates have not been used as ligands in boronate affinity chromatography, possibly because of their low stability. To fill this void, we have prepared three different boronate esters: 1-chloro-5-(3-dimethylaminophenoxy)pentane-1-boronate, 1-thiourea-5-(3-dimethylaminophenoxy)pentane-1-boronate and 1-acetamido-5-(3-dimethylaminophenoxy)pentane-1-boronate, the latter two of which have a hetero atom coordinated with the boron, creating a tetrahedral boronate. These were coupled to the hydroxylic matrix and their ability to interact with various catechols was tested. Chloroboronate gel bound a number of catechol derivatives, except DL-DOPA, quantitatively, but was rather unstable. Thiourea-boronate gel, on the other hand, was relatively stable, although chromatography using it failed. Acetamido-boronate gel did not bind catechol derivatives quantitatively, but did retard them differentially, a property which could be used for their separation. Acetamido-boronate gel was also more stable than chloro-boronate gel, although it was not stable enough for unlimited application.

INTRODUCTION

The use of boronate chromatography for the separation of nucleic acid components and carbohydrates was first reported by Weith *et al.* in 1970 [1]. Since then immobilized boronates have been used successfully for the separation of many various biomolecules containing vicinal (1,2 or 1,3) diols including nucleic acids [2–4], nucleosides [2,5–8], catechols [8–10], carbohydrates [1,8,11] and glycoproteins [12–15]. Boronate matrices are commonly used for the assay of glycosylated hemoglobin in blood, which is an important element in the diagnosis of diabetes mellitus [16–18].

The most widely used boronate matrix is 3-aminophenyl boronic acid coupled to agarose, which gives the best results in terms of operational pH and minimal secondary interactions. However, many other ligands have been tested to improve the properties of boronates, chiefly, to lower their pK_a and to eliminate hydrophobic adsorption, which are the major limitations to their utilization [8,9,19–21]. These new boronate matrices were based on the introduction of electron withdrawing groups on the aromatic ring of phenylboronates.

Because of their reported instability, aliphatic boronates have, to date, never been utilized for boronate chromatography. However, Matteson and co-workers have prepared a tetrahedral aliphatic boronic ester containing a thiourea moiety as a internal Lewis base and used it to form an ester with catechol [22,23] and an anhydride with malonic acid [24], both of which were stable under acidic conditions. Later, Matteson and Schaunberg synthesized a series of compounds with similar properties [25].

Brown and Vara Prasad [26] have investigated

Correspondence to: Professor W. H. Scouten, Baylor University, Department of Chemistry, WACO, TX 76798-7348, USA.

* Present address: Prague Institute of Chemical Technology, Department of Biochemistry and Microbiology, Technika 3, 166 28 Prague 6, Czechoslovakia.

0021-9673/92/$05.00

aliphatic boronic esters complexed with amino diols. ^{11}B NMR showed that coupling of the boron with the amine function gives a chemical shift of 12–14 ppm. These investigations demonstrated that both electronic and steric factors are influential in forming B–N bonds.

It is known that the natural tendency of boron to accept an electron pair favors the stability of tetrahedral boronic esters in contrast to trigonal forms, particularly in aqueous solution under neutral or acidic conditions. For this reason internally coordinated tetrahedral boronic acids may be very useful for affinity chromatography. Recently, Biedrzycki *et al.* [27] described a series of new aliphatic boronate esters, containing such internal coordinating agents, which were prepared as potential ligands for affinity chromatography. Beyond possessing hetero atoms, which coordinate with the boron to create a more stable tetrahedral structure, these boronate derivatives contained a dimethylaminophenoxypentane functional group for immobilization on a solid phase via a diazonium bond. In this study, we have attempted to utilize these boronate esters for boronate affinity chromatography.

EXPERIMENTAL

Chemicals and materials

Sepharose Cl-4B, 4-aminothiophenol and sodium nitrite were purchased from Sigma. 1,4-Butanediol diglycidyl ether, 1-bromo-4-chlorobutane, butyllithium, 1,1,1,3,3,3-hexamethyldisilazane, trimethylborate, catechol, pyrogallol, DL-DOPA and dopamine were obtained from Aldrich. Azomethine H was a product of Pierce.

The ligands, pinacol 1-chloro-5-(3-dimethylaminophenoxy)pentane-1-boronate, pinacol 1-thioura-5-(3-dimethylaminophenoxy)pentane-1-boronate, and pinacol 1-acetamido-5-(3-dimethylaminophenoxy)pentane-1-boronate were synthesized as described below.

Plastic chromatography columns (2 ml volume, 0.5 cm diameter) from Bio-Rad were used for chromatographic experiments. The concentration of catechol derivatives was spectroscopically measured at 280 nm on a Perkin-Elmer Coleman 124 D double beam spectrophotometer.

Synthesis of pinacol 1-chloro-5-(3-dimethylaminophenoxy)pentane-1-boronate, pinacol 1-thiourea-5-(3-dimethylaminophenoxy)pentane-1-boronate and pinacol 1-acetamido-5-(3-dimethylaminophenoxy)-pentane-1-boronate (see Fig. 1)

Pinacol 1-chloro-5-(3-dimethylaminophenoxy)pentane-1-boronate (CIPP). Dichloromethaneboronic acid (**I**) was synthesized as reported by Ranthke *et al.* [29].

Dichloromethaneboronic acid (170 mmol) was dissolved in 120 ml of dry benzene, then 170 mmol of pinacol were added and the mixture was stirred at room temperature until there was no solid left. After drying over $MgSO_4$, the product was distilled at 25 mmHg. The major fraction, which distilled at 80–82°C, was dichloromethaneboronic acid pinacol ester (**II**). The yield was 52% (16.5 g, 88 mmol).

3-Dimethylaminophenol (7 g, 51 mmol) was dissolved in ethanol, containing 1.17 g (52 mmol) of sodium and refluxed for 30 min. Then 8.75 g of 1-bromo-4-chlorobutane were added and refluxed for 9 h under nitrogen. The dark purple liquid, which was obtained after evaporating the solvent, was further purified by low-pressure silica chromatography (230–400 mesh, 60 Å, 50 × 2.5 cm column) using diethyl ether–light petroleum (b.p. 35–60°C) (1:5) to yield 5.5 g (25 mmol) of **III**. Thin-layer chromatography on Al_2O_3 plates was used to monitor the purification.

III (5.4 g) and 0.576 g of Mg (24 mmol) were added to 40 ml of dry tetrahydrofuran (THF) and refluxed for 3 h. The resulting Grignard reagent was added dropwise to 5.2 g of **II** in 50 ml dry THF at −75°C. The mixture was allowed to come to room temperature and was held overnight under nitrogen. After sequentially adding 100 ml of diethyl ether and 100 ml of hexane to precipitate by-products, the solvent was filtered and evaporated yielding 4.7 g of yellow liquid, which was CIPP (**IV**). *m/z* calculated for $C_{19}H_{31}BO_3NCl$ (M^+): 367.2086; *m/z* found: 367.2070. ^1H NMR (C^2HCl_3) δ [ppm *vs.* tetramethylsilane (TMS)] 1.30 (s, 12H, CH_3C), 1.50–2.10 (m, 6H, CH_2), 2.93 (s, 6H, NCH_3) 3.42 (t, J = 7.2 Hz, 1H, CHB), 3.95 (t, J = 6.2 Hz, 2H, OCH_2) 6.10–7.30 (m, 4H aromatic).

Pinacol 1-acetamido-5-(3-dimethylaminophenoxy)pentane-1-boronate. 1,1,1,3,3,3-Hexamethyldisilazane (2.03 g, 12.6 mmol) in 40 ml of THF was treated with 12.6 mmol of butyllithium in hexane

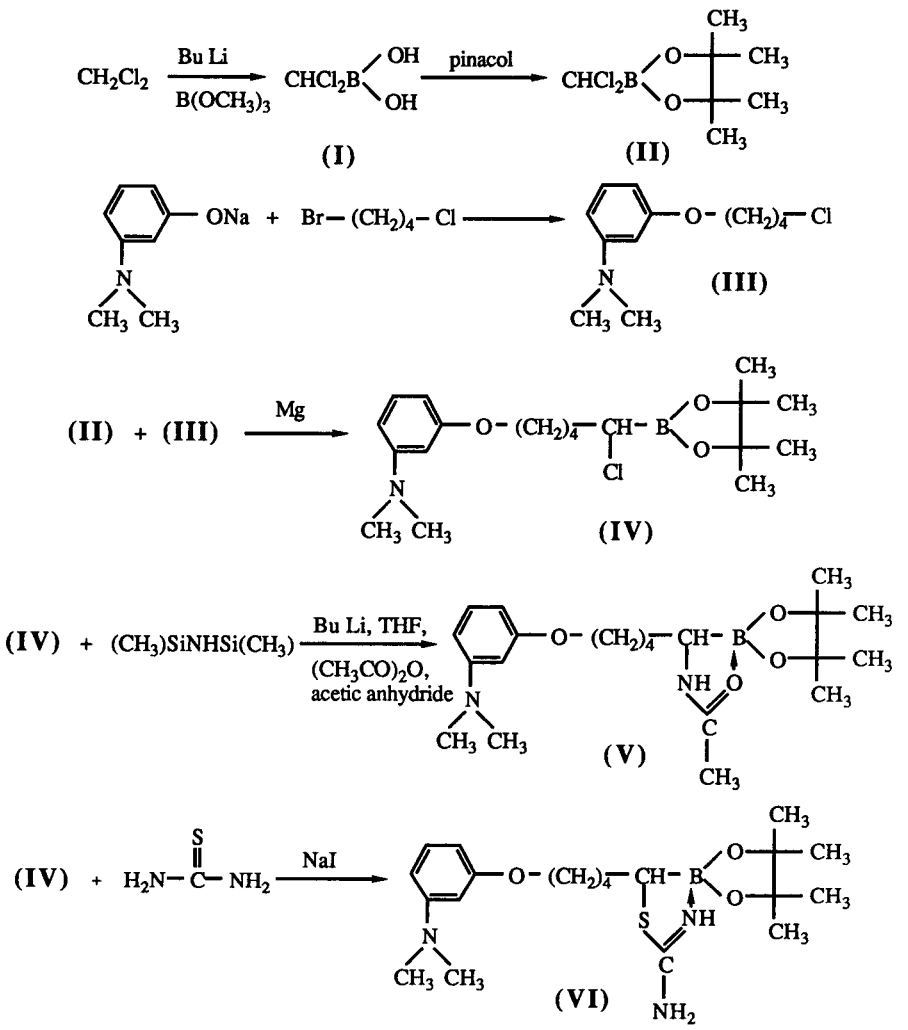

Fig. 1. Synthesis of aliphatic boronate ligands. Pinacol 1-chloro-5-(3-dimethylaminophenoxy)-1-boronate (**IV**), pinacol 1-acetaamido-5-(3-dimethylaminophenoxy)-1-boronate (**V**) and pinacol 1-thiourea-5-(3-dimethylaminophenoxy)-1-boronate (**VI**).

(5.04 ml of 2.5 *M* solution) at 0°C. The mixture was cooled to −70°C and 12 mmol of **IV** at 10 ml of THF was added at once. The mixture was allowed to reach room temperature and mixed for 5 h. The solution was cooled to −70°C and 3.86 g (37.8 mmol) of acetic anhydride were added. This was followed by adding 25.2 mmol of acetic acid. The mixture was kept overnight at 25°C and concentrated under vacuum. The residue was dried at 80°C under 0.02 Torr for 1 h and the resulting crude product was extracted three times with 10 ml of hexane. The first fraction was discarded, and the last two fractions were evaporated to yield 1.55 g (33.1%) of **V**. *m/z* calculated for $C_{21}H_{35}BO_4N_2$ (M^+): 390.2690; *m/z* found: 390.2683. ^1H NMR (C^2HCl_3) δ (ppm *vs.* TMS) 1.18 (s, 6H, CH_3C), 1.19 (s, 6H, CH'_3C), 1.31–1.76 (m, 6H, CH_2), 2,06 (s, 1H, CH_3CO) 2.38 (br. m, 1H, CHB), 2.90 (s, 6H, CH_3N) 3.92 (dt, J = 6.2 Hz, 2H, OCH_2), 6.24–6.36 (m, 3H aromatic) 7.10 (t, J = 8.2 Hz, 1H arom.) 9.74 (br. s, 1H, NH).

Pinacol 1-thiourea-5-(3-dimethylaminophenoxy) pentane-1-boronate. Sodium iodide (0.69 g, 4.61 mmol) was added to a solution of 1.69 g (4.61 mmol)

of (IV) in 40 ml of dry acetonitrile. The resulting suspension was mixed for 4 h at room temperature, after which thiourea (0.35 g, 4.61 mmol) was added and mixing was continued at room temperature for 72 h. After this, 2 g of sodium carbonate were added and the resulting suspension was stirred for additional 24 h. This mixture was then filtered and concentrated under vacuum. Extraction with diethyl ether, filtration and precipitation with hexane gave 1.22 g (3.18 mmol, 69%) of **VI**. ^{1}H NMR (C^2HCl_3) δ (ppm *vs.* TMS) 1.09 (s, 3H, CH_3C), 1.12 (s, 3H, CH_3C), 1.13 (s, 3H, CH_3C), 1.15 (s, 3H, CH_3C), 1.37–2.00 (m, 6H, CH_2), 2.38 (m, 1H, SCHB), 2.95 (s, 6H, CH_3N) 3.93 (dt, J = 6.4 Hz, 2H, OCH_2) 6.25 (s NH), 6.86–6.94 (m, 3H aromatic) 7.23–7.28 (m, 2H arom.).

Immobilization of aliphatic boronate ligands

Sepharose CL-4B (10 ml) was washed and then suspended in 7.2 ml of 1.0 *M* sodium hydroxide containing 5.8 mg sodium borohydride per ml and 7.2 ml of 1,4 butandiol diglycidyl ether. The mixture was stirred slowly at room temperature for 11 h [27]. The resulting activated gel was thoroughly washed with 500 ml of water.

The epoxy activated Sepharose CL-4B was added to 23 ml of a 4-aminothiophenol solution in buffer-ethanol (1:1, pH 10.0). The buffer contained 0.2 *M* sodium bicarbonate and 0.5 *M* sodium chloride. The coupling of 4-aminothiophenol to Sepharose CL-4B was performed at 30°C for 8 h [28]. After this, the activated gel was washed sequentially with 500 ml of binding buffer and 500 ml of 1.0 *M* sodium carbonate. To remove unreacted *p*-aminothiophenol, the gel was further washed with 500 ml of distilled water, then 3 × 250 ml of 30:70, 60:40, 80:20 ethanol–water, and finally with 500 ml of ethanol (100%). The Sepharose was subsequently washed with 3 × 250 ml of 80:20, 60:40, 30:70 ethanol–water and then with 500 ml of distilled water and 250 ml of 1 m*M* hydrochloric acid.

Wet 4-aminothiophenol activated Sepharose CL-4B (10.0 ml) was diazotized by reaction with 30 ml of 1.2 *M* hydrochloric acid and 30 ml of 1% sodium nitrite solution at 0°C for 30 min. After this, it was washed with 250 ml of distilled water and incubated in 30 ml of ethanol–water (2:1) containing 0.6 g of pinacol 1-chloro-5-(3-dimethylaminophenoxy)pentane-1-boronate, pinacol 1-thiourea-5-(3-dimethylaminophenoxy)pentane-1-boronate and pinacol 1-acetamido-5-(3-dimethylaminophenoxy)pentane-1-boronate and 2-3 drops of 1 *M* sodium carbonate. The reaction was allowed to proceed at room temperature for 5 h. The activated gel was washed four times with 100 ml each of 70:30, 60:40, 30:70, 20:80 ethanol–water and finally with 200 ml of distilled water [28]. The concentration of boronate was measured in the reaction mixture before and after reaction and in wash solutions using the Azomethine H method [30].

To hydrolyze the resulting pinacol ester, 30 ml of 1% acetic acid were added to 10 ml of wet activated Sepharose CL-4B. The reaction was allowed to continue for 20 min at room temperature after which the gel was washed with 500 ml of distilled water.

The activated gels were stored in 0.05 *M* potassium phthalate, pH 5.0, 0.05 *M* potassium phosphate monobasic, pH 7.0, or 0.05 *M* ammonium acetate, pH 8.5. The resulting gels contain 5–15 μmol of ligand per ml wet agarose.

Affinity chromatography

A 5-ml small plastic column (0.5 cm) was packed with 1 ml of the 1-chloro-5-(3-dimethylaminophenoxy)pentane-1-boronate agarose (chloro-1-boronate gel), 1-thiourea-5-(3-dimethylaminophenoxy) pentane-1-boronate agarose (thiourea-boronate gel) or 1-acetamido-5-(3-dimethylaminophenoxy)pentane-1-boronate agarose (acetamido-boronate gel) and equilibrated with wash buffer (0.25 *M* ammonium acetate, 0.1 *M* NaCl, pH 8.5). After application of 2.5 μmol of catechol, or one of its derivatives, in 50 μl of distilled water, the column was washed with the wash buffer using 1 ml fractions either (a) eight times or (b) until no further catechol derivatives emerged. The elution was accomplished using 1-ml fractions of (a) 0.1 *M* Tris, 0.2 *M* sorbitol, pH 8.5; (b) 1% acetic acid; (c) 0.25 *M* ammonium acetate, 0.1 *M* NaCl, 0.2 *M* sorbitol pH, 8.5; (d) distilled water. If elution was performed with sorbitol, the columns were regenerated before reuse by treatment with 1% acetic acid.

For the separation of DL-DOPA and catechol, the column (0.5 cm) was packed with 3 ml of the acetamido-boronate gel and equilibrated with 0.25 *M* ammonium acetate, 0.1 *M* NaCl, pH 8.5. The 50 μl mixture containing 2.5 μmol of both compounds was applied to the column and washed with the same

buffer until no further DL-DOPA emerged. After that, elution was performed using 1-ml fractions of 1% acetic acid.

Measurement of the stability of chloro-boronate, thiourea-boronate and acetamido-boronate gels under various pH

The freshly prepared gels (1 ml) were suspended in 5 ml of either 0.05 *M* potassium phthalate buffer, pH 5.0, 0.05 *M* potassium phosphate monobasic buffer, pH 7.0, or 0.05 *M* ammonium acetate buffer pH 8.5. The determination of boron [29] was performed in the buffer above the stored gels. The concentration of boron in solution above the gels corresponded with the amount of decomposed ligand. The boron assays were performed until all of the ligand was released from the matrix.

RESULTS AND DISCUSSION

The chromatograms of DL-DOPA, dopamine, pyrogallol and catechol (see Fig. 2) on chloro-boronate gel are depicted in Fig. 3. DL-DOPA was retarded, while the other catechol derivatives were bound tightly to the column. The low affinity of DL-DOPA is probably caused by repulsion by its weakly ionized carboxylic function. Complete elution of catechol, pyrogallol and dopamine was achieved with 0.1 *M* Tris, 0.2 *M* sorbitol (pH 8.5) or 1% acetic acid. Elution with either 0.1 *M* Tris, 0.2 *M* sorbitol (pH 8.5), or 1% acetic acid produced sharp peaks. If elution was performed with sorbitol, the

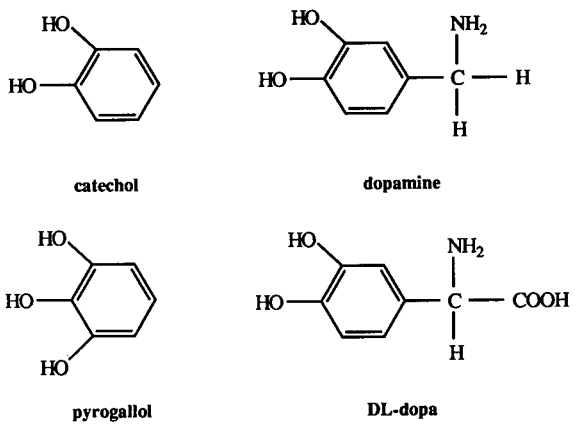

Fig. 2. Structure of catechol derivatives.

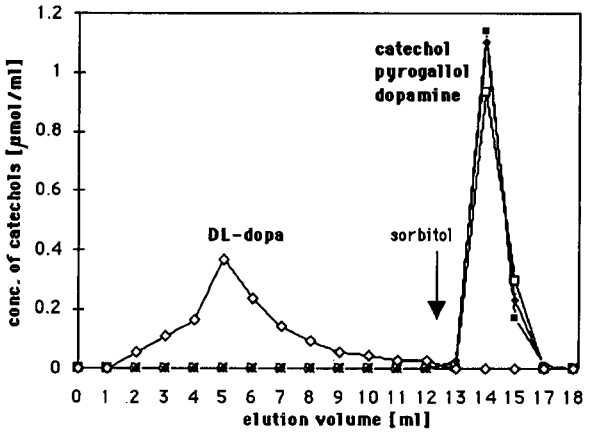

Fig. 3. Chromatography of catechol derivatives on chloro-boronate gel. The column (1 ml volume, 0.5 cm diameter) was packed with 1 ml of gel. Catechol or its derivatives (2.5 μmol in 50 μl of distilled water) was applied and the column was washed with 0.25 *M* ammonium acetate, 0.1 *M* NaCl, pH 8.5 (13 × 1 ml). Final elution was performed using 0.2 *M* sorbitol, 0.1 *M* Tris, pH 8.5.

columns had to be regenerated before reuse by treatment with 1% acetic acid. Elution using distilled water and/or binding buffer containing 0.2 *M* sorbitol wasn't effective and catechol derivatives were removed from the column as broad band.

None of the catechol derivatives were bound to

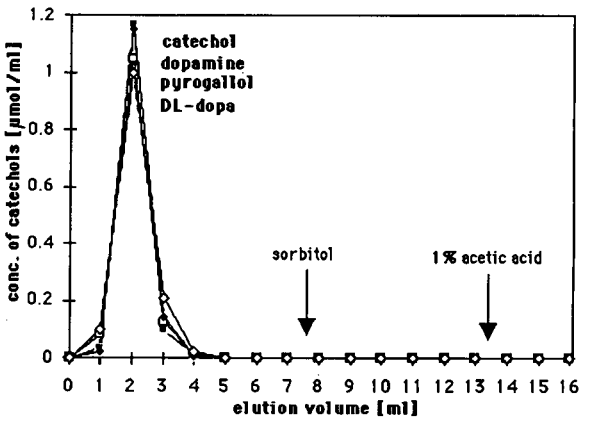

Fig. 4. Chromatography of catechol derivatives on thiourea-boronate gel. The column (1 ml volume, 0.5 cm diameter) was packed with 1 ml of gel. Catechol or its derivatives (2.5 μmol in 50 μl of distilled water) was applied and the column was washed with 0.25 *M* ammonium acetate, 0.1 *M* NaCl, pH 8.5 (7 × 1 ml). Final elution was performed using 0.2 *M* sorbitol, 0.1 *M* Tris, pH 8.5 and 1% acetic acid.

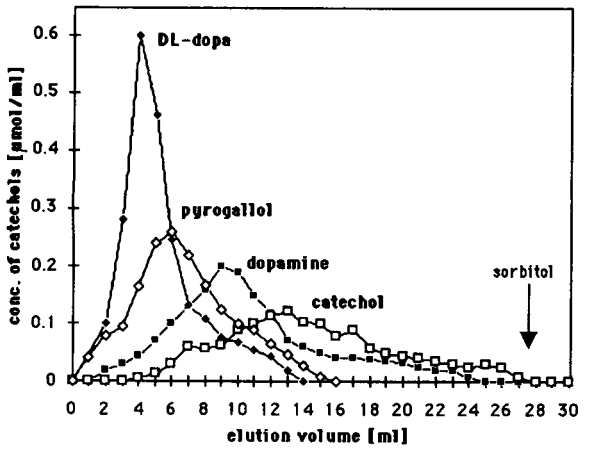

Fig. 5. Isocratic chromatography of catechol derivatives on acetamido-boronate gel. The column (1 ml volume, 0.5 cm diameter) was packed with 1 ml of gel. Catechol or its derivatives (2.5 μmol in 50 μl of distilled water) was applied and the column was washed with 0.25 *M* ammonium acetate, 0.1 *M* NaCl, pH 8.5 (27 × 1 ml). Final elution was performed using 0.2 *M* sorbitol, 0.1 *M* Tris, pH 8.5.

thiourea-boronate gel but instead eluted in the application buffer (see Fig. 4). Comparison of the chromatographic profiles of DL-DOPA on chloro-boronate gel (Fig. 3) and thiourea-boronate gel (Fig. 4) shows the difference between retardation of DL-DOPA on chloro-boronate gel (Fig. 3) and the lack of interaction with thiourea-boronate gel (Fig. 4).

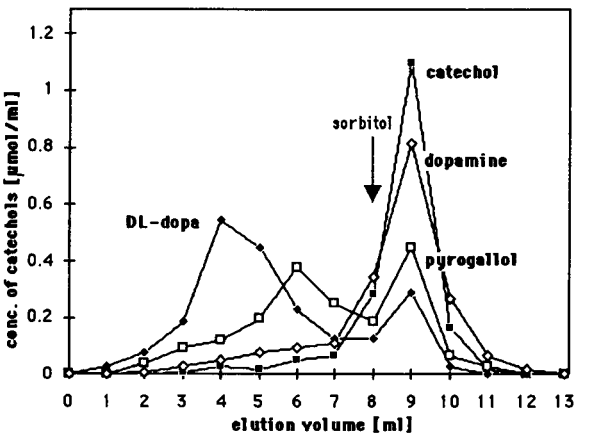

Fig. 6. Affinity elution of catechol derivatives from acetamido-boronate gel. The column (1 ml volume, 0.5 cm diameter) was packed with 1 ml of gel. Catechol or its derivatives (2.5 μmol in 50 μl of distilled water) was applied and the column was washed with 0.25 *M* ammonium acetate, 0.1 *M* NaCl, pH 8.5 (8 × 1 ml). The remaining adsorbed catechol derivatives were simultaneously eluted from the column with the addition of 0.2 *M* sorbitol, 0.1 *M* Tris, pH 8.5.

All catechol derivatives were removed from the column by wash buffer during chromatography on the acetamido-boronate gel and appeared at various retention volumes according their affinity for the sorbent (see Fig. 5). Catechol derivatives were only retarded on the column without elution in order: DL-DOPA, pyrogallol, dopamine and catechol.

Fig. 6 shows chromatograms of catechol derivatives on acetamido-boronate gel. In this experiment, the catechol derivatives were eluted from the column with the addition of sorbitol buffer before being completely eluted with binding buffer, in contrast to the experiments described previously where the catechols were eluted only with binding buffer. These results show that retardation of catechol derivatives is based on the formation of complexes between their hydroxyls and boronate groups of affinity sorbent and not on non-specific interactions based on ionic or hydrophobic effects. After application of a various elution agents (0.1 *M* Tris, 0.2 *M* sorbitol, pH 8.5, or 1% acetic acid), the catechols were released from the column in sharp peak.

Although catechol and dopamine possess different pK_a values (catechol pK_a 9.5; dopamine pK_a 10.5), both have similar affinity for acetamido-boronate gel and are not ionized under these chromatographic conditions. The relatively lower affinity of this gel for dopamine can be due to the cationic charge of primary amine group (pK_a 8.9). The presence of three hydroxylic groups in the molecule decreases affinity of pyrogallol in comparison with catechol, although their hydroxylic groups exhibit the same pK_a. The low affinity for DL-DOPA is apparently caused by the presence of the carboxylic group, which may form an intramolecular hydrogen bond with neighboring hydroxyl groups under alkaline conditions [9]. This chromatographic behavior of DL-DOPA is in agreement with the results obtained on the chloro-1-boronate gel described above (Fig. 3) and with the reports by Singhal *et al.* [8] and Sugurman *et al.* [10], who chromatographed DL-DOPA on various boronate gels.

The stability of boronate gels during storage in aqueous solutions was measured as described under Experimental. All of the gels prepared possess

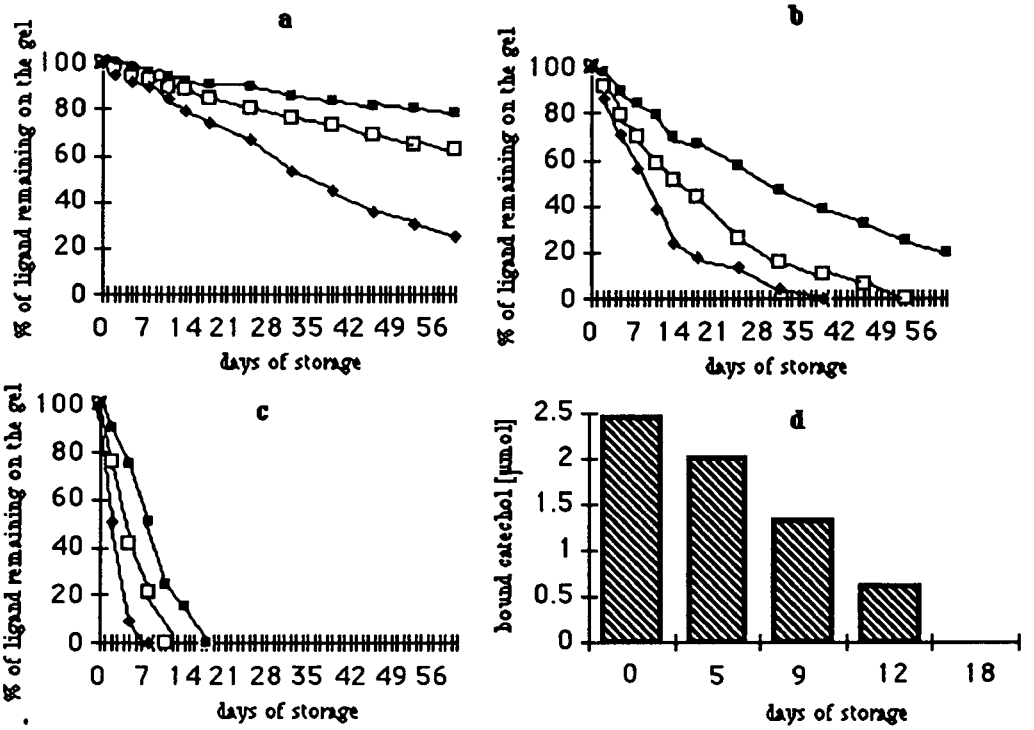

Fig. 7. Stability of aliphatic boronate gels during storage and binding capacity of catechol on the chloro-boronate-gel during storage. Stability of aliphatic boronate gels during storage at various pH; (a) thiourea-boronate gel, (b) acetamido-boronate gel, (c) chloro-boronate-gel. Gels were stored at 4°C in 0.05 *M* potassium phosphate monobasic (pH 7.0) and 0.05 *M* ammonium acetate (pH 8.5) (5 ml of buffer per 1 ml of gel) and the determination of boron was performed on buffer above the stored gels. (d) Binding capacity of catechol on the chloro-boronate-gel during storage in pH 5.0 buffer. Chromatography of catechol was performed in a column packed with 1 ml of gel. Catechol or its derivatives (2.5 μmol in 50 μl of distilled water) was applied and the column was washed with 0.25 *M* ammonium acetate, 0.1 *M* NaCl, pH 8.5 (1-ml fractions). Final elution was performed using 0.2 *M* sorbitol, 0.1 *M* Tris, pH 8.5.

higher storage stability under slightly acidic conditions, rather than neutral or alkaline conditions, as seen in Fig. 7.

Unfortunately, chloro-boronate gel, which possesses the tightest binding to catechols, was unstable even under acidic conditions, and about 50% of bound ligand decomposed after 8 days of storage (see Fig. 7c). The binding capacity for catechol on chloro-boronate gel after storage at pH 5.0 is shown in Fig. 7d. The decrease of binding capacity for catechol (Fig. 7d) corresponds with the rate of decomposition of ligand bound to the agarose (Fig. 7c). This is further evidence that binding catechol to chloro-boronate gel is based on diol interaction with boronate groups and not on non-specific interactions.

In contrast, thiourea coordinates with boron to form a relatively stable thiourea-boronate complex (see Fig. 7a). However, the resulting complex is not able to interact with vicinal diols, as described above (Fig. 4).

Although the acetamido-boronate gel (Fig. 7b) was less stable than thiourea-boronate gel, probably because the effect of the acetamido-boronate complex on ester stabilization is not as significant as in thiourea-boronate complex, the acetamido-boronate complexes were more stable than chloro-boronate.

From these results, it can be seen that the acetamido-boronate gel offers the best compromise between stability and the ability to interact with diols. Separation of DL-DOPA from catechol was chosen as an example of utilization of acetamido-boronate gel (see Fig. 8). While DL-DOPA eluted

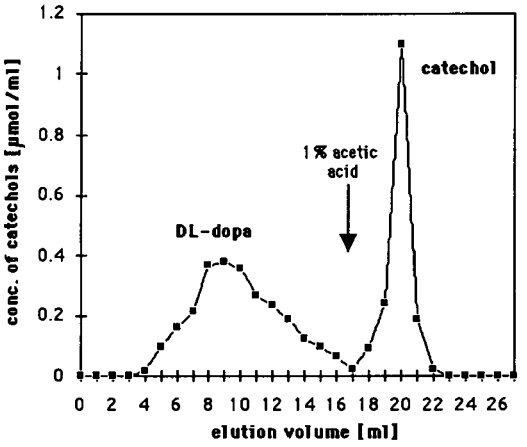

Fig. 8. Separation of DL-DOPA and catechol on acetamido-boronate gel. The column (3 ml volume, 0.5 cm diameter) was packed with 3 ml of gel. The mixture (2.5 µmol of DL-DOPA and 2.5 µmol of catechol in 50 µl of distilled water) was applied and the column was washed with 0.25 *M* ammonium acetate, 0.1 *M* NaCl, pH 8.5 (1-ml fractions). Final elution was performed using 0.2 *M* sorbitol, 0.1 *M* Tris, pH 8.5.

from the column in a low retention volume, catechol was more retarded, and its elution was accelerated using 1% acetic acid, yielding a sharp peak.

CONCLUSIONS

These experiments demonstrate that aliphatic boronate esters can be used as ligands in boronate chromatography and that an adjacent heteroatom, capable of internally coordinating to the boronate, will alter the chromatographic property of the resulting matrix. Acetamido-boronate gel can be used for separation of various catechol derivatives. Thiourea-boronate gel does not interact with catechols, while chloro-boronate gel, which bound catechols quantitatively, is rather unstable. The chief problem is the low stability of aliphatic boronates, which is the major limitation to their further utilization in boronate chromatography. Further investigations may, however, yield aliphatic boronate of sufficient stability for chromatographic application which, in turn, may reduce or eliminate non specific adsorption so often seen with aromatic boronates as ligands.

ACKNOWLEDGEMENT

This paper is based in part upon work supported by the Texas Advanced Research Program (Advanced Technology Program) under Grant No. 003545-002.

REFERENCES

1 H. L. Weith, J. L. Wiebers and P. T. Gilham, *Biochemistry*, 9 (1970) 4396–4401.
2 M. Rosenberg, J. L. Wiebers and P. T. Gilham, *Biochemistry*, 11 (1972) 3623–3628.
3 M. Rosenberg and P. T. Gilham, *Biochim. Biophys. Acta*, 246 (1973) 337–340.
4 B. Pace and N. R. Pace, *Anal. Biochem.*, 107 (1980) 128–135.
5 M. Uziel, L. H. Smith and S. A. Taylor, *Clin. Chem. (Winston-Salem, N.C.)*, 22 (1976) 1454.
6 E. Pfandenhauser and S. Tong, *J. Chromatogr.*, 162 (1979) 585.
7 R. P. Singhal, R. K. Bajaj, C. M. Buess, D. B. Smoll and V. N. Vakharia, *Anal. Biochem.*, 107 (1980) 1–22.
8 R. P. Singhal, B. Ramamurthy, N. Govindraj and Y. Sarwar, *J. Chromatogr.*, 543 (1991) 1738.
9 R. P. Singhal and S. S. M. DeSliva, *Adv. Chromatogr.*, 31 (1992) 312.
10 M. Sugurman and H. Lipke, *Anal. Biochem.*, 121 (1982) 251–256.
11 S. Higa, T. Suzuki, A. Hayashi, I. Tsuge and Y. Yamamura, *Anal. Biochem.*, 77 (1977) 25–32.
12 A. Gasion, T. Wood and L. Chiltemerere, *Anal. Biochem.*, 118 (1981) 4.
13 V. Akparov and V. Stepanov, *J. Chromatogr.*, 155 (1978) 329–336.
14 S. Cartwritght and S. Waley, *Biochem. J.*, 221 (1984) 505–512.
15 J. H. Hagaman and G. D. Kuehn, *Anal. Biochem.*, 77 (1977) 3055.
16 N. D. Cook and T. J. Peters, *Biochim. Biophys. Acta*, 828 (1985) 205–212.
17 A. K. Mallia, G. T. Hermanson, R. I. Krohn, E. K. Fujimoto and P. K. Smith, *Anal. Lett.*, 14 (1981) 649–661.
18 T. K. Mayer and Z. R. Freedman, *Clin. Chim. Acta*, 127 (1983) 147–184.
19 D. C. Klenk, G. T. Hermanson, R. I. Krohn, E. K. Fujimoto, A. K. Mallia, P. K. Smith, J. O. England, H. M. Weidmeyer, R. R. Little and D. E. Goldstein, *Clin. Chem. (Winston-Salem, N.C.)*, 28 (1982) 2088–2094.
20 S. Fulton, *Boronate Ligands in Biochemical Separations*, Amicon Corporation, Danvers, MA, 1981.
21 A. Berghold and W. H. Scouten, in W. H. Scouten (Editor), *Solid Phase Biochemistry*, Wiley, New York, 1983, pp. 1349–187.
22 D. S. Matteson and T.-C. Ceng, *J. Org. Chem.*, 33 (1968) 3055.
23 D. S. Matteson and G. D. Schaunberg, *J. Org. Chem.*, 31 (1966) 726.
24 D. S. Matteson and G. D. Schaunberg, *J. Organomet. Chem.*, 8 (1967) 359.

25 D. S. Matteson and K. M. Sadhu, *Organometallics*, 3 (1984) 614.
26 H. C. Brown and J. V. N. Vara Prasad, *J. Org. Chem.*, 51 (1986) 4526.
27 M. Biedrzycki, W. H. Scouten and Z. Biedrzycka, *J. Organomet. Chem.*, 431 (1992) 255.
28 J. Porath, *Methods Enzymol.*, 34 (1974) 13–30.
29 M. W. Rathke, E. Chao and G. Wu, *J. Organomet. Chem.*, 122 (1976) 145.
30 M. K. John, H. H. Chuan and J. H. Neufeld, *Anal. Lett.*, 8 (1975) 559–568.

Journal of Chromatography, 625 (1992) 101–108
Elsevier Science Publishers B.V., Amsterdam

CHROM. 24 496

Improved crown ether-based chiral stationary phase

Toshio Shinbo, Tomohiko Yamaguchi, Hiroshi Yanagishita, Dai Kitamoto, Keiji Sakaki and Masaaki Sugiura

National Chemical Laboratory for Industry, 1–1 Higashi, Tsukuba, Ibaraki 305 (Japan)

(First received June 18th, 1992; revised manuscript received July 13th, 1992)

ABSTRACT

An improved crown ether-based chiral stationary phase (CSP) was prepared by dynamic coating of a reversed-phase silica gel with a new chiral crown ether which was designed to have more lipophilicity than the previously used one, while preserving the basic structure responsible for chiral recognition. The CSP showed not only excellent enantioselectivity for amino acids, but also higher stability against organic solvents in the mobile phase. No desorption of the crown ether from the support was observed in a mobile phase containing up to 40% of methanol. An increase in methanol concentration in the mobile phase gave rise to a decrease in the retention of amino acids and an increase in the "apparent" enantioselectivity, *i.e.*, the separation coefficient and the resolution factor. A possible retention mechanism is proposed to explain these behaviours.

INTRODUCTION

Recently, much attention has been paid to chiral stationary phases (CSPs) based on host–guest molecular recognition [1–6]. Cram and co-workers [1,2] developed chiral packings by binding chiral crown ethers covalently to polystyrene and silica gel, and showed that a chiral crown ether-based packing is a powerful tool for the optical resolution of amino acids.

In an earlier paper [3], we also reported another crown ether-based CSP prepared by dynamic coating of the chiral crown ether **1** [(*R*)-**1** and (*S*)-**1**], on reversed-phase (RP) silica gels. The CSP showed excellent enantioselectivity toward a wide variety of amino acids and amines. However, it had a disadvantage that only aqueous solutions of inorganic species could be used as mobile phase. As the crown ether was embedded in the alkyl chain of the RP support by hydrophobic interaction, passage of methanol-containing solutions through the CSP easily desorbed the coated crown ether from the support.

In this paper, we report an improved crown ether-based CSP that can be used in methanol-containing mobile phases. The crown ether (*R*)-**2**, a derivative of (*R*)-**1** having higher lipophilicity and preserving the basic structure responsible for chiral recognition, was prepared by attaching an octyl chain to the dinaphthyl ring, and was immobilized dynamically on RP silica gel in a similar manner to that described previously. The elution behaviour of racemic amino acids on this CSP was examined, and the characteristics of the CSP is discussed in comparison with those of the previous one.

EXPERIMENTAL

Reagents and materials

Preparation of (R)-2,3:4,5-bis[1,2-(3-phenyl-6-octylnaphtho)]-1,6,9,12,15,18-hexaoxacycloeicosa-2,4-diene [(R)-2]. The *R*-enantiomer of **2** [(*R*)-**2**] was prepared according to Fig. 1.

(R)-6,6'-Dioctyl-2,2'-dimethoxy-1,1'-dinaphthyl [(R)-6]. Bromine (4 ml) was added over a 20-min period to a solution of 10 g of (*R*)-2,2'-dimeth-

Correspondence to: Dr. Toshio Shinbo, National Chemical Laboratory for Industry, 1–1 Higashi, Tsukuba, Ibaraki 305, Japan.

0021-9673/92/$05.00

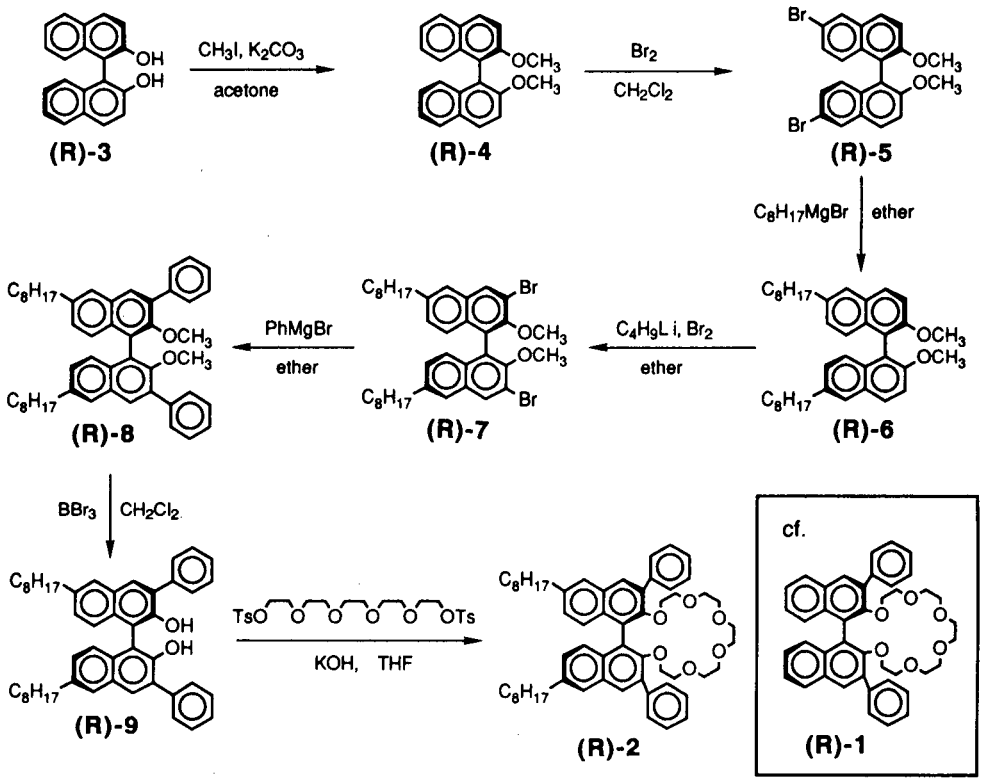

Fig. 1. Reaction scheme for the preparation of (*R*)-**2**.

oxy-1,1′-dinaphthyl [(*R*)-**4**] in 100 ml of dichloromethane stirred under nitrogen at −75°C. The mixture was stirred for 2.5 h, then gradually warmed to 25°C. After 30 min, 300 ml of 10% Na_2SO_3 were added to decompose unreacted bromine. The cake-like material that formed and the residue resulting from evaporation of the dichloromethane phase were combined and purified by column chromatography (silica gel, benzene–cyclohexane) to give 14 g (93%) of (*R*)-6,6′-dibromo-2,2′-dimethoxy-1,1′-dinaphthyl [(*R*)-**5**].

To a mixture of 10 g of (*R*)-**5** and 1.25 g of Ni[$(C_6H_5)_2P(CH_2)_3P(C_6H_5)_2$]$Cl_2$ [7] in 150 ml of diethyl ether under nitrogen were added 100 ml of a diethyl ether solution of octylmagnesium bromide (63 mmol) and the mixture was refluxed for 20 h. The reaction mixture was shaken with 800 ml each of 1 *M* HCl and dichloromethane. The organic phase was washed, dried and evaporated. The residue was chromatographed on silica gel (light petroleum–diethyl ether) and 8.1 g (72%) of (*R*)-6,6′-dioctyl-2,2′-dimethoxy-1,1′-dinaphthyl-[(*R*)-**6**] were obtained.

The following syntheses were carried out in a similar manner to those described in the literature [8].

(R)-6,6′-Dioctyl-3,3′-diphenyl-2,2′-dihydroxy-1,1′-dinaphthyl [(R)-8]. To a solution of 5.2 g of tetramethylethylenediamine in 400 ml of diethyl ether were added under nitrogen 32 ml of 1.6 *M* butyllithium in hexane. After the mixture had been stirred for 15 min at 25°C, 6.8 g of (*R*)-**6** were added and the suspension was stirred for 3 h. The mixture was cooled to −75°C and 10 ml of bromine in 30 ml of pentane were added over a 10-min period. The mixture was warmed to 25°C, stirred for 1 h, then 300 ml of a saturated solution of Na_2SO_3 were added and the mixture was stirred for an additional 4 h. The mixture was then shaken with dichloromethane and the organic layer was dried and evaporated. The residue was purified by column chromatography (silica gel, cyclohexane–benzene) to give 4.8 g

(55%) of (*R*)-6,6′-dioctyl-3,3′-dibromo-2,2′-dimethoxy-1,1′-dinaphthyl [(*R*)-**7**].

To a mixture of 4.4 g of (*R*)-**7** and 0.5 g of $Ni[P(C_6H_5)_3]_2Cl_2$ in 50 ml of diethyl ether stirred under nitrogen were added 20 mmol of phenylmagnesium bromide in 30 ml of diethyl ether and the mixture was refluxed for 20 h. After cooling, the reaction mixture was shaken with 500 ml each of 1 *M* HCl and dichloromethane. The organic layer was dried and evaporated, and the residue was purified by column chromatography (silica gel, cyclohexane–benzene) to obtain 1.66 g (38%) of (*R*)-6,6′-dioctyl-3,3′-diphenyl-2,2′-dimethoxy-1,1′-dinaphthyl [(*R*)-**8**].

To a solution of 1.5 g of (*R*)-**8** in 150 ml of dichloromethane at 0°C were added 7.5 g of BBr_3. The mixture was stirred for 24 h at 25°C, then cooled to 0°C. After the excess of BBr_3 had been decomposed with water, the organic layer was washed with water, dried, evaporated, and chromatographed on silica gel (cyclohexane–benzene) to obtain 1.55 g (80%) of (*R*)-6,6′-dioctyl-3,3′-diphenyl-2,2′-dihydroxy-1,1′-dinaphthyl [(*R*)-**9**].

*(R)-2,3:4,5-Bis[1,2-(3-phenyl-6-octylnaphtho)]-1,6,9,12,15,18-hexaoxacycloeicosa-2,4-diene [(R)-**2**].* To a solution of 0.74 g of (*R*)-**9** and 0.68 *g* of pentaethylene glycol ditosylate in 100 ml of tetrahydrofuran stirred under nitrogen was added 0.24 g of KOH and the mixture was refluxed for 72 h. The mixture was shaken with 250 ml each of dichloromethane and water and the organic layer was dried and evaporated. The residue was purified by column chromatography (silica gel, light petroleum–diethyl ether) and gel permeation chromatography (polystyrene, chloroform) to obtain 0.44 g (46%) of desired compound [(*R*)-**2**]. Specific rotation, $[\alpha]^{22}_{589}$ + 7.7° (*c* 8.68, THF). Mass spectrum, *m/z* 864 (M^+). ^1H NMR (400 MHz), d, 0.87 (t, CH_3, 6H), 1.29 (m, other CH_2, 20H), 1.70 (m, β-CH_2, 4H), 2.71 (t, α-CH_2, 4H), 3.41 (m, OCH_2, 20H), 7.47 (m, ArH, 18H).

Preparation of (R)-2-coated CSP

The preparation of (*R*)-**2**-coated CSP was performed in a similar manner to that described in a previous paper [3]. A solution of (*R*)-**2** in methanol–water (97:3) was circulated through an ODS column [LiChrospher RP-18(e) or LiChrosorb RP-18, d_p 5 μm, 125 x 4 mm I.D.] using a liquid chromatographic pump. To the solution, water was added stepwise to reduce the methanol–water ratio gradually to about 70:30. The immobilization of the crown ether on the support was monitored by the decrease in the UV absorption of the solution. The amount of crown ether coated was chosen to be 79 and 173 mg per column, because preliminary experiments revealed that, although an increase in the amount of crown ether coated gave a larger separation of enantiomers, as reported previously [3], an excessive amount (> 300 mg) of crown ether led to a severe decrease in the number of theoretical plates.

Chromatographic procedures

Chromatography was performed using a liquid chromatographic pump (DIP-1; Jasco), an injector (Model 7125; Rheodyne), a UV detector (S-310A; Soma) and an integrator (Chromatocorder11; System Instrumenz). The column temperature was controlled by placing the column in a thermostated water bath. The eluent was 0.01 *M* perchloric acid.

The resolved enantiomers were detected using UV spectrophotometry at 200 or 254 nm. The configurations of the enantiomers in the eluates were identified by comparison of their retention times with those of authentic enantiomers.

Column parameters such as capacity factors (k_L, k_D), separation coefficient (α) and resolution factor (R_s) were calculated in the usual manner.

RESULTS AND DISCUSSION

Retention and resolution of various amino acids

Fig. 2 shows some examples of the elution profiles of racemic amino acids at 25°C on the CSP coated with 173 mg of (*R*)-**2**. Racemic amino acids were clearly separated into their enantiomers on this (*R*)-**2**-coated CSP, as was observed on (*R*)-**1**-coated CSP [3]. L-Enantiomers of all the amino acids were eluted prior to D-enantiomers. As D-enantiomers of amino acids form more stable complexes with the *R*-enantiomer of the crown ether [8], this observation reflects that the enantiomer forming a more stable complex with the crown ether was eluted after the enantiomer forming a less stable complex.

Table I shows the chromatographic data obtained at 25 and 4°C using the CSP coated with 79

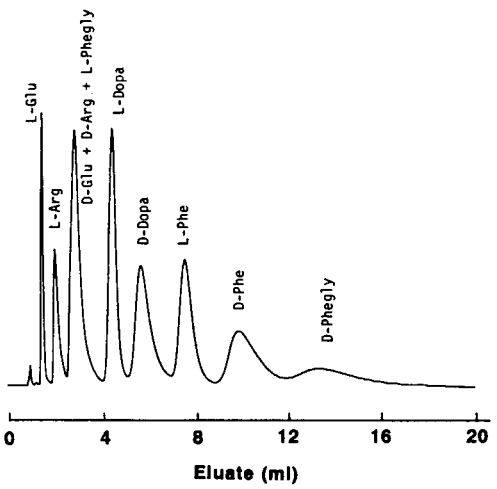

Fig. 2. Separation of five racemic amino acids on an (*R*)-**2**-coated CSP. Column, 125 mm x 4 mm I.D., LiChrospher RP-18(e) coated with 173 mg of (*R*)-**2**; eluent, 0.01 *M* perchloric acid; flow-rate, 1 ml/min; column temperature, 18°C; detection, UV (203 nm).

mg of (*R*)-**2**. Polar amino acids gave lower and hydrophobic amino acids gave higher retentions. Amino acids having one bulky substituent group at the β-carbon atom showed a large enantioselectivity, and amino acids having more than one substituent group at the β-carbon atom showed a smaller enantioselectivity (compare Leu with Ile and NVal with Val). Lower column temperatures gave higher retention and enantioselectivity.

The mechanism of the enantioselective retention of racemic amino acids on the crown ether-coated CSP can be described as follows. The injected amino acid (A^+) is distributed between the mobile and the stationary phases mainly by the following two reactions:

$$A^+ + X^- \rightleftharpoons \overline{A^+X^-} \quad (1)$$

$$A^+ + \bar{C} + X^- \rightleftharpoons \overline{(AC)^+X^-} \quad (2)$$

where X^- is the anion (perchlorate) in the mobile phase and C and AC^+ are the crown ether and the complex between the crown ether and amino acid, respectively. The bars above the letters represent the stationary phase. The crown ether-involved reaction (reaction 2) determines the enantioselectivity. The difference in the complex formation constants give rise to the difference in retention. As reaction 1 is not enantioselective, its contribution reduces the separation coefficient (*i.e.*, the apparent enantioselectivity).

This mechanism can explain the above results. The difference in retention reflects the nature of the RP stationary phase. Hydrophobic amino acids are retained strongly on RP stationary phases owing to the hydrophobic interaction and are eluted later.

The reason why the enantioselectivity depends on the number of substituent groups at the β-carbon atom is as follows. Although the bulkiness of a substituent at the α-carbon atom of an amino acid is important for chiral recognition, the presence of more than one substituent group at the β-carbon atom gives rise to extensive steric hindrance and decreases the complex formation constant of the favourable enantiomer. The small complex formation constant reduces the relative contribution of reaction 2 to the retention and hence gives small separation coefficients and resolution factors.

The temperature dependence of enantioselective retention is explained as described previously [3]. A lower temperature increases the chiral recognition of the crown ether [9], and also increases the retention due to reaction 1 [10]. The combination of these two effects causes an increase in enantioselective retention.

*Comparison of (R)-**2**-coated CSP with (R)-**1**-coated CSP*

In Table II, chromatographic data obtained using the CSP coated with 173 mg of (*R*)-**2** are compared with those obtained using the CSP coated with an equimolar amount (128 mg) of (*R*)-**1**. The retention and the enantioselectivity on the (*R*)-**2**-CSP were almost the same as those on the (*R*)-**1**-CSP, but there was a small difference between them. The capacity factors and separation coefficients of the (*R*)-**2**-CSP were slightly smaller than those of the (*R*)-**1**-CSP. As (*R*)-**2** was designed and synthesized to have the same crown ring and the same chiral barriers as (*R*)-**1**, their abilities for chiral recognition can be assumed to be the same. Therefore, the slight difference mentioned above is ascribed to the difference in their environment on the support. (*R*)-**1** is assumed to be present at the interface with the hydrophobic naphthyl group buried in the RP stationary phase and part of the relatively hydrophilic crown ring extruding toward the mobile

TABLE I

CAPACITY FACTORS AND ENANTIOSELECTIVITY FOR AMINO ACIDS ON (*R*)-**2**-COATED CSP

Column, 125 mm × 4 mm I.D. LiChrosorb RP-18 cooated with 79 mg of (*R*)-**2**; eluent, 0.01 *M* perchloric acid; flow-rate, 0.5 ml/min; detection, UV (200 nm); sample: 10^{-8} mol.

Amino acid[a]	18°C				2°C			
	k_L	k_D	α	R_s	k_L	k_D	α	R_s
Ala	0.31	0.51	1.64	0.97	0.48	0.98	2.04	2.44
AABA	0.60	0.76	1.27	0.71	0.64	1.01	1.57	1.79
Val	1.18	1.18	–	–	1.35	1.49	1.10	0.45
NVal	1.38	1.91	1.39	2.15	1.73	2.90	1.67	3.85
Leu	4.09	5.32	1.30	2.79	4.70	7.09	1.51	4.21
Ile	3.23	3.51	1.09	0.76	3.92	4.48	1.14	1.32
NLeu	4.50	5.93	1.32	2.64	5.62	8.54	1.52	4.40
Met	2.29	3.72	1.63	3.99	3.33	7.08	2.12	6.99
Phe	12.62	13.83	1.10	1.17	18.52	20.93	1.13	1.55
PGly	2.45	8.27	3.37	8.63	3.19	19.32	6.06	14.47
Ser	0.19	0.19	–	–	0.24	0.35	1.50	0.55
Thr	0.21	0.30	1.44	0.37	0.27	0.58	2.17	1.61
Cys	0.31	0.44	1.43	0.46	0.42	0.79	1.89	1.50
Tyr	9.42	10.24	1.09	1.04	20.74	22.97	1.11	1.22
Dopa	5.52	6.12	1.11	1.15	12.76	14.53	1.14	1.53
Asp	0.23	0.40	1.76	0.54	0.43	0.80	1.84	1.68
Asn	0.35	0.35	–	–	0.21	0.35	1.65	0.37
Glu	0.43	0.83	1.91	1.69	0.75	3.25	4.33	7.92
Gln	0.23	0.64	2.75	1.97	0.40	1.75	4.37	4.98
Lys	0.81	0.81	–	sh	2.00	2.36	1.18	0.97
Arg	0.47	0.81	1.73	1.61	0.92	2.40	2.60	4.11
His	0.28	0.28	–	–	0.64	0.64	–	–
PEA	17.37	19.70	1.13	0.77	22.85	27.66	1.21	1.67
AECL	1.31	1.86	1.42	2.13	1.81	3.15	1.74	3.88

[a]AABA = 2-Aminobutyric acid; NVal = norvaline; NLeu = norleucine; PGly = phenylglycine; PEA = 1-phenylethylamine; AECL = 3-amino-ε-caprolactam. Other abbreviations have their usual meanings.

TABLE II

CAPACITY FACTORS AND ENANTIOSELECTIVITY FOR AMINO ACIDS OBTAINED USING (*R*)-**1**- AND (*R*)-**2**-COATED CSPs

Column, 125 mm × 4 mm I.D., LiChrospher RP-18(e) coated with an equimolar amount of crown ether, (*R*)-**1** 128 mg and (*R*)-**2** 173 mg; temperature, 18°C; eluent 0.01 *M* perchloric acid; flow-rate, 1.0 ml/min; detection, UV (200 nm); sample, 10^{-7} mol.

Amino acid	(*R*)-**2**				(*R*)-**1**			
	k_L	k_D	α	R_s	k_L	k_D	α	R_s
Ala	0.56	1.04	1.86	1.73	0.50	1.02	2.03	2.09
Val	0.88	1.02	1.16	sh	0.98	1.22	1.25	0.86
Met	2.16	4.61	2.14	3.03	2.26	5.90	2.61	4.68
Phe	7.59	9.49	1.25	1.11	8.73	13.22	1.51	2.33
PGly	2.70	12.76	4.73	6.56	2.81	17.54	6.25	7.39
Thr	0.32	0.59	1.86	1.26	0.31	0.53	1.69	1.08
Tyr	6.29	8.13	1.29	1.03	6.15	9.39	1.53	2.38
Glu	0.66	2.38	3.63	3.87	0.59	2.34	3.95	5.05
Arg	0.88	1.80	2.06	1.75	0.71	1.36	1.93	2.10

phase. As (*R*)-**2** is more hydrophobic than (*R*)-**1** owing to the additional octyl chain on the naphthyl group, it is reasonable to assume that the crown ring of (*R*)-**2** is buried deeper than (*R*)-**1** in the RP stationary phase. Accordingly, the interaction of an amino acid in the mobile phase is weaker with (*R*)-**2** than with (*R*)-**1**. This means that with (*R*)-**2**, the contribution of reaction 2 to the retention becomes smaller, and the "apparent enantioselectivity" is decreased.

Stability of the (R)-2-CSP towards methanol-containing mobile phases

As reported previously [3], the crown ether-coated CSP is stable when aqueous mobile phases are used. However, application of this CSP to highly lipophilic amino acids (or amines) requires the addition of an organic solvent to the mobile phase, because they are strongly retained in a merely aqueous mobile phase [11].

Table III shows the stability of the (*R*)-**2**-CSP towards methanol-containing mobile phases. The amounts of crown ether desorbed from the (*R*)-**2**-CSP using mobile phases containing various concentrations of methanol are compared with those desorbed from the (*R*)-**1**-CSP. As can be seen, the (*R*)-**2**-CSP showed excellent stability and no loss of the crown ether was observed even in 40% methanol solution, whereas the (*R*)-**1**-CSP lost the crown ether gradually even in the mobile phase containing only 10% of methanol. This result indicates that octyl chain gives satisfactory hydrophobicity for the crown ether to be held on the RP stationary phase in the ordinary methanol-containing mobile phase.

Effect of methanol in the mobile phase on retention and enantioselectivity

Table IV gives column parameters obtained using mobile phases containing up to 40% of methanol. The capacity factors, as expected, decreased with increase in methanol concentration, and for Trp it was reduced to be less than one sixth on changing the methanol concentration from 0 to 40%. On the other hand, the separation coefficients were unexpectedly increased with increase in methanol concentration. Examples of elution profiles are shown in Fig. 3.

The reason for the increase in separation coefficients is not clear, but a possible explanation is as follows. According to the aforementioned mechanism, the enantioselective retention of amino acids on this CSP arises from the two distribution reactions: simple distribution (reaction 1), and crown ether-involved complex formation (reaction 2). If it is assumed that part of the crown ring is extruded into the mobile phase, an increase in methanol concentration will bring about an increase in the retention due to reaction 2 because the complex formation constant in methanol is, generally, larger than that that in water [12]. On the other hand, the retention due to reaction 1 is decreased with increase in methanol concentration. Therefore, an increase in methanol concentration leads to an increase in the relative contribution of reaction 2 to the retention, and hence to an increase in the separation coefficient.

TABLE III

AMOUNT OF CROWN ETHER DESORBED FROM (*R*)-**1**- and (*R*)-**2**-COATED CSPs IN AQUEOUS MOBILE PHASES CONTAINING METHANOL

Temperature, 18°C; flow-rate, 0.5 ml/min.

CSP	Amount of crown ether desorbed (mg/ml of eluate)				
	0% CH_3OH	10% CH_3OH	20% CH_3OH	30% CH_3OH	40% CH_3OH
(*R*)-**1**	–[a]	$3.5 \cdot 10^{-7}$	$6.7 \cdot 10^{-7}$	$9.6 \cdot 10^{-6}$	$1.5 \cdot 10^{-4}$
(*R*)-**2**	–	–	–	–	–

[a] –, Not detected (less than 10^{-7} mg/ml of eluate).

TABLE IV

EFFECT OF METHANOL CONCENTRATION IN THE MOBILE PHASE ON RETENTION AND ENANTIOSELECTIVITY FOR AMINO ACIDS

Column, 125 mm × 4 mm I.D., LiChrospher RP-18(e) coated with 173 mg of (*R*)-**2**; temperature, 18°C; eluent, 0.01 *M* perchloric acid + methanol; flow-rate, 1.0 ml/min; detection, UV (200 nm); sample, 10^{-7} mol.

Amino Acid	Enantiomer	0% CH_3OH			10% CH_3OH			20% CH_3OH			30% CH_3OH			40% CH_3OH		
		k'	α	R_s	k'	α	R_s	k'	α	R_s	k'	α	R_s	k'	α	R_s
Met	L	2.16	2.14	3.03	1.60	2.50	3.34	1.35	3.00	3.45	1.17	3.48	3.82	1.01	3.91	3.58
	D	4.61			4.01			4.06			4.08			3.96		
Phe	L	7.59	1.25	1.11	4.32	1.37	1.38	3.04	1.54	1.70	2.11	1.79	1.98	1.56	2.00	1.91
	D	9.49			5.90			4.68			3.77			3.12		
PGly	L	2.70	4.73	6.56	2.00	5.69	6.11	1.78	6.71	5.82	1.39	7.88	5.56	1.14	8.64	5.05
	D	12.76			11.39			11.92			10.97			9.82		
Trp	L	47.70	1.15	0.73	21.45	1.27	1.24	12.52	1.44	1.58	7.26	1.66	1.80	4.55	1.89	1.68
	D	54.89			27.25			17.98			12.07			8.59		
Tyr	L	6.29	1.29	1.03	3.17	1.49	1.57	2.23	1.75	1.92	1.50	2.05	2.27	1.12	2.28	2.19
	D	8.13			4.72			3.90			3.08			2.56		
Glu	L	0.61	3.63	3.87	0.58	4.17	3.65	0.54	4.78	3.61	0.53	5.15	4.12	0.50	5.41	4.02
	D	2.38			2.42			2.60			2.74			2.73		
Arg	L	0.88	2.06	1.75	0.63	2.27	1.75	0.47	2.39	1.83	0.39	2.50	1.79	0.33	2.53	1.56
	D	1.80			1.43			1.13			0.97			0.83		

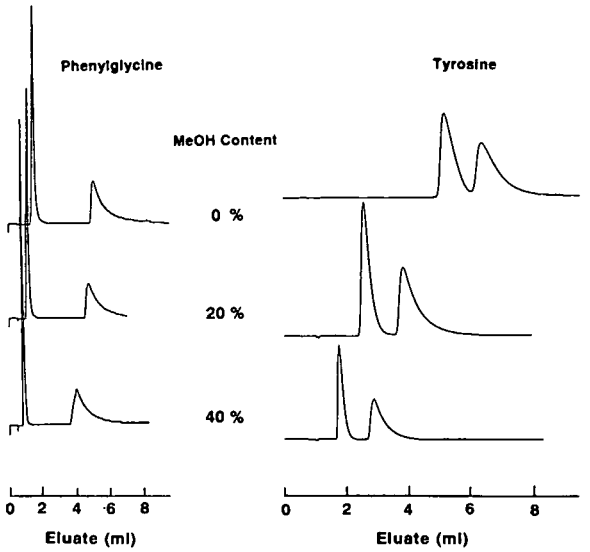

Fig. 3. Elution profiles of racemic phenylglycine and tyrosine in aqueous mobile phases containing various concentrations of methanol. Details as in Table IV.

ACKNOWLEDGEMENTS

The authors are indebted to Dr. H. Nakanishi and Dr. Y. Nagawa for the measurement and interpretation of NMR spectra.

REFERENCES

1 L. R. Sousa, G. D. Y. Sogah, D. H. Hoffman and D. J. Cram, *J. Am. Chem. Soc.*, 100 (1978) 4569.
2 G. D. Y. Sogah and D. J. Cram, *J. Am. Chem. Soc.*, 101 (1979) 3035.
3 T. Shinbo, T. Yamaguchi, K. Nishimura and M. Sugiura, *J. Chromatogr.*, 405 (1987) 145.
4 A.M. Stalcup, S. C. Chang, D. W. Armstrong and J. Pitha, *J. Chromatogr.*, 513 (1990) 181.
5 N. Thuaud, B. Sebille, A. Deratani and G. Lelièvre, *J. Chromatogr.*, 555 (1991) 53.
6 B. Sellergren, M. Lepisto and K. Mosbach, *J. Am Chem. Soc.*, 110 (1988) 5853.
7 K. Tamao, K. Sumitani, Y. Kiso, M. Zembayashi, A. Fujioka, S. Kodama, I. Nakajima, A. Minato and M. Kumada, *Bull. Chem. Soc. Jpn.*, 49 (1976) 1958.
8 D. S. Lingenfelter, R. C. Helgeson and D. J. Cram, *J. Org. Chem.*, 46 (1981) 393.
9 E. P. Kyba, J. M. Timko, L. J. Kaplan, F. de Jong, G. W. Gokel and D. J. Cram, *J. Am. Chem. Soc.*, 100 (1978) 4555.
10 B. L. Karger, J. R. Gant, A. Hartkopf and P. H. Weiner, *J. Chromatogr.*, 128 (1976) 65.
11 N. Tanaka, H. Goodell and B. L. Karger, *J. Chromatogr.*, 158 (1978) 233.
12 F. de Jong and D. N. Reinhoudt, *Advances in Physical Organic Chemistry, Vol. 17: Stability and Reactivity of Crown Ether Complexes*, Academic Press, London, 1981.

Journal of Chromatography, 625 (1992) 109–120
Elsevier Science Publishers B.V., Amsterdam

CHROM. 24 477

Direct separation of enantiomers using multiple-interaction chiral stationary phases based on the modified β-cyclodextrin-bonded stationary phase

Song Li and William C. Purdy

Department of Chemistry, McGill University, Montreal, Quebec H3A 2K6 (Canada)

(First received April 14th, 1992; revised manuscript received June 23rd, 1992)

ABSTRACT

Several multiple-interaction chiral stationary phases have been developed. These stationary phases contain a hydrophobic cavity capable of inclusion complexation, aromatic groups capable of π–π interaction, polar hydroxyl groups capable of hydrogen-bonding with the polar functional groups of the solute, and bulky non-polar groups providing steric repulsion. The characteristics and properties of these stationary phases are described. The direct separation of enantiomers of a wide variety of chiral compounds are reported. The effect of mobile phase composition on the retention and resolution is discussed.

INTRODUCTION

In recent years, direct separation of enantiomers using high-performance liquid chromatographic (HPLC) chiral stationary phases has been a very active and fast-moving field due to its importance in optical purity determination, monitoring asymmetric synthesis, pharmacokinetics studies, metabolism studies, and dating of archaelogical materials. Today, more than 50 different chiral stationary phases are commercially available.

Cyclodextrin-bonded stationary phase, especially β-cyclodextrin stationary phase, developed by Armstrong [1], is one of the most widely used chiral stationary phases. β-Cyclodextrin stationary phase offers the following advantages: (i) it is chemically and physically more robust and (ii) it can be used in a reversed-phase mode with solvents containing water and organic modifiers. However, β-cyclodextrin stationary phase has a limited range of applications. Chiral recognition is significant only for those molecules which have a large hydrophobic group in the molecule. This limitation is mainly related to the nature of β-cyclodextrin itself and the chiral recognition mechanism.

As was known, the structure of β-cyclodextrin has the shape of a toroid or hollow truncated cone. The side of the torus with the larger circumference contains the secondary hydroxyl groups (on carbons 2 and 3 of the glucose units) while the primary hydroxyl groups (on carbon 6 of the glucose units) are on the small side. The interior of the cavity contains two rings of C–H groups with a ring of glycosidic oxygens in between. As a result, the cavity is relatively hydrophobic while the external faces are hydrophillic [2]. Chiral recognition mechanism studies [3,4] show that in reversed-phase applications, chiral recognition is mainly caused by hydrophobic interaction between the cavity of cyclodextrin and the hydrophobic moiety of the solute. The chief problem is that because the interior of the cavity, with glycosidic oxygens, is not quite non-polar and both ends of the cavity are open to solvent, only those guest molecules which have large hydrophobic groups and appropriate shape can form

Correspondence to: Dr. W. C. Purdy, Department of Chemistry, McGill University, Montreal, Quebec H3A 2K6, Canada.

0021-9673/92/$05.00

strong inclusion complexes with it. Therefore, chiral recognition is significant only for these larger molecules. To overcome this problem, much work has been done to increase the binding forces by modifying the cyclodextrins through the reaction of the hydroxy groups with a variety of modifiers [5,6].

In this work, a regiospecific modification was carried out by attaching groups on the primary hydroxyl side of the β-cyclodextrin. This modified β-cyclodextrin stationary phase contains: (i) a hydrophobic cavity, capable of inclusion complexation; (ii) aromatic groups, capable of π–π interaction; (iii) polar hydrogen-bonding and/or dipole stacking sites; and (iv) bulky non-polar groups, providing steric repulsion, Van der Waals interaction, and/or confirmational control. Therefore, it can be said that it is a multiple-interaction type of chiral stationary phase. The enantiomeric separations of various compounds including amino acid derivatives, phenothiazine and related drugs, and other pharmaceuticals have been achieved on these multiple-interaction chiral stationary phases and are presented in this paper. The characteristics and chromatographic properties are discussed.

EXPERIMENTAL

Chemicals

β-Cyclodextrin was from Chemical Dynamics (South Plainfield, NJ, USA). HPLC-grade methanol and triethylamine were from Fisher Scientific (Montreal, Canada). N-(2-Aminoethyl-3-aminopropyl)trimethoxysilane was from Huls America (Bristol, PA, USA). Amino acids and their derivatives, and the phenothiazines were from Sigma (St. Louis, MO, USA). All other chemicals were from Aldrich (Milwaukee, WI, USA).

Silica gel

Silica gel purchased from Chromatographic Separation (Montreal, Canada) as Spherisorb was used as the support material. This gel consists of spherical particles with a pore diameter of 8 nm and a mean particle size of 5 μm. The surface area of the silica gel, according to the manufacturer, is 220 m^2/g. Before carrying out reactions, the silica support was acid-hydrolysed in 0.2 *M* hydrochloric acid at 90°C for 24 h, so that its surface had a maximum number of Si–OH groups per unit of surface area. After cooling and filtration, the silica was washed with distilled water until neutral, and then dried at 170°C *in vacuo* for 12 h.

Apparatus

All chromatographic experiments were performed on a liquid chromatographic system which consisted of a Model 590 pump (Waters Assoc., Milford, MA, USA), a Model 440 254-nm ultraviolet detector (Water Assoc.) and a Model 7125 injector containing a 10-μl loop (Rheodyne, Cotati, CA, USA). Injections were made on column using precision sampling syringes. All column evaluations were carried out at ambient temperature (*ca.* 20°C).

The column was 25 cm × 0.46 cm I.D. 0.655 cm O.D. stainless-steel tubing (Chromatographic Separation) with a mirror-finish. Columns were prepared by a high-pressure balanced-density slurry packing technique using a Shandon HPLC packing pump (Chromatographic Separation).

Preparation of the multiple-interaction stationary phases

The preparation procedure used in this investigation is shown in Fig. 1. It involves four steps: (i) bonding the N-(2-aminoethyl-3-aminopropyl)trimethoxysilane to the silica gel; N-(2-aminoethyl-3-aminopropyl)trimethoxysilane was used as a linkage material to join the β-cyclodextrin to the silica; (ii) regiospecific sulfonation of the primary hydroxyl groups of the β-cyclodextrin with *p*-toluenesulfonyl chloride [7]; (iii) reaction of 2-aminoethyl-3-aminopropyl-bonded silica gel (I) with toluenesulfonyl-β-cyclodextrin (II); the reaction between the amino groups of the N-(2-aminoethyl-3-aminopro-

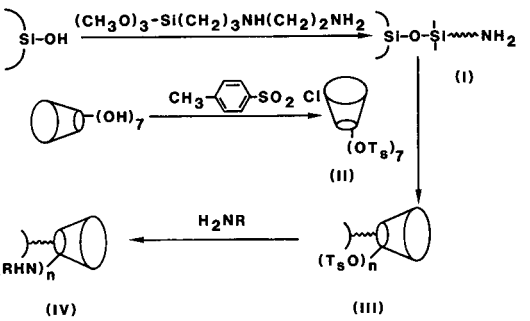

Fig. 1. General procedure for the preparation of the modified β-cyclodextrin stationary phases.

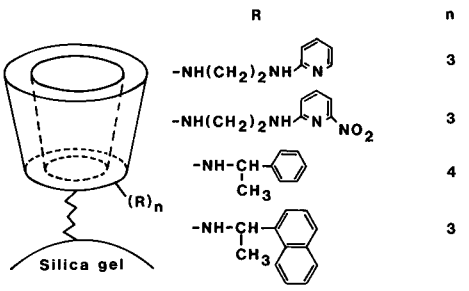

Fig. 2. Structures of modified β-cyclodextrin stationary phases.

pyl)-bonded silica and the toluenesulfonyl groups of the cyclodextrin links the cyclodextrin to the silica gel [8]; and (iv) modification of the bonded cyclodextrin by further reaction of the unreacted toluenesulfonyl groups of the cyclodextrin (III) with various modifiers.

Fig. 2 shows the structural diagrams of these modified β-cyclodextrin stationary phases.

Analyses of the surface species

Identification of the surface species is made by means of infrared spectroscopy using transmission and the attenuated total reflection techniques. In this investigation, the amounts of cyclodextrin bonded to the silica gel were determined by means of a colorimetric method based on the reaction of D-glucose with tetrazolium blue [8,9]. The stationary phase (0.5 g) was hydrolysed in 30 ml of 0.5 *M* sulfuric acid at 100°C for 5 h. The hydrolysate was neutralized with sodium hydroxide and made up to 50 ml with water. In a reaction vessel with a glass stopper, 1 ml of this solution was made to react at 50°C for 10 min with 1 ml of a solution of 0.5% tetrazolium blue in ethanol–0.2 *M* aqueous sodium hydroxide (80:20, v/v). After the vessel had cooled, 3 ml methanol were added, and sodium sulfate was removed by centrifugation. The absorbance of the clear solution was measured at 525 nm.

RESULTS AND DISCUSSION

Characteristics of the packings

Surface coverage. The most valuable parameter for characterization of bonded-phase packings is the surface concentration of bonded functional groups. However, most of the commercial chiral stationary phases are only characterized by their carbon content, which gives poor and incomplete information. In general, it is very difficult to precisely and/or accurately evaluate the content of the cyclodextrins bonded to the surface of silica gel by the method based on differences in the gel weights before and after the bonding reaction or by elemental analysis. In this work, the amount of cyclodextrin bonded to the silica gel was colorimetrically determined by a method based on the reaction of D-glucose produced by hydrolysing cyclodextrins with 3,3′-[3,3′-dimethoxy-(1,1′-biphenyl-4,4′-diyl)]bis-(2,5-diphenyl-2H-tetrazolium)dichloride, called tetrazolium blue. The maximum coverage for these stationary phases was determined to be 50.6 μmol/g.

To determine the degree of the substitution on the β-cyclodextrin of the modified β-cyclodextrin stationary phases, an HPLC method has been used. The degree of substitution for each of the stationary phases was calculated and is reported in Fig. 2.

Stability. The chemical stability of the stationary phase is primarily determined by that of silica and the bonded cyclodextrins. Consequently, most solvents can be used if they are within the pH range of 3.0–7.0. Although cyclodextrin molecules and their derivatives are fairly stable in alkaline solution, they are quite suspectible to hydrolysis in strongly acidic solution. For example, the rate constants of hydrolysis of β-cyclodextrin at pH 0.13, 40°C and 100°C, are $1.0 \cdot 10^{-5}$ and $4.8 \cdot 10^{-2}$ min^{-1}, respectively, corresponding to half-lives of 48 days and 14 min [4]. The stability in aqueous solutions of pH > 7 is influenced by the presence of organohydroxylsilyl groups resulting from the hydrolysis of Si–$(OCH_3)_3$ or Si–$(OC_2H_5)_3$ groups of the linkage materials. These stationary phases can be used at temperature up to 65°C.

Chromatographic properties

Column efficiency. Each of the slurry-packed modified β-cyclodextrin columns was conditioned with a solvent series of increasing polarity. This series consisted of isopropanol, methanol and methanol–water (50:50). After conditioning, all columns were evaluated using a test mixture of *o*-chlorophenol, *p*-chlorophenol, 3-nitroaniline, and 2-biphenylol and a mobile phase of methanol–water (50:50). The HETP values obtained on two of these columns

TABLE I

COLUMN EFFICIENCY (HETP VALUES)

Columns	HETP (cm)	
	0.5 ml/min	1.0 ml/min
β-CD	0.0014	0.0015
β-CD–NHCH(CH$_3$)–	0.0035	0.0040
β-CD–NHCH(CH$_3$)–	0.0039	0.0046

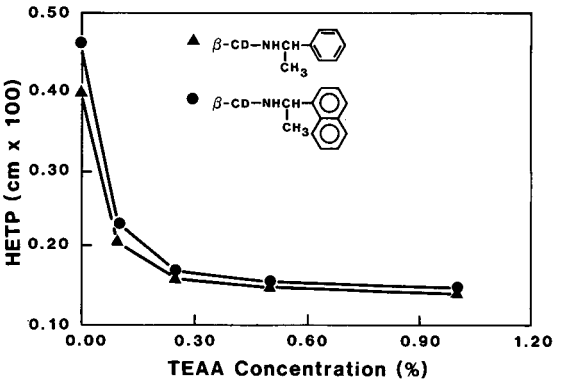

Fig. 3. Effect of TEAA on the column efficiency. Mobile phase: methanol–TEAA buffer (50:50) (pH 5.5).

at flow-rates of 0.5 and 1.0 ml/min are listed in Table I. As can be seen, the efficiences of these modified columns are lower than that of the unmodified β-cyclodextrin column.

Like the conventional β-cyclodextrin columns, the efficiency of these modified β-cyclodextrin columns is dramatically improved by adding TEAA (triethylammonium acetate) buffer in the mobile phase. As shown in Fig. 3, the presence of 0.3% TEAA in the mobile phase can produce a three-fold increase in the column efficiency.

Retention behaviour. For most solutes, the retention time on these multiple-interaction stationary phases is much longer than the retention time on the β-cyclodextrin-bonded stationary phase. For instance, the capacity factors of *o*- *m*-, and *p*-chlorophenols are more than two times larger than those on the β-cyclodextrin stationary phase (see Table II). The longer retention time means that the modification indeed increases the binding forces of inclusion complex formation between the guest and the cyclodextrin. However, the retention time for dansylamino acids is shorter than that obtained on the β-cyclodextrin column. The reason for this behaviour is that the modification may make the cyclodextrin cavity too shallow, so that the large naphthylamine group cannot completely fit into the cavity. The strength of the inclusion complex is, therefore, decreased.

TABLE II

CAPACITY FACTORS OBTAINED ON β-CYCLODEXTRIN AND MODIFIED β-CYCLODEXTRIN COLUMNS

Solute	Capacity factors		
	β-CD	β-CD–NHCH(CH$_3$)–	β-CD–NHCH(CH$_3$)–
o-Chlorophenol	0.87	2.56	2.32
m-Chlorophenol	1.00	2.35	2.15
p-Chlorophenol	1.10	2.16	2.01
COOH, CHNHSO$_2$, CH$_2$OH, –N(CH$_3$)$_2$	2.06	1.71	1.83

Enantioselectivities

It has been found that these multiple-interaction stationary phases exhibited higher enantioselectivity toward a wider variety of chiral compounds. The improved enantioselectivity may be rationalized in terms of the following two factors.

(1). The attached groups on the primary hydroxyl side of β-cyclodextrin cavity increase the capability of inclusion complexation with a wide variety of compounds.

It is believed that to achieve chiral separation on a β-cyclodextrin stationary phase, the guest molecule must form an enantioselective complex with β-cyclodextrin. Typically, cyclodextrin inclusion complex formation is associated with a favourable enthalpy and an unfavourable entropy change [4,10]. Although the exact nature of the bonding

forces involved in the complex formation still remains controversial, several proposals have been made to interpret the binding forces between the guest and the cyclodextrin molecule in solution [10–13]: (i) Van der Waals–Landon dispersion forces (the so-called "hydrophobic effect"); (ii) hydrogen bonding between the polar group of the guest molecule and the secondary hydroxyl groups of the cyclodextrin; (iii) release of high-energy water molecules in complex formation; and (iv) release of the strain energy in the ring frame system of the cyclodextrin. In most cases, a combination of these factors seems to be operative, with the first dominant. However, because the interior of the cavity, with a ring of ether oxygens, is not quite non-polar and both ends of the cavity are open to solvent, only those guest molecules which have large hydrophobic groups and appropriate shape can form strong inclusion complexes with it.

For these modified β-cyclodextrin stationary phases, the attached groups on the primary hydroxyl side can cluster to form a flexible cap on the smaller side of β-cyclodextrin cavity [14]. This will increase the hydrophobicity of the cavity, thus increasing the capability of the inclusion complex formation with the smaller molecules. It was found that the solutes which have only one benzyl ring in the molecule were indeed bound strongly on these modified β-cyclodextrin stationary phases as shown by the increased retention time on these columns.

(2). These stationary phases provide multiple-in-

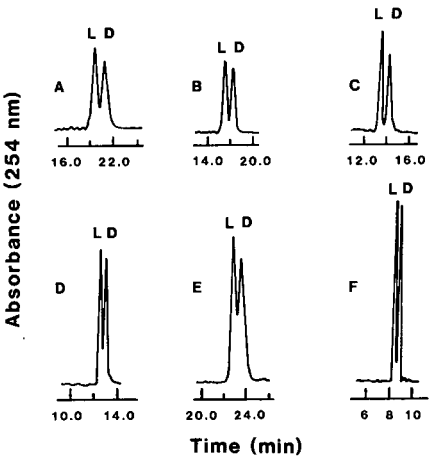

Fig. 4. Chromatograms for the resolution of dansyl-DL-amino acids. (A) dansyl-DL-norleucine; (B) dansyl-DL-valine; (C) dansyl-DL-leucine; (D) dancyl-DL-aspartic acid; (E) dansyl-DL-glutamic acid; (F) dansyl-DL-threonine. Column, (*S*)-(−)-α-methylbenzylamine-modified β-cyclodextrin-bonded column (250 × 4.6 mm I.D.); mobile phase, methanol–TEAA buffer solution (35:65) (0.3% TEAA, pH 5.5).

TABLE III

OPTICAL RESOLUTION OF THE ENANTIOMERS OF DANSYLAMINO ACIDS

Solute	β-CD–NHCH(CH$_3$)–⟨⟩				β-CD
	k'^a	α	R_s	Mobile phase[b]	R_s[c]
Norleucine	5.27	1.10	1.01	30:70	2.30
Aspartic acid	5.00	1.11	0.90	30:70	–
Serine	2.50	1.09	0.80	30:70	0.43
Leucine	4.93	1.14	1.30	30:70	–
Valine	3.13	1.10	1.10	30:70	2.10
Norvaline	3.20	1.08	0.74	30:70	0.83
Glutamic acid	3.60	1.08	0.75	30:70	–
Methionine	2.97	1.07	0.75	30:70	0.70
Threonine	2.16	1.13	1.20	30:70	2.00
Phenylalanine	6.27	1.08	0.80	30:70	1.10

[a] The capacity factor of the first-eluted enantiomer.
[b] The numbers represent the volume ratio of methanol to TEAA buffer (0.3% TEAA, pH 6.2)
[c] Data from ref. 23.

teraction sites which increase the number of specific, discrete, and simultaneous interactions between chiral solute molecules and the stationary phase.

This modified β-cyclodextrin stationary phase has the following functional groups: (i) an hydrophobic cavity, capable of inclusion complexation; (ii) aromatic groups, capable of π–π interaction; (iii) polar hydrogen-bonding sites, capable of hydrogen binding with the polar functional groups on the chiral solutes; and (iv) bulky non-polar groups, providing steric repulsion. It has been believed that the greater the number of specific, discrete, and simultaneous interactions between chiral solutes molecules and a chiral locus on the stationary phase, the greater the likelihood of effective chiral discrimination, and thus of chromatographic resolution of enantiomeric solutes [15].

Enantiomeric separations

These modified stationary phases have demonstrated a broader range of applications. The enantiomeric separations of various compounds, including amino acids and their derivatives, carboxylic acids, phenothiazine and related drugs, and other pharmaceuticals have been achieved on these modified β-cyclodextrin columns.

TABLE IV

OPTICAL RESOLUTION OF THE ENANTIOMERS OF DNP-AMINO ACIDS

Solute[a]	Structure	β-CD–NHCH(CH$_3$)–C$_6$H$_5$				β-CD
		k'[b]	α	R_s	Mobile phase[c]	R_s[d]
DNP-DL-α-amino-*n*-butyrc acid	CH_3CH_2–CHCOOH NHR	3.20	1.05	0.70	30:70	0.60
DNP-DL-norvaline	$CH_3CH_2CH_2$–CHCOOH NHR	3.87	1.12	1.20	30:70	0.80
DNP-DL-norleucine	$CH_3(CH_2)_3$–CHCOOH NHR	6.35	1.13	1,83	30:70	2.45
DNP-DL-α-amino-*n*-caprylic acid	$CH_3(CH_2)_5$–CHCOOH NHR	11.01	1.21	1.62	30:70	3.40
DNP-DL-methionine sulfone	$CH_3SO_2CH_2CH_2$–CHCOOH NHR	1.67	1.08	0.90	30:70	0.90
DNP-DL-methionine	$CH_3SCH_2CH_2$–CHCOOH NHR	3.42	1.17	2.57	25:75	1.50
DNP-DL-ethionine	$CH_3CH_2SCH_2CH_2$–CHCOOH NHR	7.22	1.17	2.37	30:70	2.50
DNP-DL-citrulline	$H_2NCONH(CH_2)_3$–CHCOOH NHR	1.75	1.07	0.80	30:70	0.80
DNP-DL-glutamic acid	$HOOCCH_2CH_2$–CHCOOH NHR	10.20	1.06	0.70	30:70	0.90

[a] R in the structures represents 2,4-dinitrophenyl.
[b] The capacity factor of the first eluted enantiomer.
[c] The number represents the volume ratio of methanol to TEAA buffer (0.3% TEAA, pH 5.5).
[d] Data from ref. 24.

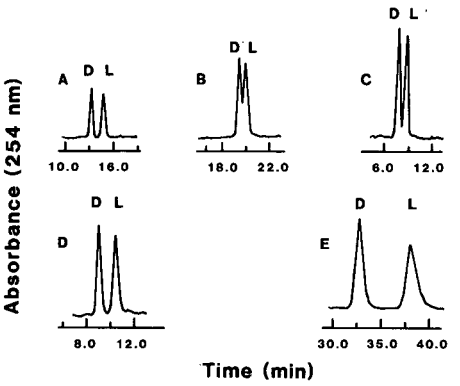

Fig. 5. Chromatograms for the resolution of DNP-DL-amino acids. (A) DNP-DL-ethionine; (B) DNP-DL-glutamic acid; (C) DNP-DL-methionine; (D) DNP-DL-norleucine; (E) DNP-DL-α-amino-*n*-caprylic acid. Column, (*S*)-(−)-α-methylbenzylamine-modified β-cyclodextrin-bonded column (250 × 4.6 mm I.D.); the mobile phase composition is given in Table IV.

Enantiomeric separation of dansylamino acids

1-Dimethylaminonaphthalene-5-sulfonyl amino acids (dansylamino acids) occupy a key position in the structural investigation of proteins and peptides, and the quantitative analysis of amino acids. Dansyl chloride reacts with free amino acids and is increasingly used in determining the amino-terminal residues of protein and peptides [16].

In this work, the enantiomeric separation of ten dansylamino acids has been achieved on the methylbenzylamine-modified β-cyclodextrin stationary phases using methanol–TEAA buffer solution (0.3% TEAA) as the mobile phase. Table III shows the optical resolution data for these ten dansylamino acids. All ten chiral compounds can be optically separated with resolution factors from 0.74 to 1.30. However, for most dansylamino acids, the resolution factor is lower than that achieved on the unmodified β-cyclodextrin column. The reason, as mentioned before, is that dansylamino acids cannot form strong inclusion complexes with modified β-cyclodextrin stationary phases.

Fig. 4 shows some typical chromatograms for the solutions of these racemic dansylamino acids. The L-enantiomers are eluted first for all the dansylamino acids.

Enantiomeric separations of dinitrophenylamino acids

Dinitrophenylamino acids (DNP-amino acids) have also been used for the quantitative amino acid estimation and the structural investigation of pro-

TABLE V

OPTICAL RESOLUTION OF THE ENANTIOMERS OF OTHER AMINO ACIDS

Solute	Structure	β-CD–NHCH(CH$_3$)–C$_6$H$_5$			
		k'^a	α	R_s	Mobile phase
3-Indoletactylaspartic acid	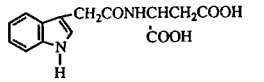	11.1	1.18	1.36	20% Methanol, 0.3% TEAA, pH 7.0
Phenylalanine	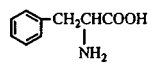	2.06	1.17	1.50	20% Methanol, 0.3% TEAA, pH 5.5
Carbobenzyloxyalanine	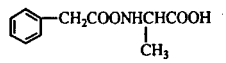	3.68	1.09	0.75	30% Methanol, 0.3% TEAA, pH 5.5
N-Phthaloylalanine	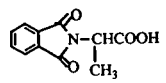	1.45	2.56	2.80	50% Methanol, 0.3% TEAA, pH 5.5

[a] The capacity factor of the first-eluted enantiomer.

teins since they were first applied by Sanger[17] to the determination of the N-terminal residues of insulin. The peptides or proteins react with fluoro-2,4-dinitrobenzene in alkaline solution to give DNP derivatives. On hydrolysis the peptide chain is broken to free amino acids but the original N-terminal amino acid remains largely in the form of its DNP derivatives which can then be extracted with diethyl ether and fractioned for identification [18]. Like the dansylamino acids, DNP-amino acid derivatives are also important in the protein chemistry.

Table IV lists the resolution data for the enantiomers of DNP-amino acids. Some typical chromatograms are shown in Fig. 5. In these cases, the D-enantiomers are eluted first.

Enantiomeric separation of some other chiral compounds

It was also found that the modified β-cyclodextrin stationary phase exhibited a very good enantioselectivity for certain aromatic amino acids and other chiral compounds which contain only one benzyl ring in their molecules. The enantiomers of these chiral compounds, including phenylalanine, phthaloylalanine, tyrosine, carboxylic acids, and some pharmaceuticals, were separated on the methylbenzylamine- and naphthylethylamine-modified β-cyclodextrin columns with methanol–TEAA buffer (0.3% TEAA) as the mobile phase. To date there have been no reports on the resolution of any enantiomers of these chiral compounds on a unmodified β-cyclodextrin column.

TABLE VI

OPTICAL RESOLUTION OF THE ENANTIOMERS OF CHIRAL COMPOUNDS

Solute	Structure	β-CD–NHCH(CH$_3$)–			
		k'^a	α	R_s	Mobile phase
Indoline-2-carboxylic acid	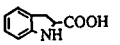	1.84	2.08	3.0	20% Methanol, 0.25% TEAA, pH 7.0
3-Indoletactic acid	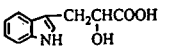	11.1	1.18	1.36	25% Methanol, 0.25% TEAA, pH 6.2
4-Methoxymandelic acid	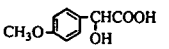	3.77	1.27	1.01	25% Methanol, 0.25% TEAA, pH 6.2
Mandelic acid	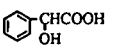	0.42	2.54	3.33	30% Methanol, 0.3% TEAA, pH 5.5
2-Phenylpropanediol	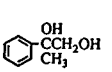	1.0	1.19	1.01	30% Methanol, 0.3% TEAA, pH 5.5
2-Phenylpropionic acid	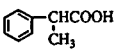	1.65	1.24	1.26	30% Methanol, 0.3% TEAA, pH 5.5
Suprofen	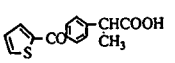	5.25	1.11	0.90	40% Methanol, 0.25% TEAA, pH 6.0

[a] The capacity factor of the first-eluted enantiomer.

Table V shows the optical resolution data for some aromatic amino acids which have only one benzene ring in the molecule. As can been seen, good resolution has been achieved for these D/L pairs with R_s values as large as 2.80 for phthaloyl-alanine.

Table VI summarizes the optical resolution data for other chiral compounds. Most of them are carboxylic acids with only one benzene ring in the molecule. Very good resolutions have been achieved on the methylbenzylamine-modified stationary phase with R_s values greater than 3.00 in several cases.

Table VII shows the optical resolution data for chiral phenothiazine drugs on a naphthylethylamine-modified β-cyclodextrin-bonded phase column. Although the enantiomers of these compounds can be separated on the unmodified β-cyclodextrin column, the resolution factors are much lower than these values.

Fig. 6 shows some typical chromatograms of the chiral compounds.

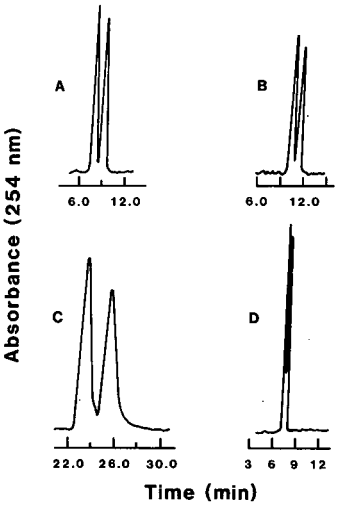

Fig. 6. Chromatograms for the enantiomeric separation of some other chiral compounds. (A) 2-phenylpropionic acid; (B) phenylalanine; (C) trimeperazine; (D) 2-indoletactylaspartic acid. Column, (*S*)-(−)-α-methylbenzylamine-modified β-cyclodextrin-bonded column (250 × 4.6 mm I.D.); mobile phase, methanol–TEAA buffer (30:70) (0.3% TEAA, pH 5.5).

Effect of mobile phase composition on the retention and resolutions

In this work, several polar solvents, such as water, methanol, ethanol, acetonitrile and tetrahydrofuran, were investigated as the potential mobile phase for these modified β-cyclodextrin stationary phases. It was found that most chiral compounds of

TABLE VII

OPTICAL RESOLUTION OF THE ENANTIOMERS OF PHENOTHIAZINES

Solute	Structure	β-CD–NHCH(CH$_3$)–			
		k'^a	α	R_s	Mobile phase
Trimeperazine	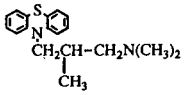	7.77	1.14	1.21	30% Methanol, 0.7% TEAA, pH 5.5
Promethazine	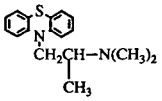	7.74	2.40	3.67	30% Methanol, 0.3% TEAA, pH 5.5
Ethopropazine	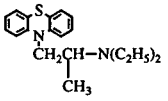	10.1	2.79	4.00	30% Methanol, 0.3% TEAA, pH 5.5

[a] The capacity factor of the first-eluted enantiomer.

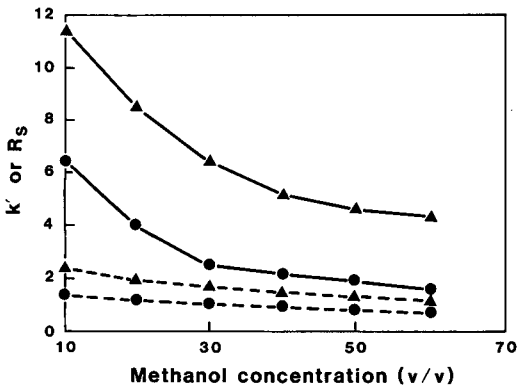

Fig. 7. Effect of methanol concentration on the retention and resolution. Column, (*S*)-(−)-α-methylbenzylamine-modified β-cyclodextrin-bonded column; mobile phase, methanol–TEAA buffer (0.5% TEAA, pH 5.5); flow-rate, 1 ml/min. ▲ = DNP-2-aminocaprylic acid, ● = 4-methoxymandelic acid. —— = k', – – – = R_s.

interest cannot be eluted within a reasonable time from the modified β-cyclodextrin columns using water alone as the mobile phase. The use of 100% methanol, ethanol, acetonitrile or tetrahydrofuran gives no resolution at all. The methanol–water and ethanol–water mobile phases were found to provide much better selectivity than acetonitrile–water and tetrahydrofuran–water mobile phases. The methanol–water system was chosen as the mobile phase.

In order to find the optimum conditions for good resolution, the effects of methanol concentration, TEAA buffer, and pH on the retention time and resolution were studied.

Effect of methanol concentration in the mobile phase

The effect of methanol concentration in the mobile phase on the retention and resolution was investigated by changing the methanol/water ratio in the mobile phase from 10:89.5 to 60:39.5 (v/v). TEAA concentration was 0.5%, and the pH was controlled at 5.5. It was found that the effect of methanol content on the retention and optical resolution gave almost the same tendencies as those observed on the unmodified β-cyclodextrin column. An increase in the methanol concentration resulted in a decrease in boh retention time and resolution factor (see Fig. 7). The effect of methanol concentration on the resolution was almost linear. When the methanol concentration reached 75%, no resolution could be observed for almost all the chiral compounds.

This is not surprising since it is known from the cyclodextrin-binding studies that methanol and other alcohols, such as ethanol, propyl alcohol, and *n*-butyl alcohol, can form inclusion complexes with β-cyclodextrin [19]. The formation constant of the β-cyclodextrin-methanol (1:1) complex has been measured by spectrophotometric examination of the effect of methanol on the association of β-cyclodextrin with sodium 4-[(4-hydroxy-1-naphthyl) azo]-1-naphthalenesulfonate and phenolphthalein [20,21], respectively. Association constants of 0.32 and 0.40 M^{-1} were reported. Assuming that the same considerations apply to our system, the following simple complexation pattern can be used to explain the results obtained:

$$G + CD = G\text{–}CD \quad (1)$$

$$K = [G\text{–}CD]/[G]\,[CD] \quad (2)$$

$$Me + CD = Me\text{–}CD \quad (3)$$

$$K_{Me\text{–}CD} = [Me\text{–}CD]/[Me]\,[CD] \quad (4)$$

Where CD, G, and Me denote β-cyclodextrin, DNP-amino acids, and methanol, respectively. G–CD and Me–CD are the inclusion complexes of β-cyclodextrin–DNP-amino acid and cyclodextrin–methanol, respectively. K and $K_{Me\text{–}CD}$ are the corresponding complex formation constants. Therefore, the true formation constant (K^*) for the inclusion complex of cyclodextrin with solute can be expressed as

$$K^* = \frac{K}{1 + K_{Me\text{–}CD}\,[Me]} \quad (5)$$

If the possible formation of higher stoichiometries between β-cyclodextrin and methanol is taken into consideration, the following equation can be derived:

$$K^* = \frac{K}{1 + K_{Me\text{–}CD}\,[Me] + K_{Me\text{–}CD}\,[Me]^2 + \ldots} \quad (6)$$

As can be seen from eqn. 6, at higher methanol concentrations, methanol can become strongly competitive for complexation with β-cyclodextrin thereby decreasing the degree of complexation between solute and β-cyclodextrin.

In addition, at high methanol concentrations, the properties of the bulk solvent begin to change substantially. Consequently, the presence of the methanol will likely make the solvent more favourable to the solute than a simple aqueous solution. The difference in hydrophobicity of the solvent and β-cyclodextrin cavity will become smaller, making inclusion complex formation between solute and β-cyclodextrin less favourable. Both of these effects could account for the decreases in retention time and resolution factor when the methanol content in the mixture is increased.

Effect of TEAA concentration in the mobile phase

Fig. 8 shows the effect of TEAA buffer concentration in the mobile phase on the retention and optical resolution. It was found that an increase in the TEAA concentration in the mobile phase results in a decreased retention time for both enantiomers. As was observed on unmodified β-cyclodextrin stationary phase, the effect of TEAA concentration on the optical resolution is somewhat more complex. When the TEAA concentration changed from 0% to 1.0%, two types of behaviour can be observed. At the beginning, the resolution increases with the increasing TEAA concentration and then it decreases when TEAA exceeds 0.3%. Resolution maxima are observed at a TEAA concentration of about 0.3%. These observations can be explained by considering the effect of TEAA on both the column efficiency (N) and the enantioselectivity (α) of β-cyclodextrin bonded phase column, and the relationship of resolution (R_s), N and α [22]:

$$R_s = \tfrac{1}{4}(\alpha - 1)\sqrt{N}\,\frac{k'}{(1 + k')} \qquad (7)$$

It has been found that the addition of TEAA buffer in the mobile phase will substantially increase the separation efficiency (N) of a modified β-cyclodextrin-bonded phase column. The increase in separation efficiency will result in an increase in the resolution factor.

On the other hand, the TEAA molecule, as an organic modifier, can include in the β-cyclodextrin cavity and there it competes with solute. The addition of TEAA in the mobile phase will weaken the strength of inclusion complexation between the solutes and the β-cyclodextrin cavity, resulting in a decrease in the enantioselectivity. The results obtained in this study indicate that at low TEAA concentrations the separation efficiency is the limiting factor for the resolution. An increase in TEAA concentration increases the column efficiency, thus increasing the resolution. As the TEAA concentration increases in the mobile phase, the enantioselectivity becomes the limiting factor, thus the resolution decreases with the increasing TEAA concentration. When TEAA concentration exceeds 2.5%, no optical resolution can be observed for most of the chiral compounds.

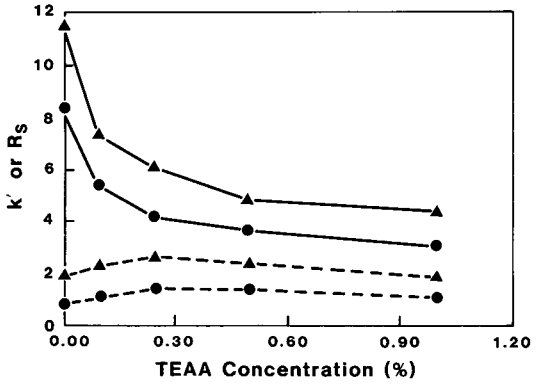

Fig. 8. Effect of TEAA concentration on the retention and resolution. Column, (*S*)-(−)-α-methylbenzylamine-modified β-cyclodextrin-bonded column; mobile phase, methanol–TEAA buffer (35% methanol, pH 5.5); flow-rate, 1 ml/min. ▲ = DNP-2-aminocaprylic acid, ● = 4-methoxymandelic acid. —— = k' − − − = R_s.

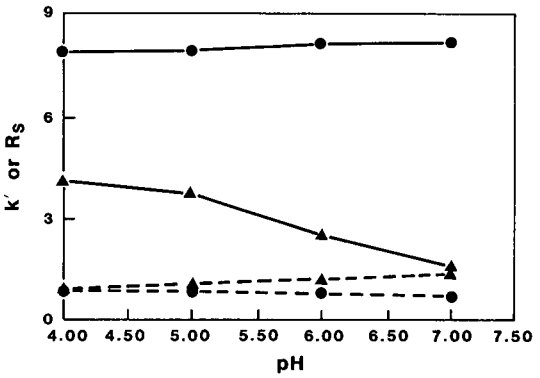

Fig. 9. Effect of pH on the retention and resolution. Column, (*S*)-(−)-α-methylbenzylamine-modified β-cyclodextrin-bonded column; mobile phase, methanol–TEAA buffer (0.3% TEAA, 35% methanol); flow-rate, 1 ml/min. ▲ = Dansyl-serine, ● = trimeperazine. —— = k', − − − = R_s.

Effect of pH

The effect of pH on the retention and resolution was investigated by changing pH of the mobile phase from 4.0 to 7.0 using a 0.5% TEAA buffer. Two typical plots are shown in Fig. 9. It was found that pH only affects the retention and resolution of those compounds which have an ionization constant in the range of 10^{-4} to 10^{-7}. For example, over this pH range the compound trimeperazine, which has a pK_a value of 9.0, will be in its molecular form. Its retention and resolution are not affected by changing pH. The other line shows the effect of pH on dansylserine. Both the retention time and resolution decreased with increasing pH. This is probably due to ionization of this compound.

In general, the effect of mobile phase composition can be summed up as follows: (i) increasing methanol content decreases the retention time and the resolution; (ii) the TEAA buffer improves column efficiency, but decreases the enantioselectivity; and (iii) neutral molecules are more readily retained than charged molecules.

CONCLUSIONS

The modified β-cyclodextrin chiral stationary phases can be seen as a combination of donor–acceptor phase and cyclodextrin phase. They have, on the molecular level, an hydrophobic cavity capable of forming inclusion complexes with the hydrophobic moiety of the solute molecule, aromatic groups capable of π–π (charge-transfer) interaction, polar hydrogen-bonds sites which can form hydrogen bonding with the polar functional groups of the solute, and bulky non-polar groups which provide steric repulsion, Van der Waals interaction and conformational control. These multiple-interaction chiral stationary phases have exhibited a high stereoselectivity toward a wide variety of chiral compounds. Enantiomeric separations of some chiral compounds which have only one benzyl ring in the molecule have been achieved without derivatization. These phases can be operated in the reversed-phase mode with mobile phase containing water and organic modifier. They are chemically and physically robust, and they have a chromatographic behaviour similar to the unmodified β-cyclodextrin column.

These multiple-interaction stationary phases have some disadvantages. (1) For some solutes the retention time is much longer than that with the unmodified β-cyclodextrin stationary phase. This may be a problem for fast analyses. (2) The stationary phases have a light brown coloration probably resulting from the formation of the nitroxide. The presence of the brown color makes the stationary phase unsuitable for thin-layer chromatography.

ACKNOWLEDGEMENT

The authors are indebted to the Natural Sciences and Engineering Research Council of Canada for financial support of this work.

REFERENCES

1 D. W. Armstrong, *US Pat.*, 4 539 399 (1985).
2 M. L. Bender and M. Komiyama, *Cyclodextrin Chemistry*, Springer, New York, 1978, pp. 3–9.
3 D. W. Armstrong, T. J. Ward, R. D. Armstrong and T. E. Beesley, *Science (Washington, D.C.)*, 232 (1986) 1132–1134.
4 S. Li and W. C. Purdy, *Anal. Chem.*, 64 (1992) 1405–1412.
5 D. W. Armstrong, A. M. Stalcup, M. L. Holton, J. D. Duncan, J. R. Faulkner, Jr. and S. C. Chang, *Anal. Chem.*, 62 (1990) 1610–1615.
6 C. D. Chang and D. W. Armstrong, presented at the *Pittsburgh Conference on Analytical Chemistry and Applied Spectroscopy, Chicago, IL, March 4–8, 1991*, paper No. 200.
7 V. W. Lautsch, R. Wiechert and H. Lehmann, *Kolloid Z.*, 135 (1954) 134–136.
8 K. Fujimura, T. Ueda and T. Ando, *Anal. Chem.*, 55 (1983) 446–450.
9 M. D'Amboise, D. Noel and T. Hanai, *Carbohydr. Res.*, 79 (1980) 1–10.
10 R. L. VanEtten, J. F. Sebastian, G. A. Clowes and M. L. Bender, *J. Am. Chem. Soc.*, 89 (1967) 3242–3253.
11 E. S. Hall and H. J. Ache, *J. Phys. Chem.*, 83 (1979) 1805–1807.
12 F. Cramer and W. Kampe, *J. Am. Chem. Soc.*, 87 (1965) 1115–1126.
13 J. Bergeron and M. P. Meeley, *Bioorg. Chem.*, 5 (1976) 197–202.
14 J. Emert and R. Breslow, *J. Am. Chem. Soc.*, 97 (1975) 670–672.
15 T. D. Doyle, in W. J. Lough (Editor), *Chiral Liquid Chromatography*, Blackie, New York, 1989, p. 102.
16 W. R. Gray and B. S. Hartley, *Biochem. J.*, 89 (1963) 379–380.
17 F. Sanger, *Biochem. J.*, 39 (1945) 507–515.
18 L. Kesner, E. Muntwyler, G. E. Griffin and J. Abrams, *Anal. Chem.*, 35 (1963) 83–89.
19 B. Siegel and R. Breslow, *J. Am. Chem. Soc.*, 97 (1975) 6869.
20 Y. Matsui and K. Mochida, *Bull. Chem. Soc. Jpn.*, 52 (1979) 2808.
21 A. Buvari, J. Szejtli and I. Barcza, *J. Inclusion Phenom.*, 1 (1983) 151.
22 L. R. Snyder and J. J. Kirkland, *Introduction to Modern Liquid Chromatography*, Wiley, New York, 2nd. ed., 1979, p. 36.
23 W. L. Hine and D. W. Armstrong, *Anal. Chem.*, 57 (1985) 237–242.
24 S. Li and W. C. Purdy, *J. Chromatogr.*, 543 (1991) 105–112.

Journal of Chromatography, 625 (1992) 121–129
Elsevier Science Publishers B.V., Amsterdam

CHROM. 24 470

Polymer-based packing materials for reversed-phase liquid chromatography

Steric selectivity of polymer gels provided by diluents and cross-linking agents in suspension polymerization

Ken Hosoya, Satoshi Maruya, Kazuhiro Kimata, Hiroshi Kinoshita, Takeo Araki and Nobuo Tanaka

Department of Polymer Science and Engineering, Kyoto Institute of Technology, Matsugasaki, Sakyo-ku, Kyoto 606 (Japan)

(First received March 26th, 1992; revised manuscript received July 2nd, 1992)

ABSTRACT

The effects of preparation conditions on the pore structures and chromatographic properties of porous polymer gels were studied. The diluents in suspension copolymerization of methyl methacrylate with a divinyl monomer affected the size and volume of micropores as well as those of the macropores. The use of a non-solvent to the polymer such as alkanes and *n*-alkyl alcohols resulted in polymer gels with micropores of smaller size and volume, accompanied by large macropores. Preferential retention of rigid, compact solutes was observed with such polymer gels due to the size-exclusion effect of the micropores. In contrast, better solvation of the polymer with cyclohexanol during polymerization resulted in gels with micropores of larger size and volume, leading to the preferential retention of bulky molecules, while producing macropores of smaller size and volume. Preferential retention of rigid, compact solutes was also observed with gels with higher cross-linking density.

INTRODUCTION

Steric selectivity in reversed-phase liquid chromatography (RPLC) has been observed with various packing materials. Octadecylsilylated silica packing materials prepared from octadecyltrichlorosilane showed preferential retention of planar compounds compared with bulky hydrocarbons [1,2]. Similar results were obtained with silica-based stationary phases with longer alkyl groups compared with those with shorter alkyl chains [3]. Ordered structures of long alkyl chains were found to be responsible for the steric selectivity. In contrast with the flexible alkyl-bonded stationary phase, graphite carbon packing materials possess rigid, planar surfaces, which resulted in the preferential retention of aryl or alkyl compounds with planar structures due to the contribution of dispersion forces and charge-transfer interactions that are strongly influenced by steric complementarity between solutes and the stationary phase [4–6].

Cross-linked polymer gels based on poly(alkyl methacrylate), esterified poly(vinyl alcohol), and polystyrene, were shown to possess common steric selectivity, leading to the preferential retention of rigid, compact compounds compared with bulky, flexible compounds [7–9]. The size-exclusion effect has been observed not only with high-molecular-weight solutes such as polypeptides but also with low-molecular-weight compounds [7–10]. The selec-

Correspondence to: Dr. N. Tanaka, Department of Polymer Science and Engineering, Kyoto Institute of Technology, Matsugasaki, Sakyo-ku, Kyoto 606, Japan.

0021-9673/92/$05.00

tivity of polymer gels for small molecules was assumed to be provided by the contribution of the microporous structure of polymer gels which gives strength to the gels. The biporous structures, macroporous gels with microporous skeletons, have been substantiated by bimodal pore size distributions [7,9,11,12].

Polymer gel packing materials for high-performance liquid chromatography (HPLC) are commonly prepared by suspension polymerization in water where a polymerization reaction takes place in oil droplets containing a monomer, a cross-linking agent, an initiator and a diluent. The presence of an inert diluent results in the formation of pores through phase separation in the oil droplets during polymerization. The effect of polymerization conditions on the macropore structures has often been studied [10–17]. Easy control of pore size is one of the advantages of polymer packing materials, as shown by the production of particles with extremely large pores [18] and continuous porous rods [19].

A study of the effect of micropore structure on chromatographic properties of styrene-divinylbenzene gels [10] suggests the importance of such a study that can relate the preparation methods of the polymer gels to the pore structures and the chromatographic properties of the products. This paper reports that polymer gels prepared from the same monomer and the cross-linking agent can show considerable difference in steric selectivity depending on the diluent in the gel preparation process. The contribution of the micropore structures determined by the diluents and cross-linking agents provides explanations for the retention mechanisms of polymer gels, which are often difficult to explain on the basis of the hydrophobic interactions that are predominant in RPLC with silica-based packing materials.

EXPERIMENTAL

Preparation of polymer gels

Cross-linked polymer gel beads were prepared by radical suspension copolymerization of methyl methacrylate (MMA) with a divinyl monomer in the presence of a diluent and 2,2′-azobis(2,4-dimethylvaleronitrile) as an initiator [20]. Typically a mixture of MMA (12.5 g), a cross-linking agent (12.5 g), a diluent (25 g) and the initiator (0.25 g) was suspended in a 1% aqueous solution (100 ml) of poly(vinyl alcohol) (degree of polymerization, DP = 2000, Nacalai-Tesque, Kyoto, Japan) by using an ultradisperser (Yamato, Model LK 21, Tokyo, Japan) for 1 min. The feed ratio, monomer/cross-linking agent/diluent (25:25:50, w/w/w), was maintained unless stated otherwise. Polymerization was carried out at 80°C for 10 h without stirring. After polymerization the resulting beads were washed successively with hot water, methanol and acetone, then refluxed in tetrahydrofuran (THF).

The beads were sieved in methanol with a 44-μm sieve. The fraction that passed through the sieve was collected and decanted three times after 15 min of sedimentation to remove fines. The beads were packed into a stainless-steel tube (100 mm × 4.6 mm I.D.) with a mixture of cyclohexanol and 2-propanol, or 2-propanol and methanol as a slurry medium.

Materials

The monomer and all the cross-linking agents, ethylene dimethacrylate (EDM), pentaerythritol tetraacrylate, butane-1,4-diol dimethacrylate, cyclohexane-1,4-diol dimethacrylate (*cis* and *trans* mixture) and divinylbenzene, were either purchased or prepared by standard procedures. The following compounds were used to illustrate the steric selectivity of each polymer gel in RPLC: (**1**) pentane, (**2**) hexane, (**3**) heptane, (**4**) octane, (**5**) nonane, (**6**) decane, (**7**) cyclohexane, (**8**) adamantane, (**9**) *trans*-decalin, (**10**) naphthalene, (**11**) anthracene, (**12**) pyrene, (**13**) phenanthrene, (**14**) diphenylmethane, (**15**) *o*-terphenyl, (**16**) triphenylene, (**17**) triptycene, (**18**) triphenylmethane, (**19**) fluorene, (**20**) benzene, (**21**) toluene, (**22**) ethylbenzene, (**23**) propylbenzene, (**24**) butylbenzene, (**25**) amylbenzene. The structures of (**8**) adamantane, (**9**) *trans*-decalin, (**11**) anthracene, (**12**) pyrene, (**15**) *o*-terphenyl, (**16**) triphenylene, and (**17**) triptycene are shown in Fig. 1. The silica C_{18} material is similar to that used in a previous study [9].

Equipment

The HPLC system consisted of an 880 PU pump (Jasco, Tokyo, Japan), a Model 440 UV detector and an R401 refractive index detector (Waters, Milford, MA, USA) and a Model 7000A data processor (System Instruments, Tokyo, Japan). The col-

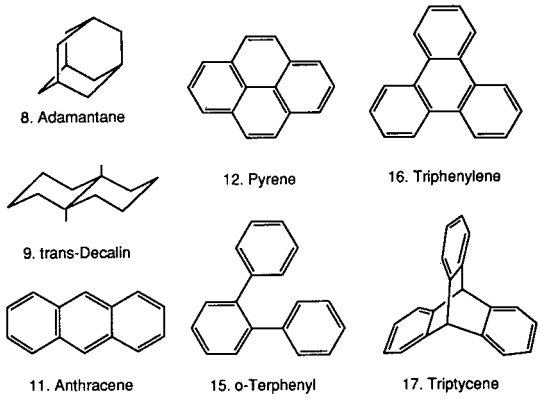

Fig. 1. Structures of hydrocarbons used to illustrate the steric selectivity of polymer gels.

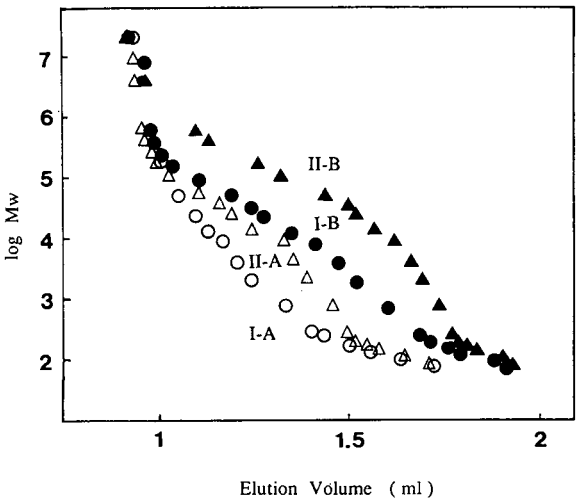

Fig. 2. Molecular weight–elution volume plots for the polymer gels prepared in cyclohexanol (I-A and I-B) and 2-octanol (II-A and II-B). Mobile phase: THF. Column size: 150 × 4.6 mm I.D. Solute: polystyrene and alkylbenzenes. ○ = I-A; ● = I-B; △ = II-A; ▲ = II-B. See Table I for gel identification.

umn temperature was maintained at 30°C with a water-bath.

RESULTS AND DISCUSSION

Characterization by size-exclusion chromatography

The pore volume and pore size of porous polymer gels, with respect to meso- and macropores, are known to be affected by the properties of diluents used for the suspension polymerization [11–17]. Series of products with various pore sizes are available for size exclusion chromatography. The effect of diluents on micropore structures was examined to explain the steric selectivity of polymer gels in RPLC.

Four types of polymer gels were prepared by copolymerization of MMA with EDM using two diluents, cyclohexanol and 2-octanol, at two monomer concentrations. The resulting gels showed no appreciable swelling in methanol or in THF.

Fig. 2 shows the results of size exclusion chromatography of polystyrene standards in THF with these polymer gels. The molecular weight–elution volume curves were bimodal in all instances, show-

TABLE I

EXCLUSION LIMITS AND PORE VOLUMES OF POLYMER GELS

Column size: 150 × 4.6 mm I.D. Mobile phase: THF.

Polymer gel No.	Diluent (monomer/diluent ratio, w/w)	Exclusion limit (log MW)[a]	Total pore volume (ml) V_p[b]	Micropore volume (ml) V_a[c]	V_b[d]
I-A	cyclohexanol (5:2)[e]	5.4	0.89	0.23	0.17
I-B	cyclohexanol (5:5)[e]	5.6	0.97	0.15	0.16
II-A	2-Octanol (5:2)[e]	5.5	0.91	0.17	0.09
II-B	2-Octanol (5:5)[e]	6.2	1.14	0.12	0.08

[a] Log (molecular weight) of polystyrene.
[b] V_p: elution volume (EV) of polystyrene standard (molecular weight > 1 000 000) was subtracted from that of benzene.
[c] V_a: EV (benzene) − EV (hexylbenzene).
[d] V_b: EV (hexylbenzene) − EV (polystyrene, molecular weight 760)
[e] (MMA + EDM)/diluent ratio in feed.

ing the presence of macropores and micropores. (In the later section of this paper, pores larger than those usually referred to as micropores, showing selective permeation for polystyrenes of molecular weight greater than 1000, are referred to as macropores.) The results indicate that the increase in the diluent content in the suspension feed resulted in the greater total pore volume and the larger macropores, as shown in Fig. 2 and in Table I.

The effect of the diluent type on gel structure is clearly observed in the comparison between I-B and II-A. Macropores are more easily formed in the presence of 2-octanol. I-B and II-A possess similar exclusion limits, or the size of macropores. These gels, however, possess considerable differences in pore volume in the macropore and micropore region. Fig. 2 and Table I indicate that the gels possessing the greater macropore volume and the greater exclusion limit generally possess smaller pore volume in the micropore region. As shown in Table I, I-B possesses the greater pore volumes in the micropore ranges, V_a and V_b, corresponding to the difference in elution volumes of benzene and hexylbenzene and that of hexylbenzene and polystyrene (molecular weight 760), respectively, than II-A. Nitrogen adsorption measurement showed two pore-volume maxima at pore sizes of 1.7 and 17 nm for I-B, and at 1.7 and 12 nm for II-A.

Selectivity towards low-molecular-weight solutes under RPLC conditions

In a previous study, the bimodal pore size distribution, particularly the presence of micropores about the size of solute molecules, was thought to be responsible for the unique selectivity of polymer gels which appeared as the preferential retention of rigid, compact solutes in RPLC [7,9]. Such steric selectivity may also be provided by the lightly cross-linked polymer chains on the gel surface [21].

Fig. 3a compares selectivities between the polymer gel I-B and silica C_{18}. The polymer gel showed the preferential retention of the rigid solutes. When the log k' values on gel II-A were plotted against those on silica C_{18} (Fig. 3b), considerable differences in selectivity were found from that in Fig. 3a. As the measurements were carried out in the same mobile phase, the selectivity difference between I-B and II-A, shown in Fig. 3c, must be explained by the difference in gel structure. Steric factors are responsible for the difference in selectivity, because the selectivity difference was also observed with the saturated compounds. The previous study showed the substantial differences in steric selectivity between the polymer gels provided by several manufacturers together with the general tendency of preferential retention of rigid, compact solutes compared with silica-based phases [9].

The steric selectivity, or the separation factor (k' value of a bulky molecule divided by that of a compact molecule), for several pairs of hydrocarbons with different rigidities and compactness is shown in Table II. The four packing materials prepared from the same monomers with the same feed ratios showed very similar hydrophobic selectivities in terms of the increase in retention caused by one methylene group, $\alpha(CH_2)$. In spite of the consid-

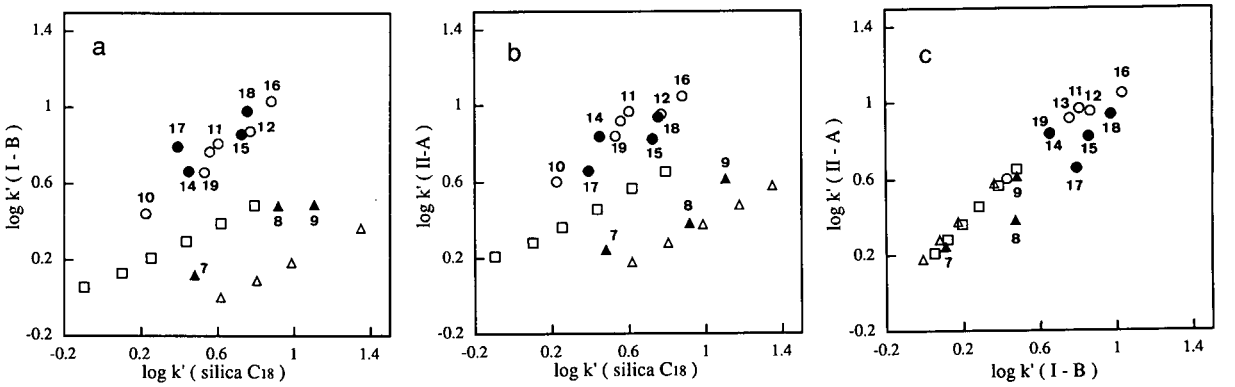

Fig. 3. Comparison of selectivity between polymer gels and octadecylsilylated silica gel in methanol–water (80:20). (a) Log k' values on I-B *versus* log k' values on silica C_{18}. (b) Log k' values on II-A *versus* log k' values on silica C_{18}. (c) Log k' values on I-B *versus* log k' values on II-A. Solutes as numbered, except alkanes (△, C_nH_{2n+2}, n = 6–10) and alkylbenzenes (□, $C_6H_5C_nH_{2n+1}$, n = 0–5).

TABLE II

EFFECT OF DILUENTS ON THE SELECTIVITY OF POLYMER GELS

Mobile phase: 80% methanol.

Solute	α^a (k')^b			
	I-A[c] (in cyclohexanol)	I-B[c] (in cyclohexanol)	II-A[c] (in 2-octanol)	II-B[c] (in 2-octanol)
$\alpha(CH_2)$[d] (No. 6)	1.24 (4.83)	1.25 (2.38)	1.24 (3.73)	1.24 (2.20)
α[**8**]/[**9**] (No. 9)	0.97 (6.67)	0.98 (3.07)	0.58 (4.11)	0.52 (2.38)
α[**17**]/[**11**] (No. 11)	1.11 (12.8)	0.97 (6.45)	0.49 (9.24)	0.45 (5.59)
α[**12**]/[**11**]	1.20	1.15	0.96	0.89
α[**15**]/[**16**] (No. 16)	0.66 (22.7)	0.67 (10.8)	0.60 (11.2)	0.61 (5.74)
V_a[e]	0.23	0.15	0.17	0.12
V_b[e]	0.17	0.16	0.09	0.08

[a] Separation factor beween the two compounds shown on the left.

[b] k' value of the compound is given in parentheses. Identification: No. 6 = decane; No. 8 = adamantane; No. 9 = *trans*-decalin; No. 11 = anthracene; No. 12 = pyrene; No. 15 = *o*-terphenyl; No. 16 = triphenylene; No. 17 = triptycene.

[c] See Table I for other preparation conditions.

[d] k'(amylbenzene)/k'(butylbenzene).

[e] See Table I for V_a and V_b. V_a: EV(benzene) − EV(hexylbenzene); V_b: EV(hexylbenzene) − EV(polystyrene, molecular weight 760) in THF.

erable difference in the size of macropores and the pore volumes in the macro- and micropore regions, the polymer gels prepared in the same diluent, I-A and I-B, and also II-A and II-B, showed very similar steric selectivity. The gels prepared in cyclohexanol consistently gave a greater preference towards bulky solutes. The greatest differences were seen for the combinations of decalin–adamantane and anthracene–triptycene, each of which possesses a considerable difference in molecular planarity and bulk.

The results shown in Table II indicate that the pore volume in a smaller micropore size range, V_a, determines the retention (k' values) of the compact solutes, whereas the retention of the bulky molecules reflects the pore volume in a larger micropore size range, V_b. Thus the steric selectivity between the planar, compact molecules and the bulky molecules can be attributed to a size-exclusion effect of micropores of polymer gels determined by the type, not the content, of the diluent used in suspension polymerization.

The size of micropores is determined by the solvation of polymer chains with the diluent in the polymerization process. Poorer solvents to the growing polymer chain result in earlier polymer precipitation, or earlier phase separation. In this instance the precipitating polymers are relatively free from the diluent due to the lack of solvation. The resulting polymer gels possess the larger macropores and smaller micropores [14], which in turn is related to the small retention of bulky solutes compared with the compact solutes in RPLC.

In contrast, when the diluent is a slightly better solvent to the polymer chain, polymerization proceeds more homogeneously, resulting in later phase separation. Precipitating polymers contain more diluent molecules, resulting in the larger micropores, whereas the size of macropores are limited [14]. The resulting gels show a preference toward bulky molecules. The explanation is compatible with the observation that the MMA homopolymer (molecular weight 20 000) is appreciably soluble in hot cyclohexanol, but not in 2-octanol. Little difference in solubility is seen either in the solubility parameters [22,23] or in experimentally obtained solubility at room temperature.

Fig. 4 shows the chromatograms obtained with gels I-B and II-A. The two gels, prepared from the same combination of a monomer and a cross-linking agent, showed a considerable selectivity difference. The largest effect was observed with bulky

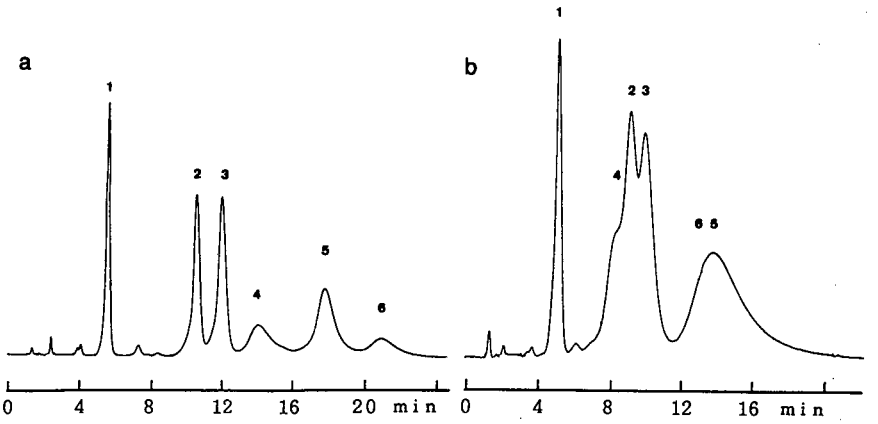

Fig. 4. Elution of some aromatic compounds on polymer gels. Stationary phase: (a) I-B and (b) II-A. Mobile phase: acetonitrile–water (60:40). Flow-rate: 0.8 ml/min. Solutes: **1** = benzene; **2** = butylbenzene; **3** = diphenylmethane; **4** = triptycene; **5** = pyrene; **6** = triphenylmethane.

triptycene (peak 4) and triphenylmethane (peak 6). Diffuse reflectance Fourier transform infrared (FTIR) spectra showed no difference between the two polymer gels prepared in the two diluents, as expected. These results suggest that the chromatographic examination can be used for characterizing or differentiating polymer gels with similar compositions, even if FTIR measurements are not useful in differentiating the preparation method.

The size-exclusion effect can be seen not only for three-dimensionally bulky molecules but also for planar polynuclear aromatic compounds such as pyrene and triphenylene with gels prepared in the presence of considerable concentrations of non-solvents. The effect, however, was not seen with anthracene or naphthalene, as shown in the plot in Fig. 3c, where pyrene and triphenylene showed a slight deviation from the general tendency found for the other more compact molecules. Although the steric selectivity inherent to polymer packing materials has been attributed to the size-exclusion effect based on micropores, the possible contribution of lightly cross-linked polymer chains on the gel surface [21] needs to be examined.

Effect of other diluents

Several other diluents and mixtures were examined with respect to their ability of forming macro- and micropores. Isooctane, a non-solvent of the polymer, resulted in large macropores and small amount of micropores when used as a mixture with cyclohexanol. Similar results were reported in the polymerization of other monomers [12,14,16]. As indicated in Fig. 5 and Table III, the polymer gel, III-B, prepared in a cyclohexanol–isooctane (60:40) mixture showed a similar selectivity to those prepared in 2-octanol or in 1-hexanol.

The diluent, cyclohexanol–isooctane (40:60), produced gels with no macropores. Similar results were obtained with decalin. The polymer gel (V) prepared in butyl acetate, possesses a similar pore structure to the gel III-A prepared in a cyclohexanol–isooctane (80:20) mixture, showing an intermediate steric selectivity. Good solvents to the polymer such as ethylbenzene, xylene and toluene produced gels with only micropores. These gels showed prolonged retention times for solutes with compact structures which can enter the micropores, whereas bulky solutes such as triptycene were excluded from the pores and eluted very early in the chromatogram, as shown in Fig. 5b. These results indicate that the pore structures and the retention selectivities in RPLC of MMA–EDM gels can be controlled by the choice of diluents in suspension polymerization.

Effect of cross-linking agents

Fig. 6 illustrates the effect of the structure of cross-linking agents on the steric selectivity of polymer gels. In each part of the figure a straight line

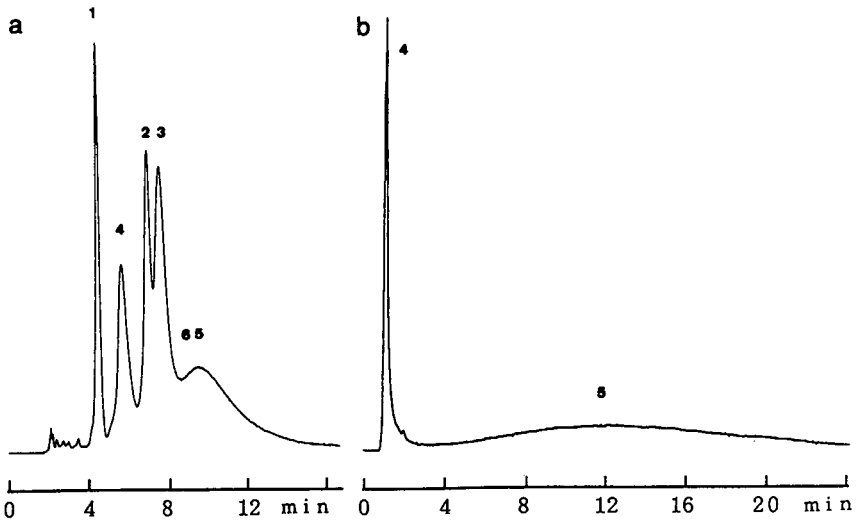

Fig. 5. Elution of some aromatic compounds on polymer gels. Stationary phase and mobile phase: (a) III-B [diluent: cyclohexanol–isooctane (60:40), acetonitrile–water (60:40)], (b) VI [diluent: xylene), methanol–water (80:20)]. Flow-rate: 0.8 ml/min. Solutes as in Fig. 4.

with a slope of unity through the origin is shown as a broken line. The gels prepared from the dimethacrylate ester of butane-1,4-diol and cyclohexane-1,4-diol (*cis* and *trans* mixture) generally resulted in a greater retention than that prepared from EDM, presumably due to the greater hydrophobic properties of the cross-linking agent.

The gels containing cyclohexane moieties

TABLE III

EFFECT OF DILUENTS ON THE SELECTIVITY OF POLYMER GELS

Mobile phase: 80% methanol.

Solute	α^a (k')^b			
	III-A[c] (in cyclohexanol–isooctane)	III-B[d] (in cyclohexanol–isooctane)	IV-A (in 1-hexanol)	V (in butyl acetate)
$\alpha(CH_2)$[e] (No. 6)	1.25 (2.58)	1.24 (2.08)	1.21 (1.84)	1.23 (2.29)
α**[8]**/**[9]** (No. 9)	0.87 (3.38)	0.54 (2.60)	0.66 (1.97)	0.71 (2.75)
α**[17]**/**[11]** (No. 11)	0.74 (6.83)	0.41 (5.64)	0.55 (4.80)	0.71 (6.13)
α**[12]**/**[11]**	1.09	0.95	0.96	1.08
α**[15]**/**[16]** (No. 16)	0.66 (10.2)	0.59 (5.91)	0.61 (6.01)	0.61 (9.17)
V_a[f]	0.15	0.11	0.15	0.14
V_b[f]	0.11	0.06	0.09	0.08

[a] Separation factor beween the two compounds shown on the left.

[b] k' value of the compound is given in parentheses. Identification: No. 6 = decane; No. 8 = adamantane; No. 9 = *trans*-decalin; No. 11 = anthracene; No. 12 = pyrene; No. 15 = *o*-terphenyl; No. 16 = triphenylene; No. 17 = triptycene.

[c] Prepared in a mixture cyclohexanol–isooctane (80:20).

[d] Prepared in a mixture cyclohexanol–isooctane (60:40).

[e] k'(amylbenzene)/k'(butylbenzene).

[f] See Table I for V_a and V_b. V_a: EV(benzene) − EV(hexylbenzene), V_b: EV(hexylbenzene) − EV(polystyrene, molecular weight 760) in THF.

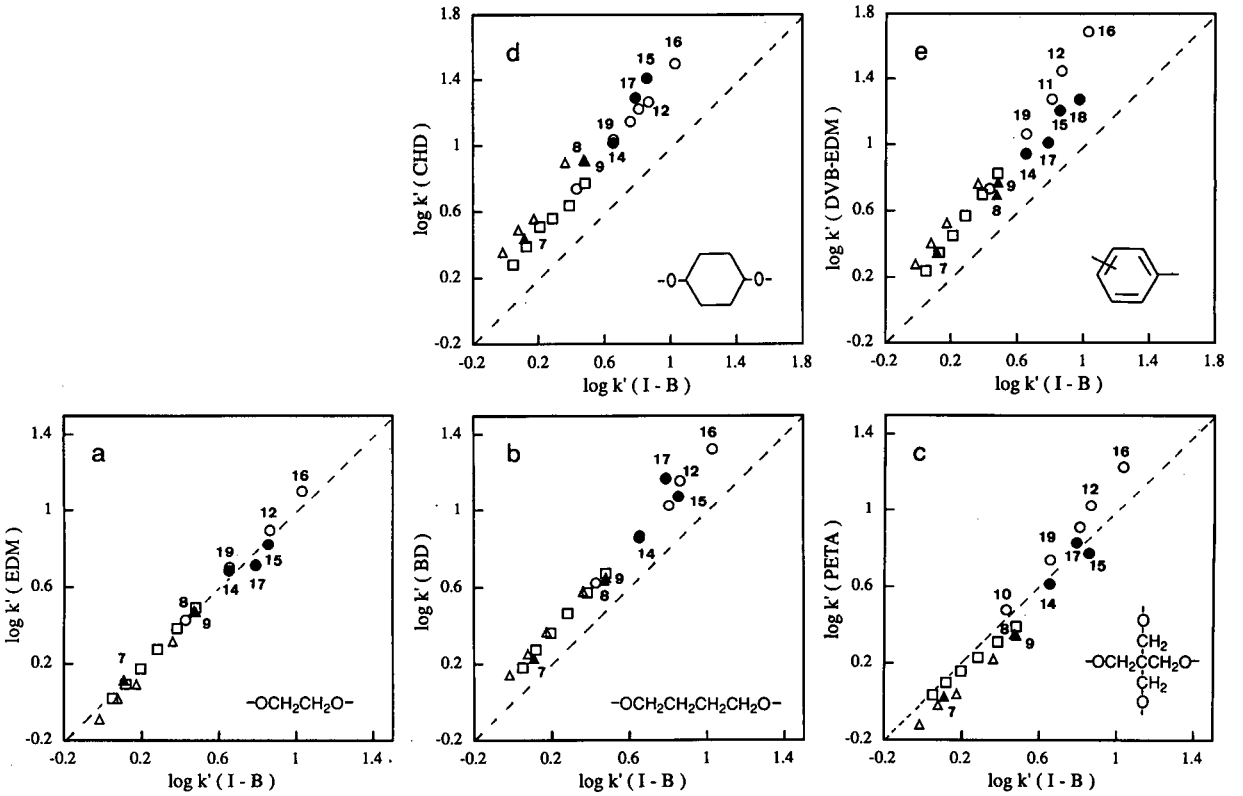

Fig. 6. Effect of cross-linking agents on steric selectivity of polymer gels. Monomer and cross-linking agent: (a) EDM 100%; (b) MMA–butane-1,4-diol dimethacrylate (BD) (40:60, w/w); (c) MMA– pentaerythritol tetraacrylate (PETA) (50:50, w/w); (d) MMA–cyclohexane-1,4-diol dimethacrylate (CHD) (45:55, w/w); (e) MMA–divinylbenzene–EDM (EDM–DVB) (50:25:25, w/w/w). Solutes as in Fig. 3.

showed preferential retention of bulky, non-planar solutes compared with I-B. The results can be explained on the basis of the lower cross-linking density or larger micropores in this gel, and the non-planarity of bridging moieties. The small retention of planar solutes on cyclohexane-bonded silica [24] and the small retention of alicyclic compounds on graphite carbon packing materials [6] are an indication of the less favourable interaction between the planar structure of the polycyclic aromatic moieties and the non-planar structure of cyclohexane rings.

Divinylbenzene resulted in a gel showing a preferential retention of planar aromatic over bulky aromatic compounds, together with a greater hydrophobic retention. Pentaerythritol tetraacrylate gave a gel with a preference towards the more rigid, compact solutes. The greater cross-linking density of these gels, resulting in the smaller micropores, can account for the greater size-exclusion effect.

CONCLUSIONS

The steric selectivity of polymer gels, or the preferential retention of rigid, compact molecules in RPLC, was shown to be a size-exclusion effect provided by the micropore structure. The effect of diluents in suspension polymerization of MMA on pore size and volume was observed in a micropore region and in a macropore region. The use of non-solvents, alkanes and n-alkyl alcohols, resulted in the smaller micropore structures leading to the greater size-exclusion effects, whereas these solvents produced the larger macropores. The pore size control of poly-MMA gels by using cyclohexanol in combination with a non-solvent will allow the con-

trol of selectivity in RPLC. The feasibility of pore size control for small molecules, shown in this study, as well as for biological macromolecules as reported previously [18,19], is an advantage of polymer-based packing materials for RPLC.

REFERENCES

1 L. C. Sander and S. A. Wise, *Anal. Chem.*, 56 (1984) 504.
2 K. Jinno, T. Nagoshi, N. Tanaka, M. Okamoto, J. C. Fetzer and W. R. Biggs, *J. Chromatogr.*, 392 (1987) 75.
3 N. Tanaka, K. Sakagami and M. Araki, *J. Chromatogr.*, 199 (1980) 327.
4 J. H. Knox, B. Kaur and G. R. Millward, *J. Chromatogr.*, 352 (1986) 3.
5 B. J. Bassler and R. A. Hartwick, *J. Chromatogr. Sci.*, 27 (1989) 162.
6 N. Tanaka, T. Tanigawa, K. Kimata, K. Hosoya and T. Araki, *J. Chromatogr.*, 549 (1991) 29.
7 N. Tanaka, K. Hashizume and M. Araki, *J. Chromatogr.*, 400 (1987) 33.
8 N. Tanaka and M. Araki, *Adv. Chromatogr.*, 30 (1989) 81.
9 N. Tanaka, T. Ebata, K. Hashizume, K. Hosoya and M. Araki, *J. Chromatogr.*, 475 (1989) 195.
10 F. Nevejans and M. Verzele, *J. Chromatogr.*, 406 (1987) 325.
11 H. Jacobelli, M. Bartholin and A. Guyot, *Angew. Makromol. Chem.*, 80 (1979) 31.
12 A. B. Wojcik, *Angew. Makromol. Chem.*, 119 (1983) 193.
13 K. A. Kun and R. Kunin, *J. Polym. Sci., Part A-1*, 6 (1968) 2689.
14 W. L. Sederel and G. J. De Jong, *J. Appl. Polym. Sci.*, 17 (1973) 2835.
15 F. Svec, J. Hradil, J. Coupek and J. Kalal, *Angew. Macromol. Chem.*, 48 (1975) 135.
16 D. Horak, Z. Pelzbauer, M. Bleha, M. Ilavsky, F. Svec and J. Kalal, *J. Appl. Polym. Sci.*, 26 (1981) 411.
17 K. Takeda and T. Yamamizu, *Kobunshi Ronbunshu*, 46 (1989) 625.
18 N. B. Afeyan, S. P. Fulton and F. E. Regnier, *J. Chromatogr.*, 544 (1991) 267.
19 F. Svec and J. M. J. Frechet, *Anal. Chem.*, 64 (1992) 820.
20 Y. Tanaka, H. Sato, K. Miyazaki and Y. Yamada, *J. Chromatogr.*, 407 (1987) 197.
21 K. Jerabek, *Anal. Chem.*, 57 (1985) 1598.
22 K. L. Hoy, *J. Paint Technol.*, 42 (1970) 76.
23 J. Brandrup and E. H. Immergut (Editors), *Polymer Handbook*, Wiley, New York, 2nd ed., 1975, p. IV-337.
24 N. Tanaka, Y. Tokuda, K. Iwaguchi and M. Araki, *J. Chromatogr.*, 239 (1982) 761.

Journal of Chromatography, 625 (1992) 131–140
Elsevier Science Publishers B.V., Amsterdam

CHROM. 24 529

Retention of C_{60} and C_{70} fullerenes on reversed-phase high-performance liquid chromatographic stationary phases

Yi Cui, Stephen T. Lee, Susan V. Olesik, Wendy Flory and Michael Mearini

Department of Chemistry, The Ohio State University, 120 W 18th Avenue, Columbus, OH 43210 (USA)

(First received July 15th, 1992; revised manuscript received July 27th, 1992)

ABSTRACT

The separation of C_{60} and C_{70} fullerenes on four different polysiloxane stationary phases was examined. It was determined that polar solvents can be used as mobile phases effectively for the separation of fullerene molecules. Unlike previously published work, a polymeric octadecyl siloxane (ODS) stationary phase provided higher separation factors for C_{70}/C_{60} than did monomeric ODS stationary phases or phenyl substituted stationary phases. For example, for a methanol–diethyl ether (50:50, v/v) mobile phase and C_{60}, $k' \approx 5.0$ separation factors, $\alpha = 3.3$, were achieved with polymeric ODS compared to $\alpha = 2.2$, with a monomeric ODS stationary phase. A linear solvation energy relationship (LSER) was used to model the importance of solvent interactions and stationary phase interaction to solute retention.

INTRODUCTION

The development of a bulk method to produce the third allotrope of carbon, buckminister fullerenes [1] has caused the development of completely new areas of chemistry and materials science. The surge of new fullerene-related discoveries continues [2]. Optical isomers of C_{76}, C_{78}, C_{82}, C_{84} were theoretically predicted [3,4] and recently experimentally separated and identified [5]. Numerous compounds with one or more metal atoms inside the fullerene cage have been produced [6].

To facilitate these new developments, various chromatographic techniques were used to separate the fullerenes. For high efficiency separations different types of HPLC columns were used. Early chromatographic separations involved use of alumina or silica stationary phases [7–9]. However, the fullerene capacity factors on these columns were low and degradation of the fullerenes was occurring when silica was used. Hawkins *et al.* [10] reasoned that a π-acid type high-performance liquid chromatographic (HPLC) stationary phase would work well for the separation of the π-basic fullerenes. To test this they separated the fullerenes on a Pirkle phenylglycine column which contains dinitrobenzamide groups on the surface of the stationary phase. With hexane as the solvent they obtained a separation factor, $\alpha = k'_{C70}/k'_{C60} = 2.25$ (k' is capacity factor). Cox *et al.* [11] used a dinitroanilinopropyl (DNAP) silica column (300 Å pore size, 5-μm particles) with a gradient from *n*-hexane to 60% methylene chloride to achieve baseline separation of C_{60} and C_{70}. Other attempts to enhance the separation of the fullerenes involved the use of a carbon stationary phase [12], multi-legged phenyl phases [13], and a size-exclusion stationary phase [14]. However, the most commonly used HPLC stationary phase is octadecyl polysiloxane (ODS). Both monomeric and polymeric ODS phases are successfully

Correspondence to: Dr. S. V. Olesik, Department of Chemistry, The Ohio State University, 120 W 18th Avenue, Columbus, OH 43210, USA.

0021-9673/92/$05.00

used for the separation of fullerenes [14–16]. Polymeric ODS is known to exhibit selectivity based on the nonplanarity of the molecule in addition to the expected dispersive interactions with ODS. However, Jinno *et al.* [13] suggested that C_{60} and C_{70} are so bulky that their retention characteristics on monomeric and polymeric should be similar.

All of the previously reported fullerene separations using ODS as the stationary phase used a nonpolar solvent such as hexane or a gradient of hexane with methylene chloride as the mobile phase. Under these conditions the separation mechanism cannot be classified as a classical normal- or reversed-phase separation. Both the stationary phase and the mobile phase are nonpolar. The fullerenes are separated solely by small differences in solubility in the nonpolar solvent and the nonpolar stationary phase. Fullerene solubility was the reason for the common preference of such nonstandard HPLC conditions. Fullerenes are most soluble in aromatic solvents (5 mg/ml); slightly soluble in hexane, pentane, chloroform and diethyl ether [9].

We report here a comparison of the separation of C_{60} and C_{70} fullerenes on five different columns with four different types of polysiloxane-based stationary phases. Commonly used solvents, such as hexane or mixtures of hexane and methylene chloride are compared to more polar mobile phases, such as, methanol and diethyl ether mixtures. Also the specific type of molecular level interactions involved in the separation of these fullerenes was evaluated. A linear solvation energy relationship (LSER) which correlates Kamlet–Taft solvent parameters with retention was used to identify these interactions.

EXPERIMENTAL

Columns

The columns included an end-capped monomeric octadecyl polysiloxane, ODS-Hypersil (Shandon Scientific), C18; an end-capped phenyl dimethylpolysiloxane, phenyl-2 Hypersil (Shandon Scientific), Phen; an experimental non end-capped diphenyl methylpolysiloxane, diphenyl Hypersil, DP-K. All the columns contained 5-μm particles with 120 Å pore size, and dimensions of 250 x 4.6 mm I.D. as supplied by Keystone Scientific, Bellefonte, PA, USA. In addition two end-capped diphenylmethylpolysiloxane, Supelcosil columns (Supelco, Bellefonte, PA, USA), with 5-μm particles, 100 Å pore size were studied. One of these columns was analytical scale with 250 x 4.6 mm I.D. dimensions, DP-S; and the other was semiprep scale with dimensions of 250 x 21.2 mm I.D. A polymeric ODS, Vydac 201TP (The Separations Group, Hesperia, CA, USA) with 5-μm particle size, 300 Å pore size, P18, was also studied.

Instrumentation

The chromatographic system included an ISCO LC-2600 syringe pump (ISCO, Lincoln NE, USA), a Valco W-series high-pressure injection valve (Valco Instruments, Houston, TX, USA) with a 20-μl injection volume and a Millipore 991 Photodiode Array Detector (Millipore, Waters Chromatography Division, Milford, MA, USA). All separations were done at room temperature, *ca.* 27°C.

Fullerene production

The raw fullerene soot was prepared by the arc welding technique which was first developed by Haufler *et al.* [17]. Detailed information on the design and operating conditions of the device have been previously published [18]. An amount of 0.5 g of raw soot was placed in a round bottom flask which was connected to a water-cooled condenser. An aliquot of 100 ml boiling benzene for 3 h was used to extract the fullerenes from the raw soot. Typical extraction yields for the fullerenes were 8% (w/w) fullerenes in soot.

Materials

All chemicals used in this study were used as delivered without further purification. Diethyl ether (>99.99%), and benzene (>99.99%) were purchased from J. T. Baker, Phillipsburgh, NJ, USA. Methanol (99.9% purity) was obtained from Mallinckrodt (Paris, KT, USA). The dyes used to determine the Kamlet–Taft solvent parameters were 4-nitroaniline (99+%), 2-nitroanisole (99+%), obtained from Aldrich and N,N-dimethyl-*p*-nitroaniline was purchased from Eastman Kodak (Rochester, NY, USA). A standard test mixture of polynuclear aromatic hydrocarbons purchased from Supelco was also used in the study. This test mix included: acenaphthene, acenaphthylene, anthracene, benzo[*a*]anthracene, benzo[*b*]fluoranthene,

benzo[*k*]fluoranthene, benzo[*ghi*]perylene, benzo[*a*]pyrene, chrysene, dibenzo[*a,h*]anthracene, fluoranthene, fluorene, indeno[1,2,3-*cd*]pyrene, naphthalene, phenanthrene and pyrene.

Density measurements

The molar volume of the methanol–diethyl ether mixtures were determined by measuring the solution densities with a DMA 512 density meter (Anton Paar USA, Warminister, PA, USA) and a TU16D constant temperature bath (Techne, Princeton, NJ, USA). The density meter was calibrated with distilled water at atmospheric pressure and 27°C.

Data analysis

A NEC 386SX PowerMate-Plus computer was used for data collection and analysis. The multivariate linear regression of the chromatographic data and the solvatochromic data was obtained using SYSTAT software (SYSTAT, Evanston, IL, USA). The statistical data provided complies with the "Recommendation for Reporting Results of Correlation Analysis in Chemistry using Regression Analysis [19]". R, the coefficient of multiple correlation is reported. An R value approaching 1 indicates excellent correlation. The standard deviation of the regression, s, is reported. The F test at the 95% confidence level is used to indicate the statistical significance of the model and the Student's t test at the 95% level was used to indicate the significance of the independent variable's coefficients. In addition to these recommendations, the adjusted coefficient of multiple determination (R_a^2) is also reported. This variable is substantially lower than the coefficient of multiple determination (R^2) when too many independent variables are used in a model. A more detailed description of the regression analysis of LSER was previously published [20].

RESULTS AND DISCUSSION

Our initial separations of fullerenes used phenyl polysiloxane columns. We anticipated that the retention and the separation factor might be higher for the phenyl columns than other reversed-phase columns, because of π–π interactions between the phenyl rings on the stationary phase and the condensed rings of the different fullerenes. Hexane and pentane were initially used as the mobile phases. The fullerenes could be separated with these mobile phases, but the efficiency was low. Fig. 1 is a sample chromatogram using a phenyl column, Phen, as stationary phase and pentane as mobile phase. Under these conditions the efficiency was low and separation factor was $\alpha = 1.33$. Mixed mobile phases which contained a low percentage of cosolvent, such as ethanol, methanol, tetrahydrofuran and diethyl ether, improved the efficiency substantially. Fig. 2 demonstrates the increased efficiency found when diethyl ether–pentane mixtures were used as the mobile phase with the Phen column. In addition, the retention of the fullerenes was practically unaffected by the addition of substantial quantities of diethyl ether to the pentane (see Fig. 3) and the selectivity decreased slightly.

Neat diethyl ether also worked well as a mobile phase for the separation of fullerenes. All five columns were tested with diethyl ether as a mobile phase. Short retention times and improved efficiency (2000–4000 plates) were achieved. Fig. 4A is a

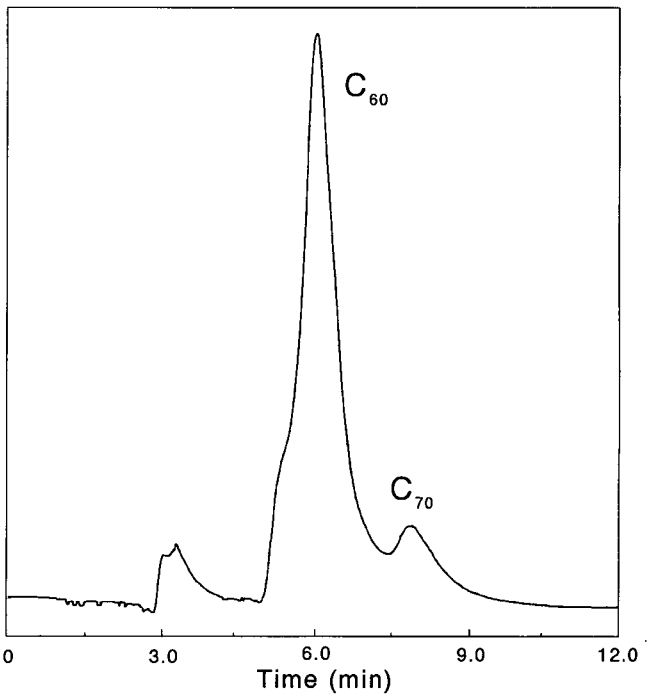

Fig. 1. Separation of C_{60} and C_{70} on the phenyl polysiloxane column (Phen). Mobile phase: pentane; flow-rate: 1 ml/min; detection wavelength: 330 nm.

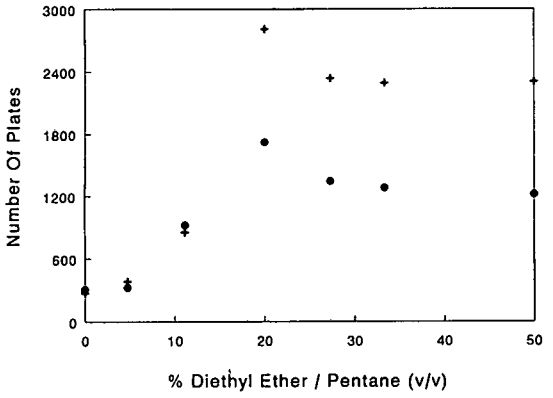

Fig. 2. Dependence of column efficiency (number of theoretical plates) on percent diethyl ether in pentane for fullerene separations on the Phen column. ● = C_{60}, + = C_{70}.

sample chromatogram of a high-molecular-weight fraction of the fullerene extract. This fullerene fraction was obtained by first extracting the soot with hot trichlorobenzene. An aliquot of 20 μl of the supernatant was injected onto and separated by the monomer ODS column. As described later, the ODS column was used because it provided the highest efficiency with diethyl ether. The high molecular weight fraction of the fullerene chromatogram (portion of the chromatogram with retention time >4.2 min) was collected for 15 injections. The resulting 250 ml sample was desolvated with a stream of N_2. The residue was then dissolved in 100 μl benzene. An aliquot of 20 μl of this yellow solution was injected onto and separated by the same column and the chromatogram in Fig. 4A was obtained. The identity of C_{60}, C_{70}, C_{76}, and C_{84} chromatographic peaks were determined from published UV–Vis spectra. Mass spectrometry was used to confirm the identification of the fullerene extract. Fig. 4B shows the Fourier transform ion cyclotron resonance (FT-ICR) mass spectrum of the concentrated high-molecular-weight fraction before the final separation shown in Fig. 4A. (Note: The relative abundance of the ions in the mass spectrum may not be indicative of the relative proportions of fullerenes because the

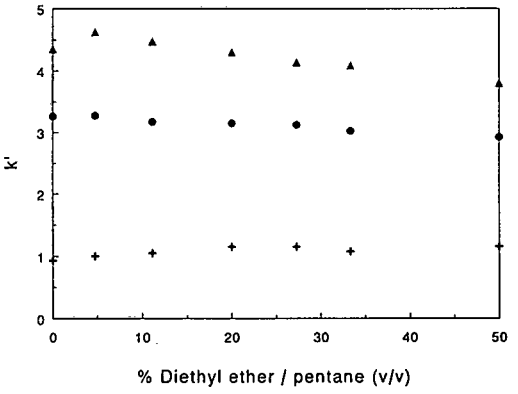

Fig. 3. Variation of capacity factor with percent diethyl ether in pentane using the phenyl polysiloxane stationary phase (Phen). + = Benzene; ● = C_{60}, ▲ = C_{70}.

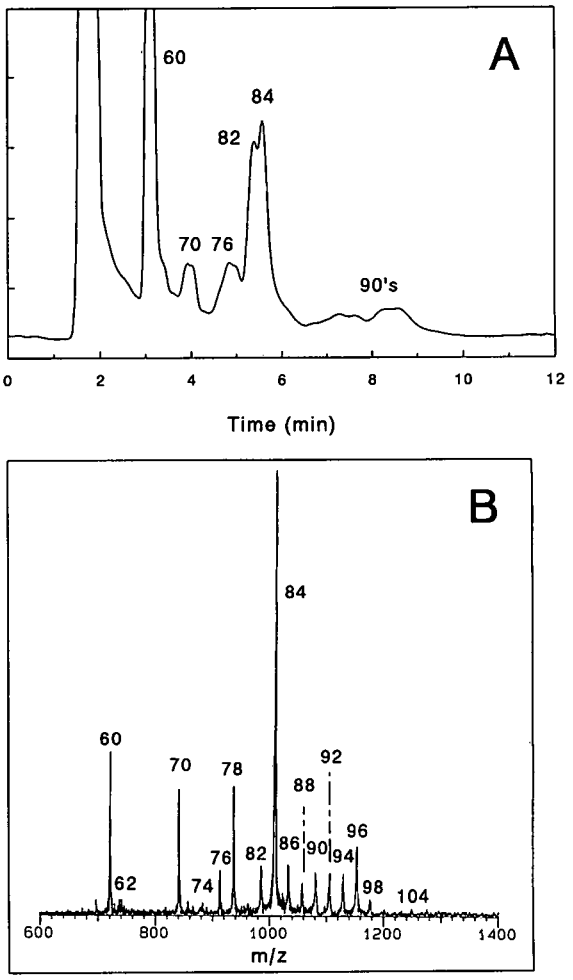

Fig. 4. (A) Chromatogram of higher molecular weight fullerenes. Mobile phase: diethyl ether; flow-rate: 1 ml/min; column: monomeric C_{18}; detector wavelength: 330 nm. (B) Laser desorption, negative ion FT-ICR mass spectrum of the sample used in (A).

relative ionization efficiencies of fullerenes are unknown).

Because diethyl ether was a good mobile phase for fullerene separations more polar co-solvents with diethyl ether were also considered. Mixtures of 20% alcohol–diethyl ether were considered. Because fullerene solubility in polar solvents was expected to be low, hexanol–diethyl ether was first considered followed by more polar alcohols such as ethanol and methanol. Of the solvents considered, methanol provided the greatest control of mobile phase solvent strength and therefore the retention and selectivity. The efficiency of C_{60} on the C18 column increased from 1400 to 2600 theoretical plates when the proportion of methanol in the mobile phase was increased from 0 to 20% and was invariant for mobile phase compositions that ranged from 20 to 70% methanol. Only for compositions >70% methanol did the efficiency lower and tailing begin due to lowered solubility in the mobile phase. Fig. 5A and B illustrates how the retention of C_{60} and C_{70} is affected by the addition of increasing amounts of methanol to diethyl ether. The ln k' increased with the percentage methanol added to the mobile phase for both C_{60} and C_{70} on all of the stationary phases studied. Cox *et al.* [11] reported that retention of C_{60} and C_{70} closely resembled the retention of planar molecules with similar molecular "footprints". They showed that under their chromatographic conditions the retention of C_{60} was similar to that of triphenylene and the retention of C_{70} was intermediate between that of benzo[*a*]pyrene and coronene. However, with the 0–50% methanol–diethyl ether mobile phases, all of the polynuclear aromatic hydrocarbon standards (listed in the experimental section), were unretained on all five columns.

Fig. 6 shows the variation of the separation factor for the methanol–diethyl ether solvent system on all five columns. Surprisingly, the separation factors were higher when ODS stationary phases were used as opposed to phenyl or diphenyl columns. The separation factors obtained with the methanol–diethyl ether ODS system were significantly higher than those previously reported by Jinno *et al.* [13] for a C_{60} and C_{70} separation using monomeric and polymeric ODS with *n*-hexane as the mobile phase. In addition, Fig. 5 and Fig. 6 show the polymeric

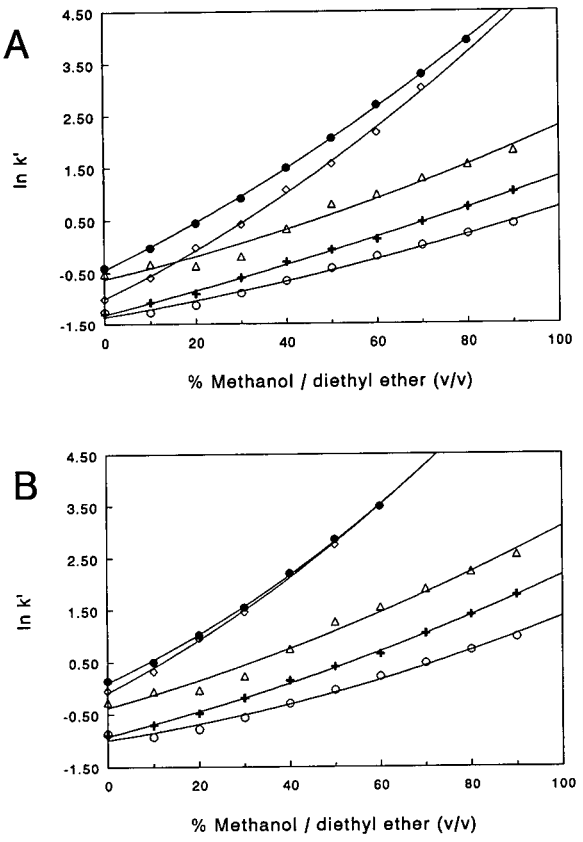

Fig. 5. Variation of capacity factors of (A) C_{60} and (B) C_{70} with percent methanol in diethyl ether mobile phase on different columns. ◇ = Polymeric ODS, P18; ● = monomeric ODS, C18; △ = diphenyl, DP-S; ○ = diphenyl, DP-K; + = phenyl, Phen.

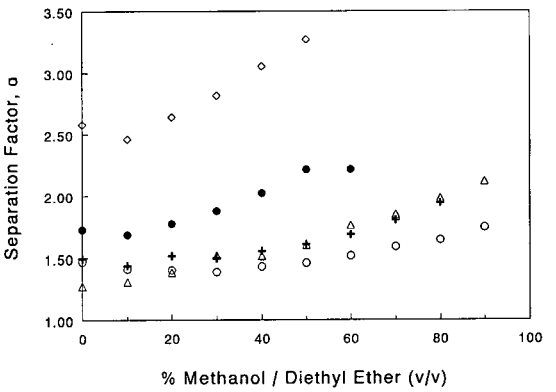

Fig. 6. Variation of separation factors with percent methanol in diethyl ether mobile phase on different columns. Symbols same as in Fig. 5.

TABLE I

NUMBER OF PLATES REQUIRED TO ACHIEVE RESOLUTION OF 1.5 WITH A 20% METHANOL–DIETHYL ETHER MIXTURE

Column	N
C18	351
Phen	2142
DP-K	4405
DP-S	1936
P18	179

phase, Vydac 201 TP, was more retentive and more selective than monomeric ODS for the separation of the fullerenes. Exactly opposite trends were found in the previous study [13] when *n*-hexane was used as the mobile phase. In the previous study, the same polymeric ODS was practically nonretentive toward C_{60} and C_{70}, while the monomer ODS provided capacity factors of 0.58 and 0.92 for C_{60} and C_{70}, respectively, and a separation factor of 1.65. The observed differences in fullerene retention and selectivity between this work and that of Jinno *et al.* is primarily caused by marked difference in the observed behavior of the polymeric ODS stationary phase. The monomeric ODS columns used in both studies performed similarly. The distinctly different behavior of the polymeric ODS is quite interesting. The different retention characteristics of the polymeric stationary phase were most likely caused by the different mobile phases use in the two studies. The observed differences cannot be explained by variation in mobile phase shielding of surface silanols. Hexane would afford minimum shielding of surface silanols compared to methanol–diethyl ether; however when hexane was used as the mobile phase lesser fullerene retention was observed. Perhaps the two mobile phases affect the surface structure of the polymeric ODS phase differently. Further investigations are needed to completely understand this phenomenon.

Using the data in Figs. 5 and 6 a comparison of the different columns was made. Table I shows a comparison of the number of theoretical plates required to achieve baseline separation ($R_s = 1.5$) for the five chromatographic columns using the data in Figs. 5 and 6 for a solvent composition of 20% methanol–diethyl ether. Due to the higher observed separation factors, the polymeric and monomeric ODS columns require the least theoretical plates to achieve baseline separation. The Phen and DP-S stationary phases require approximately 10 times the number of theoretical plates as P18 and due to the low separation factor, DP-K requires approximately double the number of theoretical plates as DP-S. However, under the experimental conditions described in Figs. 5 and 6 and for the 20% methanol–diethyl ether mobile phase composition, the measured efficiency of C_{60} and C_{70} was approximately 3000 for the C18 column and 1500–1800 for the P18, DP-K, DP-S, and Phen columns. These chromatographic conditions were scaled-up to semiprep scale using the diphenyl column described in the experimental section. This column was used because it was readily available in our laboratory. The extract used in the analytical-scale separations was first doubly concentrated. We were able to inject 100 μl of this concentrated extract directly onto the semiprep scale column and obtain resolution of 0.8–1.0 for flow velocities of 15 ml/min. From the previous discussion it is obvious that the diphenyl polysiloxane columns are the poorest choice for fullerene separations under these chromatographic conditions. Therefore much better performance should be expected when semiprep polymeric or monomeric ODS columns are used under these chromatographic conditions.

To better understand the retention mechanism involved in the separation of fullerenes with the methanol–diethyl ether mixtures on polysiloxane-based stationary phases, a linear solvent free energy relationship (LSER) between retention (ln k') and measured solvent strength parameters was developed. LSERs assume that attractive interactions can be correctly categorized by a nonspecific interaction term that measures the effect of dipolarity and specific terms that describe the effect of hydrogen bond donor and acceptor interactions on solvent properties. In addition, the aforementioned independent variables must be orthogonal and the assumption is made that there is a linear free energy relationship between the each attractive term and the specified solvent effect. Finally to complete the description of the solvent effect, an endothermic term that describes the formation of a cavity in the solvent to accommodate the solute must also be included in this model [21]. Kamlet, Taft and co-

workers [22,23] described the adsorption of gases and liquids on solids using LSER. In addition, Sadek *et al.* [24] demonstrated that LSERs can be quite useful in describing the partitioning of solutes in HPLC. Eqn. 1 is a generalized LSER that describes the transfer of a solute from mobile phase to stationary phase in HPLC.

$$\ln k' = A + B\Omega + C\pi^* + D\alpha + E\beta \quad (1)$$

Kamlet–Taft solvatochromic parameters (π^*, α, β) were used to describe the exoergetic interactions. The π^* measures the ability of the medium to stabilize charged or dipolar solutes by virtue of dipolar or induced dipolar interactions. The α parameter measures hydrogen bond donation capability and β measures the ability of solvent to accept hydrogen bonds. The most common method of modeling the cavity formation term, Ω, is to use the cohesive energy density which is the square of the Hildebrand solubility parameter [22]. We chose to use (molar volume)$^{-1}$ to represent the variation in cohesive energy density (and therefore the cavity formation term) of this mixed solvent. This is a reasonable approximation when the attractive portion of the interaction potential controls the cohesive energy density of the solvent [25].

The π^*, α, β parameters of the solvent mixture were experimentally determined by measuring the variation of the UV–Vis spectrum of solvatochromic dyes which are listed in the experimental section. More detail on the measurement of the solvent strength parameters was previously published [26]. The molar volume of the mixtures was determined from experimentally measured solution density. The cavity formation parameter used in the model was generated by dividing all the (molar volume)$^{-1}$ values by that of methanol. This was necessary to keep the cavity formation parameter in the same range as the other solvent strength parameters. Fig. 7A and B illustrates the variation in the solvent strength and cavity formation parameters as a function of percent methanol in the mixture. The hydrogen bond donator strength, α, and the hydrogen bond acceptor strength, β, of the mixture increased substantially over the composition range of 0–20% methanol, then with increasing proportions of methanol the lewis acidity and basicity varied minimally. As more diethyl ether is added methanol–methanol hydrogen bonds must break to maintain

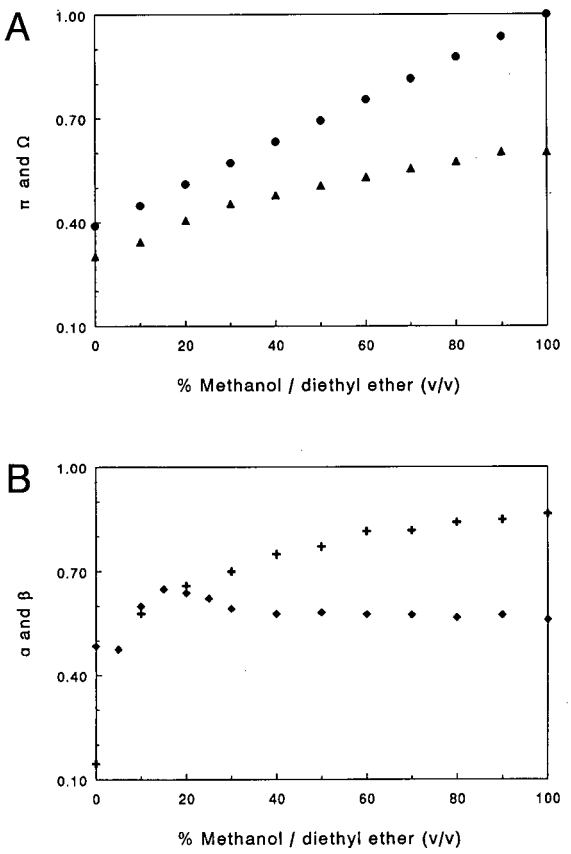

Fig. 7. Measured solvent strength parameters of methanol–diethyl ether mixtures. In A: ▲ = π^*; and ● = Ω; and in B: + = α; ◆ = β.

the polarity of the mixture at close to a constant value. The cavity formation term varies linearly with added methanol.

The relative values of the coefficients B, C, D, and E describe the relative importance of cavity formation, dipolarity, hydrogen bond accepting or donating properties of the solvent to the retention of the fullerenes. When the capacity data shown in Fig. 5A and B were fit to solvent strength parameters, models that included the α and β parameters were inadequate. They did not pass the F test even at the 75% confidence level. Only models which included exclusively the cavity formation term and the dipolarity term fit the data well. These models were valid at the 97% confidence level using the F test. For all columns, the regression coefficients for the cavity formation parameter, B, and dipolarity,

TABLE II

MODEL DESCRIBING RETENTION OF C_{60} ON DIFFERENT COLUMNS

Model $\ln k' = A + B\Omega + C\pi^*$.

Column	n^a	N^b	Coefficient (t test)[c]			Statistics					
			A	B	C	R	s	R_a^2	t_{95}	F	F_{95}
C18	9	6	−3.472 (48.0)	12.072 (39.7)	−5.570 (10.3)	1.000	0.029	1.000	2.447	1095	5.14
Phen	10	7	−2.815 (29.2)	5.019 (13.8)	−1.482 (2.2)	0.999	0.038	0.998	2.365	1853	4.74
DP-K	10	7	−2.374 (16.0)	4.799 (8.5)	−2.789 (2.7)	0.996	0.059	0.991	2.365	483	4.74
DP-S	10	7	−1.802 (5.8)	7.683 (6.5)	−5.808 (2.7)	0.992	0.124	0.979	2.365	214	4.74
P18	8	5	−4.238 (17.6)	12.651 (9.8)	−5.704 (2.7)	0.998	0.093	0.996	2.571	777	5.79

[a] Number of data points.
[b] The degrees of freedom.
[c] Number in parentheses is Student's t test value for the coefficient.

C, were positive and negative, respectively. Table II and Table III list the regression coefficients for all five columns. Fig. 8A and B shows the relative magnitude of the regression coefficients. This indicates that increased energy necessary to form a cavity in the solvent caused increased retention and increasing solvent dipolarity decreased retention. The signs of these coefficients are as expected from the endothermic and exothermic nature of the respective terms. However, the relative magnitude of these regression coefficients is interesting. For all five stationary phases the cavity formation regression coefficient was the larger of the two. However, for the monomeric and polymeric phases the cavity formation coefficient predominates. This suggests that solvophobic forces control the fullerene retention with ODS and these mobile phase mixtures.

Since the involvement of the mobile phase in retention is described by the cavity term and solvent strength parameters, the intercept term, A, of the model should represent the interaction between a solute molecule and the stationary phase. In other words, A could be treated as a measure of "pure" retention of a solute on a specific stationary phase when no mobile phase is applied, therefore all four other terms would be zero. By comparing the relative size of the A term for different columns, the retention of the fullerenes on the stationary phases is expected to decrease in the following order: diphenyl, DP-S > diphenyl, DP-K > phenyl, Phen

TABLE III

MODEL DESCRIBING RETENTION OF C_{70} ON DIFFERENT COLUMNS

Model $\ln k' = A + B\Omega + C\pi^*$.

Column	n^a	N^b	Coefficient (t test)[c]			Statistics					
			A	B	C	R	s	R_a^2	t_{95}	F	F_{95}
C18	7	4	−3.235 (21.2)	13.464 (12.8)	−6.455 (4.0)	0.999	0.059	0.998	2.776	1329	6.94
Phen	10	7	−2.488 (18.7)	6.766 (13.4)	−3.547 (3.8)	0.999	0.053	0.997	2.365	1306	4.74
DP-K	10	7	−1.950 (11.6)	6.192 (9.7)	−4.768 (4.0)	0.996	0.067	0.990	2.365	463	4.74
DP-S	10	7	−1.897 (6.8)	8.842 (8.4)	−6.225 (3.2)	0.996	0.111	0.988	2.365	387	4.74
P18	7	4	−3.682 (16.9)	14.072 (9.4)	−6.404 (2.8)	0.999	0.084	0.996	2.776	745	6.94

[a] Number of data points.
[b] The degrees of freedom.
[c] Number in parentheses is Student's t test value for the coefficient.

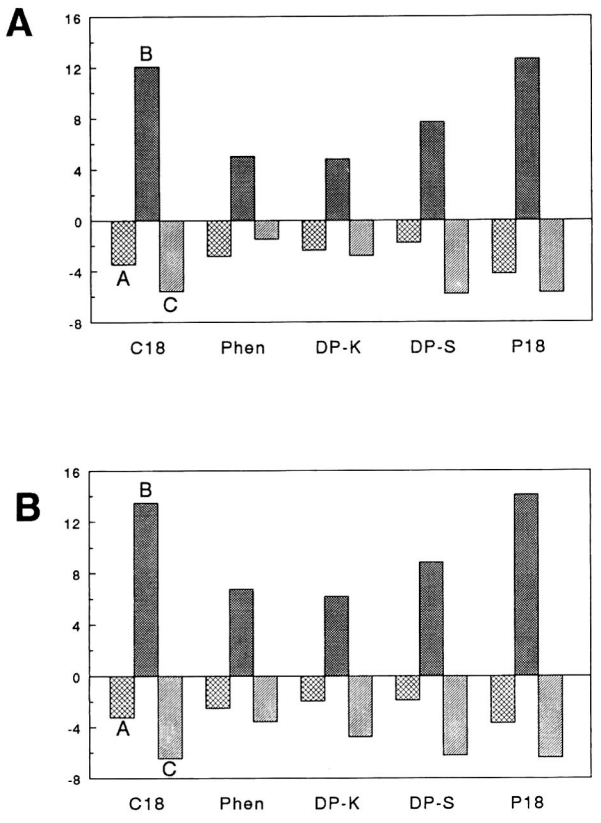

Fig. 8. Comparison of the relative values of model coefficients for different columns. (A) C_{60}; (B) C_{70}. A = model intercept; B = the coefficient for the cavity formation term; C = the coefficient for the dipolarity term.

> ODS, C18 > ODS, P18. This is exactly the order of retention that Jinno *et al.* [13] found for fullerenes with *n*-hexane as a mobile phase. We had also originally anticipated that the fullerenes would be more retentive on phenyl columns. However with the diethyl ether–methanol mobile phases the reverse retention order was observed for phenyl and ODS phases. As mentioned above, coefficients *B* and *C* describe different interactions between the solvent and the solute. However, for a chromatographic separation these parameters would be describing solvent–solute interaction in the bulk fluid and near the surface of stationary phase. Different *B* and *C* values from different columns may indicate that the solute and the solvent interactions near the surface were different. In both Table II and Table III, C18 and P18 had similar cavity formation and dipolarity coefficients; DP-K and Phen, both from the same vendor, also had similar *B* and *C* values. Therefore similar surfaces gave similar solvent–solute interaction indicators, *B* and *C*.

CONCLUSIONS

This paper demonstrates that the fullerenes are soluble enough to use solvents as polar as methanol in their separation. A nonaqueous reversed-phase method of separating C_{60} and C_{70} is described. A linear solvation energy relationship (LSER) provided significant evidence to support the proposed retention mechanism. With the methanol–diethyl ether mobile phase, monomeric and polymeric ODS provided the highest selectivity.

ACKNOWLEDGEMENTS

We are grateful for the financial support of this work through a grant from the Ohio State University Center for Materials Research. We thank Keystone Scientific, Inc., for donation of the Hypersil columns, James V. Coe and his research group for supplying the fullerene soot used in this study, and W.W. Yin for providing mass spectra from an Extrel FTMS-2000 instrument in work supported by a grant from NIH (GM-31683) to A.G. Marshall.

REFERENCES

1 W. Krätschmer, L. D. Lamb, K. Fostiropoulos and D. R. Huffman, *Nature (London)*, 347 (1990) 354.
2 F. Wudl, *Acc. Chem. Res.*, 25 (1992) 143.
3 D. E. Manolopoulos, *J. Chem. Soc. Faraday Trans.*, 87 (1991) 2861.
4 P. W. Fowler, D. E. Manolopoulos and R. C. Batten, *J. Chem. Soc. Faraday Trans.*, 87 (1991) 3103.
5 F. Diederich, R. L. Whetten, C. Thilgen, R. Ettl, I. Chao and M.M. Alvarez, *Science (Washington, DC)*, 254 (1991) 1768.
6 R. E. Smalley, *Fullerenes (ACS Symposium Series*, No. 481), American Chemical Society, Washington, DC, 1992, p. 117.
7 R. Taylor, J. P. Hare, A. K. Abdul-Sada and H. W. Kroto, *J. Chem. Soc. Chem. Commun.*, 20 (1990) 1423.
8 H. J. Ajie, M. M. Alvarez, S. J. Anz, R. D. Beck, F. Diederich, K. Fostiropoulos, D.R. Huffman, W. Krätschmer, Y. Rubin, K.E. Schriver, D. Sensharma and R. L. Whetten, *J. Phys. Chem.*, 94 (1990) 8630.
9 P. M. Allemand, A. Koch and F. Wudl, *J. Am. Chem. Soc.*, 113 (1991) 1050.
10 J. M. Hawkins, T. A. Lewis, S. D. Loren, A. Meyer, J. R. Heath, Y. Shibato and R. J. Saykally, *J. Org. Chem.*, 55 (1990) 6250.

11 D. M. Cox, S. Behal, M. Disko, S. M. Gorun, M. Greaney, C. S. Hsu, E. B. Kollin, J. Millar, J. Robbins, W. Robbins, R. D. Sherwood and P. Tindall, *J. Am. Chem. Soc.*, 113 (1991) 2940.
12 A. M. Vassallo, A. J. Palmisano and L. S. K. Pang, *J. Chem. Soc. Chem. Commun.*, 1 (1992) 60.
13 K. Jinno, K. Yamamoto, T. Ueda, H. Nagashima, K. Itoh, J. C. Fetzer and W. R. Bigg, *J. Chromatogr.*, 594 (1992) 105.
14 M. S. Meier and J. P. Selegue, *J. Org. Chem.*, 57 (1992) 1924.
15 F. Diederich and R. L. Whetten, *Acc. Chem. Res.*, 25 (1992) 119.
16 F. Diederich, R. L. Whetten, C. Thilgen, R. Ettl, I. Chao and M. M. Alvarez, *Science (Washington, DC)*, 254 (1991) 1768.
17 R. E. Haufler, J. Conceicao, L. P. F. Chibante, Y. Chai, N. E. Byrne, S. Flanagan, M. M. Haley, S. C. O'Brien, C. Pan, Z. Xiao, W. E. Billups, M. A. Ciufolini, R. H. Hauge, J. L. Margrave, L. J. Wilson, R. F. Curl and R. E. Smalley, *J. Phys. Chem.*, 94 (1990) 8634.
18 P. A. Limbach, L. Schweikhard, K. A. Cowen, M. T. McDermott, A. G. Marshall and J. V. Coe, *J. Am. Chem. Soc.*, 113 (1992) 6795.
19 M. Charton, S. Clementi, S. Ehrenson, O. Exner, J. Shorter and S. Wold, *Quant. Struct. Act. Relat.*, 4 (1985) 29.
20 T. M. Engel and S. V. Olesik, *Anal. Chem.*, 63 (1991) 1830.
21 R. W. Taft, J.-L. M. Abboud, M.J. Kamlet and M. H. Abraham, *J. Solution Chem.*, 14 (1985) 153.
22 M. J. Kamlet, R. H. Doherty, M. H. Abraham and R. W. Taft, *Carbon*, 23 (1987) 549.
23 M. H. Abraham, G. J. Buist, P. L. Grellier, R. A. McGill, R. M. Doherty, M. J. Kamlet, R. W. Taft and S. G. Maroldo, *J. Chromatogr.*, 409 (1987) 15.
24 P. Sadek, P. W. Carr, R. M. Doherty, M. J. Kamlet, R. W. Taft and M. H. Abraham, *Anal. Chem.*, 57 (1985) 2971.
25 J. E. Hildebrand and R. L. Scott, *The Solubility of Nonelectrolytes*, Dover Publications, New York, 3rd. ed., 1964, p. 98.
26 Y. Cui and S. V. Olesik, *Anal. Chem.*, 63 (1991) 1812.

Journal of Chromatography, 625 (1992) 141–149
Elsevier Science Publishers B.V., Amsterdam

CHROM. 24 478

Use of off-line gel permeation chromatography–normal-phase liquid chromatography for the determination of polycyclic aromatic compounds in environmental samples and standard reference materials (air particulate matter and marine sediment)

Pilar Fernandez and Josep M. Bayona

Environmental Chemistry Department, CID (CSIC), Jordi Girona Salgado 18, 08034 Barcelona (Spain)

(First received February 25th, 1992; revised manuscript received June 16th, 1992)

ABSTRACT

A method involving two levels of fractionation, semi-preparative gel permeation chromatography (GPC) and normal-phase liquid chromatography (NP-LC), and capillary gas chromatography with flame ionization and nitrogen–phosphorus detection coupled with mass spectrometry, was developed for the determination of polar substituted aromatic compounds (PACs) in environmental matrices. A GPC clean-up procedure (BioBeads SX-12–dichloromethane) efficiently removed lipidic matter from organic extracts, yielding an enriched PAC fraction. NP-LC (μPorasil) of that fraction provided a selectivity based on chemical classes and moderate to high recoveries for standard PAC. The application of this method to environmental samples and reference materials, air particulate matter (NIST 1649) and marine sediment (HS-4), demonstrated the validity of the procedure for the determination of polycyclic aromatic hydrocarbons (PAHs) from both qualitative and quantitative points of view. Further, a variety of aromatic ketones, quinones and aldehydes (oxy-PAHs) were determined in both matrices.

INTRODUCTION

The occurrence of polar substituted aromatic compounds (PACs) in the environment is of major concern because most of their chemical classes are carcinogenic [1]. Hence, the risk assessment associated with their occurrence requires the determination of environmental levels in the different compartments. However, whereas analytical procedures for the determination of polycyclic aromatic hydrocarbons (PAHs) in environmental samples are well established [2,3], methods for PACs require further research. In fact, because they usually occur at concentration levels several orders of magnitude lower than the corresponding parent PAHs, their characterization in environmental matrices requires multistage enrichment and fractionation techniques. In addition, the application of bioassay-directed fractionation strategies to environmental samples has revealed that a large proportion of the direct-acting mutagenicity can be accounted for by the PAC containing fractions [4,5].

Consequently, we have focused our attention on the development of a procedure for the determination of PACs in several environmental matrices, namely marine sediments and urban particulate matter. Previous workers studies have used normal- [6-8] and reversed-phase [9,10] liquid chromatographic (LC) methods to fractionate components in environmental extracts because they are fast and

Correspondence to: Dr. P. Fernandez, Environmental Chemistry Department, CID (CSIC), Jordi Girona Salgado 18, 08034 Barcelona, Spain.

0021-9673/92/$05.00

provide higher efficiencies than column chromatographic fractionation [11,12] or acid–base partitioning [13].

Although reversed-phase analytical LC is widely used, its usefulness at the semi-preparative level is limited by the low solubility of these complex organic mixtures in aqueous mobile phases [14]. On the other hand, an advantage of normal-phase LC is its selectivity, which allows the separation of PACs according to chemical functionalities [14], whereas the monomeric reversed-phase selectivity is mainly based on the number of aromatic carbon atoms in the case of the parent PAHs. Further, alkyl substitution in reversed-phase chromatography causes an appreciable increase in retention due to the decreased solubility in the polar mobile phase [15].

The approach described here is based on the use of sequential fractionation techniques of completely different selectivity. It includes the removal of the lipidic material by semi-preparative gel permeation chromatography (GPC), further fractionation of the aromatic-containing fraction (GPC-2) by semi-preparative normal-phase liquid chromatography (NP-LC) and capillary gas chromatography (cGC) with flame ionization (FID) and nitrogen–phosphorus detection (NPD) or cGC–mass spectrometry (cGC–MS) for the characterization of the PAC containing fractions. The validation of this methodology was performed with the analysis of two standard reference materials (SRMs) with certified PAH contents. Further, a wide variety of PACs, namely, aromatic ketones, quinones, aldehydes coumarins and nitroarenes, were identified in these SRMs and in environmental samples.

EXPERIMENTAL

Materials

Pesticide grade dichloromethane, hexane and isooctane were obtained from Baker (Phillipsburg, NJ,USA). Acetonitrile and methanol were HPLC grade (Teknokroma, Sant Cugat, Spain). 2-Nitrofluorene, 2-aminofluorene, 1-nitropyrene, acridine, naphthalene-1,4-dione and 9*H*-fluoren-9-one were purchased from Aldrich and Sigma (Steinheim, Germany). 7*H*-Benz[*de*]anthracen-7-one, benz[*a*]anthracene-7,12-dione, benzo[*a*]fluorenone, pyrene-*x*,*y*-dione and 1-naphthol were a gift from Professor Milton L. Lee (Brigham Young University, Provo, UT, USA). Other standards were available in our laboratory.

Urban air particulate matter (NIST 1649) and marine sediment (HS-4), both with certified values for several PAHs, were obtained from the National Institute of Science and Technology (Gaithersburg, MD, USA) and the National Research Council (Halifax, NS, Canada), respectively. A sediment sample was collected with a Reineck box corer 2 km offshore near Barcelona. The sampled superficial sediment was wrapped in aluminium foil and frozen until analysis. Air particulate matter was collected in a Whatman GF/A (20.5 x 25.4 cm) glass microfibre filter using a HI-VOL sampling system (MC.V., Collbató, Spain). Samples were collected in a heavily trafficked square in Barcelona City 8 m above the street level. Filters were replaced every 24 h.

Extraction

SRMs (2.0 g of NIST 1649, 31.3 g of HS-4) and environmental samples (24-h filter and 30 g of freeze-dried sediment) were extracted with dichloromethane (5 x 15 ml and 5 x 30 ml, respectively) by sonication in glass centrifuge tubes, which is considered to be the most efficient method for these samples and artifact formation is minimized [16]. Extracts were evaporated nearly to dryness at reduced pressure and filtered through a glass-microfibre filter (Whatman GF/F) prior to chromatographic analysis.

Chromatographic fractionation

GPC. Filtered extracts (100 mg nominal mass) were injected into a Rheodyne (Cotati, CA, USA) valve (150 μl). A stainless-steel column (500 x 10 mm I.D.) packed with styrene–divinylbenzene copolymer (200–400 mesh) (Bio-Beads SX-12, Bio-Rad Labs., Richmond, CA, USA) was used with dichloromethane as the mobile phase at flow rate of 1 ml/min as reported elsewhere [17].

NP-LC. Standard solutions or GPC-2 fraction (15 mg) in dichloromethane were fractionated through a normal-phase semi-preparative column (300 x 7.8 mm I.D.) packed with 10-μm μPorasil (Waters Assoc., Milford, MA, USA). Injection was performed via high-pressure valve (Rheodyne) equipped with a 50-μl loop.

A high pressure pump (Kontron, Zürich, Switzerland) delivered mobile phase at a flow-rate of 4.5 ml/min. A UV-VIS detector (254 nm) (Varian, Sunnyvale, CA, USA) and fluorescence detector (λ_{ex} 254 nm and λ_{em} 390 nm) (Perkin Elmer, Norwalk, CT, USA) were coupled in series. The elution programme started isocratically with hexane for 5 min, followed by a linear gradient of 1%/min of dichloromethane for 5 min and then a linear gradient of 4%/min of dichloromethane for 25 min and held isocratically at 100% dichloromethane for 10 min. Subsequently, a linear gradient of 10%/min of acetonitrile and held at these conditions for 5 min, then a step back to 100% dichloromethane (5 min) and 100% hexane for 5 min was applied. The column was re-equilibrated with 100% hexane for 15 min before the next injection. Eight fractions were collected using a Gilson (Middleton, WI, USA) fraction collector (Fig. 1). The column was backflushed with methanol as described previously [6] and the eluate was collected as fraction nine, following the last injection of each sample fractionation.

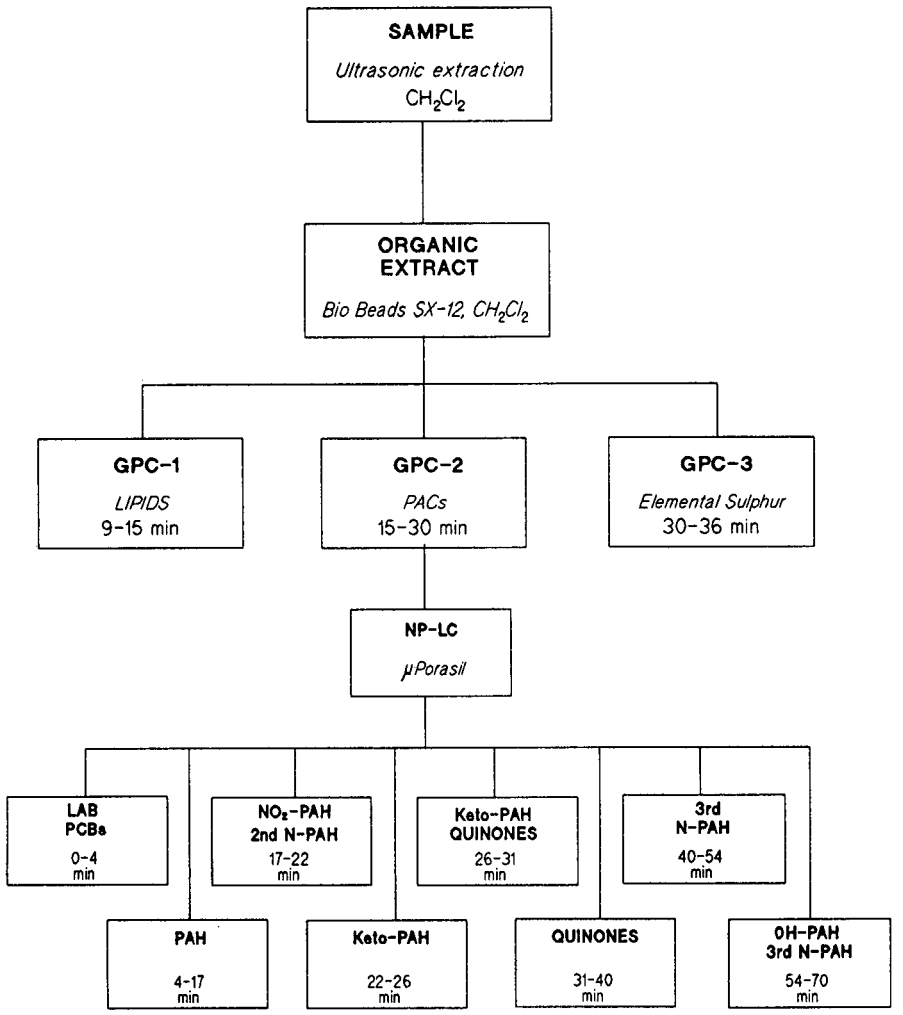

Fig. 1. Fractionation scheme. Compound-class identification as follows: LAB = long chain alquilbenzenes; PCB = polychlorobiphenyls; PAH = polycyclic aromatic hydrocarbons; NO_2-PAH = nitro substituted polycyclic aromatic hydrocarbons; 2nd N-PAH = secondary nitrogen heterocycles; Keto-PAH = polycyclic aromatic hydrocarbons with one carbonyl group; 3rd N-PAH = tertiary nitrogen heterocycles; OH-PAH = hydroxy substituted polycyclic aromatic hydrocarbons.

NP-LC fractions were evaporated nearly to dryness at reduced pressure, transferred to vials and blown down to dryness with a gentle stream of nitrogen. Blanks and spiked samples were processed in the same way as real samples.

Chromatographic Analyses

CGC. NP-LC fractions were analysed by cGC using a Carlo Erba (Milan, Italy) 5300 Mega series equipped with a split–splitless injector and with (FID) and (NPD), interfaced to a Nelson–Perkin-Elmer (Norwalk, CT, USA) data system. A fused-silica capillary column (30 m x 0.25 mm I.D.) coated with DB-5 (0.25 μm film thickness) (J & W Scientific, Folson, CA, USA) was used. Hydrogen was the carrier gas at linear velocity of 50 cm/s. The column temperature was programmed from 60 to 300°C at 6°C/min and the final temperature was held for 15 min. The injector, FID and NPD temperatures were held at 300, 330 and 310, respectively. Fractions from I to IV were analysed as solutions in isooctane, and in dichloromethane (FID) or ethyl acetate (NPD) for more polar fractions. Determinations of PAHs were accomplished as described elsewhere [18]. Nitrogen-containing PAHs were determined by cGC–NPD, using 9-nitroanthracene, 1-nitropyrene, 6-nitrochrysene and 6-nitrobenzo [*a*]pyrene.

cGC–MS. cGC–electron impact (EI) (70 eV) MS analyses were performed in a Hewlett-Packard Model 5985A quadrupole instrument interfaced to a Model 9825A data system. The injector, ion source and mass analyser temperatures were held at 300, 180 and 120°C, respectively. Helium was used as the carrier gas (30 cm/s) and scans were obtained every 0.86 s. The mass axis was calibrated with perfluorotributylamine using fragments at *m/z* 69, 219 and 502. Other chromatographic conditions were identical with those described for the cGC analysis. Positive identifications were made by injection of authentic standards and tentative identifications by the PBM algorithm search in the Wiley library.

Oxy-PAHs were determined by cGC–MS using 9*H*-fluoren-9-one, benzo[*a*]fluorenone, 7*H*-benz [*de*]anthracen-7-one, anthracene-9,10-dione and benz[*a*]antracene-7,12-dione as external standards in the multiple-ion detection (MID) and single-ion monitoring (SIM) modes for the air particulate matter and marine sediments, respectively. The SIM mode was performed using the molecular ion of these compounds as a diagnostic (*m/z* 180, 208, 230 and 258) with 2.0 cycles/s and a dwell time of

TABLE I

RETENTION AND RECOVERY BEHAVIOUR OF SELECTED STANDARD PAC BY NP-LC

Compound	t_R (min)	Fraction	Recovery (%)[a]
Octacosane	–[b]	I	79
Anthracene	6.4	II	–
Benzo[*ghi*]perylene	7.2	II	98
Coronene	7.5	II	–
2-Nitrofluorene	17.3	III	112
Carbazole	19.2	III	86
1-Nitropyrene	20.8	III	100
Naphthalene-1,4-dione	29.3	V	104
7*H*-Benz[*de*]anthracen-7-one	31.0	V	87
2-Aminofluorene	33.4	VI	36
Pyrene-*x,y*-dione[c]	37–40	VI	–
Acridine	50.4	VII	64
1,8-Naphthalic diacid anhydride	50–52	VIII	–
4-Nitrophenol	52–54	VIII	–
1-Naphtol	54.2	VIII	40

[a] Recovery experiments were perfomed at μg level.

[b] – Not determined.

[c] Mixture of : -3,8-, -8,3- and -8,10- isomers.

100 ms. Compound identification from the mass fragmentograms was accomplished by comparison with previously reported retention indices [19]. Aldehydes and coumarins were determined using the same response factor as for structurally related oxy-PAHs.

RESULTS AND DISCUSSION

The fractionation scheme applied is illustrated in Fig. 1. In the first level, organic extracts were fractionated into three fractions by semi-preparative GPC with dichloromethane. In previous work [17], we demonstrated the usefulness of this chromatographic system for the clean-up of environmental samples, allowing the removal of co-extractable lipidic material from PACs. The latter eluted in the fraction GPC-2 (15–28 min) with a recovery range from 75 to 100% depending on the chemical class of the PAC.

In this work, a separation scheme based on NP-LC using a silica gel μPorasil column, which allows the separation according to the different classes of PACs [14], was investigated (Fig. 1). The mobile phase composition and gradient programming were designed to optimize the resolution between PAHs, nitro-PAHs, oxy-PAHs, 3rdN-PAHs and hydroxy-PAHs. In this regard, Matsunaga [20] evaluated the separation of PAHs and PACs on several polar chemically bonded normal-phase (amino, nitro and cyanopropyl substituents) and silica gel. Although the amino phase had better selectivity and column stability, it is not suitable for carbonylic PAH analysis, as these compounds can react with the amino groups in the LC stationary phase to form Schiff bases [21].

On the basis of the retention time data for a standard mixture, the cut-off points between fractions were determined. This mixture was injected periodically in order to evaluate the change in reproducibility of retention times due to column deactivation.

Recoveries from NP-LC and retention time data for this mixture are summarized in Table I. Generally a good resolution between the standard compounds analysed was observed (Table II), although an overlapping between secondary nitrogen aromatic heterocycles (2ndN-PAHs) and nitro-PAHs is apparent. With nitrogen-containing PAHs, the retention times increase according to basicity. In this regard, it has been reported that basic nitrogen heterocycles are strongly retained on the μPorasil stationary phase owing to intense acid–base interactions of the basic nitrogen with the acidic silanol groups on the silica surface [14, 22] (t_R carbazole < t_R 2-aminofluorene < t_R acridine, pK_a = −1.9, 4.64 and 5.58, respectively).

The most interesting range of retention times on the NP-LC trace is that corresponding to the moderately polar fractions, where nitro- and oxy-PAHs, among other compounds, are eluted. In order to improve their resolution, a slow gradient of dichloromethane in hexane was applied. As far as the standard compounds are concerned, compound-class separation predominated. However, a slight overlapping between different chemical classes of PACs was observed with real samples, which was accounted for by a slight contribution of the number of aromatic carbons to the retention of PACs. This is the case with aromatic ketones and nitro-PAHs, but owing to the selective detection techniques used in analyse for these compounds, their

TABLE II

SELECTIVITY (α) ACCORDING TO PAH SUBSTITUTION ON NP-LC

Compound Class	PAHs	Nitro-PAHs	Keto-PAHs	Quinone	2ndN-PAHs	3rdN-PAHs
Nitro-PAHs	2.7					
Keto-PAHs	3.9	1.5				
Quinone	4.6	1.9	1.3			
2ndN-PAHs	3.0	1.1	1.3	1.5		
3rdN-PAHs	7.9	2.9	1.6	1.7	2.6	
Hydroxy-PAHs	8.5	3.1	2.2	1.8	2.8	1.1

simultaneous determination was possible, provided that the concentration ranges were comparable. Finally, the latest eluting class of PACs are hydroxy-PAHs owing to strong hydrogen bonding on the silica surface [14].

The recoveries were over 80% for most of the compounds analysed. The lowest recovery was found for hydroxy-PAHs, probably because these compounds were eluted among fractions 8 and 9, and fraction 9 was not considered in recovery determination. This polar fraction represents of 2% of the total mass of the extract of the marine sediments and 10–20% in case of air particulate matter samples.

Another group of compounds with moderate recoveries are the nitrogen-containing PAHs, especially the amino-PAHs, but this could be due to the instability of these compounds.

Application to environmental samples and standard reference materials

We evaluated the applicability of the two-step fractionation approach (Fig. 1) to environmental samples and marine sediment (HS-4, coastal sedi-

TABLE III

ANALYSIS OF URBAN PARTICULATE MATTER (UPM), NIST 1649, MARINE SEDIMENT (MS) AND HS-4 STANDARD REFERENCE MATERIALS

Peak No.	Compound	Concentration (μg/g)[a]				
		UPM	NIST 1649	MS	HS-4	
Polycyclic aromatic hydrocarbons						
1	Phenanthrene[b]	1.37	3.41 ± 0.05		0.27	(0.45 ± 0.15)
2	Anthracene	0.26	0.38 ± 0.2	0.06	0.06 ± 0.002	(0.14 ± 0.07)
3	3-Methylphenanthrene[b]	0.84	0.49 ± 0.2	0.10	0.08 ± 0.02	
4	2-Methylphenanthrene[b]	1.01	0.57 ± 0.3	0.13	0.07 ± 0.01	
5	4*H*-Cyclopenta[*def*]phenanthrene	0.44	0.10 ± 0.01	0.07	0.02 ± 0.01	
6	9-Methylphenanthrene	0.75	0.37 ± 0.2	0.11	0.08 ± 0.02	
7	1-Methylphenanthrene[b]	0.71	0.25 ± 0.01	0.10	0.04 ± 0.01	
8	Fluoranthene[b]	4.55	6.04 ± 0.8 (7.1 ± 0.5)	0.48	1.01 ± 0.2	(1.25 ± 0.2)
9	Acephenanthrylene	2.56	0.12 ± 0.01		0.07 ± 0.01	
10	Pyrene[b]	6.59	6.68 ± 0.8	0.37	0.80 ± 0.1	(0.94 ± 0.12)
11	Methylpyrenes					
12	Benzo[*ghi*]fluoranthene[b]	6.68	0.96 ± 0.3		0.21 ± 0.01	
13	Benzo[*c*]phenanthrene[b]		0.36 ± 0.05		0.12 ± 0.01	
14	Benz[*a*]anthracene[b]	5.35	2.13 ± 0.5 (2.6 ± 0.3)	0.28	0.47 ± 0.1	(0.53 ± 0.05)
15	Chrysene + triphenylene[b]	7.74	4.26 ± 0.2	0.17	0.68 ± 0.2	(0.65 ± 0.08)
16	Methylchrysenes					
17	Benzofluoranthene[c]	5.48	11.63 ± 1.5	0.23	1.46 ± 0.3	
18	Benzo[*e*]pyrene[b]	8.67	4.21 ± 0.6	0.11	0.45	
19	Benzo[*a*]pyrene[b]	9.64	3.32 ± 0.6 (2.9 ± 0.5)	0.11	0.60 ± 0.2	(0.65 ± 0.08)
20	Perylene[b]	1.85		0.02	0.32 ± 0.02	
21	Indeno[7,1,2,3-*cd*]chrysene	3.36	0.39 ± 0.04		0.14 ± 0.01	
22	Indeno[1,2,3-*cd*]pyrene[b]	10.0	3.81 ± 0.6 (3.3 ± 0.5)	0.13	0.62 ± 0.03	(0.51 ± 0.15)
23	Dibenzo[*a,h*]anthracene[b]		0.60 ± 0.05		0.13 ± 0.01	(0.12 ± 0.05)
24	Benzo[*b*]chrysene[b]		0.28 ± 0.01		0.05 ± 0.01	
25	Benzo[*ghi*]perylene[b]	26.2	4.31 ± 0.8 (4.5 ± 1.1)	0.24	0.54 ± 0.02	(0.58 ± 0.22)
26	Anthracene[b]	2.34	0.12 ± 0.02		0.09 ± 0.01	
27	Dibenzopyrenes					
28	Coronene	12.8	3.91 ± 0.4	nd[d]	0.14 ± 0.01	
Nitroarenes						
29	1-Nitropyrene[b]	0.11	0.18 ± 0.02	nd	nd	
	6-Nitrobenzo[*a*]pyrene[b]	nd	nd		0.34 ± 0.11	

TABLE III (*continued*)

Peak No.	Compound	Concentration (μg/g)[a]			
		UPM	NIST 1649	MS	HS-4
Polycyclic aromatic ketones					
30	9*H*-Fluoren-9-one[b]	0.37	0.30 ± 0.03	0.022	0.012 ± 0.001
31	C_1-9*H*-Fluoren-9-one	0.02	0.02 ± 0.01	0.002	0.001
	C_1-9*H*-Fluoren-9-one	0.01	0.02 ± 0.01	0.001	0.001
	C_1-9*H*-Fluoren-9-one	0.01	0.02 ± 0.005	0.001	0.002
32	C_2-9*H*-Fluoren-9-one	0.02	0.01 ± 0.002		
33	Anthrone[b]	0.001	0.02 ± 0.00	0.008	0.002
34	Xanthone[b]	0.005	0.07 ± 0.02		
35	4*H*-Cyclopenta[*def*]phenanthrene-4-one[b]	0.41	0.17 ± 0.05	0.003	0.13 ± 0.002
36	Benzo[*a*]fluorenone[b]	1.36	1.89 ± 0.3	0.020	0.834 ± 0.09
37	Benzo[*c*]fluorenone	0.63	0.42 ± 0.05	0.024	0.016 ± 0.003
38	Benzo[*b*]fluorenone	0.72	1.57 ± 0.02	0.004	0.010 ± 0.002
39	7*H*-Benz[*de*]anthracen-7-one[b]	2.35	1.31 ± 0.02	0.001	0.021 ± 0.005
40	Benzopyrenone isomer	0.30	nd	0.004	0.004
41	Benzopyrenone isomer	–[e]	0.19 ± 0.02	nd	0.0004
Polycyclic aromatic quinones					
42	Antracene-9,10-dione[b]	0.41	0.22 ± 0.04	–	0.009
43	Benz[*a*]anthracene-7,12-dione[b]	0.79	7.465 ± 1.1	0.005	0.159 ± 0.02
Polycyclic aromatic aldehydes					
44	Formylphenanthrene-anthracene isomer	–	0.02 ± 0.001	nd	nd
45	Formylphenanthrene-anthracene isomer	–	0.03 ± 0.002	nd	nd
Coumarines					
46	5*H*-Phenanthro[4,5-*bcd*]pyran-5-one[b]	0.84	0.16 ± 0.02	nd	nd
47	Coumarin (MW = 246)	–	0.17 ± 0.05	nd	nd

[a] Certified values in parentheses [23–25]. Procedural relative standard deviations (n = 3) are indicated as ± values.
[b] Positive identification by co-injection with an authentic standard, otherwise identifications are based on EI mass spectra, positive response in selective detectors (NPD) and retention indices.
[c] [*b*], [*j*] and [*k*] isomer mixture for the NIST 1649 and our determination but for HS-4 includes only [*b*] and [*k*] isomers.
[d] nd, Not detected.
[e] –, Not determined.

ment) and airborne particulate matter (NIST 1649, urban particulate matter) SRMs, which represent two environmental matrices with high levels of biogenic interferences. These SRMs have certified contents of some PAHs.

The levels of different chemical classes of PACs identified and the certified values are given in Table III. The identification of oxy-PAHs, reported for the first time in these SRMs is note-worthy.

The chromatographic profiles corresponding to the PAH fraction are shown in Fig. 2. From the quantitative point of view, a deviation from certified levels below the 20-30% was observed for marine sediment sample with low levels of PAHs, whereas for air particulate matter with higher levels the deviation was about the 10–15%. The highest deviation occurs with benzofluoranthene isomers ([*b*], [*j*] and [*k*]), probably owing to the lack of chromatographic resolution between these isomeric compounds in our chromatographic system. However, in the HS-4 reference material, the certified value corresponds to a mixture of [*b*] and [*k*] isomers therefore explaining the observed quantitative differences.

On the other hand, taking into account that the relative standard deviation of the whole analytical procedure is in the range 15–20% (n = 3), the values obtained in this study fall within the range of most of the certified values.

In addition, this fractionation procedure allowed the identification of several other classes of PACs, namely aromatic ketones, aldehydes, quinones and

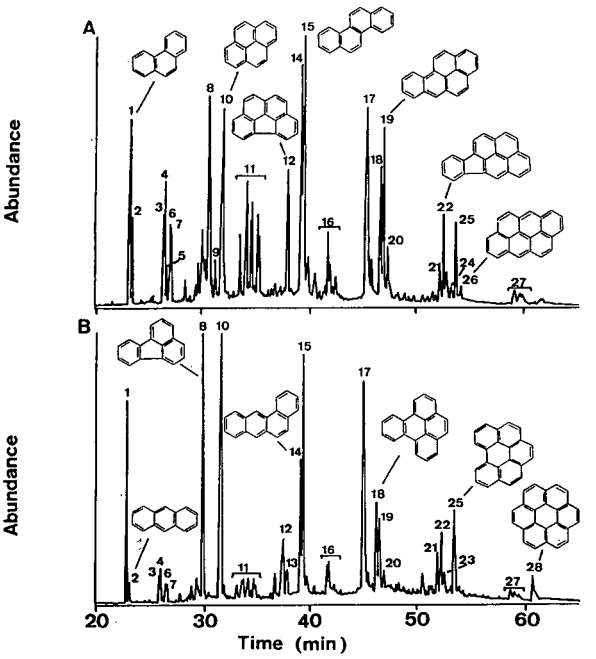

Fig. 2. cGC–MS profile of PAH fraction of SRMs isolated from (A) marine sediment (HS-4) and (B) air particulate matter (NIST 1649). For compound identification, see in Table III.

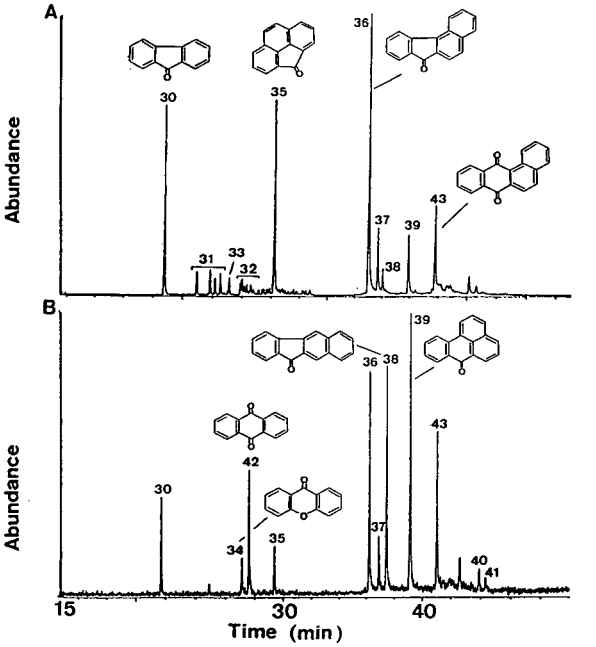

Fig. 3. cGC–MS profile of SRM fractions V and VI isolated from (A) marine sediment (HS-4) and (B) air particulate matter (NIST 1649). For compound identification, see Table III.

TABLE IV

LIMITS OF DETECTION (LOD) (ng/g) OF PACs IN SRM

Compound	NIST 1649	HS-4
PAHs[a]		
Pyrene	8.8	0.58
Benzo[*ghi*]perylene	28	1.8
Nitroarenes[b]		
9-Nitroanthracene	7.2	–
1-Nitropyrene	4.7	–
Ketones		
7*H*-Benz[*de*]anthracen-7-one	43[c]	0.008[d]

[a] FID.
[b] NPD.
[c] MS (MID).
[d] MS (SIM).

nitroarenes, in these samples, present at lower concentrations. The cGC–MS profiles obtained for the SRMs are shown in Fig. 3. Important differences between the two environmental matrices were evident. First, higher levels of these compounds were detected in the air particulate matter according to their sources. Second, as far as nitroarenes are concerned, only 1-nitropyrene was detected in NIST 1649, at a concentration similar to that reported by Ramdahl *et al.* [24] for the same sample. On the other hand, the penta- and hexa-fused aromatic ring nitroarenes are predominant in sediment samples (Table III).

Finally, the detection limits for the PAC classes were calculated, taking into account the recovery for the overall analytical procedure (extraction, GPC–NP-LC fractionation and the determination technique) (Table IV). The selection of the final determination was based on the concentration levels and on the interferences in the same fraction. In this regard, although electron-capture detection exhibited a higher sensitivity than NPD or MS for the determination of nitroarenes and oxy-PAHs, the presence of interferences precluded its application.

Further, the lower detection limit obtained with HS-4 can be accounted for by larger amount of sample extracted, as the concentration levels of PACs in sediments are lower than those in air particulate matter (Table III). Therefore, the detection and determination of oxy-PAHs in sediments required the application of the SIM detection mode.

CONCLUSIONS

A method for the simultaneous determination of several chemical classes of PACs has been developed. The main interest is the combination of GPC as a clean-up step prior to compound fractionation, yielding an enriched PAC fraction, which was further fractionated by NP-LC according to chemical classes. Finally, the applicability of these techniques to the determination analysis of PAHs and the intermediate polarity PACs in two environmental matrices has been demonstrated.

REFERENCES

1 R. C. Garner, C. N. Martin and D. B. Clayson, in C. E. Searle (Editor), *Chemical Carcinogens (A.C.S. Monograph.* Vol. 182), American Chemical Society, Washington D.C., 1984, pp. 175–276.
2 L. R. Hilpert, W. E. May, S. A. Wise, S. N. Chesler and H. S. Hertz, *Anal. Chem.*, 50 (1978) 458–463.
3 S. A. Wise, in A. Bjorseth and T. Ramdahl (Editors),*Handbook of Polycyclic Aromatic Hydrocarbons*, Vol. 2, Marcel Dekker, New York, 1985, pp 113–193.
4 P. Fernández, M. Grifoll, A. M. Solanas, J. M. Bayona and J. Albaigés, *Environ. Sci. Technol.*, 26 (1992) 817–829.
5 I. T. Salmeen, A. M. Pero, R. Zator, D. Schuetzle and T. L. Riley, *Environ. Sci. Technol.*, 18 (1984) 375–382.
6 S. P. Levine and L. M. Skewes, *J. Chromatogr.*, 235 (1982) 532–535.
7 M. C. Paputa-Peck, R. S. Marano, D. Schuetzle, T. L. Riley, C. V. Hampton, T. J. Prater, L. M. Skewes, T. E. Jensen, P. H. Ruehle, L. C. Bosch and W. P. Duncan, *Anal. Chem.*, 55 (1983) 1946–1954.
8 T. Nielsen, *Anal. Chem.*, 55 (1983) 286–290.
9 Z. Jin, S. Dong, W. Xu, Y. Li and X. Xu, *J. Chromatogr.* 386 (1987) 185–190.
10 H. Matsumoto and K. Inoue, *Arch. Environ. Contam. Toxicol.*, 16 (1987) 409–416.
11 D. W. Later, B. W. Wilson and M. L. Lee, *Anal. Chem.*, 57 (1985) 2979–2984.
12 W. R. West, P. A. Smith, G. M. Booth and M. L. Lee, *Environ. Sci. Technol.*, 22 (1988) 224–228.
13 M. G. Nishioka, C. C. Chuang, B. A. Petersen, A. Austin and J. Lewtas, *Environ. Inter.*, 11 (1985) 137–146.
14 S. C. Ruckmick and R.J. Hurtubise, *J. Chromatogr.*, 331 (1985) 55–68.
15 M. L. Lee, M.V. Novotny and K.D. Bartle, *Analytical Chemistry of Polycyclic Aromatic Compounds*, Academic Press, New York, 1981, pp. 156–187.
16 R. Williams, T. Pasley, S. Warren, R. Zweidinger, R. Watts, A. Stead and L. Claxton, *Int. J. Environ. Anal. Chem.*, 34 (1988) 137–154.
17 P. Fernández, *Ph. D. Dissertation*, Autonomous University of Barcelona, Bellaterra, 1991.
18 I. D. Brindle and X.-F. Li, *J. Chromatogr.*, 498 (1990) 11–24.
19 J. König, E. Balfanz, W. Funcke and T. Romanowski, *Anal. Chem.*, 55 (1983) 599–603.
20 A. Matsunaga, *Anal. Chem.*, 55 (1983) 1375–1379.
21 D. Karlesky, D. C. Shelly and I. Warner, *Anal. Chem.*, 53 (1981) 2146.
22 H. Colin, J.-M. Schmitter and G. Guiochon, *Anal. Chem.*, 53 (1981) 625–631.
23 *Certificate of Analysis, Standard Reference Material 1649*, National Institute of Science and Technology, Washington, DC, 1982.
24 T. Ramdahl, B. Zielinska, J. Arey, R. Atkinson, A. M. Winer and J. N. Pitts Jr., *Nature (London)*, 321 (1986) 425–427.
25 S. A. Wise, L. R. Hilpert, R. E. Rebbert, L. C. Sander, M. M. Schantz, S. N. Chesler and W. E. May, *Fresenius Z. Anal. Chem.*, 332 (1988) 573–582.

Journal of Chromatography, 625 (1992) 151–155
Elsevier Science Publishers B.V., Amsterdam

CHROM. 24 532

Determination of carbohydrates by hydrophilic interaction chromatography with pulsed amperometric detection using postcolumn pH adjustment

Tomoyoshi Soga, Yoshinori Inoue and Kenji Yamaguchi

Analytical Instruments Division, Yokogawa Analytical Systems, 2-11-19 Nakacho, Musashino-shi, Tokyo (Japan)

(First received April 1st, 1992; revised manuscript received July 28th, 1992)

ABSTRACT

An HPLC method for the determination of carbohydrates using a postcolumn pH adjustment technique with lithium hydroxide solution followed by pulsed amperometric detection was developed. In conjunction with hydrophilic interaction chromatography, the technique was used to determine reducing sugars, non-reducing sugars and sugar alcohols. Detection limits from 0.7 to 2.7 ng with a signal-to-noise ratio of 3 were achieved. The relative standard deviation for peak area was better than 2.7%. The postcolumn pH adjustment technique enabled gradient elution to be used.

INTRODUCTION

A number of chromatographic modes such as borate-complex anion exchange [1], anion exchange [2,3], ligand exchange [4], size exclusion and hydrophilic interaction [5] have been applied to carbohydrates. Hydrophilic interaction chromatography succesfully separates monosaccharides, disaccharides and higher oligosaccharides (DP3–DP10) with isocratic elution. The advantage of this mode is simplicity. Recently, a hydrophilic interaction method using a ligand-exchange column [6] was developed to achieve the separation of different monosaccharides and sugar alcohols simultaneously. Today, hydrophilic interaction chromatography is widely used to separate carbohydrates.

Carbohydrates generally cannot be detected by absorption in the ultraviolet and visible regions and refractive index (RI), absorbance [7,8], fluorescence [9–11] and electrochemical [12,13] detection methods have been used. The RI detector is not sensitive enough to detect amounts < 100 ng. Absorbance and fluorescence detection are highly sensitive, but need precolumn or postcolumn derivatization procedures. Electrochemical detection using pulsed amperometry enables permits the direct detection of sub-nanogram amounts of carbohydrates.

Pulsed amperometric detection (PAD) of carbohydrates was first reported by Hughes and Johnson [14]. Alkaline solutions were used to ionize carbohydrates, which were subsequently detected by pulsed amperometry using a flow-injection system. Pulsed amperometry removed oxidation products from the working electrode.

Rocklin and Pohl [15] applied pulsed amperometry to the HPLC of carbohydrates. In their method, reducing and non-reducing sugars were separated as anions using an ion-exchange column with an alkaline eluent and the eluates were detected with a pulsed amperometric detector. However, PAD has not been used with hydrophilic interaction chromatography of carbohydrates owing to the high concentration of acetonitrile in the mobile phase.

In this study, we developed a method for carbo-

Correspondence to: T. Soga, Analytical Instruments Division, Yokogawa Analytical Systems, 2-11-19 Nakacho, Musashino-shi, Tokyo, Japan.

0021-9673/92/$05.00

hydrate analysis by hydrophilic interaction chromatography with PAD using postcolumn pH adjustment. In addition to using isocratic elution, we performed hydrophilic interaction chromatography with gradient elution.

EXPERIMENTAL

Reagents and chemicals

D-Glucose, D-fructose, sucrose, maltose, D-xylose and xylitol were obtained from Wako (Osaka, Japan) and maltotriose, maltotetraose, maltopentaose, maltohexaose and maltoheptaose from Nacalai Tesque (Kyoto, Japan). HPLC-grade acetonitrile and amino acid analysis-grade lithium hydroxide were obtained from Wako. Deionized, distilled water was used.

HPLC system and conditions

The HPLC system consisted of a Model HP79855A autosampler (Hewlett-Packard, Waldbronn, Germany), a Model HP79852A gradient pump (Hewlett-Packard), a Model LC100T column oven (Yokogawa Analytical Systems, Tokyo, Japan), a Model LC100P reagent pump for pH adjustment (Yokogawa Analytical Systems) and a Model HP1049A electrochemical detector (Hewlett-Packerd).

The column used for isocratic elution was an Asahipak NH2P-50 (particle size 5 μm, 250 mm × 4.6 mm I.D.), (Asahi Chemical Industry, Tokyo, Japan) packed with polyamine-bonded polyvinyl alcohol gel [16]. The mobile phase was acetonitrile–water (75:25,v/v) at a flow-rate of 1.0 ml/min. The reagent solution for postcolumn pH adjustment was 0.6 mol/l lithium hydroxide at a flow-rate 0.8 ml/min. The temperature of the column oven was 40°C.

The column used with gradient elution was an Excelpak CHA-P44 (particle size 6 μm, 150 mm × 6.0 mm I.D.), (Yokogawa Analytical Systems) packed with highly cross-linked sulphonated polystyrene gel (Zn^{2+} form). Mobile phase A was acetonitrile–water (80:20, v/v) and mobile phase B was water, with a linear gradient from 5 to 40% B in 30 min at a flow-rate of 1.0 ml/min. The postcolumn conditions were as same as in isocratic elution. The oven temperature was 70°C.

The eluates from the column were mixed with the reagent solution for pH adjustment. Carbohydrates were ionized in alkaline solution (pH > 13) and introduced into the electrochemical detector. A gold working electrode was used to oxidize the carbohydrates and the potentials used in the electrochemical detector were detection potential E_1 = 0.15 V (T_1 = 30 ms), oxidative cleaning potential E_2 = 0.65 V (T_2 = 15 ms) and reductive cleaning potential E_3 = −0.95 V (T_3 = 20 ms).

RESULTS AND DISCUSSION

Lithium hydroxide, tetra-*n*-butylammonium hydroxide, sodium hydroxide and potassium hydroxide were evaluated as potential pH-adjustment agents in the presence of acetonitrile-containing mobile phases. Tetra-*n*-butylammonium hydroxide is expensive and sodium and potassium hydroxide caused phase separation when mixed with acetonitrile. When lithium hydroxide was used, the peak areas were not affected when either isocratic or gradient elution was performed. To determine the effect of the concentration of acetonitrile in the mobile phase, 10 μg of glucose were applied to an Asahipak NH2P-50 column. The flow-rate of the mobile phase was 1.0 ml/min and 0.4 mol/l lithium hydroxide at a flow-rate of 1.0 ml/min was used as the postcolumn pH agent. Changes in acetonitrile concentration did not significantly affect detection (Fig.1). Therefore, lithium hydroxide was chosen as the alkaline solution for pH adjustment.

The optimum postcolumn conditions required using the lithium hydroxide solution were investigated. The concentration of lithium hydroxide affected the peak responses of carbohydrates. Usu-

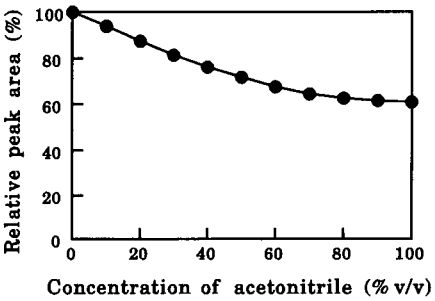

Fig. 1. Dependence of relative peak area of glucose on acetonitrile concentration in water.

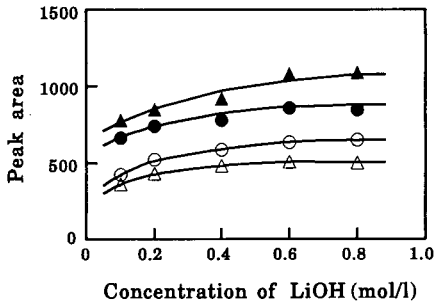

Fig. 2. Effect of concentration of lithium hydroxide on peak areas. ▲ = Fructose; ● = glucose; ○ = sucrose; △ = maltose.

ally, alkali concentrations of 0.1–0.4 mol/l are recommended [15], but we studied higher concentrations of lithium hydroxide. Chromatography was carried out with the Asahipak NH2P-50 column using an acetonitrile–water (75:25, v/v) isocratic mobile phase at a flow-rate of 1.0 ml/min. The flow-rate of lithium hydroxide solution was 0.8 ml/min. Portions of 5 μg each of fructose, glucose, sucrose and maltose were injected. Maximum peak areas were achieved at lithium hydroxide concentrations between 0.6 and 0.8 mol/l (Fig.2). The postcolumn flow-rate also altered the detector response. Lower flow-rates resulted in higher peak areas (Fig.3). However, the baseline noise increased at flow-rates of less than 0.4 ml/min. This was due to the low back-pressure on the postcolumn pump. The optimum flow-rate was 0.6–0.8 ml/min. In this study, a lithium hydroxide concentration of 0.6 mol/ml and a flow-rate of 0.8 ml/min were adopted as the optimum conditions for postcolumn pH adjustment.

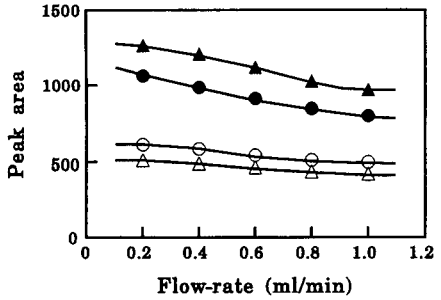

Fig. 3. Effect of postcolumn flow-rate of lithium hydroxide on peak areas. ▲ = Fructose; ● = glucose; ○ = sucrose; △ = maltose.

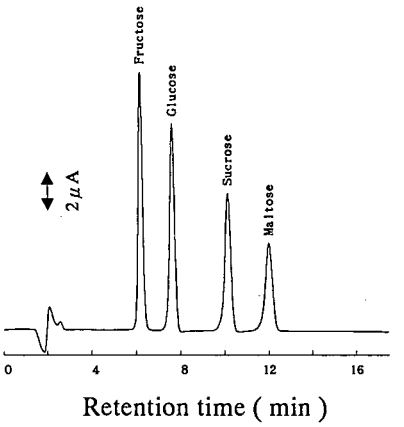

Fig. 4. Chromatography of a standard mixture of carbohydrates on the Asahipak column.

Fig. 4 shows a chromatogram of 1 μg each of fructose, glucose, sucrose and maltose standards. As reported in Table I, satisfactory reproduciblities were obtained, as reflected by the relative standard deviations (R.S.D.). The calibration graphs for all the carbohydrates were linear (40 ng–5 μg). The detection limits for fructose, glucose, sucrose and maltose were 0.9, 0.7, 2.1 and 2.7 ng (Table I), respectively, at a signal-to-noise ratio of 3. The limit of detection of sucrose was comparable to that observed with the reducing sugars.

In hydrophilic interaction chromatography, carbohydrates have generally been detected using RI detectors. However, the RI detector is not as sensitive as the PAD. Another disadvantage of RI detection is that it can only be used with isocratic elution. Chromatography with gradient elution was performed on the Excelpak CHA-P44 column. Mobile

TABLE I

CHARACTERIZATION OF THE DETERMINATION OF CARBOHYDRATES ON THE ASAHIPAK NH2P-50 COLUMN

Compound	R.S.D. ($n=10$) (%)	Correlation γ	Detection limit (ng)
Fructose	1.8	0.999	0.9
Glucose	2.1	1.000	0.7
Sucrose	0.8	0.998	2.1
Maltose	2.7	1.000	2.7

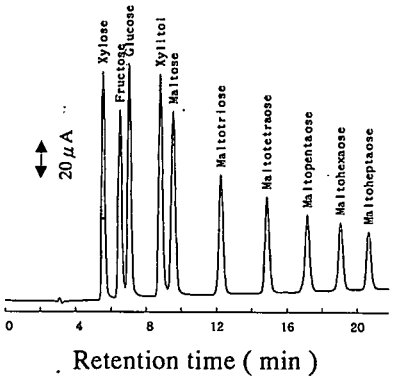

Fig. 5. Chromatography of a standard mixture of carbohydrates using gradient elution.

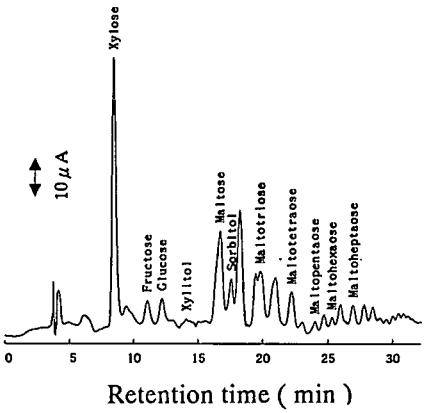

Fig. 6. Chromatography of carbohydrates in beer using gradient elution.

phase A was acetonitrile–water (80:20, v/v) and mobile phase B was water. Monosaccharide and oligosaccharides standards were separated by applying a linear gradient from 5 to 40% mobile phase B in 30 min. Fig. 5 illustrates the separation of the standards analysed with this gradient method. The standard sample contains 5 μg each of xylose, fructose, glucose and xylitol and 10 μg of other carbohydrates. The R.S.D. (n = 5) was better than 0.5% for retention times and 1.1–2.8% for peak areas (Table II). These results indicate that the proposed method can be used with gradient elution in hydrophilic interaction chromatography.

TABLE II

RELATIVE STANDARD DEVIATIONS FOR RETENTION TIMES AND PEAK AREAS OF CARBOHYDRATES AFTER GRADIENT ELUTION

Compound	R.S.D. (%) (n=5)	
	Retention time	Peak area
Xylose	0.27	2.7
Fructose	0.32	2.8
Glucose	0.29	2.5
Xylitol	0.33	2.6
Maltose	0.46	2.8
Maltotriose	0.45	2.6
Maltotetraose	0.37	2.4
Maltopentaose	0.33	2.2
Maltohexaose	0.29	1.1
Maltoheptaose	0.37	2.2

The method was applied to the analysis of beer carbohydrates. Fig. 6 shows a chromatogram of carbohydrates in beer. Glucose to maltoheptaose were well separated in 30 min.

CONCLUSIONS

A sensitive and simple method for the determination of reducing and non-reducing sugars by hydrophilic interaction chromatography has been developed. This HPLC system is based on postcolumn pH adjustment using lithium hydroxide followed by pulsed amperometric detection. It is possible that the method might also be applicable to the determination of alcohols and polyols.

REFERENCES

1 S. Honda, M. Takahashi, K. Kakei and S. Ganno, *Anal. Biochem.*, 113 (1981) 130.
2 E. Martinsson and O. Samuelson, *J. Chromatogr.*, 50 (1970) 429.
3 J. S. Hobbs and J. G. Lawrence, *J. Chromatogr.*, 72 (1972) 311.
4 R. W. Goulding, *J. Chromatogr.*, 103 (1975) 229.
5 R. T. Yang, L. P. Milligan and G. W. Mathison, *J. Chromatogr.*, 209 (1981) 316.
6 S. Honda, S. Suzuki and K. Kakei, *J. Chromatogr.*, 291 (1984) 317.
7 W. Voelter and H. Bauer, *J. Chromatogr.*, 126 (1976) 693.
8 K. Mopper, *Anal. Biochem.*, 85 (1978) 528.
9 H. Mikami and Y. Ishida, *Bunseki Kagaku*, 32 (1983) E207.

10 S. Honda, Y. Matsuda, M. Takahashi, K. Kakei and S. Ganno, *Anal. Chem.*, 52 (1980) 1079.
11 H. Takemoto, S. Hase and T. Ikenaka, *Anal. Biochem.*, 145 (1985) 245.
12 Y. Takata and G. Muto, *Anal. Chem.*, 45 (1973) 1864.
13 N. Watanabe and M. Inoue, *Anal. Chem.*, 55 (1983) 1016.
14 S. Hughes and D. C. Johnson, *Anal. Chim. Acta*, 132 (1981) 11.
15 R. D. Rocklin and C. A. Pohl, *J. Liq. Chromatogr.*, 6 (1983) 1577.
16 N. Hirata, Y. Tamura, M. Kasai, Y. Yanagihara and K. Noguchi, *J. Chromatogr.*, 592 (1992) 93.

Journal of Chromatography, 625 (1992) 157–161
Elsevier Science Publishers B.V., Amsterdam

CHROM. 24 536

Determination of the impurity profile of γ-cyclodextrin by high-performance liquid chromatography

Gregory White*, Thomas Katona, Julius P. Zodda and Michael N. Eakins

Bristol-Myers Squibb Pharmaceutical Research Institute, One Squibb Drive, P.O. Box 191, New Brunswick, NJ 08903-0191 (USA)

(First received February 6th, 1992; revised manuscript received June 15th, 1992)

ABSTRACT

High-performance liquid chromatography (HPLC) was used to determine the impurity profile of γ-cyclodextrin (γ-CD), a compound used as a stabilizer in pharmaceutical formulations. An HPLC assay was developed which separated γ-CD from potential impurities which included 7 linear (glucose to maltoheptaose) and 2 unbranched cyclic (α- and β-CD) glucose polymers. The method employed a mobile phase consisting of acetonitrile–water (73:27), a Whatman 5-μm Partisil PAC column (250 × 4.6 mm I.D.), refractive index detection, and achieved a resolution (R_s) ⩾ 1.5 for all impurities in the presence of γ-CD.The method presented provided improvements over existing methods by achieving a rapid separation (<25 min) of compounds not previously reported using moderate temperature control and quantitated impurities at the 0.1–1.2% (w/w) level of sensitivity.

INTRODUCTION

γ-Cyclodextrin (γ-CD), a cyclic octamer of D-glucose with α-(1,4)-linkages, is a water soluble compound which can form reversible complexes with poorly water soluble molecules resulting in soluble molecular inclusion complexes. This "host–guest" relationship can substantially increase the aqueous solubility of many pharmaceuticals [1–3], and act as a stabilizer by reducing rates of oxidation, decomposition, disproportionation, polymerization, and autocatalytic reactions [4]. CardioTec, a kit for the preparation of the radiopharmaceutical myocardial imaging agent Tc^{99m} teboroxime, contains γ-CD to improve the stability of the formulation. It was necessary to establish the impurity profile of γ-CD to monitor both the quality and the manufacturer to manufacturer equivalence of the material.

Commercially, γ-CD is produced from the enzymatic digestion of starch. The γ-CD is selectively purified from the crude digest containing linear glucose polymers, α- (cyclic hexamer), β- (cyclic heptamer), γ- and higher cyclodextrins [5]. An analytical method was needed to determine the level of potential linear and unbranched cyclic polymeric glucose impurities in γ-CD. Chemical structures for γ-CD and some potential impurities are shown in Fig. 1.

Various high-performance liquid chromatographic (HPLC) methods have been applied for carbohydrate analysis using such columns as μBondapak-carbohydrate [6–9], aminopropyl-bonded [10–12], aminocyano-bonded [13], specialized C_8 and C_{18} [14–18], silica [19,33], and ion exchange columns [20–32], with some investigators using a mobile phase amine modifier to affect separation [8,19,33]. Several means of detection have been employed including refractive index [6–16,19,24,30,34], pulsed amperometric [17,32], and indirect UV–vis detection with micro HPLC [18]. Koizumi *et al.* [34] compared four different amino bonded columns to successfully separate some, but not all, of the components addressed in this study, and needed highly elevated temperatures (75°C) to eliminate anomeric peak

Correspondence to: Gregory White, Bristol-Myers Squibb Pharmaceutical Research Institute, One Squibb Drive, Building 80, Room 43, P.O. Box 191, New Brunswick, NJ 08903-0191, USA.

0021-9673/92/$05.00

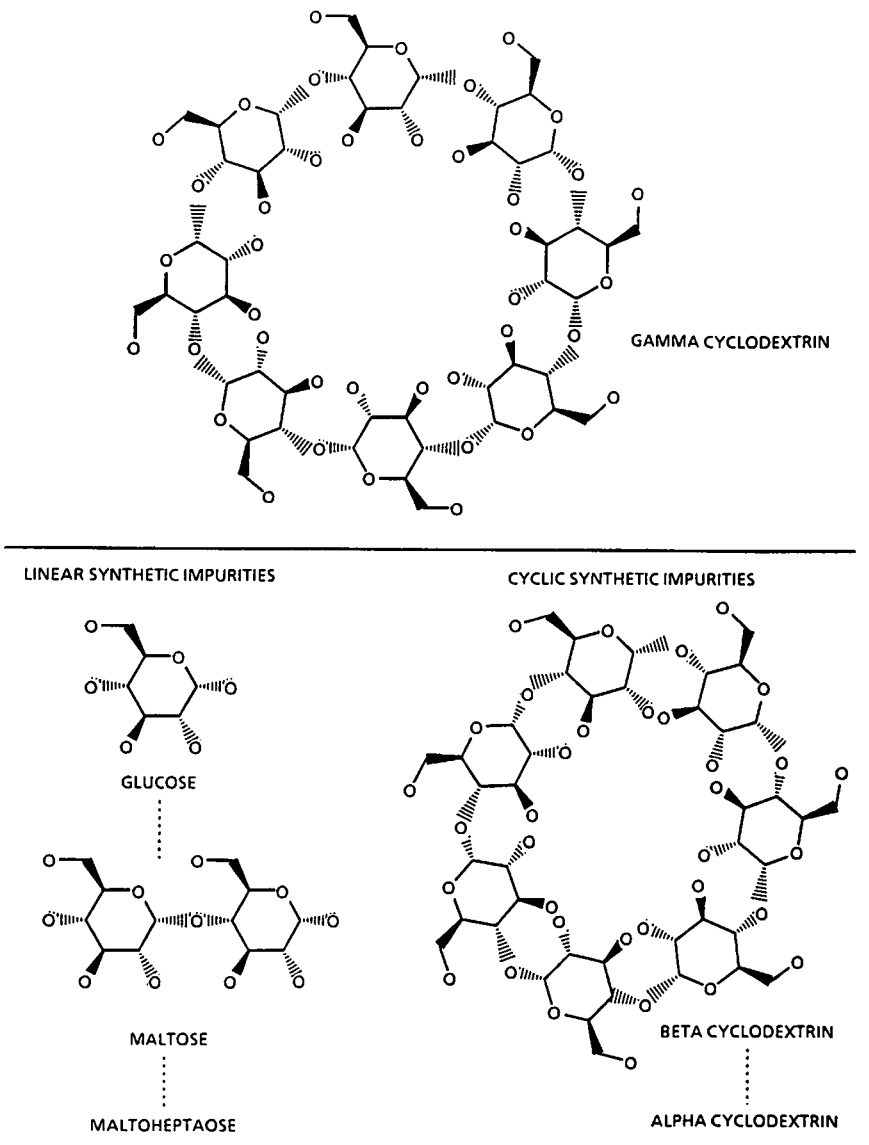

Fig. 1. Structures for γ-CD and some potential synthetic pathway impurities.

splitting on one of the columns. Rabel *et al.* [13] contended that the mode of separation for carbohydrates using polar bonded phases such as Partisil PAC is normal-phase partition chromatography since retention times are decreased by increasing the water content of the mobile phase. Historically, the most useful polar bonded phases for normal-phase separations have been ether, cyano, and amino [13]. Partisil PAC, consisting of alkyl groups containing amino-cyano groups, provides a combination of these features and was chosen as the optimal material for our analysis.

This paper details the separation of 7 linear (glucose to maltoheptaose) and 3 unbranched cyclic (α-, β- and γ-CD) glucose polymers in less than 25 min at 45°C and reports limits of detection, response factors and quantitative impurity results obtained utilizing refractive index detection.

EXPERIMENTAL

Materials

γ-CD was obtained from Advanced Separation Technologies, Astec (Whippany, NJ, USA), American Maize-Products Company, Amaizo (Hammond, IN, USA) and Fluka Chemika-BioChemika (Buchs, Switzerland). α- and β-CD and linear glucose polymers were obtained from Fluka, and Sigma Chemical Company (St. Louis, MO, USA). The acetonitrile was HPLC grade from Baxter Scientific Products (McGaw Park, IL, USA). The water was HPLC/organic free from the NANOpure II system from SYBRON/Barnstead (Boston, MA, USA).

The HPLC/data collection system consisted of a Spectra-Physics Model 4270 integrator, Model 8800 pump, and Model 8780 autosampler with a 10-μl (nominal) fixed loop injector all on Spectra-Physics LABNET from Spectra-Physics (Piscataway, NJ, USA), a Fiatron Model CH-30 column heater from Rainin Instrument (Woburn, MA, USA), and a Hewlett-Packard Model 1047A refractive index detector from Hewlett-Packard (Piscataway, NJ, USA) maintained at 45°C. A Whatman Partisil 5 PAC, 5 μm, 250 mm × 4.6 mm I.D. column from Baxter maintained at 45°C was used with a mobile phase consisting of acetonitrile–water (73:27) pumped at a flow-rate of 1.0 ml/min.

Methods

Prior to use, the column was conditioned by pumping mobile phase at 1.0 ml/min for 24 h. A solution containing 1 mg/ml each of γ-CD and maltohexaose in warm (50°C) acetonitrile–water (60:40) was injected for system suitability. The resolution, $R_s = 2(t_2 - t_1)/(W_1 + W_2)$, between the peaks should be ≥ 1.5.

For impurity determination, stock sample solutions (100 mg/ml) were prepared in warm (50°C) water. Working sample solutions (40 mg/ml) were prepared in warm (50°C) acetonitrile–water (60:40) and injected as soon as possible to prevent precipitation.

Samples were injected in duplicate and the % impurity index was calculated on an area % basis.

RESULTS AND DISCUSSION

A chromatogram of an injection of γ-CD and nine possible impurities (5 mg/ml) produced baseline resolution of all the components, $R_s \geq 1.5$ (Fig. 2). The resolution between γ-CD and maltohexaose, the closest eluting component, was 2.2. This separation represents a notable improvement over a comparable separation reported by Koizumi *et al.* [34], wherein resolution between γ-CD, maltopentaose, maltohexaose and α- and β-CD was inadequate or unreported. Relative response factors, limits of detection ($S/N = 2$), and retention times are given in Table I. Relative response factors were equivalent and limits of detection were ≤0.3 (% w/w) for the α-, β- and γ-CD. However, the response factors for the linear glucose polymers increased with increasing retention time and limits of detection were the most sensitive for the fast eluting, sharp peaks (*i.e.*, glucose, maltose) and were least sensitive for the

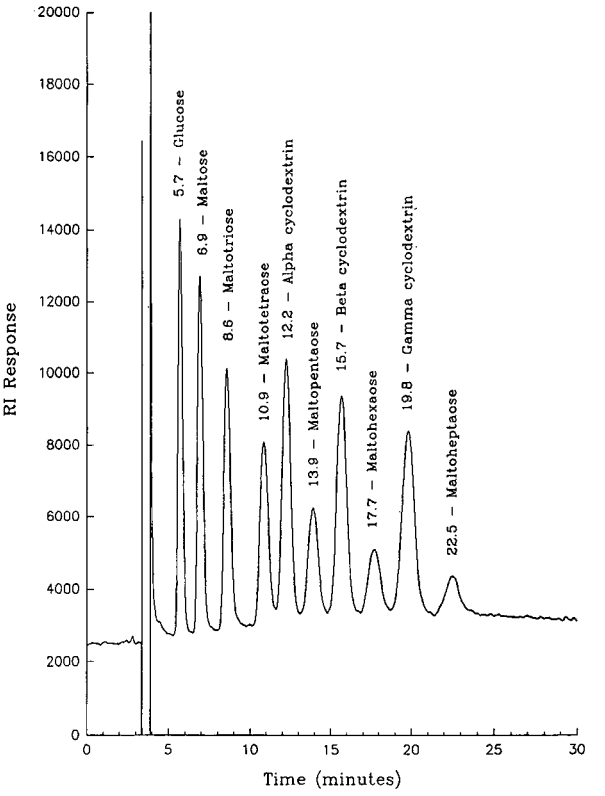

Fig. 2. Chromatogram of γ-CD and nine potential synthetic pathway impurities (10.0 μl injection containing 5 mg/ml each) using a Partisil PAC column (45°C), acetonitrile–water (73:27) at 1.0 ml/min, and refractive index detection (45°C).

TABLE I

HPLC REFRACTIVE INDEX DETECTION PARAMETERS FOR γ-CD AND IMPURITIES

Compound	Relative response factor[a]	Detectable weight on column (μg)[b]	Limit of detection (% w/w)[c]	Retention time (min)
Glucose	1.30	0.3	0.1	5.7
Maltose	1.35	0.6	0.2	6.9
Maltotriose	1.39	1.2	0.3	8.6
Maltotetraose	1.62	1.3	0.3	10.9
α-CD	1.00	0.6	0.2	12.2
Maltopentaose	1.87	2.5	0.6	13.9
β-CD	1.03	1.3	0.3	15.7
Maltohexaose	2.28	4.9	1.2	17.7
γ-CD	1.00	1.3	0.3	19.8
Maltoheptaose	2.97	4.8	1.2	22.5

[a] Relative to γ-CD as (compound concentration/compound area)/(γ-CD concentration/γ-CD area).
[b] When signal-to-noise ratio equals 2 ($S/N = 2$).
[c] Relative to maximum injectable amount of 400 μg γ-CD on the column.

long eluting, broad peaks (*i.e.*, maltohexaose, maltoheptaose). Although refractive index detection lacks the sensitivity of techniques such as pulsed amperometric detection [32], the level of sensitivity was sufficient (0.1–1.2% w/w) to provide a satisfactory impurity profile of the nine potential components of interest.

TABLE II

POTENCY AND IMPURITY INDEX RESULTS FROM TWO MANUFACTURERS OF γ-CD

Sample number	Manufacturer	Potency (% anhy.)	Impurity index (%)	Impurities found
1	I	100.0	0.00	None
2	I	99.4	0.00	None
3	II	101.0	0.00	None
4	II	–	0.65	α-, β-CD
5	II	97.8	0.00	None
6	II	98.6	0.52	α-, β-CD
7	II	99.6	0.00	None
8	II	102.0	0.00	None
9	I	100.1	0.00	None
10	II	101.1	0.00	None

To show applicability of the method, multiple samples of γ-CD raw material from two manufacturers (I and II) were assayed for total impurity index (Table II). Of 10 lots assayed, none showed any of the linear glucose impurities; however, two lots contained small amounts (< 1% w/w) of α- and β-CD impurities. The practical application of the method is graphically displayed in Fig. 3, showing overlaid chromatograms of γ-CD raw materials containing (A) α- and β-CD impurities at a level (0.65% impurity index) near the detection limit and (B) no impurities. In addition, the method was utilized to determine the potency of the 10 lots of γ-CD (Table II).

The sensitivity and accuracy of the method was demonstrated using α-CD (relative response factor = 1) as a model impurity. A 102% recovery of

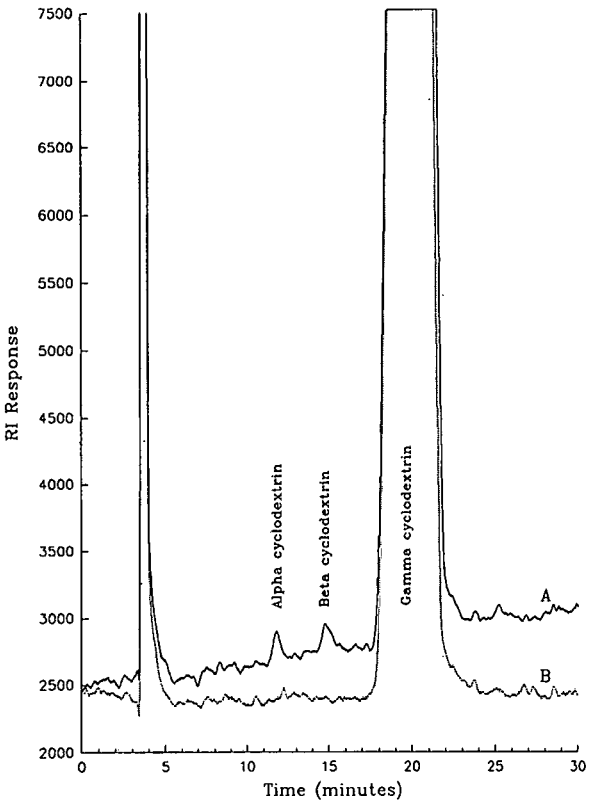

Fig. 3. Chromatograms of γ-CD raw materials containing (A) α- and β-CD impurities (at 0.65% impurity index) and (B) no impurities, using Partisil PAC column (45°C), acetonitrile–water (73:27) at 1.0 ml/min, and refractive index detection (45°C).

α-CD was obtained when γ-CD was spiked with 1% (w/w) α-CD.

The highest concentration of γ-CD in acetonitrile–water (60:40) injected was 40 mg/ml. Higher concentrations produced solubility problems. Acetonitrile–water (60:40) was chosen as an intermediate solvent between water and the mobile phase [acetonitrile–water (73:27)]. The injection solution, column, and detector were maintained at 45–50°C to enhance and stabilize the chromatography as well as to maintain the solubility of γ-CD. The optimized chromatographic conditions utilizing moderate temperature control and a mobile phase of high organic/aqueous ratio (≈3:1) produced Gaussian shaped peaks and eliminated anomeric peak splitting, a concern with other methods [34].

Ruggedness testing indicated that after approximately 250 injections were made on the column over a period of 16 days, column performance was reduced. The use of a short water rinse time (10 min) for column clean-up is recommended to eliminate possible column voids or channeling due to dissolution of silica. The use of a silica saturator column may also be employed.

In conclusion, this HPLC method provides a profile of 7 linear (glucose through maltoheptaose) and 2 unbranched cyclic (α- and β-CD) glucose polymer impurities in the presence of γ-CD. The method is rapid (< 25 min) and sensitive for quantitating impurities at the 0.1–1.2% (w/w) level, and is also suitable for use as a raw material potency assay due to its ability to eliminate potential impurity interferences. In addition, the method potentially can be used to monitor the quality of γ-CD used as a mobile phase additive for chiral separations.

ACKNOWLEDGEMENTS

The author thanks Dr. Joel Kirschbaum for his helpful comments, Karen Skupeika for her help with the structural figure and is grateful to the Bristol-Myers Squibb Library and Literature services for their assistance.

REFERENCES

1 M. E. Brewster, J. W. Simpkins, M. S. Hora, W. C. Stern and N. Bodor, *J. Parenter. Sci. Technol.*, 43 (1989) 231.
2 M. L. Bender and M. Komiyama, *Cyclodextrin Chemistry*, Springer-Verlag, Berlin, Heidelberg, New York, 1978.
3 W. Saenger, *Angew. Chem. Int. Ed. Engl.*, 19 (1980) 344.
4 J. Szejtli, *Pharm. Technol.*, 15(6) (1991) 36.
5 T. Beesley, *Advanced Separation Technologies*, Whippany, NJ, personal communication, April 4, 1990.
6 J. C. Linden and C. L. Lawhead, *J. Chromatogr.*, 105 (1975) 125.
7 K. Kainuma, T. Nakakuki and T. Ogawa, *J. Chromatogr.*, 212 (1981) 126.
8 L. A. Th. Verhaar and B. F. M. Kuster, *J. Chromatogr.*, 234 (1982) 57.
9 R. B. Meagher and A. Furst, *J. Chromatogr.*, 117 (1976) 211.
10 R. Schwarzenbach, *J. Chromatogr.*, 117 (1976) 206.
11 V. Kahle and K. Tesařík, *J. Chromatogr.*, 191 (1980) 121.
12 A. D. Jones, I. W. Burns, S. G. Sellings and J. A. Cox, *J. Chromatogr.*, 144 (1977) 169.
13 F. M. Rabel, A. G. Caputo and E. T. Butts, *J. Chromatogr.*, 126 (1976) 731.
14 P. Vrátný, J. Čoupek, S. Vozka and Z. Hostomská, *J. Chromatogr.*, 254 (1983) 143.
15 L. A. Th. Verhaar, B. F. M. Kuster and H. A. Claessens, *J. Chromatogr.*, 284 (1984) 1.
16 N. W. H. Cheetham and P. Sirimanne, *J. Chromatogr.*, 207 (1981) 439.
17 J. Haginaka, Y. Nishimura, J. Wakai, H. Yasuda, K. Koizumi and T. Nomura, *Anal. Biochem.*, 179 (1989) 336.
18 T. Takeuchi, M. Murayama and D. Ishii, *J. Chromatogr.*, 477 (1989) 147.
19 K. Aitzetmüller, *J. Chromatogr.*, 156 (1978) 354.
20 H. D. Scobell, K. M. Brobst and E. M. Steele, *Cereal Chem.*, 54 (1977) 905.
21 M. R. Ladisch, A. L. Huebner and G. T. Tsao, *J. Chromatogr.*, 147 (1978) 185.
22 L. E. Fitt, W. Hassler and D. E. Just, *J. Chromatogr.*, 187 (1980) 381.
23 H. D. Scobell and K. M. Brobst, *J. Chromatogr.*, 212 (1981) 51.
24 J. Bouchard, E. Chornet and R. P. Overend, *J. Agric. Food Chem.*, 36 (1988) 1188.
25 R. Oshima, N. Takai and J. Kumanotani, *J. Chromatogr.*, 192 (1980) 452.
26 J. Havlicek and O. Samuelson, *Carbohydr. Res.*, 22 (1972) 307.
27 O. Samuelson and J. Havlicek, *Anal. Chem.*, 47 (1975) 1854.
28 R. B. Kesler, *Anal. Chem.*, 39 (1967) 1417.
29 Z. Hostomská-Chytilová, O. Mikeš, P. Vrátný and M. Smrž, *J. Chromatogr.*, 235 (1982) 229.
30 L. A. Th. Verhaar and B. F. M. Kuster, *J. Chromatogr.*, 210 (1981) 279.
31 P. Jandera and J. Churáček, *J. Chromatogr.*, 98 (1974) 55.
32 K. Koizumi, Y. Kubota, T. Tanimoto and Y. Okada, *J. Chromatogr.*, 454 (1988) 303.
33 B. B. Wheals and P. C. White, *J. Chromatogr.*, 176 (1979) 421.
34 K. Koizumi, T. Utamura and Y. Kubota, *J. Chromatogr.*, 409 (1987) 396.

Journal of Chromatography, 625 (1992) 163–168
Elsevier Science Publishers B.V., Amsterdam

CHROM. 24 414

Effect of temperature on chiral and achiral separations of diacylglycerol derivatives by high-performance liquid chromatography on a chiral stationary phase

Toru Takagi and Toshiyuki Suzuki

Department of Chemistry, Faculty of Fisheries, Hokkaido University, Hakodate 041 (Japan)

(First received April 8th, 1992; revised manuscript received June 3rd, 1992)

ABSTRACT

Enantiomer separation of 1,2-diacyl-*rac*-glycerols (1,2-*rac*-DGs) as their 3,5-dinitrophenylurethane derivatives by high-performance liquid chromatography was carried out on a Sumichiral OA-4100 column. The separation of 1,2-DG enantiomers was improved by lowering the temperature. Linear relationships were found between the logarithm of the separation factor and the reciprocal of absolute temperature. Using thermodynamic concepts, detailed considerations are presented for the enantiomer separation and separation of molecular species differing in carbon number or olefinic bond number. Separation by carbon number is controlled by entropy differences, whereas separation by double bond number is based on enthalpy contributions.

INTRODUCTION

Recently, we reported the direct enantiomer separation of 1,2-diacylglycerols (1,2-DGs) as their 3,5-dinitrophenylurethane (3,5-DNPU) derivatives by high-performance liquid chromatography (HPLC) on the chiral stationary phases (CSPs) Sumichiral OA-2100 and OA-4100 [1–3]. The structures of the 1,2-DG 3,5-DNPU derivatives and OA-4100 stationary phase are shown in Fig. 1. The separation of enantiomers by HPLC using CSPs is based on the formation of transient diastereomeric complexes between the enantiomorphs of the solute and a chiral selector of the CSP. Typically defined chemical structures, such as π-acidic or π-basic aromatic groups and polar hydrogen bond donors/acceptors, near the chiral center, participate in the multiple attractive interactions.

All HPLC separations of 1,2-DG 3,5-DNPUs reported previously were carried out at ambient temperature. In this study, enantiomer separation was significantly improved by operating at low temperature. The selectivity, α, is related to temperature (T) and free energy difference ($\Delta\Delta G^\circ$) between analytes: $\ln \alpha = -\Delta\Delta G^\circ/RT$. Variations of the equation give the enthalpy ($\Delta\Delta H^\circ$) and entropy ($\Delta\Delta S^\circ$) differences. These values are obtained by plotting

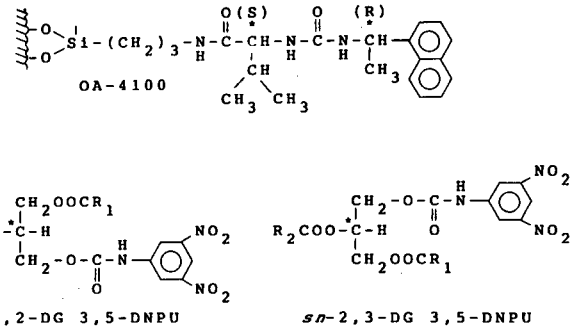

Fig. 1. Structures of Sumichiral OA-4100 stationary phase and enantiomers of 1,2-DG 3,5-DNPU derivatives.

Correspondence to: Dr. Toru Takagi, Department of Chemistry, Faculty of Fisheries, Hokkaido University, Hakodate 041, Japan.

0021-9673/92/$05.00

ln α *vs.* $1/T$. This approach has been applied to understanding chiral recognition [4,5].

In addition to chiral separations, the CSP used in this study provides achiral separations based on the number of carbon atoms and the total number of double bonds in the two constituent fatty acids. In spite of the intensive efforts that have been devoted to the study of chiral recognition on CSPs, achiral recogniton on CSPs has hardly been considered. We now present detailed thermodynamic considerations of DG enantiomer separations and achiral separations of DG molecular species differing in the number of acyl carbons and olefinic bonds.

EXPERIMENTAL

Samples

Enantiomers of 1,2- and 2,3-*sn*-DGs were synthesized by the method of Howe and Malkin [6]. DG racemates were obtained by inter-esterification of fatty acid methyl esters with glycerol in dimethylformamide medium at 90°C. The separation of 1,2-*rac*-DGs was carried out by thin-layer chromatography (TLC) on silica gel G impregnated with boric acid, using hexane–diethyl ether (60:40, v/v) and chloroform–acetone (96:4, v/v) as developing solvents. Conversion of 1,2-*rac*-DGs into 3,5-DNPU derivatives was carried out as described in previous papers [7,8].

HPLC

HPLC separation was carried out with a Hitachi (Tokyo, Japan) L-6200 instrument equipped with a Sumichiral OA-4100 chiral column (stainless steel, 50 cm × 4 mm I.D.) using hexane–1,2-dichloroethane–ethanol as the eluent at a constant flow-rate. Peaks were monitored with a Shimadzu (Kyoto, Japan) SPD-6A UV detector at 254 nm. A Hitachi Model 638-0805 recycle valve was used for recycling. The column temperature was maintained by dipping in an ethanol bath, which was cooled by an immersion cooler (Tokyo Rika, Tokyo, Japan) to within about 1.0°C with an exclusive controller.

Definitions

The structures of the fatty acids considered are expressed as follows: 16:0 = $CH_3(CH_2)_{14}COOH$; 18:0 = $CH_3(CH_2)_{16}COOH$; 20:0 = $CH_3(CH_2)_{18}COOH$; 22:0 = $CH_3(CH_2)_{20}COOH$; 18:1 = $CH_3(CH_2)_7CH = CH(CH_2)_7COOH$; 18:2 = $CH_3(CH_2)_4CH=CHCH_2CH=CH(CH_2)_7COOH$; and 18:3 = $CH_3CH_2CH = CHCH_2CH = CHCH_2CH = CH(CH_2)_7COOH$.

RESULTS AND DISCUSSION

Fig. 2 shows the HPLC separation of a saturated 1,2-*rac*-DG homologue mixture containing four acyl groups (16:0–18:0–20:0–22:0) as their 3,5-DNPU derivatives on Sumichiral OA-4100. In a previous study, we reported the separation of ten saturated enantiomers containing three acyl groups (16:0–18:0–20:0) [3]. In this study, complete separation of fourteen enantiomers was achieved at low temperature (Fig. 2B). These fourteen enamtiomer

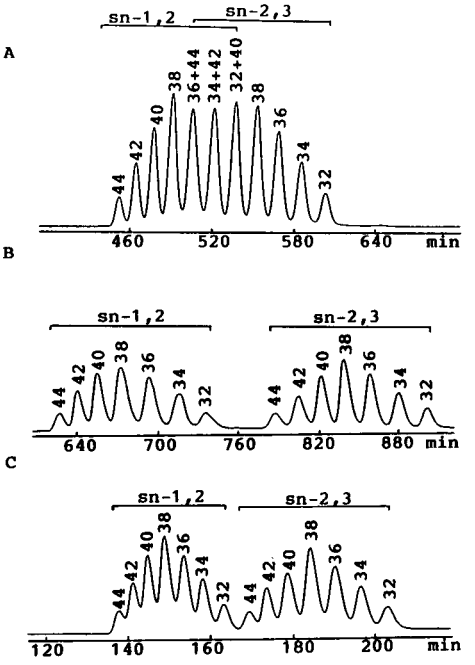

Fig. 2. Separation of saturated DG enantiomers as 3,5-DNPU derivatives on an OA-4100 chiral column. Temperature: (A) 19.5; (B) −23.0; (C) −20.0°C. Mobile phase: hexane–1.2-dichloroethane–ethanol, (A) and (B) 170:10:1 (v/v/v) and (C) 150:20:1 (v/v/v). Flow-rate: (A) and (B) 0.25 and (C) 0.5 ml/min. Peaks were monitored at 254 nm after the first recycle. Above each peak is given the acyl carbon number of the DG. 32 = C_{16} + C_{16}; 34 = C_{16} + C_{18}, C_{18} + C_{16}; 36 = C_{18} + C_{18}, C_{16} + C_{20}, C_{20} + C_{16}; 38 = C_{16} + C_{22}, C_{22} + C_{16}, C_{18} + C_{20}, C_{20} + C_{18}; 40 = C_{18} + C_{22}, C_{22} + C_{18}, C_{20} + C_{20}; 42 = C_{20} + C_{22}, C_{22} + C_{20}; 44 = C_{22} + C_{22}.

peaks were not separated at ambient temperature (Fig. 2A).

The separation factors (α) and peak resolutions (R_s) between 1,2- and 2,3-enantiomers increased from 1.13–1.14 to 1.24–1.28 and from 4.33–5.07 to 9.64–11.13, respectively, on lowering the temperature (Fig. 2A and B). On the other hand, the values of α and R_s for homologues differing by two acyl carbons were independent of temperature (Fig. 2A, α = 1.03, R_s 1.12–1.38; Fig. 1B, α = 1.02–1.03, R_s = 1.01–1.38). To obtain a rapid separation, the HPLC condition was changed (Fig. 2C). All the racemic DGs were separated into fourteen enantiomers within 220 min at −20°C.

Fig. 3 shows separation of 1,2-*rac*-DGs prepared from 18:0 and 18:1 acids. Better enantiomer resolution was obtained at low temperature. In contrast to the separation of homologues differing by two carbons, the α and R_s values obtained in the separation of DG molecular species differing by one double bond increased slightly at low temperature (Fig. 3A, α = 1.03–1.04, R_s = 0.95–1.19; Fig. 3B, α = 1.04–1.05, R_s = 1.11–1.45).

Fig. 4 shows a plot of ln α *vs.* $1/T$ for 1,2-di-18:0-*rac*-DG enantiomers. A similar linear relationship

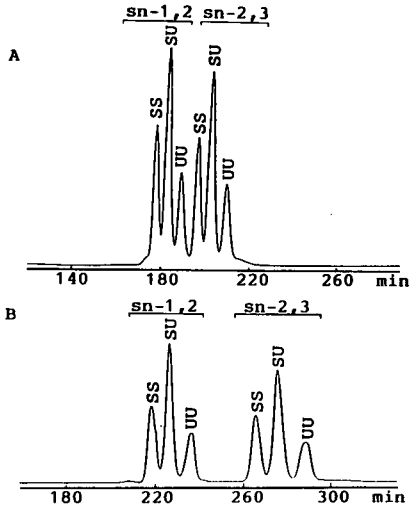

Fig. 3. Separation of DG enantiomers prepared from 18:0 and 18:1 acids as 3,5-DNPU derivatives on an OA-4100 chiral column. Temperature: (A) 27.0 and (B) −10.5°C. Mobile phase: hexane–1,2-dichloroethane–ethanol (170:10:1, v/v/v) at a flow-rate of 0.25 ml/min. SS = di-18:0-DG; SU = 18:0–18:1-DG; UU = di-18:1-DG. Peaks were monitored at 254 nm.

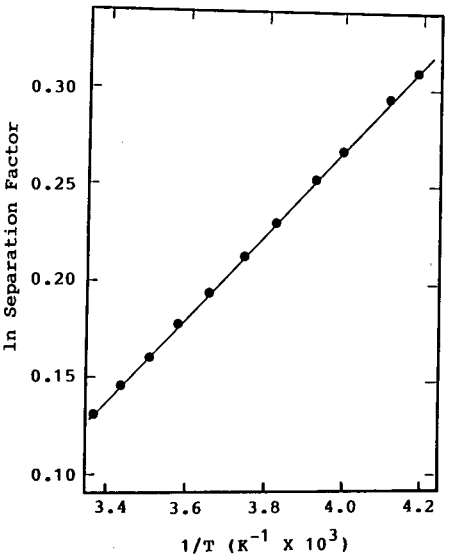

Fig. 4. Plot of ln α *vs.* $1/T$ for 1,2-di-18:0-*rac*-DG enantiomers.

was also obtained for enantiomers of various DG molecular species. This linear relationship is explained by the following well known thermodynamic equation [9]:

$$\ln \alpha = -\Delta\Delta G^\circ/RT \quad (1)$$

where $\Delta\Delta G^\circ$ is the free energy difference between the analytes and R is gas constant. Eqn. 1 and also be expressed application of the Gibbs–Helmholtz equation, $G = H - TS$, as follows:

$$\ln \alpha = -\Delta\Delta H^\circ/RT + \Delta\Delta S^\circ/R \quad (2)$$

Thus, the differences in enthalpy ($\Delta\Delta H^\circ$) and entropy ($\Delta\Delta S^\circ$) between the analytes were calculated from the slope and intercept of the line with the vertical axis.

Thermodynamic data obtained for enantiomers of various DG molecular species are given in Table I. Although the CSP gives almost the same enantioselectivity for these DGs at 25°C, the values of $\Delta\Delta H^\circ$ and $\Delta\Delta S^\circ$ increased slightly with increase in degree of unsaturation. Introduction of a *cis* double bond gives various conformations to the acyl chain [10], and the acyl conformation may produce slight differences in $\Delta\Delta H^\circ$ and $\Delta\Delta S^\circ$ on enantiomer separation.

The CSP used in this study has a polar functional

TABLE I

ENTHALPY AND ENTROPY DIFFERENCES OBTAINED IN ENANTIOMER SEPARATIONS

Mobile phase: hexane–1,2-dichloroethane–ethanol (170:10:1, v/v/v) at a flow-rate of 0.25 ml/min.

Molecular species *sn*-2,3/*sn*-1,2	α (25°)	$\Delta\Delta G°$ (25°C) (cal/mol)	$\Delta\Delta H°$ (cal/mol)	$\Delta\Delta S°$ (cal/mol · K · 0.1)
18:0–18:0	1.13	−70.39	−396.98	−10.96
18:0–18:1	1.13	−70.43	−414.92	−11.56
18:0–18:2	1.12	−68.24	−418.69	−11.76
18:0–18:3	1.12	−68.00	−428.53	−12.10
18:1–18:1	1.13	−71.56	−407.36	−11.27
18:2–18:2	1.13	−69.86	−430.17	−12.09
18:3–18:3	1.12	−68.92	−428.53	−12.07

group, N-(*R*)-1-(α-naphthyl)ethylaminocarbonyl-(*S*)-valine chemically bonded to silanized silica. This functional group provides separations according to both carbon number and degree of unsaturation. DG molecular species elute from the CSP in order of decreasing carbon number and increasing number of double bonds (Figs. 2 and 3). In this study, the temperature dependences of α on carbon number and double bond number differences were also determined. The effect of temperature on these achiral separations was extremely slight. Hence changing the temperature is not a practical means of improving the achiral separations, but out of interest we observed the temperature dependence of α.

Table II shows the thermodynamic parameters obtained in the achiral separations. The values of $\Delta\Delta H°$ based on carbon number difference were much smaller than those based on double bond difference. This indicates that separation according to carbon number is nearly independent of temperature, whereas that according to the number of double bonds is dependent on temperature.

The values of $\Delta\Delta G°$ and $\Delta\Delta H°$ were plotted against the differences in carbon number and degree of unsaturation (Figs. 5 and 6, respectively). Al-

TABLE II

ENTHALPY AND ENTROPY DIFFERENCES OBTAINED IN SEPARATIONS BASED ON CARBON NUMBER AND DOUBLE BOND NUMBER

Mobile phase: hexane–1,2-dichloroethane–ethanol (170:10:1, v/v/v) at a flow-rate of 0.25 ml/min.

Molecular species *sn*-2,3	α (25°C)	$\Delta\Delta G°$ (25°C) (cal/mol)	$\Delta\Delta H°$ (cal/mol)	$\Delta\Delta S°$ (cal/mol · K · 0.01)
20:0–18:0/20:0–20:0	1.03	−18.23	9.55	9.32
18:0–18:0/20:0–20:0	1.06	−36.44	2.98	13.23
18:0–16:0/20:0–20:0	1.10	−56.44	5.39	20.75
16:0–16:0/20:0–20:0	1.14	−78.20	5.52	28.09
18:0–18:1/18:0–18:0	1.03	−19.96	−34.87	−5.01
18:0–18:2/18:0–18:0	1.09	−52.13	−64.22	−4.06
18:1–18:1/18:0–18:0	1.08	−43.11	−73.57	−10.22
18:0–18:3/18:0–18:0	1.15	−82.60	−116.91	−11.52
18:2–18:2/18:0–18:0	1.20	−110.23	−155.88	−15.32
18:3–18:3/18:0–18:0	1.34	−173.85	−251.25	−25.97

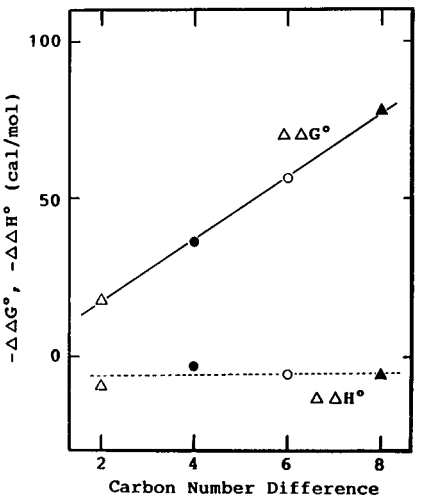

Fig. 5. Plots of $\Delta\Delta G°$ and $\Delta\Delta H°$ *vs.* difference in acyl carbon number between DG molecular species. △ = 20:0–18:0-DG/di-20:0-DG; ● = di-18:0-DG/di-20:0-DG; ○ = 18:0–16:0-DG/di-20:0-DG; ▲ = di-16:0-DG/di-20:0-DG.

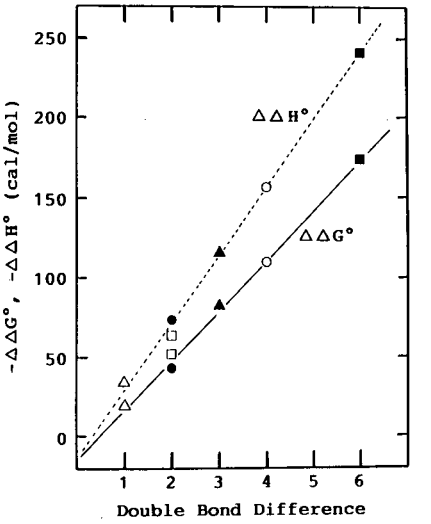

Fig. 6. Plots of $\Delta\Delta G°$ and $\Delta\Delta H°$ *vs.* difference in number of double bonds between DG molecular species. △ = 18:0–18:1-DG/di-18:0-DG; ● = di-18:1-DG/di-18:0-DG; □ = 18:0–18:2-DG/di-18:0-DG; ▲ = 18:0–18:3-DG/di-18:0-DG; ○ = di-18:2-DG/di-18:0-DG; ■ = di-18:3-DG/di-18:0-DG.

though $\Delta\Delta G°$ increased with increase in carbon number difference, the $\Delta\Delta H°$ values were nearly constant (Fig. 5). This indicates that the contribution of $\Delta\Delta H°$ to the separation according to the carbon number is relatively unimportant, and the separation is controlled by $\Delta\Delta S°$ based on shape selectivity. In contrast, separation according to the number of double bonds is controlled by $\Delta\Delta H°$ (Fig. 6), and here the contribution of $\Delta\Delta S°$ is cancelled by the large value of $\Delta\Delta H°$. The increase in $\Delta\Delta H°$ with increase in the difference in double bond number suggests a binding interaction between the CSP and double bonds, and the binding interaction is responsible for the separation according to degree of unsaturation on this CSP.

TABLE III

ENTHALPY AND ENTROPY DIFFERENCES OBTAINED IN SEPARATIONS BASED ON CARBON NUMBER AND DOUBLE BOND NUMBER

Mobile phase: hexane–1,2-dichlorethane–ethanol (170:10:1, v/v/v) at a flow-rate of 0.25 ml/min.

Molecular species *sn*-2,3	α (25°C)	$\Delta\Delta G°$ (25°C) (cal/mol)	$\Delta\Delta H°$ (cal/mol)	$\Delta\Delta S°$ (cal/mol · K · 0.01)
20:0–18:0/20:0–20:0	1.03	−17.06	−3.75	4.47
18:0–18:0/20:0–20:0	1.06	−35.78	−2.82	11.06
18:0–16:0/20:0–20:0	1.10	−55.36	−6.84	16.28
16:0–16:0/20:0–20:0	1.14	−75.98	−10.33	22.03
18:0–18:1/18:0–18:0	1.03	−19.92	−16.60	1.11
18:0–18:2/18:0–18:0	1.09	−51.99	−45.95	2.03
18:1–18:1/18:0–18:0	1.07	−41.95	−63.19	−7.13
18:0–18:3/18:0–18:0	1.15	−83.18	−98.85	−5.26
18:2–18:2/18:0–18:0	1.20	−108.48	−126.13	−5.92
18:3–18:3/18:0–18:0	1.34	−173.66	−235.59	−20.78

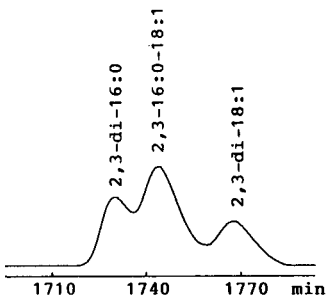

Fig. 7. Separation of critical pair prepared from 16:0 and 18:1 acids as 3,5-DNPU derivatives on an OA-4100 chiral column. Mobile phase: hexane–1,2-dichloroethane–ethanol (170:5:1, v/v/v) at a flow-rate of 0.25 ml/min. Peaks were monitored at 254 nm after the third recycle.

Dipole–induced dipole type hydrogen bonds are formed between polar X–H groups and polarizable multiple bonds such as isolated double bonds and benzene rings. The CSP used in this study contains NH groups on a chiral selector and OH groups on a silica support. A binding interaction may occur between the positively charged hydrogen of the X–H groups and π electron clouds on the double bonds. While this characteristic difference in separation according to carbon number and degree of unsaturation was also observed for the *sn*-1,2-enantiomer group (Table III), there is a problem with the results of these achiral separations. Tables II and III present the same results, but concerning the corresponding antipodes; the selectivity values are identical and also the $\Delta\Delta G^\circ$ values because enantiomers exhibit the same physico-chemical properties. Nevertheless, the data show differences in the enthalpy and entropy values for the two antipodes. The reason why the $\Delta\Delta H^\circ$ and $\Delta\Delta S^\circ$ values observed for two enantiomers are so different is unknown.

In a previous study, critical pairs were found with the DGs such as the pair of 1,2-16:0–18:0-DGs and 1,2-18:1–18:0-DGs corresponding to the same equivalent carbon number (*ECN*) [3]. These critical pairs were not separated at ambient temperature. The *ECN* value was calculated from the total acyl carbon number (*CN*) and the total number of double bonds (n) of the two constituent fatty acids according to the equation

$$ECN = CN - 2n \quad (3)$$

In this study, critical pairs were separated at low temperature. Fig. 7 shows the separation of the critical pair of *sn*-2,3-di-16:0, 2,3-16:0–18:1- and 2,3-di-18:1-DGs. The column temperature was maintained at -12.5°C for recycle chromatography. The peak area ratio is 1:2:1, and the second peak is assumed to be a mixture of *sn*-2-16:0–3-18:1- and *sn*-2-18:1–3-16:0-DGs, but detailed identification was not carried out.

In conclusion we have described the effect of temperature on DG enantiomer separation. The resolution was much improved at low temperature, but the column temperatures below -30°C caused abnormal pressure increases, irregularity of the chromatographic curve and/or deformation of peaks, hence temperatures below -30°C cannot be used for the usual analyses on this CSP. Another aspect considered is the essential difference in the mechanisms of separations according to carbon number and number of double bonds. Separation according to carbon number is controlled by $\Delta\Delta S^\circ$, whereas separation according to degree of unsaturation is based on the contribution of $\Delta\Delta H^\circ$. This characteristic difference may be expected for the other chromatographic separations.

REFERENCES

1 Y. Itabashi and T. Takagi, *J. Chromatogr.*, 402 (1987) 257.
2 T. Takagi and Y. Itabashi, *Lipids*, 22 (1987) 596.
3 T. Takagi and T. Suzuki, *J. Chromatogr.*, 519 (1990) 237.
4 W. H. Pirkle and T. C. Pochapsky, *J. Chromatogr.*, 369 (1986) 175.
5 W. H. Pirkle and T. C. Pochapsky, *Chem. Rev.*, 89 347 (1989).
6 R. J. Howe and T. Malkin, *J. Chem. Soc.*, (1951) 2663.
7 N. Oi and H. Kitahara, *J. Chromatogr.*, 265 (1983) 117.
8 N. Oi and H. Kitahara, *J. Liq. Chromatogr.*, 9 (1986) 511.
9 S. G. Allenmark, *Chromatographic Enantioseparation: Methods and Applications*, Ellis Horwood, Chichester 1988, pp. 70–71.
10 R. R. Brenner, *Prog. Lipid Res.*, 23 (1984) 69.

Journal of Chromatography, 625 (1992) 169–175
Elsevier Science Publishers B.V., Amsterdam

CHROM. 24 485

Measurement of partition coefficients by reversed-phase ion-pair liquid chromatography

Hanfa Zou, Yukui Zhang, Mingfang Hong and Peichang Lu

National Chromatographic Research and Analysis Centre, Dalian Institute of Chemical Physics, Academia Sinica, Dalian 116011 (China)

(First received January 24th, 1992; revised manuscript received June 12th, 1992)

ABSTRACT

Sixteen phenylamine- and naphthylaminesulphonic acids which are negatively charged and weakly retained or non-retained in reversed-phase high-performance liquid chromatography were used as model compounds to examine the quantitatively relationship between the calculated *n*-octanol–water partition coefficient (log *P*) and the retention value (log *k'*) (or log k_w) and solute charges in reversed-phase ion-pair liquid chromatography (RP-IPC). It was observed that the correlation of log *P vs.* log *k'* (or log k_w) for solutes with one negative charge has moderate regression coefficients of *ca.* 0.80, but, the correlation of log *P vs.* log *k'* (log k_w) and solute charges (n_e) for solutes with different charges has a regression coefficient higher than 0.98. The log *k'* (or log k_w) value in RP-IPC always make a positive contribution and the solute charges always makes a negative contribution to log *P* values. The proposed relationship between the log *P* value and the log *k'* value and solute charges makes it possible to predict the *n*-octanol–water log *P* values of ionic compounds from the retention values in RP-IPC, and is also useful in elucidating the retention mechanism in RP-IPC.

INTRODUCTION

Partition coefficients, a medicinally relevant physico-chemical property, play an influential role in many biological processes and therefore find numerous applications in quantitative structure–activity relationship (QSAR) studies [1–3] and in the determination of enviromental parameters [4–6]. Partition coefficients have been measured in nearly 100 solvent–water systems, mainly by means of the traditional shake-flask method [3]. *n*-Octanol–water is widely accepted as the reference system because of its analogy with biomembranes [3]. However, practical disadvantages and the limitation of log *P* values to between −2 and +4 have led researchers to investigate other methods for measuring partition coefficients [7,8]. In recent years, reversed-phase high-performance liquid chromatography (RP-HPLC) has become a popular alternative, capacity factors frequently being used as substitutes for *n*-octanol–water partition coefficients in QSAR studies.

The measurement of partition coefficients by RP-HPLC is based on the principle of the partition of a solute between a polar eluent and a stationary phase of low polarity [9–11]. It should be noted that many ionic organic compounds such as drugs are weakly or not retained in RP-HPLC even with pure buffer or water as the eluent, which makes it difficult to measure partition coefficients from the capacity factors in RP-HPLC. However, reversed-phase ion-pair liquid chromatography (RP-IPC) has become a well established method for the separation of ionic compounds, in which the retention can be regulated by the properties and concentration of organic modifier and ion-pair reagent and also by a competing ion with the same charges as the analyte [12–16]. Recent studies [17–19] on the retention process in RP-IPC showed that both electrostatic and hydrophobic interactions make im-

Correspondence to: Dr. H. Zou, National Chromatographic Research and Analysis Centre, Dalian Institute of Chemical Physics, Academia Sinica, Dalian 116011, China.

0021-9673/92/$05.00

portant contributions to retention. The former is directly related to the solute charges and the latter to solute hydrophobicity, which is paralleled with the partition coefficient of a solute. It is necessary to investigate the possibility of calculating partition coefficients from the capacity factors in RP-IPC if the contribution of the solute charge on the retention is corrected. In this work, the quantitative correlation of partition coefficients with capacity factors in RP-IPC and solute charges was studied.

THEORETICAL

Relationship between log P (P = partition coefficient) values and log k' (k' = capacity factor) values and solute charges

To establish a common hydrophobicity scale characterizing the partitioning of solutes in various organic–water systems, the free energies of partition should linearly related [20]:

$$\log P = -(\Delta G^0_{pm} + \Delta G^0_{pe})/RT \quad (1)$$

where ΔG^0_{pm} and ΔG^0_{pe} are the free energy of a solute transition from water to the organic phase, related to molecular and electrostatic interactions, R is the gas constant and T is absolute temperature. It can be expected that there will be a much weaker electrostatic interaction in the partitioning of an ionic compound or a natural compound in n-octanol–water system, and we then have

$$\log P = -\Delta G^0_{pm}/RT \quad (2)$$

Eqn. 2 means that the log P values of natural and ionic compounds are mainly determined by the molecular interaction, and related to ΔG^0_r (free energy of a solute transition from mobile phase to stationary phase in RP-HPLC) or retention in RP-HPLC. In RP-IPC, according to the electrostatic interaction model, the free energy change in the adsorption or partitioning of an ionic solute between the mobile and stationary phase can be divided into two parts, that is, free energy changes related to molecular and electrostatic interactions (ΔG^0_{im} and ΔG^0_{ie}), hence the capacity factor of an ionic solute can be expressed as [21]

$$\log k' = -(\Delta G^0_{im} + \Delta G^0_{ie})/RT \pm \log \phi \quad (3)$$

where ϕ is the mobile/stationary phase ratio. For a given RP-IPC column system, ΔG^0_{im} depends on the hydrophobicity of the solute and should be paralleled with the ΔG^0_{pm} of log P value; ΔG^0_{ie} can be expressed as

$$\Delta G^0_{ie} = n_e F \psi_0/RT \quad (4)$$

where ψ_0 is the electrical potential on the stationary surface and is constant under given conditions, n_e is the apparent charges of the ionic solute and F is the Faraday constant. Therefore, we have

$$\log P = A \log k' + Bn_e + C \quad (5)$$

where A, B and C are constants under given conditions. It can be seen that the partition coefficient of an ionic compound in the n-octanol–water system is related to the capacity factor and solute charges in RP-IPC.

Calculation of n-octanol–water partition coefficient

According to Hansch and co-workers [22,23], the n-octanol–water partition coefficient (log P) can be expressed as

$$\log P = \sum_1^n a_n f_n + \sum_1^m b_m F_m \quad (6)$$

where f_n is the hydrophobic fragmental constant, the lipophilicity contribution of a constituent part of a structure to the total lipophilicity, F_m represents factors affecting the partition coefficient and a_n and b_m are numerical factors indicating the incidence of

TABLE I

THE FRAGMENTAL CONSTANTS (f_n) USED TO CALCULATE THE n-OCTANOL–WATER PARTITION COEFFICIENTS OF SULPHONIC ACIDS

The fragmental constants are taken from Lyman [6] and Wang [24].

Functional group	f_n
f_{CH}	0.355
f_c	0.255
$f^{\phi}_{SO_3^-}$	−4.53
$f^{\phi}_{NH_2}$	−1.00
f^{ϕ}_{-O-}	−0.61
f_{CH_3}	0.89
f^{ϕ}_{Cl}	0.94
f_H	0.23
$f_{C_6H_5}$	1.90

the given fragmental and other factors indicating the icidence of the given fragmental and other factors in the structure of complex substance. Table I lists the fragmental constants used to calculate the partition coefficient of sixteen phenylamine- and naphthylaminesulphonic acids.

Below we give three examples of the calculation of log P values for the sulphonic acids:

1-aminobenzene-2-sulphonic acid:

$$\log P = f_{C_6H_5} + f_{NH_2} + f_{SO_3^-} + F_{p2} - f_H$$
$$= 1.90 - 1.0 - 4.53 + 0.08\ (4.53 + 1) - 0.23$$
$$= -3.42$$

1-amino-4-methoxybenzene-2-sulphonic acid:

$$\log P = f_{C_6H_5} + f_{NH_2} + f_{SO_3^-} - 2f_H + f_{-O-} + f_{CH_3}$$
$$+ F_b + F_{p2} = 1.90 - 1.0 - 4.53 - 0.46$$
$$- 0.61 + 0.89 - 0.12 + 0.08(4.53 + 1) = 3.61$$

2-aminonaphthalene-4,6,8-trisulphonic acid:

$$\log P = 8f_{CH} + 2f_c - 4f_H + 3f_{SO_3^-} + f_{NH_2}$$
$$= 8 \times 0.355 + 2 \times 0.255 - 4 \times 0.23 + 3 \times$$
$$(-4.53) - 1.0 = -12.22$$

where F_{p2} represents the combined interaction between polar substituted group and polar substituted group in orthogonal position, and F_b is a bond factor. Table II lists the calculated log P values and negative charges for sixteen sulphonic acids.

TABLE II

CALCULATED n-OCTANOL–WATER PARTITION COEFFICIENTS (log P) OF SIXTEEN SULPHONIC ACIDS AND THEIR NEGATIVE CHARGES (n_e)

Solute	n_e	Log P
1-Aminobenzene-2-sulphonic acid	1	−3.42
1-Aminobenzene-3-sulphonic acid	1	−3.86
1-Aminobenzene-4-sulphonic acid	1	−3.86
1-Amino-4-methylbenzene-2-sulphonic acid	1	−2.76
1-Amino-4-methoxybenzene-2-sulphonic acid	1	−3.61
1-Amino-6-chlorobenzene-3-sulphonic acid	1	−3.15
1,3-Diaminobenzene-4-sulphonic acid	1	−4.65
1-Aminonaphthalene-5-sulphonic acid	1	−2.70
2-Aminonaphthalene-5-sulphnonic acid	1	−2.70
2-Aminonaphthalene-6-sulphonic acid	1	−2.70
1-Aminobenzene-2,5-disulphonic acid	2	−8.18
1,3-Diaminobenzene-4,6-disulphonic acid	2	−8.97
2-Aminonaphthalene-4,8-disulphonic acid	2	−7.46
2-Aminonaphthalene-3,6-disulphonic acid	2	−7.02
2-Aminonaphthalene-4,6,8-trisulphonic acid	3	−12.22
2-Aminonaphthalene-3,6,8-trisulphonic acid	3	−11.86

EXPERIMENTAL

Materials

The phenylamine- and naphthylaminesulphonic acids analysed were obtained from the Dyestuff Laboratory, Chemical Engineering Department, Dalian University of Sciences and Technology. Standard solutions were prepared in water. Doubly distilled water was used throughout. Tetrabutylammonium iodide (TBAI) (Beijing Chemical Reagent Factory, Beijing, China), methanol, NaH_2PO_4, NaOH and HCl were of analytical-reagent grade.

Apparatus

The RP-IPC experiments were performed using a stainless-steel column (200 × 4.0 mm I.D.) that contained a Spherisorb-ODS reversed-phase packing material of 5 mm particle diameter (Phase Separations, Deeside, UK). The column was packed at the National Chromatographic Research and Analysis Centre, Dalian, China. The mobile phase was delivered by two Waters Model 510 pumps. The ratios of methanol to phosphate buffer in eluents A and B were 0.95 : 0.05 and 0.6 : 0.4 (v/v), respectively, and the concentration of the ion-pair reagent TBAI, the NaH_2PO_4 concentration and pH in both eluents were 4 mmol/l, 10 mmol/l and 7.15, respectively. The organic modifier concentration in the eluent was regulated by an NEC-APCIV computer with a Waters System Interface Module (Waters Assoc., Milford, MA, USA) by changing the ratio of eluent A to eluent B. The eluates were detected with a Waters Model 490 programmable multiwavelength detector set at 254 nm. Samples were loaded with a U6K syringe loading sample injector. The flow-rate of the eluent was 1.0 ml/min. The eluent pH was measured with an SA-720 pH meter (Orion Research, Chicago, IL, USA). All experimental data were processed on a COMPAQ-286 personal computer with Lotus software (Microsoft).

RESULTS AND DISCUSSION

The capacity factors of sixteen sulphonic acids

TABLE III

CAPACITY FACTORS OF SIXTEEN PHENYLAMINE- AND NAPHTHYLAMINESULPHONIC ACIDS AT DIFFERENT METHANOL CONCENTRATIONS IN RP-IPC

For experimental conditions, see text.

Solute	Methanol-to-buffer ratio (v/v)			
	0.325	0.281	0.239	0.198
1-Aminobenzene-2-sulphonic acid	0.46	1.00	1.64	3.04
1-Aminobenzene-3-sulphonic acid	0.26	0.54	0.84	1.34
1-Aminobenzene-4-sulphonic acid	0.15	0.30	0.49	1.01
1-Amino-4-methylbenzene-2-sulphonic acid	1.54	3.27	5.69	9.86
1-Amino-4-methoxybenzene-2-sulphonic acid	0.75	1.56	2.46	4.79
1-Amino-6-chlorobenzene-3-sulphonic acid	1.45	3.15	5.29	9.65
1,3-Diaminobenzene-4-sulphonic acid	0.14	0.28	0.43	0.95
1-Aminonaphthalene-5-sulphonic acid	0.62	1.28	2.22	4.21
2-Aminonaphthalene-5-sulphonic acid	0.78	1.63	2.94	5.25
2-Aminonaphthalene-6-sulphonic acid	1.23	2.80	5.01	9.85
1-Aminobenzene-2,5-disulphonic acid	0.29	0.68	1.11	2.46
1,3-Diaminobenzene-4,6-disulphonic acid	0.32	0.63	1.03	2.34
2-Aminonaphathalene-4,8-disulphonic acid	0.63	1.63	3.34	9.56
2-Aminonaphthalene-3,6-disulphonic acid	0.76	2.06	4.40	10.24
2-Aminonaphthalene-4,6,8-trisulphonic acid	1.09	3.04	6.98	16.79
2-Aminonaphthalene-3,6,8-trisulphonic acid	1.14	3.25	7.40	17.66

experimentally measured by RP-IPC are presented in Table III. The quantitative correlations between the calculated log P values and log k' values in RP-IPC for ten sulphonic acids with one negative charge or sixteen sulphonic acids with different negative charges and the relationship of the calculated log P values *vs.* log k' in RP-IPC and solute negative charges were established, and the results obtained are shown in Figs. 1–4. Very low regression

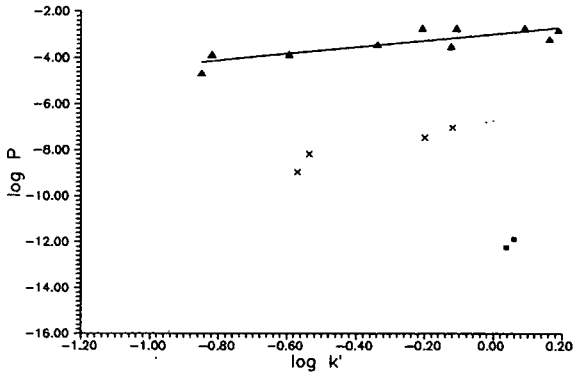

Fig. 1. Quantitative correlation of the calculated *n*-octanol–water partition coefficients (log P) *vs.* log k' and n_e in RP-IPC when the methanol concentration is 0.325; for other experimental conditions, see text. Points ▲, × and ■ represent sulphonic acids with one, two and three negative charges, respectively. For ten sulphonic acids with one negative charge: log $P = -2.899 + 1.541 \log k'$; $r = 0.773$, $n = 10$. For sixteen sulphonic acids with different negative charges: log $P = -5.830 - 1.333 \log k'$, $r = 0.017$, $n = 16$; log $P = 1.807 + 1.722 \log k' - 4.606\ n_e$, $r = 0.988$, $n = 16$.

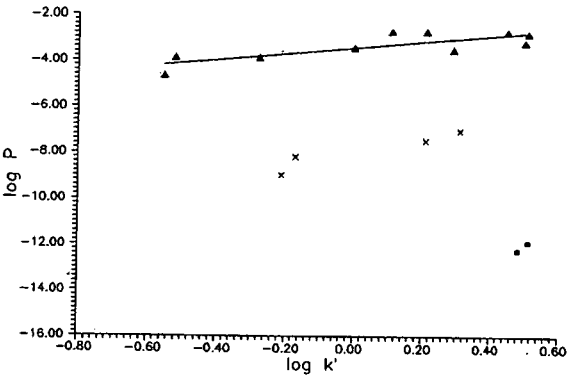

Fig. 2. Quantitative correlation of the calculated log P *vs.* log k' and n_e in RP-IPC when the methanol concentration is 0.281. Experimental conditions and symbols as in Fig. 1. For ten sulphonic acids with one negative charge: log $P = -3.393 + 1.485 \log k'$, $r = 0.771$, $n = 10$. For sixteen sulphonic acids with different negative charges: log $P = 5.166 - 2.499 \log k'$, $r = 0.075$, $n = 16$; log $P = 1.303 + 1.630 \log k' - 4.685\ n_e$, $r = 0.989$, $n = 16$.

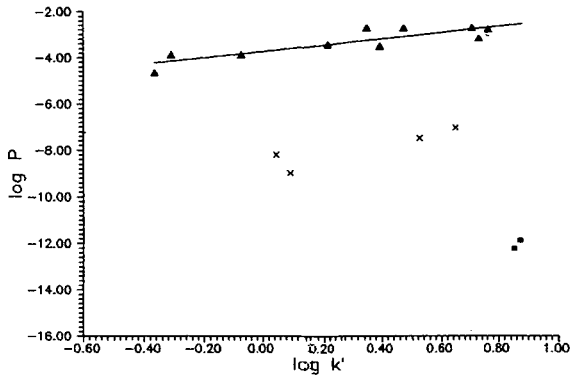

Fig. 3. Quantitative correlation of the calculated log P *vs.* log k' and n_e in RP-IPC when the methanol concentration is 0.239. Experimental conditions and symbols as in Fig. 1. For ten sulphonic acids with one negative charge: log $P = -3.714 + 1.451$ log k', $r = 0.801$, $n = 10$. For sixteen sulphonic acids with different negative charges: log $P = -4.360 - 2.923$ log k', $r = 0.125$, $n = 16$; log $P = 1.055 + 1.566$ log $k' - 4.783n_e$, $r = 0.991$, $n = 16$.

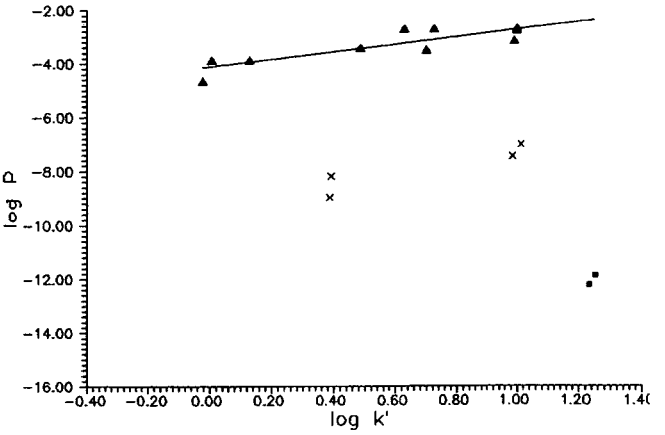

Fig. 4. Quantitative correlation of the calculated log P *vs.* log k' and n_e in RP-IPC when the methanol concentration is 0.198. Experimental conditions and symbols as in Fig. 1. For ten sulphonic acids with one negative charge: log $P = -4.128 + 1.477$ log k', $r = 0.778$, $n = 10$. For sixteen sulphonic acids with different negative charges: log $P = -2.995 - 3.557$ log k', $r = 0.200$, $n = 16$; log $P = 0.703 + 1.601$ log $k' - 4.890n_e$, $r = 0.991$, $n = 16$.

coefficients (<0.20) were obtained for the relationship of log P *vs.* log k' in RP-IPC for sixteen sulphonic acids with different negative charges, but the moderate (0.80) or high regression coefficients (>0.98) were obtained for the relationship of log P *vs.* log k' for ten sulphonic acids with one negative charge or that of log P *vs.* log k' and n_e for sixteen sulphonic acids with different negatives charges.

The retention in RP-IPC is more complex than that in RP-HPLC owing to presence of the ion-pair reagent and may be based on numerous factors [25], but the hydrophobic and electrostatic interactions play the dominant role for rigid compounds. This finding is confirmed by the fact that the correlation is greatly improved by taking into account the solute charges. However, other factors such as steric and configurational factors also play some role, especially for the complex compounds, which may cause the moderate regression coefficients (about 0.80) for ten sulphonic acids with one negative charge. We think that the effects of other factors such as steric and configurational factors on the quantitative correlation may arise in at least two ways: one is through the change in the apparent charges which may affect the electrostatic interaction of the solutes in RP-IPC; the other may result from the fact that there is a difference between the experimental solute hydrophobicity (log P) and the calculated value.

It is necessary to investigate further how these factors affect the quantitative correlation of log k' *vs.* log P. In the relationship of log P *vs.* log k' for sulphonic acids with one negative charge and log P *vs.* log k' and n_e for sulphonic acids with different negative charges, the coefficient values of the log k' and n_e terms (parameters A and B) are always positive and negative, respectively, which means that log k' and n_e make positive and negative contributions, respectively, to the log P values. There is no serious effect of methanol concentration on the values of A and B in eqn. 5, but the value of C in eqn. 5 decreases with decrease in methanol concentration, which means that the retention in RP-IPC increases with decreasing methanol concentration.

It has been reported [9,11] that there is a better correlation between extrapolated log k_w and log P values than between isocratic log k' and log P values in RP-HPLC. It has been proposed that the logarithm of the capacity factors is linearly dependent on the organic modifier concentration in RP-IPC with an adequate range of organic modifier concentrations [17,18,26–28]:

$$\log k' = \log k_w + cC_b \quad (7)$$

where k_w is the extrapolated capacity factor in RP-IPC with pure buffer as the eluent, c is the slope,

TABLE IV

PARAMETERS LOG k_w AND c OBTAINED BY REGRESSION ANALYSIS OF THE EXPERIMENTAL DATA SHOWN IN TABLE III

Solute	Log k_w	c	r
1-Aminobenzene-2-sulphonic acid	1.73	−6.30	0.997
1-Aminobenzene-3-sulphonic acid	1.26	−5.60	0.995
1-Aminobenzene-4-sulphonic acid	1.24	−6.33	0.997
1-Amino-4-methylbenzene-2-sulphonic acid	2.26	−6.30	0.998
1-Amino-4-methoxybenzene-2-sulphonic acid	1.93	−6.30	0.997
1-Amino-6-chlorobenzene-3-sulphonic acid	2.27	−6.40	0.998
1,3-Diaminobenzene-4-sulphonic acid	1.20	−6.29	0.994
1-Aminonaphthalene-5-sulphonic acid	1.90	−6.47	0.996
2-Aminonaphthalene-5-sulphonic acid	2.10	−6.77	0.999
2-Aminonaphthalene-6-sulphonic acid	2.39	−7.02	0.998
1-Aminobenzene-2,5-disulphonic acid	1.74	−7.28	0.998
1,3-Diaminobenzene-4,6-disulphonic acid	1.81	−7.16	0.998
2-Aminonaphthalene-4,8-disulphonic acid	2.77	−9.16	0.997
2-Aminonaphthalene-3,6-disulphonic acid	2.90	−9.30	0.999
2-Aminonaphthalene-4,6,8-trisulphonic acid	3.07	−9.29	0.999
2-Aminonaphthalene-3,6,8-trisulphonic acid	3.10	−9.30	0.999

mainly determined by the hydrophobic and electrostatic interaction between the solute, ion-pair reagent and the eluent, and C_b is the concentration of the organic modifier in the eluent. It should be noted that there is a quadratic relationship of log k' *vs.* C_b in RP-HPLC for a wide range of the organic modifier concentrations [29,30], and this quadratic relationship may also exist in RP-IPC when the range of organic modifier concentration is wide. It has been observed by El Tayar *et al.* [30] that there is no serious difference in the accuracy of prediction of log P values from log k_w values of linear and quadratic origin. The log k_w values derived by linear extrapolation of the isocratic capacity factors k' shown in Table III are given in Table IV. The quantitative correlation of the calculated log P values *vs.* log k_w for ten sulphonic acids with one negative charge and sixteen sulphonic acids with different negative charges and also log P *vs.* log k_w and n_e are shown in Fig. 5. It can be seen that there is no serious difference in the regression coefficients of the quantitative correlation from capacity factors and extrapolated capacity factors. It can be concluded that it is possible to calculate *n*-octanol–water log P values from the retention values (both log k' and log k_w) for rigid compounds in RP-IPC after the electrostatic interaction that is directly related to solute charges has been corrected. In order to improve the quantitative correlation, the effects of other factors such as steric and configurational factors should be taken into account, for which detailed investigations are needed.

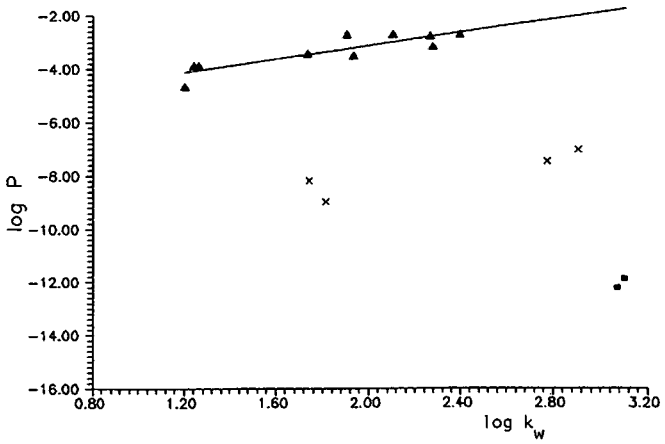

Fig. 5. Quantitative correlation of the calculated log P *vs.* log k_w and n_e in RP-IPC. Experimental conditions and symbols as in Fig. 1. For ten sulphonic acids with one negative charge: log P = $-5.717 + 1.322 \log k_w$, $r = 0.800$, $n = 10$. For sixteen sulphonic acids with different negative charges: log $P = 0.563 - 2.902 \log k_w$, $r = 0.301$, $n = 16$; log $P = -0.4385 + 1.301 \log k_w - 5.198\ n_e$, $r = 0.992$, $n = 16$.

ACKNOWLEDGEMENTS

Financial support from the Natural Sciences Foundation of China is greatfully acknowledged.

REFERENCES

1 H. Van de Waterbeemd and B. Testa, *Adv. Drug Res.*, 16 (1987) 85.
2 H. Kubinyi, *Prog. Drug Res.*, 23 (1979) 97.
3 H. Walter, D. E. Brooks and D. Fisher, *Partitioning in Aqueous Two Phase Systems*, Academic Press, London, 1985.
4 D. J. W. Blum and R. E. Speece, *Ecotoxicol. Environ. Safety*, 22 (1991) 198.
5 R. L. Lipnick, *Environ. Toxicol. Chem.*, 4 (1985) 255.
6 W. J. Lyman (Editor), *Handbook of Chemical Property Estimation Methods —Environmental Behavior of Organic Compounds*, McGraw-Hill, New York, 1982.
7 S. Yamana, A. Tsuji, E. Miyamoto and S. Kubo, *J. Pharm. Sci.*, 66 (1977) 747.
8 D. J. Minnick, D. A. Brent and J. Frenz, *J. Chromatogr.*, 461 (1989) 177.
9 T. Braumann, *J. Chromatogr.*, 373 (1986) 191.
10 R. E. Koopmans and R. F. Rekker, *J. Chromatogr.*, 285 (1984) 267.
11 A. Bechalany, A. Tsantili-Kakoulidou, N. El Tayar and B. Testa, *J. Chromatogr.*, 541 (1991) 221.
12 Cs. Horvath, W. R. Melander and I. Molnar, *Anal. Chem.*, 49 (1977) 2295.
13 B. A. Bidlingmeyer, *J. Chromatogr. Sci.*, 18 (1980) 525.
14 J. L. M. van de Venne, J. L. H. Hendrikx and R. S. Deelder, *J. Chromatogr.*, 167 (1978) 1.
15 A. Bartha and Gy. Vigh, *J. Chromatogr.*, 265 (1983) 171.
16 S. Afrashtehfar and F. F. Cantwell, *Anal. Chem.*, 54 (1982) 2422.
17 P. Lu, H. Zou and Y. Zhang, *Mikrochim. Acta, Part III*, (1990) 35.
18 H. Zou, Y. Zhang and P. Lu, *J. Chromatogr.*, 545 (1991) 599.
19 H. Liu and F. F. Cantwell, *Anal. Chem.*, 63 (1991) 2032.
20 Cs. Horvath, W. Melander and I. Molnar, *Anal. Chem.*, 49 (1977) 142.
21 A. A. Petrauskas and V. K. Svedas, *J. Chromatogr.*, 585 (1991) 3.
22 C. Hansch and A. Leo, *Substituent Constants for Correlation Analysis in Chemistry and Biology*, Wiley, New York, 1979.
23 A. Leo, P. Y. C. Jow, C. Silipo and C. Hansch, *J. Med. Chem.*, 18 (1975) 865.
24 L. Wang, *Chemistry of Pollutant Organic Compounds*, Academia Press, Beijing, 1990, (in Chinese).
25 C. M. Riley, E. Tomlinson and T. M. Jefferies, *J. Chromatogr.*, 185 (1979) 197.
26 H. Zou, Y. Zhang, M. Hong and P. Lu, *Chromatographia*, 32 (1991) 329.
27 A. Bartha, Gy. Vigh and J. Stahlberg, *J. Chromatogr.*, 506 (1990) 85.
28 P. Jandera, J. Churacek and B. Taraba, *J. Chromatogr.*, 262 (1983) 121.
29 P. J. Schoenmakers, H. A. H. Billiet, R. Tijssen and L. de Galan, *J. Chromatogr.*, 149 (1978) 519.
30 N. El Tayar, H. van de Waterbeemd and B. Testa, *J. Chromatogr.*, 320 (1985) 305.

Journal of Chromatography, 625 (1992) 177–181
Elsevier Science Publishers B.V., Amsterdam

CHROM. 24 511

Studies on an abnormally sharpened elution peak observed in counter-current chromatography

Yoichiro Ito, Yoichi Shibusawa and Henry M. Fales

Laboratory of Biophysical Chemistry, National Heart, Lung, and Blood Institute, Building 10, Room 7N322, National Institutes of Health, Bethesda, MD 20892 (USA)

Hans J. Cahnmann

National Institute of Diabetes, Digestive and Kidney Diseases, National Institutes of Health, Bethesda, MD 20892 (USA)

(First received June 2nd, 1992; revised manuscript received July 15th, 1992)

ABSTRACT

Counter-current chromatography (CCC) of the bromoacetylation product of 3,3',5-triiodo-L-thyronine (T_3) produced an unusually sharp peak for the desired product, N-bromoacetyl T_3 ($BrAcT_3$). A series of experiments revealed that bromoacetic acid, probably present as a side reaction product in the sample solution, was responsible. This compound repressed the ionization of the carboxyl group of $BrAcT_3$ forcing it into the less polar stationary phase until the bromoacetic acid had eluted completely from the apparatus. At this point, the sudden increase of pH and consequent ionization of the $BrAcT_3$ allowed the ammonium salt of the latter to enter the more polar moving phase where it eluted rapidly from the column as a sharp peak. The same phenomenon was observed in the CCC fractionation of a series of indole auxins where addition of trifluoroacetic acid to the sample caused peak sharpening by the same process. The phenomenon recalls pH gradient elution and isoelectric focussing except that the substance responsible for the pH range here is added along with the sample in one bolus forming a sharp pH gradient at its trailing edge. As with gradient elution, the technique is of practical interest since it permits collection of the eluting compounds with increased detectability in fewer fractions. The technique can also enhance separation of compounds whose partition coefficients differ with a change in pH.

INTRODUCTION

Counter-current chromatography (CCC) is a continuous chromatographic process [1,2] depending on counter-current partitioning of two liquid phases [3]. The partitioning action takes place in an open column space free of the support matrix found in ordinary liquid chromatography systems. Because of this, the adsorption and peak tailing sometimes encountered in liquid chromatography is absent and the CCC method is expected to provide symmetrical peaks as long as the partitioning phases are not overloaded with sample. As with other chromatographic systems using isocratic elution, peak width increases with retention time due to distribution and diffusion or when more than one species is present as in the case of ionization of a carboxylic acid.

During the CCC purification of a synthetic sample of N-bromoacetyl-3,3',5-triiodo-L-thyronine ($BrAcT_3$), we encountered an unexpectedly sharp elution peak (Fig. 1A) for this substance [4]. The present note describes a series of experiments which revealed the agent responsible for the peak sharpening to be bromoacetic acid, probably a side reaction product, that had been introduced with the sample. A mechanism for the effect is proposed and

Correspondence to: Dr. Y. Ito, Laboratory of Biophysical Chemistry, National Heart, Lung, and Blood Institute, Building 10, Room 7N322, National Institutes of Health, Bethesda, MD 20892, USA.

0021-9673/92/$05.00

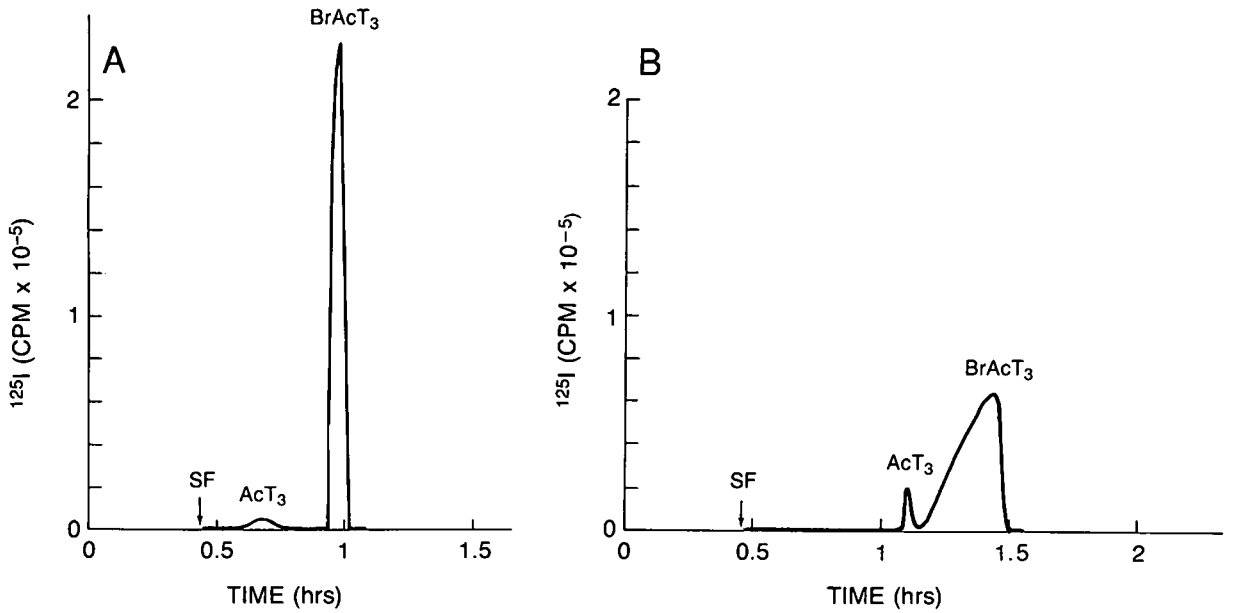

Fig. 1. Chromatograms of $BrAcT_3$ obtained with a standard two-phase solvent system composed of hexane, ethyl acetate, methanol and 15 m*M* ammonium acetate (pH 4) at two different volume ratios, (A) 1:1:1:1 and (B) 4:5:4:5, but otherwise identical experimental conditions. Other experimental conditions are as follows: sample: crude bromoacetylation mixture (from 0.1 mmol T_3) and a minute amount of [^{125}I]T_3 in 4 ml of solvent consisting of equal volumes of upper and lower phases; mobile phase: lower aqueous phase (pH 5.2); flow-rate: 3 ml/min; speed: 800 rpm; detection: ^{125}I radioactivity; retention of stationary phase: 69.8% (A) and 64.7% (B). SF = Solvent front. Note that the peak profile of $BrAcT_3$ and AcT_3 was reversed by changing the solvent ratio.

extension of the technique to other eluates and peak sharpening agents is demonstrated.

EXPERIMENTAL

All separations were performed with a commercial model of the high-speed CCC centrifuge (Ito Multilayer Separator/Extractor from P.C. Inc., Potomac, MD, USA). The design of the apparatus has been reported earlier [4].

The two-phase solvent system was prepared by mixing hexane, ethyl acetate, methanol and an aqueous solution of 15 m*M* ammonium acetate at a volume ratio of 1:1:1:1, where the pH of the ammonium acetate solution was adjusted by adding acetic acid. The solvent mixture was thoroughly equilibrated at room temperature in a separatory funnel and the two phases were separated shortly before use.

In each separation, the entire column was first filled with the stationary non-aqueous phase followed by injection of 2 to 4 ml of sample solution containing crude $BrAcT_3$ [4] or a mixture of indole auxins through the sample port. The mobile aqueous phase was then pumped into the head of the column at a flow-rate of 3 ml/min while the apparatus was spun at 800 rpm. The effluent from the outlet of the column was continuously monitored with a UV monitor (Uvicord S; LKB, Bromma Stockholm, Sweden) at 280 nm and collected in glass tubes to obtain 3-ml fractions. After all desired peaks had been eluted, the run was terminated and the column contents were collected in a graduated cylinder to determine the volume of the stationary phase retained in the column.

In the separation of radioactive samples, the radioactivity of each fraction was measured with a gamma scintillation counter (Auto-Gamma 500 Series; Packard Instruments, Downers, IL, USA). The pH of each fraction was also determined by a portable pH meter (Accumet Portable Laboratory; Fisher Scientific, Pittsburgh, PA, USA).

RESULTS AND DISCUSSION

Fig. 1A illustrates the sharp $BrAcT_3$ peak mentioned earlier [4]. To examine the effect of the solvent system on the elution of $BrAcT_3$, the mixture was reexamined using a slightly more polar solvent system. As expected, both the $BrAcT_3$ and the by-product eluted later due to the increased polarity of the solvent (Fig. 1B), however the sharpening effect was reversed. More importantly, merely diluting the original sample of $BrAcT_3$ resulted in a chromatogram in which both peaks were of normal shape. These facts suggested that a substance was present in the original sample that, though invisible to the detector, was strongly affecting the partitioning action. Mass spectrometric analysis showed that the original sample contained much bromoacetic acid. To prove the point, a solution of 2.5 mmol of bromoacetic acid was deliberately added to an amount of prepurified $BrAcT_3$ corresponding to that seen in Fig. 1A and monitored by pH as it eluted (Fig. 2, dotted line). Because of the quantity used, the stationary phase is considerably overloaded and it elutes with a sharply defined trailing edge just before the sharp peak of $BrAcT_3$ (Fig. 2, solid line). Clearly, the bromoacetic acid has acted to delay elution of the $BrAcT_3$ by repressing its ionization and forcing it to partition more completely into the non-polar stationary phase.

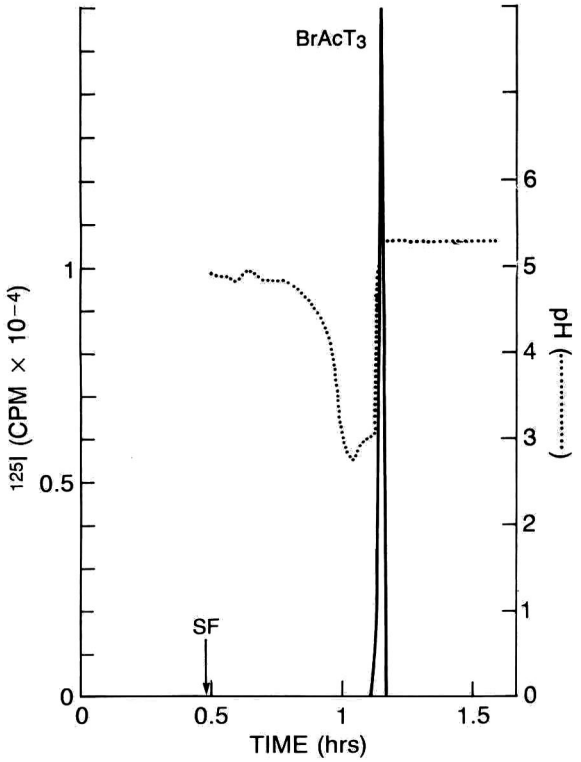

Fig. 2. Chromatogram of prepurified $BrAcT_3$ obtained with 2.5 mmol bromoacetic acid in the sample solution. A sharp peak profile of $BrAcT_3$ in Fig. 1A was reproduced by adding bromoacetic acid in the sample solution. Close association between the abrupt return point of pH curve and the sharp $BrAcT_3$ peak strongly suggests that bromoacetic acid is the causative agent of the sharp peak. Sample solution: CCC-purified $BrAcT_3$ (*ca.* 0.04 mmol) with bromoacetic acid (2.5 mmol) in 3.5 ml lower phase. Other experimental conditions as in Fig. 1A. Retention of the stationary phase was 67%. SF = Solvent front.

The above peak sharpening effect can be seen in detail in Fig. 3A where a schematic view of the column is shown with the stationary and moving phases arbitrarily separated. Thus, $BrAcT_3$ anions, that happen to be at location 1 in the presence of bromoacetic acid will rapidly protonate due to the lower pK_a of the excess bromoacetic acid and enter the nonpolar stationary phase (location 2). As the sharply defined trailing edge moves forward, the compound finds itself in location 3 where the stationary phase is in contact with the higher pH mobile phase. Ionization of the carboxylic acid occurs and the $BrAcT_3$ enters the mobile phase (location 4) whereupon it rapidly migrates to location 1 and the process is repeated. Thus, although elution of the sample is delayed, it undergoes the same partitioning action with distribution and diffusion lessened by the focussing action of the bromoacetic acid edge. Clearly, for the focussing action to take place there must be a particular relationship between the partition coefficients of the sample and causative agent. Fig. 3B details further the general requirements for the effect to be manifest. Thus when partition coefficients $[C_{s(\text{tationary})}/C_{m(\text{obile})}]$ of both the free acid (K_a) and its salt (K_b) are less than the partition coefficient of the causative acid (K_{pH}), the solute will elute earlier (peak 1) than the pH gradient and there will be no sharpening. On the other hand, when both K_a and K_b are greater than K_{pH}, the solute will elute after the gradient (peak 4), again without sharpening. Sharpening occurs only when K_{pH} falls between K_a and K_b as shown in peaks 2 and 3.

At first glance, the focussing effect recalls ordinary gradient elution [5] used extensively to reduce

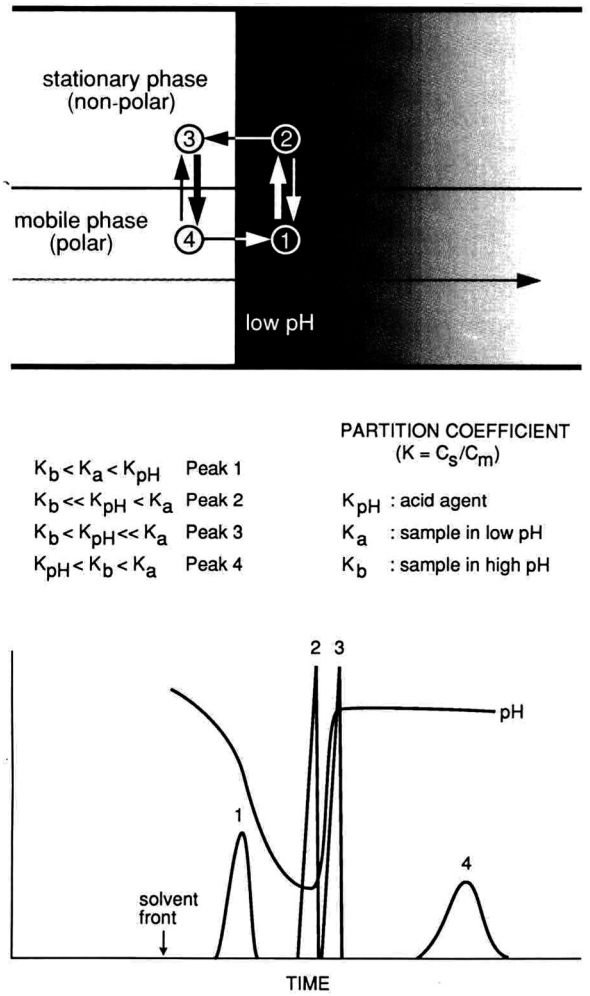

Fig. 3. (A) Schematic illustration of the peak sharpening process in the separation column. A portion of the column contains the non-polar stationary phase in the upper half and the polar mobile phase in the lower half where the solute molecules circulate at the sharp edge of the low pH region (shaded). For more detailed description, see the Results and Discussion section. (B) General requirements for sharp peak formation. Peak 1 is obtained when both K_a and K_b are smaller than K_{pH} while peak 4 is obtained when both K_a and K_b are greater than K_{pH}. Sharp peaks 2 and 3 are formed when K_{pH} falls between K_a and K_b as indicated above.

elution times and sharpen peaks in column chromatography of amino acids [6] and counter-current separation of alkaloids [7,8] where the specific relations between partition coefficients and ionization constants are discussed. Another apparently related process is isoelectric focusing [9] where an eluting ampholyte is trapped at a point in an established gradient where its effective charge is zero. However, in the present case, the shape of the pH gradient is unique since it is caused by the addition of the acid in one bolus along with the sample. Its effect on the eluting sample is therefore determined both by its quantity and its specific elution characteristics in the solvent system employed.

Inorganic acids including HCl and HBr elute rapidly due to their high polarity and, as expected from the above analysis, we have found that they do not sharpen the $BrAcT_3$ peak. However, trifluoroacetic acid (TFA), selected as a more convenient pH gradient-forming agent because of its easy removal

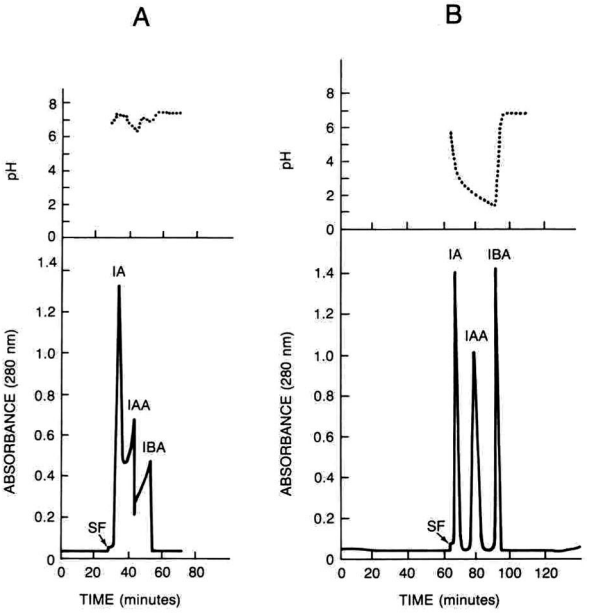

Fig. 4. Chromatograms of indole auxins obtained with a neutral solvent system using sample mixtures containing 2 μl TFA (A) and 400 μl TFA (B). Note that the amount of TFA in the sample solution determines the retention volume of the abrupt return point of the effluent pH which coincides with the sharp peak of one of the auxins. Solvent system: hexane–ethyl acetate–methanol–15 m*M* ammonium acetate, pH 7 (1:1:1:1); sample: indole auxins, IA, IAA and IBA (2 mg each) + 2 μl TFA (A) and 400 μl TFA (B) in 2 ml of solvent (1 ml of each phase); mobile phase: lower aqueous phase (pH 7.4); flow-rate: 3 ml/min; speed: 800 rpm. Retention of the stationary phase was 66.8% (A) and 28.1% (B). The low stationary phase retention in B is apparently due to introduction of a large volume of TFA in the sample solution. SF = Solvent front.

from the fractions (b.p. 72.4°C), served equally well for the chromatography of $BrAcT_3$.

To illustrate the generality of the technique, a set of indole auxins, indole-3 acetamide (IA), indole-3-acetic acid (IAA) and indole-3-butyric acid (IBA), was selected as a further example since these compounds have suitable partition coefficients in the above two-phase solvent system. With a trace of TFA added to the sample, the mixture at this pH produces broad and skewed peaks at short elution times as expected for dissociating substances (Fig. 4A). Addition of 400 μl of TFA results in a considerable shift of the pH edge toward longer times (Fig. 4B) to coincide with the elution of the IBA which is now sharpened. Under these conditions, the IAA peak is now beginning to return to the normal profile.

CONCLUSIONS

Since this peak sharpening phenomenon is dependent only on the partioning process, the present technique should be generally useful in liquid chromatography of ionizable substance wherever it is necessary to concentrate solutions in as few fractions as possible for enhanced detection or simplification of workup. The method should work as well for basic compounds by using a weak base to establish the pH profile. Of course, successful sharpening can be brought about only by careful consideration of the partition coefficients involved and these are not always easy to obtain particularly with unknown compounds.

An important feature of the method is its ability to cause a change in the *relative* elution times of components. This may be of use where impurities coelute with the desired analyte. Separation can be brought about as long as the impurities do not respond to a pH change in similar fashion. Thus, the technique is effective in shifting organic acids and bases away from neutral compounds.

Recently we have found that the causative acid can also be added to the stationary phase instead of the sample solution. We are expanding the application to preparative-scale separations.

REFERENCES

1 Y. Ito, in N. B. Mandava and Y. Ito (Editors), *Countercurrent Chromatography: Theory and Practice*, Marcel Dekker, New York, 1988, Ch. 3, pp. 79–442.
2 W. D. Conway, *Countercurrent Chromatography: Apparatus, Theory and Applications*; VCH, New York, 1990.
3 L. C. Craig and D. Craig, in A. Weissberger (Editor), *Techniques of Organic Chemistry*, Vol. 3, Interscience, New York, 1956, pp. 149–331.
4 H. J. Cahnmann, E. Gonçalves, Y. Ito, H. M. Fales and E. A. Sokoloski, *J. Chromatogr.*, 538 (1991) 165.
5 L. R. Snyder, in Cs. Horváth (Editor), *High-Performance Liquid Chromatography —Advances and Perspectives*, Vol. 1, Academic Press, New York, 1980, pp. 208–224.
6 T. Kuster and A. Niederweisen, in E. Heftmann (Editor), *Chromatography —Fundamentals and Applications of Chromatographic and Electrophoretic Methods, Part B; Applications*, Elsevier, Amsterdam, New York, 1983, pp. 1–52.
7 C. Galeffi, M. A. Ciasca-Rendina, E. Miranda Delle Monache, A. Villar del Fresno and G. B. Marini-Bettolo, *J. Chromatogr.*, 45 (1969) 407.
8 G. B. Marini-Bettòlo and C. Galeffi, in F. Bruner (Editor), *The Science of Chromatography*, Elsevier, Amsterdam, New York, 1985, pp. 283–303.
9 N. Catsimpoolas, in Z. Deyl (Editor), *Electrophoresis —A Survey of Techniques and Applications, Part A: Techniques*, Elsevier, Amsterdam, New York, 1979, pp. 167–192.

Journal of Chromatography, 625 (1992) 183–190
Elsevier Science Publishers B.V., Amsterdam

CHROM. 24 484

Reversed-phase high-performance liquid chromatography of S-alk(en)yl-L-cysteine derivatives in *Allium sativum* including the determination of (+)-S-allyl-L-cysteine sulphoxide, γ-L-glutamyl-S-allyl-L-cysteine and γ-L-glutamyl-S-(*trans*-1-propenyl)-L-cysteine

M. Mütsch-Eckner and O. Sticher

Department of Pharmacy, Swiss Federal Institute of Technology (ETH) Zurich, CH-8092 Zürich (Switzerland)

B. Meier

Zeller AG, CH-8590 Romanshorn (Switzerland)

(First received April 24th, 1992; revised manuscript received June 22nd, 1992)

ABSTRACT

The separation of six S-alk(en)yl-L-cysteine sulphoxides and γ-L-glutamyl-S-alk(en)yl-L-cysteines as genuine constituents of *Allium sativum* L. is reported. After automated precolumn derivatization with *o*-phthaldialdehyde–*tert.*-butanethiol the reaction products, sulphur-substituted isoindole derivatives, were analysed by reversed-phase high-performance liquid chromatography (RP-HPLC) followed by UV detection at 337 and 260 nm or fluorescence detection (excitation wavelength 230 nm, emission wavelength 420 nm). The method described allowed the qualitative and quantitative determination of the characteristic genuine polar garlic components in a single run. The accuracy and precision of the assay method, including external calibration, were evaluated. To validate the system the two main γ-glutamyl peptides, γ-L-glutamyl-S-allyl-L-cysteine and γ-L-glutamyl-S-(*trans*-1-propenyl)-L-cysteine, were determined using two different chromatographic procedures: they were determined as isoindole derivatives with UV detection as described above and by RP-HPLC with UV detection at 210 nm without previous derivatization. The method can be applied to the standardization of garlic and garlic preparations. Several garlic bulb samples were investigated and the total amount of the three main compounds was found to vary by a factor of about 2.5.

INTRODUCTION

Sulphur containing L-cysteine derivatives have been reported to be characteristic, genuine constituents of various *Allium* species [1,2]. The S-alk(en)yl-L-cysteine sulphoxides, especially (+)-S-allyl-L-cysteine sulphoxide (alliin), are precursors of a variety of more lipophilic products derived from enzymatic conversion of, *e.g.* alliin to allicin by the alliinase after cell rupture and further transformation to ajoenes, vinyldithiins or sulphides [3]. Most of the previous chromatographic analyses tended to concentrate on the latter compounds [4–12], because they are considered to be associated with the biological activity of garlic [13,14]. In this case the cysteine sulphoxides act as prodrugs. Less is known about the biological activity of the γ-glutamyl peptides [15] or the pharmacokinetic properties of all the cysteine derivatives mentioned.

The determination of alliin was presented for the

Correspondence to: Professor Dr. O. Sticher, Department of Pharmacy, Swiss Federal Institute of Technology (ETH) Zurich, CH-8092 Zürich, Switzerland.

0021-9673/92/$05.00

first time by Ziegler and Sticher [16] and Mochizuki *et al.* [17]. After precolumn derivatization, alliin was analyzed as isoindole and a fluorophore derivative, respectively. Recently Lawson *et al.* [18] reported the separation of the γ-glutamyl peptides by reversed-phase high-performance liquid chromatography (RP-HPLC) and their determination after UV detection at 220 nm. Lancaster and Kelly [19] developed a rather complicated method using a combination of electrophoresis, two-dimensional thin-layer chromatography and densitometric detection for the quantitative analysis of garlic extracts. Kappenberg and Glasl [20] described an assay method using thin-layer chromatography and detected alliin after derivatization with ninhydrin.

The aim of this work was to develop an RP-HPLC method for the selective qualitative analysis of cysteine derivatives in garlic and a validated chromatographic procedure for the determination of the main γ-glutamyl peptides, γ-L-glutamyl-S-allyl-L-cysteine (GLUACS) and γ-L-glutamyl-S-(*trans*-1-propenyl)-L-cysteine (GLUPRENCS), and (+)-S-allyl-L-cysteine sulphoxide [alliin, (+)-ACSO] in garlic in a single run.

EXPERIMENTAL

Plant material

All of the garlic bulb samples were purchased in 1991 at local markets in Zürich (Switzerland). They were cultivated either in France, Switzerland or Spain.

Reference compounds

S-Alk(en)yl-L-cysteine sulphoxide derivatives, (+)-S-allyl-L-cysteine sulphoxide [alliin, (+)-ACSO] and (±)-S-methyl-L-cysteine sulphoxide [(±)-MCSO] were synthesized; details are given in ref. 21. Additionally, alliin was isolated from garlic leaves [22]. (+)-S-(*trans*-1-Propenyl)-L-cysteine sulphoxide [(+)-PRENCSO] and the two γ-glutamyl peptides, γ-L-glutamyl-S-allyl-L-cysteine (GLUACS) and γ-L-glutamyl-S-(*trans*-1-propenyl)-L-cysteine (GLUPRENCS), were isolated as monoammonium salts from garlic bulbs, details of the isolation procedure and the analytical data have been described in ref. 22. γ-L-Glutamyl-S-methyl-L-cysteine (GLUMCS) was isolated from chive seeds [18] and was a gift from Dr. L.D. Lawson (Murdock

γ-L-Glutamyl peptides

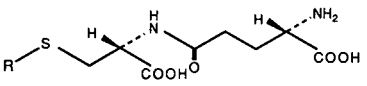

L-Cysteine sulphoxides

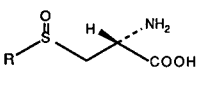

	-R:
GLUMCS:	$-CH_3$
GLUACS:	$-CH_2CHCH_2$
GLUPRENCS:	$-CHCHCH_3$

	-R:
(+)-MCSO:	$-CH_3$
(+)-ACSO:	$-CH_2CHCH_2$
(+)-PRENCSO:	$-CHCHCH_3$

Healthcare, Springville, UT, USA). The purity of the reference compounds was checked by means of reversed-phase HPLC and on normal-phase thin-layer chromatography.

Solvents

Methanol, acetonitrile, tetrahydrofuran and 1,4-dioxane were of HPLC quality (Romil Chemicals, Shepshed, UK). Water was obtained using a NANOpure Cartridge system (Skan, Basle-Allschwil, Switzerland). All other reagents employed for the preparation of buffer solutions or derivatization procedures were of analytical-reagent grade and were obtained from Merck (Darmstadt, Germany) or Fluka (Buchs, Switzerland). Aqueous buffer solutions needed for the mobile phases were prepared with sodium dihydrogenphosphate dihydrate, adjusted to the desired pH value and passed through a 0.45 μm membrane filter.

Instrumentation

HPLC analyses were performed using a Hewlett-Packard instrument (Model 79994A analytical workstation, Model 1090M liquid chromatograph, Model 1040 diode-array detector, Model 1046A fluorescence detector). UV detection was performed at 337 nm and 260 nm; for fluorescence detection the excitation wavelength (λ_{ex}) was set at 230 nm and emission was recorded at wavelength (λ_{em}) 420 nm.

Chromatographic conditions

The analytical column for method 1 (100 x 4.6 mm I.D.) was packed with Spherisorb ODS II, 3 μm (Phase Separations, Queensferry, UK); for method 2 the column (250 x 4 mm I.D.) was filled with Lichrosorb RP-18, 5 μm (Merck). The column temperature was maintained at 25°C.

For method 1 the mobile phase consisted of sol-

vent A [tetrahydrofuran–1,4-dioxane–acetonitrile–0.045 *M* aqueous phosphate buffer (pH 7.10) (1.6:6.0:13.1:79.3)] and solvent B [tetrahydrofuran–1,4-dioxane–acetonitrile–0.045 *M* aqueous phosphate buffer (pH 7.10) (3.4:12.9:28.1:55.6)] with the following gradient 0 to 5 min, 100% A; 10 min, 90% A; 15 min, 65% A; 20 min, 60% A. The isocratic analyses of method 2 were performed with methanol–0.015 *M* aqueous phosphate buffer (pH 3.2) (14:86) as the eluent. The flow-rate was maintained at 1.0 ml/min for method 1 and 1.1 ml/min for method 2.

Sample preparation

About 0.8–1.0 g (accurately weighed) of freeze-dried and pulverized plant material was extracted for 5 min with 50.0 ml of methanol–water (50:50) containing 0.05% of formic acid using a Polytron (Kinematica, Kriens, Switzerland). After filtration, 5.0 ml of the filtrate were passed through a Bond Elut C_{18} cartridge. To ensure complete elution, an additional volume of about 4.5 ml of the extraction solvent was passed through. The solution obtained was adjusted to a final volume of 10.0 ml in a volumetric flask. From each specimen three samples were prepared. According to method 2, 15 μl were injected into the chromatographic system.

Derivatization

The reagent used for precolumn derivatization of the cysteine derivatives was prepared as follows: 81 mg of *o*-phthaldialdehyde and 60 μl of *tert.*-butanethiol were dissolved in 5 ml of methanol and diluted to 20.0 ml in a volumetric flask with 0.07 *M* aqueous borate buffer (pH 9.60). The reagent was stored at room temperature and replaced every week. The automated precolumn derivatization was performed at ambient temperature by mixing 9 μl of the reagent with 3 μl of the extract sample for four times. After waiting for 5 min the derivatized sample was injected into the chromatographic system.

Standard solutions

The reference compounds, (+)-S-allyl-L-cysteine sulphoxide [alliin, (+)-ACSO], γ-L-glutamyl-S-allyl-L-cysteine (GLUACS) and γ-L-glutamyl-S-(*trans*-1-propenyl)-L-cysteine (GLUPRENCS) were dissolved in methanol–water (50:50) containing 0.05% of formic acid. The solutions were stored at low temperature for not more than 1 day except for the solutions of alliin, which were stable at room temperature for several days.

Calibration was performed using the external standard method and calculating the peak areas. For the determination of the linearity, eight-point calibration lines were obtained with concentrations of the standard solutions between about 0.030 and 0.400 mg/ml. Each calibration point was measured three times. The correlation coefficient (r^2) was $\geqslant$ 0.997.

RESULTS AND DISCUSSION

Extraction and sample preparation

Freeze-drying and pulverizing the plant material guaranteed a homogeneous sample for the subsequent extraction. The relative standard deviation of the constituents determined was thereby slightly reduced with respect to the freshly extracted specimen. Extraction in an acidic methanolic–aqueous medium using a Polytron was rapid to perform, protected the extract components from enzymatic activity (*e.g.* by alliinase) and therefore favoured the stability of the extracts; a decrease in the peak areas could not be measured for at least 5 h. The stability of extracts is often a crucial problem in the automation of the chromatographic procedure. Extraction with a methanolic–aqueous solution of O-(carboxymethyl)hydroxylamine, reported to be a specific inhibitor of alliinase [23], did not result in a higher yield of either alliin or GLUACS and GLU-

TABLE I

RESULTS OF RECOVERY EXPERIMENTS

For conditions, see Experimental.

Compound	Recovery (%)[a]	
	Method 1 (337 nm)	Method 2 (210 nm)
GLUACS	99.2 (1.7)	98.9 (1.3)
GLUPRENCS	98.1 (2.1)	98.4 (1.4)
(+)-ACSO	99.5 (2.6)	–[b]

[a] Mean (n = 3) with relative standard deviation (%) in parentheses.

[b] Not determined.

PRENCS. The recovery of all three compounds added to the extraction medium was not less than 98% (n = 3, Table I), confirming not only their quantitative extraction but also their complete elution from the reversed-phase sample clean-up cartridges.

Precolumn derivatization

Improved detection possibilities of primary amines, especially of amino acids and smaller peptides, could be achieved by their reaction with *o*-phthaldialdehyde and *tert.*-butanethiol in an alkaline medium to give 1-butylthio-N-substituted isoindole derivatives [21]. In the investigation presented, the precolumn derivatization was automated and the conditions of the derivatization were optimized: the concentrations of the reagents were adjusted to guarantee a complete reaction on the one hand and to avoid precipitation during derivatization on the other. Owing to its buffer capacity especially at more basic pH values, borate buffer was preferred to phosphate buffer. The reaction time of the cysteine derivatives at ambient temperature was varied between 2 and 15 min and a waiting time of 5 min was found to be adequate. The reproducibility of the automated derivatization step was checked by injection of replicate derivatized standards and extracts. Relative standard deviations for the peak areas of reference compounds were 0.53% (GLUACS), 0.49% (GLUPRENCS) and 0.60% [(+)-ACSO)], (n = 4, detection at 337 nm). The linearity of the reaction system and of the detector employed was controlled by derivatizing alliin,

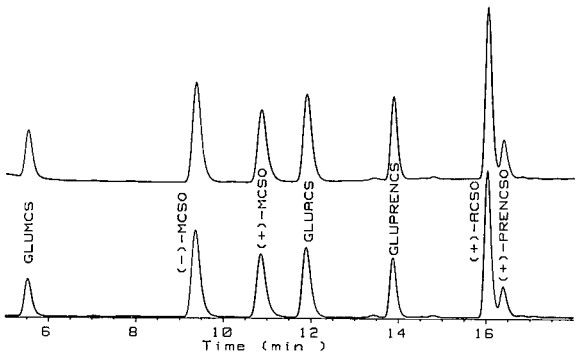

Fig. 1. Chromatographic separation of the derivatized reference compounds (method 1) with UV detection at 260 nm (top) and 337 nm (bottom). For conditions, see Experimental.

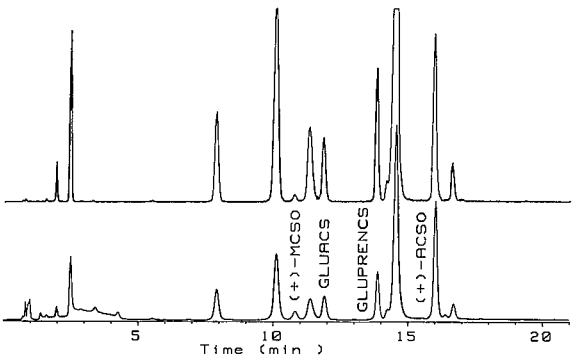

Fig. 2. Typical elution profile of a derivatized garlic bulb extract (method 1) with fluorescence detection (top) and UV detection at 337 nm (bottom). For conditions, see Experimental. Further main peaks eluted were mainly identified as ubiquitous amino acids or γ-glutamyl peptides of ubiquitous amino acids (see text).

GLUACS and GLUPRENCS in amounts ranging from about 0.15 to 1.5 μg.

Qualitative analysis

The separation of the derivatized extract components was performed using a reversed-phase C_{18} stationary phase. Owing to the different chemical properties of the compounds to be separated, an efficient and selective procedure for the optimization of the mobile phase was required. Satisfactory resolution was achieved by means of a four solvent system applying the PRISMA model [24]. Performing a gradient elution, the solvent strength of the mobile phase was increased as a factor of time. Figs. 1 and 2 show chromatograms of the separation of the derivatized reference compounds and a derivatized extract sample. To obtain highly reproducible results the column temperature was maintained at 25°C.

There is great versatility for the selective and sensitive detection of the 1-butylthio-N-substituted isoindole derivatives. The UV characteristics are fixed primarily by the chromophoric system of the isoindole moiety. It shows a UV maximum at 337 nm and a shoulder at 260 nm. In addition to specific UV detection, more sensitive electrochemical or fluorescence detectors can be employed. Ziegler and Sticher [25] investigated the advantages and disadvantages of these detection techniques and also described results of in-series coupling experiments with two detectors (*e.g.* fluorescence and electro-

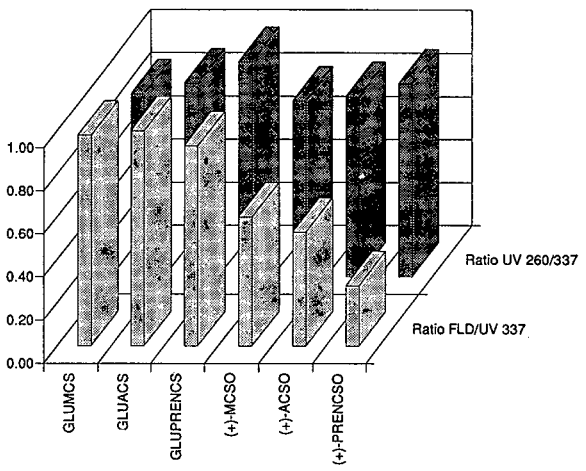

Fig. 3. Graphical representation of detector ratios of derivatized cysteine derivatives. Results were obtained by calculating ratios of integrated peak areas. Ratios were normalized to a value of 1.0 for the largest value calculated. UV = ultraviolet detection; FLD = fluorescence detection.

chemical). In this work, UV detection at two different wavelengths (260 and 337 nm) was combined with fluorescence detection. Optimum detector settings which were consistent with the results of Ziegler and Sticher [25] for (+)-ACSO were λ_{ex} 230 nm and λ_{em} 420 nm. The baseline disturbance in the front region of the chromatogram obtained with UV detection was due to the excess of derivatization reagent and did not interfere with the separation or determination of the cysteine derivatives.

Within the chromatographic system described not only the isomeric pairs GLUACS–GLUPRENCS and (+)-ACSO–(+)-PRENCSO, could be separated, but also epimeric mixtures of the synthesized sulphoxides [*e.g.* (±)-MCSO, see Fig. 1]. The identification and peak purity control of the plant constituents was established by comparing their retention times and the ratios of the signals measured at two different wavelengths or by in-series coupling of UV and fluorescence detection with the corresponding values for the reference substances (Fig. 3). Both detector ratios determined for the γ-glutamyl peptides and the cysteine sulphoxides differed significantly; compared with the cysteine sulphoxides the γ-glutamyl peptides showed increased fluorescence activities and higher UV absorbance values at 260 nm.

The fingerprint chromatogram (Fig. 2) of the garlic bulb samples examined exhibited similar elution profiles for all extracts, whereas the relative concentrations of the eluted substances varied. Under standard chromatographic conditions (+)-S-methyl-L-cysteine sulphoxide [(+)-MCSO], (+)-S-allyl-L-cysteine sulphoxide [alliin, (+)-ACSO], γ-L-glutamyl-S-allyl-L-cysteine (GLUACS) and γ-L-glutamyl-S-(*trans*-1-propenyl)-L-cysteine (GLUPRENCS) were detected in all of the garlic bulb samples analysed. γ-L-Glutamyl-S-methyl-L-cysteine (GLUMCS) could be identified in two garlic bulb samples as a minor compound. (+)-S-(*trans*-1-Propenyl)-L-cysteine sulphoxide [(+)-PRENCSO] occurred in very small amounts. In the extract samples the compound could not be detected by fluorescence detection owing to its low fluorescence activity when compared with UV detection. Further peaks eluted were mainly identified as ubiquitous amino acids (*e.g.* aspartic acid, glutamic acid, glutamine, arginine, alanine; other chromatographic conditions [22]) or γ-glutamyl dipeptides (γ-glutamylmethionine and γ-glutamylphenylalanine [22]). They showed no interference with the S-alk(en)ylcysteine derivatives.

Determination

The relevant major compounds of garlic bulb extracts, (+)-S-allyl-L-cysteine sulphoxide [alliin, (+)-ACSO], γ-L-glutamyl-S-allyl-L-cysteine (GLUACS) and γ-L-glutamyl-S-(*trans*-1-propenyl)-L-cysteine (GLUPRENCS), were determined. To validate the reproducibility and precision of the method described above (method 1) the determination of the γ-glutamyl peptides in garlic bulb samples was performed by an additional chromatographic procedure (method 2). Applying the more specific and sensitive method 1 the cysteine derivatives were separated as their isoindole derivatives and the detection limit of (+)-ACSO was found to be in the picomole range (detection at 337 nm) [25]. Method 2 (see experimental) allowed the isocratic determination of the γ-glutamyl peptides avoiding any chemical reaction. Both systems were calibrated using the pure compounds, (+)-ACSO, GLUACS and GLUPRENCS, as external standards and the linearity of the determination was ensured by regression analysis (eight-point measurements, $r^2 \geqslant 0.997$).

Using method 2, the two γ-glutamyl peptides

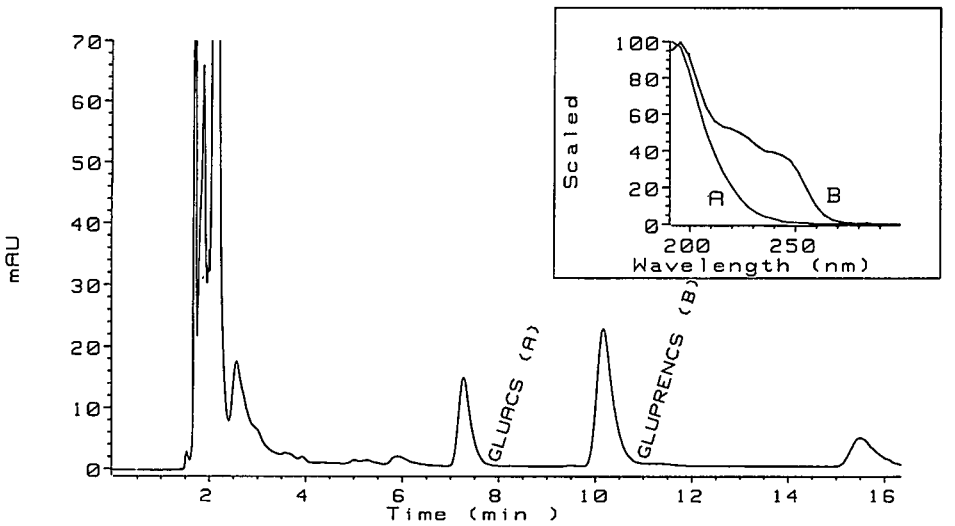

Fig. 4. Chromatogram of a garlic bulb extract according to method 2 with UV detection at 210 nm and on-line recorded UV spectra of the two γ-glutamyl peptides. For conditions, see Experimental.

were separated in an isocratic run within less than 12 min using RP-HPLC. Fig. 4 shows the chromatogram of the separation of a garlic bulb sample. The acidic buffered mobile phase decreased the fronting of the γ-glutamyl peptide peaks due to ionized carboxyl groups. In the chromatographic system described, alliin eluted in the front region of the chromatogram and overlapped with ubiquitous amino

TABLE II

RESULTS OF ALLIIN AND γ-GLUTAMYL PEPTIDE ASSAYS OF SELECTED GARLIC BULB SAMPLES

For conditions, see Experimental.

Sample No.	Origin	Compound	Content (% dry weight)[a]		
			Method 1		Method 2 (210 nm)
			260 nm	337 nm	
I	Switzerland	GLUACS	0.36 (1.38)	0.36 (1.60)	0.35 (1.02)
		GLUPRENCS	0.63 (2.76)	0.63 (2.47)	0.63 (0.87)
		(+)-ACSO	0.98 (2.70)	1.00 (2.31)	–[b]
II	Spain	GLUACS	0.99 (1.23)	0.99 (1.75)	1.02 (0.56)
		GLUPRENCS	0.63 (1.70)	0.63 (1.59)	0.65 (0.87)
		(+)-ACSO	2.62 (2.29)	2.70 (2.43)	–[b]
III	France	GLUACS	1.08 (0.93)	1.09 (0.88)	1.06 (1.58)
		GLUPRENCS	0.59 (2.88)	0.59 (1.18)	0.58 (1.03)
		(+)-ACSO	1.41 (2.51)	1.45 (2.79)	–[b]
IV	Switzerland	GLUACS	1.77 (2.07)	1.78 (1.32)	1.77 (0.86)
		GLUPRENCS	1.44 (1.30)	1.44 (1.60)	1.43 (0.75)
		(+)-ACSO	2.52 (2.06)	2.58 (1.36)	–[b]

[a] Mean (n = 3) with relative standard deviation (%) in parentheses.
[b] Not determined.

acids. Owing to the lack of a chromophoric system, UV detection was performed at 210 nm. Peak identity and homogeneity were established by comparing the retention times and on-line recorded UV spectra of the reference and extract compounds. The detection limit of method 2 at a signal-to-noise ratio of *ca.* 2 was at 20–30 ng of injected γ-glutamyl peptide.

In order to obtain some information on the precision and accuracy of both methods, the recoveries of the reference substances added to the garlic bulb samples prior to extraction were determined. The results indicated complete recovery and suggested that there is no loss of compounds during sample clean-up (Table I).

Yields of sample III (Table II), determined six times applying both methods 1 and 2, revealed no significant difference between the two methods by means of the two-tailed Student's *t*-test. Results of the analyses of several garlic extract samples are summarized in Table II. The relative standard deviations did not exceed 3.0% for GLUACS, GLUPRENCS and (+)-ACSO ($n=3$). Comparable results of the quantitative analyses based on the mean values and the standard deviations were obtained by performing UV detection at either 260 or 337 nm.

The results presented in Table II revealed striking variable contents of all three compounds determined, probably owing to the origin, variety, cultivation, harvesting and storage conditions. Assuming a water content of about 65%, total values of all three compounds constituted up to 2.0% of the fresh material. Varying contents are in agreement with the results of Lawson *et al.* [18] for the γ-glutamyl peptides and Ziegler *et al.* [26] and Iberl *et al.* [27] for alliin. The alliin content was always higher than that of either of the γ-glutamyl peptides. The ratio of the content of the two γ-glutamyl peptides was not constant between the samples tested, although there is a tendency towards higher levels of GLUACS which could be explained with an accelerated transformation of GLUPRENCS during storage [18].

Conclusions

The chromatographic analysis of polar garlic bulb extracts revealed a characteristic pattern of genuine amino acids and dipeptides. (+)-S-Allyl-L-cysteine sulphoxide (alliin), γ-L-glutamyl-S-allyl-L-cysteine and γ-L-glutamyl-S-(*trans*-1-propenyl)-L-cysteine were found to be the major cysteine derivatives of garlic bulbs. They are not only the main compounds in garlic under the conditions described but as sulphur-containing constituents also relevant for *Allium* species in general.

The assay method presented emphasized the occurrence of two main groups of cysteine derivatives in garlic: the sulphoxides and the γ-glutamyl peptides. Biosynthetic investigations confirmed the latter to be precursors of the cysteine sulphoxide derivatives [28]. Their qualitative and quantitative determination including fingerprint profiles, provided some information for quality control of the raw material and of pharmaceutical garlic preparations and should also be suitable for investigations of the pattern of cysteine derivatives in various *Allium* species.

In addition, the three cysteine derivatives are prodrugs and could therefore act as marker compounds for the pharmacologically active transformation products. Their yield in garlic samples provides concise information about the proportion of the various known transformation products to be formed, *e.g.*, after enzymatic conversion.

ACKNOWLEDGEMENTS

Financial support from the Alpha Foundation (Fribourg, Switzerland) is gratefully acknowledged. We thank Dr. S.J. Ziegler for the synthesis of alliin and (±)-S-methyl-L-cysteine sulphoxide and Dr. L.D. Lawson for supplying γ-L-glutamyl-S-methyl-L-cysteine as reference compound.

REFERENCES

1 G. R. Fenwick and A. B. Hanley, *CRC Crit. Rev. Food Sci. Nutrit.*, 22 (1985) 296.
2 J. R. Whitaker, *Adv. Food Res.*, 22 (1976) 199.
3 E. Block, S. Ahmad, J. L. Catalfamo, M. K. Jain and R. Apitz-Castro, *J. Am. Chem. Soc.*, 108 (1986) 7045.
4 G. Blania and B. Spangenberg, *Planta Med.*, 57 (1991) 371.
5 M. H. Brodnitz, J. V. Pascale and L. Van Derslice, *J. Agric. Food Chem.*, 19 (1971) 273.
6 B. Iberl, G. Winkler and K. Knobloch, *Planta Med.*, 56 (1990) 202.
7 H. Jansen, B. Müller and K. Knobloch, *Planta Med.*, 53 (1987) 559.

8 J. Koch, L. Berger and Ch. Vieregge-Reiter, *Planta Med.*, 55 (1989) 327.
9 I. Laakso, T. Seppänen-Laakso, R. Hiltunen, B. Müller, H. Jansen and K. Knobloch, *Planta Med.*, 55 (1989) 257.
10 B. Müller, *Dtsch. Apoth. Ztg.*, 129 (1989) 2500.
11 G. Vernin, J. Metzger, D. Fraisse and C. Scharff, *Planta Med.*, 52 (1986) 96.
12 M. Voigt and E. Wolf, *Dtsch. Apoth. Ztg.*, 126 (1986) 591.
13 H. D. Reuter, *Spektrum Allium sativum L.*, Aesopus, Zug, 1988.
14 H. Wagner, M. Wierer and B. Fessler, *Planta Med.*, 53 (1987) 305.
15 A. Sendl, G. Elbl, B. Steinke, K. Redl, W. Breu and H. Wagner, *Planta Med.*, 58 (1992) 1.
16 S. J. Ziegler and O. Sticher, *Planta Med.*, 55 (1989) 372.
17 E. Mochizuki, A. Nakayama, Y. Kitada, K. Saito, H. Nakazawa, S. Suzuki and M. Fujita, *J. Chromatogr.*, 455 (1988) 271.
18 L. D. Lawson, Z-Y. Wang and B. G. Hughes, *J. Nat. Prod.*, 54 (1991) 436.
19 J. E. Lancaster and K. E. Kelly, *J. Sci. Food Agric.*, 34 (1983) 1229.
20 F.-J. Kappenberg and H. Glasl, *Pharm. Ztg. Wiss.*, 135 (1990) 189.
21 S. J. Ziegler, *Thesis*, ETH Zürich, No. 8721, 1988.
22 M. Mütsch-Eckner, *Thesis*, ETH Zürich, No. 9462, 1991.
23 H. Jansen, B. Müller and K. Knobloch, *Planta Med.*, 55 (1989) 434.
24 Sz. Nyiredy, B. Meier, C. A. J. Erdelmeier and O. Sticher, *J. High Resolut. Chromatogr. Chromatogr. Commun.*, 8 (1985) 186.
25 S. J. Ziegler and O. Sticher, *J. High Resolut. Chromatogr. Chromatogr. Commun.*, 11 (1988) 639.
26 S. J. Ziegler, B. Meier and O. Sticher, *Dtsch. Apoth. Ztg.*, 129 (1989) 318.
27 B. Iberl, G. Winkler, B. Müller and K. Knobloch, *Planta Med.*, 56 (1990) 320.
28 J.E. Lancaster and M.L. Shaw, *Phytochemistry*, 28 (1989) 455.

Journal of Chromatography, 625 (1992) 191–198
Elsevier Science Publishers B.V., Amsterdam

CHROM. 24 552

Anomalous reversed-phase high-performance liquid chromatographic behavior of synthetic peptides related to antigenic helper T cell sites

Klaus Büttner*, Clemencia Pinilla, Jon R. Appel and Richard A. Houghten

Torrey Pines Institute for Molecular Studies, 3550 General Atomics Court, San Diego, CA 92121 (USA)

(First received June 15th, 1992; revised manuscript received August 7th, 1992)

ABSTRACT

Sets of overlapping synthetic peptides for three well characterized proteins (sperm whale myoglobin, hen egg lysozyme, and the circumsporozoite protein from *Plasmodium falciparum*) were prepared and examined by reversed-phase high-performance liquid chromatography (RP-HPLC). Using retention coefficients to predict the retention time of each peptide, several peptides in each protein set were found that exhibited anomalous behavior (*i.e.* eluted significantly later than predicted). Previous work with model peptides has shown that this anomalous behavior can be attributed to specific amphipathic arrangements induced by the lipid stationary phase during the RP-HPLC process. In the current study it was found that although not all of the peptides containing an antigenic T cell site displayed anomalously late behavior, all of the peptides which eluted anomalously late during RP-HPLC included the regions of these proteins known from earlier studies to be antigenic T cell sites.

INTRODUCTION

T cell immune response involves a multi-step process that begins with the internalization of a foreign protein antigen by antigen presenting cells (APC). The protein antigen is then unfolded and/or processed into smaller peptide fragments by a still incompletely understood mechanism. These peptide fragments are then presented in association with class I or class II major histocompatilitity complex (MHC) membrane protein on the surface of the APC. The specific T cell receptors that recognize the peptide antigen-MHC protein bimolecular complex initiate T cell activation and proliferation. It has been proposed that the processed antigen adopts, maintains, and/or is induced into a specific conformation which is stabilized by hydrophobic forces upon its interaction with MHC [1,2]. In a recent review [3], however, evidence was presented for and against the fact that T cell determinants adopt specific secondary structures. Also, a number of prediction programs based on secondary structural motifs have been developed to identify potential antigenic T cell sites [1,4–7]. Nevertheless, the fact that T cell recognition requires that a protein antigen be processed, and ultimately presented as defined peptide fragments, permits the use of synthetic peptides for the study of the structural requirements of antigenic T cell sites.

In aqueous solution, peptides exist in a vast number of conformational arrays which are ultimately dependent upon a given peptide's amino acid sequence. However, in lipid or other hydrophobic environments, peptides display highly ordered and/or stabilized conformations [8]. We and others have found that reversed-phase high performance liquid chromatography (RP-HPLC) is a simple and useful

Correspondence to: Dr. R. A. Houghten, Torrey Pines Institute for Molecular Studies, 3550 General Atomics Court, San Diego, CA 92121, USA.

* Present address: Fournier Pharma GmbH, Justus-von-Liebig Strasse 16, D-6603 Sulzbach, Germany.

0021-9673/92/$05.00

tool for the study of induced secondary structure of peptides [9–12]. As a simple model system, the aqueous mobile phase and the octadecyl (C_{18}) of the stationary phase can be considered to mimic the anisotropic aqueous–lipid environment which exists when peptides interact with membranes. We reasoned that if a correlation could be found between induced secondary structure of peptides (as determined by RP-HPLC retention times) and antigenic T cell sites (given their postulated tendency to adopt α-helical amphipathic structures [1]) then RP-HPLC could be used to determine the antigenic T cell sites of proteins.

Retention coefficients have been widely used for the prediction of the retention times of peptides during RP-HPLC [13,14]. These values, which are based solely on the amino acid composition (irrespective of sequence) of a peptide, involve the assignment of specific, empirically determined hydrophobicity values for each amino acid. We have found, however, that a significant number of peptides exhibit anomalous RP-HPLC behavior relative to their predicted retention times [15,16]. We reasoned that differences between the theoretically calculated and experimentally determined retention times must result from specific conformational effects induced during the RP-HPLC process. For instance, in studies involving model peptides expected to have amphipathic conformations when induced into an α-helix, decreases in RP-HPLC retention times correlated well with the expected perturbations in amphipathicity caused by single residue substitutions [12,17–19].

In the current study we prepared complete sets of overlapping peptides for three proteins for which helper T cell determinants have been identified, namely sperm whale myoglobin (SWM), hen egg lysozyme (HEL), and the circumsporozoite protein (CSP) of *Plasmodium falciparum*. The RP-HPLC behavior of the peptides in each series (*i.e.*, the differences found between predicted and experimentally determined retention times) was then correlated with the MHC class II antigenic helper T cell sites for each of these three proteins.

EXPERIMENTAL

Peptide synthesis

Peptide resins were synthesized using the method of simultaneous multiple peptide synthesis [20] using Boc chemistry. Twenty-four peptide resins were cleaved simultaneously by liquid hydrogen fluoride using a multiple vessel cleavage apparatus [21]. Peptide purity was determined by analytical RP-HPLC (pH 2.1). Purities of the crude peptides ranged from 70 to 85%. No further purification or analyses were carried out. Numbering for each set of overlapping synthetic peptides was begun at the N-terminus of each of the three proteins. The peptides for the SWM and HEL were 15 residues in length and overlapped by 5 residues (*i.e.*, 1–15, 6–20, 11–25, etc.), resulting in a total of 29 peptides for SWM and 24 peptides for HEL. In the case of CSP 22, 20-residue peptides were prepared which overlapped by 10 residues(*i.e.*, 1–20, 11–30, etc.). The central repeat region of the protein (NANP 121–292) was not included.

Reversed-phase high-performance liquid chromatography

The RP-HPLC system utilized consisted of two Altex Model 110A pumps, a Beckman Model 421 microprocessor (Beckman Instruments, Anaheim, CA, USA), a Hitachi Model 100-20 variable-wavelength spectrophotometer (Baxter Scientific Products, Los Angeles, CA, USA), a Shimadzu CR3A integrator (Cole Scientific, Calabasas, CA, USA) and a Bio-Rad Model AS-48 autosampler (Bio-Rad Labs., Richmond, CA, USA). Samples (20 μl, 0.2 mg/ml) were analyzed on Vydac 218TP54 C_{18} columns, 250 mm × 4.6 mm I.D., 5 μm particle size (Alltech Assoc., Los Altos, CA, USA), and a solvent system consisting of buffer A (0.01 *M* $(NH_4)_2HPO_4$, pH 7.0) and buffer B (acetonitrile) was used. A 1% gradient consisting of 5% B to 50% B in 45 min was used throughout. Elution was measured at 215 nm. The experimentally determined retention times of each peptide were normalized by the inclusion of the same peptide reference standard in each run to eliminate deviations in the results due to variations in column performance and injection times.

Retention time prediction

A modification based on Meek's procedure [22] for the calculation of the individual retention coefficients for each amino acid was used. The differences in predicted and experimentally determined reten-

tion times were averaged and a standard deviation was calculated for each set of synthetic peptides associated with the three proteins. Peptides found to have differences in retention times that exceeded ±1 S.D. standard deviation from the average were considered to exhibit anomalous elution behavior during the RP-HPLC process.

RESULTS

Sperm whale myoglobin

The RP-HPLC elution behavior for the 29 overlapping peptides of SWM are shown in Table I. The average difference between the experimentally determined and predicted retention times (Δ retention time) of the peptides of the SWM series were found to be −0.8 min with an S.D. of 3.3 min (Fig. 1). RP-HPLC elution behavior within ±1 S.D. of the average was found for 22 of the 29 peptides. Four peptides eluted significantly later than predicted in the SWM series, namely, peptide 4 (SWM 16–30), peptide 14 (SWM 66–80), peptide 22 (SWM 106–120), and peptide 26 (SWM 126–140). The majority of the residues of these 4 peptides correspond to regions of the SWM sequence that have been reported to be antigenic helper T cell sites for MHC class II (Table I, ref. 23).

Hen egg lysozyme

The RP-HPLC elution behavior of the 24 overlapping peptides of HEL are shown in Table II. The differences between the experimentally determined

TABLE I

RETENTION TIMES FOR OVERLAPPING PEPTIDES OF SWM

No.	Peptide residue	Sequence	RP-HPLC retention time (min)			Known T cell site[a]
			Experimental	Predicted	Experimental − predicted	
1	1–15	VLSEGEWQLVLHVWA-NH_2	28.5	32.6	−4.1	
2	6–20	EWQLVLHVWAKVEAD-NH_2	28.9	28.5	0.4	
3	11–25	LHVWAKVEADVAGHG-NH_2	23.7	23.4	0.2	
4	16–30	KVEADVAGHGQDILI-NH_2	23.7	20.3	3.4	15–22
5	21–35	VAGHGQDILIRLFKS-NH_2	31.0	29.5	1.5	
6	26–40	QDILIRLFKSHPETL-NH_2	29.8	29.6	0.2	
7	31–45	RLFKSHPETLEKFDR-NH_2	20.3	25.0	−4.7	
8	36–50	HPETLEKFDRFKHLK-NH_2	21.4	25.1	−3.8	
9	41–55	EKFDRFKHLKTEAEM-NH_2	21.8	22.2	−0.4	
10	46–60	FKHLKTEAEMKASED-NH_2	17.6	17.7	−0.1	
11	51–65	TEAEMKASEDLKKHG-NH_2	10.2	13.6	−3.3	
12	56–70	KASEDLKKHGVTVLT-NH_2	18.2	20.9	−2.7	
13	61–75	LKKHGVTVLTALGAI-NH_2	30.2	29.8	0.5	
14	66–80	VTVLTALGAILKKKG-NH_2	38.7	29.8	8.9	70–78
15	71–85	ALGAILKKKGHHEAE-NH_2	20.2	20.7	−0.5	
16	76–90	LKKKGHHEAELKPLA-NH_2	17.2	21.4	−4.3	
17	81–95	HHEAELKPLAQSHAT-NH_2	15.3	17.9	−2.7	
18	86–100	LKPLAQSHATKHKIP-NH_2	15.5	24.4	−8.9	
19	91–105	QSHATKHKIPIKYLE-NH_2	21.4	23.4	−2.0	
20	96–110	KHKIPIKYLEFISEA-NH_2	28.4	28.3	0.1	
21	101–115	IKYLEFISEAIIHVL-NH_2	35.1	34.6	0.6	
22	106–120	FISEAIIHVLHSRHP-NH_2	35.1	30.2	4.9	106–118
23	111–125	IIHVLHSRHPGDFGA-NH_2	26.3	27.4	−1.1	
24	116–130	HSRHPGDFGADAQGA-NH_2	12.9	15.2	−2.3	
25	121–135	GDFGADAQGAMNKAL-NH_2	16.2	19.3	−3.0	
26	126–140	DAQGAMNKALELFRK-NH_2	28.1	23.1	5.0	132–153
27	131–145	MNKALELFRKDIAAK-NH_2	25.6	26.4	−0.9	
28	136–150	ELFRKDIAAKYKELG-NH_2	21.1	24.6	−3.5	
29	141–153	DIAAKYKELGYQG-NH_2	18.2	19.0	−0.8	

[a] Reported helper T cell sites as reviewed by Millich [23].

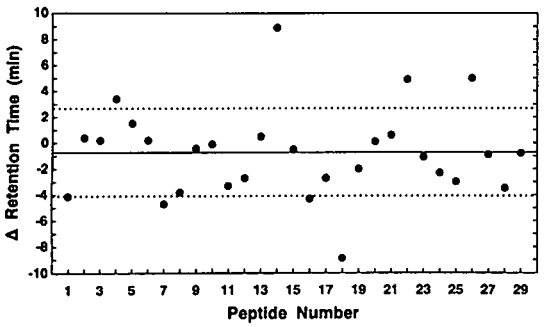

Fig. 1. RP-HPLC elution behavior for overlapping peptides of SWM. Each solid circle represents differences between the experimental retention time and the predicted retention time for each peptide. The solid line represents the average of the differences in the retention times for this set of peptides. The dotted lines represent ±1 S.D. from the average.

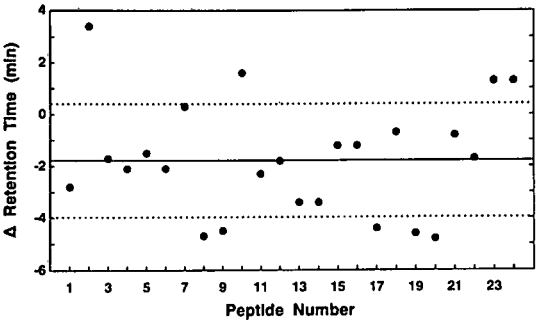

Fig. 2. RP-HPLC elution behavior for overlapping peptides of HEL. Each solid circle represents differences between the experimental retention time and the predicted retention time for each peptide. The solid line represents the average of the differences in the retention times for this set of peptides. The dotted lines represent ±1 S.D. from the average.

and predicted retention times for each peptide of the HEL series were found to average −1.8 min with an S.D. of 2.2 min (Fig. 2). RP-HPLC elution behavior for 15 of the 24 peptides fell within ±1 S.D. (2.2 min) of the average (−1.8 min). Four peptides eluted significantly later than predicted, name-

TABLE II

RETENTION TIMES FOR OVERLAPPING PEPTIDES OF HEL

No.	Peptide residue	Sequence	RP-HPLC retention time (min)			Known T cell site[a]
			Experimental	Predicted	Experimental − predicted	
1	1–15	KVFGRCELAAAMKRH-NH_2	23.1	26.0	−2.8	
2	6–20	CELAAAMKRHGLDNY-NH_2	25.2	21.8	3.4	1–18
3	11–25	AMKRHGLDNYRGYSL-NH_2	22.1	23.9	−1.7	
4	16–30	GLDNYRGYSLGNWVC-NH_2	25.0	27.0	−2.1	
5	21–35	RGYSLGNWVCAAKFE-NH_2	26.5	28.0	−1.5	
6	26–40	GNWVCAAKFESNFNT-NH_2	24.5	26.7	−2.1	
7	31–45	AAKFESNFNTQATNR-NH_2	20.7	20.4	0.3	
8	36–50	SNFNTQATNRNTDGS-NH_2	10.8	15.6	−4.7	
9	41–55	QATNRNTDGSTDYGI-NH_2	10.7	15.2	−4.5	
10	46–60	NTDGSTDYGILQINS-NH_2	20.6	18.9	1.6	46–61
11	51–65	TDYGILQINSRWWCN-NH_2	28.7	31.0	−2.3	
12	56–70	LQINSRWWCNDGRTP-NH_2	26.0	27.8	−1.8	
13	61–75	RWWCNDGRTPGSRNL-NH_2	22.5	25.9	−3.4	
14	66–80	DGRTPGSRNLCNIPC-NH_2	17.0	20.5	−3.4	
15	71–85	GSRNLCNIPCSALLS-NH_2	25.8	27.0	−1.2	
16	76–90	CNIPCSALLSSDITA-NH_2	24.2	25.4	−1.2	
17	81–95	SALLSSDITASVNCA-NH_2	18.6	23.0	−4.4	
18	86–100	SDITASVNCAKKIVS-NH_2	21.1	21.9	−0.7	
19	91–105	SVNCAKKIVSDGDGM-NH_2	14.5	19.1	−4.6	
20	96–110	KKIVSDGDGMNAWVA-NH_2	17.9	22.7	−4.8	
21	101–115	DGDGMNAWVAWRNRC-NH_2	23.3	24.2	−0.8	
22	106–120	NAWVAWRNRCKGTDV-NH_2	24.2	26.0	−1.7	
23	111–125	WRNRCKGTDVQAWIR-NH_2	28.9	27.6	1.3	112–129
24	116–129	KGTDVQAWIRGCRL-NH_2	27.2	25.9	1.3	112–129

[a] Reported helper T cell sites as reviewed by Millich [23].

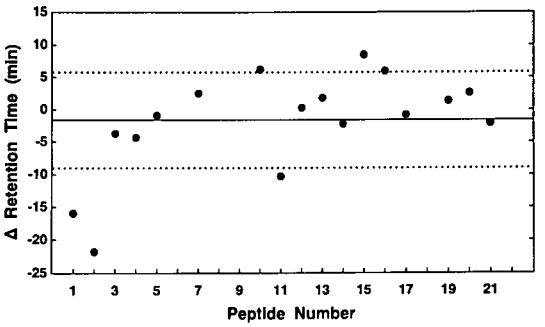

Fig. 3. RP-HPLC elution behavior for overlapping peptides of CSP. Each solid circle represents differences between the experimental retention time and the predicted retention time for each peptide. The solid line represents the average of the differences in the retention times for this set of peptides. The dotted lines represent ±1 S.D. from the average.

ly peptide 2 (HEL 6–20), peptide 10 (HEL 46–60), peptide 23 (HEL 111–125), and peptide 24 (HEL 116–129). The majority of the residues in each of these peptides are found in known HEL antigenic helper T cell sites for MHC class II (Table II, ref. 23).

Circumsporozoite protein

The RP-HPLC elution behavior of the 22 overlapping peptides of CSP are shown in Table III. The differences between the experimentally determined and predicted retention times for each peptide of the CSP series were found to average −1.8 min with a standard deviation of 7.4 min [Fig. 3]. RP-HPLC elution behavior was found for 11 of the 22 peptides fell within ±1 S.D. (7.4 min) of the average (−1.8 min). Peptides 10 (CSP 91–110), 15 (321–340), and 16 (331–350) eluted significantly later than predicted. The regions of CSP represented by peptides 15 and 16 correspond to the antigenic helper T cell sites found for both mice (IA^k) and humans (Table III, refs. 24 and 25). CSP 91–110 borders a region that is a known antigenic T cell site in hu-

TABLE III

RETENTION TIMES FOR OVERLAPPING PEPTIDES OF CSP

No.	Peptide residue	Sequence	RP-HPLC retention time (min)			Known T cell site[a]
			Experimental	Predicted	Experimental − predicted	
1	1–20	MMRKLAILSVSSFLFVEALF-NH_2	33.2	29.1	−15.9	
2	11–30	SSFLFVEALFQEYQCYGSSS-NH_2	13.1	34.9	−21.8	
3	21–40	QEYQCYGSSSNTRVLNELNY-NH_2	19.9	23.6	−3.7	
4	31–50	NTRVLNELNYDNAGTNLYNE-NH_2	18.3	22.5	−4.3	
5	41–60	DNAGTNLYNELEMNYYGKQE-NH_2	18.8	19.7	−0.9	
6	51–70	LEMNYYGKQENWYSLKKNSR-NH_2	N.D.[b]	26.2		
7	61–80	NWYSLKKNSRSLGENDDGNN-NH_2	21.1	18.6	2.5	
8	71–90	SLGENDDGNNNNGDNGRFGK-NH_2	N.D.	4.5		
9	81–100	NNGDNGREGKDEDKRDGNNE-NH_2	N.D.	0.6		
10	91–110	DEDKRDGNNEDNEKLRKPKH-NH_2	11.9	5.7	6.2	103–122
11	101–120	DNEKLRKPKHKKLKQPGDGN-NH_2	5.6	15.8	−10.3	
12	291–310	NQGNGQGHNMPMDPNRNVDE-NH_2	12.6	12.3	0.3	
13	301–320	PNDPNRNVDENANANNAVKN-NH_2	11.6	9.8	1.8	
14	311–330	NANANNAVKNNNNEEPSDKH-NH_2	5.9	8.1	−2.2	
15	321–340	NNNEEPSDKHIEQYLKKIKN-NH_2	24.4	15.9	8.5	326–343
16	331–350	IEQYLKKIKNSISTEWSPCS-NH_2	34.2	28.2	6.0	326–343
17	341–360	SISTEWSPCSVTCGNGIQVR-NH_2	25.3	26.1	−0.8	
18	351–370	VTCGNGIQVRIKPGSANKPK-NH_2	N.D.	24.1		
19	361–380	IKPGSANKPKDELDYENDIE-NH_2	14.8	13.4	1.4	
20	371–390	DELDYENDIEKKICKMEKCS-NH_2	18.4	15.8	2.6	
21	381–400	KKICKMEKCSSVFNVVNSSI-NH_2	27.7	29.8	−2.1	
22	391–412	SVFNVVNSSIGLIMVLSFLFLN-NH_2	N.D.	49.2		

[a] Reported helper T cell sites as reviewed by Millich [23].
[b] N.D. = Not determined.

mans [26]. The experimental retention times could not be determined in this RP-HPLC system utilized for peptides 6, 8, 9, 18, and 22 due to insolubility or extreme hydrophilicity.

DISCUSSION

In earlier studies, RP-HPLC was found to be useful in the determination of induced secondary structures of peptides [10,12,17–19]. In the current study, this method was extended to examine the correlation of induced peptide structure as evidenced by anomalous RP-HPLC retention time behavior with the known antigenic T cell sites of three proteins. SWM, HEL, and CSP were chosen for this study because their T cell sites have been extensively characterized for both mice and humans (reviewed in ref. 23). The predicted retention time of each peptide used in this study was calculated using retention coefficients [13,14,22]. It was hoped that this approach would permit RP-HPLC to be used as a functional model system for the interaction of peptides with class II MHC as well as for the prediction of T cell sites in proteins.

Peptides with an intrinsic potential for the adoption of amphipathic α-helical conformations have been shown to have increased retention times relative to their elution times calculated using retention coefficients [12,17–19]. This behavior can be explained if one assumes that a specific amphipathic secondary structure for these peptides is induced during hydrophobic interaction of their side chains with the C_{18} of the stationary phase of RP-HPLC. This is not only intuitively reasonable but also reflects an energy-minimized ordered conformation in which an amphipathic arrangement of the peptide's amino acid side-chains has occurred in which all of the hydrophobic residues interact optimally with the lipid-like C_{18} stationary phase while the internal hydrogen bonding expected for α-helices is maintained. Based on these earlier findings, we examined overlapping peptides spanning three different proteins in an effort to correlate their known MHC class II antigenic T cell sites with their RP-HPLC behavior. This approach is based on the assumption that the basic principles of partitioning of a peptide's amino acid side-chain between the solvent and the C_{18} lipid layer of the stationary phase during RP-HPLC are analogous to those involved in peptide–MHC-T cell interactions. Physiological pH conditions were utilized during RP-HPLC for the determination of retention coefficients and retention times.

The most striking finding in this study was that for the three proteins examined all of the peptides which eluted significantly later than predicted corresponded to regions of known T cell helper sites (11 peptides). Peptides 4, 14, 22, and 26, covering the SWM sequence 16–30, 66–80, 106–120 and 126–140, respectively, were found to elute significantly later than predicted (Table I) suggesting that an amphipathic conformation was induced during RP-HPLC for each peptide. In a recent study, a synthetic peptide comprising residues 102–118 of SWM (corresponding to peptide 22, SWM 106–120, from this study) was found by circular dichroism spectroscopy to be 80% helical [in 50% trifluoroethanol (TFE)] and is known to be an immunodominant helper T cell site [27–29]. In the same study SWM 132–146 was found to be 35–40% helical (in 60% TFE). In the current study, peptide 26 (SWM 126–140) shares nine residues with SWM 132–146 and is amphipathic when viewed in a helical wheel array. This region has also been suggested to be an immunodominant T cell site for SWM [28,29]. Myoglobin, however, consists of six amphipathic helical regions folded against one another and the current analysis for this protein may therefore contain an inherent selection bias for amphipathic peptides.

For the CSP, peptides 10, 15, and 16, corresponding to CSP 91–110, CSP 321–340, and CSP 331–350, were found to elute significantly later than their predicted times. Peptides 15 and 16 are found in the polymorphic region of CSP and correspond to a previously determined immunodominant T cell site [24,25]. The peptides chosen to be studied by Good and co-workers [24,25] were selected based on predictive algorithms for amphipathicity and therefore are expected to be biased in the current study [1]. Peptide 10 shares less than half (8 of 20 residues) of known antigenic helper T cell site CSP 103–122 (26), however, peptide 11 (CSP 101–120), which eluted earlier than predicted, contains nearly this entire T cell site. These results suggest that α-helical amphipathicity may not be the sole structural motif responsible for T cell antigenicity. Antigenic helper T cell sites have also been found in earlier studies for CSP 300–310 and CSP 361–380

[25], however, the peptides representing these regions display no anomalous behavior during RP-HPLC. It must also be pointed out that experimental retention times for peptides 6 (CSP 51–70), 8 (CSP 71–90), 9 (81–100), 18 (351–370), and 22 (CSP 391–412) could not be determined in this system due to their extreme hydrophilic nature or poor solubility.

For the HEL peptides 2, 10, 23, and 24, respectively, covering sequences 6–20, 46–60, 111–125, and 116–129, eluted significantly later than predicted (Table II). All of these peptides correspond to reported T cell sites [23]. Since peptides 23 and 24 overlap each other by only 5 amino acids, they are essentially representing only one T cell site. Peptide 10 (46–60) includes the majority of a region of HEL which has been found to be an immunodominant helper T cell site for HEL [30,31]. By helical wheel representation this peptide is amphipathic. Another known immunodominant helper T cell site is HEL 74–86 [32], however, in the current study peptides representing this region of HEL displayed no anomalous behavior by RP-HPLC. HEL is known to have little or no helical nature and is the least likely of the three proteins examined here to contain inherent bias.

The peptides which elute significantly earlier than predicted for each of the proteins studied (Tables I–III) illustrate a markedly different and unclear behavior. One possible explanation for this behavior may be that prior to interaction with the C_{18}, they fold back upon themselves, or become self-associated by hydrophobic interactions, thus exposing only their hydrophilic residues while shielding their hydrophobic residues. This would be expected to effectively decrease the interaction of the hydrophobic residues with the C_{18} and cause the peptide to elute earlier. Additionally, 3 out of the 5 HEL peptides which eluted significantly earlier than predicted correspond to known antigenic helper T cell sites. This also suggests that there may be other conformational arrays (such as the self-interaction of 2 peptides linked by a disulfide bridge) which bind to MHC class II in addition to single amphipathic α-helices.

Every peptide found to elute later than predicted for the three proteins studied contained regions of reported helper T cell sites, and the majority could be configured into an amphipathic array. As found in this study, however, it is evident that amphipathicity may not be the only secondary structural feature governing T cell antigenicity since a number of known helper T cell sites were not confirmed by this method. Those peptides which eluted significantly earlier than predicted, and correspond to known antigenic helper T cell sites, may adopt other structural motifs in their MHC class II interaction. Conformational studies using circular dichromism spectroscopy to determine the secondary structure of those peptides found to exhibit anomalous RP-HPLC behavior would be useful in clarifying alternative structural motifs. If one considers just immunodominant T cell sites for these 3 proteins, 4 out of 7 peptides containing regions of immunodominant T cell sites were found to elute significantly later than their predicted retention times. In conclusion, we have found RP-HPLC to be a useful tool for the study of induced secondary structure of peptides.

ACKNOWLEDGEMENTS

The authors wish to thank Eileen Silva for her help in preparing this manuscript. This work was supported in part by National Science Foundation Grant (DIR8713707).

REFERENCES

1 J. L. Spouge, H. R. Guy, J. L. Cornette, H. Margalit, K. Cease, J. A. Berzofsky and C. Delisi, *J. Immunol.*, 138 (1987) 204.
2 J. A. Berzofsky, *Immunol. Lett.*, 18 (1988) 83.
3 P. Kourilsky and J.M Claverie, in F. J. Dixon (Editor), *Advances in Immunology*, Vol. 45, Academic Press, San Diego, CA, 1989, p.107.
4 H. Margalit, J. L. Spouge, J. L. Cornette, K. B. Cease, C. Delisi and J. A. Berzofsky, *J. Immunol.*, 138 (1987) 2213.
5 C. J. Stille, L. J. Thomas, V. E. Reyes and R. E. Humphreys, *Mol. Immunol.*, 24 (1987) 1021.
6 J. B. Rothbard and W. R. Taylor, *EMBO J.*, 7 (1988) 93.
7 S. Fraga, E. San-Fabian, S. Thornton and B. Singh, *J. Mol. Recognit.*, 3 (1990) 65.
8 E. T. Kaiser and F. J. Kézdy, *Proc. Natl. Acad. Sci. U.S.A.*, 80 (1983) 1137.
9 W. R. Melander and C. Horvath, in C. Horvath (Editor), *High Performance Liquid Chromatography*, Academic Press, San Diego, CA, 1980, p. 224.
10 W. S. Hancock, D. R. Knighton and D. R. K. Harding, in U. Ragnarsson (Editor), *Peptides 1984: Proceedings of the 18th European Peptide Symposium*, Almqvist & Wiksell International, Stockholm, 1984, p.145.

11 N. E. Zhou, C. T. Mant and R. S. Hodges, *Pept. Res.*, 3 (1990) 8.
12 J. M. Ostresh, K. Büttner and R. A. Houghten, in R. Hodges (Editor), *HPLC of Peptides and Proteins: Separation, Analysis and Conformation,* CRC Press, Boca Raton, FL, 1991, p. 633.
13 J. L. Meek and Z. L. Rossetti, *J. Chromatogr.*, 211 (1981) 15.
14 T. Sasagawa, T. Okuyama and D. C. Teller, *J. Chromatogr.*, 240 (1982) 329.
15 R. A. Houghten and S. T. DeGraw, *J. Chromatogr.*, 386 (1987) 223.
16 R. A. Houghten and J. M. Ostresh, *Biochromatography*, 2 (1987) 80.
17 K. Büttner, O. Arad, J. Ostresh and R. A. Houghten, in R. Epton (Editor), *Innovation and Perspectives in Solid Phase Synthesis,* Solid Phase Conference Coordination, Oxford, 1990, p. 325.
18 S. E. Blondelle and R. A. Houghten, *Pept. Res.*, 4 (1991) 12.
19 S. E. Blondelle and R. A. Houghten, *Biochemistry*, 30 (1991) 4671.
20 R. A. Houghten, *Proc. Natl. Acad. Sci. U.S.A.*, 82 (1985) 5131.
21 R. A. Houghten, M. K. Bray, S. T. DeGraw and C. J. Kirby, *Int. J. Pept. Protein Res.*, 27 (1986) 673.
22 D. Guo, C. T. Mant, A. K. Tameja, J. M. R. Parker and R. S. Hodges, *J. Chromatogr.*, 359 (1986) 499.
23 D. R. Milich, in F. J. Dixon (Editor), *Advances in Immunology*, Vol. 45., Academic Press, San Diego, CA, 1989, p.195.
24 M. F. Good, W. L. Maloy, M. N. Lunde, H. Margalit, J. L. Cornette, G. L. Smith, B. Moss, L. H. Miller and J. A. Berzofsky, *Science*, 235 (1987) 1059.
25 M. F. Good, D. Pombo, W. E. Maloy, V. F. de la Cruz, L. H. Miller and J. A. Berzofsky, *J. Immunol.*, 140 (1988) 1645.
26 F. Sinigaglia, M. Gutttinger, D. Gillenssen, D. M. Doran, B. Takacs, H. Matile, A. Trzeciak and J. R. Pink, *Eur. J. Immunol.*, 18 (1988) 633.
27 L. R. Lark, J. A. Berzofsky and L. M. Gierasch, *Pept. Res.*, 2 (1989) 314.
28 I. Berkower, H. Kawamura, L. A. Matis and J. A. Berzofsky, *J. Immunol.*, 135 (1985) 2628.
29 I. Berkower, G. K. Buckenmeyer and J. A. Berzofsky, *J. Immunol.*, 136 (1986) 2498.
30 S. Bixler, T. Yoshida and M. Z. Atassi, *Immunology*, 56 (1985) 103.
31 P. M. Allen, D. J. McKean, B. N. Beck, J. Sheffield and L. H. Glimcher, *J. Exp. Med.*, 162 (1985) 1264.
32 N. Shastri, A. Oki, A. Miller and E. E. Sercarz, *J. Exp. Med.*, 162 (1985) 332.

Journal of Chromatography, 625 (1992) 199–206
Elsevier Science Publishers B.V., Amsterdam

CHROM. 24 562

Evaluation of peptide–peptide interactions using reversed-phase high-performance liquid chromatography

Sylvie E. Blondelle, Klaus Büttner* and Richard A. Houghten

Torrey Pines Institute for Molecular Studies, 3550 General Atomics Court, San Diego, CA 92121 (USA)

(First received June 2nd, 1992; revised manuscript received August 14th, 1992)

ABSTRACT

The separation of peptides during RP-HPLC depends mainly upon differential hydrophobic interactions of the individual peptides being separated with the C_{18} group of the stationary phase. We have examined the behavior of dimeric disulfide-linked model peptides during RP-HPLC in order to study self-induced conformational effects. A set of 18 analogues of the amphipathic α-helical sequence Ac-LKLLKKLLKKLKKLLKKL-NH_2 was used for this study. These analogues differed only by the successive replacement of each position with a cysteine. Strong peptide–peptide interactions, occurring through interchain hydrophobic forces, resulted in a presenting face to the C_{18} group, consisting primarily of lysine residues and, in turn, in early retention times. Three homo-dimers were also found to be strongly α-helical in water as determined by circular dichroism spectroscopy.

INTRODUCTION

The induced secondary structures of peptides, such as amphipathic α-helicity [1], are known to be essential for many peptide–peptide or peptide–protein interactions. Examples include the binding of melittin [2], or specific model amphipathic peptides [3,4], to calmodulin. Amphipathicity, as well as other general structural effects such as dipole–dipole interactions [5], hydrophobic interactions [6], and salt bridge formation [7], have also been established as important stabilizing elements in peptide and protein tertiary and quaternary structures.

Hydrophobic forces, which dominate peptide–peptide interactions as well as protein folding and stability, are generally counterbalanced by the solvation of hydrophilic residues which renders the proteins soluble in water. As a result, in globular proteins hydrophilic external surfaces interact with and are solvated by water, whereas hydrophobic amino acids are "buried" and form a lipid-core environment [6]. Often, hydrophilic–hydrophobic amino acid segregation follows an initial non-specific binding of a peptide to a protein, lipid, cell membrane, etc. This type of induced segregation of hydrophilic and hydrophobic amino acids is suggested for a variety of important physiological processes, such as hormone–receptor [8] and T-cell–major histocompatibility complex (MHC) interactions [9]. For instance, using disulfide-linked peptide dimers, O'Shea *et al.* [10] was able to mimic the conformations of proximal sequences (not covalently linked) found in native proteins. Others have designed and synthesized artificial "proteins" whose overall structures are formed and/or stabilized by hydrophobic interactions [11–13]. Recently, Hahn *et al.* [14] reported the *de novo* chemical synthesis of a 4-barrel helix bundle having enzymatic activity.

In earlier studies carried out in this laboratory, induced conformational factors (especially amphipathic α-helical arrangements) were found to influ-

Correspondence to: Dr. R. A. Houghten, Torrey Pines Institute for Molecular Studies, 3550 General Atomics Court, San Diego, CA 92121, USA.

* Present address: Fournier Pharma GmbH, Justus-von-Liebig Strasse 16, D-6603 Sulzbach, Germany.

0021-9673/92/$05.00

ence the retention behavior of peptides during reversed-phase high-performance liquid chromatography (RP-HPLC) [15–18]. This earlier work has lead us to the general hypothesis that every peptide has a small number of energetically favored conformations which are induced by the interaction of the peptide with the hydrophobic groups of the stationary phase. For instance, three peptides having the same composition (nine leucine and nine lysine residues) but different linear sequences representing several potential structural motifs, eluted over a range of 20 min [17]. Those which adopted classically and segmentally amphipathic α-helical conformations eluted later than anticipated [19]. By systematically studying the RP-HPLC behavior of single substitution analogues of a given sequence, we were able to evaluate the induced conformation of this peptide [17,18,20]. In particular, the model peptide Ac-LKLLKKLLKKLKKLLKKL-NH_2 was found to be induced into a classically amphipathic α-helical conformation during RP-HPLC [17,20]. Since an important factor in peptide–peptide and peptide-protein interactions involves conformational effects induced by hydrophobic constituents, we have investigated in the present study the use of RP-HPLC for the study of such interactions. To facilitate the study of such peptide–peptide interactions, we have synthesized a complete series of individual cysteine substitution analogs of the model peptide studied in earlier studies: Ac-LKLLKKLL-KKLKKLLKKL-NH_2. We then examined peptide–peptide interactions of these dimeric disulfide-linked model peptides using RP-HPLC, along with circular dichroism spectroscopy (CD) as a complementary and contrasting means of investigation. Since this set of peptide analogues represents two closely related compositions (*i.e.*, either 9 leucines, 8 lysines and 1 cysteine or 8 leucines, 9 lysines and 1 cysteine), only two distinct retention times would be expected to be seen if conformation was not a factor contributing to elution behavior [19]. Our working hypothesis, however, was that dimerization of each individual monomer by disulfide bridge formation would result in homo-dimeric peptides, which through self interactions would be induced into specific secondary structures. The overall surface hydrophobicity of these cysteine homo-dimers would be expected to differ depending on the conformation of the two peptide chains, which in turn would be dependent on the position of the cysteine.

MATERIALS AND METHODS

Peptide synthesis

Peptides were prepared by simultaneous multiple peptide synthesis (SMPS) [21]. Final cleavage and deprotection were carried out with liquid hydrogen fluoride (HF), using Tam *et al.* "low–high" HF cleavage protocol [22] with a 24-vessel cleavage apparatus [23] (Multiple Peptide Systems, San Diego, CA, USA). Oxidized peptides were produced by stirring a solution of the peptides (5 mg/ml) in 0.1 *M* NH_4HCO_3, pH 8, overnight at room temperature. The peptides were purified prior to CD studies using a DeltaPrep 3000 preparative RP-HPLC with a Foxy Fraction collector (Millipore, Waters Division, San Francisco, CA, USA). Analytical RP-HPLC was used to determine which fractions of the desired purity were to be pooled and lyophilized. The identities of the peptides were confirmed by time-of-flight mass spectroscopy analyses on a BIOION 20 spectrometer.

Analytical RP-HPLC

Relative retention times were determined using a Beckman gradient HPLC system consisting of two Model 110A pumps, a Beckman Model 421 microprocessor (Beckman Instruments, Anaheim, CA, USA), a Hitachi Model 100-20 variable wavelength spectrophotometer (Baxter Scientific Products, Los Angeles, CA, USA), a Shimadzu C-R3A Integrator (Cole Scientific, Calabasas, CA, USA), and a Bio-Rad Model AS-48 autosampler (Bio-Rad Laboratories, Richmond, CA, USA). Samples (20 μl, 0.2 mg/ml) were analyzed on Vydac 218TP54 C_{18} columns (Alltech Associates, Los Altos, CA, USA) (250 mm × 4.6 mm I.D., 5μm). Peptide elution was monitored at 215 nm. Buffer A consisted of 0.05% trifluoroacetic acid (TFA) in water and buffer B consisted of 0.05% TFA in acetonitrile. The peptides were analyzed using a 1%/min increasing gradient, starting at 5% buffer B.

RP-HPLC determinations of the monomeric forms were carried out by adding 50 μl of 5 m*M* dithiothreitol to a RP-HPLC sample of peptide (500 μl of a 1 mg/ml solution) in 0.1 *M* NH_4HCO_3, pH 8 [24]. After 1 h at room temperature, the pH was lowered prior to RP-HPLC by the addition of 50 μl of 10% AcOH. The samples were then analyzed by analytical RP-HPLC.

Circular dichroism measurements

All measurements were performed at ambient temperature on a Jasco J-720 circular dichroism spectrometer (Jasco, Easton, MD, USA). The instrument was routinely calibrated with an aqueous solution of ammonium [$^2H_{10}$]camphorsulfonic acid. Constant nitrogen flushing was employed. The measurements were carried out using quartz cells of 0.1 cm pathlength at a peptide concentration of 0.050 mg/ml (*i.e.*, $1.2 \cdot 10^{-5}$ mol/l). The relative concentration of each peptide was determined by its UV absorption at 210 nm prior to the measurements. The mean residue ellipticities ([θ]) were calculated using the relationship $[\theta] = 100/cnl$, where θ is the ellipticity (mdeg), c is the peptide concentration (m*M*), *n* is the number of residues in the peptide, and *l* is the pathlength (cm). The approximate percent helicity for the homo-dimeric peptides was calculated using $[\theta]_{222}$ (at 222 nm) with the assumption that a 100% helical peptide yields $[\theta]_{222} = -33\,400$ deg cm^2 dmol^{-1} [25].

TABLE I

PEPTIDE SEQUENCES

Sequence	Substituted residue
Ac-LKLLKKLLKKLKKLLKKL-NH_2	None
Ac-CKLLKKLLKKLKKLLKKL-NH_2	L-1
Ac-LCLLKKLLKKLKKLLKKL-NH_2	K-2
Ac-LKCLKKLLKKLKKLLKKL-NH_2	L-3
Ac-LKLCKKLLKKLKKLLKKL-NH_2	L-4
Ac-LKLLCKLLKKLKKLLKKL-NH_2	K-5
Ac-LKLLKCLLKKLKKLLKKL-NH_2	K-6
Ac-LKLLKKCLKKLKKLLKKL-NH_2	L-7
Ac-LKLLKKLCKKLKKLLKKL-NH_2	L-8
Ac-LKLLKKLLCKLKKLLKKL-NH_2	K-9
Ac-LKLLKKLLKCLKKLLKKL-NH_2	K-10
Ac-LKLLKKLLKKCKKLLKKL-NH_2	L-11
Ac-LKLLKKLLKKLCKLLKKL-NH_2	K-12
Ac-LKLLKKLLKKLKCLLKKL-NH_2	K-13
Ac-LKLLKKLLKKLKKCLKKL-NH_2	L-14
Ac-LKLLKKLLKKLKKLCKKL-NH_2	L-15
Ac-LKLLKKLLKKLKKLLCKL-NH_2	K-16
Ac-LKLLKKLLKKLKKLLKCL-NH_2	K-17
Ac-LKLLKKLLKKLKKLLKKC-NH_2	L-18

RESULTS

Peptide Synthesis

A set of 18 analogues of the peptide Ac-LKLLKKLLKKLKKLLKKL-NH_2, found in earlier studies to be induced into a classically amphipathic α-helical conformation during RP-HPLC [17,20], was synthesized. This starting sequence is illustrated in helical wheel [26] and lateral representations in Fig. 1. The analogues differed only in the successive replacement of each position with a cysteine (Table I). Each peptide was prepared by the SMPS method [21]. The homo-dimers contained in the crude synthetic peptides ranged from 20 to 80% of the total.

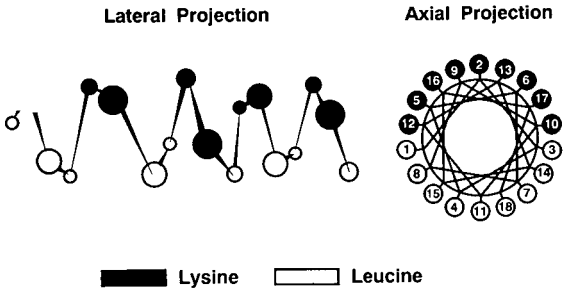

Fig. 1. Helical wheel and lateral representation of Ac-LKLLKKLLKKLKKLLKKL-NH_2

Peptide–peptide interactions as estimated by RP-HPLC

The homo-dimers contained in the crude synthetic peptides were readily reduced with dithiothreitol [24], enabling the determination of the respective retention times of both the monomeric and homo-dimeric forms of each analogue. The relative retention times for these analogues were the same in three separate determinations. The retention times of the monomeric and homo-dimeric forms (Table II) were plotted from the N-terminus relative to the position of the cysteine residue in the peptide (Fig. 2). A larger, overall variation in retention times (35 min) was observed for the homo-dimers than for the monomers (10 min). When the cysteine was located on the lysine side of this amphipathic α-helix, except for the extreme N- and C- terminal residues, both the monomeric and homo-dimeric forms eluted later than the starting peptide (X in Fig. 2). In contrast, when the cysteine was located on the leucine side of the amphipathic α-helix, all of the pep-

TABLE II

RETENTION TIME OF MONOMERS AND HOMO-DIMERS

The retention times were determined using a 1% gradient starting at 5% B.

Substituted residue	Retention time (min)	
	Monomers	Homo-dimers
None	46.2	
L-1	42.9	48.2
K-2	47.7	51.2
L-3	42.6	49.4
L-4	41.6	36.3
K-5	48.6	54.8
K-6	48.0	48.7
L-7	42.4	31.9
L-8	42.8	40.0
K-9	47.3	46.4
K-10	51.2	50.6
L-11	41.5	30.5
K-12	50.2	53.1
K-13	47.7	54.2
L-14	41.9	43.6
L-15	41.9	39.3
K-16	47.3	64.2
K-17	49.3	44.6
L-18	43.1	47.9

tides eluted earlier than the starting peptide. In particular, a substantially prolonged retention time for the homo-dimeric form was observed when lysine-16 was replaced with a cysteine, while much earlier retention times were found upon replacement of either leucine-7 or leucine-11.

If one envisions the hydrophobic alkyl groups of the amphipathic α-helix as being imbedded in the C_{18} layer of the stationary phase, then a more informative way to plot the results obtained relates to the position of the cysteine substitution in a helical wheel format. Thus, these substitutions were viewed counter-clockwise for those analogues in which a leucine has been replaced by a cysteine, and clockwise for those analogues in which a lysine was replaced by a cysteine (Fig. 3). In each case, the plot was started at the "nine o'clock" position (see helical wheel representation, Fig. 1). This representation emphasizes the effects of the position being replaced by the single cysteine residue relative to the location of the C_{18} interface. Large variations in retention times were observed in the 9 different homo-dimeric analogues in each set: the retention times varied by 20 min when either leucine or lysine was replaced by a cysteine (Fig. 3A). The retention times of those homo-dimers resulting from replacements of a leucine by a cysteine follow a pattern (except for position 18), which indicates that the closer a cysteine substitution is to the C_{18} interface, the longer its retention time (*i.e.*, the stronger its interaction with the C_{18}). In contrast, only small variations in retention times were found for the cor-

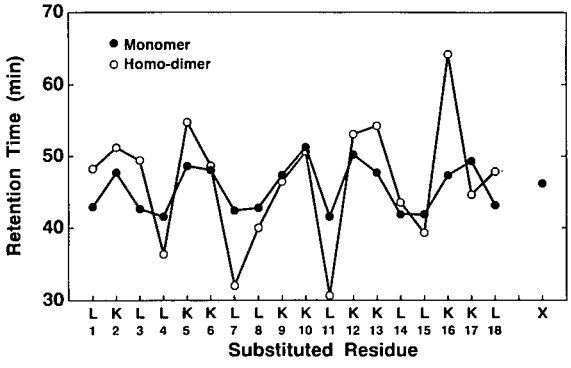

Fig. 2. RP-HPLC retention times of the monomeric and dimeric forms of the cysteine substitution analogues. The retention times were determined using a 1% gradient (5–75% B in 70 min). X = parent sequence.

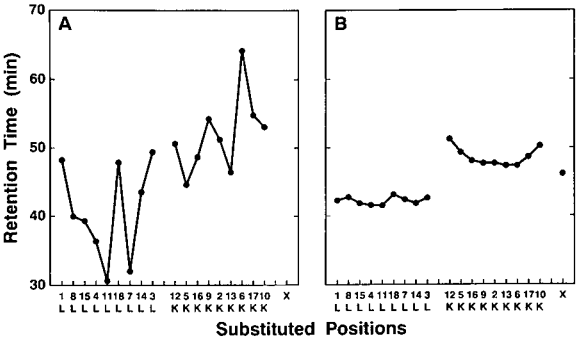

Fig. 3. Variation of the RP-HPLC retention times of the cysteine substitution analogues as viewed in a helical wheel representation. The substituted leucine positions are plotted as viewed counter-clockwise, while the substituted lysine positions are plotted as viewed clockwise on the helical wheel representation shown in Fig. 1. Both plots started at the "nine o'clock" position. (A) homo-dimeric forms; (B) monomeric forms; X = Parent sequence.

responding monomers (a 2-min and 3-min range when a cysteine replaced either a leucine or a lysine, respectively; Fig. 3B).

Peptide–peptide interactions as estimated by circular dichroism

CD spectroscopy has long been used for the estimation of the secondary structures of peptides or proteins in solution [27]. CD investigations were carried out to confirm or contrast the induced conformation predicted by RP-HPLC. Following air oxidation to their homo-dimeric forms in 0.1 *M* NH_4HCO_3, the analogues were purified to greater than 95% by RP-HPLC. RP-HPLC was used to confirm the absence of the monomeric forms of the peptides. Their dimeric states were confirmed by mass spectroscopy ($M+H=4443\pm2$ when a cysteine replaced a leucine, $M+H=4413\pm2$ when a cysteine replaced a lysine). The induced conformations of these homo-dimers were examined in salt-free aqueous solution. The CD spectra showed that only those analogues in which leucine-7, leucine-8, leucine-11, lysine-12 or leucine-18 were replaced with a cysteine adopted any significant percentage of defined secondary structure in aqueous solution (*i.e.*, α-helical conformation; Fig. 4 and Table III).

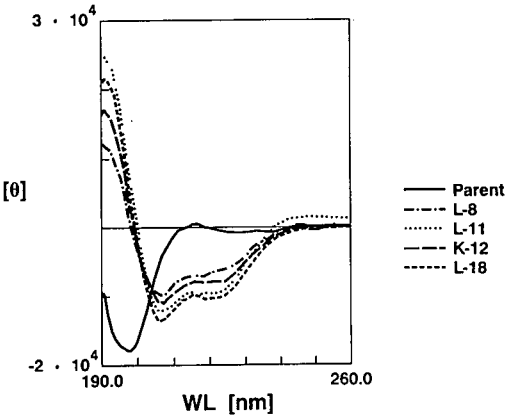

Fig. 4. Circular dichroism spectra in aqueous solution. The CD spectra show the mean residue molar ellipticities in deg cm^2 $dmol^{-1}$ as a function of wavelength (WL) for 0.050 mg/ml peptide in water.

TABLE III

α-HELICITY OF PEPTIDES AS ESTIMATED BY CD AT 222 nm

ND = Not determined. All of the peptides are in their dimeric form.

Substituted residue	% α-Helicity				
	H_2O	10% TFE[a]	20% TFE	30% TFE	40% TFE
None	>5	11	33	39	49
L-1	9	43	41	42	44
K-2	<5	37	42	47	58
L-3	<5	33	39	41	44
L-4	8	54	50	52	55
K-5	<5	53	54	ND	ND
K-6	<5	20	39	42	45
L-7	32	44	48	50	48
L-8	19	32	32	38	34
K-9	<5	18	29	30	40
K-10	11	31	49	43	46
L-11	29	46	54	60	58
K-12	24	34	35	38	ND
K-13	8	31	ND	42	42
L-14	<5	28	34	40	36
L-15	<5	37	41	44	50
K-16	<5	24	26	28	36
K-17	<5	21	22	ND	33
L-18	31	43	ND	45	43

[a] A v/v mixture of TFE in water.

TABLE IV

RELATIVE α-HELICITY AS DETERMINED BY CD USING RATIOS OF CD INTENSITIES [29]

All of the peptides are in their dimeric forms.

Substituted Residue	$R1 = [\theta]_{max}/[\theta]_{min}$		$R2 = [\theta]_{222}/[\theta]_{min}$	
	H_2O	10% TFE[a]	H_2O	10% TFE
None	0.52	−0.74	0.02	0.37
K-6	0.43	−0.85	0.10	0.50
L-7	−1.62	−2.16	0.79	0.88
K-9	0.46	−0.93	0.01	0.53
L-11	−2.00	−1.73	0.79	0.81
K-16	0.12	−1.92	0.15	0.73
K-17	0.54	−1.61	0.02	0.64
L-18	−1.58	−2.26	0.76	0.79

[a] A v/v mixture of TFE in water.

The propensity of the homo-dimeric analogues to adopt an α-helical conformation in the presence of trifluoroethanol (TFE), a solvent that induces helicity in potentially α-helical polypeptides [28], was then examined. The relative percentages of helicity for each analogue in the presence of increasing amounts of TFE are shown in Table III. The maximum helicity (ranging from 33% to 60%) was reached for each analogue in the highest percent TFE used (40%). The greatest amount of α-helicity was observed upon substitution of leucine-11 with a cysteine, while the lowest amount of α-helicity was found for those analogues in which a cysteine replaced a lysine at positions 16 or 17. Substitutions analogues at position 6 and 9, as well as the starting sequence, also had low helicity in 10% TFE.

To avoid misinterpretation of the data due to small variations in concentration, Bruch *et al.* [29] proposed the use of two parameters, $R1 = [\theta]_{max}/[\theta]_{min}$ and $R2 = [\theta]_{222}/[\theta]_{min}$. These ratios are based on the fact that in a two-state equilibrium between α-helix and random coil, the absolute value of $[\theta]_{222}$ and the maximum ellipticity $[\theta]_{max}$, increase relative to the minimum ellipticity $[\theta]_{min}$ as a function of α-helicity, independent of the peptide concentration. $R1$ values should decrease and $R2$ values should increase with an increase in α-helicity. For each peptide analogue studied, the CD spectra exhibited an isodichroic point at 203 nm as a function of %TFE, indicating a two-state equilibrium between a random coil and an α-helical conformation. The relative ratios calculated for the homo-dimer analogues confirmed that the highest percent α-helicity in water is reached when a cysteine replaced leucine-11, followed next by a cysteine replacement of leucine-7 and leucine-18 (lowest $R1$ and highest $R2$ values, Table IV). In 10% TFE, the low levels of helicity observed for the parent peptide and for those analogues in which a cysteine replaced either lysine-6 or lysine-9 were supported by high $R1$ and low $R2$ ratios (Table IV).

DISCUSSION

In anisotropic environments such as RP-HPLC, dimerization of the parent sequence by disulfide bridge formation results in homo-dimeric peptides that are induced into specific secondary structures. These specific self-induced conformations were entirely dependent on the location of the cysteine in the linear chain of the peptide, and in turn on the position of the peptide chains relative to one another. Since two closely related compositions are being studied (*i.e.*, either 9 leucines, 8 lysines and 1 cysteine or 8 leucines, 9 lysines and 1 cysteine), only two distinct retention times would be expected to be seen if conformation was not a factor contributing to elution behavior [19]. However, large variations (20 min) were observed in the retention times of the homo-dimers. This indicates that the specific secondary structures self-induced by peptide-peptide interactions are affecting RP-HPLC behavior. In support of this hypothesis, only small variations in retention times were found for the corresponding monomers (a 2-min and 3-min range when a cysteine replaced leucine or lysine, respectively; Fig. 3B).

The shortest retention time found for a homo-dimer resulted from replacing leucine-11 with a cysteine. This can be explained by the occurrence of strong peptide–peptide interactions through the two leucine faces of the two induced amphipathic helices. Since leucine-11 is located in the central region of the hydrophobic side of the amphipathic helix (see helical wheel representation, Fig. 1), this self-induced conformation results in a C_{18} surface presentation consisting almost entirely of lysine residues, and thus in an early retention time. The

adoption of an α-helical conformation for this analogue observed by CD in aqueous solution strengthens our belief that strong interchain hydrophobic interactions occur between the leucine residues, and in turn result in a stabilized double-stranded α-helical conformation. Similar but smaller effects are seen upon replacing leucine-7 with a cysteine.

The α-helical conformation calculated by CD in water for the substitution analogue of leucine-18 may result from the location of the cysteine at the far end of the chain. Thus, one chain may be folding over onto the other, again resulting in stabilization of a double-stranded α-helical structure through hydrophobic interactions between the leucine residues, as seen by Hodges and co-workers [11,12] for double-stranded coiled-coils conformation. However, the prolonged retention time found for this analogue relative to the others in this series indicates that an extended, or partially extended, conformation exists upon interactions between the leucines and the C_{18} group of the stationary phase.

In contrast to a folding process, the prolonged retention time observed when lysine-16 was replaced by a cysteine can be considered to be due to a juxtaposition of the two peptide chains in an antiparallel manner, resulting in a functionally extended C_{18} group hydrophobic presenting face (*i.e.*, equivalent to a 36-residue chain presenting 18 leucines on one face). This would result in a much stronger interaction of this dimer with the C_{18} group of the stationary phase. The low helical content found by CD for this analogue reconciles better with a single-stranded α-helical conformation than a double-stranded structure. The disulfide bridge appears, therefore, not to be contributing directly to its α-helical stability in aqueous solution.

In conclusion, we believe that RP-HPLC is a useful tool for the comparative study of self-induced conformations resulting from peptide–peptide interactions. The significant variations found between retention times of the homo-dimeric analogues studied here confirm the predominant role of amphipathicity in peptide–peptide interactions.

ACKNOWLEDGEMENTS

The authors thank David Burcin and James Winkle for their technical assistance, and Eileen Silva for the editing and preparation of this manuscript.

REFERENCES

1 J. P. Segrest, M. K. Jones, H. De Loof, C. G. Brouillette, Y. V. Venkatachalapathi and G. M. Anantharamaiah, *J. Lipid. Res.*, 33 (1992) 141.
2 M. Kataoka, J. F. Head, B. A. Seaton and D. M. Engelman, *Proc. Natl. Acad. Sci. USA*, 86 (1989) 6944.
3 K. T. O'Neil and W. F. DeGrado, *Trends Biochem. Sci.*, 15 (1990) 59.
4 M. Ikura, G. M. Clore, A. M. Gronenborn, G. Zhu, C. B. Klee and A. Bax, *Science (Washington, D.C.)*, 256 (1992) 632.
5 W. G. J. Hol, L. M. Halie and C. Sander, *Nature (London)*, 294 (1981) 532.
6 C. R. Cantor and P. R. Schimmel, in A. C. Bartlett, P. C. Vapnek and L. W. McCombs (Editors), *Biophysical Chemistry Part I: The Conformation of Biological Macromolecules*, W.H. Freeman & Co, New York, 1980, p. 279.
7 P. C. Lyu, L. A. Marky and N. R. Kallenbach, *J. Am. Chem. Soc.*, 111 (1989) 2733.
8 J. W. Taylor, in B. N. Dhawan and R. S. Rapaka (Editors), *Recent Progress in Chemistry and Biology of Centrally Acting Peptides*, Central Drug Research Institute, Lucknow, India, 1988, p. 25.
9 M. R. Pincus, F. Gerewitz, R. H. Schwartz and H. A. Scheraga, *Proc. Natl. Acad. Sci. USA*, 80 (1983) 3297.
10 E. K. O'Shea, R. Rutkowski, W. F. Stafford,III and P. S. Kim, *Science (Washington, D.C.)*, 245 (1989) 646.
11 R. S. Hodges, N. E. Zhou, C. M. Kay and P. D. Semchuk, *Pept. Res.*, 3 (1990) 123.
12 N. E. Zhou, C. M. Kay and R. S. Hodges, *J. Biol. Chem.*, 267 (1992) 2664.
13 S. P. Ho and W. F. DeGrado, *J. Am. Chem. Soc.*, 109 (1987) 6751.
14 K. W. Hahn, W. A. Klis and J. M. Stewart, *Science (Washington, D.C.)*, 248 (1990) 1544.
15 R. A. Houghten and J. M. Ostresh, *BioChromatography*, 2 (1987) 80.
16 R. A. Houghten and S. T. De Graw, *J. Chromatogr.*, 386 (1987) 223.
17 J. M. Ostresh, K. Büttner and R. A. Houghten, in C. Mant and R. S. Hodges (Editors), *HPLC of Peptides and Proteins: Separation, Analysis, and Conformation*, CRC Press, Boca Raton, FL, 1991, p. 633.
18 K. Büttner, S. E. Blondelle, J. M. Ostresh and R. A. Houghten, *Biopolymers*, 32 (1992) 575.
19 J. L. Meek and Z. L. Rossetti, *J. Chromatogr.*, 211 (1981) 15.
20 K. Büttner and R. A. Houghten, in E. Giralt and D. Andreu (Editors), *Peptides 1990, Proceedings of the Twenty-First European Peptide Symposium*, Escom, Leiden, 1991, p. 478.
21 R. A. Houghten, *Proc. Natl. Acad. Sci. USA*, 82 (1985) 5131.
22 J. P. Tam, W. F. Heath and R. B. Merrifield, *J. Am. Chem. Soc.*, 105 (1983) 6442.
23 R. A. Houghten, M. K. Bray, S. T. De Graw and C. J. Kirby, *Int. J. Pept. Protein Res.*, 27 (1986) 673.
24 W. W. Cleland, *Biochemistry*, 3 (1964) 480.
25 C. H. Chen and M. Sonenberg, *Biochemistry*, 16 (1977) 2110.
26 M. Schiffer and A. B. Edmundson, *Biophys. J.*, 7 (1967) 121.
27 W. C. Johnson, in D. Glick (Editor), *Methods of Biochemical Analysis*, Interscience, New York, 1985, p. 61.

28 S. R. Lehrman, J. L. Tuls and M. Lund, *Biochemistry*, 29 (1990) 5590.

29 M. D. Bruch, M. M. Dhingra and L. M. Gierasch, *Proteins: Struct. Func. Genet.*, 10 (1991) 130.

Journal of Chromatography, 625 (1992) 207–215
Elsevier Science Publishers B.V., Amsterdam

CHROM. 24 538

Separation of oxidized human growth hormone variants by reversed-phase high-performance liquid chromatography

Effect of mobile phase pH and organic modifier

Glen Teshima and Eleanor Canova-Davis

Genentech, Inc., 460 Pt. San Bruno Avenue, South San Francisco, CA 94080 (USA)

(First received May 19th, 1992; revised manuscript received August 3rd, 1992)

ABSTRACT

Human growth hormone (hGH), a polypeptide of 191 amino acids, contains three methionine residues, two of which are susceptible to oxidation by both chemical and photochemical means (Met14 and Met125). To date, no method has existed for resolving the various mono- and di-oxidation products. We report on the resolution of these oxidized variants and native hGH at weakly (pH 3.5) acidic pH. Although all of the oxidized species can be resolved at pH 3.5, use of low pH and neutral pH mobile phases confer some advantages. For example, the Met14 oxidized variant (MetSO-14) and native hGH are best resolved at neutral pH and the mono-oxidized variants (MetSO-125 and MetSO-14) are best resolved at low pH. The effect of organic modifier on the separation of the oxidized variants was also evaluated. 1-Propanol was more effective than acetonitrile in the separation of MetSO-14 and native hGH while acetonitrile was more effective than 1-propanol in the separation of MetSO-125 and MetSO-14. In summary, mobile phase pH and organic modifier were shown to be important parameters in the separation of oxidized hGH variants.

INTRODUCTION

Oxidation of methionine to methionine sulphoxide is a common chemical reaction known to occur in proteins [1–5]. Human growth hormone (hGH), produced by recombinant DNA technology, contains three potential sites for methionine oxidation; Met14, Met125, and Met170. Oxidation has been detected at both Met14 and Met125 in hGH [6–9], although there has been some discrepancy concerning the relative rates of oxidation at the two sites. Met170 is not oxidized in the native state [10] consistent with its location in the interior of the molecule according to the recently published hGH-receptor crystal structure [11].

Teh *et al.* [6] have reported a greater susceptibility of Met125 to chemical oxidation whereas Becker *et al.* [7] detected oxidation primarily at Met14. In the study by Teh *et al.* [6], relative rates were deduced from the peak heights of tryptic peptides generated from digestion of hydrogen peroxide-treated hGH. In the study by Becker *et al.* [7], relative rates were deduced from the peak heights of tryptic peptides generated from digestion of an oxidized fraction isolated by neutral pH reversed-phase high-performance liquid chromatography (HPLC). Canova-Davis *et al.* [8] isolated and characterized a Met125 oxidized hGH variant produced from exposure to light. The oxidized variant was isolated by reversed-phase HPLC at low pH. The results from the studies

Correspondence to: G. Teshima, Genentech, Inc., 460 Pt. San Bruno Avenue, South San Francisco, CA 94080, USA.

0021-9673/92/$05.00

of Becker *et al.* [7] and Canova-Davis *et al.* [8] suggest that the Met14 and Met125 oxidized hGH variants have different mobile phase pH selectivities; that is the Met14 oxidized variant is better resolved from native hGH at neutral pH whereas the Met125 oxidized variant is better resolved from native hGH at low pH. To better understand the separation mechanism and chromatographic behavior of human growth hormone and its oxidized variants, the effect of mobile phase pH and type of organic modifier was evaluated.

EXPERIMENTAL

Preparation of oxidized hGH

An amount of 15 mg of recombinant hGH (lyophilized) was dissolved in 1.5 ml water (final pH 7.4). An aliquot of 30 μl of 3% hydrogen peroxide (J. T. Baker) was added. The reaction was carried out at ambient temperature for 4 h.

Preparative reversed-phase chromatography at neutral pH

The oxidized hGH solution (15 mg) was loaded onto a Polymer Labs PLRP-S 10 μm, 300 Å (300 × 7.5 mm) column. Buffer A consisted of 25 m*M* ammonium acetate, pH 7.5. Solvent B was 1-propanol. Protein was eluted with a linear gradient from 34% B to 39% B over 100 min. Column temperature was 40°C and the flow-rate was 1 ml/min.

Rechromatography and characterization of oxidized fractions

Oxidized and main peak fractions isolated by preparative reversed-phase chromatography at neutral pH were analyzed on a Vydac C_{18} column (5 μm, 300 Å, 250 × 4.6 mm I.D.). Buffer A was aqueous 0.1% trifluoroacetic acid (TFA). Solvent B was 0.1% TFA in acetonitrile. Protein was eluted with a gradient from 57% B to 77% B in 40 min. Column temperature was 40°C and the flow-rate was 0.5 ml/min. The oxidized fraction from neutral pH reversed-phase chromatography was separated into two peaks. The less retained, minor fraction (12% by peak area) and major fraction were dried using a Savant Speed-vac. The dried fractions were reconstituted in a 10 m*M* Tris buffer, pH 8.2, containing 100 m*M* sodium acetate and 0.1 m*M* calcium chloride, and digested with L-1-tosylamido 2-phenylethyl chloromethyl ketone-treated trypsin (Worthington) at a 1:50 enzyme to substrate weight ratio for 4 h at 37°C. The trypsin-digested protein was loaded onto a Nucleosil C_{18} column (150 × 4.6 mm I.D.) equilibrated with 0.1% aqueous TFA and eluted with a linear gradient to 40% acetonitrile over 120 min at a flow-rate of 1 ml/min. UV absorbance was monitored at 214 nm. The native and oxidized tryptic peptides were collected, dried, and reconstituted in methanol–water (50:50) in preparation for analysis by electrospray ionization mass spectrometry (MS). This solution was infused at 10 μl/min into the ionspray probe of a Sciex API 111 triple quadrupole mass spectrometer. The mass axis was previously calibrated with a mixture of polypropylene glycols. The mass spectrum was analyzed using the Sciex Hypermass program to calculate the molecular mass from multiple-charged ions.

Analytical chromatography

A mixture of the oxidized and main peak fraction from the preparative reversed-phase HPLC separation were analyzed isocratically by reversed-phase HPLC on a Polymer Labs PLRP-S 8 μm, 300 Å (250 × 4.6 mm I.D.) column. Column temperature was 40°C and the flow-rate was 0.5 ml/min. The following mobile phase systems were evaluated: (1) Buffer A: 0.1 *M* sodium phosphate, pH 2.0, 1% sodium chloride. Solvent B: 1-propanol or acetonitrile. (2) Buffer A: 0.1 *M* sodium phosphate, pH 3.5, 1% sodium chloride. Solvent B: 1-propanol or acetonitrile. (3) Buffer A: 0.1 *M* sodium phosphate, pH 7.0, 1% sodium chloride. Solvent B: 1-propanol or acetonitrile.

RESULTS

Hydrogen peroxide-treated hGH (15 mg) was separated by reversed-phase HPLC at neutral pH on a PLRP-S (Polymer Labs) column. Lesser retained minor (peak a, Fig. 1) and major (peak b, Fig. 1) peaks were resolved from native hGH (peak c, Fig. 1). The two side fractions (peak a and b) and the main peak (native hGH) were then rechromatographed by reversed-phase HPLC on a Vydac C_{18} column using an 0.1% aqueous TFA–acetonitrile solvent system (Fig. 2). HPLC analysis of the minor

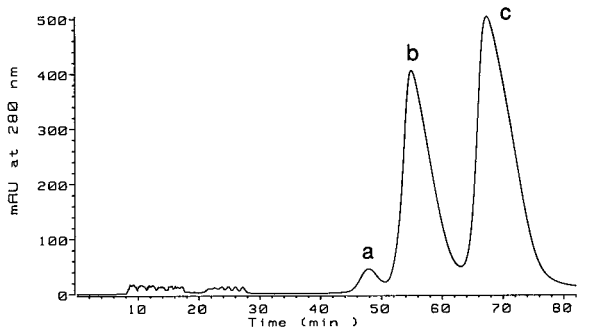

Fig. 1. Preparative reversed-phase HPLC at neutral pH of hydrogen peroxide-treated hGH (15 mg). Chromatography was performed on a Polymer Labs PLRP-S column equilibrated with ammonium acetate and eluted with a 1-propanol linear gradient as described in Experimental section.

TABLE I

ELECTROSPRAY IONIZATION MASS SPECTRAL ANALYSES

	Mass (dalton)	Theoretical mass
T2 (residues 9 to 16)	979.1	979.5[a]
T2 (oxidized at Met14)	995.1	995.5[a]
T11 (residues 116 to 127)	1361.3	1361.7[a]
T11 (oxidized at Met125)	1377.3	1377.67[a]
hGH (native)	22 126.5	22 125[b]
hGH (oxidized at Met125)	22 143.1	22 141[b]

[a] Mono-isotopic.
[b] Average.

side fraction (peak a, Fig. 1) resulted in the separation of a lesser retained peak (peak a-1, Fig. 2A). The corresponding fraction was collected, dried, and analyzed by tryptic mapping (Fig. 3A). The native T2 (residues 9 to 16, Leu-Phe-Asp-Asn-Ala-Met-Leu-Arg) and T11 (residues 116 to 127, Asp-Leu-Glu-Glu-Gly-Ile-Gln-Thr-Leu-Met-Gly-Arg) peptides are absent in the map and two new peptides represented by their oxidized counterparts appeared indicating that the minor peak from the neutral pH separation (Fig. 1) was a di-oxidized hGH variant.

HPLC analysis of the major side fraction (peak b, Fig. 1) resulted in the separation of an earlier eluting peak (peak b-1, Fig. 2B) in addition to a peak with the same retention time as native hGH (peak b-2, Fig. 2B). The fraction representing the earlier eluting fraction (peak b-1, Fig. 2B) was collected, dried, and analyzed by electrospray ionization MS. The mass of the earlier eluting component was 22 143.1 u as compared to 22 126.5 u for native hGH (Table I). The increase of 16.5 u is consistent with the oxidation of a single methionine residue. Tryptic mapping (Fig. 3) was carried out in order to localize the site of oxidation, since hGH contains three potential sites for methionine oxidation (residues 14, 125, and 170). The T11 peptide (residues 116 to 127) was absent from the tryptic map and a new peptide appeared on the ascending shoulder of T2 (residues 9 to 16) (Fig. 3B, inset). The new peptide had a mass of 1377.3 u as compared with 1361.3 u for the native T11 peptide (Table I). The increase in mass of 16 u is consistent with the oxidation of Met125 to methionine sulphoxide. Other amino acids which can react with hydrogen peroxide at neutral pH (cysteine, tryptophan, histidine, or tyrosine residues) are not present in the T11 peptide. A fraction representing the major peak (peak b-2, Fig. 2B), which co-eluted with native hGH (peak c-1, Fig. 2C), was also analyzed by tryptic mapping and electrospray ionization MS. The T2 peptide (residues 9 to 16) was absent from the tryptic map and a new peptide eluting at 56 min appeared (Fig. 3C). The new peptide had a mass of 995.1 u as compared with 979.1 u for the native T2 peptide. This increase in mass of 16 u is consistent with the oxidation of Met14 to methionine sulphoxide. The tryptic map of native hGH (peak c-1, Fig. 2C) is shown in Fig. 3D. The T2 and T11 peptides elute at 66 min and 81 min, respectively, as compared to 56 min and 63 min for their oxidized counterparts. In summary, the tryptic mapping and mass spectrometry results demonstrate that the major side fraction isolated from neutral pH reversed-phase HPLC consists of two mono-oxidized hGH variants; a minor variant (12%) oxidized at Met125 and a major variant oxidized at Met14.

To better understand the effect of pH and organic modifier on the separation of the oxidized variants; acidic, weakly acidic, and neutral pH mobile phases were evaluated with either acetonitrile or 1-propanol as the organic modifier (Fig. 4). The sample analyzed was a mixture of the di-oxidized, mono-

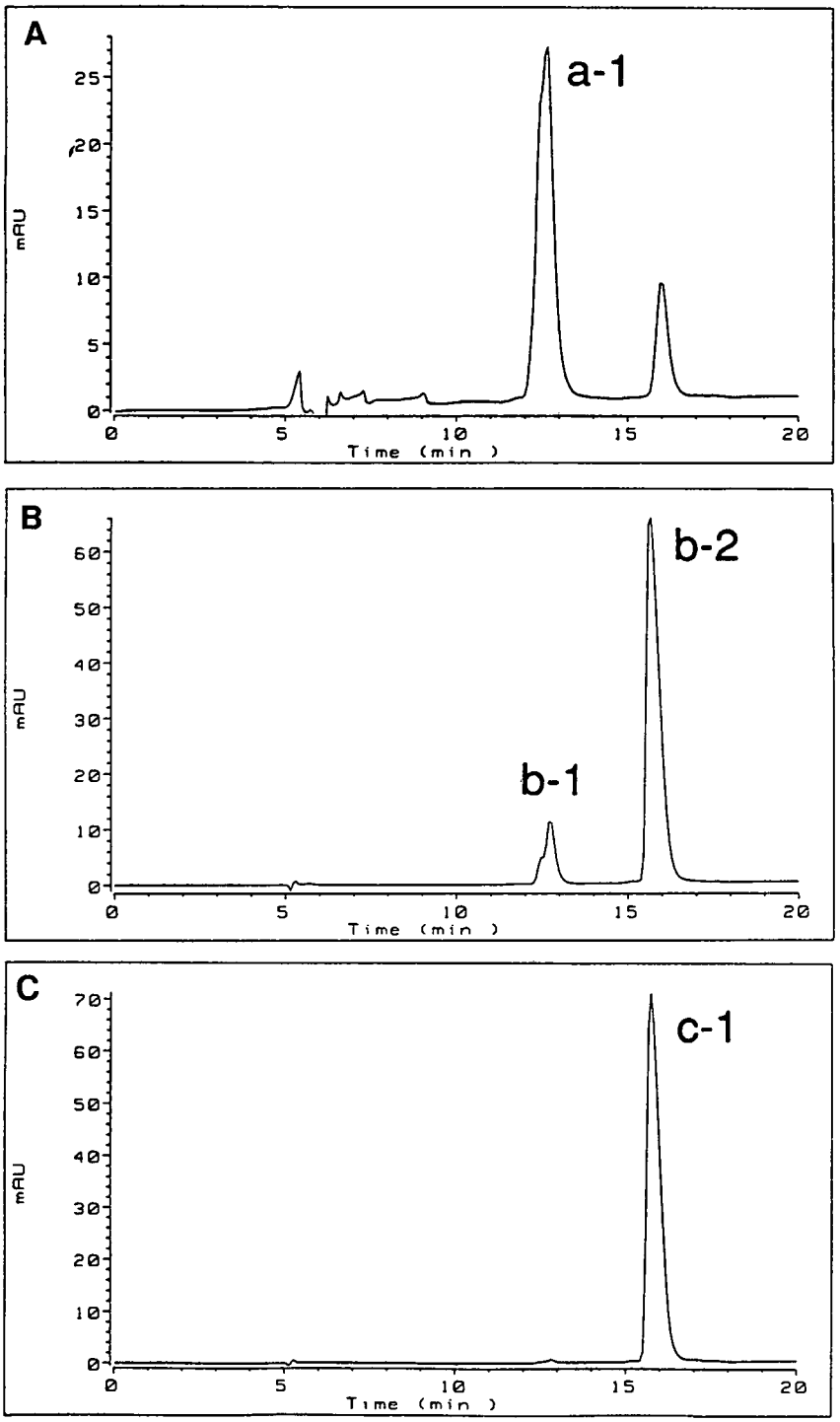

Fig. 2. Rechromatography at acidic pH of fractions isolated from reversed-phase HPLC at neutral pH. Chromatography was performed on a Vydac C_{18} column equilibrated with 57% acetonitrile containing 0.1% TFA and eluted with a linear acetonitrile gradient as described in Experimental section. (A) Reversed-phase HPLC of peak a in Fig. 1; (B) reversed-phase HPLC of peak b in Fig. 1; (C) reversed-phase HPLC of peak c in Fig. 1.

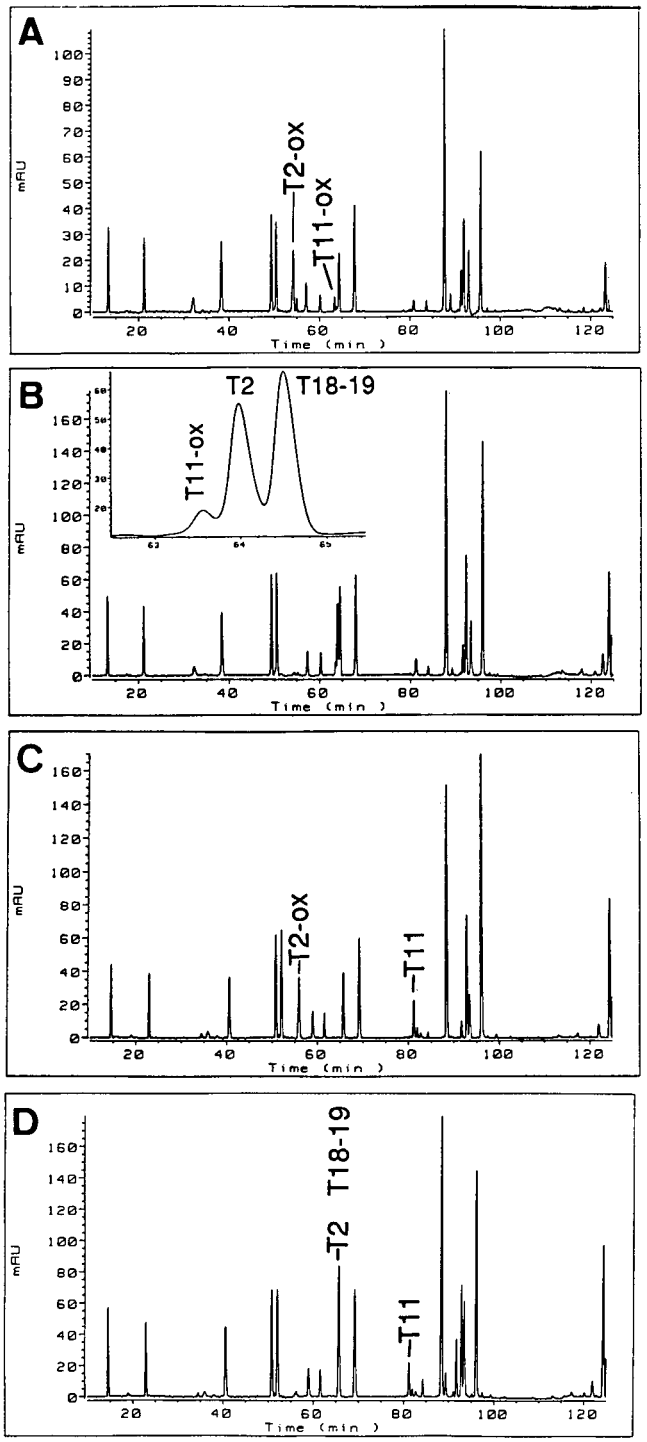

Fig. 3. Reversed-phase HPLC tryptic maps of oxidized and native hGH fractions. Insert: blow-up of the chromatogram between $t = 62.5$ min and $t = 65.5$ min. Chromatography was performed on a Nucleosil C_{18} column equilibrated with 0.1% TFA and eluted with a linear acetonitrile gradient as described in Experimental section. (A) Tryptic map of di-oxidized hGH (peak a-1, Fig. 2A); (B) tryptic map of mono-oxidized (methionine sulphoxide-125) hGH (peak b-1, Fig. 2B); (C) tryptic map of mono-oxidized (methionine sulphoxide-14) hGH (peak b-2, Fig. 2B); (D) tryptic map of native hGH (peak c-1, Fig. 2C).

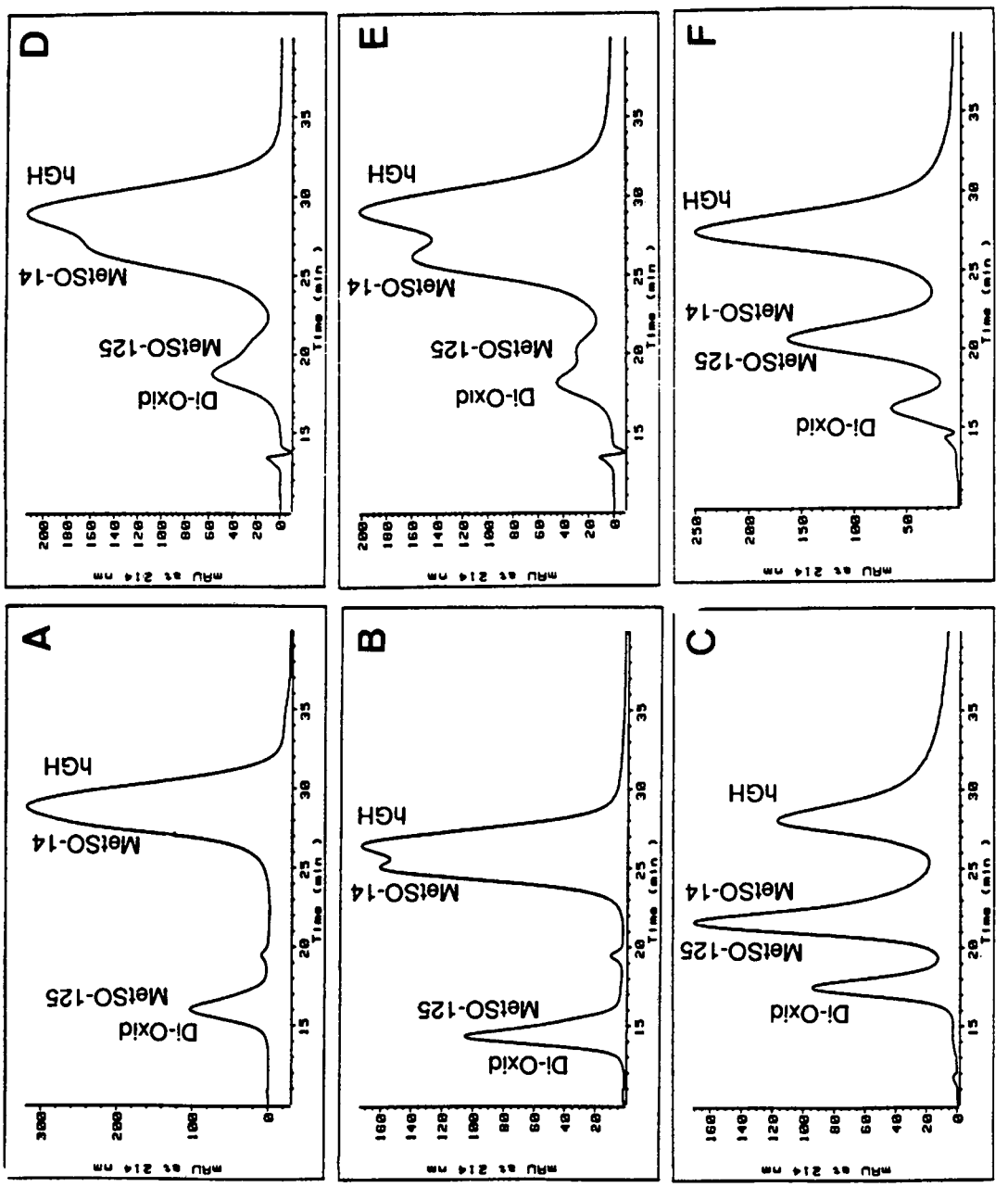

Fig. 4. The effect of pH and organic modifier on the separation of hGH and its oxidized variants by reversed-phase HPLC. The sample analyzed was a mixture of the di-oxidized, mono-oxidized and main peak fractions isolated from the preparative reversed-phase HPLC separation at neutral pH. The sample (100 μg) was eluted isocratically from a Polymer Labs PLRP-S 8 μm, 300 Å (250 × 4.6 mm I.D.). The column temperature was 40°C and the flow-rate was 0.5 ml/min. The concentration of organic modifier in the mobile phase was adjusted to maintain a constant k' (4.2 ± 0.3). The following mobile phase systems were evaluated: (A) 0.1 *M* sodium phosphate pH 2.0–acetonitrile; (B) 0.1 *M* sodium phosphate pH 3.5–acetonitrile; (C) 0.1 *M* sodium phosphate pH 7.0–acetonitrile; (D) 0.1 *M* sodium phosphate pH 2.0–1-propanol; (E) 0.1 *M* sodium phosphate pH 3.5–1-propanol; (F) 0.1 *M* sodium phosphate pH 7.0–1-propanol.

TABLE II

SELECTIVITY FACTORS (α) FOR hGH VARIANTS

Selectivity factor $(\alpha) = (t_{R2} - t_0)/(t_{R1} - t_0) = k'_2/k'_1$, where t_{R2} is the retention time of the more retained component and t_{R1} is the retention time of the lesser retained component.

	Acetonitrile			1-Propanol		
	pH 2.0	pH 3.5	pH 7.0	pH 2.0	pH 3.5	pH 7.0
B/A[a]	1	1	1.34	1	1.14	1.42
C/B[a]	2.20	2.18	1	1.6	1.39	1
D/C[a]	1	1.06	1.40	1	1.13	1.44
k' (native)[b]	4.44	3.99	4.31	4.46	4.38	4.20
% Organic	47.5	47.5	40.8	36	36	32.1

[a] A = Di-oxidized hGH; B = hGH methionine sulphoxide at 125; C = hGH methionine sulphoxide at 14; D = native hGH.
[b] Capacity factor $(k') = t_R - t_0$, where t_R is the retention time and t_0 is the void time.

oxidized, and main peak fractions collected from the preparative neutral pH separation. Elution was done in the isocratic mode and retention times held constant from run to run. The selectivity factors for the separation of (MetSO-125-containing and di-oxidized hGH), (MetSO-14 hGH and MetSO-125 hGH), and (native hGH and MetSO-14 hGH) are shown in Table II.

The optimal pH for the separation of MetSO-125-containing and di-oxidized hGH was 7.0 (α = 1.34 with acetonitrile, α = 1.42 with 1-propanol). Partial resolution was attained at pH 3.5 with 1-propanol as the organic modifier (α = 1.14). MetSO-125 and di-oxidized hGH co-eluted at pH 2.0 and at pH 3.5 with acetonitrile as the organic modifier. A substantially lower organic concentration eluted hGH at pH 7 (40.8% acetonitrile, 32% 1-propanol) than at pH 2 and 3.5 (47.5% acetonitrile, 36% 1-propanol) indicating that hGH is less denatured at neutral pH than at low pH.

MetSO-14 and MetSO-125 hGH were not separated at pH 7.0 (α = 1) but were well resolved at pH 2 and 3.5 using either acetonitrile or 1-propanol. Resolution was considerably better using acetonitrile (α = 2.18 at pH 3.5) as compared to 1-propanol (α = 1.39 at pH 3.5).

MetSO-14 and native hGH were best resolved at pH 7.0 using either acetonitrile or 1-propanol as the organic modifier (α = 1.40 with acetonitrile, α = 1.44 with 1-propanol). Partial resolution was achieved at pH 3.5, with 1-propanol giving a slightly better separation than acetonitrile (α = 1.13 with 1-propanol, α = 1.06 with acetonitrile). MetSO-14 and native hGH co-eluted at pH 2.0.

Sodium phosphate, pH 3.5, with 1-propanol was the only mobile phase system capable of resolving the mono- and di-oxidized variants and native hGH. In order to further improve the separation, the column residence time was increased (Fig. 5). The oxidized hGH variants are sufficiently well resolved to allow quantitation of the various oxidized species. Using this method, it was estimated that there was 2% di-oxidized hGH, 5% mono-oxidized at Met125, and 35% mono-oxidized at Met14 in the hydrogen peroxide-treated hGH sample.

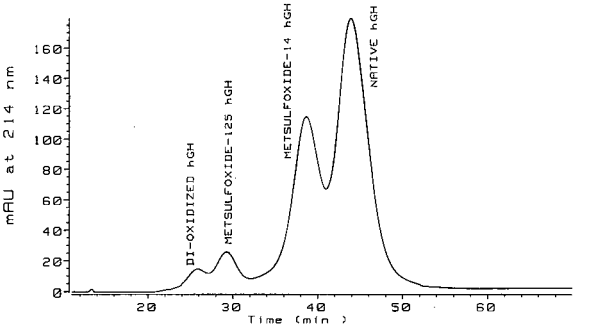

Fig. 5. Optimized reversed-phase HPLC analysis of hydrogen peroxide-treated hGH. Hydrogen peroxide-treated hGH (100 μg = 10 μl of 10 mg/ml solution) was eluted isocratically from a Polymer Labs PLRP-S 8 μm, 300 Å (250 × 4.6 mm I.D.) column. Column temperature was 40°C. The mobile phase consisted of 32.5% 1-propanol in 100 m*M* sodium phosphate, pH 3.5, with 1% sodium chloride. The flow-rate was 0.5 ml/min.

DISCUSSION

Mobile phase parameters such as pH, type of organic modifier, and column temperature have been shown to influence the reversed-phase HPLC separation of proteins [12,13]. Although reversed-phase chromatography is denaturing due to interaction of the protein with the hydrophobic matrix, the extent of denaturation can be modified by the mobile phase selection [14]. Use of less denaturing conditions (neutral pH) has been employed in the separation of native hGH and hGH with an additional methionine at the N-terminus [12,13]. More denaturing conditions (low pH and acetonitrile) failed to resolve the pair. Partial resolution was attained at low pH with 1-propanol as the organic modifier and at intermediate pH (3.5–4.5).

In our study, less denaturing conditions (neutral pH) favored the resolution of the Met14 oxidized hGH variant and native hGH while more denaturing conditions (low pH) favored the separation of the Met125 oxidized hGH variant and native hGH. These results suggest that Met125 is less solvent accessible than Met14; that is more denaturing conditions are required to expose it for interaction with the matrix.

Since Met14 is most likely solvent accessible under all of the mobile phase conditions evaluated, more strongly denaturing conditions which expose additional residues for interaction with the matrix results in a poorer separation. A possible explanation is that exposure of these additional residues dilutes out the effect of the modification at Met14. A similar explanation was described by Canova-Davis *et al.* [12] and Frenz *et al.* [13] for the separation of native hGH and hGH with an additional N-terminal methionine. It is interesting to note that the selectivity factors for the separation of the Met14 oxidized hGH variant and native hGH and the N-terminal hGH variant and native hGH are similar. For example, both are well resolved at neutral pH, partially resolved at intermediate pH and at low pH with 1-propanol as the organic modifier and not resolved at low pH with acetonitrile as the organic modifier. This suggests that they have similar solvent accessibilities in the column matrix-mobile phase environment. In contrast, Met14 and Met125 appear to have different solvent accessibilities in the column matrix-mobile phase environment.

Changing the conformation (by varying the mobile phase composition as discussed above) and therefore the contact region such that a lesser or greater number of residues are involved in binding to the matrix is one mechanism through which selectivity could be altered. Other possible mechanisms involve a change in local conformation due to oxidation at Met14 and/or Met125, local pH changes affecting the ionization of nearby residues (*i.e.*, Asp11 and His18), and a disruption of secondary interactions, in particular, the salt bridge between His18 (one turn remove from Met14 in α-helix 1) and Glu174. It cannot be determined with any degree of certainty what mechanism is involved in the separation of oxidized and native hGH, however, the fact that a substantially lower organic concentration eluted hGH at neutral pH as compared to low pH suggests that conformational changes induced by the mobile phase play a major role.

Use of a weakly acidic pH (3.5) mobile phase provided a compromise between the contrasting selectivities obtained at low *versus* neutral pH and resulted in the separation of the Met125 and Met14 mono-oxidized hGH variants, the di-oxidized hGH variant and native hGH. Development of a single method for separating the mono- and di-oxidized variants and native hGH at weakly acidic pH (3.5) with 1-propanol was useful for directly determining the relative reactivity of Met14 and Met125 in hGH rather than indirectly by measurement of the peak heights of tryptic peptides as was the case in the study by Teh *et al.* [6]. Our results are in agreement with Becker *et al.* [7] that Met14 is the primary site of oxidation in hGH. This was not unexpected since our reaction conditions (pH, temperature, concentration of hydrogen peroxide) were the same as used by Becker *et al.* [7]. Perhaps the different reaction conditions (*i.e.*, higher concentration of hydrogen peroxide) used by Teh *et al.* [6] explains the greater reactivity of Met125 reported in their study. Our tryptic map of the oxidized hGH fraction separated by reversed-phase HPLC at neutral pH appeared similar to the one shown by Becker *et al.* [7]. A modified T2 peptide containing methionine sulphoxide at residue 14 was identified; however, the methionine sulphoxide-125 containing T11 peptide was not detected nor was a significant decrease in the native T11 peptide observed. Rechromatography of the oxidized fraction at low pH resulted in the

separation of the Met14 and Met125 oxidized hGH variants. The Met125 variant represented 12% of the mono-oxidized hGH fraction by peak area calculations. The fact that its corresponding oxidized peptide was not detected in the tryptic map emphasizes the importance of a direct chromatographic assay for monitoring oxidation in hGH.

CONCLUSIONS

We have shown that the selectivity factors for the separation of native hGH and its oxidized variants can be varied by manipulating the mobile phase conditions. Both pH and type of organic modifier were shown to be important parameters in the separation of the oxidized hGH variants and native hGH.

Met14 and Met125 appeared to have very different solvent accessibilities under reversed-phase chromatographic conditions since more denaturing mobile phase conditions favored the separation of MetSO-125 and less denaturing conditions favored the separation of MetSO-14.

This suggests a general strategy for separating protein variants assuming that the residues involved have dissimilar solvents accessibilities; that is one could vary the strength of protein interaction by adjusting the pH and type of organic modifier.

ACKNOWLEDGEMENTS

The authors thank Victor Ling for the mass spectral analyses and acknowledge helpful discussions with Drs. William S. Hancock, S.-L. Wu, and A. M. DeVoss. We acknowledge John Battersby for his contributions to hGH chromatography and Barbara O'Connor for previous work resulting in the characterization of oxidation at Met125.

REFERENCES

1 N. Brot and H. Weissbach, *BioFactors*, 3 (1991) 91–96.
2 P. H. Tobler, A. Johl, W. Born, R. Maier and J. A. Fischer, *Biochim. Biophys. Acta*, 707 (1982) 59–65.
3 P. H. Tobler, F. A. Tschopp, M. A. Dambacher, W. Born and J. A. Fischer, *J. Clin. Endocrinol. Metab.*, 57 (1982) 749–753.
4 J. Wolff, G. H. Cook, A. R. Goldhammer and S. A. Berkowitz, *Proc. Natl. Acad. Sci. USA*, 77 (1980) 3841–3844.
5 A. L. Frelinger and J. E. Zull, *Arch. Biochem. Biophys.*, 244 (1986) 641–649.
6 L.-C. Teh, L. J. Murphy, N. L. Huq, A. S. Surus, H. G. Friesen, L. Lazarus and G. E. Chapman, *J. Biol. Chem.*, 262 (1987) 6472–6477.
7 G. W. Becker, P. M. Tackitt, W. W. Bromer, D. S. Lefeber and R. M. Riggin, *Biotech. Appl. Biochem.*, 10 (1988) 326–337.
8 E. Canova-Davis, R. C. Chloupek, I. P. Baldonado, J. E. Battersby, M. W. Spellman, L. J. Basa, B. O'Connor, R. Pearlman, C. Quan, J. A. Chakel, J. T. Stults and W. S. Hancock, *Am. Biotechnol. Lab.*, 5 (1988).
9 P. Gellerfors, B. Pavlu, K. Axelsson, C. Nyhlen and S. Johansson, *Acta Paediatr. Scand. Suppl.*, 370 (1990) 93–100.
10 R. A. Houghten, C. B. Glaser and C. H. Li, *Arch. Biochem. Biophys.*, 178 (1977) 350–355.
11 A. M. DeVos, M. Ultsch and A. A. Kossiakoff, *Science (Washington, D.C.)*, 255 (1992) 306–312.
12 E. Canova-Davis, G. Teshima, J. Kessler, P.-J. Lee, A. Guzzetta and W. S. Hancock, in Cs. Horváth and J. G. Nikelly (Editors), *Analytical Biotechnology (ACS Symposium Series*, No. 434), American Chemical Society, Washington, DC, 1990, pp. 90–112.
13 J. Frenz, W. S. Hancock, W. J. Henzel and Cs. Horváth, in K. M. Gooding and F. E. Regnier (Editors), *HPLC of Biological Macromolecules*, Marcel Dekker, 1990, pp. 145–177.
14 Y. M. Lau, A. K. Taneja and R. S. Hodges, *J. Chromatogr.*, 317 (1984) 129–140.

Journal of Chromatography, 625 (1992) 217–222
Elsevier Science Publishers B.V., Amsterdam

CHROM. 24 481

Effect of column length and elution mechanism on the separation of proteins by reversed-phase high-performance liquid chromatography

Junichi Koyama, Junko Nomura, Yoshihiro Shiojima, Yutaka Ohtsu and Izumi Horii

Shiseido Research Centre, Skin Biology Research Laboratories, 1050 Nippa-cho, Kohoku-ku, Yokohama 223 (Japan)

(First received April 23rd, 1992; revised manuscript received June 23rd, 1992)

ABSTRACT

Different theories have been proposed for the elution of proteins in reversed-phase high-performance liquid chromatography. To establish the correct elution mechanism, the effects of column length and the concentration of the organic solvent on column efficiency and the elution of high- and low-molecular-weight compounds were examined. It was concluded that protein elution principally involves the same retention process as for low-molecular-weight compounds, although the influence of partition is small under steep gradient conditions. In accordance with this, wide-pore packings in a short column (35 mm) gave excellent separations of proteins and were usable with a wide range of gradients.

INTRODUCTION

Reversed-phase high-performance liquid chromatography (RP-HPLC) has become an important technique for protein analysis owing to its high resolution [1–9]. A gradient elution technique is commonly used for protein analysis. However, the behaviour of proteins is different from that of low-molecular-weight compounds, and new mechanisms, such as the so-called "on–off" or "critical behaviour" mechanism, which differs from that of conventional partitioning, have been proposed [10–22]. According to these mechanisms, proteins are trapped at the top of the column initially and then, after the concentration of organic solvent reaches a value sufficient for protein desorption from the packing material, the proteins are eluted through the column without further interaction with the packing. Recently, Nimura *et al.* [23] reported a high-speed protein analysis based on this adsorption–desorption mechanism. If these proposed concepts are valid, the structure of the packing material, such as pore size and particle size, and column length should have no influence on protein elution. Nevertheless, many studies concerning the influence of pore size and particle size on protein analysis have appeared [24–30]. Further, Snyder and coworkers [31–39] reported that protein elution can be explained by the same mechanism as for of small molecules. Therefore, the influence of the structure of the packing material and the protein elution mechanism still remain to be established. In order to clarify the mechanism of protein elution and to identify the best packings for protein analysis, we have studied the elution of proteins in RP-HPLC with variations in the column length and the concentration of organic solvent.

Our previous studies demonstrated that small amounts of metallic impurities in packing materials have a greater influence than pore size, alkyl chain length and residual silanols on protein elution [40]. In this study, capsule-type packings, the surface of

Correspondence to: Dr. J. Koyama, Shiseido Research Centre, Skin Biology Research Laboratories, 1050 Nippa-cho, Kohoku-ku, Yokohama 223, Japan.

0021-9673/92/$05.00

which is covered with silicone polymer, were used to avoid the influence of metallic impurities in silica gels.

EXPERIMENTAL

Reagents and materials

Capsule-type packings having C_8-alkyl groups were prepared by using high-purity silica gels [41]. The pore size was 300 Å and particle diameter 5 μm. The materials were packed into 0.46 cm I.D. stainless-steel tubes of length 10, 35, 100 and 250 mm.

Bovine serum albumin (BSA), ovalbumin, cytochrome *c*, lysozyme, myoglobin and ribonuclease A were purchased from Sigma (St. Louis, MO, USA), peptides, alkylphenones (C_4–C_6) and trifluoroacetic acid (TFA) from Wako (Osaka, Japan) and HPLC-grade acetonitrile from Nacalai Tesque (Kyoto, Japan).Water was purified using a Milli-R/Q system (Millipore, Bedford, MA, USA).

Apparatus

A Shimadzu LC-6A system equipped with a high-pressure gradient mixer was used.Elution gradients were prepared from solvents A and B (A, 0.1% TFA in water; B, 0.1% TFA in acetonitrile) and the gradient programmes are illustrated in the figures. The column temperature was maintained at 40°C, the flow-rate was 1.5 ml/min and the eluate was monitored at 214 nm.

Each protein was dissolved in water at a concentration of 1 mg/ml and each solution was mixed as an equal volume. An aliquot of the mixture (20 μl) was injected into the HPLC system.

RESULTS AND DISCUSSION

Gradient elution

Fig. 1 shows the effect of column length on the elution profile. The retentions of low-molecular-weight compounds, alkylphenones and peptides, decreased as the column was made shorter. The retention capacity of the 35-mm column was only 10–30% of that of the 250-mm column. On the other hand, the decrease in protein retentions was smaller than that with low-molecular-weight substances. Even the 10-mm column maintained more than 60% of the retention capacity as compared with the 250-mm column.

Fig. 2 shows the influence of column length on band width. The values for low-molecular-weight compounds became smaller as the column length became longer, from 10 to 250 mm, as shown in Fig. 2A. These results indicate that the column efficiency for small compounds is improved by increasing the column length. In contrast, the band width of proteins was almost constant for lengths > 35 mm, as shown in Fig. 2B. These results indicate that for proteins, a longer column does not give a high separation efficiency. Hence there is a clear difference

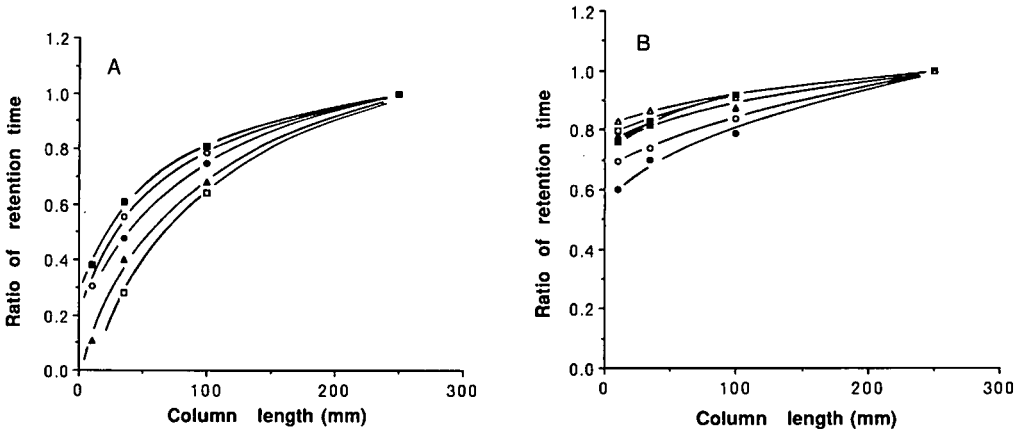

Fig. 1 Effect of column length on retention time of solutes of various molecular size. (A) Low-molecular-weight compounds: ● = C_4-phenone; ○ = C_5-phenone; ■ = C_6-phenone; □ = Lys-bradykinin; ▲ = Met-Lys-bradykinin. (B) Proteins: ● = ribonuclease A; ○ = cytochrome *c*; ■ = lysozyme; □ = BSA; ▲ = myoglobin; △ = ovalbumin. Conditions: linear gradient from 15 to 60% eluent B in 15 min.

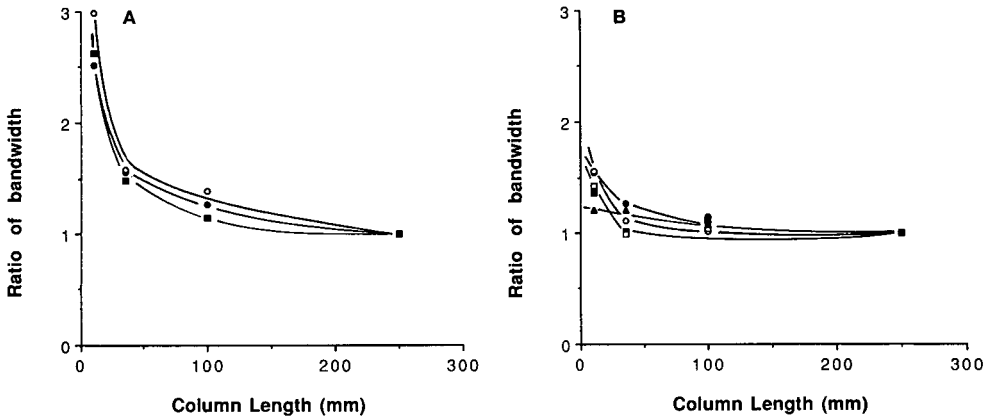

Fig. 2. Effect of column length on peak band width. (A) Low-molecular-weight compounds: ● = C_4-phenone; ○ = C_5-phenone; ■ = C_6-phenone. (B) Proteins: ● = ribonuclease A; ○ = lysozyme; ■ = BSA; △ = myoglobin; ▲ = ovalbumin. Conditions as in Fig. 1.

in elution behaviour between proteins and low-molecular-weight compounds.

The effect of the initial concentration of the organic solvent on elution behaviour is shown in Fig. 3. The retention times of small compounds decreased in proportion to the increase in initial organic solvent concentration. Proteins showed similar behaviour. However, when the concentration of organic solvent exceeded a critical value, which was different for each protein, the elution rate increased rapidly. This phenomenon indicates that proteins are no longer retained when the organic solvent concentration exceeds this critical value. This is a second difference between proteins and low-molecular-weight compounds. These phenomena suggested us that protein elution involves a different mechanism to that from the theory for low-molecular-weight compounds.

Isocratic elution

The effect of column length on capacity factor underisocratic conditions is shown in Fig. 4. Under isocratic conditions, high-molecular-weight compounds showed similar elution profiles to low-molecular-weight compounds, *i.e.*, delayed retentions and higher theoretical plate numbers were obtained with longer columns.

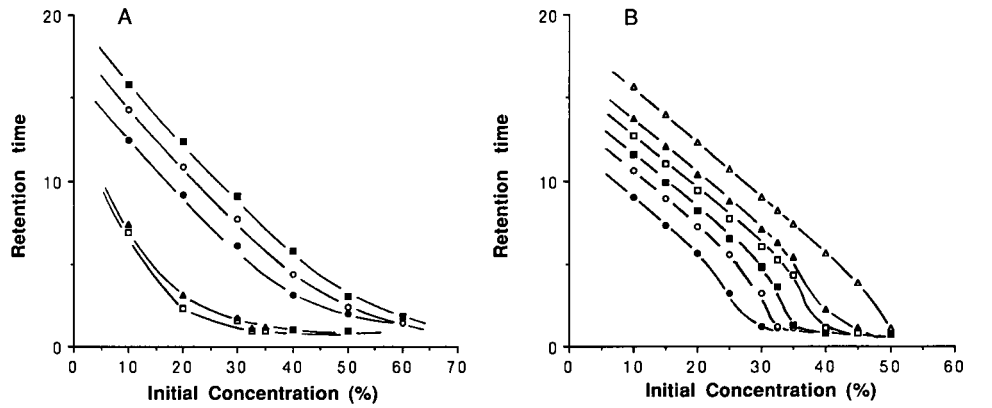

Fig. 3. Effect of initial concentration of organic solvent on retention time for (A) low-molecular-weight compounds and (B) proteins. Symbols as in Fig. 1 Conditions: linear gradient from the indicated initial concentration to 60% eluent B at 3%/min; column length, 250 mm.

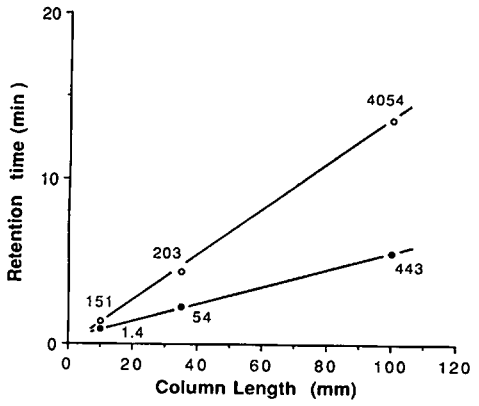

Fig. 4 Effect of column length on retention time and column plate number. The ratio of retention time is represented on the basis of the retention time of a 250-mm column. ● = Lysozyme; ○ = C_6-phenone. Numbers indicate the column plate number. Conditions; isocratic, 31% eluent B.

Fig. 5 shows the variation of the capacity factor with change in the concentration of the organic solvent. The capacity factors of low-molecular-weight solutes decreased linearly with increase in organic solvent concentration. In isocratic elution, proteins gave similar results to small compounds, although the changes in capacity factors were far greater for the proteins. From this result, it is concluded that protein elution in RP-HPLC is not based on the putative "on–off" or "critical behaviour" mechanism, but on the same repeated partition mode as operates for low-molecular-weight substances. However, the influence of organic solvent concentration on the capacity factors of proteins is very large. This steep change in capacity factor is the reason why proteins show curious behaviour in gradient elution.

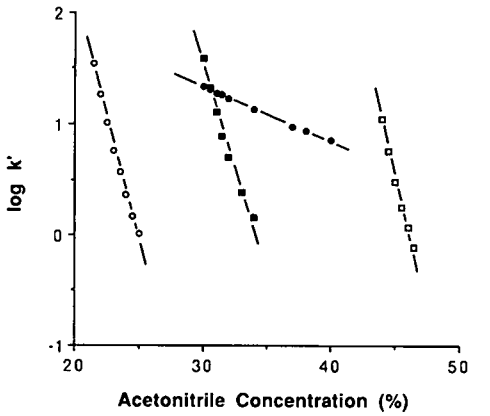

Fig. 5. Variation of capacity factor (k') with the concentration of acetonitrile. Column length, 250 mm. ● = C_6-phenone; ○ = ribonuclease A; ■ = lysozyme; □ = ovalbumin.

Protein elution mechanism

In gradient elution, the behaviour of proteins was apparently different from that of low-molecular-weight compounds, as if a peculiar "on–off" or "critical behaviour" elution mechanism were operating. These observations have been explained by a model proposed by Armstrong and co-workers [16,19], in which macromolecules are precipitated at the head of a column in the presence of a low-strength mobile phase and they never migrate until the mobile phase strength increases to some critical composition which induces dissolution and subsequent elution. However from our isocratic results, it was considered that protein elution involves essentially the same partition mode as for low-molecular-weight compounds. Evidently, as shown in Fig. 5, the plot of k' *versus* volume of organic solvent is far steeper than that for hexanophenone.

Snyder and co-workers [31,37,38] have shown that the separation of proteins by gradient elution can be described quantitatively by a model based on a small-molecule separation mechanism.The retention time in gradient elution can be predicted from data for corresponding isocratic systems. For isocratic systems there is a linear relationship between the k' value of a sample and the volume fraction of organic solvent (φ) in the mobile phase:

$$\log k' = \log K_w - S\varphi$$

where S is the slope of the plot of $\log k'$ *vs.* φ, and K_w is the k' value for water as mobile phase. In gradient elution, at any point in time during the separation, the composition of the mobile phase in contact with the solute band determines an isocratic value of k', and this in turn determines the instantaneous velocity of the band through the column. Consequently, a band elutes under a given set of gradient conditions with some average value of k' [38]. It was demonstrated that the large values of S is the reason for the curious behaviour in gradient elution.

Because proteins take a large value of K_w, despite the large value of S for proteins, k' will not change much with increase in organic solvent with a low-strength mobile phase. However, after the organic solvent has reached a sufficient concentration for elution, k' changes considerably owing to the large value of S, as shown in Fig. 5. This is the reason for the unchanging retention time in Fig. 1B and critical point in Fig. 3B.

The range of concentration of organic solvent within which proteins can have the appropriate value of k' for separation is very narrow, at most within a few per cent. This means that when the concentration of the organic solvent is less than the lower limit, the k' value of proteins become very large, and so proteins move through the column only very slowly, as reported by Bussolo and Gant [39]. In contrast, at an organic solvent concentration even slightly over the upper limit, the k' value of proteins becomes too small for retention on the stationary phase. Therefore, under gradient conditions, an injected protein moves very slowly in the column until the organic solvent concentration reaches the value at which the protein has the appropriate value of k' for elution. Beyond this point, the protein moves through the column, being repeatedly partitioned on the stationary phase, for a while until the organic solvent concentration reaches the upper limit. Above this upper limit, the protein has only small value of k', so it moves through the column very rapidly and the interaction with the stationary phase is very small.

Because the suitable range of organic solvent concentration for the partition mode is very narrow, as described above, when the gradient rate is high the participation of the partition mode becomes very small. As a result, the peak shape and elution profile of proteins are almost independent of the column length, as shown in Figs. 1 and 6. Differences in retention time essentially reflect the void volume of each column, and under this condition protein elution apparently looks like "on–off" or "critical behaviour" elution. When the gradient rate was low, a shorter column exhibited peak broadening, as shown in Fig. 7. This result is ex-

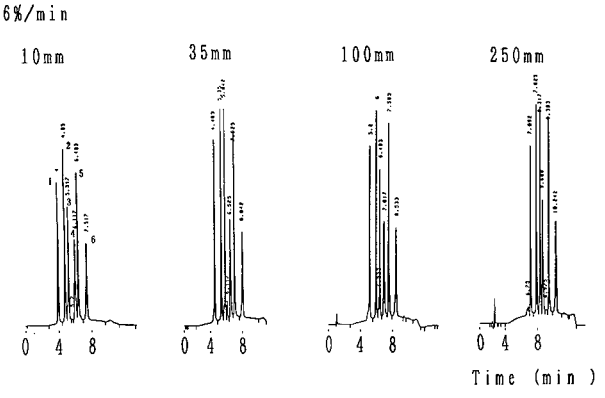

Fig. 6. Effect of column length (10–250 mm) on protein elution under fast gradient conditions. Conditions: linear gradient from 15 to 75% eluent B in 10 min. Peaks: 1 = ribonuclease A; 2 = cytochrome *c*; 3 = lysozyme; 4 = BSA; 5 = myoglobin; 6 = ovalbumin.

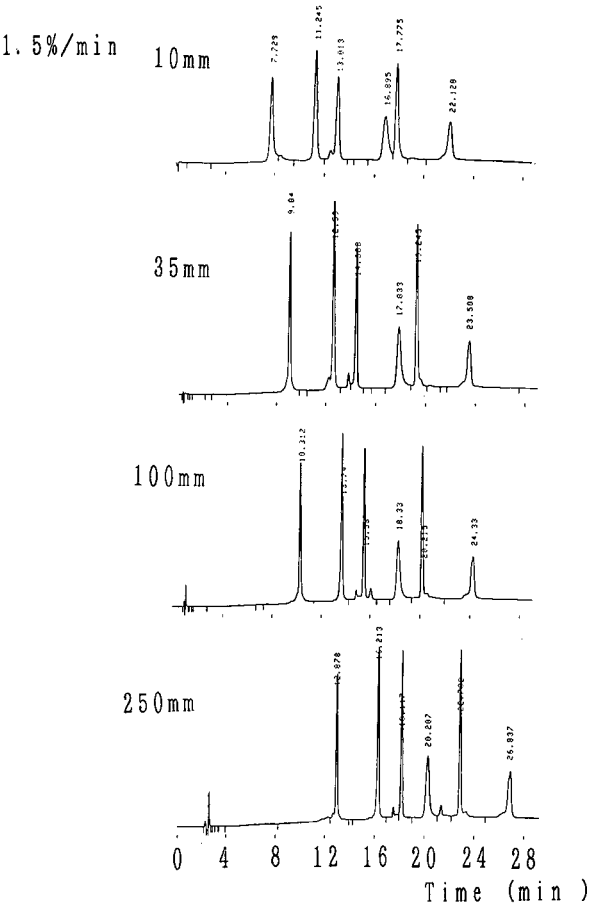

Fig. 7. Effect of column length (10–250 mm) on protein elution under slow gradient conditions. Conditions: linear gradient from 15 to 60% eluent B in 30 min. Peaks as in Fig. 6.

plained by the greater participation of the partition mode. Under such a slow gradient rate condition, the increase in organic solvent concentration is slower, so the time for which the partition mode dominates is extended. The peak widening obtained in a short column is considered to reflect the limited surface area where the protein can be repeatedly partitioned on the stationary phase. If the protein elution occurred in an "on–off" or "critical behaviour" elution mode, peak broadening should not be seen even in a short column. Hence the results also support the idea that protein elution involves a partition mode.

In conclusion, this study has indicated that protein elution occurs principally in the partition mode. Therefore, wide-pore packings, which have a sufficient surface area for protein partition, are expected to be more suitable for protein analysis than small-pore or non-porous packings, especially under low gradient rate conditions.

REFERENCES

1 J. D. Pearson, N. T. Lin and F. E. Regnier, *Anal. Biochem.*, 103 (1980) 1.
2 S. Terabe, H. Nishi and T. Ando, *J. Chromatogr.*, 212 (1981) 295.
3 K. K. Unger, J. N. Kinkel, B. Anspach and H. Giesche, *J. Chromatogr.*, 296 (1984) 3.
4 K. K. Unger, G. Jilge, N. Kinkel and M. T. W. Hearn, *J. Chromatogr.*, 359 (1986) 61.
5 G. Jilge, R. Janzen, H. Giesche, K. K. Unger, J. N. Nikel and M. T. W. Hearn, *J. Chromatogr.*, 397 (1987) 71.
6 R. Janzen, K. K. Unger, H. Giesche, J. N. Kinkel and M. T. W. Hearn, *J. Chromatogr.*, 397 (1987) 81.
7 R. Janzen, K. K. Unger, H. Giesche, J. N. Kinkel and M. T. W. Hearn, *J. Chromatogr.*, 397 (1987) 91.
8 M. A. Stadalius, B. F. D. Ghrist and L. R. Snyder, *J. Chromatogr.*, 387 (1987) 21.
9 M. T. W. Hearn, *J. Chromatogr.*, 418 (1987) 3.
10 J. D. Pearson, W. C. Mahoney, M. A. Hermodson and F. E. Regnier, *J. Chromatogr.*, 207 (1981) 15.
11 J. D. Pearson, N. T. Lin and F. E. Regnier, *Anal. Biochem.*, 124 (1982) 217.
12 F. E. Regnier, *Science*, 222 (1983) 245.
13 J. D. Pearson and F. E. Regnier, *J. Liq. Chromatogr.*, 6 (1983) 497.
14 X. Geng and F. E. Regnier, *J. Chromatogr.*, 296 (1984) 15.
15 J. L. Fausnaugh, L. A. Kennedy and F. E. Regnier, *J. Chromatogr.*, 387 (1987) 21.
16 D. W. Armstrong and R. E. Boehm, *J. Chromatogr. Sci.*, 22 (1984) 378.
17 D. W. Armstrong and K. H. Bui, *Anal. Chem.*, 54 (1982) 706.
18 D. W. Armstrong, K. H. Bui and R. E. Boehm, *J. Liq. Chromatogr.*, 6 (1983) 1.
19 K. H. Bui, D. W. Armstrong and R. E. Boehm, *J. Chromatogr.*, 288 (1984) 15.
20 K. H. Bui and D. W. Armstrong, *J. Liq. Chromatogr.*, 7 (1984) 29.
21 R. E. Boehm, D. E. Martire, D. W. Armstrong and K. H. Bui, *Macromolecules*, 16 (1983) 466.
22 R. E. Boehm, D. E. Martire, D. W. Armstrong and K. H. Bui, *Macromolecules*, 17 (1984) 4003.
23 N. Nimura, H. Itoh, T. Kinoshita, N. Nagae and M. Nomura, *J. Chromatogr.*, 585 (1991) 207.
24 M. T. W. Hearn and B. Gergo, *J. Chromatogr.*, 296 (1984) 61.
25 M. A. Stadalius, H. S. Gold and L. R. Snyder, *J. Chromatogr.*, 327 (1985) 27.
26 B. W. Sands, Y. S. Kim and J. L. Bass, *J. Chromatogr.*, 360 (1986) 353.
27 L. F. Colwel and R. A. Hartwick, *J. Liq. Chromatogr.*, 10 (1987) 2721.
28 Y. Kato, T. Kitamura, A. Mitsui and T. Hashimoto, *J. Chromatogr.*, 398 (1987) 327.
29 W. G. Burton, K. D. Nugent, T. K. Slattery, B. R. Summers and L. R. Snyder, *J. Chromatogr.*, 443 (1988) 363.
30 N. Tanaka, K. Kimata, Y. Mikawa, K. Hosoya, T. Araki, Y. Ohtsu, Y. Siojima, R. Tsuboi and H. Tsuchiya, *J. Chromatogr.*, 535 (1990) 13.
31 L. R. Snyder, M. A. Stadalius and M. A. Quarry, *Anal. Chem.*, 55 (1983) 1412A.
32 M. A. Stadalius, H. S. Gold and L. R. Snyder, *J. Chromatogr.*, 296 (1984) 31.
33 A. J. Banes, G. W. Link and L. R. Snyder, *J. Chromatogr.*, 326 (1985) 419.
34 M. A. Stadalius, H. S. Gold and L. R. Snyder, *J. Chromatogr.*, 327 (1985) 93.
36 R. W. Stout, S. I. Sivakoff, R. D. Ricker and L. R. Snyder, *J. Chromatogr.*, 353 (1986) 439.
37 M. A. Stadalius, M. A. Quarry, T. H. Mourey and L. R. Snyder, *J. Chromatogr.*, 358 (1986) 17.
38 M. A. Stadalius and L. R. Snyder, in Cs. Horvath (Editor), *High-Performance Liquid Chromatography. Advances and Perspectives*, Vol. 4, Academic Press, New York, 1984, p. 195.
39 J. M. D. Bussolo and R. Gant, *J. Chromatogr.*, 327 (1985) 67.
40 J. Koyama, J. Nomura, Y. Ohtsu, O. Nakata and M. Takahashi, *Chem. Lett.*, (1990) 687.
41 Y. Ohtsu, H. Fukui, T. Kanda, K. Nakamura., M. Nakano, O. Nakata and Y. Fujiyama, *Chromatographia*, 24 (1986) 380.

Journal of Chromatography, 625 (1992) 223–230
Elsevier Science Publishers B.V., Amsterdam

CHROM. 24 494

Improvement of the liquid chromatographic separation of the enantiomers of tetracyclic eudistomins by the combination of a β-cyclodextrin stationary phase and camphorsulphonic acid as mobile phase additive

Peter H. Kuijpers, Thijs K. Gerding and Gerhardus J. de Jong

Analytical Development Department, Solvay Duphar BV, P.O. Box 900, 1380 DA Weesp (Netherlands)

(First received April 9th, 1992; revised manuscript received July 6th, 1992)

ABSTRACT

Tetracyclic eudistomins, a class of compounds with potent antiviral and antitumour activity, contain two asymmetric centres, resulting into two (*d,l*) pairs called "*cis*" and "*trans*". The *cis*-enantiomers can be separated on the chiral stationary phase β-cyclodextrin using a mobile phase consisting of acetonitrile–triethylamine (99.5:0.5), adjusted to an apparent pH of 3.5 with trifluoroacetic acid. Separation of the *trans*-enantiomers was only achieved after the addition of camphorsulphonic acid to the mobile phase. The influence of the pH of the mobile phase, nature [D-(+) or L-(−)] and concentration of camphorsulphonic acid on retention and enantioselectivity was investigated.

INTRODUCTION

Tetracyclic eudistomins (1-amino-1,2,7,8,13,13b-hexahydro-[1,6,2]oxathiazepino[2′,3′:1,2]pyrido-[3,4-b]indole) are a class of indole alkaloids containing a tetrahydro-β-carboline fragment annulated with an oxathiazepine unit. These compounds display potent antiviral and antitumour activity [1,2]. At first, the tetracyclic eudistomins were isolated from natural sources, but recently the total synthesis of this class of compounds with interesting pharmacological activities was achieved [3]. Tetracyclic eudistomins contain two asymmetric centres, resulting into two (*d,l*) pairs called "*cis*" and "*trans*" (see Fig. 1). In order to follow the stereoselectivity of the synthesis, chiral liquid chromatographic (LC) systems were developed.

It was found that the *cis*-enantiomers can be separated on a β-cyclodextrine (β-CD) stationary phase, using as mobile phase acetonitrile–triethylamine (TEA) (99.5:0.5), adjusted to an apparent pH of 3.5 with trifluoroacetic acid (TFA). Using this system, the *trans*-enantiomers cannot be separated. A new possibility for the separation of enantiomers by using a combination of ion pairing and inclusion complexation was described by Szepesi and Gazdag [4]. They combined an achiral Nucleosil-10-CN column and a mobile phase containing a combination of α-, β and γ-CDs and D-(+)-10-camphorsulphon-

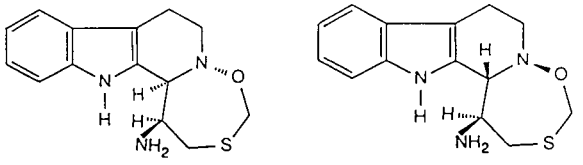

Fig. 1. Structures of *cis*-enantiomers (left) and *trans*-enantiomers (right) of tetracyclic eudistomins.

Correspondence to: Dr. T. K. Gerding, Analytical Development Department, Solvay Duphar BV, P.O. Box 900, 1380 DA Weesp, Netherlands.

0021-9673/92/$05.00

ic acid [D-(+)-CSA] and found an improvement in selectivity for the enantiomers of Yutac and Tobanum. Pettersson and Gioeli [5] found an improved resolution for the enantiomers of naproxen by the simultaneous use of a chiral acetylquinidine-silica stationary phase and quinine as chiral mobile phase additive. Based on the results presented in both papers, we have studied the addition of the enantiomers of 10-camphorsulphonic acid to the mobile phase, which is used for the separation of the *cis*-enantiomers. We investigated the effects of nature [D-(+) or L-(−)] and concentration of camphorsulphonic acid and the pH of the mobile phase on retention and selectivity for the *cis*- and *trans*-enantiomers. Further, a comparison was made with a conventional chiral ion-pair system, using a LiChrosorb-Diol column and D-(+)-CSA as mobile phase additive [6].

EXPERIMENTAL

Apparatus

The liquid chromatographic system consisted of an HP 1050 pump (Hewlett-Packard, Waldbronn, Germany), a Model 7125 injector fitted with a 10-μl loop (Rheodyne, Cotati, CA, USA) and a variable-wavelength UV detector (Kratos Spectroflow 757, ABI, Ramsey, NJ, USA). The chromatograms were recorded on an HP 3396 integrator (Hewlett-Packard). The column temperature was controlled through a Type M57020-88-2 column oven (Chrompack, Middelburg, Netherlands).

A β-cyclodextrin column (Cyclobond I) (250 x 4.6 mm I.D.) was purchased from Advanced Separation Technologies (Whippany, NJ, USA). The Diol-bonded silica column (250 x 4.6 mm I.D., particle size 5 μm) was packed with a slurry technique using tetrachloromethane–1-propanol (80:20) as the slurry medium and LiChrosorb-Diol from Merck (Darmstadt, Germany) as packing material.

Chemicals

The tetracyclic eudistomins were synthesized by Hermkens *et al.* [3]. High-performance liquid chromatographic-grade acetonitrile, technical-grade 2-propanol, TFA and TEA were purchased from Baker (Deventer, Netherlands). Technical grade dichloromethane was obtained from Baker and purified by distillation. D-(+)-CSA was used as the sodium salt and purchased from Merck (Darmstadt, Germany), while L-(−)-CSA and racemic CSA were used as acids and obtained from Fluka (Buchs, Switzerland).

Chromatographic conditions

The samples were dissolved in the eluent to a concentration of about 0.1 mg/ml. The injection volume was 10 μl and the tetracyclic eudistomins were detected by their UV-absorption at 275 nm. All separations were performed at a temperature of 30°C.

At first, enantiomeric separations of tetracyclic eudistomins were done on a β-CD stationary phase, using a mobile phase consisting of acetonitrile–TEA (99.5:0.5), adjusted to an apparent pH of 3.5 with TFA. The flow rate was 1.0 ml/min.

In subsequent experiments different types of CSA [D-(+), L-(−) or the racemate] were added to the mobile phase. The concentration of CSA was varied between 0 and 8 m*M*. The influence of the pH on the capacity factors and selectivity was investigated by varying the pH of the mobile phase, acetonitrile–4 m*M* D-(+)-CSA, from 10 to 3.5 using 0.5% TEA–TFA buffer. In all experiments in which CSA was added, the flow-rate was increased from 1.0 to 2.0 ml/min in order to reduce the analysis time.

The conventional chiral ion-pair system consisted of a LiChrosorb-Diol column and as mobile phase 2-propanol–dichloromethane (4:96) containing 4 m*M* D-(+)-CSA. Chromatography was carried out at a flow rate of 2.0 ml/min.

RESULTS AND DISCUSSION

In Fig 2, the chromatograms of the separations of *cis*- and *trans*-enantiomers of tetracyclic eudistomins on a β-CD stationary phase are shown. As can be seen, the β-CD column exhibits high enantioselectivity towards the *cis*-enantiomers, whereas the *trans*-enantiomers are not separated. The chiral recognition mechanism of CDs is attributed to inclusion complex formation between the cavity of the CD and the hydrophobic moiety of the solute, in combination with hydrogen bonding between the polar functional groups of the solute in the vicinity of its chiral centre and the hydroxyl groups of the CD [7–10]. It is generally assumed that aqueous–organic mobile phases are required for the formation of inclusion complexes [11–13]. In our experi-

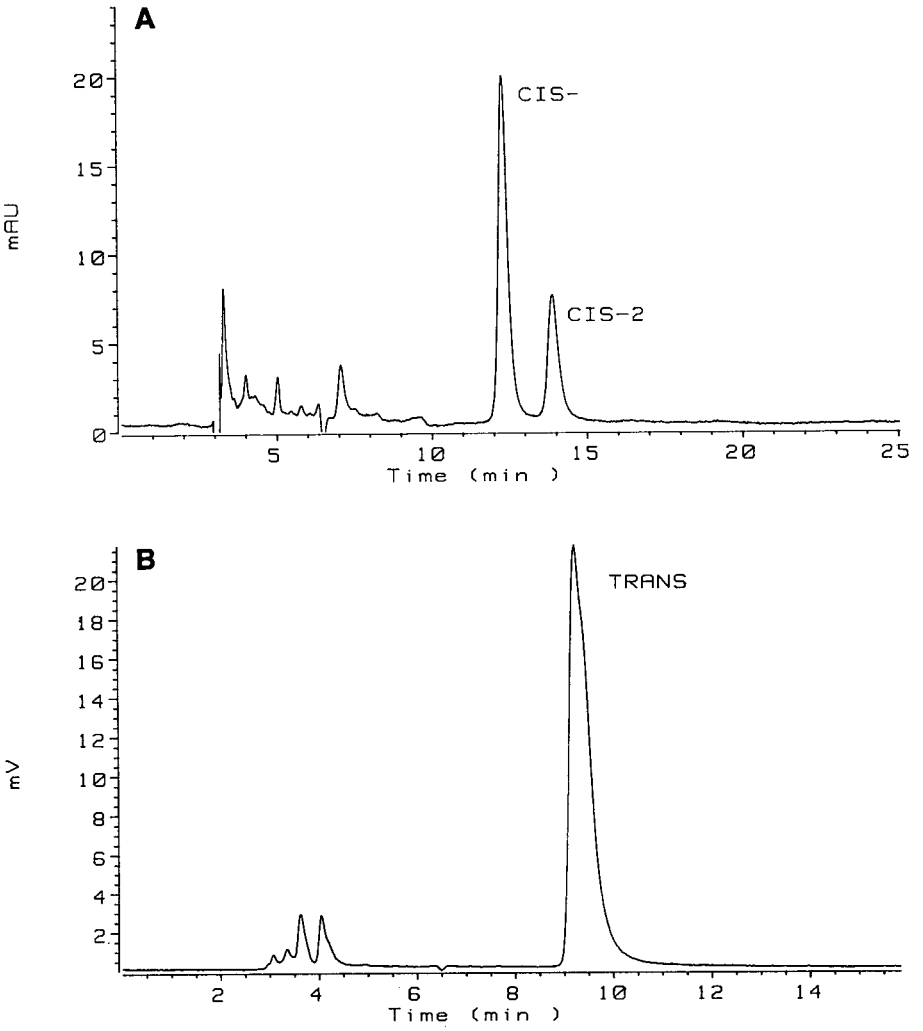

Fig. 2. Chromatograms of (A) *cis*- and (B) *trans*-enantiomers of tetracyclic eudistomins. Column, 250 × 4.6 mm I.D. β-cyclodextrin; mobile phase, acetonitrile–TEA (99.5:0.5), adjusted to pH 3.5 with TFA; flow rate, 1.0 ml/min.

ments, we succeeded in separating the *cis*-enantiomers using acetonitrile as mobile phase. Therefore, we assume that also in a non-aqueous mobile phase inclusion complexes can be formed.

The observed enantioselectivity may be attributed to the use of acetonitrile, as it is known from a study of Seeman *et al.* [13] that this modifier can cause anomalous retention behaviour on a β-CD column. They found that the retention times of the enantiomers of N′-benzylnornicotine decreased when the proportion of acetonitrile in the aqueous mobile phase was increased from 10% up to about 80%, but an increase in retention was observed when the proportion of acetonitrile was increased further up to 100%. Compared with an eluent containing 60–80% of acetonitrile, they demonstrated an improvement in enantioselectivity for acetonitrile contents above 80% and suggested that the mechanism of chiral recognition has changed. In the presence of non-polar solvents (such as hexane–2-propanol mixtures), inclusion of the solute in the cavities of CDs is probably hampered because

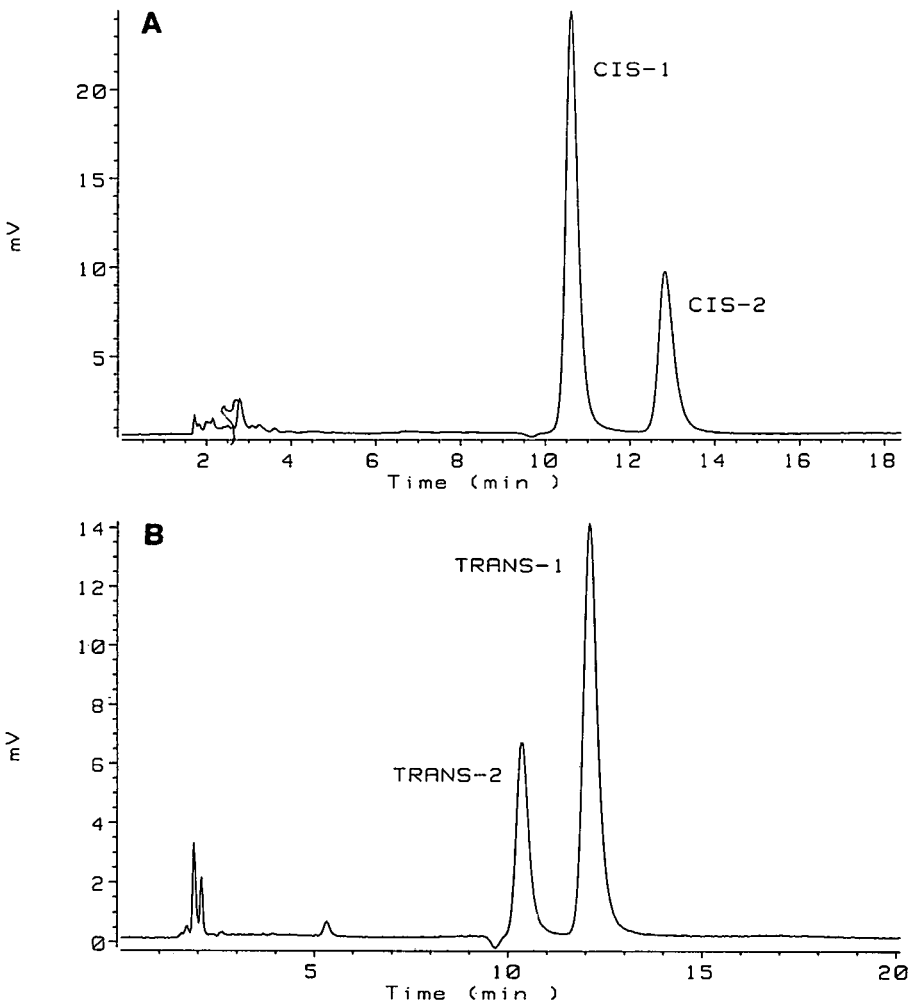

Fig. 3. Chromatograms of (A) *cis*- and (B) *trans*-enantiomers of tetracyclic eudistomins after the addition of 4 m*M* D-(+)-CSA to the mobile phase. Flow-rate, 2.0 ml/min; other chromatographic conditions as in Fig. 2.

the non-polar component of the mobile phase occupies the cavity. However, our results indicate that the modifier acetonitrile does not completely occupy the cavity of β-CD, as inclusion complexes can still be formed.

By adding D-(+)-CSA to the mobile phase, the enantioselectivity of the *trans*-enantiomers is improved significantly, and for the *cis*-enantiomers an improvement in selectivity is obtained also. The chromatograms of the enantiomeric separations after the addition of D-(+)-CSA to the mobile phase are shown in Fig. 3. It is well known that chiral amines can form diastereomeric ion pairs with CSA [6,14–17]. The gain in selectivity for the *trans*-enantiomers and, to a lesser extent, also for the *cis*-enantiomers may be ascribed to the ion-pair complexation followed by a different distribution of the ion pairs into the cavities of CD [4].

Effect of nature and concentration of CSA

The influence of nature and concentration of CSA on the capacity factors (k') and enantioselectivities (α) was studied. The results of these experiments are presented in Table I. The addition of 2

TABLE I

INFLUENCE OF NATURE AND CONCENTRATION OF CSA ON CAPACITY FACTORS (k') AND SELECTIVITIES (α) OF THE CIS- AND TRANS-ENANTIOMERS OF TETRACYCLIC EUDISTOMINS

CSA	Concentration (m*M*)	*trans*-enantiomers			*cis*-enantiomers		
		k'_1	k'_2	α^a	k'_1	k'_2	α
D-(+)-CSA	0	2.1	2.1	1.00	2.9	3.5	1.18
	2	5.6	6.6	1.19	5.8	7.2	1.24
	4	6.8	8.1	1.19	7.0	8.9	1.27
	6	7.4	8.8	1.19	7.6	9.8	1.28
	8	8.7	10.3	1.18	8.5	11.0	1.28
L-(−)-CSA	2	4.2	4.7	−1.12	4.3	4.8	1.11
	4	9.0	10.5	−1.17	8.0	8.8	1.09
	8	8.6	9.9	−1.15	8.1	8.6	1.07
(D,L)-CSA	4	5.5	5.5	1.00	4.9	5.6	1.15

[a] The minus sign before a selectivity value indicates that the elution order of the enantiomers is reversed.

m*M* D-(+)-CSA increases the capacity factors of all the enantiomers, whereas the enantioselectivity improves markedly for the *trans*-enantiomers and, to a lesser extent, also for the *cis*-enantiomers. On further increasing the concentration of D-(+)-CSA, the capacity factors of all enantiomers increase, while no further gain in selectivity is obtained for the *trans*-enantiomers and only a minor improvement for the *cis*-enantiomers is found.

When 2 m*M* L-(−)-CSA is added to the mobile phase, for the *trans*-enantiomers a higher selectivity is obtained. However, it is striking that compared with the addition of D-(+)-CSA, the elution order of both *trans*-enantiomers is reversed, which is indicated in Table I by a minus sign before the selectivity value. This reversal could be detected as we analysed non-racemic mixtures of both (*d,l*) pairs. For the *cis*-enantiomers, the selectivity decreases after the addition of L-(−)-CSA to the eluent, whereas no reversal of the elution order of the two enantiomers is found. On increasing the concentration of L-(−)-CSA, no significant influence on the selectivity for the *trans*-enantiomers is found, whereas for the *cis*-enantiomers the selectivity seems to decrease slightly. The inversion of the elution order of the *trans*-enantiomers after the addition of L-(−)-CSA can be explained by the fact that diastereomeric ion pairs of opposite configuration are formed. These results are comparable to a situation when an optically impure chiral selector is added to the mobile phase. With a decreasing optical purity of the chiral selector, the resolution between the enantiomers decreases and a reversed selectivity is found if the antipode of the chiral selector is added [4,18].

After the addition of (D,L)-CSA to the mobile phase, no separation is obtained for the *trans*-enantiomers, whereas the enantioselectivity for the *cis*-enantiomers is comparable to that for the system in which no CSA is added. However, in contrast to the latter situation, the capacity factors of all enantiomers have increased significantly, demonstrating ion-pair formation with CSA.

Effect of pH

As can be expected for ion-pair chromatography, the pH of the mobile phase is an important factor. The results of variation of the pH of the mobile phase, acetonitrile–4 m*M* D-(+)-CSA, from 10 to 3.5 are summarized in Table II. It can be seen that at a pH of 6 or lower, a pronounced improvement in enantioselectivity is obtained for the *trans*- and *cis*-enantiomers. Moreover, the capacity factors also increase if the pH decreases. The pK_a values of all three nitrogen atoms were calculated by QSAR studies and estimated to be about 9.5 for the primary amino group, less than zero for the indolic nitrogen and about 6 for the tertiary nitrogen atom.

TABLE II

INFLUENCE OF THE pH OF THE MOBILE PHASE, WITH AND WITHOUT D-(+)-CSA, ON CAPACITY FACTORS (k') AND SELECTIVITIES (α) OF CIS- AND TRANS-ENANTIOMERS OF TETRACYCLIC EUDISTOMINS

pH	D-(+)CSA (m*M*)	*trans*-enantiomers			*cis*-enantiomers		
		k'_1	k'_2	α	k'_1	k'_2	α
10	0	0.19	0.19	1.00	2.8	3.2	1.15
	4	0.29	0.29	1.00	2.9	3.1	1.07
8	0	0.23	0.23	1.00	3.4	3.8	1.13
	4	0.40	0.40	1.00	4.3	4.9	1.12
6	0	2.4	2.4	1.00	5.1	6.0	1.17
	4	3.3	3.7	1.12	7.3	9.1	1.24
5	0	2.8	2.8	1.00	4.1	4.9	1.17
	4	8.0	9.3	1.16	8.6	10.8	1.25
3.5	0	2.9	2.9	1.00	3.6	4.2	1.17
	4	8.1	9.8	1.20	7.7	9.8	1.26

At a pH of 6 or lower, the tertiary amine function is (partly) protonated resulting into the formation of ion pairs and a separation of the *trans*-enantiomers. Therefore, it can be concluded that for ion pairing, electrostatic interaction of the protonated tertiary nitrogen with the sulphonic group of CSA is essential. As the *cis*-enantiomers are separated over the whole pH range investigated, it can be concluded that ion pairing is no prerequisite for the chiral recognition of the *cis*-enantiomers. In the system without CSA, the capacity factors of the *trans*-enantiomers increase with decreasing pH, whereas for the *cis*-enantiomers an increase in the capacity factors is observed in the pH range from 10 to 6, followed by a decrease at lower pH values. The observation that very low capacity factors for the *trans*-enantiomers are found at high pH may be explained by the fact that TEA will bind to the hydroxyl groups of CD and thereby compete with hydrogen bonding of the solute. Therefore, it can be concluded that especially for the *trans*-enantiomers, interaction with the external hydroxyl groups at the mouth of the CD cavity play an essential role in the retention.

Comparison with a conventional chiral ion-pair system

For the LiChrosorb-Diol stationary phase, it has been reported that a large enantioselectivity is obtained under conditions that favour a high degree of ion-pair formation [6]. Water, even in very low concentrations, can have an adverse influence on the enantioseparation. In our experiments, this condition is fulfilled as we used a mobile phase of 100% acetonitrile. Further, it is known that for good complexation with CSA, a hydrogen-donating function at a distance of two carbon atoms from the hydrogen-accepting amine function is essential for the stereoselectivity [17]. In the present system, tetracyclic eudistomins contain a protonated amino group two carbon atoms from the tertiary amine function. This amino group can interact by hydrogen bonding with the oxo group of CSA. The electrostatic interaction of the tertiary amine nitrogen with the sulphonic group of CSA in combination with the hydrophobic interaction between the ring systems of CSA and tetracyclic eudistomins provide for three interaction points (Dalgliesh's "three-point" rule [19]), so in principle efficient enantioselective ion-pair formation can occur.

Therefore, the results described above, obtained with a combination of a chiral column and a chiral mobile phase additive, were compared with those obtained on a conventional chiral ion-pair system using a LiChrosorb-Diol column. From the chromatogram shown in Fig. 4, it can be concluded that separation of *cis*- and *trans*-enantiomers is also possible on a LiChrosorb-Diol column with D-(+)-CSA in the mobile phase, although the selectivity [α(*cis*-enantiomers) = 1.08; α(*trans*-enantiomers) = 1.10] and efficiency of this system are lower. For this system, the plate number is about 2900 (*trans*-

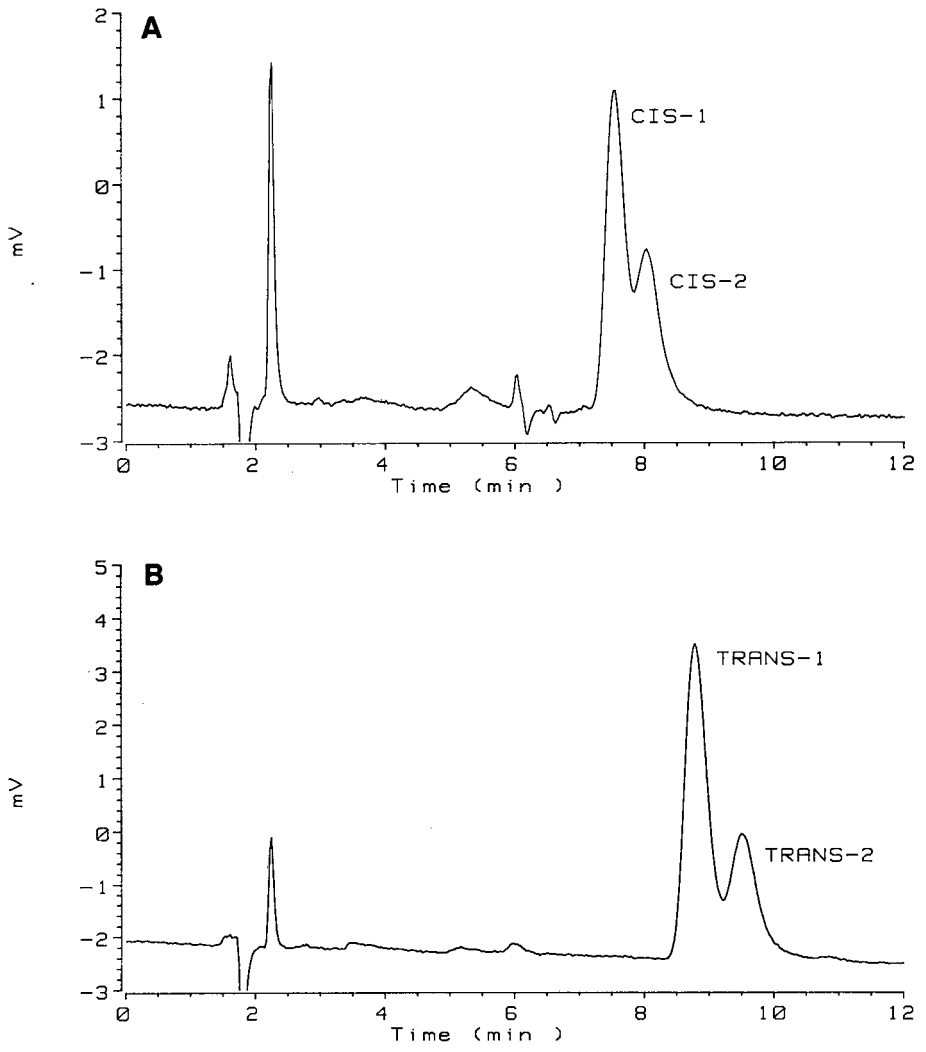

Fig. 4. Chromatograms of (A) *cis*- and (B) *trans*-enantiomers of tetracyclic eudistomins. Column, 250 × 4.6 mm I.D. LiChrosorb-Diol; mobile phase, 2-propanol–dichloromethane (4:96) containing 4 m*M* D-(+)-CSA; flow-rate, 2.0 ml/min.

enantiomers) or 2600 (*cis*-enantiomers) against 4500 (*trans*-enantiomers) or 5600 (*cis*-enantiomers) in the CD system. It should be noted that in comparison with the chromatogram presented in Fig. 3, a reversal in elution order for the *trans*-enantiomers occurs, whereas for the *cis*-enantiomers the elution order is identical in both chromatographic systems. The reversal of elution order for the *trans*-enantiomers suggests that the stationary phases LiChrosorb-Diol and β-CD have a different separation mechanism, as in both LC systems the same amount and nature of CSA were added to the mobile phase. For a LiChrosorb-Diol column, the stereoselectivity is obtained by a different distribution of the diastereomeric ion pairs between the mobile and the stationary phases. Evidently, for a β-CD column the different inclusion complexation of the diastereomeric ion pairs may cause a change in retention behaviour for the *trans*-enantiomers in comparison with the LiChrosorb-Diol column.

CONCLUSIONS

In contrast to what is commonly assumed, our results indicate that inclusion complex formation can occur on a β-CD bonded phase using a non-aqueous mobile phase. Moreover, by choosing the proper conditions for ion-pair chromatography, using camphorsulphonic acid as ion-pair reagent, an increase in stereoselectivity can be obtained, probably as a consequence of a more effective discrimination of β-CD for the diastereomeric ion pairs. The pH of the mobile phase and the nature and concentration of CSA added are important factors in the chiral selectivity.

We have frequently applied the combination of a β-CD stationary phase and D-(+)-CSA in the mobile phase to separate the enantiomers of various new chemical entities with similar structural features to the tetracyclic eudistomins. For those compounds which can form ion pairs, this combination was found to offer an excellent possibility of improving enantioselectivity. Further studies are in progress to investigate if this approach can be exploited to improve enantioselectivity by adding other chiral counter ions, *e.g.* N-benzoxycarbonyl-glycyl-L-proline (ZGP), to the mobile phase.

ACKNOWLEDGEMENT

The authors thank Dr. M. R. Linschoten for calculating the pK_a values of the tetracyclic eudistomins.

REFERENCES

1 A. C. Schroeder, R. G. Hughes and A. J. Bloch, *J. Med. Chem.*, 24 (1981) 1078.
2 R. J. Lake, J. W. Blunt and M. H. G. Munro, *Aust. J. Chem.*, 42 (1989) 1201.
3 P. H. H. Hermkens, J. H. van Maarseveen, H. C. J. Ottenheijm, C. G. Kruse and J. W. Scheeren, *J. Org. Chem.*, 55 (1990) 3998.
4 G. Szepesi and M. Gazdag, *J. Pharm. Biomed. Anal.*, 6 (1988) 623.
5 C. Pettersson and C. Gioeli, *J. Chromatogr.*, 435 (1988) 225.
6 C. Pettersson and G. Schill, *J. Chromatogr.*, 204 (1981) 179.
7 W. L. Hinze, T. E. Riehl, D. W. Armstrong, W. DeMond, A. Alak and T. Ward, *Anal. Chem.*, 57 (1985) 237.
8 D. W. Armstrong, *J. Liq. Chromatogr.*, 7 (1984) 353.
9 D. W. Armstrong and W. DeMond, *J. Chromatogr. Sci.*, 22 (1984) 411.
10 D. W. Armstrong, W. DeMond, A. Alah, W. L. Hinze, T. E. Riehl and K. H. Bui, *Anal. Chem.*, 57 (1985) 234.
11 S. Li and W. C. Purdy, *J. Chromatogr.*, 543 (1991) 105.
12 D. A. Armstrong, A. M. Stalcup, M. L. Hilton, J. D. Duncan, J. R. Faulkner, Jr., and S.-C. Chang, *Anal. Chem.*, 62 (1990) 1610.
13 J. I. Seeman, H. V. Secor, D. A. Armstrong, K. D. Timmons and T. J. Ward, *Anal. Chem.*, 60 (1988) 2120.
14 G. Szepesi, M. Gazdag and R. Ivancsics, *J. Chromatogr.*, 241 (1982) 153.
15 G. Szepesi, M. Gazdag and R. Ivancsics, *J. Chromatogr.*, 244 (1982) 33.
16 C. Pettersson and G. Schill, *Chromatographia*, 16 (1982) 192.
17 C. Pettersson and M. Josefsson, *Chromatographia*, 21 (1986) 321.
18 C. Pettersson, A. Karlsson and C. Gioeli, *J. Chromatogr.*, 407 (1987) 217.
19 C. E. Dalgliesh, *J. Chem. Soc.*, 137 (1952) 3940.

Journal of Chromatography, 625 (1992) 231–235
Elsevier Science Publishers B.V., Amsterdam

CHROM. 24 605

Liquid chromatographic separation of the enantiomers of diniconazole using a β-cyclodextrin-bonded column

Ritsuko Furuta and Hiroshi Nakazawa

Environmental Health Science Laboratory, Sumitomo Chemical Co. Ltd., 3-1-98, Kasugade Naka, Konohana-ku, Osaka 554 (Japan)

(First received July 16th, 1992; revised manuscript received September 4th, 1992)

ABSTRACT

Enantiomers of the fungicide diniconazole were separated by reversed-phase high-performance liquid chromatography on a commercially available β-cyclodextrin (β-CD)-bonded column. The effects of organic modifier in the mobile phase, mobile phase pH and column temperature on the retention and resolution of the enantiomers were studied and optimum conditions were established. The retention behaviour of some structurally related compounds of diniconazole under the optimum conditions were examined to clarify the separation mechanism on the β-CD-bonded column. Optical separation of diniconazole using β-CD as a mobile phase modifier on an octadecylsilanized (ODS) silica gel column was also investigated for comparison with separation by the above method.

INTRODUCTION

Diniconazole (Fig.1), which has fungicidal activity, is an optically active compound and the enantiomers are very different in their activity, like many other bioactive reagents. In this instance the activity of the *R*-enantiomer is much higher than that of the *S*-enantiomer, and diniconazole-M, containing a high proportion of the *R*-enantiomer, was developed for the purpose of obtaining a high activity of the product [1]. Consequently, analytical methods for separating the enantiomers are very important for studies of biological action and activity, dynamics and kinetics and also for quality control of the compound. Although some normal-phase high-performance liquid chromatographic (HPLC) methods for diniconazole using chiral stationary phases based mainly on π–π interactions and hydrogen bonding have already been reported [2–4], no reversed-phase methods have been reported.

Cyclodextrin (CD)-bonded stationary phases have recently been developed for use in the reversed-phase mode for the separation of enantiomers [5–8]. CDs are torus-shaped cyclic oligosaccharides containing from six to twelve D-(+)-glucopyranose units, which are bonded through α-(1,4) linkages. The most common CDs are α-, β- and γ-CDs, containing six, seven and eight glucose units, respectively. The interior of the CD cavities is relatively hydrophobic, thus allowing them to form inclusion complexes with a variety of molecules.

The basic property of CDs that allows them to affect chiral separations is their ability to form enantioselective inclusion complexes with guest molecules. There are several requirements for chiral

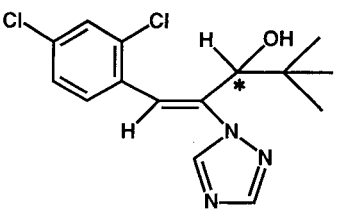

Fig. 1. Structure of diniconazole.

Correspondence to: R. Furuta, Environmental Health Science Laboratory, Sumitomo Chemical Co. Ltd., 3-1-98, Kasugade Naka, Konohana-ku, Osaka 554, Japan.

0021-9673/92/$05.00

recognition by CDs. The size of the CD cavity with respect to the size of the enantiomer to be complexed is of critical importance; tighter fitting molecules are preferable. Additionally, it is beneficial if the substituents attached to the chiral centre of the compound to be resolved interact with the secondary hydroxyl groups at the mouth of the CD cavity by hydrogen bonding [9].

We found that enantiomers of diniconazole were separated on a β-CD-bonded column, but not on an α-CD-bonded column, and were partly separated on a γ-CD-bonded column. In this study, the enantiomeric separation of diniconazole with respect to the chromatographic conditions and elution behaviour of structurally related compounds on the β-CD-bonded column were investigated and possible mechanisms are discussed.

EXPERIMENTAL

Apparatus

Chromatography was performed using a liquid chromatographic system which consisted of a Model L-6200 pump equipped with a Model L-4000 variable-wavelength spectrometric detector (Hitachi, Tokyo, Japan). The chromatograms were recorded on a Model C-R4A integrator (Shimadzu, Kyoto, Japan). The column temperature was controlled through a Model UC-55N water-bath (Tokyo Rikakikai, Tokyo, Japan).

Cyclobond I, II and III columns (250 mm × 4.6 mm I.D.) packed with 5-μm spherical silica gel with chemically bonded β-, γ- and α-CD, respectively. were purchased from Advanced Separation Technologies (Whippany, NJ, USA). A Sumipax ODS A-212 column (150 mm × 6 mm I.D., 5 μm) was purchased from Sumika Chemical Analysis Service (Osaka, Japan).

Chemicals

Diniconazole and structurally related compounds were synthesized by Sumitomo Chemical (Osaka, Japan). β-CD was purchased from Kanto (Tokyo, Japan). Organic solvents and other reagents were of analytical-reagent grade from Kanto or Wako (Osaka, Japan). Water was processed through an RO/NANOpure II system (Barnstead, Dubuque, IA, USA).

Chiral stationary phase system

Experiments were carried out with Cyclobond I unless specified otherwise. The mobile phase was prepared by mixing an organic solvent with water or 0.1% triethylammonium acetate (TEAA) buffer. Sample solutions were prepared by dissolving each compound in methanol to give a concentration of 0.3 mg/ml. A 5-μl portion of the sample solutions was injected. The column temperature was kept at 20°C unless specified otherwise. The flow-rate was 0.5 ml/min and the detector was set at 254 nm. The void volume was determined by injecting methanol.

Chiral mobile phase system

The column used was Sumipax ODS A-212. For the mobile phase, β-CD was dissolved in 4.0 or 4.5 *M* aqueous urea, the pH of the solution was adjusted to 6.0 with diluted phosphoric acid and then acetonitrile was added. Sample solutions were 0.03 mg/ml in methanol. Separations were performed at controlled room temperature (*ca.* 25°C) with a flow-rate of 1.0 ml/min; the other conditions were the same as above.

RESULTS AND DISCUSSION

Chiral recognition of CDs

The effect of the type of CDs on the chiral recognition of diniconazole was investigated by using α-, β- and γ-CD-bonded columns.

The enantiomers of diniconazole were separated completely only on the β-CD-bonded column; they were not separated at all on the α-CD-bonded column and only partly separated on the γ-CD-bonded column (Table I). This shows that the formation of an inclusion complex depends on the size of the CD

TABLE I

ENANTIOMERIC SEPARATION OF DINICONAZOLE ON CYCLODEXTRIN-BONDED COLUMNS

Column	k_1'[a]	α[b]	Mobile phase[c]
Cyclobond I	6.47	1.19	80:20
Cyclobond II	4.96	1.04	87:13
Cyclobond III	4.99	1.00	90:10

[a] Capacity factor of first-eluted enantiomers.
[b] Separation factor.
[c] Mobile phase, acetonitrile–water (v/v).

cavity. The molecule of diniconazole can fit in the cavity of β-CD. Although complexation is also possible with γ-CD, the large cavity probably includes the molecule loosely, not differentiating between the enantiomers. The cavity of α-CD is too small for the molecule to enter. The β-CD bonded column was used in all subsequent experiments.

Effect of the structure of organic modifier

Because CDs form inclusion complexes with various hydrophobic compounds, organic solvent molecules in the mobile phase compete with the solute in occupying the CD cavity. The effects of the hydrophobicity and bulkiness of the organic modifier in the mobile phase on the separation of diniconazole were investigated using series of primary and secondary alcohols, and also acetonitrile. Each organic solvent concentration was adjusted so that the capacity factor of the first-eluted enantiomer was about 7.

As shown in Table II, the separation factors and resolutions decreased with increase in the number of carbon atoms. In a comparison of 1-propanol and 2-propanol, or 1-butanol, 2-methyl-1-propanol and 2-methyl-2-propanol, when the branched-chain isomers were used the peaks tended to tail and smaller resolution values were obtained, although the separation factors were almost the same as when the corresponding straight-chain alcohol was used. This result could be explained as follows; an increase in the bulkiness and hydrophobicity of the alcohol would increase the interaction between the alcohol and the CD cavity, shown as association constants, log K_a [10] in Table II , and then the alcohol would compete more strongly with the solute.

Acetonitrile–water was found to provide much better resolution than alcohol–water systems, probably because of its low interaction with hydroxyl groups of CD, and was therefore chosen as the mobile phase in subsequent experiments.

TABLE II

EFFECT OF ORGANIC MODIFIERS ON SEPARATION FACTORS, α, AND RESOLUTION, R_s

Column, Cyclobond I.

Organic modifier[a]	α	R_s	Log K_a[b]
Acetonitrile (20:80)	1.19	2.75	–
Methanol (36:64)	1.19	2.23	−0.49
Ethanol (25:75)	1.20	2.18	−0.03
1-Propanol (14:86)	1.16	1.93	0.57
2-Propanol (15:85)	1.17	1.76	0.58
1-Butanol (7:93)	1.13	1.70	1.22
2-Butanol (9:91)	1.16	1.78	1.19
2-Methyl-1-propanol (6:94)	1.13	1.59	1.62
2-Methyl-2-propanol (10:90)	1.14	1.06	1.68

[a] Mobile phase, organic modifier–water(v/v).

[b] Logarithm of association constant for β-CD–alcohol complex [10].

Effect of acetonitrile content

The effects of the acetonitrile content on the retention and resolution were investigated by changing the acetonitrile–water ratio in the mobile phase. Fig. 2 shows plots of the capacity factors of the first-eluted enantiomers and separation factors *versus* acetonitrile content. Both the retention time and selectivity decreased with increase in the acetonitrile content. A 20% acetonitrile content was adopted in subsequent experiments because a good separation was achieved in a reasonable time.

Effect of pH

The influence of pH on the capacity factors and separation factors of diniconazole was investigated by changing the pH of the mobile phase using 0.1% TEAA buffer. pH had no effect on the separation factors, as expected for this non-ionic compound,

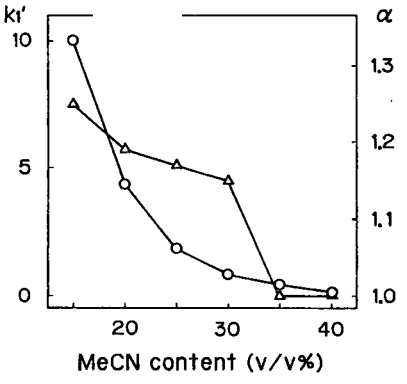

Fig. 2. Effect of acetonitrile content in the mobile phase on (○) capacity factors, k'_1 (capacity factors of the first-eluted enantiomers), and (△) separation factors, α. Column, Cyclobond I; mobile phase, acetonitrile–water.

TABLE III

EFFECT OF pH ON CAPACITY FACTORS, k'_1[a], AND SEPARATION FACTORS, α

Column, Cyclobond I; mobile phase, acetonitrile-0.1% TEAA buffer or water (20:80, v/v).

pH	k'_1[a]	α
4.0	4.39	1.18
5.0	4.56	1.18
6.0	4.98	1.19
7.0	4.48	1.19
Water	6.47	1.19

[a] Capacity factor of first-eluted enantiomer.

although the capacity factors were smaller when TEAA buffer was used than that when water was used, as shown in Table III.

Effect of column temperature

The effect of column temperature on the retention and resolution was examined over the range 0–60°C. The retention and resolution were significantly influenced by the column temperature, as can be seen in Fig.3. The capacity factors and the separation factors decreased with increase in the column temperature, and the enantiomers were not resolved at 60°C (k'_1 = 1.14). It is interesting to compare this result with that shown in Fig. 2 at the lower temperature, in which optical resolution was

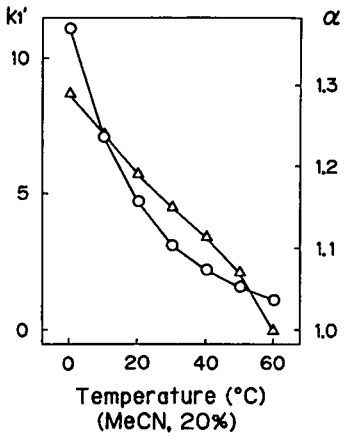

Fig. 3. Effect of column temperature on capacity factors, k'_1 and separation factors, α. Symbols as in Fig. 2; column, Cyclobond I; mobile phase, acetonitrile–water (20:80, v/v).

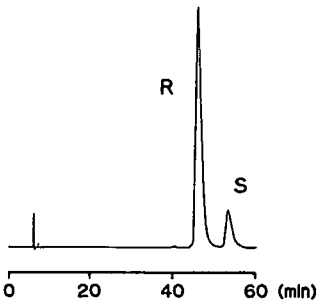

Fig. 4. Enantiomeric separation of diniconazole-M on Cyclobond I. Mobile phase, acetonitrile–water (20:80, v/v); temperature, 20°C.

still achieved when k'_1 was 0.86 (at a 30% acetonitrile content). These results indicate that inclusion complex formation is prevented at temperatures higher than 60°C, as reported previously [11].

Retention behavior of structurally related compounds

Fig. 4 shows the optical resolution of diniconazole-M under the optimum conditions and Table IV

TABLE IV

RETENTION BEHAVIOUR OF STRUCTURALLY RELATED COMPOUNDS OF DINICONAZOLE ON CYCLOBOND I

Chromatographic conditions as in Fig. 4.

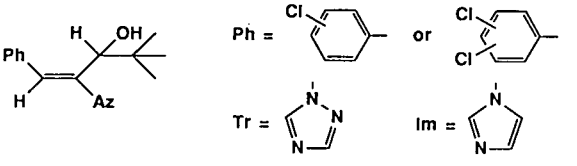

Ph	Az	k'_1[a]	α[b]
2-Cl	Tr	2.77	1.08
3-Cl	Tr	2.64	1.00
4-Cl	Tr	3.23	1.00
4-Cl	Im	4.95	1.00
2,3-Cl_2	Tr	2.56	1.00
2,4-Cl_2	Tr[c]	3.20	1.18
2,4-Cl_2	Im	6.71	1.17
3,4-Cl_2	Tr	4.23	1.10
3,5-Cl_2	Tr	1.81	1.00

[a] Capacity factor of first-eluted enantiomer.
[b] Separation factor.
[c] Diniconazole.

lists the capacity factors and separation factors of structurally related compounds of diniconazole under the same conditions. Among the triazoles, the 2-chlorophenyl and 3,4-dichlorophenyl analogues were resolved into the enantiomers, in addition to diniconazole, and the other substituents were not resolved. Imidazoles were retained longer than triazoles because of their higher hydrophobicity [12], but the enantioselectivity was not affected by the triazole or imidazole ring in the molecule.

From these results, it was concluded that the benzene ring of the solute inserted into the CD cavity and its substituent(s) played an important role from a steric point of view, a tight fit being important. The hydroxyl group at the chiral centre and a nitrogen atom in the triazole ring could interact with the hydroxyl groups at the mouth of the CD cavity by hydrogen bonding at the same time.

β-CD as a chiral additive

The method using β-CD as a chiral mobile phase additive was applied to the separations of diniconazole enantiomers. The enantiomers were slightly resolved on the Sumipax ODS A-212 column with 30 m*M* β-CD in 4.5 *M* aqueous urea (pH 6.0)–acetonitrile (60:40, v/v). Higher concentrations of β-CD seem to be necessary for complete separation, but it could not be achieved owing to the limited solubility of β-CD.

In this method, the *S*-enantiomer eluted first, in contrast to the above method using the chiral stationary phase. This phenomenon is explained as follows: the enantiomer forming a more stable complex with the CD elutes first in the chiral mobile phase method because CDs interact little with the hydrophobic stationary phase owing to the hydrophilic nature of the external faces of them; on the other hand, this enantiomer elutes later in the chiral stationary phase method because it is retained longer on the CD-bonded phase.

CONCLUSIONS

It has been demonstrated that a β-CD-bonded column exhibits a high enantioselectivity for diniconazole and some analogues. The investigation of the effects of the size of CDs, the mobile phase composition, column temperature and the small changes in the structure of the solute on the retention and resolution suggested that inclusion complex formation between the benzene ring of the solute and the CD cavity is the most important factor in the chiral recognition.

REFERENCES

1 H. Takano, Y. Oguri and T. Kato, *Nippon Noyaku Gakkaishi*, 11 (1986)373.
2 N. Ôi and H. Kitahara, *J. Liq. Chromatogr.*, 9 (1986) 511.
3 N. Ôi, H. Kitahara, Y. Matsumoto, H. Nakajima and Y. Horikawa, *J. Chromatogr.*, 462 (1989) 382.
4 N. Ôi, H. Kitahara and R. Kira, *J. Chromatogr.*, 535 (1990) 213.
5 D. W. Armstrong and W. DeMond, *J. Chromatogr. Sci.*, 22 (1984) 411.
6 D. W. Armstrong, T. J. Ward, R. D. Armstrong and T. E. Beesley, *Science (Washington, D.C.)*, 232 (1986) 1132.
7 D. W. Armstrong, S. M. Han and Y. I. Han, *Anal. Biochem.*, 167 (1987) 261.
8 D. W. Armstrong, Y. I. Han and S. M. Han, *Anal. Chim. Acta*, 208 (1988) 275.
9 A. M. Krstulovic (Editor), *Chiral Separations by HPLC*, Ellis Horwood, Chichester, 1989, Ch.10, pp. 213–214.
10 Y. Matsui and K. Mochida, *Bull. Chem. Soc. Jpn.*, 52 (1979) 2808.
11 W. L. Hinze, T. E. Riehl, D. W. Armstrong, W. DeMond, A. Alak and T. Ward, *Anal. Chem.*, 57 (1985) 237.
12 Japan Society for Bioscience, Biotechnology, and Agrochemistry, *Biorational Approach for Pesticide Design*, Soft Science, Tokyo, 1986, Ch.9, p. 184.

Journal of Chromatography, 625 (1992) 237–245
Elsevier Science Publishers B.V., Amsterdam

CHROM. 24 504

Drying step for introduction of water-free desorption solvent into a gas chromatograph after on-line liquid chromatographic trace enrichment of aqueous samples

Jolan J. Vreuls, Rudy T. Ghijsen, Gerhardus J. de Jong☆ and Udo A. Th. Brinkman

Department of Analytical Chemistry, Free University, De Boelelaan 1083, 1081 HV Amsterdam (Netherlands)

(Received May 15th, 1992)

ABSTRACT

Two procedures are described which effect the rigorous removal of water from the liquid chromatographic (LC) precolumn during the on-line LC trace enrichment–capillary gas chromatography (GC) of aqueous samples, thereby preventing the deterioration of the performance of the retention gap and, thus, the loss of analytes. After LC preconcentration of an aqueous sample on a polymer-packed precolumn, the ethyl acetate used for desorption is led to the GC system either via a small cartridge containing a drying agent (anhydrous sodium sulphate or silica) or after removal of residual water from the precolumn by means of a 30-min nitrogen purge. Regeneration of the drying agents by electric heating permits re-use of the cartridges for about 20 runs. For both procedures, experiments with a series of *s*-triazine herbicides and several volatile test compounds showed that analyte losses are negligible, even at the sub-ppb level and the repeatability is satisfactory.

INTRODUCTION

In recent papers we have discussed a system for column liquid chromatography (LC) coupled on-line with gas chromatography (GC) that can be used for the LC-type preconcentration of aqueous samples [1] and for trapping compounds eluting from either a reversed-phase LC [2] or an immunoselective preconcentration system [3]. After (re)concentration of the compounds on a short LC precolumn, they are introduced into the GC system using ethyl acetate as desorption solvent. Direct introduction of traces of water which are still present in the LC precolumn into the gas chromatograph is prevented by optimizing the time to fill the LC precolumn and capillary tubing with ethyl acetate and push the water to waste, the so-called delay time. Although the method has been used successfully, problems sometimes arose with compounds that elute at high temperatures, *i.e.* above about 200°C, in GC. The origin of these problem has been described in detail by Grob [4]. A short discussion is as follows.

The deactivation layer in silylated retention gaps is hydrolysed by water present in the ethyl acetate. This results in an active surface of the retention gap. In subsequent runs at low temperatures such a retention gap will be deactivated by the few per cent of water that are dissolved in the ethyl acetate. Consequently, compounds that pass through the retention gap under these conditions have a normal peak shape in GC. However, once the water has been removed as a result of the steadily increasing temperature in the GC programme, compounds then still present in the retention gap can interact with the surface. As a result, peaks will be distorted or no

Correspondence to: Professor U. A. Th. Brinkman, Department of Analytical Chemistry, Free University, De Boelelaan 1083, 1081 HV Amsterdam, Netherlands.

☆ Present address: Analytical Development Department, Solvay-Duphar BV, P.O. Box 900, 1380 DA Weesp, Netherlands.

0021-9673/92/$05.00

peak will show up at all. In other words, the weak point of such an LC–GC system is that up to 3% of water can dissolve in the ethyl acetate. The introduction of 50–75 μl of ethyl acetate used as desorption solvent into the retention gap has the consequence that several microlitres of water also enter, which has the deleterious effect already described.

Self-evidently, solving the above problem is highly desirable in order to extend the application range and improve the robustness of on-line (reversed-phase) LC–GC. A practical solution should preferably require no major hardware changes. In addition, it should not cause contamination nor lead to loss of compounds, and regeneration of the system should be automatable. One option is removal of the water via a postcolumn reaction. However, the reaction conditions generally will not be favourable, requiring the presence of chemicals or a catalyst, a high temperature and/or a long reaction time. The reaction of water with triethyl orthoformate or 2,2-dimethoxypropane is a typical example [5]. Another solution is the use of Nafion tubing (DuPont), which allows the selective removal of water through the pores in the tube [6]. Apart from the fact that loss of small polar compounds can be a problem (reported for drying of gaseous samples [7]), in our case incorporating the tubing in the existing LC–GC set-up cannot easily be achieved. Actually, adapting drying procedures which are routinely used in liquid–liquid and solid-phase extraction, such as the addition of anhydrous sodium sulphate or drying a column by sucking air through it, provides much simpler solutions to remove water rigorously from an organic desorption solvent. Such procedures do not cause analyte losses, even at very low concentration levels [8,9].

In this work, two approaches were examined. One alternative is to incorporate a cartridge containing a drying agent (sodium sulphate or silica) into the existing LC–GC apparatus in order that drying of the desorption solvent can be carried out on-line with trace enrichment and desorption. Water present in the desorption solvent binds to the agent when passing it. Regeneration of the drying agent is done by heating the cartridge in combination with a helium purge. The other approach is to remove the water present in the LC-type precolumn by a nitrogen purge before the analyte desorption [10,11]. The main aspect studied was the recovery of compounds after trace enrichment and on-line drying.

EXPERIMENTAL

Reagents

Nitrogen used as a drying gas was of 5.0 grade from Hoekloos (Schiedam, Netherlands). The drying agents silica and anhydrous sodium sulphate were obtained from J.T. Baker (Deventer, Netherlands). Ethyl acetate (J.T. Baker) was freshly distilled before use and HPLC-grade water was prepared by purifying demineralized water in a Milli-Q filtration system (Millipore, Bedford, MD, USA). Two aqueous test mixtures were used: (i) a solution of twelve *s*-triazines (97–99% purity; Dr. Ehrenstorfer, Augsburg, Germany) and (ii) a solution containing nitrobenzene, *m*-cresol, phenanthrene, tributyl phosphate, atrazine and cyanazine.

System for on-line trace enrichment, drying and desorption

The scheme of the LC trace enrichment–GC set-up is shown in Fig. 1. Aqueous standards were enriched using a Gilson (Villiers-le-Bel, France) Model 302 pump, a valve switching unit (Kontron, Zürich, Switzerland) and a laboratory-made 10 mm × 2 mm I.D. preconcentration column (LC precolumn) packed with 10 μm PLRP-S styrene–divinylbenzene copolymer (Polymer Labs., Church Stretton, UK). The valve switching unit consisted of a solvent-delivery valve and four six-port valves. Desorption with ethyl acetate into the GC system was carried out with a Phoenix 20 syringe pump (Carlo Erba, Milan, Italy) through a 20 cm × 0.075 mm I.D. fused-silica capillary permanently mounted in the on-column injector of the gas chromatograph. All steps in the procedure, *i.e.*, changing the solvents during trace enrichment by switching the solvent-delivery valve, flushing the capillaries between solvent exchanging, trace enrichment, optional drying with nitrogen, desorption, transfer into the retention gap, starting data acquisition and optional heating of the drying cartridge, were executed by adequate programming of the four six-port valves and the auxiliary outputs of the time programmer of the valve switching unit.

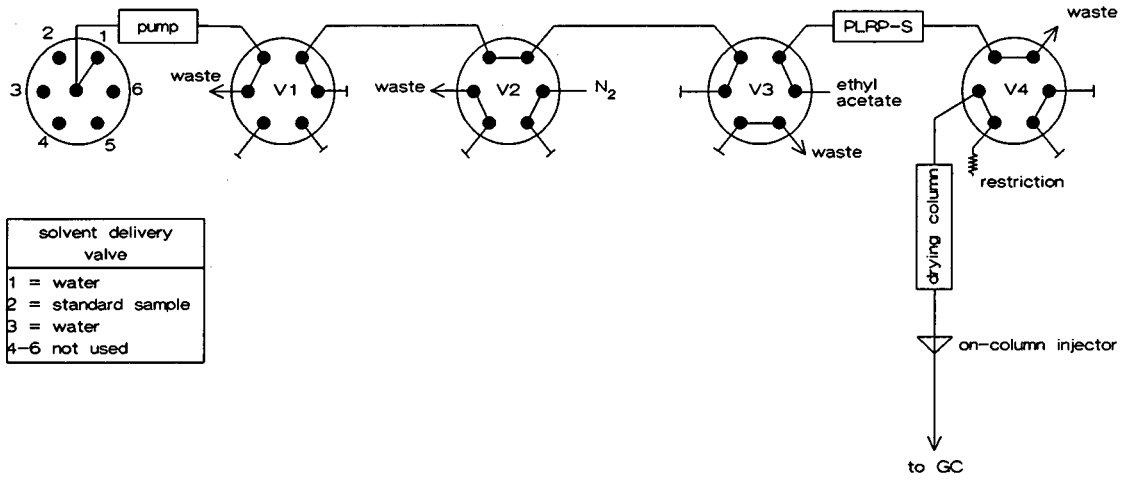

Fig. 1. Scheme of the system used for on-line LC trace enrichment on a PLRP-S column, clean-up, drying and desorption into the GC system, consisting of a solvent-delivery valve and four six-port valves (V1–V4). Drying was carried out using either a drying agent packed in a cartridge positioned between valve V4 and the on-column injector or a nitrogen purge of the PLRP-S column introduced via valve V2.

GC system

A Carlo Erba Mega gas chromatograph equipped with an on-column injector, a flame ionization detector and a Nelson data storage system (Perkin Elmer, Gouda, Netherlands) was used. The 7.5 m × 0.32 mm I.D. diphenyltetramethyldisilazane-deactivated retention gap, (DPTMDS; B. Schilling, Zürich, Switzerland), was used for the introduction of 50–75 μl of ethyl acetate under partially concurrent solvent evaporation conditions [12]. It was connected to the 15 m × 0.25 mm I.D. GC column (DB 1701, d_f 0.25 μm) via a glass press-fit connector. Helium was used as the carrier gas at an inlet pressure of 90 kPa. After elution of the solvent peak a temperature programme from 84 to 285°C at different ramps was used.

Procedure

Table I lists the two time schedules that were used to run the fully automated system, *viz.* steps I and II or steps I and III.

Steps I and II. The PLRP-S precolumn is subsequently flushed with 2.5 ml of HPLC-grade water to remove ethyl acetate from the previous run, with 10 ml of the aqueous sample (trace enrichment) and again with 2.5 ml of HPLC-grade water (to provide further clean-up in real analyses) at 5 ml/min by switching of valves V1 and V3. Next, desorption with ethyl acetate is started at a flow-rate of 25 μl/min by switching valve V3 again. During this step water is removed from the precolumn and capillary tubing and pushed to waste by ethyl acetate. When ethyl acetate reaches valve V4, *i.e.*, after 1.25 min, it is introduced into the system through the 10 mm × 2 mm I.D. cartridge filled with the drying agent by switching this particular valve. When the cartridge is filled with ethyl acetate, which takes 0.67 min with the 10 mm × 2 mm I.D. cartridge used in this study, the data acquisition and GC programme are started, and ethyl acetate is introduced into the retention gap for 2.00 min at a flow-rate of 25 μl/min. After completion of the transfer, valve V4 is switched and ethyl acetate, still present in the cartridge and capillaries, is pushed out by the helium back-pressure in the on-column injector.

Prior to the next run, the sodium sulphate- or silica-containing cartridge is dried for 30 min at 150 and 180°C, respectively. Drying is promoted by the small helium purge through the cartridge. During the whole procedure, the PLRP-S precolumn is continuously flushed with ethyl acetate. The next run is started after the end of the GC programme in order that the introduction of the desorption solvent takes place when the oven has cooled down.

Steps I and III. When a nitrogen purge is used as a drying step after loading and flushing of the

TABLE I

TIME SCHEDULES FOR AUTOMATED LC TRACE ENRICHMENT–CAPILLARY GC OF AQUEOUS SAMPLES WITH AN IN-LINE DRYING STEP

Conditions: loading of sample at 5 ml/min; desorption with ethyl acetate at 25 μl/min; GC–FID as reported in the text; in-line drying with drying agent in a cartridge or with a nitrogen purge of 40 ml/min.

Step	Time (min)	S[a]	V1[b]	V2[b]	V3[b]	V4[b]	Comments
I. Preconcentration	0.00	Water	A	A	A	A	Flush capillaries with water
	0.50		B		B		Flush PLRP-S column (2.5 ml)
	1.00	Sample	A				Flush capillaries with sample
	1.50		B				Load sample (10 ml)
	3.50	Water	A				Flush capillaries with water
	4.00		B				Clean-up step (2.5 ml); pump switched off at end
II. Drying	4.50		A		A		Start desorption (displacing water from PLRP-S column)
	5.75					B	Introduction into cartridge (filling with ethyl acetate)
	6.42						Actual transfer; start GC programme and data acquisition
	8.42					A	Stop transfer; further cleaning of PLRP-S column until next run
	10.00						Drying agent heated for 30 min to 150 or 180°C during GC programme
	45.00						System ready for next run
III. Nitrogen purge	4.50		A	B			Drying with nitrogen
	34.50			A	A		Start desorption
	35.70					B	Switch just before actual introduction into GC system; filling of transfer line
	35.80						Start GC programme and data acquisition
	37.80					A	Further cleaning of PLRP-S column
	45.00						System ready for next run

[a] S = Solvent pumped by Gilson pump selected by solvent-delivery valve.
[b] V1–V4 = Positions of six-port valves (position A refers to position in Fig. 1).

PLRP-S precolumn (for details, see above), the precolumn is purged for 30 min at ambient temperature (40 ml/min of gas). Next, desorption is started. When the precolumn has just been filled with ethyl acetate, the introduction valve V4 is switched and kept in that position for 2.1 min (0.1 min to fill the transfer line; 2.0 min to transfer the analytes into the retention gap). While the GC separation proceeds, first the PLRP-S precolumn is flushed with ethyl acetate. Then the next run can be started after 45 min, as preconcentration and drying of the LC precolumn can be carried out at the same time as the GC separation of the previous sample.

RESULTS AND DISCUSSION

Trace enrichment

In the LC trace enrichment of aqueous samples coupled on-line with GC analysis there are several main parameters. First, the PLRP-S precolumn, which is not discarded after a single analysis but is repeatedly re-used, should be cleaned after each run by flushing with ethyl acetate (at least *ca.* 150 μl) and, next be reconditioned with water (2.5 ml). Second, breakthrough of analytes on the precolumn should be avoided while on the other hand a sufficient amount of these analytes should be trapped to allow the desired overall sensitivity to be obtained. If the limit of detection is set at 10–30 ppt (w/w), at least *ca.* 10 ml of an *s*-triazine-containing sample has to be loaded to permit detection by means of GC with flame ionization detection (FID). Fortunately, the breakthrough volumes of the s-triazines on a 10 mm × 2 mm I.D. polymer-packed column are of the order of 30–100 ml [13], that is, no loss of analytes will occur during this step.

As regards desorption of analytes from the precolumn, earlier work has convincingly shown that

50–75 μl of ethyl acetate suffice for their quantitative transfer to the retention gap [2,3]. During transfer, the speed of introduction into the retention gap should be higher than the evaporation rate of the solvent to ensure solvent trapping of volatile compounds [14]. For the present GC system, the evaporation rate of ethyl acetate was found to be 12 μl/min. As the retention gap should have such a length that the solvent film created on its wall does not reach the stationary phase of the analytical GC column, the amount of solvent that is introduced into the retention gap in the liquid state, *i.e.*, (25 − 12) μl/min × 2.0 min = 26 μl, should be multiplied by the so-called flooded zone, which is about 20 cm/μl for ethyl acetate in a DPTMDS-deactivated retention gap [15]. In other words, the retention gap should have a length of at least 5 m. In all our experiments we used a 7.5 m × 0.32 mm I.D. retention gap.

Drying procedure

In this study, the main aspect of interest was to prevent any water from reaching the retention gap, *i.e.*, to prevent any deterioration of the retention gap performance. The presence of a trace amount of water in the desorption solvent can easily be detected by leading it into 100 μl of *n*-hexane rather than into the retention gap after the optimum delay time, the *n*-hexane turns opaque if water is present. Two alternatives were studied in order to remove water rigorously from the ethyl acetate, *viz.*, the on-line insertion of a small cartridge filled with anhydrous sodium sulphate or silica, or drying by purging with nitrogen.

When a sorbent-packed drying column was used, the ethyl acetate was found to contain no water at all. However, whereas with the silica column the *n*-hexane turned opaque already after the second analysis, with the sodium sulphate there was no breakthrough of water even after ten consecutive runs. Obviously, with the present configuration, 15 μl of water can be removed by the latter sorbent as against only 1–2 μl with silica. In order to improve the practicality of the system, the drying module was modified to include an electrical heating unit. If heating of the cartridge for 30 min at 150–180°C was combined with a small helium purge, the hexane receiving solvent did not turn opaque even after 25 runs (the largest number tested at this stage), irrespective of whether sodium sulphate or silica was used as the sorbent.

One note of warning should be added here. Under actual operating conditions (see the next section), it was occasionally observed that the sodium sulphate particles partially disintegrated, with the fines so formed being swept through the outlet screen of the cartridge and into the GC part of the system. The disintegration is probably the result of water present within the particles becoming overheated. As this never occurred with a sodium sulphate packing that had been used for less than 25 runs, in all final experiments a fresh cartridge was installed after each 20 runs.

As regards drying of the PLRP-S precolumn by means of a nitrogen purge, recent experience with the drying of alkyl-bonded silica- and polymer-bonded membrane extraction discs has shown that purging should be continued for at least 20 and 10 min, respectively, at ambient temperature [16]. In this work it was found that a nitrogen purge of 30 min, at a flow rate of 40 ml/min, obtained by applying a pressure of 3 bar, sufficed to remove water completely from the precolumn. Because the use of a nitrogen purge as drying step has been considered in some detail elsewhere [16], in the final part of this work most attention was devoted to the LC trace enrichment–drying sorbent–GC–FID set-up.

On-line drying for LC trace enrichment–GC

Drying over a sorbent. Preliminary experiments revealed that using sodium sulphate or silica as drying agent without any further clean-up caused severe contamination and a high background in GC–FID. As an example, Fig. 2a shows a chromatogram obtained using a freshly packed sodium sulphate cartridge. In this instance, 75 μl of ethyl acetate containing 7.5 ng of each of twelve *s*-triazines were injected directly on to the drying cartridge; these analytes elute between 21 and 27 min. For comparison, Fig. b shows the chromatogram obtained when using sodium sulphate purified for 4 h by Soxhlet extraction with ethyl acetate. A similarly dramatically improved result was observed, for both sodium sulphate and silica, after flushing the packed cartridge overnight with 10 μl/min of ethyl acetate.

Inserting the sorbent cartridge did not cause a noticeable loss of analytes with either sodium sul-

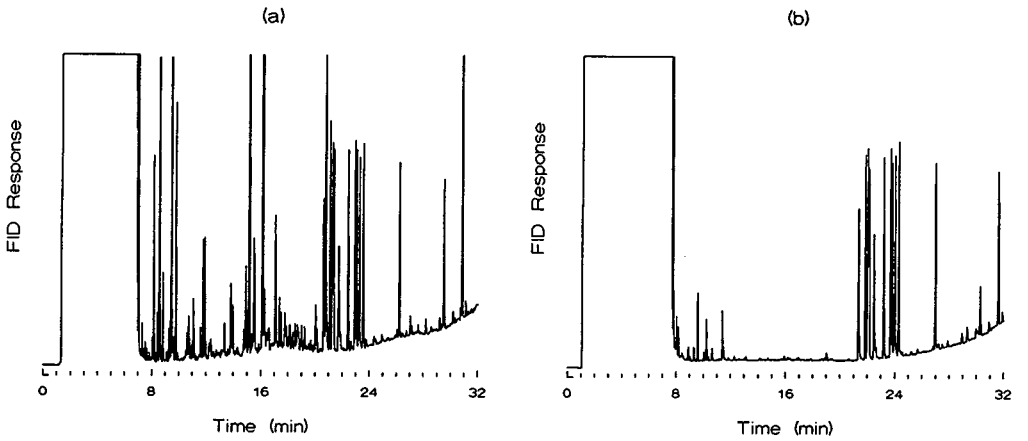

Fig. 2. GC–FIC trace obtained after introduction of 75 μl of *s*-triazine standard (7.5 ng per compound) through a cartridge filled with anhydrous sodium sulphate either (a) used as received or (b) purified for 4 h by Soxhlet extraction with ethyl acetate. GC temperature programme: 84°C until complete solvent elution, then increased to 285°C at 6°C/min; for other conditions, see Experimental. The twelve *s*-triazine herbicides elute between 21 and 27 min.

phate or silica. This is illustrated in Fig. 3, in which part of the chromatogram obtained after the injection of 75 μl of the *s*-triazine standard on to a sodium sulphate cartridge is compared with the corresponding part of the chromatogram of a 75-fold concentrated 1-μl on-column injection. All twelve analyte peaks had the same area to within 3% in Fig. 3a and b. The tails on the peaks in both chromatograms due to atraton and secbumeton are caused by active sites in the retention gap. The slightly different elution times in Fig. 3a and b are the result of slightly different linear velocities.

Using the complete system, with the cartridge packed with either sodium sulphate or silica, on-line LC–GC–FID was carried out for 10-ml samples containing 27 ppt–2 ppb of the test solutes. Results of two such runs are shown in Fig. 4. Above the 0.1 ppb level (the 0.2 ppb level is given as an example in Fig. 4), all twelve analytes showed up well, indicating that real trace-level analysis is possible. At the

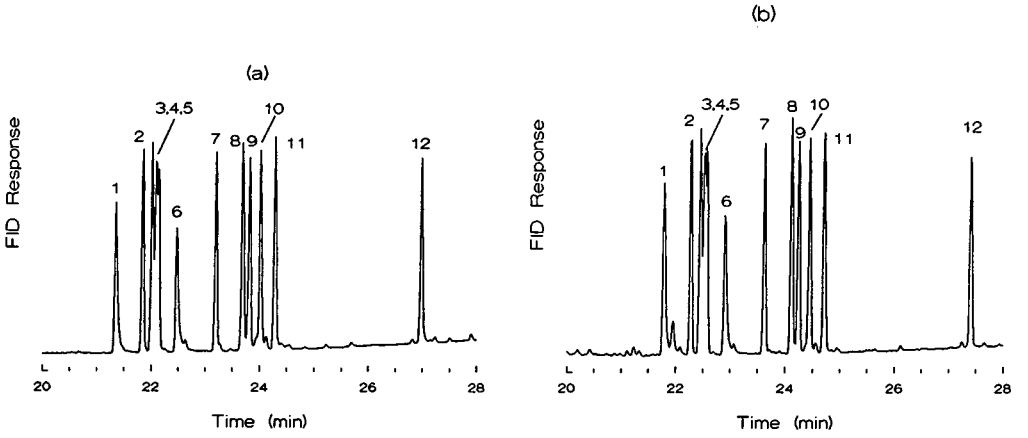

Fig. 3. Part of GC–FID trace obtained after introduction of (a) 75 μl of *s*-triazine standard (7.5 ng per compound) through a Soxhlet-extracted sodium sulphate column and (b) 1 μl of 75-fold concentrated *s*-triazine standard. Same conditions as in Fig. 2. Peak assignment: 1 = atraton; 2 = trietazine; 3 = simazine; 4 = atrazine; 5 = propazine; 6 = secbumeton; 7 = sebutylazine; 8 = prometryn; 9 = simetryn; 10 = terbutryn; 11 = dipropetryn; 12 = cyanazine.

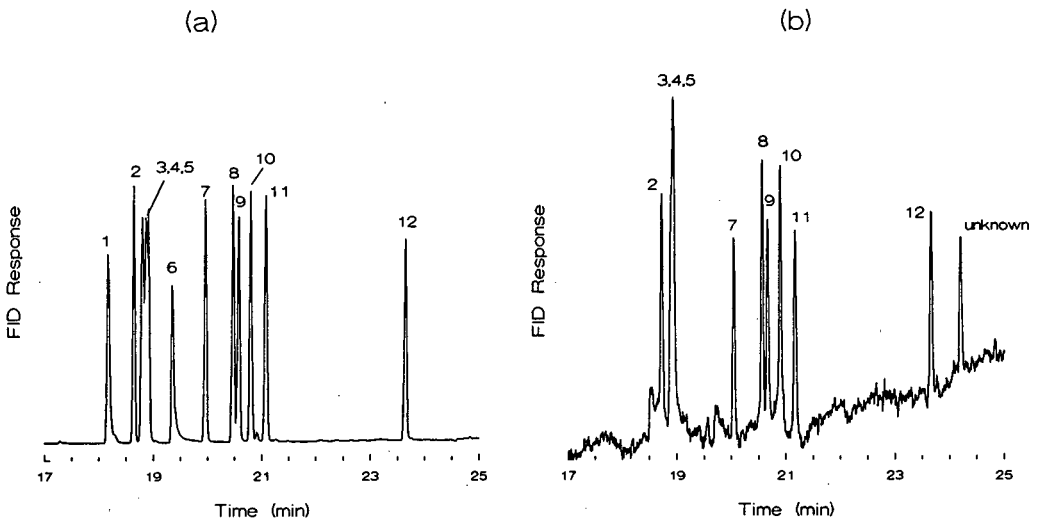

Fig. 4. Part of GC–FID trace obtained after preconcentration of 10 ml of an aqueous standard containing twelve *s*-triazines at a concentration of (a) 0.2 ng/ml or (b) 27 pg/ml. Desorption with ethyl acetate through a cartridge containing 45 mg of sodium sulphate; total volume introduced into the GC system, 50 μl. GC temperature programme: 84°C until complete solvent elution, then increased to 285 °C at 8°C/min. Peak assignment as in Fig. 3.

TABLE II

AVERAGE RECOVERY OF *s*-TRIAZINES AT THREE CONCENTRATION LEVELS (n = 4) USING LC TACE ENRICHMENT–CAPILLARY GC OF 10 ml OF STANDARD WATER SAMPLES WITH IN-LINE DRYING OVER A SORBENT BED

Conditions: loading of sample at 5 ml/min; desorption with 50 μl of ethyl acetate at 25 μl/min; GC–FID as in Fig. 4; in-line drying with sodium sulphate or silica.

Compound	Recovery (%)					
	Sodium sulphate			Silica		
	2 ppb[a]	0.2 ppb[b]	27 ppt[c]	2 ppb[a]	).2 ppb[b]	27 ppt[c]
Trietazine	103	98	91	109	108	89
Simazine	90	112	95	93	106	98
Atrazine	109	93	91	105	105	94
Propazine	105	93	91	110	93	94
Sebutylazine	103	93	93	111	103	97
Prometryn	105	99	96	103	104	98
Simetryn	109	95	97	105	97	101
Terbutryn	106	91	90	102	99	90
Dipropetryn	104	99	98	102	103	100
Cyanazine	104	95	94	106	107	95

[a] Relative standard deviation (R.S.D.) range, 0.4–3.9%.
[b] R.S.D. range, 0.2–6.2%.
[c] R.S.D. range, 4.3–21.1%.

extremely low level of 30 ppt, ten of the twelve *s*-triazines could still be easily recognized, although peaks 3, 4 and 5 were not resolved at all (Fig. 4b). As expected, at this sub-ppb level, atraton and secbumeton are attacked to such an extent by the active sites in the retention gap that they have completely disappeared from the chromatogram. Actually, when a new DPTMDS-deactivated retention gap was installed these analytes were lost even when using conventional 1-μl on-column injections containing the same amount of analyte (270 pg).

Some relevant data on the analytical performance of the on-line LC trace enrichment–sorbent drying–GC–FID system are given in Table II. For obvious reasons, no data are given for atraton and secbumeton. With both drying agents tested, the FID response was linear over the range 27 ppt–2 ppb with regression coefficients between 0.991 and 0.999 for all ten analytes. Analyte recoveries were quantitative (89–112%) compared with 1-μl on-column injections. The repeatability was good above the 0.2 ppb level (0.2–6.2%) and acceptable at the 27 ppt level (4.3–21%). The limits of detection with 10-ml aqueous standards typically were between 10 and 20 ppt (*cf.*, Fig. 4).

Purging with nitrogen. With the present set-up, using a nitrogen purge instead of drying over a sorbent bed presents no technical problems. The nitrogen supply can be connected to valve V2, and a pressure of 3 bar suffices to obtain a gas flow-rate of 40 ml/min. Because of the large volume of gas used, care should be taken to use extremely pure nitrogen, such as, *e.g.* 5.0 grade, or to install suitable filters in the supply line. We preferred the former option.

The main risk with nitrogen purging is the loss of volatile analytes of interest. Therefore, in this instance the test mixture contained, in addition to two triazines, compounds such as nitrobenzene and *m*-cresol. However, even though some of these compounds elute just after the solvent peak [1], they were quantitatively recovered at the 0.1–0.4 ppb level, as is evident from the data in Table III. For the two *s*-triazines tested, the repeatability (2.4 and 2.6%) was the same as observed with drying over a sorbent bed at the 0.2 ppb spiking level (2.3 and 2.6%; individual data not shown).

TABLE III

AVERAGE RECOVERIES OF SIX ANALYTES USING LC TRACE ENRICHMENT–CAPILLARY GC OF 10 ml OF STANDARD WATER SAMPLES WITH IN-LINE DRYING BY MEANS OF A NITROGEN PURGE

Conditions: loading of sample at 5 ml/min; desorption with 50 μl of ethyl acetate at 25 μl/min; GC–FID as in Fig. 4; 30-min nitrogen purge at 40 ml/min.

Compound	Concentration (ppb)	Recovery (%)	R.S.D. (%)
Nitrobenzene	0.41	93	2.4
m-Cresol	0.25	88	3.3
Phenanthrene	0.12	96	0.5
Tributyl phosphate	0.14	91	3.6
Atrazine	0.10	95	2.6
Cyanazine	0.12	97	2.4

CONCLUSIONS

The main problem in on-line LC trace enrichment–capillary GC of aqueous samples is deterioration of the performance of the retention gap caused by the introduction of traces of water dissolved in the ethyl acetate used for the desorption of the analytes of interest from the LC precolumn into the GC system. This work has shown that this problem can be solved either by the on-line insertion of a small column containing a drying agent between the LC trace enrichment module and the on-column injector or by purging the trace enrichment column with nitrogen. With a series of *s*-triazine herbicides and some rather volatile analytes as test compounds, it was demonstrated that no noticeable losses occur even at the sub-ppb level.

With the present LC trace enrichment–capillary GC system, at least *ca.* 20 analyses can be performed without exchanging the drying cartridge, provided that the drying agent is regenerated after each run by electric heating at 150–180°C. Drying by means of a nitrogen purge is even easier to perform. The *ca.* 30-min purge time cannot be considered a real disadvantage, as drying can be carried out during the GC analysis of the previous sample. In order to reduce the drying time (if necessary), polymer-loaded membrane extraction discs can be used as an alternative to a polymer-packed precolumn [16]. Current research is aimed at using the present system for the fully automated analysis of drinking and surface water samples and at testing more vola-

tile desorption solvents to extend the volatility range of the analytes.

ACKNOWLEDGEMENT

The authors thank DSM, Geleen, Netherlands, for financial support.

REFERENCES

1 J. J. Vreuls, W. J. G. M. Cuppen, G. J. de Jong and U. A. Th. Brinkman, *J. High Resolut. Chromatogr.*, 13 (1990) 157.
2 J. J. Vreuls, V. P. Goudriaan, U. A. Th. Brinkman and G. J. de Jong, *J. High Resolut. Chromatogr.*, 14 (1991) 475.
3 A. Farjam, J. J. Vreuls, W. J. G. M. Cuppen, G. J. de Jong and U. A. Th. Brinkman, *Anal. Chem.*, 63 (1991) 2481.
4 K. Grob, in W. Bertsch, W. G. Jennings and P. Sandra (Editors), *On-line Coupled LC-GC*, Hüthig, Heidelberg, 1991, pp. 200–205.
5 J. Chen and J. S. Fritz, *Anal. Chem.*, 63 (1991) 2016.
6 R. W. Coutant and G. W. Keighley, *Anal. Chem.*, 60 (1988) 2536.
7 W. F. Burns, D. T. Tingey, R. C. Evans and E. H. Bates, *J. Chromatogr.*, 269 (1983) 1.
8 J. M. Vinuesa, J. C. M. Cortes, C. I. Cañas and G. F. Perez, *J. Chromatogr.*, 472 (1989) 365.
9 J. C. Moltó, Y. Picó, G. Font and J. Mañes, *J. Chromatogr.*, 555 (1991) 137.
10 A. T. Boo and J. Krohn, *J. Chromatogr.*, 301 (1984) 335.
11 E. Noroozian, F. A. Maris, M. W. F. Nielen, R. W. Frei, G. J. de Jong and U. A. Th. Brinkman, *J. High Resolut. Chromatogr. Chromatogr. Commun.*, 10 (1987) 17.
12 F. Munari, A. Trisciani, G. Mapelli, S. Trestianu, K. Grob, Jr. and J. M. Colin, *J. High Resolut. Chromatogr. Chromatogr. Commun.*, 8 (1985) 601.
13 J. Slobodnik, E. R. Brouwer, R. B. Geerdink, W. H. Mulder, H. Lingeman and U. A. Th. Brinkman, *Int. J. Environ. Anal. Chem.*, in press.
14 K. Grob, Jr., *J. Chromatogr.*, 253 (1982) 17.
15 K. Grob, in W. Bertsch, W. G. Jennings and P. Sandra (Editors), *On-line Coupled LC-GC*, Hüthig, Heidelberg, 1991, p. 209-210
16 P. J. M. Kwakman, J. J. Vreuls, R. T. Ghijsen and U. A. Th. Brinkman, *Chromatographia*, 34 (1992) 41.

Journal of Chromatography, 625 (1992) 247–255
Elsevier Science Publishers B.V., Amsterdam

CHROM. 24 530

Detection of substituted benzenes in water at the pg/ml level using solid-phase microextraction and gas chromatography–ion trap mass spectrometry

David W. Potter and Janusz Pawliszyn

Guelph–Waterloo Center for Graduate Work in Chemistry and the Waterloo Center for Groundwater Research, University of Waterloo, Waterloo, Ontario N2L 3G1 (Canada)

(First received April 28th, 1992; revised manuscript received July 28th, 1992)

ABSTRACT

Solid-phase microextraction (SPME) is combined with gas chromatography–ion trap mass spectrometry (GC–IT-MS) for the analysis of benzene, toluene, ethyl benzene and xylene isomers (BTEX) in water. SPME is a recent technique for extracting organics from an aqueous matrix into a stationary phase immobilized on a fused-silica fiber. The analytes are thermally desorbed directly in the injector of a gas chromatograph.

The wide linear dynamic range (five orders of magnitude) and pg sensitivity of the ion trap mass spectrometer in its full scan mode is an ideal detector for identifying and quantifying the analytes extracted with an SPME device.

The combined method SPME–GC–IT-MS, using fibers coated with a 100-μm polydimethylsiloxane coating, showed a limit of quantitation (LOQ) of 50 pg/ml benzene in water. This corresponds to 5 pg of benzene absorbed onto the fiber. The limit of detection (LOD) was 15 pg/ml benzene. For *o*-xylene spiked at 50 pg/ml in water 50 pg were absorbed by the fiber indicating an LOQ and LOD 10 times better than for benzene. The detection limits obtained exceed the requirements of both the United States Environmental Protection Agency method 524.2 and the Ontario Municipal/Industrial Strategy for Abatement program, which range from 30 to 80 pg/ml and 500 to 1100 pg/ml, respectively.

The linearity of the method extended over five orders of magnitude. Relative standard deviation ranged from 2.7 to 5.2% for 15 ng/ml BTEX in water and from 5.5 to 7.5% for 50 pg/ml BTEX in water. SPME–GC–IT-MS was used to evaluate the contamination level in laboratory, potable and wastewater sources.

INTRODUCTION

Contamination of water by organic pollutants is a common environmental problem. Simple highly sensitive analytical techniques are required to detect and quantitate pollutants in water at trace levels. The first step in the analytical process involves extraction of the contaminants from the water matrix. This step is commonly achieved using liquid–liquid extraction, solid-phase extraction or purge-and-trap techniques. These methods either use large amounts of organic solvents, are labour intensive, difficult to automate and apply in the field or are expensive.

Solid-phase microextraction (SPME) is an excellent alternative to the aforementioned techniques. In SPME the analytes are extracted into a stationary phase which is attached to a length of fused-silica fiber [1]. The fiber is contained within a microsyringe for protection and ease of sampling. SPME completely eliminates solvents and consists of only a few simple steps. The fiber is withdrawn into the needle of the microsyringe and the needle of the syringe is used to pierce the sample vial. The fiber is then exposed to the aqueous sample where the ana-

Correspondence to: Dr. J. Pawliszyn, Guelph–Waterloo Center for Graduate Work in Chemistry and the Waterloo Center for Groundwater Research, University of Waterloo, Waterloo, Ontario N2L 3G1, Canada.

0021-9673/92/$05.00

lytes partition between the stationary film on the fiber and the aqueous phase. The fiber is then withdrawn from the sample and inserted into the injector of a gas chromatograph where the analytes are thermally desorbed. In SPME an exhaustive extraction does not occur but an equilibrium is established as analytes partition between the stationary phase and the aqueous phase. At equilibrium a linear relationship exists between the number of moles of an analyte absorbed by the fiber and the analyte concentration in the aqueous phase [1]. For a large aqueous sample volume this relationship is described by:

$$n_s = KV_sC_{aq} \quad (1)$$

where n_s is the number of moles of the analyte in the stationary phase, K is the distribution constant of the analyte partitioning between the stationary and aqueous phase, V_s is the volume of the stationary phase and C_{aq} is the concentration of the analyte in the aqueous phase. High sensitivity can be ensured by using thick (large V_s) and selective (large K) stationary phases. The whole extraction and analyte transfer process usually takes only a few minutes [2] and can be easily automated [3].

The main objective of this paper is to demonstrate that in addition to its simplicity, SPME can be implemented in methods which meet both the United States Environmental Protection Agency (USEPA) and the Ontario Municipal/Industrial Strategy for Abatement (MISA) specifications for the analysis of environmental samples. These methods usually require gas chromatography (GC)–mass spectrometry (MS) separation and quantitation. Ion trap mass spectrometry (IT-MS) was used in this study. With the introduction of automatic gain control (AGC) [4] and axial modulation [5] quadrupole ion trap mass spectrometers have become an attractive alternative to conventional quadrupole mass filter spectrometers for environmental analysis. Ion trap mass spectrometers are capable of picogram detection limits in a full scan mode. Picogram detection limits can be achieved with a conventional quadrupole spectrometer when operating in the selected ion monitoring (SIM) mode, but in this case valuable spectral information is lost.

EXPERIMENTAL

An SPME device is shown in Fig. 1 and was prepared as follows. A 12-inch length of 30 gauge stainless steel tubing was obtained from Hamilton (Reno, NV, USA). Fused-silica capillary fibers coated with a 100 μm (± 5 μm) polydimethylsiloxane film were obtained from Polymicro Technologies (Tuscon, AZ, USA). A 1-cm portion of the coating was scraped from a short length (5 cm) of coated fiber. The stripped portion of fiber was then dipped into epoxy resin (Epo-Tek 353ND, Billerica, MA, USA) and inserted into the stainless steel tubing. The glue was cured for 1 min at approximately 150°C. The stainless steel was then inserted up through the needle of a Hamilton (7105) syringe (plunger wire removed) until it protruded from the top, cut to a length of 20.5 cm and glued in place with a dab of standard 5-min epoxy glue. Once the glue had cured the plunger button was replaced, the exposed fiber was trimmed to 1 cm and the syringe assembly was leak checked in a gas chromatograph injector using a Gow-Mac helium leak detector. Leaks may arise where the needle joins the syringe body and also at the top of the syringe barrel. These can be corrected by tightening the knurled nut which holds the needle in place.

A Varian Saturn benchtop gas chromatograph–ion trap mass spectrometer was used for the separation and analysis of benzene, toluene, ethyl benzene and xylene isomers (BTEX). The gas chromatograph was a Varian 3400 equipped with a Septum Programmable Injector and oven cryogenics. Separations were conducted using a Supelco 60 m x 0.25 mm I.D. VOCOL column (1.0 μm film) or a Supelco 30 m x 0.25 mm I.D. VOCOL column (1.5 μm film). The chromatographic conditions were as follows for the 60 m column:

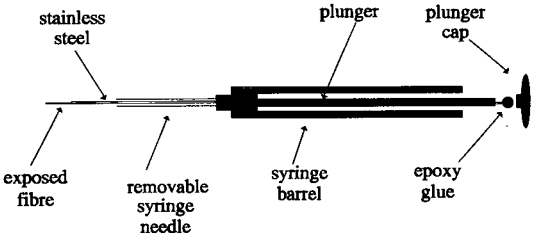

Fig. 1. A solid-phase microextraction device.

Injector:	25°C for 0.10 min, 250°C/min to 150°C, hold 3 min.
Column:	− 5°C for 2 min, 20°C/min to 150°C, hold 3.25 min, ramp ballistically to 200°C, hold 3 min.
Transfer line:	220°C
Ion trap manifold:	220°C

For the 30-m column the oven was programmed as follows: 10°C for 1 min, 15°C/min to 90°C, 3°C/min to 105°C, ramp ballistically to 200°C, hold 2 min.

The mass spectrometer was tuned to perfluorotributylamine (PFTBA) in accordance with the MISA program. When tuned to PFTBA the ITS also met the tuning criteria for 4-bromofluorobenzene (BFB) as required by USEPA method 524.2 [6]. The electron multiplier and the AGC target were set automatically. The electron multiplier sets to give a multiplier gain of 10^5 and the target sets to achieve a valley to isotope ratio of 25% for mass 131 of perfluorotributylamine and its isotope 132. The filament emission current was set so that the ionization time was almost at the maximum value (25 ms) for the lowest concentration of BTEX analyzed. The segment breaks were left at their default values of 10–99/100–249/250–399/400–650 amu; however, the segment tune factors were set at 115/100/100/85 in order to pass both the PFTBA and BFB tune. The mass range scanned was 35–250 amu during BTEX analysis. The ions used for quantitation were as follows: benzene = 78, toluene = 91, 92, ethyl benzene = 91, 106 and xylene isomers = 106, 91.

Spiking standards were prepared in methanol (OmniSolve; BDH, Toronto, Canada) and spiked into Milli-Q (Millipore, USA) reagent water inside sealed 60-ml hypovials. The hypovials contained a stirbar and 0.5 ml of headspace to prevent the sample from wicking up the syringe needle. An absorption time of 30 min was used to ensure that equilibrium had been reached. Desorption was performed with the fiber just above the restriction in the glass insert of the SPI injector as this is the optimum location [3]. Each day a column blank was followed by a fiber blank and a water blank to determine the extent of any laboratory contamination.

The limit of quantitation (LOQ) and limit of detection (LOD) were determined initially from calibration curves and confirmed by analyzing five standards spiked with BTEX at the LOQ. The LOQ was defined as an analyte signal ten times the baseline noise. The LOD was defined as a signal three times the baseline noise.

The mass absorbed at equilibrium was obtained from a calibration curve constructed by injecting (1 μl) triplicate injections of BTEX standards prepared in methylene chloride (OmniSolve; BDH, Toronto, Canada).

Precision was determined by analyzing nine solutions containing 15 ng/ml BTEX on a single day with a single experimenter. This was repeated with five solutions containing 50 pg/ml BTEX. The relative standard deviation was calculated by dividing the standard deviation by the mean and multiplying by 100.

Carryover was investigated by analyzing a 1.5 ng/ml standard and then running consecutive fiber blanks to determine the fraction of the original mass desorbed remaining on the fiber.

Background contamination was examined in Milli-Q reagent water, deionized water, tap water and natural spring water (Aberfoyle, Canada).

RESULTS AND DISCUSSION

Benzene, toluene, ethyl benzene, and xylene isomers were used as target analytes in the investigation of SPME–GC–IT-MS since they are common groundwater pollutants. Their presence may arise from incomplete combustion of gasoline, leaking storage tanks or accidental spills into the environ-

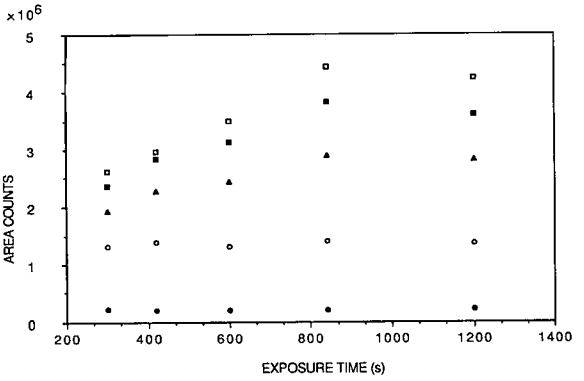

Fig. 2. Absorption profile for benzene, toluene, ethyl benzene and xylene isomers using 1 cm of a 100-μm polydimethylsiloxane-coated fiber. All compounds have reached equilibrium in 14 min using a conventional laboratory magnetic stirring plate. ● = Benzene; ○ = toluene; ■ = ethyl benzene; □ = *m*- and *p*-xylene; ▲ = *o*-xylene.

TABLE I

DISTRIBUTION CONSTANTS, LIMITS OF DETECTION, LIMITS OF QUANTITATION, PRECISION OF SPME, K_{ow} VALUES, AND METHOD DETECTION LIMITS (MDL) AS REQUIRED BY MISA AND USEPA REGULATIONS

Analyte	$\log_{10} K^a$	$\log_{10} K_{ow}$	LOD (pg/ml)	LOQ (pg/ml)	Precision 50 pg/ml (%)	Precision 15 ng/ml (%)	MDL	
							(MISA) (pg/ml)	USEPA (pg/ml)
Benzene	2.30	2.13[b]	15	50	7.3	5.3	500	30
Toluene	2.88	2.69[b]	5	15	6.7	3.2	500	80
Ethyl benzene	3.33	2.84[c]	2	7	7.2	3.6	600	60
m- and *p*-Xylene	3.31	3.20[d] *meta* 3.15 *para*	1	4	6.5	6.5	1100	90
o-Xylene	3.26	2.77	1.5	5	5.5	2.7	500	60

[a] Experimentally determined.
[b] Ref. 8.
[c] Ref. 9.
[d] Ref. 10.

ment. A quick, sensitive method is required to detect the presence of these contaminants in groundwater at the pg/ml level.

The first step in developing a method for SPME is to establish the time required for all target analytes to reach equilibrium. Previous work with a 56-μm film thickness showed that all BTEX components had reached equilibrium in under 6 min [3]. The distribution constants for BTEX analytes partitioning between the 56-μm coating and water were found to be similar to the analytes octanol–water partition coefficients (K_{ow}) [3]. In order to maximize the sensitivity of this technique the thickest available polydimethylsiloxane coated fiber (100 μm) that could be accommodated inside the syringe needle was used. Fig. 2 shows that all analytes have attained equilibrium in 14 min when using a 100-μm coating. The extraction process is limited by the mass transfer of analytes through a thin static aqueous layer at the fiber–solution interface [2]. The longer equilibration times for ethyl benzene and the xylene isomers relative to benzene and toluene are to be expected since these compounds have higher (K_{ow}) values and a greater mass must diffuse across the unstirred layer before equilibrium is reached. Using eqn. 1 the distribution constants for BTEX in water can be calculated for the 100-μm polydimethylsiloxane coating. As shown in Table I, using a 100 μm coating the calculated distribution constants are similar to the K_{ow} values.

In the following experiments a 30-min extraction time was chosen. This is twice the equilibration time but convenient since the time required to complete one chromatographic run and cool down for the next was about half an hour.

After establishing the equilibration time, the linear dynamic range and mass detection limits of the ion trap were investigated by injecting the target analytes dissolved in methylene chloride. A signal-to-noise ratio of 10:1 was obtained for 4 pg of benzene, which is at the LOQ and suggests a LOD of approximately 1 pg. Similar values were obtained

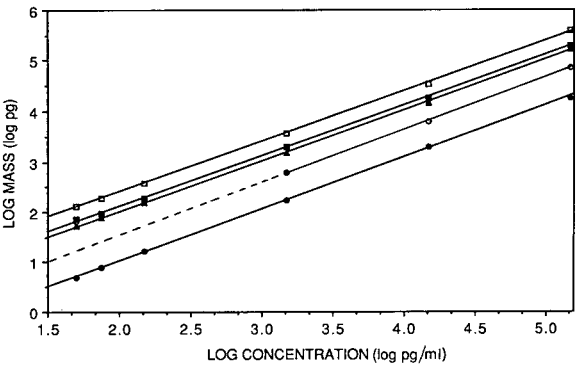

Fig. 3. The linearity of the 100-μm coated fiber and the mass spectrometer is shown over four orders of magnitude from 50 pg/ml to 150 ng/ml. Toluene is linear from 1.5 ng/ml upwards because of background contamination. Symbols as in Fig. 2.

for toluene, ethyl benzene and the xylene isomers. The mass spectrometer was found to give a linear response over five orders of magnitude, up to 100 ng BTEX using conventional syringe injections.

To determine the LODs and the dynamic range of the SPME–GC–IT-MS method aqueous standards were prepared ranging from 50 pg/ml to 1.5 μg/ml BTEX in water. Excellent linearity was obtained for 50 pg/ml to 150 ng/ml for all compounds except toluene (Fig. 3). Toluene was linear from 1.5 pg/ml to 150 pg/ml. This poor linear range was due to reagent water contamination and is discussed below. A signal-to-noise ratio of 10:1 was obtained for 50 ppt benzene in water indicating an LOD of 15 ppt and an LOQ of 50 ppt. The mass of benzene absorbed by the fiber at the LOQ was 5 pg. This agrees favourably with the results obtained using syringe injections. This low LOQ demonstrates that the coating on the fiber is sufficiently stable to withstand the thermal stress of desorption and does not produce background which might coelute with the target compounds. The mass absorbed at equilibrium for 50 pg/ml *o*-xylene was 50 pg, indicating an LOQ and LOD ten times lower than that obtained for benzene. A signal-to-noise ratio in excess of 100:1 confirms this. This greater sensitivity results from the higher K values (Table I) since for analytes with large distribution constants a greater amount of analyte diffuses into the coating before equilibrium is reached [2]. These extremely low detection limits were obtained without any sample preconcentration or special tuning of the mass spectrometer.

LODs and LOQs were determined for all compounds by examining the signal-to-noise ratios at 50 pg ml and extrapolating from Fig. 3. The method detection limits for BTEX were all less than those required by the USEPA method 524.2 [6] and also by the MISA program [7] In fact, with the exception of benzene, even without extrapolation 50 pg/ml is below the detection limits required by the more stringent USEPA method. Based upon the signal-to-noise ratios obtained for 50 pg/ml BTEX the calculated LODs and LOQs should be easily attainable but, preparing standards at these low levels requires an extremely clean room for sample preparation. A summary of these results is shown in Table I.

BTEX analytes with the largest distribution constants have the lowest detection limits and therefore the maximum concentration that can be analyzed will also be lower. For example when sampling a 1.5 μg/ml BTEX sample the mass of ethyl benzene and xylene isomers absorbed exceeds the capacity of the ion trap. This results in peak splitting and extremely poor resolution between ethyl benzene and *m*- and *p*-xylenes. In this case a thinner stationary phase could be used. Benzene which has a low K value remains linear up to 1.5 μg/ml.

The relative standard deviation of this method for samples containing 15 ng/ml BTEX ranged from 2.7 for *o*–xylene to 5.2 for benzene (Table I). The precision is expected to be the worst for benzene since this is the most volatile compound present. At 50 pg/ml the precision ranged from 5.5 to 7.3% (Table I).

Carryover is an important issue to address since before any trace sampling can be undertaken a pristine fiber is required. The extent of carryover after sampling a 1.5 ng/ml standard is shown in Table II. The results indicate there is no detectable carryover for either benzene or toluene after sampling a 1.5 ng/ml BTEX standard. The amount of ethyl benzene, *m*- and *p*-xylenes, and *o*-xylene present after one injection was 0.17, 0.19 and 0.05%, respectively. Since a greater mass is absorbed at equilibrium

TABLE II

PERCENT OF BTEX REMAINING ON FIBER AFTER 1.5 ng/ml STANDARD

n/d = Not detected.

	Benzene	Toluene	Ethyl benzene	*m*- and *p*-Xylene	*o*-Xylene
1.5 ng/ml	100	100	100	100	100
1st blank	n/d	n/d	0.17	0.19	0.05
2nd blank	n/d	n/d	0.03	0.02	0.03

for those compounds with larger K_{ow} values and they tend to have higher boiling points it is not surprising that they show the greatest carryover [2]. All compounds have decreased to less than 0.03% of their original levels by the second fiber blank. Carryover can be reduced by increasing the desorption temperature, but this results in the slow degradation of the coating. In the experiments reported in this work a fiber blank was analyzed before and after the analysis of any standards or unknown samples to ensure proper quantitation.

Samples of a totally unknown composition or suspected to have an extremely high level of contamination should be screened using a thin film (15 μm) polydimethylsiloxane coating or a shorter fiber beforehand. A new fiber could also be used for each sample since the cost of a fiber is negligible. Alternatively, a less sensitive detector such as a flame

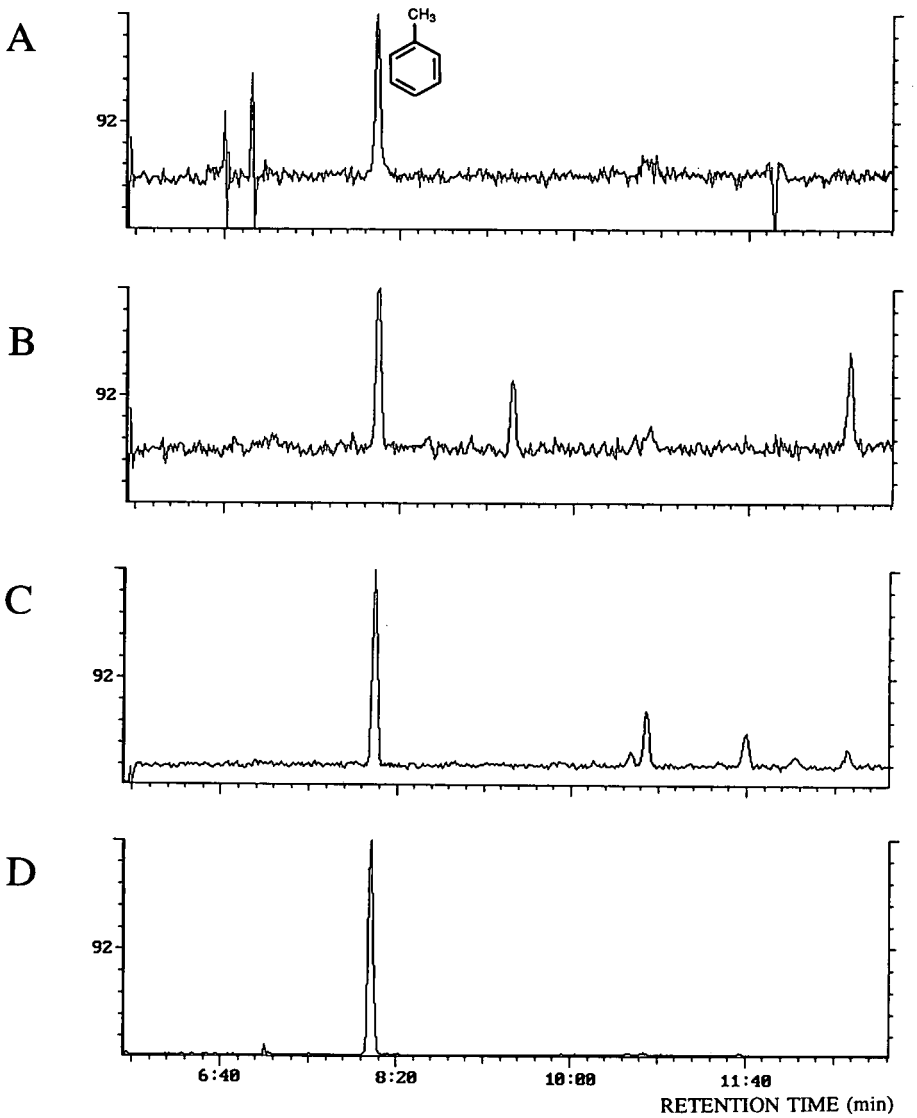

Fig. 4. Comparison of toluene background contamination in four different water sources. (A) Milli-Q reagent water, (B) regular tap water, (C) natural spring water and (D) deionized tap water.

ionization detector could be used if the positive identification a mass spectrometer provides is not required.

Milli-Q purified water was used in all experiments to prepare the standard solutions. When analyzing blanks toluene was found to be present in this water at about 15 pg/ml (see Fig. 4A) but was also detected at levels as high as 150 pg/ml, which explains the nonlinearity of the calibration curve in Fig. 3 for this analyte.

In the search for a clean water blank several sources were examined. The chemistry building tap water contained approximately 15 pg/ml toluene (Fig. 4B). Natural spring water purchased in a local grocery store contained toluene at 90 pg/ml (Fig. 4C). The biggest surprise was associated with the large amount of toluene in the deionized water of the chemistry building (Fig. 4D). Toluene contamination in the deionized water ranged from 0.5 ng/ml to greater than 10 ng/ml. It appears that there is

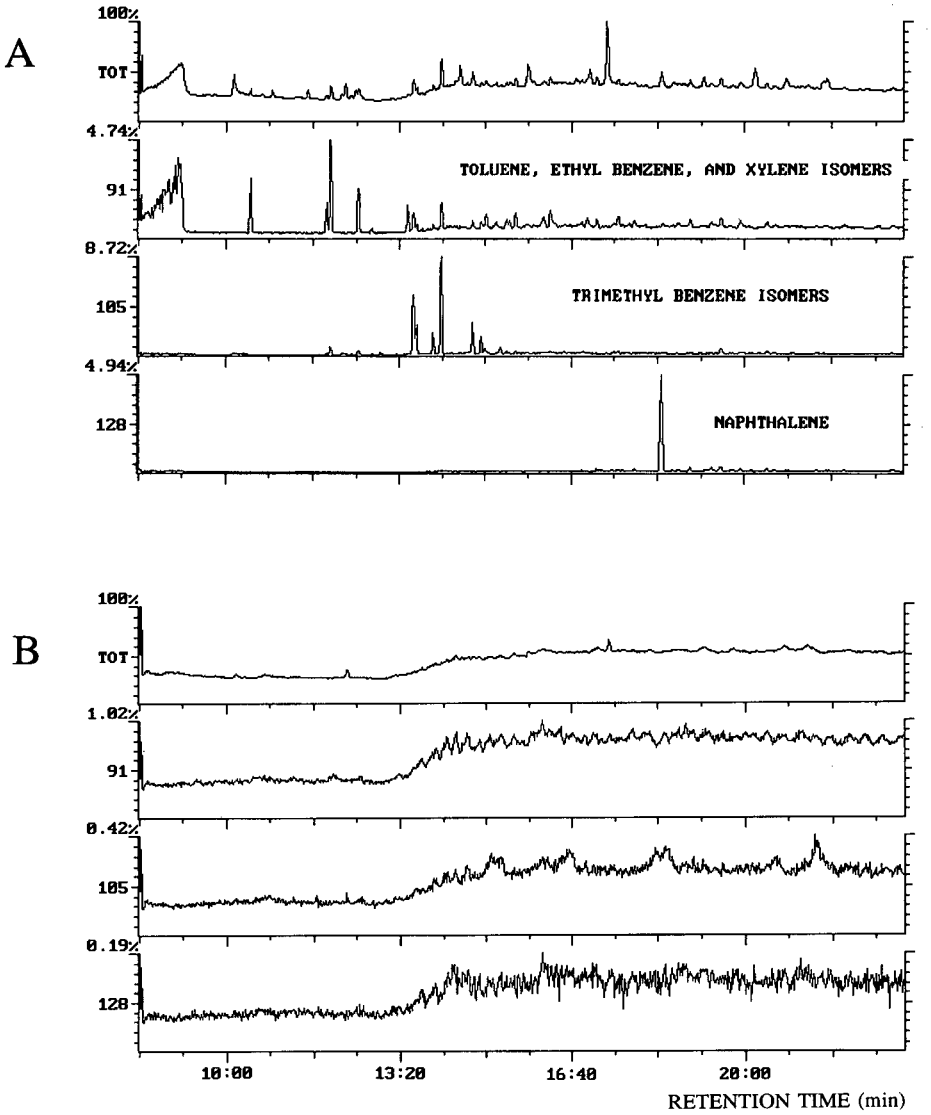

Fig. 5. (A) BTEX is present at the ng/ml level in parking lot runoff water, (B) BTEX is undetected in a fiber blank analyzed immediately afterwards.

TABLE III

BTEX DETECTED IN PARKING LOT RUNOFF WATER (ng/ml)

n/d = Not detected.

	Benzene	Toluene	Ethyl benzene	*m*- and *p*-Xylene	*o*-Xylene
Bottle A	n/d	17.4	10.7	18.1	18.9
Bottle B	n/d	16.9	10.6	17.3	17.7
Bottle B (2nd injection)	n/d	18.1	11.4	18.7	18.5

contamination somewhere in the lines or ion-exchange resin.

Toluene is used in our laboratory as a solvent for silanizing glassware and in soxhlet extractions. It is also used extensively by other laboratories in the same building. Contamination by adsorption to glassware was prevented by heating glassware in a muffle furnace at 400°C for several h. The possibility of the fiber being contaminated with analytes in laboratory air was also examined. A fiber exposed to laboratory air for 1 h was equivalent to sampling water containing 7.0 ng/ml toluene. The exact volume of air sampled is not known, however the extreme sensitivity of this technique is shown as well as the possibility of using SPME for air sampling. It is not surprising that toluene showed significant contamination considering the problems encountered with this analyte in aqueous samples. During transfer of the fiber from the sample vessel to the injector the fiber is retracted into the needle of the syringe. Contamination during the transfer process (10 s) can be ruled out since even after several min

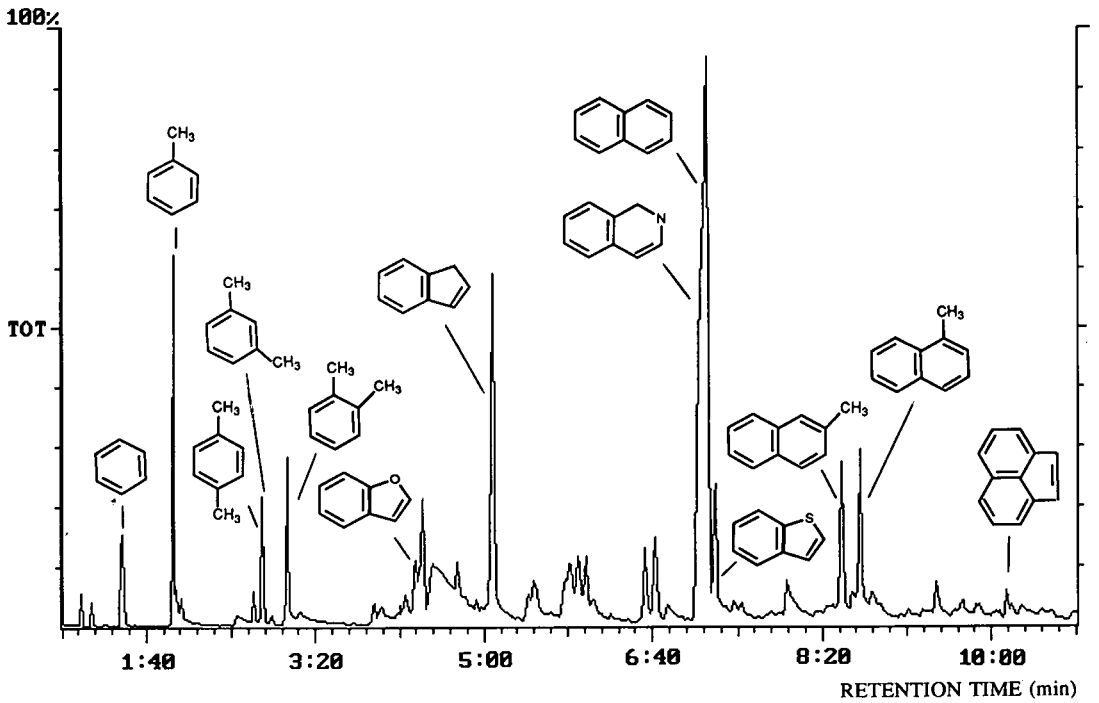

Fig. 6. Total ion chromatogram showing organics detected and identified in a coal gasification wastewater sample.

on a laboratory bench with the fiber sheathed no analytes were detected. However, the ultra sensitivity of this technique requires that extreme care be taken so that fibers are not inadvertently contaminated. In order to avoid contamination and incorrect results it is advisable to run a fiber blank before each sample when analyzing for ultra trace levels of pollutants.

In order to demonstrate the practicality of SPME–GC–IT-MS duplicate water samples were collected from parking lot runoff after a recent snowfall. A typical total ion and selected ion chromatograms for BTEX and other contaminants are shown in Fig. 5A, and can be compared to a fiber blank in Fig. 5B. Trimethyl benzenes and naphthalene were detected but not quantitated. The first sample collected was analyzed once while the second water sample was analyzed twice. The results are tabulated in Table III.

Detection limits required by USEPA and MISA for BTEX in water are easily obtainable in a full scan acquisition mode thus eliminating any ambiguity that may arise when acquiring data using selected ion monitoring. Since low pg/ml detection limits have been achieved for BTEX components with only one aromatic ring, pg/ml detection limits for compounds with larger K_{ow} values such as polynuclear aromatic hydrocarbons should be easily attainable. Polynuclear aromatic hydrocarbons have K_{ow} values up to several orders of magnitude larger than for the BTEX compounds studied in this paper. A total ion chromatogram showing many compounds with high K values extracted from a coal gasification wastewater sample is shown in Fig. 6. This was obtained with a relatively thick coating (56 μm) and only a 5-min absorption time so it does not necessarily reflect the relative concentrations of analytes in the sample, but rather constitutes qualitative information which can be used for screening purposes. It may be preferable to use a thinner stationary phase for quantitation. A thinner film will require shorter equilibration times and absorb fewer contaminants with low K values which could constitute interferences.

ACKNOWLEDGEMENTS

This work was supported in part by the Natural Sciences and Engineering Council of Canada, Imperial Oil of Canada, the University Research Incentive Fund, Varian Canada and Supelco Canada. We also wish to thank Catherine Arthur for her invaluable comments and suggestions.

REFERENCES

1 C. L. Arthur and J. Pawliszyn, *Anal. Chem.*, 62 (1990) 2145.
2 D. Louch, S. Motlagh and J. Pawliszyn, *Anal. Chem.*, 64 (1992) 1188.
3 C. L. Arthur, L. M. Killam, K. D. Buchholz and J. Pawliszyn, *Anal. Chem.*, 64 (1992) 1960.
4 R. A. Yost, W. McClennen and L.C. Meuzelaar, *Finnigan MAT Application Report 209; Enhanced Full Scan Sensitivity and Dynamic Range in the Finnigan MAT Ion Trap Detector with the New Automatic Gain Control Software*, Finnigan MAT, San Jose, CA, 1986.
5 M. Weber-Grabau, P. E. Kelley, S. C. Bradshaw and D. J. Hoekman, presented at the *36th ASMS Conference on Mass Spectrometry and Allied Topics, San Francisco, CA*, 1988.
6 J. W. Eichelberger and W. L. Budde, *Method 524.2, Revision 3.0; Measurement of Purgeable Organic Compounds in Water by Capillary Column Gas Chromatography/Mass Spectrometry*, Environmental Monitoring Systems Laboratory, Office of Research and Development, US Environmental Protection Agency, Cincinnati, OH, 1989.
7 *The Determination of Volatile Organics in Water and Aqueous Effluent by GC/MS*; SMY-PBVOL-H20.1N, MISA Section 1.7.1 (no publication date).
8 T. Fujita, J. Iwasa and C. Hansch, *J. Am. Chem. Soc.*, 86 (1964) 5175.
9 C. T. Chiou, D. W. Schmedding and M. Manes, *Environ. Sci. Technol.*, 16 (1982) 4.
10 K. Verschueren, *Handbook of Environmental Data on Organic Chemicals*, Van Nostrand Reinhold, New York, 2nd ed., 1983.

Journal of Chromatography, 625 (1992) 257–269
Elsevier Science Publishers B.V., Amsterdam

CHROM. 24 462

Identification of chlorinated fatty acids in fish lipids by partitioning studies and by gas chromatography with Hall electrolytic conductivity detection

Clas Wesén and Huiling Mu

Department of Technical Analytical Chemistry, Chemical Center, P.O. Box 124, S-221 00 Lund (Sweden)

Arne Lund Kvernheim

Center for Industrial Research, P.O. Box 124, Blindern, N-0314 Oslo 3 (Norway)

Peter Larsson

Department of Technical Analytical Chemistry, Chemical Center, P.O. Box 124, S-221 00 Lund (Sweden)

(First received March 13th, 1992; revised manuscript received June 24th, 1992)

ABSTRACT

Chlorinated compounds in fish lipids [determined by neutron activation analysis as extractable, organically bound chlorine (EOCl)] were characterized by liquid–liquid extractions after enzymatic hydrolysis and after forming fatty acid methyl esters (FAMEs). Most of the chlorinated compounds in lipids from four different fish samples could be hydrolysed. Comparison with results of methanolysis of two of the fish lipids indicated that chlorinated fatty acids made up the major portion of EOCl. Using gas chromatography (GC) with electrolytic conductivity detection (ELCD), chlorinated compounds were found among FAMEs of eel lipids containing 1200 ppm of EOCl. Approximately 90% of EOCl was detected by GC–ELCD. The GC-detectable compounds are suggested to be methyl esters of chlorinated fatty acids and 9,10-dichlorostearic acid was tentatively identified after co-injection of the synthesized compound.

INTRODUCTION

Much work has been devoted to the identification of organochlorine compounds in fish. Organochlorine pollutants, such as polychlorinated biphenyls (PCBs), DDT and DDE, in fish tissues are normally traced by gas chromatography (GC) with electron-capture detection (ECD) or mass spectrometric (MS) detection. The chlorinated pollutants are first isolated in a crude extract, which also contains the fish lipids. After thorough purification and removal of lipid components, the sample can be subjected to GC and the amount of chlorine connected with the identified substances can be calculated. The total content of chlorine in hydrophobic compounds can be measured by neutron activation analysis (NAA) after elimination of chloride from the lipid-containing extract [1–3]. This measure expresses the extractable, organically bound chlorine (EOCl) and assesses the upper limit of chlorine that is to be accounted for by other techniques. By comparing the results obtained with GC and NAA, it has been found that compounds identified by GC–ECD or GC–MS can account for 0.1–16% of the EOCl in fish tissues [4–6] and 1–8% of the EOCl in sediments [5,7]. The major portion of EOCl in fish and

Correspondence to: Dr. C. Wesen, Department of Technical Analytical Chemistry, Chemical Center, P.O. Box 124, S-221 00 Lund, Sweden.

0021-9673/92/$05.00

sediments is of relatively high molecular weight [2,8,9], and part of the chlorinated material in fish lipids can be hydrolyzed, resulting in the release of acidic compounds from neutral (non-acidic) material [10]. These findings suggest that the unidentified organochlorine substances in fish lipids to a large extent are chemically bound in acylglycerols or similar esters and that the acidic hydrolysis products are either chlorinated carboxylic acids or chlorinated phenols.

As ECD has been reported to have a low sensitivity for methyl esters of chlorinated stearic acids [7,11], it is of limited value for studies of chlorinated lipid constituents such as chlorinated fatty acids. In addition to ECD, other halogen-sensitive GC detection methods have been developed. Karmen [12] coupled two flame ionization detectors in series, and studied the ionization due to metal chlorides in the upper flame. The detection limit was in the range of 1 ng and could not compete with ECD. Atomic emission detection (AED) and electrolytic conductivity detection (ELCD) are halogen-selective detection methods which are commercially available. AED can identify individual halogens and the response is based on their spectral emission produced by the high temperature in a plasma. Although the principle has been known for a long time, it is only lately that AED has become commercially available. ELCD was first developed by Piringer and Pascalau [13] for the determination of carbon. Coulson [14] used a similar system for the selective detection of compounds containing either halogens, nitrogen or sulphur. In this type of detector, the GC eluate is pyrolyzed. The reaction products are transported to a mixing chamber, mixed with a suitable solvent and the conducting properties of the solvent are registered. The Coulson detector has been further improved by Hall [15] and, in a recent configuration, the detection limit using ELCD was lowered to the picogram range. The US Environmental Protection Agency has recommended ELCD for the detection of PCBs and other halogenated substances in certain environmental samples.

In this study, fish lipids were subjected to enzymatic hydrolysis and methanolysis. The products were partitioned by liquid–liquid extraction at different pH and NAA was used to measure the chlorine in fractions containing acidic and neutral (non-acidic) compounds. The chlorine in chlorinated carboxylic acids was then determined. Fatty acid methyl esters (FAMEs) were detected by GC–ELCD and by GC-flame ionization detection (FID), used in parallel. Methyl esters of chlorinated stearic acids were used as external standards for calibrating the ELCD response and the total ELCD response was compared with the amounts of organically bound chlorine that were injected. The ECD response was also studied for some samples containing FAMEs.

EXPERIMENTAL

Preparation of fish lipids and EOCl determination

Eels (*Anguilla anguilla*) were obtained from the receiving waters of two Norwegian pulp mills producing bleached pulp, as described in Håkansson *et al.* [6]. One eel sample, A (39 fish), was obtained from the vicinity of a magnesium acid sulphite mill (chlorine bleaching) in the narrow fiord Idefjord, between Sweden and Norway. The other eel sample, B (sixteen fish), was obtained from the receiving waters of a kraft mill (chlorine dioxide/chlorine bleaching), discharging to a coastal area of the Oslo fiord (after determining EOCl in this sample, it served as a reference to eel A in the GC analysis). Flounders (*Platichtys flesus*) were caught in the bight of Hanö in southern Sweden. Samples C and D (three flounders each) were obtained from the receiving waters of a kraft mill, using chlorine/chlorine dioxide bleaching after an oxygen delignification stage. Sample E (five flounders) was obtained from an open, coastal area in the bight of Hanö, 10 km north of Simrishamn, about 300 m offshore, at a distance of 45 km from any point source of chlorinated material.

The determination of EOCl included homogenization of the fish fillets, extraction with cyclohexane–2-propanol (1:1), removal of 2-propanol and inorganic chlorine by subsequent washings with distilled water (pH 2, H_2SO_4) and drying the cyclohexane phase over anhydrous Na_2SO_4 [1,2]. The concentration of EOCl in the extract was determined by NAA according to Gether *et al.* [1]. The relative standard deviation of the method is about 10% [2,16].

Enzymatic hydrolysis and partitioning of lipids

Enzymatic hydrolysis of fish lipids, dissolved in

cyclohexane, was performed for 20 h using an immobilized *Mucor miehei* lipase (Lipozyme IM 20, activity 64 BIU/g) (Novo Industry, Copenhagen, Denmark) and distilled water [10].

The partitioning of hydrolysed and unhydrolysed lipids into neutral (non-acidic) and acidic substances was effected by liquid–liquid extractions between cyclohexane and aqueous buffers at different pH (Fig. 1). 2-Propanol was added to break emulsions [10]. After partitioning, the dry mass of the lipid residues that could be extracted with cyclohexane was determined gravimetrically after evaporating the solvent under nitrogen at 30°C. Each residue was dissolved in a small volume of cyclohexane and the chlorine content was determined by NAA.

Esterification and partitioning of lipids

Two methods were used for esterification of the unhydrolysed lipids to FAMEs, following Christie [17]. The methods were slightly modified by merely selecting solvents that were known to maintain low concentrations of EOCl in blank procedures. In one method, eel lipids were subjected to alkaline transesterification. Four portions of eel lipid, *ca.* 50 mg each, were each dissolved in 1 ml of cyclohexane, mixed with a solution of 0.5 *M* Na in methanol (2 ml) and heated at 50°C for 10 min. Water (3 ml) was added and the FAMEs in each sample were extracted three times with 3 ml of cyclohexane [17]. The FAME solutions were transferred to a separation funnel.

The aqueous phases were combined to one sample, which was acidified with H_2SO_4 from a pH of about 12 to 2 (Fig. 1), and shaken three times with 12 ml of cyclohexane. The cyclohexane solutions, containing uncharged, acidic substances (possibly chlorophenolic compounds and free fatty acids), were transferred into another separation funnel.

The two extracts were rinsed twice with water (pH 2), dried, concentrated by evaporation to small volumes and analysed for chlorine by NAA. The dry masses were determined as described above.

The alkaline transesterification was also performed with one sample containing 212 mg of eel lipid, the procedure being the same but on a four times larger scale.

In the other method, flounder lipids were subjected to acidic methanolysis. Six portions of flounder lipid, about 25 mg each, were each dissolved in 1 ml of cyclohexane, mixed with a solution of 1.5% (w/v) H_2SO_4 in methanol (2 ml), and heated at 60°C for 12 h [17]. The solutions were combined into one sample. Lipid residues in the small tubes were washed out by two additions of cyclohexane and transferred to the combined sample (a total cyclohexane volume of 30 ml). Acidic substances were removed by shaking the extract against a pH 9 buffer (50 ml). After centrifugation, the cyclohexane, containing FAMEs, was transferred into a separation funnel. The extraction of FAMEs was repeated once with another portion of cyclohexane (24 ml).

After acidifying the buffer to pH 2, uncharged, acidic substances were twice extracted from the water phase with cyclohexane (25 + 25 ml).

The two extracts were rinsed with water, dried, analysed for chlorine and the dry masses determined as above.

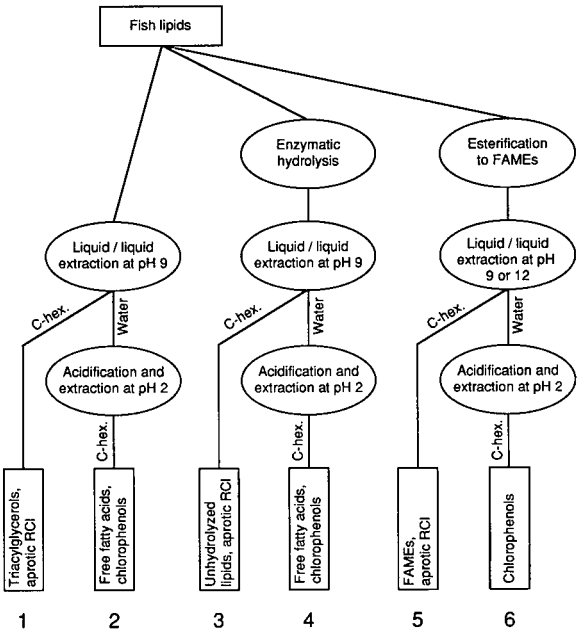

Fig. 1. Partitioning scheme used for characterizing chlorinated organic substances (RCl) in untreated fish lipids, lipids hydrolysed with lipase and esterified lipids. The partitioning of triolein and oleic acid was studied by silica gel thin-layer chromatography according to Håkansson *et al.* [6]. FAMEs were determined by GC–FID. PCBs in hydrolysed samples were determined by GC–ECD after treatment with concentrated sulphuric acid. Free chlorophenols (added as reference substances) were determined previously [10] by reversed-phase liquid chromatography. The numbers 1–6 at the bottom are used in Tables I and II.

Free fatty acids, obtained by enzymatic hydrolysis of the eel lipids A, were converted into FAMEs by acidic esterification, using 2 *M* HCl in methanol (60°C, 30 min [17]). Water was added and the FAMEs were extracted with cyclohexane.

GC conditions

The samples that were obtained after the esterification procedures were dissolved in cyclohexane and the FAMEs were studied by GC (Varian 3500) with FID and ELCD, used in parallel. A glass splitter (Pressfit, Schmidlin Labor + Service) divided the column flow to the two detectors with a splitting ratio close to 1:1. In part of the study, the electrolytic conductivity detector was replaced with an electron-capture detector.

The samples were injected on-column into a NB-54 fused-silica capillary column (18 m × 0.32 mm I.D., film thickness 0.25 μm) (HNU-Nordion). Helium was used as the carrier gas (4 ml/min). After a delay of 1 min, the injector was programmed from 90 to 280°C at a rate of 200°C/min. The column temperature was programmed from 90°C (held for 3 min) to 280°C at 6°C/min.

The ELCD instrument (Tracor/Varian, Model 1000) was mounted above a hole drilled in the column oven ceiling, close to the FID instrument. It was operated at a base temperature of 280°C and a temperature of 830°C in the nickel reactor tube. Helium (99.995%) was used as make-up gas (26 ml/min) and hydrogen (99.9995%) as reaction gas (23 ml/min). The detector was bypassed by vent during the first 2 min, which prevented the solvent from reaching the reactor tube. A PTFE tube transferred the pyrolysis products from the reactor tube to the electrolytic conductivity cell, through which 1-propanol was passed at a flow-rate of 0.53 ml/min. Before entering the cell, the 1-propanol was pumped through an ion-exchange resin (halogen form) which removed halogen ions. When used in the halogen-selective mode, other solutes containing nitrogen or sulphur do not interfere in ELCD. The ion-exchange resin and solvent were supplied in assembly by Varian. Any 1-propanol that evaporated was replaced with new solvent (>99.8%, Aristar) (BDH).

The FID and ECD systems were operated at 320°C and nitrogen was used as make-up gas (20 ml/min in each detector).

A series of homologous FAMEs (FA mix ME 62, Larodan) and a fish fat (methyl esters) of known constituency (Qualmix fish, Larodan) were used for the tentative identification of the FID peaks in the sample chromatograms. The FAMEs in the samples were then determined in relation to methyl nonadecanoate (internal standard) and the amounts of FAMEs were compared with the gravimetrically determined dry masses.

Methyl esters of 9,10-dichlorostearic acid and a mixture of 9- and 10-monochlorostearic acid (Synthelec, Lund, Sweden) were prepared by acidic esterification. The identity of these chlorinated standards has been verified by GC–MS [11]. These substances were used as external standards for ELCD. A PCB mixture (Clophen A 50, Bayer) was also used for reference purposes.

RESULTS AND DISCUSSION

Concentrations of halogenated compounds in fish

The eels, caught in the vicinity of the sulphite mill, contained about 1200 μg of EOCl per gram of lipid. Eels from the receiving waters of the Norwegian kraft mill and the flounders caught in the vicinity of the Swedish kraft mill had EOCl concentrations of 30–60 μg/g lipid. Flounders from the low-impact area of Simrishamn had an EOCl concentration of slightly less than 30 μg/g lipid. It can be argued that the reported data cannot be used directly for comparing the effects on the environment of the two pulp production methods because the Idefjord fiord, into which the sulphite mill discharged its effluent, is narrow and has a low water exchange rate. However, high EOCl concentrations (200–2000 μg/g lipid) have been found in freshwater fish close to a discharge of bleach effluents from an old calcium-based sulphite mill [18]. Additionally, sulphite mills producing bleached pulp can be expected to have a greater impact on the EOCl concentrations in fish in the receiving waters than can be expected for kraft mills, because EOCl in bleach liquors from sulphite mills and from kraft mills makes up about 3–15% and 0.5–2%, respectively, of the total content of organically bound halogens in the liquors [19–21]. Bleaching of pulp, produced according to the sulphite process, can therefore probably produce more organochlorine compounds that can bioaccumulate than the bleaching of kraft pulp.

TABLE I

PARTITIONING OF LIPIDS, EOCl AND EOBr IN NEUTRAL AND ACIDIC SUBSTANCES BEFORE AND AFTER AN ENZYMATIC HYDROLYSIS

The EOCl blank values are substracted and include all solvents and (when used) enzyme.

Sample	Original lipid extract			Fraction[a]	Recovered lipid		Recovered EOCl		Recovered EOBr		EOCl blank (μg)
	Lipid (g)	EOCl (μg)	EOBr (μg)		g	%	μg	%	μg	%	
Undrolysed eel lipid (A)	1.003	1220	2.6	1 (neutral)	0.932	93	1200	98	n.a.	–	3.8
(EOCl: 1220 μg/g fat)				2 (acidic)	0.005	1	25	2	n.a.	–	0.6
Hydrolysed eel lipid (A)	1.002	1220	2.6	3 (neutral)	0.205	20	190	16	n.a.	–	1.2
				4 (acidic)	0.546	55	530	43	n.a.	–	1.1
Hydrolysed eel lipid (A)	1.009	1230	2.6	3 (neutral)	0.211	21	210	17	n.a.	–	1.2
				4 (acidic)	0.562	56	560	46	n.a.	–	1.1
Unhydrolysed flounder lipid (C)	0.346	16.6	n.a.[b]	1 (neutral)	0.280	81	13	78	n.a.	–	0.3
(EOCl: 48 μg/g fat)				2 (acidic)	0.055	16	0.5	3	n.a.	–	0.4
Hydrolysed flounder lipid (C)	0.356	17.1	n.a.	3 (neutral)	0.068	19	3.1	18	n.a.	–	0.6
				4 (acidic)	0.224	63	4.3	25	n.a.	–	0.2
Hydrolysed flounder lipid (C)	0.366	17.6	n.a.	3 (neutral)	0.070	19	3.0	17	n.a.	–	0.6
				4 (acidic)	0.238	65	6.3	36	n.a.	–	0.2
Unhydrolysed flounder lipid (D)	0.347	10.4	n.a.	1 (neutral)	0.275	79	11	106	n.a.	–	0.3
(EOCl: 30 μg/g fat)				2 (acidic)	0.062	18	1.7	16	n.a.	–	0.4
Hydrolysed flounder lipid (D)	0.409	12.3	n.a.	3 (neutral)	0.070	17	3.3	27	n.a.	–	0.6
				4 (acidic)	0.276	67	3.2	26	n.a.	–	0.2
Hydrolysed flounder lipid (D)	0.348	10.4	n.a.	3 (neutral)	0.064	18	2.9	28	n.a.	–	0.6
				4 (acidic)	0.235	68	2.3	22	n.a.	–	0.2
Unhydrolysed flounder lipid (E)	0.299	8.4	1.1	1 (neutral)	0.295	99	7.6	91	1.1	104	0.2[d]
(EOCl: 28 μg/g fat)				2 (acidic)	n.d.[c]	–	n.d.	–	n.d.	–	0.2[d]
Hydrolysed flounder lipid (E)	0.316	8.8	1.2	3 (neutral)	0.031	10	1.7	19	0.2	16	0.1[d]
				4 (acidic)	0.228	72	2.7	31	0.2	16	0.2[d]

[a] The numbers 1–4 characterizing the fractions refer to Fig. 1.
[b] n.a. = Not analysed.
[c] n.d. = Not detected.
[d] EOBr blanks were 0.08 μg.

Characterization of chlorinated compounds and lipids

Untreated lipids. Partitioning with liquid–liquid extractions showed that most lipids and chlorinated compounds in the untreated samples of eel A and flounder E were of a neutral (non-acidic) character (Table I). This result agreed with that for a previously performed characterization of EOCl in cod liver lipids [10]. However, some hydrolysis (lipolysis) had occurred with the flounder samples C and D during storing the fish at −20°C for 15 months before homogenization and extraction. This led to 16–18% of the lipid dry mass and part of the chlorinated substances to be recovered as acidic material. The lipolysis found with the two flounder samples is a phenomenon well known by lipid chemists, but is usually disregarded when persistent, organochlorine pollutants are studied.

Enzymatic hydrolysis of lipids. After the enzymatic hydrolysis, neutral material made up 10–20% of the supplied lipids (Table I). The enzymatic hydrolysis also reduced the proportion of chlorinated compounds of neutral character (to 15–30% of the supplied EOCl) and part of the chlorinated material (22–45%) was recovered as acidic compounds. The neutral lipids, remaining after the enzymatic hydrolysis, were again treated with lipase but no further hydrolysis could be detected. The extent of hydrolysis was therefore not limited by the amount of water added.

Each experimental set-up for testing the partitioning of chlorinated compounds was accompanied by a blank sample. In spite of this, the recovered EOCl for one flounder sample exceeded 100%, showing the difficulties in handling small amounts of EOCl in the laboratory.

The partitioning studies showed that most of the chlorinated compounds in fish, exposed to pulp bleach liquors, did not consist of aprotic compounds, otherwise they should be recovered as neutral material after the enzymatic hydrolysis. Further, there was no evident difference in the hydrolysable properties of the chlorinated compounds in fish from the receiving waters of the two pulp mills and fish from the area of Simrishamn with a low anthropogenic impact. The main result of this study agrees with an earlier observation [10] that most chlorinated compounds in marine fish can be hydrolysed by lipase, and the result was independent of the EOCl levels and catch localities. The observation also corresponds to that obtained for brominated compounds [characterized with NAA as extractable, organically bound bromine (EOBr)] in marine fish [22,23] (Table I). It can therefore be concluded that halogenated compounds make up part of the fish lipids.

Alkaline transesterification of eel lipids. The lipids that were extracted from eel caught in the receiving waters of a sulphite mill (eel A) were converted into FAMEs. On performing the alkaline transesterification in one batch, the dry mass in the FAME fraction corresponded to slightly more than 90% of the supplied eel lipids (Table II). This corresponds reasonably well with the theoretical recovery from a triacylglycerol. A lower recovery was obtained when the eel lipids were transesterified in several small portions. However, it was necessary to establish the percentage of the neutral material that was actually in the form of FAMEs because a triacylglycerol and a FAME would be partitioned similarly. Comparisons with the results of GC–FID showed that FAMEs made up 95–102% of the dry mass of the neutral material, *i.e.*, the esterification yield (Table II), showing that the transesterification was complete. The finding also indicates that lipids extracted according to the EOCl method are dominated by triacylglycerols, as glycerophosphatides carry only two fatty acids in each molecule. Håkansson *et al.* [6] drew the same conclusion after separating similar fish lipids by silica gel chromatography, finding that 93–97% of the untreated lipids was eluted in a fraction characterized by triacylglycerols.

Acidic esterification of flounder lipids. The partitioning of the unhydrolysed flounder sample C showed that acidic compounds made up about 17% of the lipid dry mass (Table I). The esterification to FAMEs was therefore performed under acidic conditions because an alkaline transesterification cannot transform free fatty acids into their methyl esters. After the acidic esterification, which can form FAMEs from both acylglycerols and free fatty acids, 105–106% of the supplied lipids were recovered as neutral substances (Table II). The recovery of > 100% was probably due to the fact that part of the lipids were free fatty acids, which on acidic esterification became the corresponding methyl esters, thereby increasing the weight. By correlating the FAMEs determined by GC–FID with the dry

TABLE II

PARTITIONING OF LIPIDS AND EOCl IN NEUTRAL AND ACIDIC SUBSTANCES AFTER TRANSESTERIFICATION

The EOCl blank values are subtracted.

Sample	Original lipid extract		Fraction[a]	Recovered lipid		Recovered EOCl		EOCl blank (μg)	Esterification yield (%)
	Lipid (g)	EOCl (μg)		g	%	μg	%		
Esterified eel fat (A)	0.212[b]	260[b]	5 (neutral)	0.193	91	265	102	7.5	95
(EOCl: 1220 μg/g fat)			6 (acidic)	0.003	1	8	3	6.0	
Esterified eel fat (A)	0.211[c]	260[c]	5 (neutral)	0.157	74	170	65	12.2	102
			6 (acidic)	0.011	5	40	15	5.0	
Esterified flounder fat (C)	0.155[d]	7.5[d]	5 (neutral)	0.164	106	6.7	90	0.1	98
(EOCl: 48 μg/g fat)			6 (acidic)	0.003	2	n.d.[e]	–	0.0	
Esterified flounder fat (C)	0.149[d]	7.2[d]	5 (neutral)	0.156	105	5.9	82	0.1	95
			6 (acidic)	0.003	2	0.1	1	0.0	

[a] The numbers 5 and 6 characterizing the fractions refer to Fig. 1.
[b] One sample.
[c] Four samples of *ca.* 50 mg.
[d] Six samples of *ca.* 25 mg.
[e] n.d. = Not detected.

mass of the samples, the esterification yield was calculated to be 95–98%. The acidic esterification of flounder lipids therefore proceeded similarly to the alkaline transesterification of eel lipids and the esterification experiments could be used for discussions about EOCl as part of the fish lipids.

Contribution to EOCl from chlorinated carboxylic acids. The hydrolysis experiments alone could not ascertain whether the chlorine-containing esters were chlorinated phenols esterified with fatty acids or acylglycerols containing chlorinated carboxylic acids. However, after forming FAMEs from acylglycerols by transesterification (alkaline and acidic) and from free fatty acids by acidic esterification, there was a close relationship between the dry masses and the amounts of EOCl in fractions containing FAMEs and acidic substances, respectively (Table II). As repeated hydrolysis did not increase the yield of hydrolysis products, the chlorinated material remaining in the neutral fraction after hydrolysis was regarded as aprotic substances. The chlorine associated with carboxylic acids was therefore calculated as the difference between the percentage of EOCl in the neutral fraction containing FAMEs (Table II) and the percentage of EOCl in the neutral fraction after the enzymatic hydrolysis (Table I). Using this approach, chlorine in chlorinated carboxylic acids was calculated to account for 50–85% of EOCl in eels exposed to chlorinated compounds from the sulphite mill and 65–75% of the EOCl in flounders caught in the receiving waters of a kraft mill.

The reasoning above assumes that any fatty acids, esterified with chlorophenols, were transesterified to methyl esters in the esterification procedures, thereby releasing free chlorophenols. If this should not hold, part of the EOCl recovered in the neutral fraction might actually have been fatty acid esters of chlorophenols. However, transesterification is a reversible reaction and the position of the equilibrium depends on the relationship between the concentrations of the alcohol added and the ester. The large excess of methanol thus favours the transesterification reaction in general. Particularly under alkaline conditions, the phenolate ion is a better leaving group than an alkoxide in the transesterification of esters, because phenols are stronger acids than alcohols, and the acidity increases as the benzene nucleus carries electron-attracting substituents such as halogens or nitro groups [24]. The possibility that chlorophenol/fatty acid esters would remain unaffected during the transesterification procedures was therefore considered to be low. In a previous study [10], 90% of free chlorophenols dissolved in cyclohexane were recovered as acidic substances on liquid–liquid extraction with a pH 9 buffer. Hence esterified chlorophenols ought to be released from their fatty acid esters and the majority of them recovered in the acidic fraction.

As only a small part (< 1–15%) of the EOCl was recovered as acidic material after the transesterification procedures (Table II), it is therefore suggested that chlorinated phenolic compounds were of minor significance to the hydrolysable chlorinated compounds in the fish lipids studied. More direct methods should be chosen, however, if the amount of chlorine in esterified chlorophenolic compounds is to be assessed. A combination of the results given above with the general picture that the compounds representing EOCl have relatively high molecular weights (> 300 [2,8,9]) and are hydrolysable strongly supports the suggestion that the major portion of EOCl in fish is associated with chlorinated carboxylic acids bound in acylglycerols.

Detection of chlorinated FAMEs with ELCD

ELCD detected chlorinated but not unchlorinated FAMEs (Fig. 2). The detection limit (DL), defined as a peak height larger than twice the noise, found with GC–ELCD was about 50 pg of chlorine, which equalled 400 pg of monochloro- and 250 pg of dichlorostearic acid methyl esters (Fig. 2). GC–FID showed about the same DL (300 pg) for the reference substances as did ELCD. In spite of the high DL obtained with GC–ELCD (20–30 times higher than expected), possibly depending on an insufficiently pure make-up gas or excessive column bleeding, the results achieved are presented because of the novel application.

It was possible to detect halogenated compounds among FAMEs produced from the eel lipids A, containing 1200 ppm of EOCl (Fig. 3). The bromine concentration (EOBr) was only 0.2% of EOCl and all the detected compounds were, therefore, chlorinated substances. The ELCD response is almost proportional to the amount of chlorine injected and independent of the compound structure [25,26]. It was therefore possible to determine how much of the injected EOCl that was accounted for by the

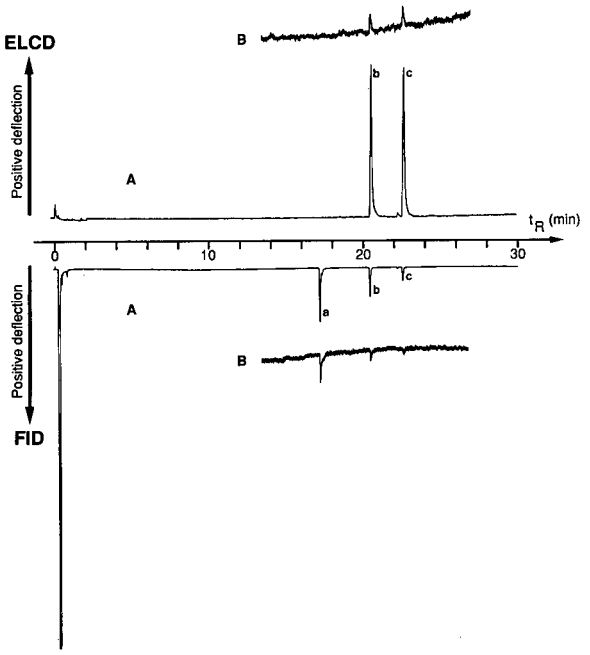

Fig. 2. Simultaneous detection with GC–ELCD and GC–FID of methyl esters of the reference compounds: (a) oleic acid, (b) monochlorostearic acid and (c) dichlorostearic acid. Chromatograms labelled A refer to an injection of 30 ng, 17 ng (1.8 ng chlorine) and 10 ng (1.9 ng chlorine) of compounds a, b and c, respectively. The inserted chromatograms labelled B, obtained at the limit of detection, refer to an injection of 0.74 ng, 0.42 ng (46 pg chlorine) and 0.25 ng (48 pg chlorine) of compounds a, b and c, respectively. t_R = Retention time.

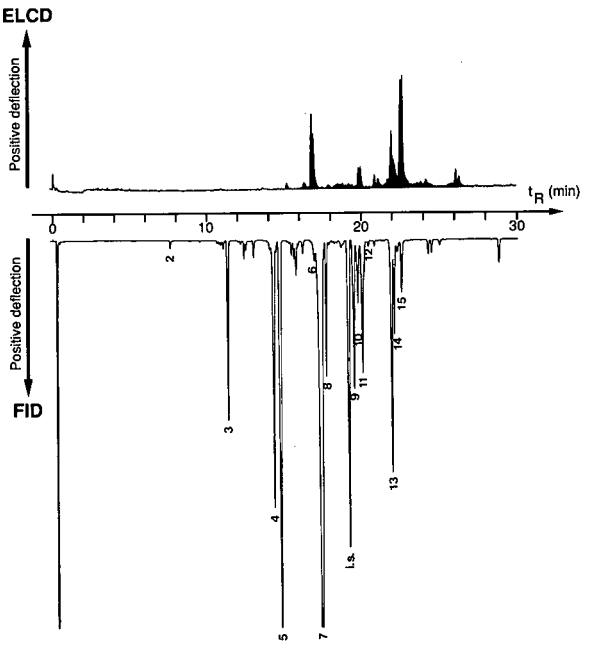

Fig. 3. Simultaneous detection with GC–ELCD and GC–FID of 7.2 μg of FAMEs from eel lipids containing 8.6 ng of organically bound chlorine. The dark area used for integration of the total ELCD response corresponds to 7.8 ng of chlorine. The FAMEs shown in the FID chromatogram, given by the numbers of carbon atoms and double bonds, are tentatively identified as 2 = 12:0, 3 = 14:0, 4 = 16:1, 5 = 16:0, 6 = 18:4, 7 = 18:2 and 18:1, 8 = 18:0, 9 = 20:5, 10 = 20:4, 11 = 20:1, 12 = 20:0, 13 = 22:6, 14 = 22:5, 15 = 22:1 and i.s. = 19:0 (internal standard).

GC–ELCD technique. An injection of 7.2 μg of FAMEs containing 1200 ppm of EOCl equalled 8.6 ng of chlorine. By comparison with the reference compounds, the total ELCD response of the eel sample corresponded to 7.8 ng of chlorine and the individual compounds contained less than 1 ng of chlorine. This means that ELCD accounted for 90% of the chlorine of the chlorinated substances in the eel lipids after their conversion into FAMEs. The ELCD chromatograms obtained with the other fish samples (30–60 ppm of EOCl) showed only minute peaks, which indicated that no solutes other than chlorinated compounds produced a measurable ELCD response. The other fish samples had 20–40 times lower EOCl concentrations than the eel caught in the receiving waters of the sulphite mill. If the chlorine in those lipids was distributed over a similar number of compounds, most of the constituents would be below the detection limit obtained.

The solution containing FAMEs (eels A) was treated three times with concentrated sulphuric acid to investigate whether the substances detected with ELCD were persistent compounds like PCBs. As this treatment eliminated the compounds that could be detected with ELCD (Fig. 4), the chlorinated substances were not regarded as persistent. It was also verified that the chlorinated reference substances (methyl esters) were not resistant to this treatment. Some small ELCD peaks were found with the sulphuric acid-treated eel sample after concentrating it by evaporation (Fig. 4). The pattern did not fit with that of a PCB mixture. The peaks were more likely derived from chlorinated fatty acids (see below).

The free fatty acids that were produced by enzymatic hydrolysis of the eel lipids had been sep-

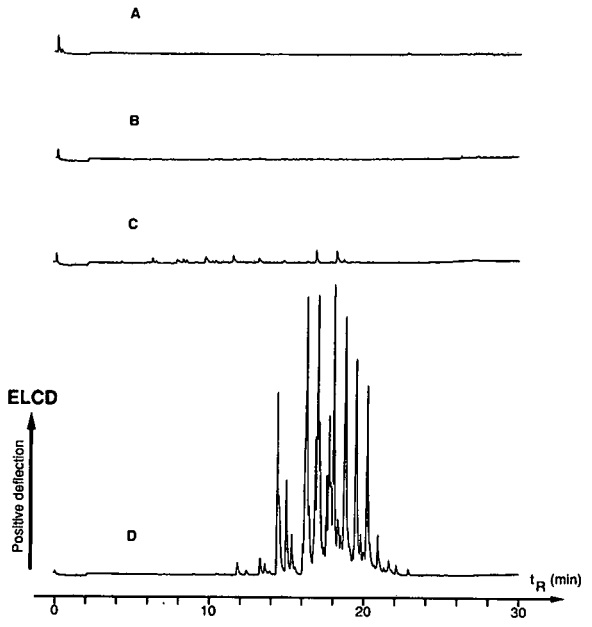

Fig. 4. GC–ELCD traces obtained after treating FAMEs of (A) the reference compounds (*cf.*, Fig. 2) and (B) the eel sample (*cf.*, Fig. 3) with concentrated H_2SO_4. After evaporation to a small volume, minor amounts of chlorinated material were found in the treated eel sample (C). Chromatogram D shows the ELCD response to 36 ng of PCBs (Clophen A50) equalling 18 ng of chlorine.

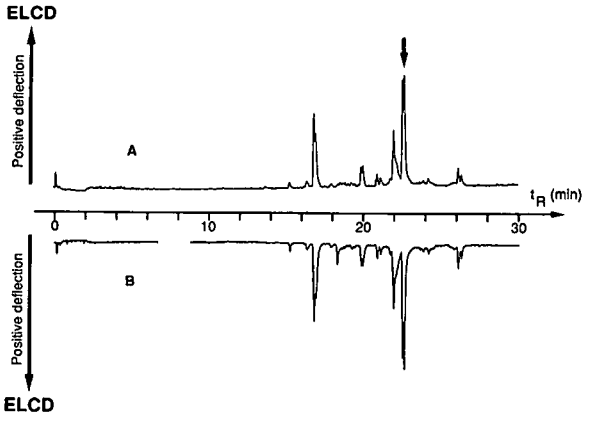

Fig. 5. (A) GC–ELCD of eel lipids subjected to alkaline transesterification and (B) GC–ELCD of FAMEs produced by acidic esterification of free fatty acids (separated from non-acidic compounds after enzymatic hydrolysis; *cf.*, Fig. 1). The arrow shows the retention time of methyl 9,10-dichlorostearate.

arated from non-acidic compounds by extraction into an alkaline buffer, followed by re-extraction into cyclohexane after acidification (Fig. 1). The free fatty acids were converted into FAMEs by acidic esterification and their GC–ELCD (Fig. 5) and GC–FID patterns were almost identical with those obtained after the alkaline transesterification. This implies that the chlorinated compounds detected with ELCD were chlorinated carboxylic acids. By co-injection, methyl 9,10-dichlorostearate was tentatively identified by its retention time as the largest peak in the ELCD chromatogram (Fig. 5). The presence of dichlorostearic acid in the eel lipids has recently been established by mass spectrometry [27]. Judging from the peak area, the concentration of dichlorostearic acid (having a chlorine content of 20%) in the eel lipid was calculated to be 600 ppm.

After the acidic esterification of the free fatty acids isolated from the hydrolysed eel lipids, one extra peak was found (Fig. 5), suggesting that this substance was degraded during the alkaline transesterification. Tinsley and Lowry [23] reported that 50% of a brominated stearic acid was degraded during alkaline hydrolysis whereas Sundin *et al.* [11] observed no degradation of dichlorostearic acid during alkaline transesterification from its triacylglycerol to the methyl ester. However, when working with yet unidentified compounds, the risk of producing artifacts must be considered. As HCl was used as a catalyst for this acidic esterification, it cannot be excluded that HCl had been added to some double bond in an unsaturated fatty acid. The acidic esterification with sulphuric acid might have been more appropriate.

The two isomers of the synthesized monochlorinated stearic acids, 9- and 10-monochlorostearic acid, could not be separated with the GC system used. Similar results were also reported by Haken and Korhonen [28], who studied the GC retention indices of different isomers of monochlorinated FAME. Using an SE-30 column, they found a negligible influence on the GC retention from the location of the chlorine when the chlorine was located at the mid-positions of a long-chain FAME. However, they found a considerable enhancement in the retention with chlorine in terminal (ω) or near-terminal positions.

Several compounds could be detected by ELCD after treating a solution of FAMEs (eels A) with

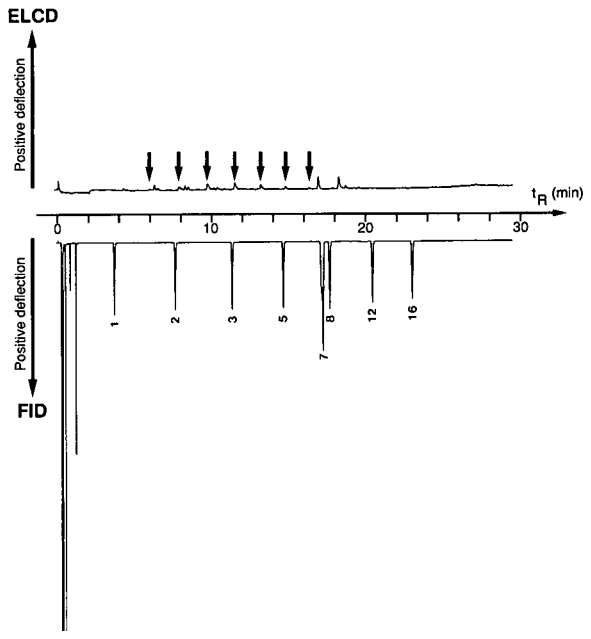

Fig. 6. GC–ELCD of FAMEs treated with H_2SO_4 (*cf.*, Fig. 4) and GC–FID of a synthetic mixture of FAMEs, containing members of a homologous series. The FID peaks correspond to 1 = 10:0, 2 = 12:0, 3 = 14:0, 5 = 16:0, 7 = 18:2 and 18:1, 8 = 18:0, 12 = 20:0 and 16 = 22:0. A possible homologous series is shown by arrows on the ELCD trace. The ELCD retention times seem to indicate that each compound is separated from the previous one by one CH_2 group.

concentrated sulphuric acid and thereafter concentrating the sample by evaporation. Their retention times were compared with the GC–FID pattern of a homologous series of $C_{10:0}$–$C_{22:0}$ FAMEs. The similar elution patterns of the homologous series and some of the ELCD-detectable compounds (Fig. 6) suggest that some of the latter compounds might belong to a homologous series of chlorinated fatty acids and that each compound is separated from the previous one by one CH_2 group. The compounds were not present after treating the reference compounds with concentrated acid and therefore did not originate from the sulphuric acid. It cannot be concluded if the compounds were degradation products from longer fatty acids, became detectable after destroying the major compounds with concentrated sulphuric acid or were reaction products formed from unsaturated fatty acids and inorganic HCl released from the eel lipids during the treatment with sulphuric acid.

By treating a sample with concentrated sulphuric acid, the persistent EOCl (EPOCl) can be assessed [2]. The proportion of EPOCl that can be identified by GC–ECD has been found to be in the range 40–100% for fish from a fiord area polluted by industrial effluents from magnesium production [29]. In tissues of seal caught off the Norwegian coast, the identified EPOCl has been found to be in the range 10–100% [30] and, in a recent study of salmon and eel lipids [6], the sum of chlorine in PCBs, DDT and DDE amounted to 7–36% of EPOCl. As ECD seems not to be a suitable detection method for chlorinated fatty acids (see below), it is possible that part of the unidentified EPOCl belongs to chlorinated fatty acids remaining after, or formed during, the treatment with concentrated sulphuric acid.

Detection of FAMEs with ECD

When working with GC–ECD, negative peaks are occasionally encountered in the chromatograms. An extreme result was obtained when FAMEs of eel lipids A were injected into the GC system and studied using ECD and FID in parallel. It was not possible to obtain any positive signal from ECD (Fig. 7) comparable to the ELCD response (Fig. 3). Owing to a high background with ECD, the unchlorinated FAMEs were less electron capturing and were therefore detected as negative peaks. This result was found both with the Varian detector and with a Carlo Erba Model 4160 gas chromatograph and a Model HT-25 electron-capture detector using argon–4% methane as the make-up gas and nitrogen as the carrier gas. The negative ECD response from unchlorinated FAMEs has been reported previously [31].

Sundin *et al.* [11] found a GC–ECD detection limit for methyl dichlorostearate of about 500 pg. In this study, the peak representing methyl dichlorostearate changed from a positive to a negative appearance on reducing the injected amount to 2.5 ng (Fig. 7). This problem was encountered after injecting several samples containing fish FAMEs. It was not investigated whether the problem resulted from residues of the transesterification reagent or from other solutes. However, the problem must be solved otherwise ECD is not suitable for the detection of chlorinated fatty acids in fish lipids.

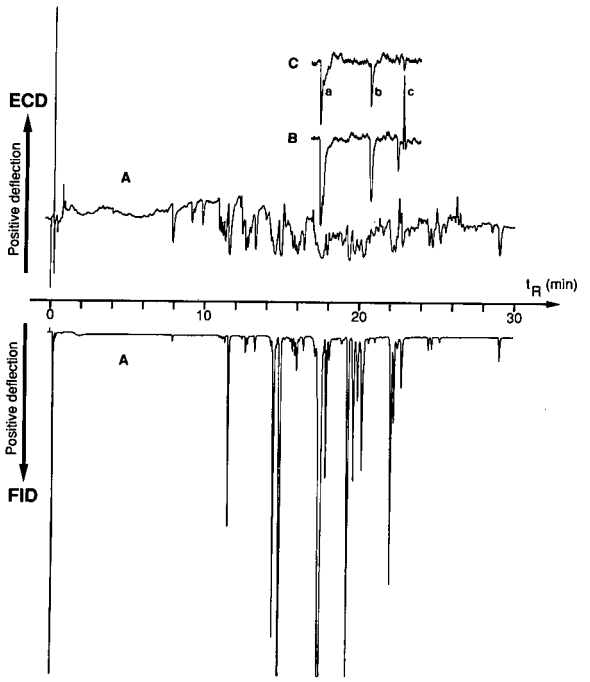

Fig. 7. Simultaneous detection with GC–ECD and GC–FID. (A) 4.5 μg of FAMEs of eel lipids (*cf.*, Fig. 3). The inserted ECD traces B and C were obtained with methyl esters of the reference compounds (a) oleic acid, (b) monochlorostearic acid and (c) dichlorostearic acid [(B) 30, 17 and 10 ng; (C) 7, 4 and 2.5 ng].

General considerations

This work indicates that chlorinated carboxylic acids bound in acylglycerols make up an important part of EOCl in fish tissues and that a fungal lipase can hydrolyse such substances. The chlorinated carboxylic acids are presumably of fatty acid character, as they have similar GC retention times to the normal fish FAMEs. This is the first report in which as much as 90% of EOCl in fish lipids could be detected after GC separation and, thus, the GC–ELCD technique can be successful in detecting new halogenated substance groups in environmental samples.

In the first study on the hydrolysable properties of organochlorine compounds in fish and sediments [10], it was assumed that short-chain fatty acids containing chlorine were liberated by the hydrolysis and then lost in the washing procedure, thereby causing a considerable loss of EOCl after hydrolysis. In this study, the ELCD chromatograms revealed that there was only a small difference between FAMEs produced by alkaline transesterification of the untreated eel lipids and FAMEs produced from free fatty acids that were isolated after an enzymatic hydrolysis (Fig. 5). As the ELCD chromatograms of FAMEs of the eel lipids A could be estimated to represent about 90% of the EOCl, the loss of EOCl after the enzymatic hydrolysis, *ca.* 40% (Table I), more likely depended on adsorption on the immobilized enzyme or to its carrier.

The incorporation of chlorinated fatty acids in fish lipids has been overlooked, although some workers have discussed their possible occurrence [10,32,33]. However, in connection with investigations on chlorinated cake flour, it has been demonstrated that chlorinated fatty acids can be taken up and distributed in rat tissues and that the substances can be transferred from mother to suckling rats and also, to some extent, to the foetuses via the placenta (reviewed by Cunningham [34]).

The chlorinated carboxylic acids found in the eel lipids were probably derived from compounds in the sulphite mill bleach effluents. Fatty acids in the wood are dissolved during the pulping processes and chlorinated fatty acids can occur in bleach liquors if the pulp is not thoroughly washed before bleaching. Dichlorostearic acid has been detected in effluents from Canadian kraft mills [35,36] and di- and tetrachlorostearic acids have been found in sediments from the receiving waters of three Scandinavian kraft mills [7]. A modern kraft mill normally has an oxygen prebleaching stage ahead of the chlorine and chlorine dioxide stages. The oxygen stage effectively reduces the concentration of fatty acids and resin acids in the pulp [37], thereby reducing the formation of chlorinated acids in the effluents. However, it ought to be considered whether the chlorinated fatty acids in fish are directly taken up from the effluents or are metabolites from other compounds formed during the bleaching processes. The Coulson electrolytic conductivity detector has been used for the GC detection of brominated fatty acids in rat tissues after administering di- and tetrabromostearic acids to rats via the food [38]. In addition to the administered substances, di- and tetrabrominated metabolites (palmitic and myristic acids) were found. At least part of the chlorinated carboxylic acids indicated by GC–ELCD in this work might be metabolites produced in the fish or in its prey organisms.

ACKNOWLEDGEMENTS

We thank Professor Karl-Gustav Wahlund, Dr. Peter Sundin and Professor Georg E. Carlberg for their constructive criticisms of this manuscript. We also thank employees at Varian in Sweden and the USA for encouraging us in experimenting with ELCD. Neutron activation analysis was performed by Sylviane Sieglé at the Institute for Energy Technology, Kjeller, Norway, and the flounders from the bight of Hanö were supplied by Peter Göransson. This work was supported by the Swedish Council for Forestry and Agricultural Research, the National Swedish Environmental Protection Board and the Royal Norwegian Council for Technical and Industrial Science.

REFERENCES

1 J. Gether, G. Lunde and E. Steinnes, *Anal. Chim. Acta*, 108 (1979) 137.
2 K. Martinsen, A. Kringstad and G. E. Carlberg, *Water Sci. Technol.*, 20 No. 2 (1988) 13.
3 C. Wesén, *Vatten*, 3 (1988) 213.
4 G. Lunde, J. Gether and E. Steinnes, *Ambio*, 5 (1976) 180.
5 A. Södergren, B. E. Bengtsson, P. Jonsson, S. Lagergren, Å. Larsson, M. Olsson and L. Renberg, *Water Sci. Technol.*, 20 No. 1 (1988) 49.
6 H. Håkansson, P. Sundin, T. Andersson, B. Brunström, L. Dencker, M. Engwall, G. Ewald, M. Gilek, G. Holm, S. Honkasalo, J. Idestam-Almquist, P. Jonsson, N. Kautsky, G. Lundberg, A. Lund Kvernheim, K. Martinsen, L. Norrgren, M. Pesonen, M. Rundgren, M. Stålberg, M. Tarkpea and C. Wesen, *Pharmacol. Toxicol.*, 69 (1991) 459.
7 M. Remberger, P.-Å. Hynning and A. H. Neilson, *J. Chromatogr.*, 508 (1990) 159.
8 C. Wesén, *Water Sci. Technol.*, 20 (1988) 185.
9 J. Hemming and K.-J. Lehtinen, *Nord. Pulp Pap. Res. J.*, 4 (1988) 185.
10 C. Wesén, G. E. Carlberg and K. Martinsen, *Ambio*, 19 (1990) 36.
11 P. Sundin, P. Larsson, C. Wesén and G. Odham, *Biol. Mass Spectrom.*, in press.
12 A. Karmen, *Anal. Chem.*, 36 (1964) 1416.
13 O. Piringer and M. Pascalau, *J. Chromatogr.*, 8 (1962) 410.
14 D. M. Coulson, *J. Gas Chromatogr.*, 3 (1965) 134.
15 R. C. Hall, *J. Chromatogr. Sci.*, 12 (1974) 152.
16 A. Bjørseth, G. E. Carlberg, E. Baumann Ofstad, J. P. Rambæk and C. Halvorsen, *Anal. Chim. Acta*, 160 (1984) 257.
17 W. W. Christie, *Gas Chromatography and Lipids*, Oily Press, Ayr, 1989, pp. 68–69.
18 G. E. Carlberg, A. Kringstad, K. Martinsen and O. Nashaug, *Pap. Puu*, 69 (1987) 337.
19 T. Källquist, G. E. Carlberg and A. Kringstad, *Ecotoxicol. Environ. Saf.*, 18 (1989) 321.
20 N. Soteland, E. Lystad, G. E. Carlberg, G. Tveten and T. Källquist, *Tappi*, 74, No. 5 (1991) 119.
21 G. E. Carlberg, S. Johnsen, L. H. Landmark, B.-E. Bengtsson, B. Bergström, J. Skramstad and H. Storflor, *Water Sci. Technol.*, 20 No. 2 (1988) 37.
22 G. Lunde, *J. Am. Oil Chem. Soc.*, 49 (1972) 44.
23 I. J. Tinsley and R. R. Lowry, *J. Am. Oil Chem. Soc.*, 57 (1980) 31.
24 F. A. Carey and R. J. Sundberg, *Advanced Organic Chemistry, Part A*, Plenum Press, New York, 3rd ed., 1990, pp. 465–470.
25 T. L. Ramus, S. J. Hein and L. C. Thomas, *J. Chromatogr.*, 314 (1984) 243.
26 Q. Wu, Q. Ou and W. Yu, *Fenxi Huaxiu*, 15 (1987) 390.
27 P. Sundin, Lund University, personal communication.
28 J. K. Haken and I. O. O. Korhonen, *J. Chromatogr.*, 298 (1984) 89.
29 E. Baumann Ofstad, G. Lunde and K. Martinsen, *Sci. Total Environ.*, 10 (1978) 219.
30 E. Baumann Ofstad and K. Martinsen, *Ambio*, 12 (1983) 262.
31 A. Södergren, *J. Chromatogr.*, 160 (1978) 271.
32 R. F. Addison, *Prog. Lipid Res.*, 21 (1982) 47.
33 A. Jernelöv, *Kem. Tidskr.*, 4 (1989) 119.
34 H. M. Cunningham, in R. L. Jolley, W. A. Brungs and R. B. Cumming (Editors), *Water Chlorination, Environmental Impact and Health Effects*, Vol. 3, Ann Arbor Sci. Publ., Ann Arbor, MI, 1980, pp. 995–1005.
35 J. M. Leach and A. N. Thakore, *Prog. Water Technol.*, 9 (1977) 787.
36 R. H. Voss and A. Rapsomatiotis, *J. Chromatogr.*, 346 (1985) 205.
37 O. Dahlman, R. Mörck, L. Johansson and F. deSousa, in A. Södergren (Editor), *Environmental Fate and Effects of Bleached Pulp Mill Effluents, Report 4301*, Swedish Environmental Protection Agency, Stockholm, 1992, pp. 47–56.
38 J. F. Lawrence, R. K. Chadha, F. Iverson, P. McGuire and H. B. S. Conacher, *Lipids*, 19 (1984) 704.

Journal of Chromatography, 625 (1992) 271–276
Elsevier Science Publishers B.V., Amsterdam

CHROM. 24 488

Gas chromatography–mass spectrometry of the picolinyl ester derivatives of deuterated acetylenic fatty acids

M. S. F. Lie Ken Jie and Y. C. Choi

Department of Chemistry, University of Hong Kong, Pokfulam Road, Hong Kong (Hong Kong)

(Received April 28th, 1992)

ABSTRACT

Deuteration (with Wilkinson's catalyst) of methyl 12:1(3*a*), 14:1(5*a*), 15:1(6*a*), 16:1(7*a*), 18:1(9*a*), 18:2(9*a*,11*a*), 17:2(10*a*,12*a*) and 18:2(5*a*,10*c*) gave the corresponding deuterium-labelled saturated fatty esters. The mass spectral analysis of their picolinyl esters gave predictable diagnostic ion fragments for most isomers. In the case of 12:1(3*a*) and 14:1(5*a*) isomers, hydrogen–deuterium scrambling occurred during electron impact to give unique fragmentation patterns. This method allows the accurate determination of the positions of the unsaturated centres in the alkyl chain of the fatty esters.

INTRODUCTION

Acetylenic bonds in fatty acids have been located by mass spectrometry following conversion into keto groups by oxymercuration and demercuration [1,2], or more simply as the pyrrolidides [3] or 4,4-dimethyloxazoline derivatives [4]. Christie *et al.* [5] have studied the mass spectra of the picolinyl ester derivatives of a series of positional isomers of dimethylene-interrupted octadecadiynoic acids. This study shows that the triple bond more remote from the carboxyl group is identifiable because of the presence of diagnostic ions, but the proximal triple bond is not. Mass spectral study of the picolinyl esters of a series of positional isomers of conjugated diacetylenic acids has also been performed [6].

We have recently reported the single and accurate determination of the positions of the double bonds (up to six) in the alkyl chain of fatty esters, by examining the mass spectra of the picolinyl esters of the corresponding deuterated fatty acids [7]. As heterogenous catalytic deuteration causes extensive hydrogen–deuterium scrambling during the reduction process [8], palladium and platinum catalysts cannot be used to "add" deuterium across unsaturated centres. Homogeneous catalysts, such as Wilkinson's catalyst [$(Ph_3P)_3RhCl(I)$], permit deuteration of unsaturated fatty acids to take place without scrambling [9,10].

This paper describes the gas chromatography–mass spectrometry (GC–MS) of picolinyl esters of deuterated 12:1(3*a*), 14:1(5*a*), 15:1(6*a*), 16:1(7*a*), 18:1(9*a*), 18:2(9*a*,11*a*), 17:2(10*a*,12*a*) and 18:2 (5*a*,10*c*) acids.

EXPERIMENTAL

Wilkinsons's catalyst [$(Ph_3P)_3RhCl(I)$] was purchased from Strem Chemical (Newburyport, MA, USA). Deuterium was obtained from Alpha Products (Ward Hill, MA, USA). The mono-acetylenic fatty acids were synthesized by known methods [11], and the conjugated diacetylenic acids [6] and enynoic acid [12] were prepared as described elsewhere. Deuteration of the unsaturated methyl esters was performed according to the procedure described by Rakoff and Emken [13], and the deuterium-labelled saturated methyl esters were trans-

Correspondence to: Dr. M. S. F. Lie Ken Jie, Department of Chemistry, University of Hong Kong, Pokfulam Road, Hong Kong, Hong Kong. Telefax: (852) 5170217.

0021-9673/92/$05.00

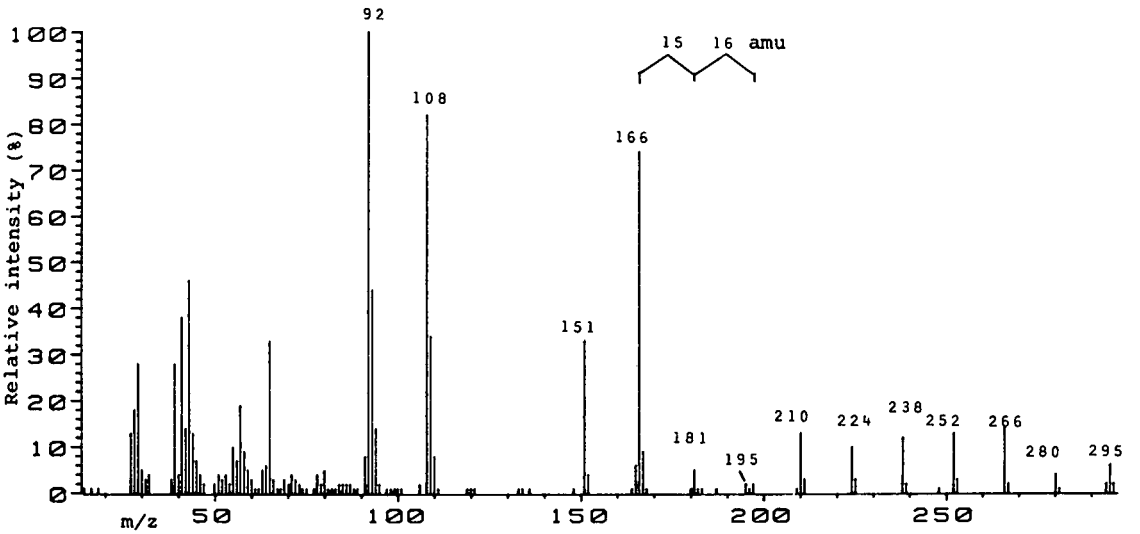

Fig. 1. Mass spectrum of deuteriated 12:1(3*a*).

formed into the picolinyl esters as described by Christie and Stefanov [14].

The picolinyl esters were submitted to GC–MS by means of on-column injection into a Hewlett Packard GC (Model HP5970). The GC column was a fused-silica capillary (12 m × 0.2 mm I.D., 0.33 μm film thickness) coated with cross-linked methyl silicone gum, Ultra 1. Helium was used as the carrier gas. The column oven temperature was 190°C. The outlet of the column was connected directly to the source of a Hewlett Packard mass selective detector, operated at an ionization energy of 70 eV (Hewlett-Packard Asia, Hong Kong, Hong Kong).

RESULTS AND DISCUSSION

The mass spectra of the picolinyl esters of deuterated 12:1(3*a*), 14:1(5*a*), 15:1(6*a*), 16:1(7*a*) and 18:1 (9*a*) acids are shown in Figs. 1–5. In all cases the molecular ion (M^+) indicated the addition of two

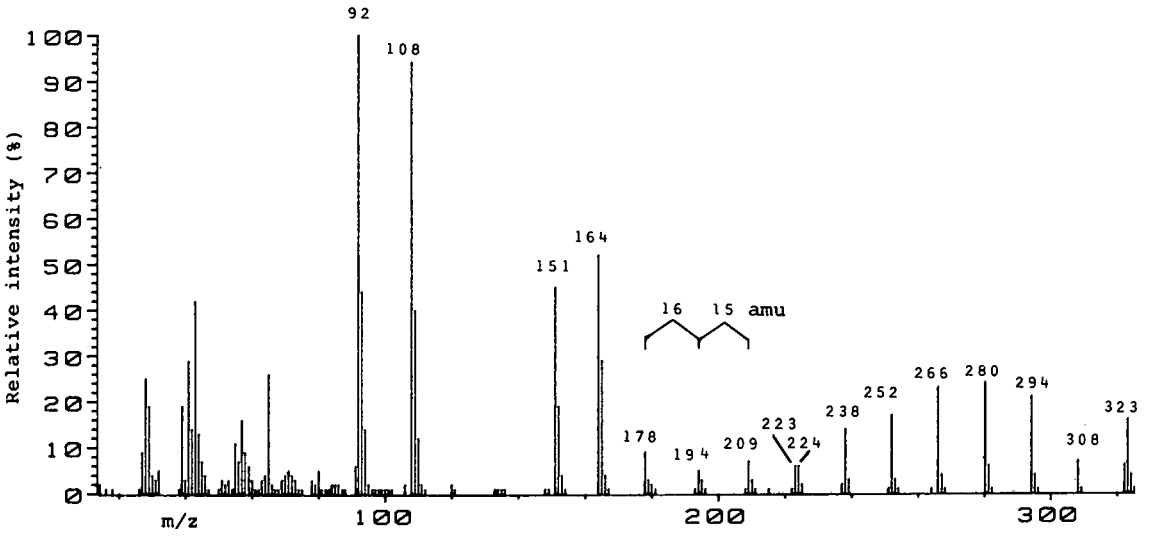

Fig. 2. Mass spectrum of deuteriated 14:1(5*a*).

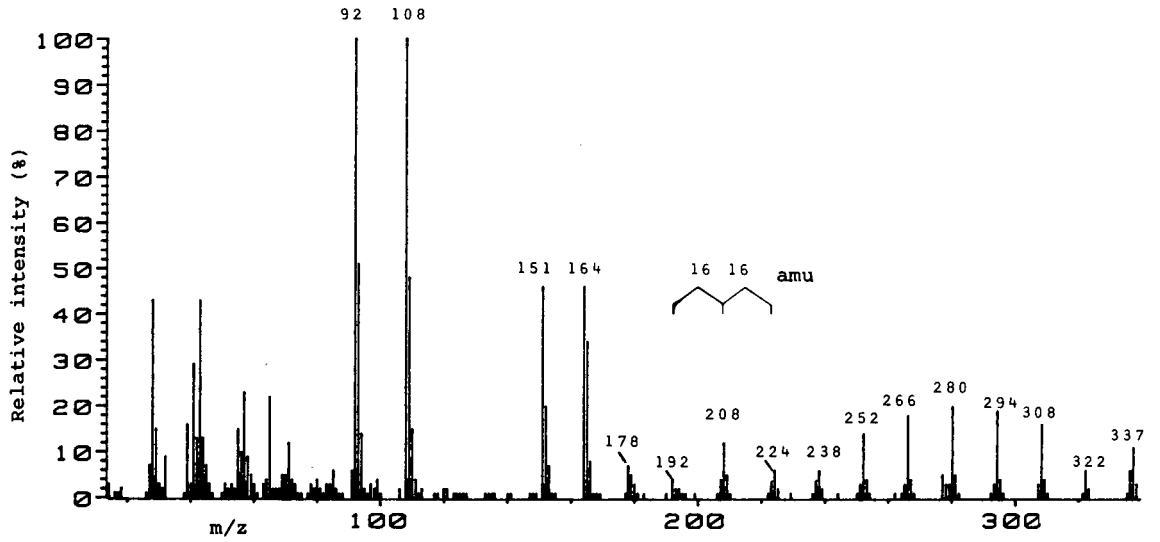

Fig. 3. Mass spectrum of deuteriated 15:1(6*a*).

molar equivalents of deuterium to the unsaturated centre of the mono-acetylenic substrate. Ion fragments of *m/z* greater than 200 were generally of medium intensity (10–25% relative intensity), except for the M − 15 ion fragment (*ca.* 5%). Ion fragments of *m/z* between 170–200 were low in relative abundance (5–10%). The picolinyl moiety was readily characterized by the appearance of very intense peaks at *m/z* 92, 108, 151 and 164. However, in the spectrum of the deuterated 12:1(3*a*) isomer, the peak at *m/z* 164 was replaced by a very intense peak at *m/z* 166 (72%), which indicated that the C-3 methylene carbon of the alkyl chain carried two deuterium atoms (Fig. 1). Cleavage of the C-4/C-5 bond gave an unexpected peak at *m/z* 181 instead of 182, implying that there was an exchange of one of

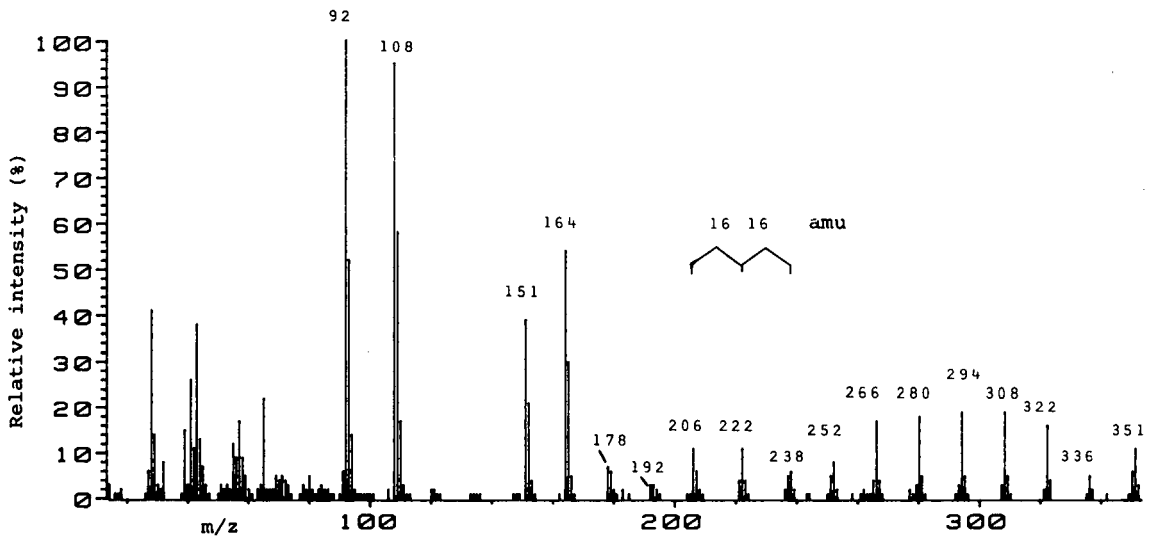

Fig. 4. Mass spectrum of deuteriated 16:1(7*a*).

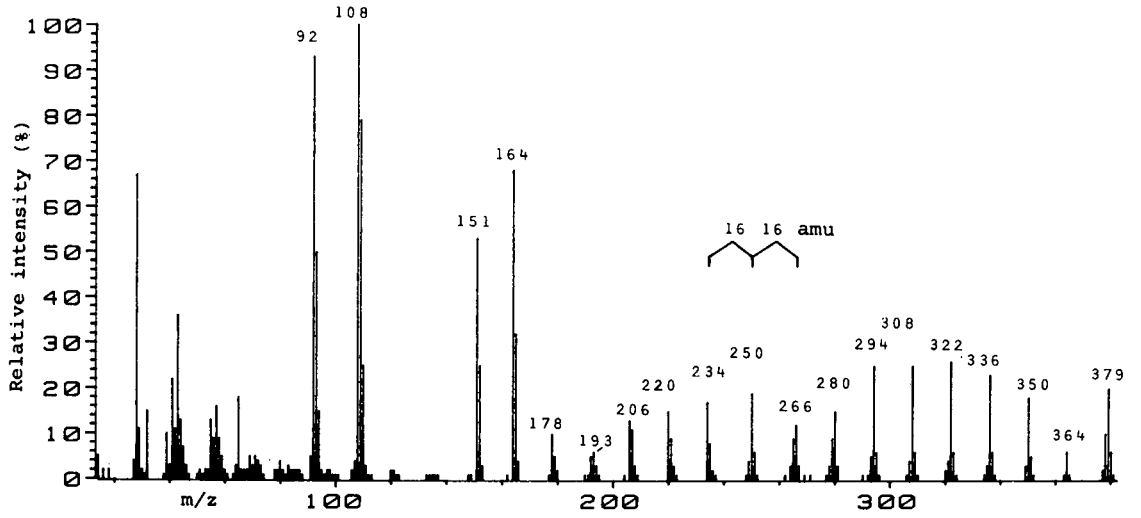

Fig. 5. Mass spectrum of deuteriated 18:1(9*a*).

the two deuterium atoms for a hydrogen at the C-4 carbon atom. Cleavage at the C-5/C-6 bond resulted in a cluster of three peaks of very low intensity at *m/z* 195 (2%), 196 (1%) and 197 (2%). This phenomenon was indicative of further hydrogen–deuterium scrambling. However, these hydrogen–deuterium exchanges appeared to be limited to the C-4 and C-5 carbon atoms of the alkyl chain of this isomer, as the cleavage of the C-6/C-7 bond gave the expected single ion fragment of *m/z* 210. The remaining peaks of the spectrum were spaced 14 amu apart until reaching the terminal methyl group, where the M − 15 peak appeared. From these results, it can be concluded that isomers containing a triple bond at the C-3/C-4 position are characterized by peaks at *m/z* 166 and 181 in their mass spectra.

In the analysis of the deuterated 14:1(5*a*) isomer (Fig. 2), cleavage of the C-5/C-6 bond gave a characteristic peak at *m/z* 194 (5%), which was 16 amu apart from the peak at *m/z* 178 (9%). This ion fragment showed that the C-5 carbon atom contained two deuterium atoms. However, scrambling involving one of the two deuterium atoms at C-6 resulted in two sets of low intensity twin peaks (1 amu apart) at *m/z* 209 (7%), 210 (3%) and 223 (6%), 224 (6%). The remaining ion fragments were 14 amu apart except for the M − 15 peak. From these two positional isomers, it was evident that hydrogen–deuterium scrambling occurred only when C–C bond cleavage took place at the α- and β-positions from the site containing the deuterium atoms.

In the spectrum of the deuteriated 15:1(6*a*) isomer (Fig. 3), there were two distinct 16-amu gaps between the peaks at *m/z* 192, 208 and 224, which allowed the position of the triple bond to be fixed at C-6/C-7 of the alkyl chain. A simple method of calculating the position of the triple bond from the values obtained in the mass spectrum is to substract 164 from the *m/z* value of the middle peak (the peak flanked by the two 16-amu gaps), divide the remainder by 14 and add 3 to the quotient. The whole number obtained corresponds to the first carbon atom of the triple bond in the alkyl chain. Thus in the case of the deuterated 15:1 isomer, the position of the triple bond is calculated as follows: [(208 − 164):14 + 3 = 6.14]. This result locates the triple bond at the C-6/C-7 position of the alkyl chain.

In the spectrum of the picolinyl ester of the deuterated 16:1(7*a*) isomer (Fig. 4), the 16-amu gaps appeared at *m/z* 206, 222 and 238. The position of the triple bond was located between the C-7 and C-8 atoms of the alkyl chain. The 16-amu gaps in the deuterated 18:1 isomer (Fig. 5) were found at *m/z* 234, 250 and 266, which confirmed the structure of 18:1(9*a*). From the spectra of the last three isomers [15:1(6*a*), 16:1(7*a*) and 18:1(9*a*)], it was evident that

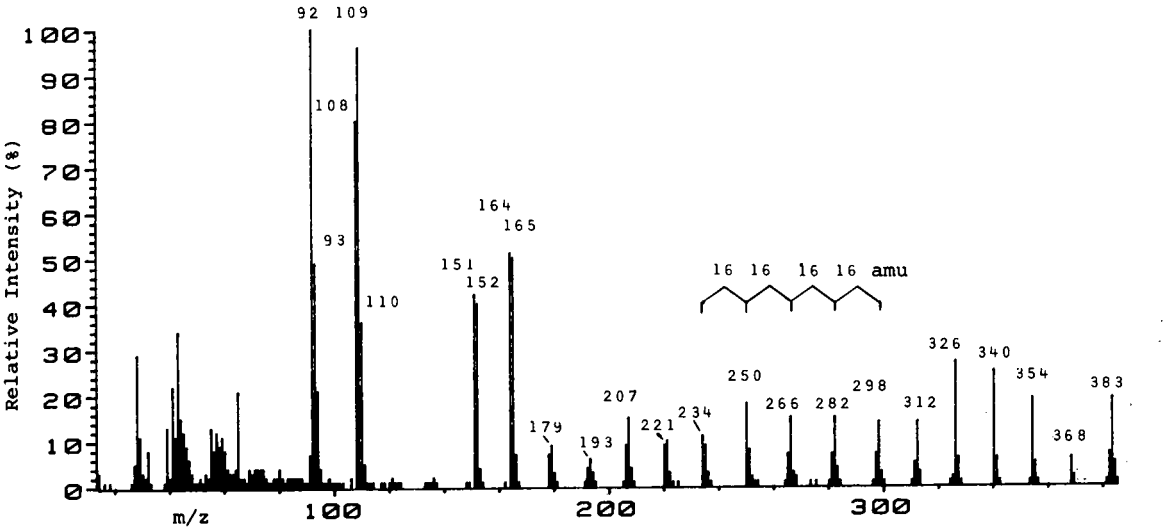

Fig. 6. Mass spectrum of deuteriated 18:2(9*a*,11*a*).

isomers with triple bonds located at the C-6 atom or at positions more distant than C-6 from the ester function produce distinct and diagnostic ion fragmentation patterns, which allow the accurate location of the triple bonds. There was no sign of significant hydrogen–deuterium scrambling during mass spectral analysis of these positional isomers.

In the mass spectrum of the picolinyl ester derivative of the 18:2(9*a*,11*a*) isomer, four distinct and consecutive 16-amu gaps at *m/z* 234, 250, 266, 282 and 298 were observed (Fig. 6). The positions of the triple bonds were therefore located between the C-9 and C-10 and the C-11 and C-12 atoms of the alkyl chain. In the case of the 17:2(10*a*,12*a*) isomer, a similar set of four consecutive 16-amu gaps at *m/z* 248, 264, 280, 296 and 312 were found (Fig. 7). From this fragmentation pattern, the locations of the triple bonds were in full agreement with the structure of 17:2(10*a*,12*a*). No hydrogen–deuterium scrambling was observed during the analysis of these isomers.

We extended this study to a mixed diunsaturated

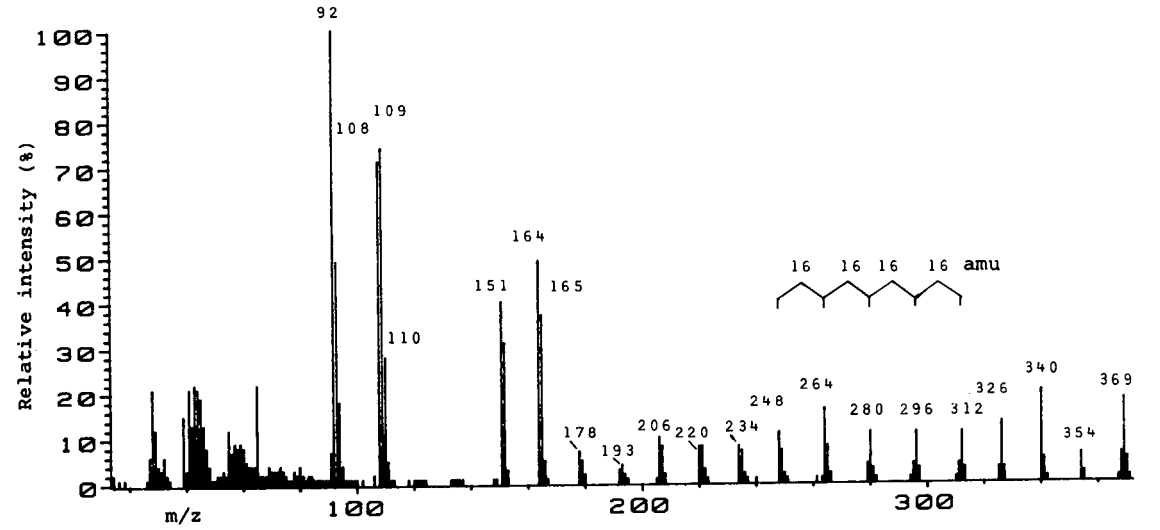

Fig. 7. Mass spectrum of deuteriated 17:2(10*a*,12*a*).

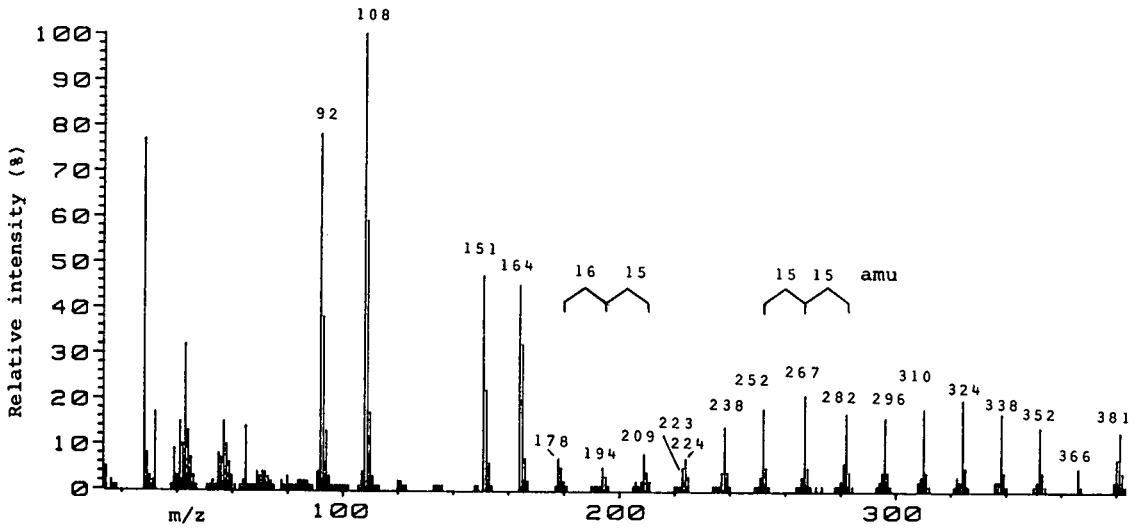

Fig. 8. Mass spectrum of deuteriated 18:2(5*a*,10*c*).

fatty acid, 18:2(5*a*,10*c*). Analysis of the corresponding picolinyl ester of the deuterated substrate gave a set of low intensity peaks at *m/z* 178 (8%), 194 (6%), 209 (9%), 210 (4%), 223 (6%) and 224 (7%) (Fig. 8). This part of the spectrum matched the characteristic pattern observed for the 14:1(5*a*) homologue (Fig. 2). From this result, the position of the triple bond was located at C-5/C-6 of the alkyl chain. In the same spectrum, there were two 15-amu gaps at *m/z* 252, 267 and 282, which confirmed the position of the double bond at C-10/C-11 of the alkyl chain.

This study demonstrates that mass spectral analysis of picolinyl esters of deuterated unsaturated fatty acids gives a predictable fragmentation pattern, which provides a simple and accurate means of locating the positions of triple bonds. Isomers with unsaturated centres in the proximal part in the alkyl chain from the ester function furnish unique mass spectral fragmentation patterns of their own, owing to hydrogen–deuterium scrambling.

ACKNOWLEDGEMENTS

We thank Lipid Research Fund, the Strategic Research Grants Committee, the Research Grants Committee of the University of Hong Kong for financial assistance and the University of Hong Kong for a Research Studentship (CYC).

REFERENCES

1 J. D. Bu'Lock and G. N. Smith, *J. Chem. Soc. C*, 1967, 332–336.
2 R. Kleiman, M. B. Bohannon, F. D. Gunstone and J. A. Barve, *Lipids*, 11 (1976) 599–603.
3 A. J. Valicenti, W. H. Heimermann and R. T. Holman, *J. Org. Chem.*, 44 (1979) 1068–1073..
4 J. Y. Zhang, X. J. Yu, H. Y. Wang, B. N. Liu, Q. T. Yu and Z. H. Huang, *J. Am. Oil Chem. Soc.*, 66 (1989) 256–259.
5 W. W. Christie, E. Y. Brechany and M. S. F. Lie Ken Jie, *J. Chromatogr.*, 46 (1988) 225–229.
6 M. S. F. Lie Ken Jie, Y. K. Cheung, S. H. Chau, W. W. Christie and E. Y. Brechany, *Chem. Phys. Lipids*, (1992) in press.
7 M. S. F. Lie Ken Jie and Y. C. Choi, *J. Am. Oil. Chem. Soc.*, in press.
8 M. Gungor, F. H. Jardine and J. D. Wheatley, *J. Chem. Soc. Dalton Trans.*, (1988) 1653–1656.
9 R. O. Adlof, *J. Am. Oil Chem. Soc.*, 67 (1990) 52–54.
10 A. P. Tulloch, *Progr. Lipid Res.*, 22 (1983) 235–256.
11 F. D. Gunstone and I. A. Ismail, *Chem. Phys. Lipids*, 1 (1967) 209–224.
12 M. S. F. Lie Ken and G. Tsang, *Chem. Phys. Lipids*, 13 (1974) 21–26.
13 H. Rakoff and E. M. Emken, *J. Labelled Comp. Radiopharm.*, 15 (1978) 223–252.
14 W. W. Christie and K. Stefanov, *J. Chromatogr.*, 392 (1987) 259–265.

Journal of Chromatography, 625 (1992) 277–288
Elsevier Science Publishers B.V., Amsterdam

CHROM. 24 546

Field detection of organochlorine pesticides by thermal desorption gas chromatography–mass spectrometry

Albert Robbat, Jr., Chengjie Liu and Tyng-Yun Liu

Trace Analytical Measurement Laboratory, Department of Chemistry, Tufts University, Medford, MA 02155 (USA)

(First received June 11th, 1992; revised manuscript received August 5th, 1992)

ABSTRACT

Thermal desorption gas chromatography–mass spectrometry (TDGC–MS) was evaluated for field detection of organochlorine pesticides in soil/sediment and water. Rapid, 3 min/sample, TDGC–MS selected ion monitoring (SIM) yielded detection limits of 50 ng/g and 40 ng/l pesticide in soil (2 g) and water (500 ml), respectively, with measurement precision <40%. MS total ion current–selected ion extraction (TIC–SIE) measurements yielded somewhat higher detection limits with measurement precision <20%. Examples of selective pesticide detection in the presence of a wide variety of environmental contaminants in soils, pond and sea waters are provided.

INTRODUCTION

Because of their acute and chronic toxicities as well as resistance to environmental degradation, the detection of organochlorine pesticides and metabolites has received much attention [1–11]. The ability to provide rapid, on-site analyses of complex samples collected from hazardous waste sites as well as livestock and agricultural farms has grown in importance over the last five years. High-resolution capillary gas chromatography (GC) with either mass spectrometry (MS) or electron-capture detection (ECD) provide the most often employed analytical techniques. Although MS can provide positive compound identification, extensive sample preparation procedures are required compared to the more selective ECD for highly contaminated samples. On the other hand, the ECD is especially useful when chlorinated pesticide concentrations are below the GC–MS detection limit. The non-descriptive nature of ECD, however, raises concerns about data reliability [12]. Multi-step sample preparation procedures in addtion to the significant difference in MS and ECD hardware costs presumably account for the 7-fold difference in commercial laboratory analytical costs between GC–MS and GC–ECD analyses.

In this paper, we describe an approach based on thermal desorption (TD) GC sample introduction and selected ion monitoring (SIM) MS detection for 14 organochlorine pesticides and metabolites in soil and water. The research presented is, in part, an on-going effort to provide rapid "field-practical" screening technologies for the analysis of complex hazardous waste site and agricultural samples. Toward that end, TDGC–MS has been developed and "field-validated" for polychlorinated biphenyls (PCBs) and polycyclic aromatic hydrocarbons (PAHs) in soil/sediment as well as the US Environmental Protection Agency (EPA) listed volatile organic compounds (VOCs) in soil and water [13–16]. For example, 2 min/sample PCB and PAH screening level measurements, with $\leqslant$ 40% measurement precision, have been shown to compare favorably against EPA standardized procedures [14–16]. In contrast, the more quantitative PCB,

Correspondence to: Professor A. Robbat, Jr., Trace Analytical Measurement Laboratory, Department of Chemistry, Tufts University, Medford, MA 02155, USA.

0021-9673/92/$05.00

PAH and VOC methods required 10–25 min/analysis and yielded run-to-run relative standard deviations (R.S.D.s) within 30%. The more quantitative TDGC–MS methods provide data comparable to current EPA standardized methods. Results delineating linear dynamic range, minimum detectable amount as well as simple, field-practical pesticide soil–solvent and water–solid-phase extraction procedures are provided. Data will be presented documenting SIM selectivity for pesticide detection in the presence of large quantities of background organics. Rapid, field-practical, TDGS–MS measurements should provide increased data output/unit time and thus, better delineation of hazardous waste site conditions.

EXPERIMENTAL

A thermal desorption gas chromatography–mass spectrometer (Bruker, Billerica, MA, USA) was used in this study. The instrument was powered in the field by 24 V of direct current supply by four 6-V batteries (Trojan J250 Deep Cycle, North Wales, PA, USA). For laboratory MS operation, electrical service was provided through conversion of 110 V a.c. to 24 V d.c. by a VF Series power supply (Deltron). The TDGC–MS instrument consisted of a 3.5-m flexible hose which was attached to the sample inlet system of the mass spectrometer on one end, and on the other a stainless-steel mesh sampling head. The sampling probe head and the hose (GC oven) can be heated from ambient temperature to 260 and 240°C, respectively. Fitted within the hose was a 3.5-m DB-5 capillary column (J&W Scientific). Ambient air served as the carrier gas. Fitted between the sample probe assembly and the mass spectrometer inlet was a methyl silicone membrane which excluded oxygen from entering the electron impact (EI) ionization source. Sample was introduced by placing the heated sampling probe head directly onto the analyte, which was previously injected onto an aluminum foil-covered dish, followed by direct thermal desorption into the GC column. The mass spectrometer was auto-tuned to $H_2O(g)$ (18 amu) and Ar (40 amu) in air *and* a mixture of fluorinated hydrocarbons (FC-77; 69, 100, 119, 169, 219, 269, 331, 397 amu).

In this study, SIM and total ion current–selected ion extraction (TIC–SIE) mass spectrometry were evaluated. Data acquisition was provided by either an on-board microprocessor (SIM) or by a portable computer (TIC–SIE). For confirmatory analyses a HP5890 GC with an electron capture detector, (Hewlett Packard, Avondale, PA, USA) was used. The TDGC–MS and GC–ECD operating conditions are shown in Table I. Detailed description of the TDGC–MS hardware has been reported elsewhere [14,15].

The linear dynamic range was evaluated for the pesticides over a wide concentration range using both the SIM and TIC–SIE-MS detection modes. A 10-μl portion of a standard pesticide mixture (100 ng/μl per pesticide for SIM and 200 ng/μl per pesticide for TIC–SIE) was co-injected with 100 ng of an internal standard ($[^2H_{10}]$phenanthrene) onto an aluminum foil-covered dish. After TDGC–MS analysis, the solution was diluted and each dilution analyzed under the same conditions. This process was continued until signals from these concentrations were no longer observable. In the SIM mode, signal response was the peak height of the selected

TABLE I

EXPERIMENTAL CONDITIONS FOR TDGC–MS AND GC–ECD DETECTION OF THE ORGANOCHLORINE PESTICIDES

TDGC–MS conditions	
GC column	DB-5 (5% phenyl, 95% methyl), 3.5 m × 0.32 I.D., 0.25 μm film
Carrier gas	ambient air, 3.5 ml/min (120°C)
Temperature program	(1) Semi-quantitative: 120 to 240°C at 18°C/min (2) Quantitative: 100 to 180°C at 6°C/min
Sample probe temperature	260°C
Mass range	99–390 amu
Mass scan time	1 s
GC–ECD conditions	
GC column	DB-5, 30 m × 0.25 I.D., 0.25 μm film
Carrier gas	Helium, 1 ml/min (150°C)
ECD make-up gas	5% methane in argon, 30 ml/min
Temperature program	150 to 280°C at 15°C/min, 280°C for 5 min
Injection port temperature	170°C
ECD temperature	325°C

TABLE II

SIM AND TIC–SIE FRAGMENT IONS AND RELATIVE ABUNDANCES (%)

No.	Compound	Ion (relative abundance, %)	
		SIM	TIC
1	α-Benzene hexachloride (BHC)	219 (74,9), 181 (100) 221 (38.8), 263 (0.0)	219, 217, 221
2	β-BHC	(same as α-BHC)	
3	γ-BHC	(same as α-BHC)	
4	δ-BHC	(same as α-BHC)	
5	Heptachlor	100 (100), 274 (51.9) 272 (64,7), 261 (0.0)	100, 274, 272
6	Aldrin	263 (100), 261 (64.7) 101 (100), 293 (41.6)	263, 261, 101 293
7	Heptachlor epoxide	353 (100), 355 (80.5) 351 (51.9), 357 (38.8)	353, 355, 351 351
8	Endosulfan 1	195 (100), 241 (86.5) 207 (74.9), 387 (0.0)	195, 241, 207
9	Dieldrin	108 (100), 263 (20.1) 277 (15.0), 207 (0.0)	108, 263, 277
10	4,4′-DDE	246 (100), 318 (80.5) 316 (60.1), 235 (0.0)	246, 318, 248
11	Endosulfan 2	(same as Endosulfan 1)	
12	4,4′-DDD	235 (100), 237 (64.7) 165 (44.8), 178 (11.2)	235, 237, 165
13	Endosulfan sulfate	272 (100), 274 (92.8) 277 (44.8), 195 (0.0)	272, 274, 277
14	4,4′-DDT	246 (20.1), 235 (100) 237 (69.6), 178 (0.0)	235, 237, 165
15	[$^2H_{10}$]Phenanthrene (internal standard)	188 (100), 187 (21.6) 189 (16.2), 263 (0.0)	188, 187, 189
16	Endrin	317 (55.9), 315 (38.8) 345 (25.0), 343 (18.7)	317, 315, 345
17	Endrin aldehyde	345 (44.8), 347 (25.0) 343 (28.9), 349 (9.7)	345, 347, 343
18	Endrin ketone	317 (51.9), 319 (33.5) 315 (35.9), 321 (11.2)	317, 319, 315

ion current (in logarithmic scale). In the TIC–SIE mode, the selected ion current for each target analyte was manually extracted and integrated from the TIC chromatogram. The identification and quantitation ions and their relative abundances selected for each pesticide are listed in Table II. Response factors (*RF*) were calculated over the linear concentration range; $RF = (A_{std}C_{is})/A_{is}C_{std})$, where A_{std} or A_{is} and C_{std} or C_{is} are TIC–SIE and SIM signals and concentrations for the pesticides or [$^2H_{10}$]phenanthrene, respectively.

Soil samples were prepared as follows: 2 g of soil were placed in a 4 ml sample vial with PTFE-lined screw cap, 2 ml hexane were added and the vial was shaken for 2 min. The extract was then filtered through a disposable 0.45-μm pore size PTFE microfilter (Supelco, Bellefonte, PA, USA) and was analyzed by TDGC–MS without any additional cleanup steps. Two soil types were studied: a poorly to moderately sorted fine to medium sand and a very poorly sorted clay to coarse sand.

For water samples: a 500-ml water sample was drawn by vacuum through a disposable C_{18} Sep-Pak Plus solid-phase extraction (SPE) cartridge (Waters, Milford, MA, USA) at a flow-rate of *ca.* 100 ml/min. The cartridge was dried by drawing

purified air through the cartridge under vacuum for 8–10 min. HPLC-grade hexane was used to elute the pesticides with the analyte collected within the first 1 ml. The extract was analyzed as described above. Three different water samples were used: deionized water, pond water (Mystic Lake, Medford, MA, USA) and sea water (Revere, MA, USA). Pond water and sea water were pre-filtrated by a 0.45-μm nylon 66 membrane before SPE. Field blanks were extracted using the same procedure.

SIM and TIC–SIE conditions were used as described above. C_{18} cartridges were used as supplied by the manufacturer.

Evaluation of SIM detection as a selective detector was accomplished by analyzing known quantities of a standard pesticide solution in the presence of either a PCB standard solution or a mixture of Acid–Base–Neutral (A/B/N) standards. The PCB standard contained 1 isomer from 9 of the 10 chlorination levels (Concentration Calibration Standard

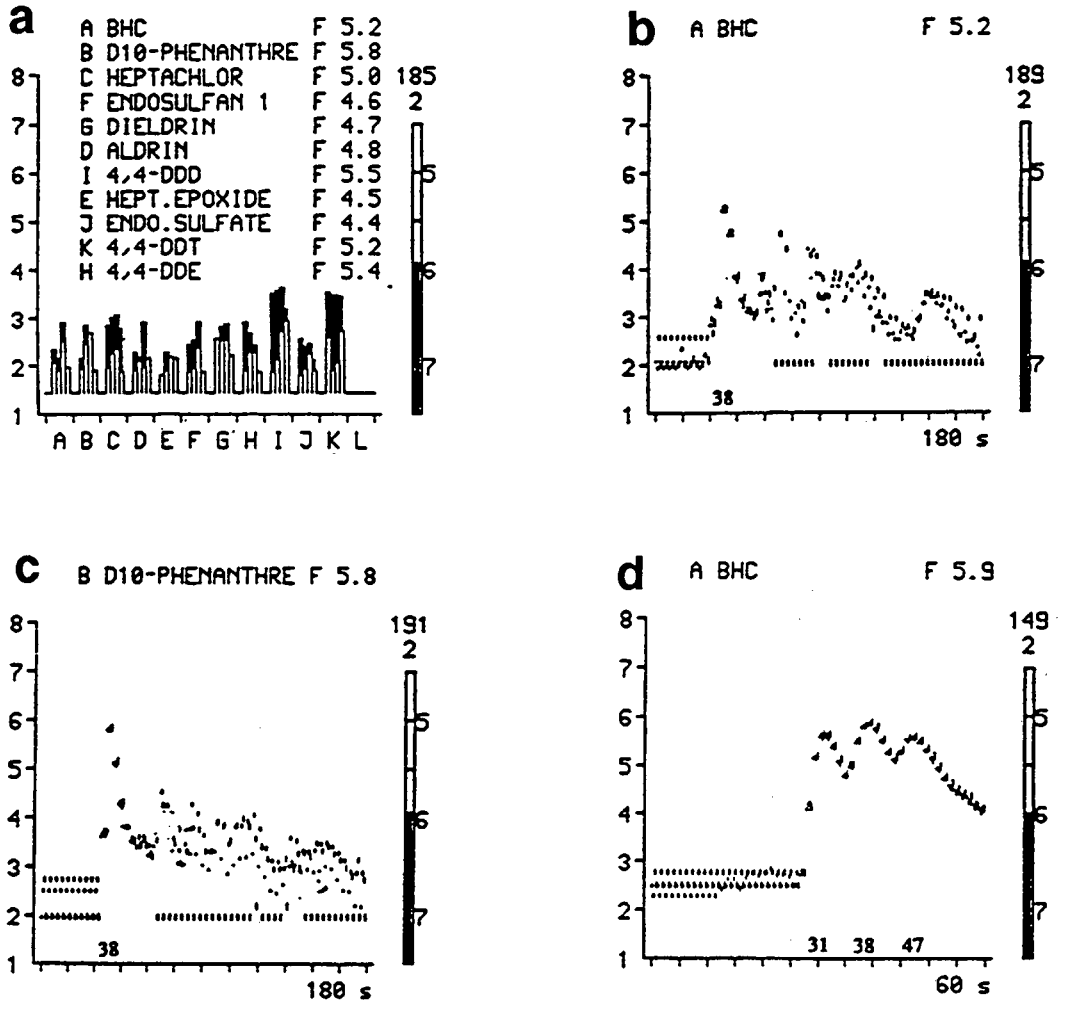

Fig. 1. (a) Typical pesticide (200 ng/compound) and [$^2H_{10}$]phenanthrene (100 ng) SIM signal readout; A = BHC; B = [$^2H_{10}$]phenanthrene; C = heptachlor; D = aldrin; E = heptachlor epoxide; F = endosulfan I; G = dieldrin; H = 4,4'-DDE; I = 4,4'-DDD; J = endosulfan sulfate; K = 4,4'-DDT. (b–d) Selective ion chromatograms (signal *vs.* time curves) for (b) γ-BHC (retention time: 38 s), (c) [$^2H_{10}$]phenanthrene (retention time 38 s) and (d) BHC isomers (retention times: α-BHC: 31 s; β- and γ-BHC: 38 s; δ-BHC: 47 s). F values represent log values of SIM ion current.

Mixture, Ultra Scientific, North Kingstown, RI, USA). The A/B/N mixture consisted of 63 semivolatile organics and was prepared by mixing 6 commercial standards (Supelpreme-HC Benzidines Mix, Supelpreme-HC Phenols Mix, Supelpreme-HC Polynuclear Aromatic Hydrocarbons Mix, Supelpreme-HC Base-Neutrals Mix 1, Supelpreme-HC Base-Neutrals Mix 2 and Supelpreme-HC Internal standards Mix, Supelco).

Organochlorine pesticides were purchased from Chem Service (West Chester, PA, USA) and the internal standard, [$^2H_{10}$]phenanthrene, from Cambridge Isotope Laboratories (Woburn, MA, USA). A standard pesticide solution was also purchased from Accustandard (New Haven, CT, USA). HPLC-grade methanol and hexane were purchased from Aldrich (Milwaukee, WI, USA) and used as received.

RESULTS AND DISCUSSION

Rapid on-site TDGC–MS analysis has been developed for organochlorine pesticides in soil and water. Results are based on "field-practical" sample preparation procedures, direct TD of analyte from an organic extract *and* SIM (semi-quantitative) or TIC–SIE (quantitative) detection. Figs. 1a and 2a illustrate SIM signal response and the corresponding TIC chromatogram under the same temperature-programmed GC conditions (see Table I, program 1). Table II lists peak numbers, associated compound identities and their relative intensities. For SIM, cells A–K depict signal intensities for the four ions monitored for 10 of the pesticides and the internal standard, [$^2H_{10}$]phenanthrene. The white bars represent the background levels of the four ions selected for detection while the black bars indicate the amount of signal detected. Note that the signals are reported as logarithmic values (left *y*-axis). Compound identity was reported when the selected ions normalized to 100% were above background signal at the peak maxima and on either side of one-half peak maxima on three consecutive scans through the chromatographic peak. In some cases, impossible ions were selected, *i.e.*, relative abundance set at 0%, which served to filter out possible matrix (background) interferant ions resulting in SIM selective detection analogous to an electron-capture detector. Fig. 2a reveals that at the temperature program employed many of the pesticides and the internal standard co-eluted. Nonetheless, SIM detection employing the MS algorithm described above provided sufficient differentiation to yield compound identity as well as semi-quantitative analyses in less than 3 min. For example, by monitoring specific ions for γ-BHC (No. 3) and [$^2H_{10}$]phenanthrene (No. 15), these two co-eluted compounds were easily differentiated. Typical signal *versus* time curves for these compounds are shown in Fig. 1b and c. Note that the four ions monitored for each compound reach the same signal height at 38 s while their relative contribution to total peak height (see Fig. 2a) are monitored separately. Retention matching, *i.e.*, $t_{R(unknown)} \leqslant t_{R(standard)} \pm 5$ s (where t_R = retention time), provides a second means for compound confirmation.

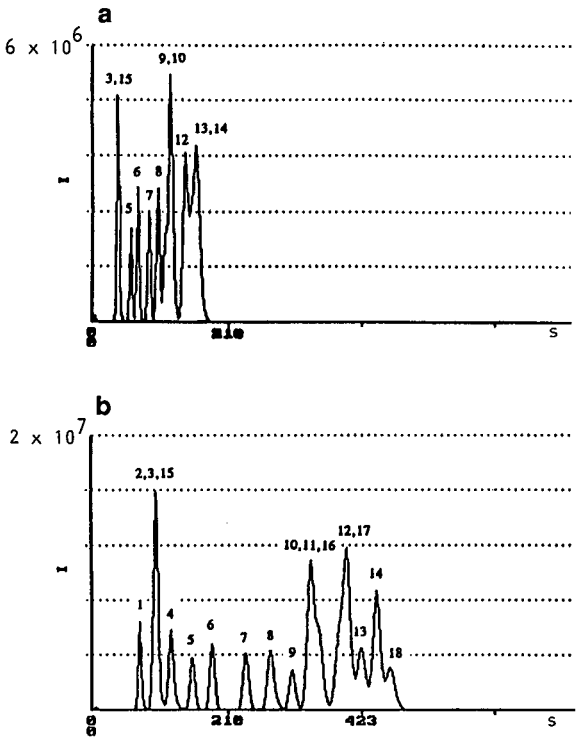

Fig. 2. Total ion current chromatograms for the same standards as shown in Fig. 1 at two different temperature programs: (a) 120 to 240°C at 18°C/min and (b) 100 to 180°C at 6°C/min. See Table II for compound identities. I = total ion current signal.

An additional advantage of SIM detection is that it provides simple visual observation of the chro-

matogram. For example, Fig. 1d shows the signal *versus* time curves for the four BHC isomers. Isomers β-BHC and γ-BHC co-elute at 38 s while α- and δ-BHC elute at 31 s and 47 s, respectively. Because the SIM reports current signal based on the peak height, visual estimation of the log response against the left y-axis can be made providing qualitative isomer concentration measurements. This approach can also be employed for the determination of the endosulfans 1 and 2. For screening level purposes, one can employ rapid GC temperature programs with SIM detection to obtain semi-quantitative or qualitative information as to pesticide presence in complex environmental samples.

For improved compound separation, a slower temperature program was employed (see Table I, program 2). Fig. 2b illustrates the separation of 17 pesticides, metabolites and internal standard. Peaks 16, 17 and 18 are endrin, endrin aldehyde and endrin ketone (endrin breakdown product), respectively. The purpose of this program was to obtain sufficient GC separation for compound identification by MS as well as to provide more quantitative analysis by TIC–SIE.

To obtain maximum TD of pesticide into the GC column and thus, optimum detection limit, a tempeature of 260°C was required. The possible breakdown of 4,4'-DDT and endrin was evaluated. Negligible breakdown was observed for DDT while endrin thermal degradation produced 30% endrin aldehyde and 64% endrin ketone. Therefore, if endrin and its metabolites are present in the sample, care must be taken when quantitative concentration assignments are made.

TABLE III

SIM AND TIC–SIE DYNAMIC RANGE AND MINIMUM DETECTABLE AMOUNT (MDA; n = 3 AT EACH CONCENTRATION)

Concentration range studied: SIM: 1000, 640; 400, 200, 10, 2, 1, 0.5, 0.2 and 0.1 ng/pesticide; TIC–SIE: 2000, 1500, 1000, 500, 50, 20 and 5 ng/pesticide except for compounds 2 and 3 which coeluted under the GC temperature program employed, 3000 to 10 ng total pesticide injected.

Compound	MDA (ng)	Slope	Intercept		Average signal R.S.D. (%)
SIM					
3	0.1	1918 ± 67	+20936 ± 25663	0.995	22
5	1	1377 ± 46	−27596 ± 20631	0.997	14
6	0.2	789 ± 27	+9867 ± 11018	0.995	12
7	0.5	796 ± 30	+2450 ± 12708	0.995	16
8	0.5	647 ± 14	+4883 ± 5750	0.998	12
9	2	802 ± 50	+15071 ± 23879	0.991	10
10	0.1	2904 ± 111	+22811 ± 27693	0.994	13
12	0.2	6492 ± 119	+17298 ± 48003	0.999	15
13	2	643 ± 18	+6145 ± 8590	0.998	11
14	0.5	3410 ± 129	+70677 ± 54881	0.995	14
TIC–SIE					
1	5	10529 ± 231	+272620 ± 224045	0.999	4
2 and 3	10	10052 ± 433	+730030 ± 616600	0.995	8
4	5	12384 ± 299	+367182 ± 289853	0.999	6
5	5	28059 ± 470	−1126654 ± 456386	0.999	9
6	5	17586 ± 247	+56029 ± 240179	0.999	5
7	20	8481 ± 195	+12362 ± 202103	0.999	6
8	20	8590 ± 135	+58417 ± 140079	0.999	4
9	5	11858 ± 441	−567177 ± 428517	0.996	14
10	5	66659 ± 1009	+839694 ± 980148	0.999	2
11	20	10221 ± 152	−133768 ± 157265	0.999	7
12	5	125899 ± 1527	−3364743 ± 1482553	0.9996	4
13	20	7560 ± 185	−48833 ± 192339	0.999	7
14	5	135139 ± 2810	+5557163 ± 2728885	0.999	6

TABLE IV

SIM AND TIC–SIE AVERAGE RESPONSE FACTOR (*RF*) AND THE PERCENT RELATIVE STANDARD DEVIATION

Average *RF* over the concentration range: SIM: 1000, 640, 400, 200, 100 and 10 ng/pesticide; TIC: 2000, 1500, 1000, 500, 200 and 50 ng/pesticide and for compounds β and γ-BHC, 3000, 2000, 1000, 400, 100, and 40 ng total amount injected.

Compound	SIM		TIC–SIE	
	Average RF	R.S.D. (%)	Average RF	R.S.D. (%)
α-BHC			0.070	17
β-BHC			0.076	17
γ-BHC (lindane)	0.093	18	(coetlutes with β-BHC)	
δ-BHC			0.085	18
Heptachlor	0.047	30	0.14	17
Aldrin	0.037	12	0.11	11
Heptachlor epoxide	0.031	15	0.050	13
Endosulfan 1	0.028	15	0.053	10
Dieldrin	0.038	14	0.060	9
4,4'-DDE	0.14	20	0.43	13
Endosulfan 2			0.061	8
4,4'-DDD	0.26	20	0.67	10
Endosulfan sulfate	0.028	13	0.046	13
4,4'-DDT	0.17	22	0.67	15

Differences in SIM and TIC–SIE measurement precision and detection limit were evaluated by determining their linear dynamic ranges and *RF* values. Temperature programs 1 and 2 were used for the SIM and TIC–SIE measurements, respectively. Plots of signal *versus* concentration yielded correlation coefficient, r, values closer to 1 for TIC–SIE indicating a higher degree of linearity than for SIM detection (see Table III). Moreover, the average signal R.S.D. calculated over the linear plot was typically 2–3 times lower for TIC–SIE than for SIM. Greater measurement precision was further evidenced for TIC–SIE by the lower average response factor (average *RF*) % R.S.D.s shown in Table IV.

TABLE V

COMPARISON OF INJECTED AMOUNT (10 ng/PESTICIDE) AND DETECTED PESTICIDE AMOUNT BY SIM IN THE PRESENCE OF OTHER ORGANIC COMPOUNDS (n = 3)

Compound	PCBs (10000 ng total)		A/B/N (1000 ng/compound)	
	Detected (ng)	Difference (%)	Detected (ng)	Difference (%)
3	10.0	0	8.1	−19
5	13.1	+31	18.8	+88
6	8.8	−11	10.0	0
7	8.2	−18	10.0	0
8	8.0	−20	18.5	+85
9	14.8	+48	16.9	+69
10	8.5	−15	7.9	−21
12	8.7	−13	10.0	0
13	18.5	+85	10.6	+6
14	10.7	+7	10.8	+8

Evident was the greater measurement precision obtained by TIC–SIE than from SIM. This is explained by the fact that the SIM readout is based on the logarithm of the signal measured, rounded to the nearest decimal point, as compared to TIC which provides actual current signals. For SIM, the error in the current output is highly dependent on the log value mantissa roundoff. On the other hand, the detection limit of SIM was *ca.* 30 times more sensitive.

To determine SIM selectivity, pesticide detection in the presence of significant amounts of other organic pollutants including PCBs as well as a wide variety of A/B/N organics was studied. The A/B/N standard solution contained 63 compounds comprising benzidines, phenols, PAHs, chlorinated ethers, nitrosoamines, halogenated and nitrated benzenes, phthalates and deuterated PAHs. Two experiments were conducted: standard solutions containing 10 pesticides, 10 ng/pesticide, were analyzed in the presence of (1) 10 000 ng PCBs or (2) 63 000 ng A/B/N, 1000 ng/compound. Table V illustrates the comparison of injected (thermally desorbed) *versus* detected amounts for each pesticide (n = 3 for each experiment). The percent difference for most pesticides was less than 30%. Out of the 20 measurements, 4 pesticides were over-estimated presumably due to the rise in background current as a result of matrix interference ions. Recall, that no sample cleanup was performed, that is, TDGC–SIM measurements were made in the presence of a wide range and high concentration of EPA monitored organics. It is unlikely that this level of highly contaminated sample will be present at hazardous waste or agricultural sites. Nevertheless, judicious selection of solvent-type (*i.e.*, solvent strength) should preclude many of the A/B/N organics from being extracted from soil or aqueous media. In contrast, typical EPA methods require multi-column organic fraction "cutting" for highly contaminated samples before analysis by either MS or non-descriptive, selective detectors. For example, GC–ECD analysis without pre-fractionation is unlikely to provide unabiguous pesticide identification in the presence of a wide range of chlorinated organics [12]. Therefore, the purpose of this experiment was to simulate extreme matrix interference conditions for a sample collected from a hazardous waste site.

Toward this end, a study was conducted to determine optimum solvent composition and extraction times for the puposes of providing a field-practical pesticide soil–solvent extraction. Two soil types were analyzed: soil 1 consisted of an oil stained, poorly to moderately sorted fine to medium sand and soil 2, a very poorly sorted clay to coarse sand. A variety of solvents from high to low polarity as well as some mixed solvents over a range of extraction times from 0.5 min to 20 min were studied. The bar graph shown in Fig. 3 depicts optimum pesticide recovery for the dried soils and the same soils with 10–30% moisture. For example, 4 μg/g/pesticide added to 2 g dry soil and extracted with 2 ml hexane for 2 min yielded pesticide recoveries > 90% with the exception of endosulfan sulfate whose recovery was about 65%. Decreased pesticide recovery was obtained as soil moisture content increased. Extraction with hexane–methanol (4:1, v/v) resulted in comparable recoveries as the dried soil extracted with hexane.

Five oil-stained soil 1 (2 g) samples were prepared containing 4000 to 50 ng/g/pesticide. The samples were extracted as described above and analyzed by TDGC–SIM-MS and TCGC–TIC–SIE-MS *and* GC–ECD. Several observations are apparent from Table VI. First TIC–SIE and ECD provided comparable measurement precision while SIM precision was higher but within the 40% R.S.D. obtained for

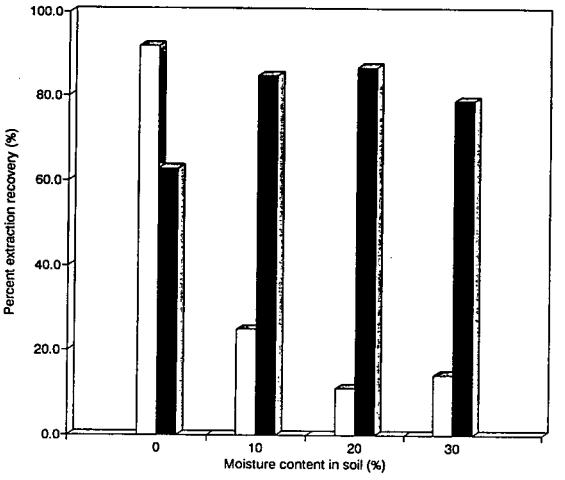

Fig. 3. Effect of soil moisture content on the average percent recovery of 10 pesticides extracted from soil 1: solvent compositions, hexane (2 ml) (open bars) and hexane–methanol (2 ml/0.5 ml) (solid bars).

TABLE VI

COMPARISON OF SIM, TIC–SIE AND GC–ECD RESULTS FOR KNOWN PESTICIDE CONCENTRATIONS IN 2 g OF SOIL 1

ND = pesticide not detected. For this experiment, no recovery data were used in the calculation of amount detected. Note that 65% extraction efficiency was found for compound 13 (endosulfan sulfate).

Compound	Detected amount, ppb (R.S.D. %[a])				
	SIM	TIC	GC–ECD	Average	R.S.D. (%)
4000 ppb/pesticide					
3	4283 (11)	4049 (3)	3739 (3)	4024	6
5	4788 (35)	4047 (7)	3715 (4)	4183	11
6	4425 (34)	4407 (5)	3617 (4)	4150	9
7	3939 (19)	4174 (4)	3735 (4)	3949	5
8	4881 (27)	4830 (4)	3808 (6)	4506	11
9	3667 (30)	4681 (5)	3583 (2)	3977	13
10	4795 (19)	4142 (6)	4042 (1)	4326	8
12	4395 (20)	4173 (6)	3803 (5)	4124	6
13	2814 (27)	2397 (7)	6475 (1)[b]	–	
14	4881 (20)	4506 (4)		–	
1000 ppb/pesticide					
3	801 (19)	941 (1)	948 (1)	897	8
5	906 (42)	904 (4)	922 (2)	911	1
6	1081 (30)	992 (4)	920 (6)	998	7
7	989 (19)	964 (3)	940 (5)	964	2
8	1098 (11)	1088 (0)	934 (7)	1040	7
9	1230 (23)	1067 (4)	987 (6)	1095	9
10	1252 (35)	998 (3)	953 (7)	1068	11
12	1194 (23)	1001 (0)	1132 (7)	1109	7
13	656 (30)	678 (3)	1606 (9)[b]	–	
14	1054 (23)	1028 (0)		–	
500 ppb/pesticide					
3	435 (20)	520 (6)	472 (16)	476	7
5	335 (10)	551 (5)	485 (14)	457	20
6	481 (0)	555 (3)	476 (11)	504	7
7	453 (10)	417 (2)	476 (13)	449	5
8	571 (10)	710 (7)	461 (12)	581	18
9	516 (0)	630 (10)	477 (13)	541	12
10	471 (0)	515 (2)	484 (13)	490	4
12	544 (11)	527 (8)	492 (14)	521	4
13	292 (0)	330 (7)	770 (25)[b]	–	
14	557 (0)	596 (5)		–	
100 ppb/pesticide					
3	92 (10)	34 (49)	98 (10)	75	39
5	98 (11)	51 (22)	100 (12)	83	27
6	89 (10)	ND	93 (13)	–	
7	99 (19)	ND	99 (15)	–	
8	96 (11)[c]	ND	87 (17)	–	
9	100 (23)[c]	ND	100 (23)	–	
10	96 (19)	96 (16)	102 (21)	98	3
12	109 (11)	121 (18)	97 (27)	109	9
13	70 (23)	ND	152 (29)[b]	–	
14	168 (23)[c]	111 (6)		–	

(Continued on p. 286)

TABLE VI *(continued)*

Compound	Detected amount, ppb (R.S.D. %[a])				
	SIM	TIC	GC–ECD	Average	R.S.D. (%)
50 ppb/pesticide					
3	47 (23)	10 (62)	49 (3)	35	51
5	45 (0)	ND	58 (3)	–	
6	46 (23)	ND	50 (1)	–	
7	39 (19)	ND	52 (1)	–	
8	49 (20)[c]	ND	48 (3)	–	
9	42 (0)[c]	ND	54 (1)	–	
10	41 (11)	37 (31)	54 (4)	44	16
12	48 (23)	45 (40)	50 (9)	48	4
13	32 (11)	ND	89 (8)[b]	–	
14	72 (19)[c]	50 (20)		–	

[a] $n = 3$ for SIM, TIC, GC–ECD.
[b] Pesticides 13 and 14 co-eluted by GC–ECD, therefore, the average and R.S.D. were not calculated.
[c] Detected amount calculated using one-point RF calibration

the standard solution linear dynamic range of *RF* studies. In general, TIC–SIE produced better run-to-run measurement precision, *ca.* 5% R.S.D., than did SIM, *ca.* 20% R.S.D. Second, as anticipated SIM provided increased sensntivity over TIC–SIE. However, compounds 8, 9 and 14 were over-estimated at the lower pesticide concentrations using the linear dynamic range *RF* value. These concentrations are near the SIM detection limit. Over-estimation occurs presumably due to log current roundoff as a function of decreased analyte signal-to-noise ratio and the *RF* falling outside the linear dynamic range at these concentrations. For a more quantitative SIM measurement, a "one-point" *RF* calibration can be made. For example, by calculating the *RF* value of endosulfan 1 at an injection amount of 2.5 ng, the SIM measurement for the 100 ppb and 50 ppb samples yielded 96 ± 11 ppb and 49 ± 10 ppb, respectively. Third, the average pesticide concentration R.S.D. calculated from the SIM, TIC–SIE and ECD detected amounts were well-within the acceptable range for intermethod comparisons [14,15].

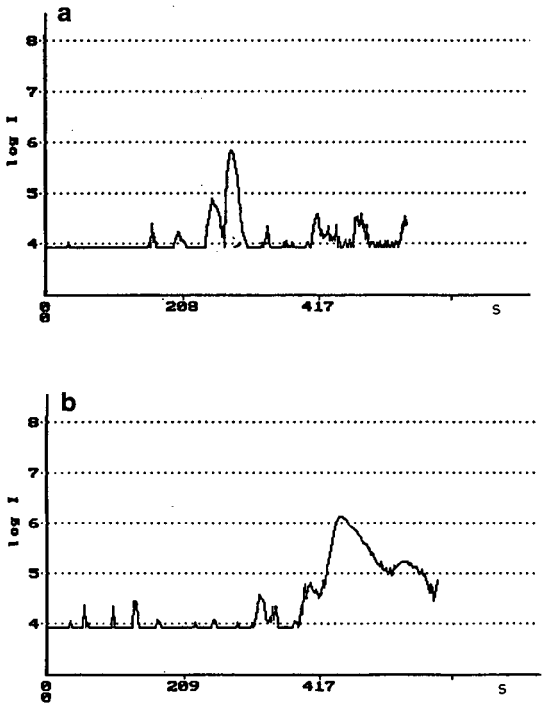

Fig. 4. Total ion current chromatograms of hexane—C_{18} extracted pond (a) and sea (b) waters. Temperature program: 100 to 180°C at 6°C/min. I = total ion current.

SPE using a C_{18} bonded phase silica cartridge was employed as a field-practical means for extracting pesticides from aqueous samples. To test the method, known amounts of pesticide were added to 500 ml deionized water and passed through the cartridge at a rate of 90–130 ml/min. The pesticides were eluted off the cartridge with hexane and collected in the first 1 ml. The extraction procedure was repeated three times and each extract analyzed three times. Table VII lists the SPE recoveries for

TABLE VII

PESTICIDE PERCENT RECOVERY (%) OF DEIONIZED WATER–C_{18} SOLID-PHASE EXTRACTION WITH SIM DETECTION

For each concentration 3 extractions were prepared and each extract analyzed 3 times; ND = not detected.

Compound	Pesticide concentration (ng/l)						
	40[a]	100[a]	2000	6000	10000	20000	Average (R.S.D., %)
3	81 ± 5	95 ± 6	68 ± 19	55 ± 9	55 ± 9	54 ± 5	68 (23)
5	69 ± 8	86 ± 18	69 ± 9	79 ± 18	71 ± 1	83 ± 12	76 (9)
6	67 ± 17	89 ± 14	85 ± 13	72 ± 12	67 ± 5	73 ± 6	76 (11)
7	61 ± 24	77 ± 17	92 ± 14	91 ± 18	82 ± 19	100 ± 13	84 (15)
8	ND	93 ± 15	93 ± 5	96 ± 12	85 ± 16	96 ± 14	93 (5)
9	ND	94 ± 16	98 ± 25	96 ± 8	95 ± 4	115 ± 13	100 (9)
10	93 ± 25	77 ± 6	84 ± 13	91 ± 3	65 ± 8	62 ± 7	79 (15)
12	106 ± 17	86 ± 6	96 ± 16	92 ± 12	71 ± 5	87 ± 7	90 (12)
13	ND	77 ± 11	75 ± 9	81 ± 8	70 ± 5	97 ± 9	80 (13)
14	126 ± 18	108 ± 25	78 ± 10	70 ± 7	73 ± 13	67 ± 9	87 (25)

[a] Calculated using one-point *RF* calibration.

the pesticides between the concentration range of 20 000 ng/l and 100 ng/l for each pesticide. At each concentration, the SIM measurement precision was $< 25\%$ ($n = 9$) and the average recovery R.S.D. over the concentration range was $< 30\%$ ($n = 54$). The average recovery R.S.Ds over the concentration range studied suggest that the pesticide recoveries were linear. This was evident by the plots of the average SIM signal *versus* concentration which yielded $r > 0.996$.

Pond and sea water samples were collected, filtered and analyzed as field blanks. Shown in Fig. 4 are the TIC chromatograms for both the pond and sea waters: apparent are the presence of organics eluting during the retention times of interest. Pesticides were added to the water at 2000 ng/l per compound (500 ml). The pesticide average recovery value shown in Table VII was used in the calculation. Table VIII illustrates the SIM detected amount and percent differences after SPE. The percent differ-

TABLE VIII

COMPARISON OF FORTIFIED AND SIM DETECTED AMOUNTS OF PESTICIDES FROM POND AND SEA WATER SAMPLES: FORTIFIED CONCENTRATION 2000 ng/l PER PESTICIDE

The water samples were extracted 3 times and each extract analyzed 3 times.

Compound	Pond water		Sea water	
	Detected (ng/l)	Difference (%)	Detected (ng/l)	Difference (%)
3	2324 ± 147	+16	2412 ± 470	+21
5	2053 ± 237	+3	1806 ± 184	−10
6	2000 ± 369	0	2369 ± 211	+18
7	2428 ± 309	+21	2310 ± 357	+16
8	2946 ± 258	+47	2129 ± 237	+6
9	2160 ± 220	+8	2240 ± 220	+12
10	2278 ± 127	+14	1924 ± 51	−4
12	2311 ± 89	+16	2200 ± 289	+10
13	2150 ± 350	+8	1900 ± 400	−5
14	1701 ± 0	−15	1701 ± 245	−15

ence was within 30% for all of the pesticides except endosulfan 1 in pond water. Experiments at the 40 ng/l per pesticide levels indicated that all of the pesticides were detected with the same method precision as above with the exception of dieldrin, endosulfan 1, and endosulfan sulfate whose concentrations were at the SIM detection limit.

The results of a 6-commercial laboratory GC–MS detection study of chlorinated pesticides were reported [7]. Uniform calibration solutions and EPA standardized analytical procedures were followed. Five soil sediment samples were prepared to contain known concentrations of pesticides with the exception of 1 sample. Two different sample clean-up procedures for solids were employed resulting in duplicates of 4 different extracts, *viz.*, mechanical shaking and/or ultrasonication followed by Florisil and/or gel permeation chromatography fractionation. The solid samples, fortified to contain 0.2–20 ppm/pesticide (in 10 to 50 g), had mean R.S.Ds typically between 10 and 70% with several > 100%. These findings were consistent with the reported results for multilaboratory studies of PCB and PAH soil sediment samples [7,14–17]. Although this paper does not provide data with respect to interlaboratory comparisons, the SIM, TIC–SIE and ECD produced average concentration measurement precision well-within the multilaboratory R.S.Ds reported above and over a much wider pesticide/soil concentration range. In addition to the solids results described above, the authors conducted a multilaboratory GC–MS comparison study for the detection of pesticides fortified, 3–30 μg/l, in water. Water samples were prepared for analysis by performing several liquid–liquid extraction steps. The 6-commercial laboratory measured mean concentration R.S.D.s for 2 different water samples were found to be between 30 and 60%. Although the results reported in Table VII in this paper are not based on multiple laboratory or method comparisons, the SIM average measured concentration R.S.D.s over the concentration range studied were well under the 6-laboratory R.S.D. range and suggests that multimethod precision should be no worse than the soil results shown in Table VI.

Semi-quantitative TDGC–SIM-MS as well as more quantitative TIC–SIE measurements have been developed for field detection of organochlorine pesticides in soil and water. In general, SIM produced < 40% measurement precision with analysis times of less than 3 min/sample while TIC–SIE produces data comparable to standardized EPA methods (*i.e.*, < 30% R.S.D.). Although SIM measurement precision was somewhat less than TIC–SIE, measurement accuracies were comparable. The ability to obtain rapid, on-site chemical data should support activities in hazardous waste site assessment *and* routine regulatory programs in environmental and agricultural monitoring.

ACKNOWLEDGEMENTS

We appreciate the financial assistance for this work which was in part, funded by the US EPA and Army (USATHAMA) through New Jersey Institute of Technology, Northeast Hazardous Substance Research Center and through Tufts University, Center for Environmental Management.

REFERENCES

1 W. A. Telliard, *Spectra*, 10 (1986) 4–9.
2 J. P. Hsu, H. G. Wheeler, Jr., D. E. Camann, H. J. Schattenberg, III, R. G. Lewis and A. E. Bond, *J. Chromatogr. Sci.*, 26 (1988) 181–189.
3 H.-J. Stan, *J. Chromatogr.*, 467 (1989) 85–98.
4 D. Rood and M. Feeney, *Environmental Lab.*, October (1989) 10–13.
5 G. S. Durell and T. C. Sauer, *Anal. Chem.*, 62 (1990) 1867–1871.
6 A. L. Alford-Stevens, T. A. Bellar, J. W. Eichelberger and W. L. Budde, *Anal. Chem.*, 58 (1986) 2022–2029.
7 A. L. Alford-Stevens, J. W. Eichelberger and W. L. Budde, *Environ. Sci. Technol.*, 22 (1988) 304–312.
8 D. J. Munch, R. L. Graves, R. A. Maxey and T. M. Engel, *Environ. Sci. Technol.*, 24 (1990) 1446–1451.
9 M. P. Seymour, T. M. Jefferies, A. J. Floyd and L. J. Natarianni, *Analyst (London)*, 112 (1987) 427–431.
10 L. Torreti, A. Simonella, A. Falgiani, C. Filipponi and F. Gramenzi, *J. High Resolut. Chromatogr. Chromatogr. Commun.*, 10 (1987) 510–515.
11 *Method 680; Determination of Pesticides and PCBs in Water and Soil/Sediment by Gas Chromatography/Mass Spectrometry*, US Environmental Protection Agency, Cincinnati, OH, July 1985.
12 A. L. Alford-Stevens, *Environ. Sci. Technol.*, 20 (1986) 1194–1199.
13 A. Robbat, Jr. and G. Xyrafas, Proceedings of the *1st International Symposium on Field Screening Methods for Hazardous Waste Site Investigations, Las Vegas, NV, October 11–13, 1988*, U.S. EPA, Environmental Monitoring Systems Laboratory, Las Vegas, NV.
14 A. Robbat, Jr., T. Y. Liu and B. M. Abraham, *Anal. Chem.*, 64 (1992) 358–364.
15 A. Robbat, Jr., T. Y. Liu and B. M. Abraham, *Anal. Chem.*, 64 (1982) 1477–1483.
16 Superfund Innovative Technology Evaluation Program, *Technology Evaluation Report, EPA/600/x-91/079*, U.S. EPA, Environmental Monitoring Systems Laboratory, Las Vegas, NV, June 1991.
17 A. L. Alford-Stevens, W. L. Budde and T. A. Bellar, *Anal. Chem.*, 57 (1985) 2452–2457.

Journal of Chromatography, 625 (1992) 289–298
Elsevier Science Publishers B.V., Amsterdam

CHROM. 24 491

Stereoselective determination of cucurbitine in *Cucurbita* spp. seeds by gas chromatography and gas chromatography–mass spectrometry

E. Schenkel, P. Duez and M. Hanocq

Unité de Chimie Bioanalytique, de Toxicologie et de Chimie Physique Appliquée, Université Libre de Bruxelles, C. P. 205/1, Boulevard du Triomphe, 1050 Brussels (Belgium)

(First received March 20th, 1992; revised manuscript received July 2nd, 1992)

ABSTRACT

The use of Chirasil-L-Val, a chiral stationary phase, was investigated for the resolution of D,L-cucurbitine as esters of N-trifluoroacetyl derivatives; the influence of the esterifying alcohol on resolution and retention times was studied in comparison with those of different proteic amino acids. The separation mechanism was studied by the thermodynamic analysis of retention data. With flame ionization detection, linear calibration was found between 2 and 40 ng of each isomer detected and the detection limit was *ca.* 1 ng; the internal standard was methyl pentadecanoate. Comparison was made with high-performance thin-layer chromatographic determination. Gas chromatography–mass spectrometry allowed the determination of the structure of synthesized derivatives and positive identification of L-cucurbitine in aqueous extracts of *Cucurbita* seeds.

INTRODUCTION

Cucurbitine [(−)-3-aminopyrrolidine-3-carboxylic acid] is responsible for the anthelmintic, notably taenicidal and schistosomicidal, properties of *Cucurbita* spp. seeds [1,2]; cytotoxicity has recently been demonstrated on *Amoeba proteus* [3]. This amino acid, apparently limited to the *Cucurbita* genus [4], has already been analysed qualitatively by two-dimensional paper chromatography [1,4,5], thin-layer chromatography (TLC) [5], paper electrophoresis [5] and ion-exchange liquid chromatography [5] and also quantitatively by paper [5] and high-performance TLC (HPTLC)–densitometry [6] with post-chromatographic ninhydrin detection and by HPLC on a cyanide column with phenyl isothiocyanate pre-chromatographic derivatization [6].

In this work, stereoselective determination of N-trifluoroacetyl cucurbitine esters was developed using gas chromatography (GC) on a Chirasil-L-Val capillary column with a view to further studies on the preparative resolution of isomers and applications to biological media.

EXPERIMENTAL

Methanol, ethanol, 1- and 2-propanol, 1-, 2- and 3-butanol, isoamyl alcohol and methyl pentadecanoate were analytical-reagent grade reagents supplied by Merck (Darmstadt, Germany). Anhydrous ethyl acetate, acetyl chloride, chloroform and trifluoroacetic anhydride were provided by Aldrich (Milwaukee, WI, USA).

Racemic cucurbitine hydrobromide was synthesized according to Sun *et al.* [7] from 1,3-dicarbethoxy-4-pyrrolidone, obtained by condensation of ethyl acrylate and N-carbethoxyglycine ethyl ester

Correspondence to: E. Schenkel, Unité de Chimie Bioanalytique, de Toxicologie et de Chimie Physique Appliquée, Université Libre de Bruxelles, C.P. 205/1, Boulevard du Triomphe, 1050 Brussels, Belgium.

0021-9673/92/$05.00

[8]; this compound was prepared from ethyl chloroformate and glycine ethyl ester hydrochloride [9].

The identity of the synthesized cucurbitine hydrobromide was checked by melting point determination (decomposition at 286°C), carbon-13 NMR [6] and elemental analysis (calculated: H 5.25, C 28.45, N 13.27, O 15.16, Br 37.86; found: H 5.25, C 28.42, N 13.19, O 15.21, Br 37.92).

Cucurbita moschata seeds were harvested in Burkina Faso (Farako Bâ Agronomical Research Station), reduced to coarse powder and extracted as described previously [6]. The seed powder was defatted with light petroleum (b.p. 40–60°C) and extracted with boiling water; the aqueous extract was adsorbed on Amberlite IR-120 (H^+ form), desorbed with 1 *M* aqueous ammonia and evaporated to dryness under reduced pressure. Weights were corrected for residual water as determined on aliquots by drying in an oven at 105°C.

HPTLC–densitometry

Volumes of 0.5 μl of standard or sample solutions in methanol–water (1:1, v/v) were applied to precoated HPTLC plates of silica gel 60 F_{254} provided by Merck and developed with methanol–chloroform–25% aqueous ammonia–acetic acid (80:10:8.5:1.5, v/v) (saturated tank) to a distance of 90 mm. After drying at 105°C for 1 h and dipping in ninhydrin reagent [80 mg of ninhydrin in a solution of water–acetone–acetic acid (18:80:2, v/v), the plates were left for 10 min at ambient temperature and 15 min at 60°C. Spots were measured with a Shimadzu CS-930 high-speed TLC scanner (linear scan at 370 nm) [6].

Chromatographic analysis

GC analyses were performed either on a Perkin-Elmer Sigma 2000 insrument with flame ionization detection or on a Hewlett-Packard Model 5890 instrument with a Model 5970 quadrupole mass-selective detector interfaced to Model 59940 A Chem Station. The mass-selective detector was operated in the electron impact ionization mode with an ionization potential of 70 eV; the scanning range was *m/z* 40–800.

The chromatographic column was a 25 m × 0.25 mm I.D. WCOT fused-silica column coated with a 0.12-μm Chirasil-L-Val film (Chrompack, Bergen op Zoom, Netherlands). The carrier gas was nitrogen (purified on a high-capacity gas purifier coupled with an OMI-1 indicating purifier (Supelco, Bellefonte, PA, USA)) at 0.5 bar; the oven temperature ranged from 100 to 175°C and the injector and detector temperatures were 220°C. Injection was in split mode with a splitting ratio ranging from 40:1 to 20:1.

Derivatization

Derivatization was carried out in 100 × 14 mm I.D. glass tubes with PTFE-lined screw-caps (Sovirel, Bagneaux-sur-Loing, France). Heating was performed using a block heater (Pierce, Rockford, IL, USA) and an aluminium block in which 35-mm deep holes 16 mm in diameter were drilled. Evaporation was carried out in a 40°C vacuum vortex evaporator (Buchler, Fort Lee, N.J., USA). Samples containing 10–200 μl of amino acid solutions [10–50 μmol/ml in water or methanol–water (1:1, v/v] or *Cucurbita* extracts [extract from 150 mg of seeds dissolved in 1 ml methanol–water (1:1, v/v)] were evaporated, dissolved in 300 μl of the esterifying solution [acetyl chloride–alcohol (methanol, ethanol, 1-propanol, 2-propanol, 1-butanol, 2-butanol, 3-butanol or isoamyl alcohol) (1:2, v/v)], heated for 1 h at 110°C, evaporated to dryness, the residue dissolved in 400 μl of anhydrous chloroform, 200 μl of trifluoroacetic anhydride added, heated for 10 min at 110°C, evaporated to dryness and the residue dissolved in 200 μl of ethyl acetate [10–12] containing 50–100 nl of methyl pentadecanoate (internal standard).

RESULTS AND DISCUSSION

According to previous studies [13–15], N-TFA-isopropyl derivatives of amino acid enantiomers can be readily separated by GC on a Chirasil-L-Val capillary column. Application to cucurbitine of the described derivatization resulted in long retention times and poor enantiomeric resolution. These observations led to further investigations concerning the modification of the esterifying agent and the influence of the chromatographic conditions.

Influence of esterifying alcohol on resolution

In comparison with the 2-propyl derivatives, an increase in retention times with a better resolution was observed with 1-butyl derivatives. However, 2-

TABLE I

EXPERIMENTAL ISOTHERMAL t'_R VALUES OF THE DIFFERENT N-TFA ESTERS OF D-AND L-CUCURBITINE, t_M OF METHANE, NET CAPACITY FACTOR k' OF EACH ENANTIOMER, RESOLUTION FACTOR α AND PEAK RESOLUTION R

Chromatographic conditions: column, Chirasil-L-Val (25 m × 0.25 mm I.D.); injector and detector temperatures, 220°C; carrier gas, nitrogen at 0.5 bar; oven temperature, 145°C; 0.2 μg of racemic mixture injected; splitting ratio, 20:1. N-TFA-1-butyl D- and L-cucurbitine derivatives were not eluted at 125°C. No separation of the N-TFA-2-propyl D- and L-cucurbitine derivatives occurred at 155 and 165°C.

Compound	T(°C)	t_M (min)	$t'_{R(D)}$ (min)	$t'_{R(L)}$ (min)	k'_D	k'_L	α	R
Methyl ester	125	2.23	77.17	80.97	34.61	36.31	1.0491	1.38
	135	2.27	45.03	47.13	19.84	20.76	1.0464	1.49
	145	2.32	26.28	27.38	11.33	11.80	1.0415	1.24
	155	2.35	15.35	15.95	6.53	6.79	1.0398	1.05
	165	2.38	10.02	10.42	4.21	4.38	1.0404	0.89
Ethyl ester	125	2.23	84.57	87.67	37.92	39.31	1.0367	1.22
	135	2.27	51.23	52.93	22.57	23.32	1.0332	1.20
	145	2.32	27.68	28.68	11.93	12.36	1.0360	1.15
	155	2.35	17.15	17.65	7.30	7.51	1.0288	0.98
	165	2.38	10.92	11.22	4.59	4.71	1.0261	0.67
1-Propyl ester	125	2.23	132.67	136.37	59.49	61.15	1.0279	1.03
	135	2.27	75.13	77.13	33.10	33.98	1.0266	1.16
	145	2.32	42.28	43.38	18.22	18.70	1.0263	1.14
	155	2.35	25.05	25.75	10.66	10.96	1.0281	0.99
	165	2.38	15.52	15.82	6.52	6.65	1.0199	0.62
2-Propyl ester	125	2.23	82.47	83.85	36.98	37.60	1.0168	0.30
	135	2.27	48.53	49.23	21.38	21.69	1.0145	0.29
	145	2.32	27.58	27.88	11.89	12.02	1.0109	0.28
	155	2.35	16.85	16.85	7.17	7.17	1.000	
	165	2.38	10.72	10.72	4.50	4.50	1.000	
1-Butyl ester	125	2.23						
	135	2.27	113.63	115.83	50.06	51.03	1.0194	1.14
	145	2.32	60.88	61.98	26.24	26.72	1.0183	1.05
	155	2.35	36.35	37.05	15.47	15.77	1.0194	0.84
	165	2.38	22.72	23.02	9.55	9.67	1.0126	0.56

butyl, 3-butyl and isoamyl derivatives could not be eluted under experimental conditions. From *n*-propyl to methyl derivatives the retention times were found to decrease and the resolution to increase at all tested temperatures with a maximum resolution at the lower temperatures (Table I).

Thermodynamic analysis of retention data is an important source of information about the chiral discrimination process in the separation of enantiomers on chiral stationary phases [16,17]. The interpolation and extrapolation of the retention data such as the net retention time, t'_R (Table II) allow the different thermodynamic properties of each derivative (Table III) and the best chromatographic conditions to be established. The thermodynamic treatment of retention data could be done according to Koppenhoefer and co-workers [16,17] using nomograms [ln k' or ln t'_R (min) *versus* $1/T$ (K^{-1}) and ln α *versus* $1/T$]. We used an original algorithm (FADHA) which permitted the fitting of $1/T$–t'_R or $1/T$–α curves by optimizing a non-linear cost function by the simplex method and allowed the best fit from our experimental data to be assessed statistically [18]; the equation used was $y = e^{a+bx}$, where y is t'_R, x is $1/T$ and b is $(-\Delta H + C_1)/R$, with $C_1 = -0.50$ kcal mol^{-1} for 0.5 bar N_2,

TABLE II

CALCULATED ISOTHERMAL t'_R and α VALUES FOR METHYL, ETHYL AND 1-PROPYL D- AND L-CUCURBITINE DERIVATIVES

Chromatographic conditions as in Table I.

T (°C)	Methyl ester			Ethyl ester			1-Propyl ester		
	$t'_{R(D)}$ (min)	$t'_{R(L)}$ (min)	α	$t'_{R(D)}$ (min)	$t'_{R(L)}$ (min)	α	$t'_{R(D)}$ (min)	$t'_{R(L)}$ (min)	α
50	16 075	17 374	1.0786	18 450	19 230	1.0631	39 339	41 311	1.0548
	±119	±125	±1.0123	±150	±170	±0.0104	±357	±378	±0.0104
	0.7%	0.7%	1.1%	0.8%	0.9%	1.0%	0.9%	0.9%	1.0%
75	2119	2266	1.0675	2403	2539	1.0528	4571	4763	1.0457
	±15	±16	±0.0114	±20	±21	±0.0101	±42	±43	±0.0099
	0.7%	0.7%	1.1%	0.8%	0.8%	1.0%	0.9%	0.9%	0.9%
100	366.6	388.2	1.0572	411.3	430.1	1.0440	708.6	733.7	1.0378
	±2.8	±2.8	±0.0113	±3.4	±3.5	±0.0095	±6.5	±6.7	±0.0095
	0.8%	0.7%	1.1%	0.8%	0.8%	0.9%	0.9%	0.9%	0.9%
145	26.45	27.60	1.0426	29.20	30.07	1.0308	43.37	44.48	1.0261
	±0.20	±0.20	±0.0106	±0.24	±.25	±0.0088	±0.39	±0.41	±0.0088
	0.8%	0.7%	1.0%	0.8%	0.8%	0.9%	0.9%	0.9%	0.9%
190	3.180	3.281	1.0310	3.466	3.526	1.0204	4.569	4.649	1.0168
	±0.024	±0.024	±0.0101	±0.029	±0.029	±0.0083	±0.041	±0.042	±0.0083
	0.8%	0.7%	1.0%	0.8%	0.8%	0.8%	0.9%	0.9%	0.8%

or where y is α, x is $1/T$, b is $-\Delta\Delta H/R$ and a is $\Delta\Delta S/R$.

The three enantiomeric pairs show similar thermodynamic properties (Table III); the $\Delta\Delta S$ values are very similar but the $-\Delta\Delta H$ values are different, with methyl > ethyl > 1-propyl. This is represented when plotting ln α *versus* $1/T$ as three straight lines, which do not intersect. Therefore, whatever the temperature, the methyl ester derivatives will always show a greater resolution than the other derivatives.

Structure of cucurbitine derivatives

Owing to the two amino functions of cucurbitine, and depending on reagent concentration, the possibility arises in the course of N-trifluoroacetylation of the formation of two different monoacyl derivatives, a diacyl derivative or even a mixture of these compounds [19]. However, with the various acetylation reagents tested (33.3%, 50%, 66.6% and 83.3% TFAA in anhydrous chloroform), no differences were observed in the retention times and peak shapes of the end product derivatives and no further peak occurred.

The GC–MS analysis, initially undertaken to confirm peak identity in chromatograms of plant extracts, allowed the exact structure of the derivatives formed to be specified. A series of proteic racemic amino acids (D,L-alanine, D,L-proline, L-leucine, D,L-aspartic acid, D,L-methionine, D,L-glutamic acid, L-arginine and D,L-tryptophan) was similarly derivatized (N-TFA acylation and methyl, ethyl or 1-propyl esterification) and analysed (Fig. 1). Molecular ions were generally not detected but individual mass spectra of the different N-TFA esters allowed similar fragmentation patterns to be deduced (Fig. 2) irrespective of the esterifying alcohol.

The mass spectra of the N-TFA esters of cucurbitine (Table IV) suggest strong evidence for the formation of a diacyl (di-TFA) compound under the conditions of the derivatization reaction; the observed ions cannot be satisfactorily explained by a monoacyl cucurbitine derivative even when rearrangement reactions are considered.

TABLE III

THERMODYNAMIC PROPERTIES OF METHYL, ETHYL AND 1-PROPYL D- AND L-CUCURBITINE DERIVATIVES

Chromatographic conditions as in Table I.

Property		Methyl ester			Ethyl ester			1-Propyl ester		
		Specified units		SI units[a]	Specified units		SI units[a]	Specified units		SI units[a]
$-\Delta H_{(D)}$	(kcal mol^{-1})	17.60 ±0.01	0.06%[b]	73.57 ±0.04	17.71 ±0.01	0.06%[b]	74.03 ±0.04	18.73 ±0.01	0.05%[b]	78.29 ±0.04
$-\Delta H_{(L)}$	(kcal mol^{-1})	17.70 ±0.01	0.06%	73.99 ±0.04	17.82 ±0.01	0.06%	74.49 ±0.04	18.80 ±0.01	0.05%	78.58 ±0.04
$-\Delta\Delta H$	(cal mol^{-1})	95.9 ±3.6	3.8%	400.9 ±15.0	87.1 ±3.6	4.1%	364.1 ±15.0	77.7 ±3.6	4.6%	324.8 ±15.0
$\Delta\Delta S$	(cal K^{-1} mol^{-1})	−0.147 ±0.012	8.0%	−0.614 ±0.050	−0.148 ±0.009	6.1%	−0.619 ±0.038	−0.135 ±0.009	6.7%	−0.564 ±0.038
$-\Delta\Delta G^{323}$	(cal mol^{-1})	48.4 ±0.6	1.2%	202.3 ±2.5	39.3 ±0.7	1.8%	164.3 ±2.9	34.1 ±1.4	4.4%	142.5 ±5.9
$-\Delta\Delta G^{373}$	(cal mol^{-1})	41.1 ±1.8	4.4%	171.8 ±7.5	31.9 ±0.3	0.9%	133.3 ±1.3	27.3 ±0.5	1.8%	114.1 ±2.1
$-\Delta\Delta G^{418}$	(cal mol^{-1})	34.4 ±2.8	8%	144.2 ±11.7	25.2 ±0.2	0.8%	105.3 ±0.8	21.3 ±0.3	1.4%	89.0 ±1.3
T_s	(°C)		382 ±29 8.0%			316 ±12 3.8%			303 ±12 4.0%	

[a] SI units: kJ mol^{-1} or J mol^{-1}.

[b] Relative error.

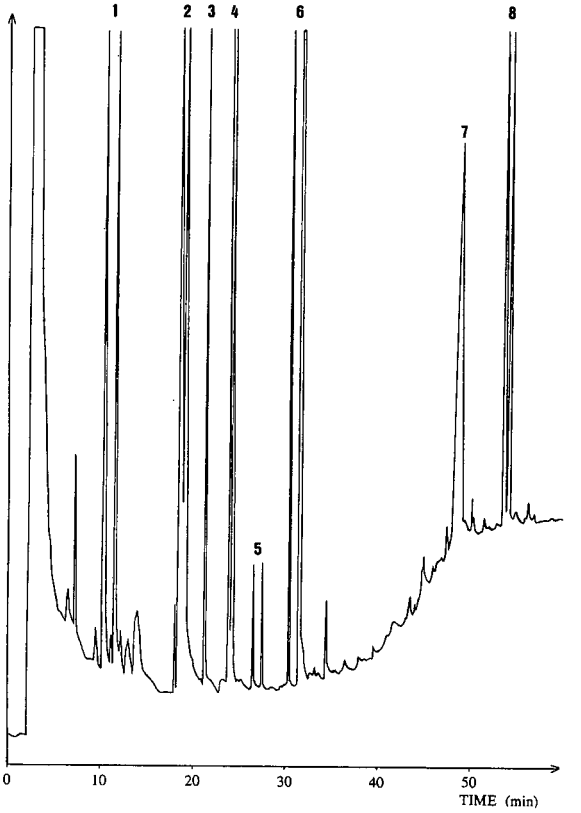

Fig. 1. GC separation of the enantiomers of several amino acids. Chromatographic conditions: column, Chirasil-L-Val (25 m × 0.25 mm I.D.); injector and detector temperatures, 220°C; carrier gas, nitrogen at 0.5 bar; temperature programme, 60°C for 3 min. then increased at 3°C/min to 190°C, held for 3 min. Peaks: 1 = D,L-alanine; 2 = D,L-proline; 3 = L-leucine; 4 = D,L-aspartic acid; 5 = D,L-methionine; 6 = D,L-glutamic acid; 7 = L-arginine; 8 = D,L-tryptophan. In all instances the D-enantiomer was eluted prior to the L-enantiomer.

For all the investigated esters of proteic amino acids, the principal ion (100% relative abundance) was the fragmentation product resulting from the loss of the –COOR radical (R = methyl, ethyl or propyl) even in the case of diacids (glutamic and aspartic acid). However, when applied to cucurbitine derivatives, this rule was found to be invalid; in this instance, the principal ion (100% relative abundance) resulted from the loss of one $-NHCOCF_3$ radical. This can probably be explained by steric factors.

Fig. 3 shows the corresponding mass spectra of N-TFA-methyl, -ethyl and -1-propyl esters of L-cucurbitine derivatives and the possible fragmentation patterns with principal ions.

For every amino acid investigated, including cucurbitine, the mass spectra were similar for both enantiomers.

Quantitative limits of the method

The N-TFA-methyl ester was the derivative used for quantitative work; isocratic elution at 145°C allowed perfect resolution of the two cucurbitine isomer peaks.

It is widely accepted that on Chirasil-L-Val, the elution order of amino acid enantiomers is correlated with stereochemistry; in chromatograms of *Cucurbita* seeds, a single cucurbitine isomer, which was assigned the L stereochemistry from its retention time (Fig. 4), could be detected. This is in accordance with previous stereochemical studies [1]. Assays also permitted the absence of racemization during the derivatization process to be confirmed, as can be seen by the exceedingly high enantiomeric purity of L-cucurbitine from *Cucurbita* seeds (Fig. 4) [20]. Quantitative work was developed with the flame ionization detector; methyl pentadecanoate was used as the internal standard and the splitting ratio was fixed at 20:1.

The method was found to give a linear response for each isomer between 2 and 40 ng; the detection limit was *ca.* 1 ng [the equation of the regression line was $y = 0.00262x - 0.01234$, where y is the peak area (cm^2) and x is the amount of L-cucurbitine injected (ng); $r = 0.9860$; $n = 21$].

The assay was applied to different samples of *Cucurtine* spp. seeds cultivated in Burkina Faso and compared with HPTLC determination. GC appeared to give good accuracy when compared with HPTLC, but with a tenfold better precision (Table V) and also a 10–100-fold greater sensitivity.

Recovery was calculated by the standard addition method, which requires the determination of a calibration line for a particular sample. Results obtained with the standard addition method were compared with those obtained by using direct determination [the equation of the regression line for the standard addition method was $y = 0.00268x + 0.3338$, where y is the peak area (cm^2) and x the amount of L-cucurbitine injected (ng); $r = 0.9985$; $n = 22$]. The mean recovery was 106.8% ($n = 3$).

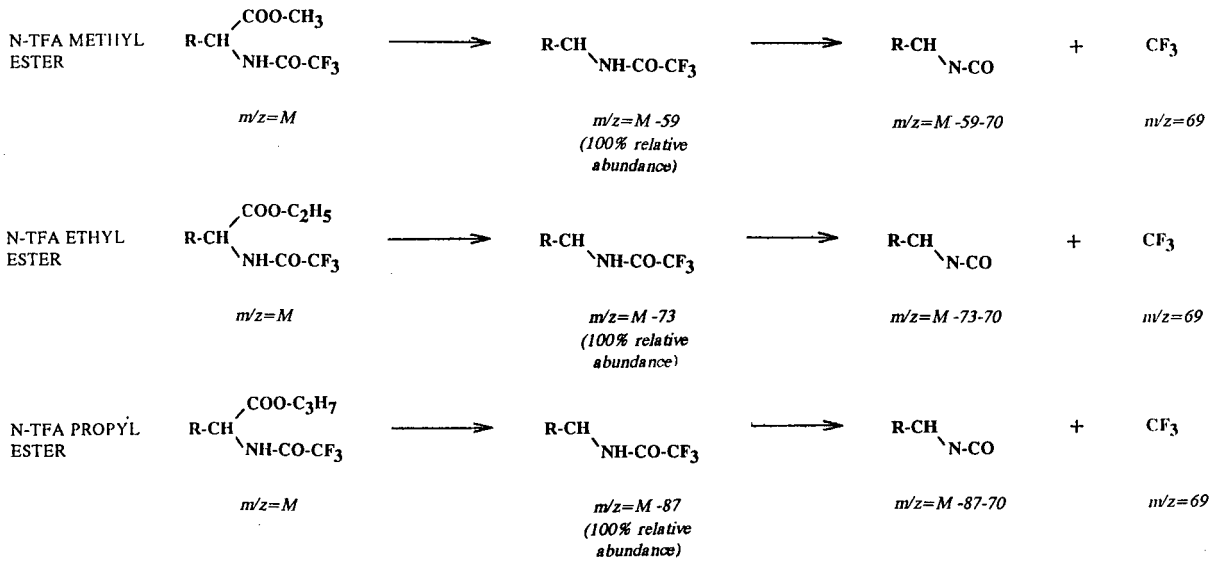

Fig. 2. Deduced fragmentation patterns of N-TFA-methyl, -ethyl and -1-propyl esters of proteic racemic amino acids. Chromatographic conditions as in Fig. 1. Quadrupole mass-selective detector; electron impact ionization potential, 70 eV; scanning from *m/z* 40 to 800.

TABLE IV

PRINCIPAL IONS OF THE MASS SPECTRA OF THE DIFFERENT N-TFA ESTERS OF SYNTHETIC D- AND L-CUCURBITINE

m/z of observed fragments[a]											
N-TFA-methyl ester (molecular mass of di-N-TFA-methyl ester: 336)				N-TFA-ethyl ester (molecular mass of di-N--TFA-ethyl ester: 350)				N-TFA-1-propyl ester (molecular mass of di-N--TFA-1-propyl ester: 364)			
D-Isomer		L-Isomer		D-Isomer		L-Isomer		D-Isomer		L-Isomer	
267	(12)	267	(8)	281	(9)	281	(7)				
277	(23)	277	(22)	277	(23)	277	(19)	277	(20)	277	(27)
		224	(11)	238	(9)	238	(9)			252	(9)
223	(100)	223	(100)	237	(100)	237	(100)	251	(58)	251	(73)
				209	(27)	209	(17)	209	(100)	209	(100)
				208	(32)	208	(30)	208	(10)	208	(17)
207	(9)	207	(6)	207	(14)	207	(9)	207	(12)	207	(7)
193	(7)	193	(6)	193	(9)	193	(4)	193	(10)		
192	(37)	192	(20)	192	(53)	192	(32)	192	(27)	192	(37)
165	(9)	165	(10)	165	(24)	165	(15)	165	(10)	165	(21)
164	(48)	164	(28)	164	(41)	164	(36)	164	(40)	164	(44)
163	(30)	163	(30)	163	(14)	163	(16)	163	(14)	163	(16)
				112	(10)	112	(12)	112	(25)	112	(23)
96	(13)	96	(4)	96	(16)	96	(8)	96	(13)	96	(18)
94	(13)	94	(10)	94	(19)	94	(15)	94	(17)	94	(14)
83	(15)	83	(7)	83	(14)	83	(10)	83	(8)	83	(9)
69	(65)	69	(44)	69	(50)	69	(41)	69	(29)	69	(36)
						68	(11)	68	(14)	68	(10)
67	(13)	67	(7)	67	(12)	67	(8)	67	(13)	67	(14)

[a] Relative abundances (%) in parentheses.

CONCLUSIONS

GC–MS analysis confirmed the formation of a di-N-TFA cucurbitine derivative. The thermodynamic analysis results show that the methyl ester derivative is preferred because of its greater resolution and its shorter retention times. Chirasil-L-Val is a valuable stationary phase for the separation of optical isomers of cucurbitine. The method allows the identification and determination (nanograms level) of optical isomers of cucurbitine and the efficient resolution of L-cucurbitine in *Cucurbita* seed extracts, and has better precision and sensitivity than HPTLC.

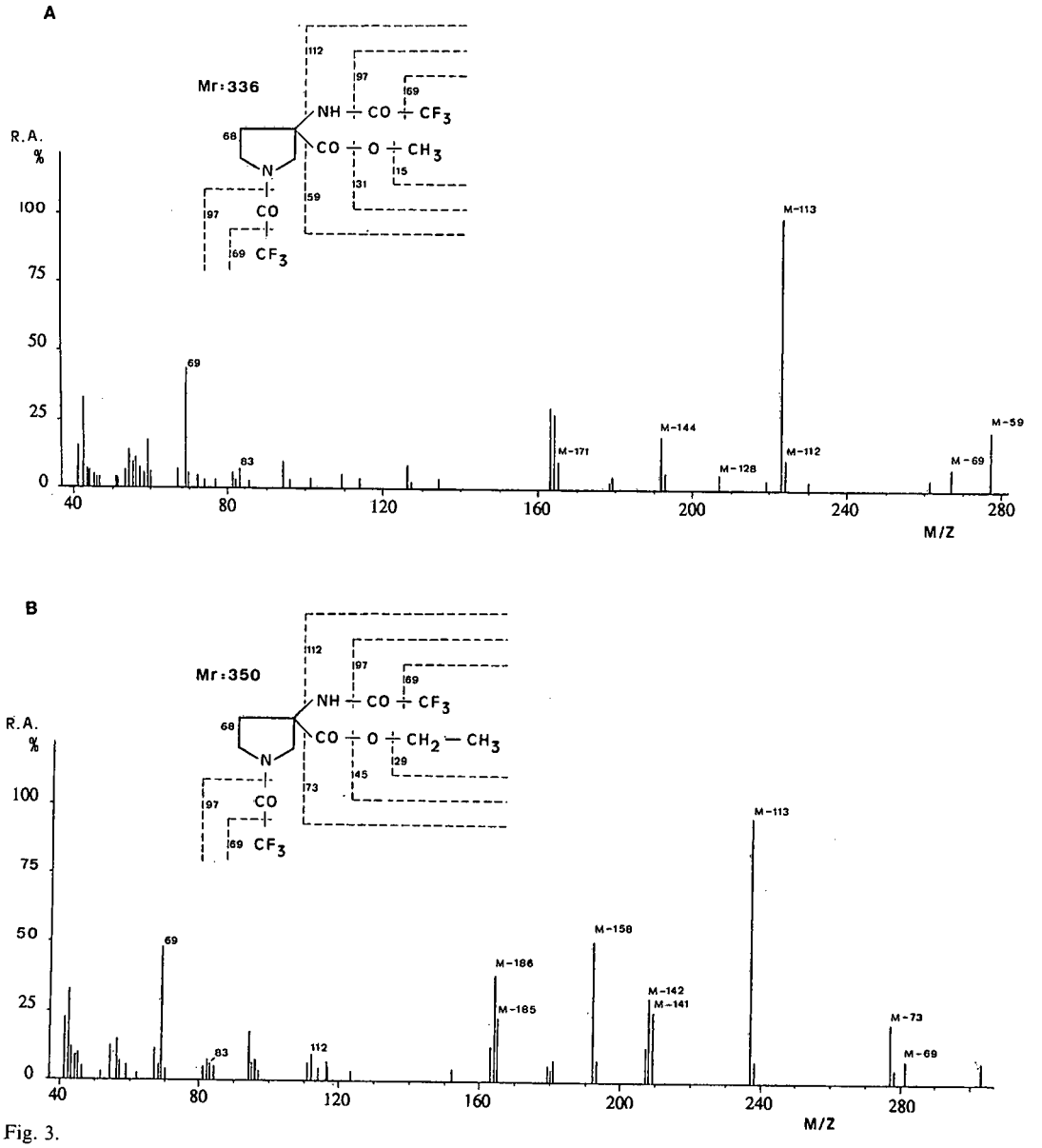

Fig. 3.

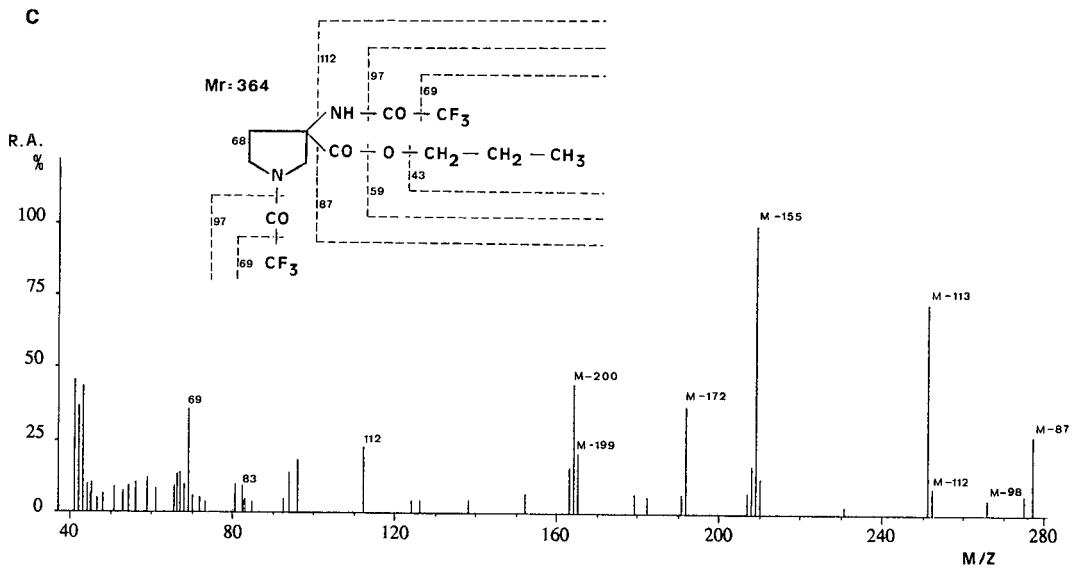

Fig. 3. Mass spectra of N-TFA (A) methyl, (B) ethyl and (C) 1-propyl esters of L-cucurbitine with possible fragmentation patterns explaining principal ions. Mass spectra were similar for both enantiomers. R.A. = Relative abundance.

ACKNOWLEDGEMENTS

The authors thank Professor Y. Mardens, Dr. A. Kumps and Miss C. Wurth for the use of the GC–MS equipment and valuable advice.

TABLE V

GC AND HPTLC DETERMINATION OF DIFFERENT *CUCURBITA PEPO* AND *MOSCHATA* SEED EXTRACTS

Cucurbita seed studied		L-Cucurbitine in defatted seed powder (%)			
Species	Line	GC (n = 5)		HPTLC (n = 11)	
		Mean	S.D.	Mean	S.D.
pepo	L 34	0.201	0.007	0.15	0.04[a]
pepo	L 5	0.441	0.004	0.43	0.03
pepo	L 149	0.776	0.004	0.76	0.01[b]
moschata	B 7 6b	0.292	0.006	0.27	0.04
moschata	E 3	0.462	0.007	0.48	0.05
moschata	B 7 3b	0.457	0.008	0.48	0.05

[a] Cochran statistical test allowed a statistical significant difference to be concluded only between the two means of *Cucurbita pepo* L34.

[b] n = 3.

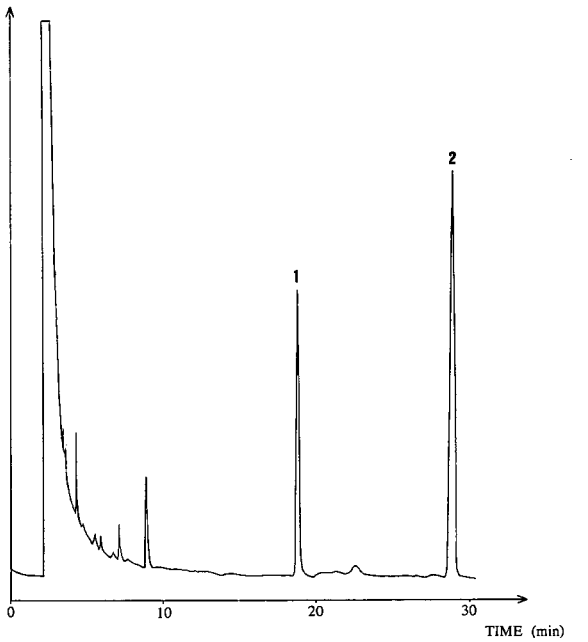

Fig. 4. Chromatogram of *Cucurbita* seed extract. Chromatographic conditions as in Fig. 1. Oven temperature, 145°C. Peaks: 1 = methyl pentadecanoate; 2 = L-cucurbitine.

REFERENCES

1 S. Fang, L. Li, C. Niu and K. Tsing, *Sci. Sin.*, 10 (1961) 845–851.
2 S. J. Shiao, B. J. Shao, Y. H. Ho, Y. C. Yang and C. P. Mao, *Sci. Sin.*, 11 (1962) 1527–1534.
3 P. Duez, A. Livaditis, P. I. Guissou, M. Sawadogo and M. Hanocq, *J. Ethnopharmacol.*, 34 (1991) 235–246.
4 M. P. Dunnhil and L. Fowden, *Phytochemistry*, 4 (1965) 933–934.
5 V. H. Mihranian and C. I. Abou-Chaar, *Lloydia*, 31 (1968) 23–29.
6 P. Duez, S. Chamart, M. Hanocq and M. Sawadogo, *J. Planar Chromatogr.*, 1 (1988) 313–316.
7 T. Sun, S. Loh, C. Chow and Z. Kyi, *Sci. Sin.*, 10 (1961) 852–859.
8 R. Khun and G. Osswald, *Chem. Ber.*, 89 (1956) 1423–1442.
9 E. Fischer and E. Otto, *Chem. Ber.*, 36 (1903) 2106–2116.
10 G. Gamerith, *J. Chromatogr.*, 256 (1983) 326–330.
11 P. Husek and K. Macek, *J. Chromatogr.*, 113 (1975) 139–230.
12 H. Frank, N. Vujtovic-Ockenga and A. Rettenmeier, *J. Chromatogr.*, 279 (1983) 507–514.
13 H. Frank, G. J. Nicholson and E. Bayer, *J. Chromatogr.*, 146 (1978) 197–206.
14 H. Frank, G. J. Nicholson and E. Bayer, *J. Chromatogr.*, 167 (1978) 187–196.
15 C. H. Lochmüller and R. W. Souter, *J. Chromatogr.*, 113 (1975) 283–302.
16 B. Koppenhoefer, S. Abdalla and M. Hummel, *Chromatographia*, 31 (1991) 31–40.
17 B. Koppenhoefer and E. Bayer, *Chromatographia*, 19 (1984) 123–130.
18 J. Dubois, F. Abi Khalil, M. Hanocq, G. Atassi and R. Arnould, *J. Pharm. Belg.*, 44 (1989) 181–191.
19 G. Gamerith, *J. Chromatogr.*, 318 (1985) 65–74.
20 B. Koppenhoefer, V. Muschalek, M. Hummel and E. Bayer, *J. Chromatogr.*, 477 (1989) 139–145.

Journal of Chromatography, 625 (1992) 299–309
Elsevier Science Publishers B.V., Amsterdam

CHROM. 24 512

Model for retention and efficiency in open-tubular supercritical fluid chromatography

Donald P. Poe

Department of Chemistry, University of Minnesota, Duluth, MN 55812 (USA)

(First received May 17th, 1992; revised manuscript received July 16th, 1992)

ABSTRACT

A model for open-tubular supercritical fluid chromatography at constant mass flow-rate, which takes into account the effects of temperature, density and pressure drop on solute retention and dispersion, is developed and applied to the elution of normal alkanes (C_8–C_{40}) on a polysiloxane stationary phase using CO_2 mobile phase at 40 to 120°C. An exact expression for resolution is derived in terms of observed chromatographic parameters, and the effect of swelling on solute diffusion coefficients in the stationary phase is considered. Plots of apparent plate height *vs.* temporal average velocity show the onset of gradient-induced band spreading for a variety of conditions. Swelling of the stationary phase is shown to be critical to the achievement of acceptable efficiency for heavy solutes at low temperatures, and the prediction of a second maximum in resolution at high mobile phase velocities suggests the possibility of extremely fast separations by supercritical fluid chromatography.

INTRODUCTION

The complex dependence of retention and dispersion processes in supercritical fluid chromatography (SFC) on temperature, pressure and pressure drop has been the subject of a number of investigations dealing with both packed [1–7] and open-tubular [8,9] columns. It is generally acknowledged that large pressure drops in SFC, especially near the critical point of the mobile phase, may lead to variations in retention and to a loss of efficiency beyond that which is predicted by the simple Van Deemter or Golay equations. Recent advances in chromatographic theory provide explanations for these phenomena. A unified molecular theory of chromatographic retention developed by Martire and Boehm [10,11] has provided a firm theoretical basis for the dependence of retention on temperature and mobile phase density in SFC. Further work by Martire and co-workers [12–14] developed the use of appropriate temporal and spatial column parameters in chromatography, with one specific result being that the observed capacity factor is the temporal average value. Recently, Poe and Martire [15] provided a theoretical basis for the effect of pressure drop on efficiency in gas, liquid and supercritical fluid chromatography. The theory, which is an extension of Giddings' theory for the effect of pressure drop in gas chromatography [16], was applied to retention and band spreading for several solutes in packed column SFC, and the prediction from the theory agreed well with experimental observations. More recently Janssen *et al.* [17], using a similar approach, obtained reasonably good agreement between theory and experiment for both packed and open-tubular columns. Of particular relevance to the present investigation is that they obtained well-shaped peaks for elution of *n*-alkanes from an open-tubular column at very high velocities and large pressure drops. A general treatment of the variance of a zone in a non-uniform medium was recently published [18].

The purpose of the present study is to extend the

Correspondence to: Dr. D. P. Poe, Department of Chemistry, University of Minnesota, Duluth, MN 55812, USA.

0021-9673/92/$05.00

earlier treatment of the theory for apparent plate height to provide a model for retention and efficiency in open-tubular SFC over a wide range of operating conditions, and especially to examine the effects of pressure drop and stationary phase swelling of efficiency. The column dimensions selected for application of the model represent a typical modern-day system, and in some cases the linear velocities required to generate large pressure drops are much greater than would normally be encountered in a typical laboratory setting. It is hoped that the data generated by the model will provide a basis for further experimental verification of the theory for apparent plate height, and will provide insight into open-tubular column design and operation for SFC.

THEORY

The relevant theories for retention and efficiency in SFC are provided elsewhere [10,12,13,15]. Some of the major arguments are presented here for clarity with specific emphasis on open-tubular columns, and an exact equation for resolution is developed. In the treatment that follows, the following assumptions are made.

(1) Mass flow-rate is constant. Density programming is not considered.

(2) The column is a uniform tube, and except for the effect of mobile phase density on film thickness, it is coated with a uniform film of stationary phase.

(3) Temperature is constant, and the column and mobile phase are at thermal equilibrium. Temperature gradients due to expansion of the mobile phase and viscous flow are assumed to be negligible.

(4) Laminar flow is maintained. In the model, the Reynolds number is not allowed to exceed 1400.

Retention

The dependence of capacity factor on temperature and density in SFC was expressed in general form by Martire and Boehm [10] as

$$\ln k' = \ln k'^0 + \Delta + a\rho_R - b\rho_R/T_R + c\rho_R^2/T_R \qquad (1)$$

where k'^0 is the ideal gas chromatography (GC) capacity factor, T_R and ρ_R are reduced temperature and density of the mobile phase, a, b and c depend on solute and mobile phase properties, and Δ accounts for sorption of mobile phase by the stationary phase.

The apparent capacity factor, which is the value observed at the column outlet, has been shown to be the temporal average of the local value [12,14]

$$\hat{k}' = <k'>_t \qquad (2)$$

Details for calculating $<k'>_t$ and other average quantities are given in ref. 13.

Efficiency

For an open-tubular column under conditions of laminar flow the Golay equation describes the solute dispersion exactly.

$$H = \frac{2D_m}{u} + \frac{ud_c^2(1 + 6k' + 11k'^2)}{96D_m(1 + k')^2} + \frac{2ud_f^2k'}{3D_s(1 + k')^2} \qquad (3)$$

where H is plate height, D_m and D_s are diffusion coefficients in the mobile and stationary phases, u is linear velocity of the mobile phase, d_c is column diameter, and d_f is the stationary phase film thickness.

In a previous paper [15] it was shown that the variation of k' and ρ along the axis of the column generates solute velocity gradients, which in turn give rise to gradient-induced band spreading (GIBS). For a column of uniform geometry operated under isothermal, steady-state conditions, the apparent plate height observed at the outlet of the column was shown to be

$$\hat{H} = \frac{<H(1 + k')^2\rho^2>_z}{<(1 + k')\rho>_z^2} \qquad (4)$$

or the equivalent expression

$$\hat{H} = \frac{<H(1 + k')^2\rho>_t}{<1 + k'>_t^2<\rho>_z} \qquad (5)$$

where the subscripts z and t indicate the spatial and temporal averages of the quantities in brackets.

In open-tubular SFC the internal diameter of the column may vary due to swelling of the stationary phase, resulting in variations in the column permeability and specific mass flow-rate (F, the mass flow-rate per unit area). It may be shown that for this case the exact expression for apparent plate height is

$$\hat{H} = \frac{<H(1 + k')^2\rho^2/F^2>_z}{<(1 + k')\rho/F>_z^2} \qquad (6)$$

If the variation in column diameter is on the order of a few percent or less, as it appears to be in open-tubular SFC with a typical phase ratio of 50 (see below), this variation will produce no significant effect on the apparent plate height, and eqn. 4 or 5 may be used.

Application of eqn. 5 to the Golay equation yields the desired expression for apparent plate height in open-tubular SFC,

$$\hat{H} = \frac{1}{<1+k'>_t^2 <\rho>_z}\left[2<D_m\rho(1+k')^2/u>_t + \frac{1}{96}<ud_c^2(1+6k'+11k'^2)\rho/D_m>_t + \frac{2}{3}<ud_f^2k'\rho/D_s>_t\right] \quad (7)$$

The corresponding expression for the apparent reduced plate height is

$$\hat{h} = \frac{1}{<1+k'>_t^2 <\rho>_z}\left[2<(1+k')^2\rho/v>_t + \frac{1}{96}<v(1+6k'+11k'^2)\rho>_t + \frac{2}{3}<vD_m d_f^2 k'\rho/D_s d_c^2>_t\right] \quad (8)$$

where the reduced velocity v is defined

$$v = ud_c/D_m \quad (9)$$

Eqns. 4–8 may also be written using reduced density, $\rho_R = \rho/\rho_{cr}$, where ρ_{cr} is the critical density of the mobile phase fluid.

Resolution

Because of the significant effect of pressure drop on retention and efficiency in SFC, an exact expression for the general resolution equation is necessary. For a pair of Gaussian-shaped peaks, the resolution is

$$R_s = \frac{\Delta t_r}{2(\tau_1 + \tau_2)} \quad (10)$$

where t_r is retention time and τ_1 is the standard deviation of the first eluting peak expressed in units of time. In the usual derivation of the general resolution equation, an approximate equation is arrived at by assuming that for closely spaced peaks $\tau_1 = \tau_2$. This may not be an appropriate assumption in SFC, and the following equations are based on eqn. 10 as written. The apparent plate height is

$$\hat{H} = L\tau^2/t_r^2 = L/\hat{N} \quad (11)$$

where L is column length and $\hat{N}$ is the apparent number of theoretical plates. The retention time is [12,13]

$$t_r = t_0(1 + \hat{k}') \quad (12)$$

where t_0 is the time required to elute an unretained species.

Combining eqns. 10–12 and rearranging yields

$$R_s = \frac{0.5(\hat{k}'_2 - \hat{k}'_1)\sqrt{L}}{(1+\hat{k}'_1)\sqrt{\hat{H}_1} + (1+\hat{k}'_2)\sqrt{\hat{H}_2}} \quad (13)$$

which is the desired equation expressing resolution in terms of apparent capacity factor and apparent plate height.

DEVELOPMENT OF THE MODEL

Selection of a model system

Prediction of retention and efficiency from the equations presented above requires a knowledge of the effects of temperature and density on k', D_m, D_s, d_c, and d_f. Examination of the literature did not yield all of the desired experimental data for a single system. The expectation that the effect of density on k' is the most important factor in the generation of gradient-induced band spreading led to the selection of *n*-alkanes–CO_2–polysiloxane as the solute–mobile phase–stationary phase system. The effect of temperature and density on retention for such systems has been treated theoretically [10], and extensive experimental data for a specific system have been recently obtained by Riester and Martire [19]. These data, for *n*-alkanes (C_3–C_{22}) on SB-octyl stationary phase (a methyloctylpolysiloxane, 50% methyl, 50% octyl substitution) over a wide range of temperature (320–380 K) and density (0.20–0.75 g/cm^3), were subjected to an empirical fit to eqn. 1 to allow precise estimation of local and apparent capacity factors.

Effect of temperature and density on diffusion in the mobile phase

Solute diffusion coefficients were estimated from a modified form of the Wilke–Chang equation (see ref. 20) in which mobile phase density replaces viscosity

$$D_a \propto \frac{M_b^{0.5} T}{\rho_b V_a^{0.6}} \quad (14)$$

where the subscript a indicates the solute and b the solvent, and D, M and V represent the diffusion coefficient, molecular mass and molar volume, respectively. This relation is based on data from several studies [21–23] of solute diffusivity in dense gases, including supercritical CO_2, which show that the product ρD varies in a fairly well-defined fashion. Using naphthalene as a model solute, which is well-studied, the diffusivity of other non-polar solutes may be estimated.

Effect of temperature and density on film thickness, column diameter and diffusion in the stationary phase

The stationary phase in absorption SFC may absorb significant amounts of mobile phase, with concomitant changes in film thickness, effective column diameter, and the solute diffusion coefficient in the stationary phase. Changes in k' are reflected in the experimental data used in the model, and as such the effect of mobile phase sorption on retention will not be addressed directly. The impact on efficiency is treated here.

The swelling of the stationary phase due to uptake of mobile phase is represented by the swelling factor (SF)

$$SF = (V - V^0)/V^0 \quad (15)$$

where V and V^0 are the volumes of the swollen and unswollen film, respectively. Since the length of the film in an open tube is fixed, and if the thickness is small compared to the column radius, the volumetric change is proportional to the change in film thickness, and

$$SF = (d_f - d_f^0)/d_f^0 \quad (16)$$

where d_f and d_f^0 are the thickness of the swollen and unswollen film. The effective column diameter is

$$d_c = d_c^{00} - 2d_f \quad (17)$$

where d_c^{00} is the diameter of the uncoated tube. Thus both d_c and d_f can be easily estimated if the swelling factor is known.

Springston *et al.* [24] reported a swelling factor of 1.0 ± 0.6 for SE-30 in the presence of supercritical CO_2 at 40°C and 88.8 atm (ρ_R = 1.05). Swelling factors for SE-30 in the presence of butane were

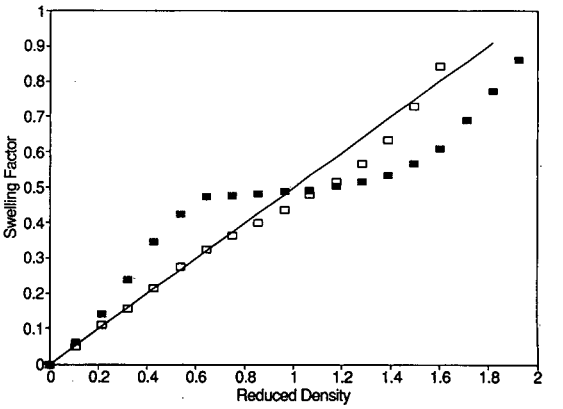

Fig. 1. Effect of CO_2 density on swelling of silicone rubber. ■ = 35°C; □ = 75°C; — = model. Experimental data taken from ref. 25.

greater and increased with increasing temperature. Shim and Johnston [25] measured the swelling of a silicone rubber film in the presence of CO_2 at pressures up to 300 bar and temperatures of 35°C and 75°C. Their experimental data are plotted as SF *vs.* reduced density in Fig. 1. The swelling factor increases almost linearly up to a reduced density of 0.5, levels off around a reduced density of 1, especially at the lower temperature, and then increases again with no indication of a maximum volume being reached. The swelling can be represented approximately by the simple equation

$$SF = 0.50\rho_R \quad (18)$$

While this is a much oversimplified expression, there is no reason to expect that the silicone rubber used by Shim and Johnston would behave identically to a polysiloxane stationary phase in an open capillary tube.

While knowledge of the swelling factor yields d_f and d_c, it yields no direct information about solute diffusion coefficients in the stationary phase. Rather, D_s can be related to the mass fraction of mobile phase in the stationary phase, which bears no simple relationship to the swelling factor. Fujita [26] has shown that for a rubbery polymer impregnated with a low-molecular-mass diluent with diffusivity D_a^s in the swollen polymer, a plot of log D_a^s *vs.* mass fraction of diluent in the polymer, ϕ, is approximately linear. Assuming that this relationship exists

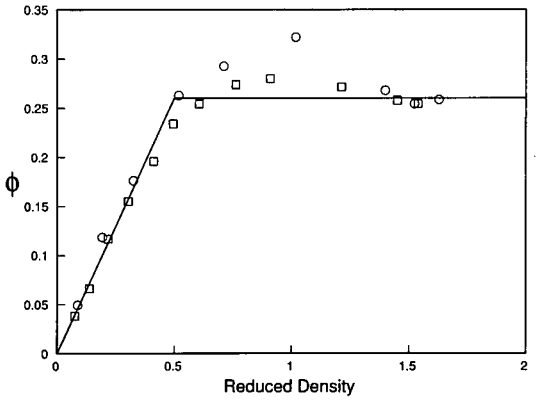

Fig. 2. Sorption of CO_2 by SE-30. ○ = 40°C; □ = 50°C; — = model. Experimental data taken from ref. 28.

across the entire range of concentrations, we have the equation

$$\log D_a^s = (1 - \phi)\log D_a^{s0} + \phi \log D_a^m \quad (19)$$

where D_a^{s0} and D_a^m are the diffusion coefficients of the diluent in the pure polymer (stationary phase) and pure diluent (mobile phase), respectively. We will assume that the equation also applies to *solute* diffusion coefficients in the stationary and mobile phases, where D_a^s and D_a^{s0} are equivalent to D_s and D_s^0, the solute diffusion coefficients in the swollen and unswollen stationary phase, respectively.

In order to utilize eqn. 19, we must evaluate ϕ, D_a^{s0} and D_a^m. The value of D_a^{s0} is estimated from the equation developed by Kong and Hawkes [27] for diffusion of normal alkanes in polysiloxane stationary phases. The estimations of ϕ and D_a^m are discussed in the following paragraphs.

Mass sorption isotherms for CO_2 in polysiloxanes have been reported by several workers [28–30]. Of these only the report by Strubinger *et al.* [28] provides data for the CO_2–SE-30 system at temperatures and pressures of interest in SFC. Their data for 40 and 50°C at pressures up to 160 bar are presented in Fig. 2 in terms of reduced density as the independent variable. Both sets of data exhibit a maximum around the critical density, a phenomenon also observed by Yonker and Smith [29] for the CO_2–SE-54 system. At high densities, all curves (including the isotherm for 35°C, not shown) converge to a value of $\phi = 0.26$. These phenomena, especially the occurrence of maxima, are not well understood. Yonker and Smith have suggested that surface adsorption may play a significant role in these systems. One possible explanation is that both absorption and adsorption occur, where the sorption of CO_2 occurs largely by *absorption*, as represented by the solid line in Fig. 2, and the excess sorption is due to *adsorption*, leading to the maxima observed around the critical density. Whatever the case, the situation poses some uncertainty with regard to the effect of ϕ on D_s. For the purpose of the application of eqn. 19 to the model, then, let us choose the simple case represented by the solid line in Fig. 2, where

$$\phi = 2\rho_R\phi_{max} \qquad (\rho_R \leqslant 0.5) \quad (20a)$$

$$\phi = \phi_{max} \qquad (\rho_R > 0.5) \quad (20b)$$

For the CO_2–polysiloxane system, we set $\phi_{max} = 0.26$ for all temperatures.

Next we examine the value of D_a^m in eqn. 19. D_a^m in this case represents the solute diffusion coefficient in the mobile phase at a density corresponding to the specific volume of the mobile phase component in the swollen stationary phase. Strubinger *et al.* [28] have shown that the specific volume of CO_2 in SE-30, $\hat{V}_1^L$, is about 1.1 cm^3/g at low values of pressure and ϕ, but that it increases significantly at increased pressure. This is a result of the fact that, while the amount of CO_2 sorbed reaches a maximum at high pressures (Fig. 2), the swelling factor increases continuously as pressure is increased (Fig. 1). In our model, the value of $\hat{V}_1^L$ can be calculated from the relation

$$\hat{V}_1^L = \frac{SF(1 - \phi)}{\phi\rho_s^0} \quad (21)$$

where ρ_s^0 is the density of the pure stationary phase [27]. The value of D_a^m used in eqn. 19 is then calculated from the modified Wilke–Chang equation (as D_a in eqn. 14) at a CO_2 reduced density of

$$\rho_R = \frac{1}{\hat{V}_1^L\rho_{cr}} \quad (22)$$

The critical density of CO_2, ρ_{cr}, is taken as 0.468 g/cm^3.

The net effect of SF and ϕ on D_s is shown in Fig. 3 for C_{24} at 40°C. The model predicts that D_s increases more than ten-fold as CO_2 density is increased from $\rho_R = 0$ to $\rho_R = 0.5$. While ϕ is assumed to be constant above $\rho_R = 0.5$, D_s continues to increase

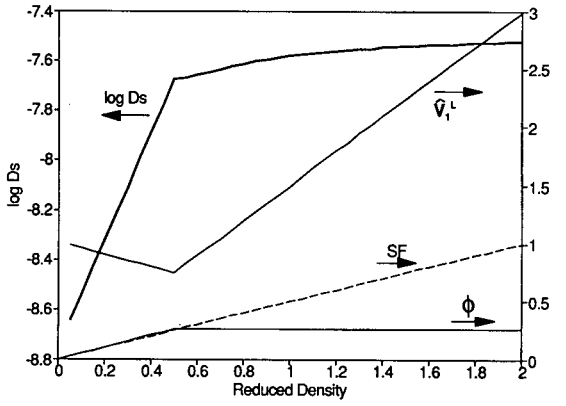

Fig. 3. Effect of stationary phase swelling on diffusivity. Predictions of the model for n-$C_{24}H_{50}$ at 40°C.

slightly due to continued swelling of the stationary phase. The value of $\hat{V}_1^L$ decreases from 1.0 to 0.8 at $\rho_R < 0.5$, in reasonably good agreement with the value of 1.1 predicted by Strubinger *et al.* [28], and then rises continuously as density increases due to the combined effects of a continuously increasing SF while ϕ remains constant. The negative slope at low densities is an artifact of the treatment, arising from a somewhat inexact description of the swelling behavior.

There is a substantial difference between this system and those treated by Fujita. In the latter systems the penetrants were condensed phases such as benzene at room temperature, for which the partial molar volume of the penetrant inside the polymer is assumed to be equal to the bulk liquid value. For the CO_2–polysiloxane system, the specific volume of CO_2 rises dramatically for $\rho_R > 0.5$. The treatment here accounts for this by adjusting the value of D_b in eqn. 19, so that even though ϕ is assumed constant at $\rho_R > 0.5$, log D_s continues to increase with ρ_R at a moderate rate. However, the large increase in $\hat{V}_1^L$ at $\rho_R > 0.5$ suggests a loosening of the cross-linked polymer network, which would further enhance diffusion in the swollen polymer. Even though the present treatment predicts substantial increases in D_s at low mobile phase densities, it may in fact severely underestimate the values of D_s at higher densities.

COMPUTATIONAL APPROACH

The calculation of temporal and spatial average quantities has been described elsewhere [12,13]. Computations were performed on an IBM-compatible personal computer with an Intel 80386 microprocessor and 80387 math coprocessor, using an extension of a program written in Microsoft QuickBASIC for modelling retention and efficiency of packed columns [15].

A Van Deemter plot is typically prepared by measuring apparent plate height as a function of velocity while maintaining other conditions constant so that, among other things, $\hat{k}'$ does not vary with flow-rate. This is not possible in SFC because k' varies along the column. However, at low pressure drops $\hat{k}'$ is approximately a quadratic function of $<\rho>_t$ [12]

$$\ln \hat{k}' = \ln <k'>_t \approx \ln k'^0 - a<\rho_R>_t + b<\rho_R>_t^2 \quad (23)$$

In order to obtain results at constant $\hat{k}'$, at least in the low velocity, low pressure-drop region, all measurements should be done at the same temporal average density. Results obtained in this fashion may be compared with results obtained for non-compressible fluids.

The basic computational approach therefore mimics a series of isothermal SFC experiments for the elution of a pair of n-alkanes in which the mass flow-rate, which is held constant for a given experiment, is incremented while maintaining the same temporal average mobile phase density for all experiments. This is done for $<\rho_R>_t$ = 1.0, 1.2, 1.4, 1.6 and 1.8, at temperatures of 40, 80 and 120°C. The result is a set of Van Deemter plots, each corresponding to a single temperature and temporal average density. All calculations for this study were done for an open-tubular column of 30 m × 50 μm I.D. with a 0.25-μm thick film of stationary phase. For successive experiments, the mass flow-rate is increased by simultaneously increasing the inlet pressure and decreasing the outlet pressure so that the selected temporal average density is maintained. This approach yields Van Deemter plots which, at low flow-rates, are similar to those traditionally produced for liquid or gas chromatography.

PREDICTIONS OF THE MODEL

Mobile phase density, velocity and pressure

The inlet and outlet pressures required to achieve

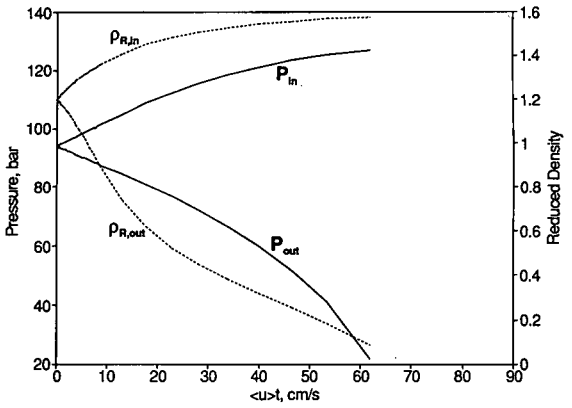

Fig. 4. Pressure and reduced density at column inlet and outlet for CO_2 at 40°C and $<\rho_R>_t$ = 1.2. Column: open-tubular, 30 m × 50 μm I.D. × 0.25 μm film, SB-octyl stationary phase. Dashed lines are plotted against right axis.

desired flow-rates while maintaining the same temporal average density are shown in Fig. 4 for $<\rho_R>_t$ = 1.2 at 40°C. Values of the corresponding inlet and outlet reduced densities (dashed curves) are plotted against the right axis. In general, the curves for low temperature (40°C) and low density showed a non-linearity similar to that in Fig. 4, whereas at higher temperatures and densities the curves were more linear. Fig. 4 demonstrates that simply maintaining the same average column pressure while adjusting the flow-rate will not in general result in maintaining the same temporal average density.

Effect of temperature, density and solute on efficiency

Fig. 5 shows a family of curves for apparent plate

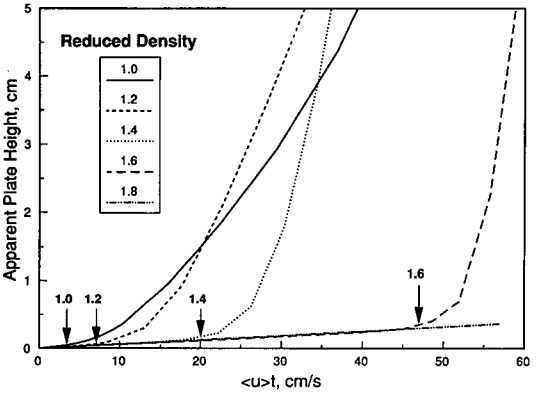

Fig. 5. Apparent plate height *vs.* temporal average linear velocity at various mobile phase densities for C_{16} at 40°C.

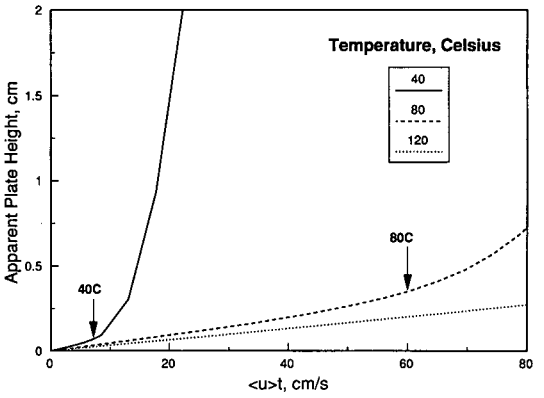

Fig. 6. Apparent plate height *vs.* temporal average linear velocity at different temperatures for C_{16} at $<\rho_R>_t$ = 1.2.

height *vs.* temporal average linear velocity, $<u>_t$, for C_{16} at 40°C and various mobile phase densities. The curves at lower $<\rho_R>_t$ show significant loss of efficiency as the linear velocity is increased. These curves are similar to those reported elsewhere [1,15, 17]. Extremely large plate height values are observed at high velocities, especially at low mobile phase densities. The arrows identify the onset of GIBS (see below).

The effect of temperature on $\hat{H}$ for elution of C_{16} at $<\rho_R>_t$ = 1.2 is shown in Fig. 6. At elevated temperatures it should be possible to operate at much higher velocities before GIBS becomes a significant problem. This is due to the decreased compressibility of CO_2 at the higher temperatures.

The effect of solute on $\hat{H}$ at 40°C and $<\rho_R>_t$ =

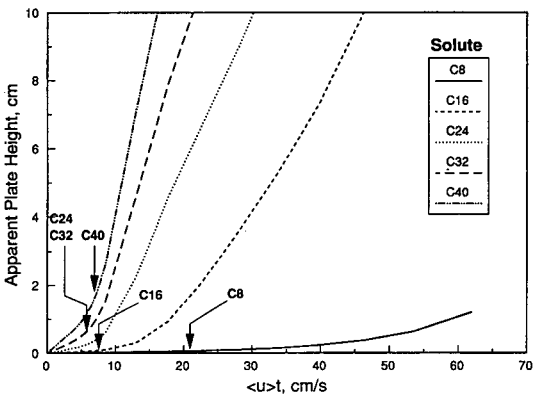

Fig. 7. Apparent plate height *vs.* temporal average linear velocity for five *n*-alkanes at 40°C and $<\rho_R>_t$ = 1.2.

1.2 is shown in Fig. 7. Severe losses in efficiency occur for the long-chain alkanes at even moderate velocities. These systems are examined in greater detail below.

Contribution of gradient-induced band spreading to apparent plate height

The loss of efficiency at higher velocities in Figs. 5–7 is attributable to the presence of solute velocity gradients [15]. These gradients arise from the expansion of the mobile phase and the corresponding increases in mobile phase velocity and solute capacity factor as the solute band travels along the column. An estimate of the relative contribution of this effect to the overall dispersion can be obtained by examination of the following terms:

(i) the reduced plate height assuming density is constant at $<\rho_R>_t$ with no swelling

$$h_{set} = \frac{2}{v_{set}} + \frac{v_{set}(1 + 6k'_{set} + 11k'^2_{set})}{96(1 + k'_{set})^2} + \frac{2v_{set}D_{mset}(d_f^0)^2k'_{set}}{3D_s^0(d_c^0)^2(1 + k'_{set})^2} \quad (24)$$

(ii) the reduced plate height assuming constant conditions at $k' = <k'>_t$ with no swelling

$$h_{est} = \frac{2}{v_{set}} + \frac{v_{set}(1 + 6<k'>_t + 11<k>'^2_t)}{96(1 + <k'>_t)^2} + \frac{2v_{set}D_{mset}(d_f^0)^2<k'>_t}{3D_s^0(d_c^0)^2(1 + <k'>_t)^2} \quad (25)$$

(iii) the reduced plate height assuming mobile phase GIBS with no swelling

$$h_{set2} = \frac{1}{<1 + k'>_t^2 <\rho_R>_z}\left[\frac{2}{v_{set2}}<(1 + k')^2\rho_R>_t + \frac{v_{set2}}{96}<(1 + 6k' + 11k'^2)\rho_R>_t + \frac{2v_{set2}(d_f^0)^2}{3D_s^0(d_c^0)^2}<D_m\rho_R k'>_t\right] \quad (26)$$

The subscript "set" sets the corresponding mobile phase parameter to its value at a reduced density equal to $<\rho_R>_t$, and the superscript "0" sets the stationary phase parameter to its value in the absence of swelling. The subscript "set2" indicates that the mobile phase parameters are allowed to vary, but the stationary phase parameters are constant with no swelling. Both h_{set} and h_{est} are estimates of the reduced plate height which would be obtained in the absence of GIBS and stationary phase swelling, *i.e.*, all column parameters are constant. These two terms differ only in that h_{set} employs k'_{set}, whereas h_{est} employs $<k'>_t$ as the value of the capacity factor. h_{set2} provides an estimate of the apparent plate height which would be observed due to mobile phase GIBS only, with no swelling of the stationary phase.

The dependence of $\hat{h}$, h_{est}, h_{set}, h_{set2} and $<k'>_t$ on reduced velocity is shown in Fig. 8 for the elution of C_{16} at 40°C and $<\rho_R>_t = 1.2$. [*Note. To facilitate comparison with other figures, the point at which* $<u>_t = 5$ *cm/s is indicated in Figs. 8–10. The relationship between* $<u>_t$ *and* $<v>_t$ *may be taken as approximately linear.*] At $<v>_t = 2900$, $\hat{h}$ reaches a value of 5000, about 50 times greater than h_{set}, and about 18 times greater than h_{est}. In contrast, h_{set2} is essentially identical to $\hat{h}$ over the entire range of velocities, indicating that the increased band spreading (relative to h_{set} or h_{est}) is due almost entirely to mobile phase GIBS. For this system, then, GIBS is by far the major contribution to dispersion at high velocities for this system, and essentially all of the GIBS is due to changes in the mobile phase.

An estimate of the onset of GIBS is given by the ratio of h_{set2} over h_{set} or by h_{set2} over h_{est}. The point at which the ratio h_{set2}/h_{est} exceeds 1.1 is marked by an arrow on each of the curves in Figs. 5–7. The onset of GIBS occurs at higher velocities as $<\rho_R>_t$

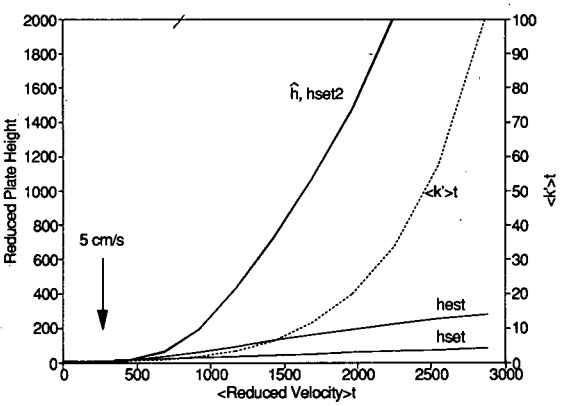

Fig. 8. Estimates of reduced plate height for elution of C_{16} at 40°C and $<\rho_R>_t = 1.2$. Dashed line is plotted against right axis.

is increased (Fig. 5). Higher operating temperatures also increase the velocity for onset of GIBS (Fig. 6). Fig. 7 shows that GIBS occurs at roughly the same velocity for C_{16}–C_{40} at 40°C and $<\rho_R>_t = 1.2$, but at a significantly higher velocity for C_8.

Contributions from the individual plate height terms

Under conditions of laminar flow, the apparent reduced plate height in open-tubular chromatography is the sum of three terms,

$$\hat{h} = \hat{h}_l + \hat{h}_m + \hat{h}_s \quad (27)$$

where the subscripts l, m, and s refer, respectively, to longitudinal diffusion in the mobile phase, radial mixing in the mobile phase, and resistance to mass transfer in the stationary phase. A plot of the apparent reduced plate height *vs.* $<v>_t$ for C_{16} at 40° and $<\rho_R>_t = 1.2$ appears in Fig. 9, along with h_{set} and $<k'>_t$. At high reduced velocities, where $\hat{h} \gg h_{set}$, the total dispersion is due almost entirely to the mobile phase mixing term $\hat{h}_m$; the $\hat{h}_l$ and $\hat{h}_s$ terms are insignificant and are not visible in the figure. This is true also at the lower velocities, and in general for C_{16} at other temperatures and densities. A much different result is obtained for C_{32} at 40°C and $<\rho_R>_t = 1.4$ (Fig. 10). At reduced velocities below 1500, $\hat{h}_s$ is the dominant term. At higher velocities $\hat{h}_m$ becomes the dominant term because of the onset of GIBS, and $\hat{h}_s$ decreases because of the increase in capacity factor.

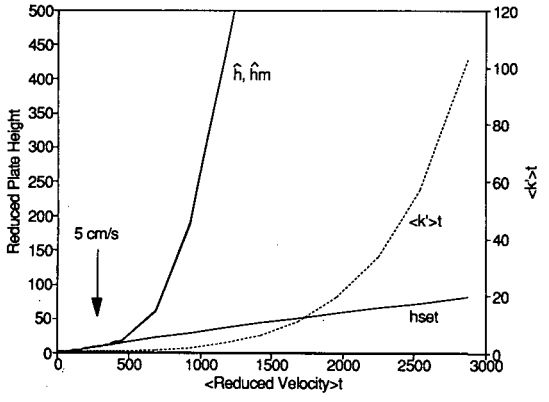

Fig. 9. Contributions of individual plate height terms to apparent reduced plate height for C_{16} at 40°C and $<\rho_R>_t = 1.2$. The $\hat{h}_l$ and $\hat{h}_s$ terms are too small to be seen. The h_{set} curve shows expected efficiency in absence of GIBS and swelling. Dashed line is plotted against right axis.

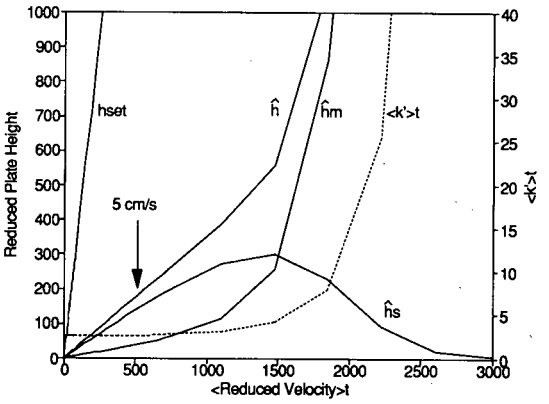

Fig. 10. Contributions of individual plate height terms to apparent reduced plate height for C_{32} at 40°C and $<\rho_R>_t = 1.4$. Dashed line is plotted against right axis.

Effects of temperature and swelling on the stationary phase term

Note that the h_{set} term for C_{32} in Fig. 10 is much larger than the apparent plate height. This large value of h_{set} is due to the stationary phase term, resulting from a very small predicted value of D_s^0 for C_{32} at this temperature [27]. The true magnitude of the stationary phase term at low temperatures is somewhat questionable because the value of D_s^0 used represents an extrapolation of the experimental data obtained by Kong and Hawkes. Normally in gas chromatography the stationary phase term for C_{32} would be much smaller due to the higher temperatures used and better diffusivity in the stationary phase; at lower temperatures poor diffusion in that stationary phase would be a problem even if reasonable retention times could be obtained. These predictions of the model suggest that the sorption of mobile phase by stationary phase, and the attendant swelling which results, may be largely responsible for the achievement of acceptable efficiency in the separation of high-molecular-mass solutes at low temperatures by SFC.

Retention time and resolution

Retention time and resolution are two parameters which are of great practical importance in chromatography. Other parameters held constant, a decrease in retention time produced by an increase in flow-rate is generally obtained at the expense of decreased resolution. The extremely large values of

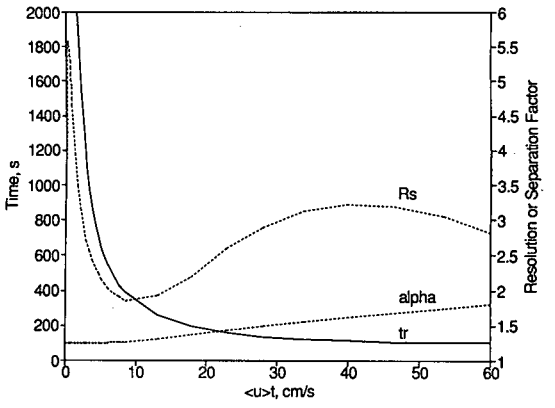

Fig. 11. Retention time for C_9 and its resolution from C_8 at 40°C and $<\rho_R>_t$ = 1.2. Symbols: tr = retention time; alpha = separation factor; Rs = resolution. Dashed lines are plotted against right axis.

apparent plate height due to GIBS which are generated at high velocities in SFC strongly suggest that one should avoid large pressure drops in SFC. However, the data presented in Fig. 11 show that it should be possible to simultaneously reduce the retention time and improve resolution by increasing the flow-rate. Fig. 11 shows the predicted retention time for C_9 and its resolution from C_8 for their elution at 40°C and $<\rho_R>_t$ = 1.2. The resolution was calculated using eqn. 13. Two maxima appear in the R_s *vs.* $<u>_t$ curve; one as expected at very low velocity (R_s = 5.5 at $<u>_t$ = 0.35 cm/s, t_r = 2.7 h, barely visible near the origin), and the other at a very high velocity (R_s = 3.2 at $<u>_t$ = 40 cm/s, t_r = 110 s). The latter resolution is also obtained at $<u>_t$ = 2.0 cm/s with t_r = 1700 s, or about 28 min. The second resolution maximum occurs under conditions where GIBS is the dominant source of dispersion and the apparent reduced plate height is greater than 100 (Fig. 12). This unusual behavior is produced by the simulated experimental conditions (see Computational approach section), and appears to be due to an increase in the separation factor, α, at high velocities, also shown in Fig. 11. The separation factor is defined [13]

$$\alpha = \hat{k}'_2/\hat{k}'_1; \qquad \hat{k}'_2 > \hat{k}'_1 \tag{28}$$

While $\hat{k}'$ for C_9 increases at high flow-rates, it increases somewhat less rapidly for C_8, leading to the increased separation factor and the improved resolution at high flow-rates. As the velocity increases beyond 40 cm/s, α continues to increase, but resolution decreases due to the overwhelming effect of GIBS. Resolution curves with two maxima were observed for other solutes and at other conditions in this study, but in most cases the rapid increase in GIBS prevented significant improvements in resolution at high velocities. This example does however point out the possibility of performing very rapid separations by using large pressure drops and flow-rates in SFC.

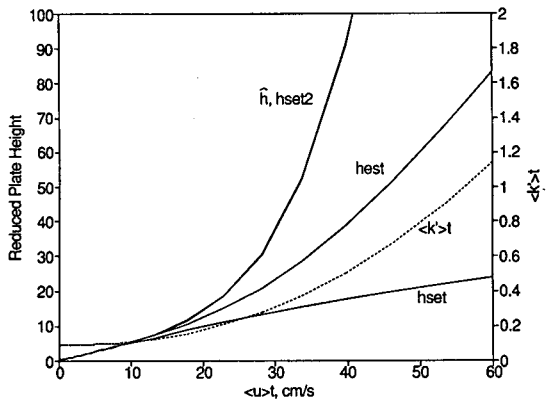

Fig. 12. Estimates of reduced plate height for elution of C_9 at 40°C and $<\rho_R>_t$ = 1.2. Dashed line is plotted against right axis.

CONCLUSIONS

This model takes into account recently developed theories for retention and efficiency, as well as the observed effects of temperature and mobile phase density on system parameters, to produce realistic predictions of retention, efficiency and resolution in open-tubular SFC. The excessive band spreading often observed at high pressure drops, or GIBS, is due primarily to mobile phase processes. The maximum pressure drop and linear velocity which can be used before GIBS becomes significant depends on a combination of temperature, temporal average density and solute. In general, GIBS may be largely avoided by working at densities and temperatures well above the critical values. Sorption of mobile phase by the stationary phase appears to be critical to the achievement of acceptable efficiency in the separation of high-molecular-mass solutes at the

low temperatures commonly used in SFC, due to the improved solute diffusivity in the swollen stationary phase. However, a better understanding of the effect of swelling on diffusivity is required to accurately predict the magnitude of the effect. Finally, the effect of density drop on separation factor has the potential to make possible very fast separations by SFC.

ACKNOWLEDGEMENTS

The author thanks Rebecca Riester of Georgetown University for supplying experimental retention data, and appreciates the useful discussions with Daniel Martire of Georgetown University and Tim Lodge of the University of Minnesota, Twin Cities. Support for this work was provided through a Grant-in-Aid of Research from the Graduate School of the University of Minnesota. The basic theoretical work was initiated while the author was on sabbatical leave at Georgetown University with support from the Bush Sabbatical Program of the University of Minnesota, and the National Science Foundation grant number CHE-8902735.

REFERENCES

1 P. A. Mourier, M. H. Caude and R. H. Rosset, *Chromatographia*, 23 (1987) 21.
2 P. J. Schoenmakers and L. G. M. Uunk, *Chromatographia*, 24 (1987) 51.
3 T. A. Berger and J. F. Deye, *Chromatographia*, 30 (1990) 57.
4 H. Engelhardt, A. Gross, R. Mertens and M. Petersen, *J. Chromatogr.*, 477 (1989) 169.
5 D. R. Gere, R. Board and D. McManigill, *Anal. Chem.*, 54 (1982) 736.
6 T. A. Dean and C. F. Poole, *J. Chromatogr.*, 468 (1989) 127.
7 B. P. Semonian and L. B. Rogers, *J. Chromatogr. Sci.*, 16 (1978) 49.
8 P. A. Peaden and M. L. Lee, *J. Chromatogr.*, 259 (1983) 1.
9 S. M. Fields, R. C. Kong, J. C. Fjelstad, M. L. Lee and P. A. Peaden, *J. High Resolut. Chromatogr. Chromatogr. Commun.*, 7 (1984) 312.
10 D. E. Martire and R. E. Boehm, *J. Phys. Chem.*, 91 (1987) 2433.
11 D. E. Martire, *J. Liq. Chromatogr.*, 10 (1987) 1569.
12 D. E. Martire, *J. Chromatogr.*, 461 (1989) 165.
13 D. E. Martire, R. L. Riester, T. J. Bruno, A. Hussam and D. P. Poe, *J. Chromatogr.*, 545 (1991) 135.
14 X. Zhang, D. E. Martire and R. G. Christiansen, Georgetown University and National Institute for Science and Technology, Washington, DC, 1990, unpublished results.
15 D. P. Poe and D. E. Martire, *J. Chromatogr.*, 517 (1990) 3.
16 J. C. Giddings, *Dynamics of Chromatography*, Marcel Dekker, New York, 1965, pp. 79–82.
17 H.-G. Janssen, P. J. Schoenmakers, H. M. J. Snijders, J. A. Rijks and C. A. Cramers, *J. High Resolut. Chromatogr.*, 14 (1991) 438.
18 L. M. Blumberg and T. A. Berger, *J. Chromatogr.*, 596 (1992) 1.
19 R. Riester and D. E. Martire, Georgetown University, Washington, DC, 1991, unpublished results.
20 R. C. Reid, J. M. Prausnitz and B. E. Poling, *The Properties of Liquids and Gases*, McGraw-Hill, New York, 4th ed., 1987.
21 I. Swaid and G. M. Schneider, *Ber. Bunsenges. Phys. Chem.*, 83 (1979) 969.
22 R. Feist and G. M. Schneider, *Sep. Sci. Technol.*, 17 (1982) 261.
23 Z. Balenovic, M. N. Myers and J. C. Giddings, *J. Chem. Phys.*, 52 (1970) 915.
24 S. R. Springston, P. David, J. Steger and M. Novotny, *Anal. Chem.*, 58 (1986) 997.
25 J.-J. Shim and K. P. Johnston, *AIChE J.*, 35 (1989) 1097.
26 H. Fujita, *Fortschr. Hochpolym.-Forsch.*, 3 (1961) 1.
27 J. M. Kong and S. J. Hawkes, *J. Chromatogr. Sci.*, 14 (1976) 279.
28 J. R. Strubinger, H. Song and J. F. Parcher, *Anal. Chem.*, 63 (1991) 98.
29 C. R. Yonker and R. D. Smith, *J. Chromatogr.*, 505 (1990) 139.
30 G. K. Fleming and W. J. Koros, *Macromolecules*, 19 (1986) 2285.

Journal of Chromatography, 625 (1992) 311–321
Elsevier Science Publishers B.V., Amsterdam

CHROM. 24 503

Universal set-up for measurement of diffusion coefficients in supercritical carbon dioxide with flame ionization detection

Karel Janák*, Ingela Hägglund and Lars G. Blomberg

Department of Analytical Chemistry, University of Stockholm, Arrhenius Laboratory, S-106 91 Stockholm (Sweden)

Agneta K. Bemgård and Anders L. Colmsjö

Department of Analytical Chemistry, National Institute of Occupational Health, S-171 84 Solna (Sweden)

(Received May 7th, 1992)

ABSTRACT

Improvements to the chromatographic apparatus for diffusivity measurements in supercritical carbon dioxide with flame ionization detection have been designed and evaluated. Modifications concerned the injection with partial solvent evaporation in the injector loop, separation of solutes and solvent in a short precolumn coated with a thin film of PS 264 stationary phase, and a back-pressure device. Diffusion coefficients of C_{15}–C_{18} *n*-alkanes, dodecanone, pentadecanone, methyl myristate and biphenyl in supercritical carbon dioxide at 100°C and 125°C at 100 atm were determined. The method of optimization of D_g to a plot of H *vs.* v was evaluated for the estimation of diffusion coefficients. The estimated diffusion coefficients have been compared with the average diffusion coefficients and diffusion coefficients calculated from the Wilke–Chang equation. Relatively good agreement of measured diffusion coefficients and those calculated from the modified Wilke–Chang equation has been obtained for biphenyl and polar solutes.

INTRODUCTION

During the past decade, supercritical fluid chromatography (SFC) has been developed as a widely accepted analytical separation method, which complements gas chromatography and high-performance liquid chromatography. A large number of applications [1,2] have been described. However, interactions of the solute with the supercritical mobile phase and the stationary phase, swollen with the mobile phase, are not yet fully understood [3,4]. It is believed that diffusion in the mobile phase has a decisive influence on band broadening in SFC [5]. Knowledge of the diffusion in supercritical fluids may be useful also in areas other than SFC, such as supercritical fluid extraction and in industrial supercritical processes, *e.g.*, polymer fractionation and/or impregnation. Regardless of the many publications devoted to diffusivity measurements in supercritical fluids [6–24], diffusion data in the literature are still scarce and, often, inaccurate. Further, mathematical models for the prediction of diffusion coefficients are known to be unreliable in the region around the critical point [25]. The present state of diffusion and thermodynamic measurements by SFC has recently been reviewed [26].

The Taylor dispersion technique, also known as the chromatographic band-broadening method, has been applied to diffusion measurements in supercritical fluids. Measurements are based on the

Correspondence to: Dr. L. G. Blomberg, Department of Analytical Chemistry, University of Stockholm, Arrhenius Laboratory, S-106 91 Stockholm, Sweden.

* On leave from Institute of Analytical Chemistry, Czechoslovak Academy of Sciences, 611 42 Brno, Czechoslovakia.

0021-9673/92/$05.00

dispersion of a narrow concentration pulse in a fully developed laminar flow of the supercritical mobile phase through a tube of circular cross-section. Although the mathematical treatment is relatively complete [27–30], the experimental measurements are subject to many errors. These errors originate from non-ideal behaviour of the system, such as (1) non-zero width of the pulse at the tube inlet, (2) extra-column band broadening, (3) solute–solvent interactions, if the injected solute is dissolved in a solvent, (4) solute adsorption on the inner walls of the diffusion tube, (5) density changes due to the pressure drop along the diffusion tube, (6) coiling-induced secondary flow within the tube, and (7) concentration dependence of the diffusion coefficient.

The first diffusivity measurements in supercritical carbon dioxide were done by Swaid and Schneider [6]. Since that time, much effort has been devoted to the development of instrumentation for the determination of binary diffusion coefficients in supercritical fluids. Dahmen *et al.* [22] applied a subtraction method, originally proposed by Giddings and Seager [31]. In this method, the effects of the initial variance of the solute and of dead volume on peak broadening are eliminated. A symmetrical initial band of the solute, eluted from a short precolumn, was recorded with a UV detector. The observed variance was subtracted from the variance measured when the solute had passed the diffusion tube. This method is limited to UV-detectable solutes and necessitates the use of two UV detectors with identical time constants and dead volumes. The influence of extra-column band broadening has, in many cases, been decreased by the use of diffusion tubes with large volumes, and/or by the application of an off-line subtraction method, in which two diffusion tubes of different lengths are used [6]. The latter method can, however, give inaccurate data, as the dead volumes of the connections must be absolutely identical in both cases [32].

Some authors studied the effect of the solvent used for solute injection into the diffusion tube on the measurements of diffusion coefficients [9,19,20]. However, no solvent effect on the solute diffusion coefficients in supercritical CO_2 was observed [9,19, 20,22]. Olesik *et al.* [33] recommended injection of the pure compound in the supercritical fluid in order to obtain exact binary diffusion coefficients. When a solvent is used, interdiffusion coefficients of a solute in an undefined mixture of supercritical fluid and solvent are being measured; dissolution of the sample in the mobile phase can be achieved in an extraction cell [33].

The effect of solute adsorption is reduced with increasing tube diameter and solute concentration [11]. However, its presence can be easily recognized by the appearance of asymmetric peak shapes; it is difficult to avoid adsorption in SFC when the aim is the measurement of solute diffusion coefficients at a broad density interval. Recently, a method for the determination of solute diffusion coefficients in gases from diffusivity measurements affected by solute adsorption has been described [34].

A pressure drop in the column results in a drop in both density and viscosity. The diffusion coefficient of the solute in a supercritical mobile phase, D_m, is affected by density and viscosity, so that the term $D_m v^{-1}$, where v is the kinematic viscosity, is constant at high densities. As the changes of v^{-1} at pressures above 100 atm are small [35], D_m should be changed only slightly. In SFC with open tubular columns, the pressure drop under typical conditions is quite small [35]. The pressure drop in wide-bore tubes used for diffusivity measurements does not exceed 1 atm and can be neglected.

Under certain conditions ($De^2\ Sc > 100$, where De and Sc are the Dean and Schmidt numbers, respectively), the peak variance is affected by the column coiling, which causes secondary flow effects [36]. This can easily be avoided if mobile phase velocities are used that are lower than the maximum calculated for the column diameter and coiling radius.

Recently, a method for processing the data obtained from diffusivity measurements in gas chromatography has been published [34]. For the evaluation of the band broadening in a diffusion tube, possible contributions from solute adsorption on the column wall, extra-column band broadening and non-laminar flow effects have been included. Thus, the height equivalent to the theoretical plate (H) can be expressed as:

$$H = 2D_{g0}f_1/v_0 + r^2 f_1 v_0/(24D_{g0}) + G_a f_2 v_0 + D(f_2 v_0)^2 \quad (1)$$

where D_{g0} is the diffusion coefficient in the gas phase

at the outlet pressure, v_0 is the carrier gas velocity at the outlet of the tube, r is the tube radius and f_1 and f_2 are pressure drop factors. The first two terms describe ideal band broadening in a diffusion tube due to actions of the molecular diffusion and the parabolic velocity profile. The effects of a v_0-dependent adsorption and non-laminar flow are expressed by the C_a term, and the diffusion-independent extra-column band broadening contributes to H as the D term. An optimization programme has been used by means of a least-squares fit of the measured values (H_i, v_{0i}) to eqn. 1. Making a number of assumptions, D_{g0}, C_a and D have been estimated [34]. For low pressure drops, *i.e.*, f_1 and f_2 approach unity, the outlet velocity can be replaced by the average mobile phase velocity, and the diffusion coefficient at outlet pressure can be replaced by the average binary diffusion coefficient, D_g. Eqn. 1 becomes:

$$H = 2D_g/v + r^2v/(24D_g) + C_av + D(v)^2 \quad (2)$$

If v approaches zero, then the last two terms of eqn. 2 approach zero and the diffusion coefficient in mobile phase can be calculated from eqn. 3 as if no adsorption and/or extra-column effects occurred:

$$D_g = L/(4t_r)[H \pm \sqrt{H^2 - (r^2/3)}] \quad (3)$$

where L/t_r is the average mobile phase velocity in the column.

It seems that chromatographic measurements at low mobile phase velocities are preferable for the determination of diffusion coefficients, although the effects that decrease the accuracy of the determination of diffusion coefficients, as mentioned above, become in most cases negligible at such velocities.

Attention must, however, be paid to the diffusion-dependent extra-column band broadening, originating from the injector and couplings. Although this has been proven to be negligible in GC [32], the contribution in SFC can be significant owing to the much lower diffusion coefficients in the mobile phase.

Instrumentation for diffusivity measurements in supercritical fluids should, for a given inlet pressure, provide a means for convenient changes of the mobile phase velocity. As the flow of mobile phase in SFC is controlled by a restrictor, a back-pressure device, regulating the pressure drop over the restrictor, has been used to adjust the mobile phase velocity [26]. Back-pressure devices compatible with post-restrictor detection usually consist of a system of linear restrictors [24]. Back-pressure can be applied either by compressed gas from a tube or by carbon dioxide from a second syringe pump. Other devices, such as a high-pressure sheath-flow nozzle [38] and a back-pressure regulator based on a low-dead-volume high-speed switching solenoid valve [39], have not been proven to be suitable for flame ionization detection (FID).

This paper describes improvements to the apparatus for diffusivity measurements in supercritical carbon dioxide with FID. Average mobile phase diffusion coefficients were calculated from chromatographic data obtained at low mobile phase velocities. The method of optimization of D_g to a plot of H *vs.* v was further evaluated for an estimation of diffusion coefficients in supercritical carbon dioxide.

EXPERIMENTAL

Instrumentation

A schematic diagram of the apparatus is shown in Fig. 1. A Suprex SFC/200A supercritical fluid chromatograph (Pittsburgh, PA, USA) was equipped with a pneumatically actuated Valco injection valve (Model CI4W, Valco Instruments, Houston, TX, USA) with a 0.06-μl internal loop. The waste line of the injector was equipped with a piece of fused-silica capillary tubing (0.10 m × 50 μm I.D.) (Polymicro Technologies, Phoenix, AZ, USA). A short precol-

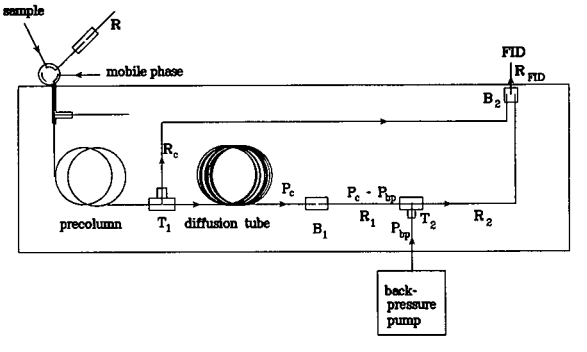

Fig. 1. Schematic diagram of the apparatus for the measurement of diffusion coefficients. R_c, R_1, R_2 and R_{FID} are restrictors, T_1 and T_2 are T-pieces, B_1 is a low-dead-volume butt connector, and B_2 is an outlet splitter.

umn coated with methylpolysiloxane PS-264 (Fluka, Buchs, Switzerland) (0.55 m × 259 μm I.D., d_f = 0.18 μm, or 1.50 m × 50 μm I.D., d_f = 0.24 μm) was connected at one end to the injection valve via a flow-splitter, the other end being connected to a linear restrictor R_c (0.20 m × 11 μm I.D.) and to the diffusion tube (25.01 m × 259 μm I.D.) with a coiling radius of 65 mm, via a low-dead-volume ZT.5 Valco T-piece (Valco Instruments). The mobile phase velocity was controlled by a variable-flow restrictor R_1 (0.50 m × 21 μm I.D.), which was connected to a feeding capillary from a back-pressure μLC-500 micropump (Isco, Lincoln, NE, USA) and restrictor R_2 (0.50 m × 21 μm I.D.) via another ZT.5 Valco T-piece. The variable-flow restrictor R_1 was coupled to the diffusion tube using a low-dead-volume butt connector MVSU 004 (SGE, Austin, TX, USA). The mobile phase flows issuing from restrictors R_c and R_2 were combined using a low-dead-volume VSOS outlet splitter (SGE) into a restrictor R_{FID} (21 μm I.D.) ending in the jet of the flame ionization detector. The chromatograph was connceted to an ELDS 900 laboratory data system (Chromatography Data Systems, Kungshög, Stenhamra, Sweden).

Diffusivity measurements

A solution of one to three solutes in pentane, 10 mg/ml, was injected on the precolumn at 40°C by partial evaporation of the solvent in the internal loop of the injector. The loop was washed out with the sample and the syringe was withdrawn, thus allowing evaporation through the injector inlet. After a delay of 30–60 s, the injection was carried out using a 50–100 ms injection period and a split ratio of 1:4 to 1:6. The mobile phase velocity, 4–20 mm/s, was adjusted by the back-pressure of supercritical carbon dioxide. Each solute was injected three to five times under the same conditions, the time between two injections being chosen so that overlapping of the peaks from the precolumn and the diffusion tube was avoided. After alteration of the test parameters, an equilibration time of 30 min was sufficient to attain stable conditions. The diffusivity measurements were performed for C_{15}–C_{18} *n*-alkanes, dodecanone, pentadecanone, methyl myristate and biphenyl at 100 atm and at 100°C and 125°C.

Data handling

Chromatograms were registered at 3.03 Hz, and FID chromatograms were obtained first from the precolumn and then after the precolumn and the diffusion tube. Band broadening arising from the diffusion tube was estimated by computerized subtraction of the square of the peak width at half height from the precolumn from the square of the peak width at half height after the precolumn and diffusion tube. The HETP was then calculated from the estimated peak width at half height, and the binary diffusion coefficients corresponding to each mobile phase velocity were calculated by use of eqns. 2 and 3.

RESULTS AND DISCUSSION

Instrumentation

The requirement of generally applicable, accurate measurements of binary diffusion coefficients in supercritical carbon dioxide made some modifications of the chromatograph necessary. These modifications concerned the injection, the separation of solute(s) and solvent, and the back-pressure device.

The on-line subtraction procedure was modified by use of a small precolumn for the separation of solute and solvent. In general, this is not a problem [40,41], but for diffusivity measurements, band broadening in the precolumn must be very low,

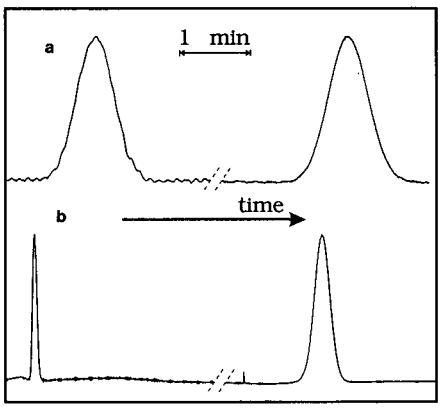

Fig. 2. SFC-FID chromatograms of pentadecane. On-line elution of the solute from (a) a precolumn (4.50 m × 250 μm I.D.) coated with PS 264 stationary phase, d_f = 1.57 μm, and (b) a precolumn (1.50 m × 50 μm I.D.) coated with PS 264 stationary phase, d_f = 0.24 μm, and a diffusion tube (25.01 m × 259 μm I.D.). Temperature, 100°C; pressure, 100 atm.

otherwise the accuracy of the measurements will be decreased. Thus, the attempt to use a thick-film precolumn (4.50 m × 250 μm I.D., d_f = 1.57 μm) failed (Fig. 2a). Even when the length of the precolumn was only one fifth of that of the diffusion tube, it can be seen from the comparison of the peak widths from the precolumn and from the total bandwidth in Fig. 2a, that the precolumn contributed more to the total bandwidth than the diffusion tube. In addition to the diffusion in supercritical fluids, other factors (excluding extra-column effects) contributing to the band broadening in SFC seem to be more significant than is commonly considered. In Fig. 2b, a short 1.50 m × 50 μm I.D. column, coated with a thin film, 0.24 μm, was used as the precolumn.

Two precolumns were used. The first was coated with a thin film of PS-264, the I.D. being the same as the I.D. of the diffusion tube; the second had an I.D. of 50 μm. The contribution of this precolumn to the peak width was significantly lower than that of the first type of column. However, it was sensitive to overloading, and sometimes distorted peaks were generated. Further, the separation of solutes from the solvent was more difficult, owing to very high mobile phase velocities in the precolumn. These factors caused a higher standard deviation of the measured diffusion coefficients than when the first precolumn was applied.

Both precolumns had rather low retention power, and they could accept only small volumes of solvent. In this case, the total separation of early eluting solutes from the solvent under isobaric conditions is difficult. In order to facilitate the separation, partial evaporation of solvent and a preconcentration of the solutes in the internal loop of the injector have been applied. The injector was accordingly thermostatted at around the boiling temperature of the solvent. It was thus possible to inject similar amounts of solute and solvent (Table I). Consequently, their separation in the precolumn was readily achieved (Fig. 3). The degree of solvent evaporation and solute concentration in the sample was dependent on several factors, such as the time between the filling of the loop with the test solution and the moment of injection (Table I), the length of the restrictor in the waste line of the injector, and the type of solute and its concentration in the solvent. It is evident that this technique has low reproducibility from a quantitative point of view and most likely suffers from discrimination effects.

TABLE I

EFFECT OF SAMPLE EVAPORATION TIME IN THE INJECTOR LOOP ON THE SOLVENT EVAPORATION AND SOLUTE PRECONCENTRATION

Conditions: timed split 50 ms; separation on a 1.50 m × 50 μm I.D. column coated with PS 264, d_f = 0.23 μm, at 100°C, 100 atm; mobile phase velocity, 43 mm/s; sample, 10 mg/ml naphthalene in dichloromethane; injector loop thermostatted at 40°C.

Time (s)	Injected sample (%)[a]	Injected solute (%)[a]	c_s (%)[b]	Preconcentration factor
0	15 ± 5	17 ± 8	3 ± 2	1.1 ± 0
15	5 ± 1	67 ± 7	53 ± 2	4.7 ± 0.4
30	7 ± 2	100 ± 18	54 ± 3	6.7 ± 1.2
60	4 ± 1	53 ± 3	47 ± 1	3.5 ± 0.6

[a] The amounts of injected sample and solute compared with those injected with the injector cooled to 15°C.
[b] Solute concentration in the preconcentrated sample (w/w %).

A plain back-pressure device has been applied for the control of the mass flow-rate in the column (Fig. 1). A similar device has been proposed by Hirata and Nakata [42] and tested using UV detection. In the present work, a slightly modified set-up was used with post-restrictor FID. The mass flow-rate in the column is identical with a mass flow-rate in a variable-flow restrictor. With high pressure at the restrictor outlet, it can be assumed that mobile phase behaviour is more liquid-like than gas-like and that the mass flow-rate, F, in a linear type of restrictor R_1, can be approximated by the Poiseuille equation for laminar flow:

$$F = [(\pi\rho d^4)/(128\eta L)](P_c - P_{bp}) \quad (4)$$

where ρ and η are the fluid density and viscosity, respectively, d and L are the restrictor diameter and length, respectively, and P_c and P_{bp} are the column inlet pressure and back-pressure, respectively. Accordingly, the mass flow-rate in the column is proportional to the pressure drop over the variable-flow restrictor. Fig. 4 shows the linear dependence of the mass flow-rate in the column on the pressure drop over the variable-flow restrictor for high pressures at the restrictor outlet (curve 1 in Fig. 4). For back-pressures lower than 150 atm (at an oven temperature of 100°C) deviations from the linearity of the dependence appear, because reciprocal kine-

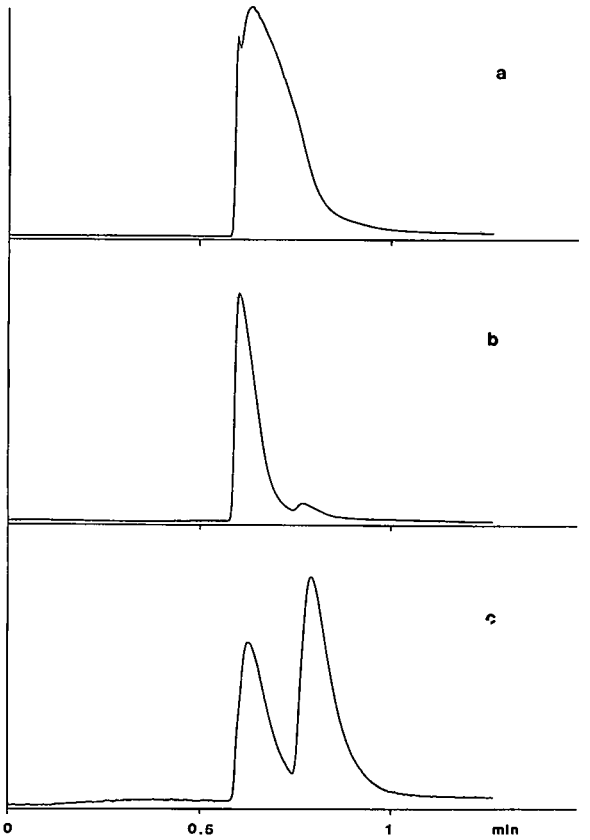

Fig. 3. Influence of injection temperature and sample evaporation time in the injector loop on the separation of dichloromethane (solvent) and naphthalene (solute) on a precolumn (1.50 m × 50 μm I.D.). (a) Injection at 15°C; (b) injection at 40°C, evaporation time 0 s; (c) injection at 40°C, evaporation time 30 s.

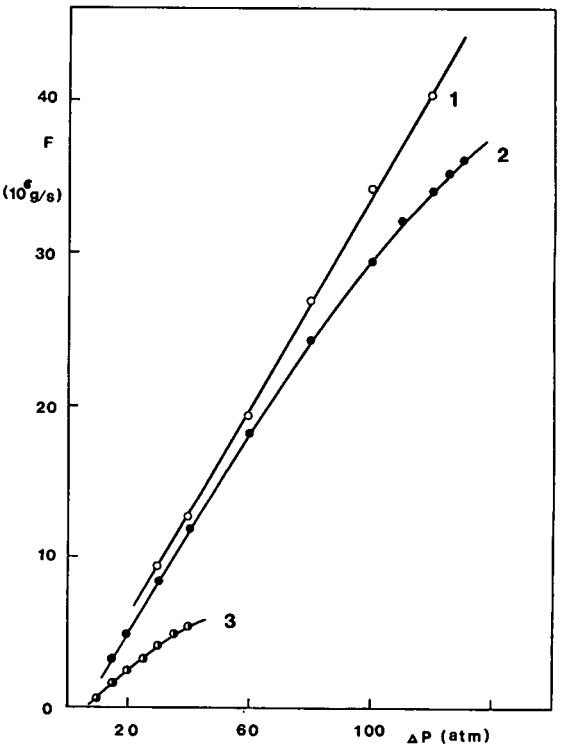

Fig. 4. Column mass flow-rate at different pressure drops, ΔP, over the variable-flow restrictor for different column-inlet pressures: (1) 300 atm; (2) 200 atm; (3) 100 atm.

matic viscosity is markedly dependent on the pressure [35]. The stability of the whole system resulted in low standard deviations of solvent as well as solute hold-up times in the diffusion tube (Table II). Reproducible adjustment of the back-pressure was tested by the measurement of solvent (pentane) hold-up time in the diffusion tube. Good reproducibility was obtained, as shown in Table II. Adequate control of the mass flow-rate was obtained.

The present back-pressure device is much simpler than the one designed for use with FID by Janssen *et al.* [24]. The column flow is not split, and consequently, the detection limit is not decreased with increasing mobile phase velocity. Further, the back-pressure flow also functions as a make-up fluid and decreases possible extra-column band broadening. It is easy to match the dimensions of restrictors to the desired range of column flow-rates. Easy control of the maximum column velocity was achieved by changing the restrictor R_{FID}.

Extra-column band broadening of the whole apparatus was either minimized and/or subtracted from the column band broadening. Subtraction was applied in order to exclude the influence of band broadening in the injector and the first T-piece. Band broadening in the second T-piece, in butt connector B_2 and in the detector was decreased by application of the back-pressure flow. In order to investigate possible band broadening in connector B_2, measurements have been made without restrictor R_{FID}; restrictors R_c and R_2 were thereby inserted into the jet of the detector. Such an arrangement resulted in an unstable baseline, but peak widths were unaffected. It can therefore be anticipated that the connector B_2 has no effect on the band broad-

TABLE II

SOLUTE AND SOLVENT HOLD-UP TIMES IN THE DIFFUSION TUBE AT DIFFERENT VELOCITIES

t_r = Solute hold-up time in diffusion tube, 25.01 m × 259 μm I.D.; t_m = pentane hold-up time considered as dead time at 125°C and 100 atm; k'_i = solute capacity factor at the given mobile phase velocity; $\bar{k}'$ = average capacity factor. Solutes: C_{15}–C_{18} = *n*-alkanes; C_{12on} = 2-dodecanone; C_{15on} = 2-pentadecanone; C_{14es} = methyl myristate.

Solute	v = 14.6 mm/s				v = 12.4 mm/s				v = 10.4 mm/s				v = 8.3 mm/s				$\bar{k}'$
	t_r (s)	S.D. (%)	t_m (s)	$10^2k'_i$	t_r (s)	S.D. (%)	t_m (s)	$10^2k'_i$	t_r (s)	S.D. (%)	t_m (s)	$10^2k'_i$	t_r (s)	S.D. (%)	t_m (s)	$10^2k'_i$	
C_{15}	1730	0.06	1721	0.52	2016	0.06	2008	0.40	2416	0.15	2408	0.33	3008	0.12	2994	0.47	0.0043 ± 0.0009
C_{16}	1735	0.34	1721	0.81	2030	0.09	2019	0.54	2429	0.07	2418	0.46	3020	0.12	2999	0.70	0.0063 ± 0.0018
C_{17}	1718	0.06	1704	0.82	2032	0.09	2017	0.74	2398	0.08	2381	0.71	3031	0.08	3009	0.73	0.0075 ± 0.0006
C_{18}	1722	0.12	1704	1.06	2038	0.05	2017	1.04	2408	0.10	2381	1.13	3041	0.06	3009	1.06	0.0107 ± 0.0004
C_{12on}	–	–	–	–	2027	0.09	2019	0.40	2431	0.04	2418	0.54	3011	0.03	2994	0.57	0.0050 ± 0.0007
C_{15on}	1748	0.17	1721	1.57	2033	0.12	2008	1.25	2442	0.10	2408	1.41	3039	0.08	2994	1.50	0.0143 ± 0.0016
C_{14es}	1742	0.12	1721	1.22	2037	0.09	2008	1.44	2447	0.03	2418	1.20	3031	0.03	2994	1.24	0.0127 ± 0.0013
Biphenyl	1711	0.03	1704	0.41	2026	0.05	2017	0.45	2390	0.05	2381	0.38	3023	0.04	3009	0.46	0.0042 ± 0.0004
S.D.[a]		0.44				0.35				0.75				0.27			

[a] Standard deviation of solvent hold-up time resulting from reproducibility of back-pressure adjustment.

TABLE III

SOLUTE DIFFUSION COEFFICIENTS IN SUPERCRITICAL CARBON DIOXIDE AT 125°C AND 100 ATM

$\bar{D}_m$ = Average measured solute diffusion coefficient, data from eqn. 3; D_m(opt) = solute diffusion coefficient calculated by optimization of eqn. 2; D_m(opt $C_a = 0$) = solute diffusion coefficient calculated by optimization of eqn. 2 with the C_a term set to zero; D_mW and D_mW′ = solute diffusion coefficient calculated from Wilke–Chang equation and modified Wilke–Chang equation, respectively.

Solute	$\bar{D}_m$ (mm²/s)	D_m(opt) (mm²/s)	D_m(opt $C_a = 0$) (mm²/s)	k'	C_a (μs)	D_mW (mm²/s)	D_mW′ (mm²/s)
C_{15}[a]	0.0404 (±0.0034)	0.0406	0.0406	0.0043	−10	0.0290	0.0344
C_{16}[b]	0.0386 (±0.0036)	0.0389	0.0389	0.0063	7	0.0285	0.0331
C_{17}[a]	0.0374 (±0.0045)	0.0379	0.0379	0.0075	14	0.0275	0.0320
C_{18}[c]	0.0375 (±0.0039)	0.0373	0.0372	0.0107	90	0.0266	0.0309
C_{12on}[d]	0.0420 (±0.0026)	0.0427	0.0427	0.0050	−3	0.0337	0.0392
C_{15on}[c]	0.0346 (±0.0026)	0.0355	0.0355	0.0143	45	0.0296	0.0344
C_{14es}[e]	0.0371 (±0.0022)	0.0373	0.0373	0.0127	11	0.0290	0.0336
Biphenyl[e]	0.0499 (±0.0014)	0.0502	0.0502	0.0042	−3	0.0427	0.0496

[a] $n = 14$.
[b] $n = 13$.
[c] $n = 11$.
[d] $n = 8$.
[e] $n = 10$.

ening. Thus, the only section sensitive to extra-column band broadening is the low-dead-volume butt connector B_1, connecting the diffusion tube and the variable-flow restrictor.

Diffusivity measurements

Diffusion coefficients of each solute at 100 atm and 125°C, calculated from measured data according to eqn. 3, are summarized in Table III. An average diffusion coefficient was obtained for each solute as an average of all values estimated at low mobile phase velocities. Possible effects of solute adsorption on the walls of the diffusion tube, of insufficient solute solvation at low densities, of extra-column band broadening and of other possible effects described above have thus been neglected. Relatively good precision was obtained for biphenyl (2.8% relative standard deviation). The standard deviation of D_m for other solutes was much higher, increasing to almost 10%. This is quite high in comparison with the precision obtained in some investigations [19,20,33], and could be due to the above-mentioned effects. However, the spread of values measured at individual velocities was not significantly lower. In several investigations of D_m in supercritical media, the diffusion tube has been immersed in a thermostatted bath [19,20,33], and it was thought that the less stringent temperature control, ±1°C, applied in this work might make a contribution to the standard deviation. However, the diffusion coefficients are, at given conditions, not very dependent on small temperature differences (calculated from Wilke–Chang equation [43] for pentadecane D_m(124°C) = 0.0295 mm²/s, D_m(126°C) = 0.0296 mm²/s). A much stronger effect can be expected from adsorption and condensation of the solutes. Another source of errors may be asymmetric solute bands in the inlet of the diffusion tube. At low carbon dioxide densities, the precolumn was easily overloaded. Leading peaks were, however, not eval-

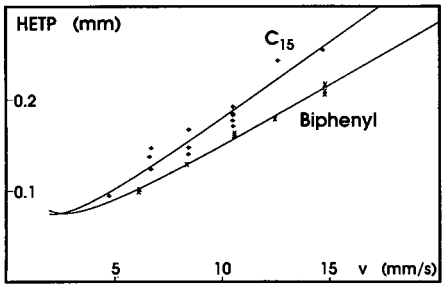

Fig. 5. Optimized HETP *versus* υ plots for pentadecane and biphenyl at 125°C and 100 atm.

uated. Both effects probably contributed to the increased standard deviations of diffusion coefficient measurements for polar and higher-molecular-mass solutes.

Solute diffusion coefficients obtained by optimization of D_m or C_a and D_m to the best fit of H *vs.* υ, according to eqn. 2 are presented in Table III. Either the coefficient of adsorption, C_a, was set to zero or the computer had to optimize both D_m and C_a, respectively (third and fourth column in Table III). As can be seen in Table III, the contribution of a C_a term to the total band broadening is negligible. Thus, the D_m values are not significantly affected by column adsorption for any of the solutes at 125°C. A close fit of the optimized HETP curve to the data points was observed for all solutes. An example is demonstrated in Fig. 5 where two optimized HETP curves, derived from *n*-pentadecane and biphenyl at 125°C, are shown.

Diffusion coefficients in liquids can be calculated according to the Wilke–Chang equation [43]:

$$D_{12} = (1.9 \cdot 10^{-18}) \frac{(\phi M)^{1/2} T}{\eta V_b^{0.6}} \quad (5)$$

where η is the viscosity of the liquid (in Pa s), V_b is the molecular volume of the solute at its boiling temperature at atmospheric pressure (in m^3/mol), M is the molecular mass of the liquid, and ϕ is the association factor of the liquid. When applying this equation for supercritical fluids, some uncertainty originating from prediction of the association factor, the viscosity of the fluid and the solute molar volume at its boiling temperature can be expected. Sassiat *et al.* [19] have modified the Wilke–Chang equation for estimation of diffusion coefficients in supercritical carbon dioxide, introducing molar volume at ambient temperature instead of V_b. As these molar volumes obey eqn. 6:

$$V_b = -5.31 + 130V \approx 1.3V \quad (6)$$

the modified Wilke–Chang equation gives higher values for solute diffusion coefficients than the original equation. Good agreement between measured diffusion coefficients and those calculated according to the modified Wilke–Chang equation has been found for aromatic compounds in high-density supercritical carbon dioxide [19]. Funazukuri *et al.* [20] have applied the modified equation for calculation of diffusion coefficients of linoleic acid methyl ester in supercritical CO_2 at different temperatures for a given pressure and for a given density. Good agreement with the measured values was obtained for the dependence at constant pressure, but at constant density the measured values gave steeper temperature dependence.

In Table III, diffusion coefficients calculated according to Wilke–Chang and according to the modified Wilke–Chang equation are given. As the modified equation was derived from the diffusion coefficients measured for aromatic compounds, very good agreement was obtained for biphenyl. Measured values for polar compounds are in most cases somewhat higher but, within experimental error, they fit to the values calculated from the modified equation. Relatively large differences have been found between the measured and the calculated values for alkanes, the measured values being higher. In Fig. 6, D_m values for the alkanes are plotted *versus* carbon number. The optimized values are signifi-

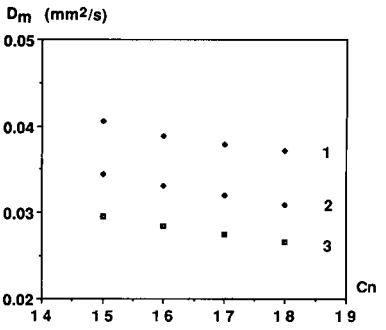

Fig. 6. Correlation of solute diffusion coefficients of *n*-alkanes with the carbon number at 125°C: (1) optimized diffusion coefficients; (2) calculated from modified Wilke–Chang equation; (3) calculated from Wilke–Chang equation.

TABLE IV

SOLUTE DIFFUSION COEFFICIENTS IN SUPERCRITICAL CARBON DIOXIDE AT 100°C AND 100 ATM

Symbols as in Table III; n = 7–11.

Solute	$\bar{D}_m$ (mm²/s)	D_m(opt) (mm²/s)	D_m(opt $C_a = 0$) (mm²/s)	k'	C_a (μs)	$D_m W$ (mm²/s)	$D_m W'$ (mm²/s)
C_{15}	0.0342 (±0.0026)	0.0312	0.0333	0.006	375	0.0277	0.0322
C_{16}	0.0329 (±0.0041)	–	0.0351	0.008	–	0.0267	0.0310
C_{17}	–	–	–	0.010	–	0.0257	0.0299
C_{18}	0.0305 (±0.0067)	–	0.0343	0.014	–	0.0249	0.0289
C_{12on}	0.0387 (±0.0058)	0.0405	0.0403	0.007	100	0.0316	0.0367
C_{15on}	0.0296 (±0.0034)	0.0297	0.0295	0.025	160	0.0277	0.0322
C_{14cs}	0.0283 (±0.0071)	0.0289	0.0288	0.021	120	0.0272	0.0316
Biphenyl	0.0373 (±0.0044)	0.0412	0.0407	0.007	150	0.0400	0.0465

cantly higher than those obtained by the Wilke–Chang and the modified Wilke–Chang equations. However, the shapes of the curves are similar.

The same approach as for data obtained at 125°C was applied to data obtained at 100°C. However, the peak shapes were not of the same quality as at 125°C, *i.e.*, adsorption appeared to be greater.

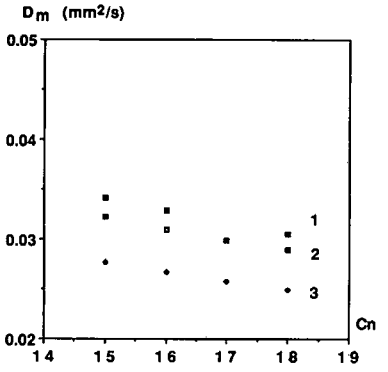

Fig. 7. Correlation of solute diffusion coefficients of *n*-alkanes with the carbon number at 100°C: (1) average diffusion coefficients; (2) calculated from modified Wilke–Chang equation; (3) calculated from Wilke–Chang equation.

Solute diffusion coefficients obtained at 100°C are listed in Table IV, and it can be seen that the C_a term has some influence on the optimized diffusion coefficients. Though only symmetrical peaks were evaluated, the number of measurements at different velocities was too small to be able to optimize D_m and C_a from eqn. 2 for all solutes. However, in Fig. 7, the calculated average diffusion coefficients from Table IV and the D_m values from Wilke–Chang and from the modified Wilke–Chang are plotted *versus* carbon number for the alkanes. A similar trend as at 125°C is observed at 100°C, but the calculated values are closer to the modified Wilke–Chang values at 100°C than at 125°C. No literature data can be found for diffusion coefficients of the alkanes measured at the same conditions as applied in the present work.

ACKNOWLEDGEMENTS

Thanks are due to M. Demirbüker for the idea to apply solvent evaporation in the injector. Economic support from the Swedish Natural Science Research Council is acknowledged.

REFERENCES

1 K. E. Markides and M. L. Lee (Editors), *SFC Applications, Symposium/Workshop on Supercritical Fluid Chromatography*, Brigham Young University Press, Provo, UT, 1989.
2 M. L. Lee and K. E. Markides, *Analytical Supercritical Fluid Chromatography and Extraction*, Chromatography Conferences, Inc., Provo, UT, 1990.
3 C. R. Yonker and R. D. Smith, *J. Chromatogr.*, 505 (1990) 139.
4 J. R. Strubinger, H. Song and J. F. Parcher, *Anal. Chem.*, 63 (1991) 98.
5 S. R. Springston, P. David, J. Steger and M. Novotny, *Anal. Chem.*, 58 (1986) 997.
6 I. Swaid and G. M. Schneider, *Ber. Bunsenges. Phys. Chem.*, 83 (1979) 969.
7 R. Feist and G. M. Schneider, *Sep. Sci. Technol.*, 17 (1982) 261.
8 A. Wilsch, R. Feist and G. M. Schneider, *Fluid Phase Equilibria*, 10 (1983) 299.
9 H. H. Lauer, D. McManigill and R. D. Board, *Anal. Chem.*, 55 (1983) 1370.
10 H. Saad and E. Gulari, *Ber. Bunsenges. Phys. Chem.*, 88 (1984) 834.
11 S. R. Springston and M. Novotny, *Anal. Chem.*, 56 (1984) 1762.
12 M. Roth, J. L. Steger and M. V. Novotny, *J. Phys. Chem.*, 91 (1987) 1645.
13 C. K. J. Sun and S. H. Chen, *AIChE J.*, 31 (1985) 1510.
14 C. K. J. Sun and S. H. Chen, *AIChE J.*, 31 (1985) 1904.
15 C. K. J. Sun and S. H. Chen, *Chem. Eng. Sci.*, 40 (1985) 2217.
16 C. K. J. Sun and S. H. Chen, *AIChE J.*, 32 (1986) 1367.
17 C. K. J. Sun and S. H. Chen, *Ind. Eng Chem. Res.*, 26 (1987) 815.
18 A. Kopner, A. Hamm, J. Ellert, R. Feist and G. M. Schneider, *Chem. Eng. Sci.*, 42 (1987) 2213.
19 P. R. Sassiat, P. Mourier, M. H. Caude and R. H. Rosset, *Anal. Chem.*, 59 (1987) 1164.
20 T. Funazukuri, S. Hachisu and N. Wakao, *Anal. Chem.*, 61 (1989) 118.
21 T. J. Bruno, *J. Res. Natl. Inst. Stand. Technol.*, 94 (1989) 105.
22 N. Dahmen, A. Kordikowski and G. M. Schneider, *J. Chromatogr.*, 505 (1990) 169.
23 N. Dahmen, A. Dülberg and G. M. Schneider, *Ber. Bunsenges. Phys. Chem.*, 94 (1990) 384.
24 H.-G. Janssen, J. A. Rijks and C. A. Cramers, *J. Microcol. Sep.*, 2 (1990) 26.
25 Z. Balenovic, M. N. Myers and J. C. Giddings, *J. Chem. Phys.*, 52 (1970) 915.
26 M. Roth, *J. Microcol. Sep.*, 3 (1991) 173.
27 G. Taylor, *Proc. Roy. Soc. London, Ser. A*, 219 (1953) 186.
28 G. Taylor, *Proc. Roy. Soc. London, Ser. A*, 225 (1954) 473.
29 R. Aris, *Proc. Roy. Soc. London, Ser. A*, 235 (1956) 67.
30 A. R. Mansour, *Sep. Sci. Technol.*, 24 (1989/1990) 1437.
31 J. C. Giddings and S. L. Seager, *J. Chem. Phys.*, 33 (1960) 1579.
32 A. K. Bemgård and A. L. Colmsjö, *J. High Resolut. Chromatogr.*, 13 (1990) 689.
33 S. V. Olesik, J. L. Steger, N. Kiba, M. Roth and M. V. Novotny, *J. Chromatogr.*, 392 (1987) 165.
34 A. K. Bemgård and A. L. Colmsjö, *J. Chromatogr.*, 522 (1990) 277.
35 M. Roth and A. Ansorgová, *J. Chromatogr.*, 465 (1989) 169.
36 S. R. Sumpter and M. L. Lee, *J. Microcol. Sep.*, 3 (1991) 91.
37 J. C. Giddings, S. L. Seager, L. R. Stucki and G. H. Stewart, *Anal. Chem.*, 36 (1964) 741.
38 D. E. Raynie, K. E. Markides, M. L. Lee and S. R. Goates, *Anal. Chem.*, 61 (1989) 1178.
39 M. Saito, Y. Yamauchi, H. Kaishiwazaki and M. Sugawara, *Chromatographia*, 25 (1988) 801.
40 A. F. Buskhe, B. E. Berg, O. Gyllenhaal and T. Greibrokk, *J. High Resolut. Chromatogr. Chromatogr. Commun.*, 11 (1988) 16.
41 Y. Hirata, M. Tanaka and K. Inomata, *J. Chromatogr. Sci.*, 27 (1989) 395.
42 Y. Hirata and F. Nakata, *Chromatographia*, 21 (1986) 627.
43 C. R. Wilke and P. Chang, *AIChE J.*, 1 (1955) 264.

Journal of Chromatography, 625 (1992) 323–330
Elsevier Science Publishers B.V., Amsterdam

CHROM. 24 493

Prediction of current–voltage dependence and electrochemical calibration for capillary zone electrophoresis

Mikhail S. Bello*, Marcella Chiari, Marina Nesi and Pier Giorgio Righetti

Department of Biomedical Sciences and Technologies, University of Milan, Via Celoria 2, Milan 20133 (Italy)

Marco Saracchi

Institute of Plant Pathology, University of Milan, Via Celoria 2, Milan 20133 (Italy)

(First received February 21st, 1992; revised manuscript received July 6th, 1992)

ABSTRACT

An experimental procedure is described for predicting the current–voltage dependence and temperature rise due to Joule heating in capillary zone electrophoresis. An equation is given for calculating the Biot number from known values of capillary electric resistance in the absence of thermal effects (R_0) and the new value of the resistance when thermal effects become pronounced. Once the R_0 and Biot number have been obtained for a given capillary, one can easily predict the electric current and temperature inside it. Current–voltage plots theoretically derived for phosphate (pH 6.87) and acetate (pH 4.7) buffers and for two capillary diameters (75 and 100 μm I.D.) were found to coincide accurately with experimentally measured data. An equation is also given allowing the determination of a capillary inner diameter from current readings in low-voltage runs (where thermal effects would be negligible) in buffers of known conductivity. A reasonable agreement was found between "electrochemical" and "optical" (or electron microscope) measurements of a capillary lumen. The equations presented allow the prediction of the maximum voltage gradient compatible with minimum band spreading from a single preliminary run in buffers of known conductivity.

INTRODUCTION

Reproducibility of results is essential for any separation method and all factors that influence the separation process have to be accounted for in order to secure it. In capillary zone electrophoresis (CZE), it was understood that reproducibility is related to a great extent to temperature effects and cooling conditions of a capillary [1–5].

Electric current within a capillary generates internal heating of the buffer solution. This heating elevates the average temperature of the buffer and produces a radial temperature gradient in the capillary. It is very important that the electric conductivity of the buffer increases with increasing temperature. The temperature dependence of the electric conductivity has been shown by Gobie and Ivory [2] to be a cause of non-Ohmic behaviour of a current–voltage characteristic of the capillary. This means that, *e.g.*, a twofold increase in an applied voltage does not lead to a twofold increase in the electric current. Moreover, if the voltage exceeds a certain value the electric current and temperature rise dramatically. This phenomenon has been studied and called "autothermal runaway" [2]. Heating of the buffer and deviations from Ohm's law strongly

Correspondence to: Professor P. G. Righetti, Department of Biomedical Sciences and Technologies, University of Milan, Via Celoria 2, Milan 20133, Italy.

* Permanent address: Institute of Macromolecular Compounds, Bolshoi 31, 199004 St. Petersburg, Russia.

0021-9673/92/$05.00

depend on the cooling conditions of the capillary [1].

By assuming that longitudinal diffusion is the major source of zone broadening (in the absence of interactions of the analyte with the capillary wall) [6], it follows that high applied voltages are the most direct way to achieve high separation efficiencies. However, this relationship breaks down at very high voltages (*e.g.*, >500 V/cm) because the high heat generated promotes strong dispersion of the analyte.

Issaq *et al.* [3] considered the beginning of the deviation of the current–voltage dependence from a straight line to be the upper limit for the voltage applied to the capillary. We assume, however, that this deviation, indicating of course a reasonable temperature rise of the buffer within the capillary, has no adverse effect on the separation (provided that the sample is thermostable enough) and reproducibility.

If a high voltage is used for rapid separations, it is necessary to have a reliable method allowing an experimenter to predict the current–voltage dependence and the buffer temperature rise in the capillary. However, the autothermal theory of Gobie and Ivory [2], which could in principle be applied to this problem, gives only qualitatively correct predictions. In addition, this theory needs a precise knowledge of the diameters of a capillary lumen, fused-silica wall and polyimide coating, the exact determination of which would require considerable efforts.

Although the dimensions of a capillary (inner diameter, diameter of the fused-silica wall and diameter of the polyimide coating) are usually given by the producer, the tolerance intervals are too large for use in quantitative predictions. Thus, Gobie and Ivory [2] reported considerable deviations (from the point of view of quantitative predictions) of capillary dimensions from their nominal values.

In order to predict the current–voltage dependence and temperature rise within a capillary, we suggest a procedure of electrochemical calibration of a capillary based on the approximate thermal theory developed by Bello and Righetti [4,5]. This procedure allows one, after measurements of current at low and high voltages, to calculate current–voltage and temperature–voltage dependences. In addition, the capillary inner diameter can be calculated if the specific conductivity of the buffer solution is known.

The aim of this paper is to propose and verify experimentally the procedure of electrochemical calibration and to compare the approximate thermal theory with experimental results. This paper consists of a theoretical section, with all relevant equations and a description of the calibration procedure, followed by an experimental section that includes measurements of buffer solution conductivities at different temperatures, measurements of the capillary inner diameters by using electron and optical microscopes, a comparison of the theoretical and experimental results and a discussion with practical guidelines.

THEORY

Determination of the capillary resistance and its inner diameter

According to Ohm's law, the relationship between current and voltage drop for a conductor of cylindrical cross-section is given by

$$RI = V \tag{1a}$$

$$R = \frac{4L}{\sigma\pi d^2} \tag{1b}$$

where I is the electric current, V the voltage applied, R the electrical resistance of the capillary filled with the buffer solution, σ the buffer electric conductivity, d the capillary inner diameter and L its length.

We use eqn. 1a and b for the determination of the capillary diameter by applying them when the voltage is relativley low and thermal effects are negligible:

$$d = \sqrt{\frac{4IL}{\sigma_0\pi V}} \tag{2}$$

where σ_0 is the buffer conductivity at the reference temperature $T_0 = 25$°C.

We identify the voltage applied to electrodes with the voltage applied to the ends of the capillary and neglect the voltage drop at the electrode compartment (note also that in most instruments the capillary extremities and the platinum wires are only a few millimetres apart).

Prediction of the temperature and current and determination of the Biot number

The temperature elevation of the buffer inside the capillary depends on the cooling conditions of the

capillary. These conditions can be classified as lack of forced cooling (natural cooling), forced air cooling and liquid cooling. Deviations from Ohm's law have been shown to be significant for the cases of natural cooling and forced air cooling [1]. These conditions determine the heat removal from the external surface of the capillary. At the steady state, heat exchange between the heated buffer and the coolant surrounding the capillary is characterized by the overall Biot number. The latter is the coefficient of proportionality between dimensionless heat flux and dimensionless difference of the inner surface temperature of the capillary and the temperature of the coolant in the bulk. It is assumed that the law of proportionality is valid, which is, in fact, a reasonable approximation. If the Biot number, capillary inner diameter, its length and the properties of the buffer are known then it is possible to calculate the temperature inside the capillary and electric current for any given voltage [2,4]. Direct calculation of the Biot number is possible for some particular cases [1,2] but in general it is a complex problem. We propose not to calculate the Biot number but to obtain it from fitting experimental points on a current–voltage plot with the curves given by the approximate thermal theory [4]. This theory is assumed to be valid for the natural and forced air cooled capillaries. In these cases the temperature profile within the capillary is flat and can be replaced by its average value. It simplifies significantly solutions of equations of heat transfer and leads to simple equations for the electric current and average temperature [5].

All thermal theories assume the buffer conductivity to be linearly dependent on temperature:

$$\sigma = \sigma_0[1 + \alpha(T - T_0)] \tag{3a}$$

where T is the buffer temperature within the capillary and α is the temperature coefficient of conductivity.

The capillary resistance, according to eqns. 1b and 3a, is given by the following relationship:

$$R = R_0/[1 + \alpha(T - T_0)] \tag{3b}$$

where R_0 is the reference resistance at 25°C.

Experimentally, R_0 can easily be evaluated from eqns. 1a and 3b applied for low voltage conditions. As elsewhere [2,4,5], we introduce a characteristic temperature difference as

$$\Delta T_{ref} = \sigma_0 E^2 d^2/4\chi \tag{4a}$$

where E is the electric field intensity and χ the thermal conductivity of the buffer solution set equal to the water thermal conductivity ($\chi = 0.61$ W m^{-1} K^{-1}). The characteristic temperature difference can be also expressed as

$$\Delta T_{ref} = \frac{V^2}{\pi\chi L R_0} \tag{4b}$$

The electric current and average buffer temperature within the capillary are given by [4]

$$T = \frac{2Bi_{0A}(T_C - T_0) + \Delta T_{ref}}{2Bi_{0A} - k^2} + T_0 \tag{5}$$

$$I = \frac{V}{R_0}\left\{\frac{2Bi_{0A}[1 + \alpha(T_C - T_0)]}{2Bi_{0A} - k^2}\right\} \tag{6}$$

where $k^2 = \alpha\Delta T_{ref}$ is the autothermal parameter, T_C is the temperature of the surrounding medium and Bi_{0A} is the Biot number.

When $k^2 \ll 2Bi_{0A}$ (low voltage, small capillary diameter, low conductivity and liquid cooling), eqn. 6 reflects currents variations due to the coolant temperature changes. In order to separate these changes of current from the changes caused by internal heating, we denote by I_{25} the value of current corresponding to a given voltage if the temperature of the coolant were equal to the reference temperature of 25°C. Then eqn. 6 can be represented in the following form:

$$I = I_{25}[1 + \alpha(T_C - T_0)] \tag{7a}$$

$$I_{25} = \frac{V}{R_0}\left(\frac{2Bi_{0A}}{2Bi_{0A} - k^2}\right) \tag{7b}$$

Eqns. 7 allow one to evaluate the Biot number by measuring the current I for a given voltage, applying eqn. 7a to calculate I_{25} and using the following equation, derived from eqn. 7b:

$$Bi_{0A} = \frac{I_{25}k^2}{2(I_{25} - V/R_0)} \tag{8a}$$

Eqn. 8a can be also rewritten as follows:

$$Bi_{0A} = \frac{k^2}{2(1 - R_{25}/R_0)} \tag{8b}$$

where $R_{25} = V/I_{25}$ is the capillary electric resistance at a given voltage provided that the coolant temperature is equal to 25°C.

Calibration of capillary

The procedure for electrochemical calibration of the capillary is as follows. At low voltage, when thermal effects are negligible, one determines the capillary resistance R_0 by using eqn. 1a. The capillary diameter can be calculated from eqn. 1b. By measuring the electric current I at a given voltage V, which should be high enough to produce a deviation from Ohm's law, and knowing the coolant temperature T_C and thermal coefficient of conductivity α, one finds the value of I_{25} or R_{25} (the values of current and electric resistance which would be generated if the temperature of the coolant or surrounding medium is equal to the reference temperature). The values of R_0 and I_{25} thus obtained are then used for calculating ΔT_{ref} (eqn. 4b), k^2 and, finally, Bi_{0A} (eqn. 8a or 8b). Knowing both R_0 and Bi_{0A}, one can easily predict the electric current and temperature within a capillary. Note that Bi_{0A} is a characteristic of the given capillary in the given system and does not vary when the buffer solution is changed.

EXPERIMENTAL

All chemicals were purchased from Merck (Darmstadt, Germany).

Two buffer solutions were used, phosphate and acetate. The phosphate buffer was 10 m*M* Na_2HPO_4–10 m*M* $NaH_2PO_4 \cdot H_2O$–50 m*M* KCl (pH 6.87) and the acetate buffer was 50 m*M* CH_3COOH–25 m*M* NaOH (pH 4.7). The specific conductivity of buffer solutions was measured in the temperature range 25–45°C with an Orion Research conductimeter at a frequency of 1 kHz. The temperature was stabilized with a thermostat and controlled by a Digiterm Quartz 1505 thermocouple (Hanhart, Schwennigen, Germany). Before measurements, the conductimeter was calibrated by using standard solutions of KCl and the temperature dependence of the specific conductivity of the standard solution was measured and shown to be in agreement with the reference values [7]. Capillaries of length 50 cm and with nominal inner diameters of 50, 75 and 100 μm were obtained from Polymicro Technologies (Phoenix, AZ, USA). All measurements of current–voltage dependence were performed on a Waters Quanta 4000 capillary electrophoresis system (Millipore, Milford, MA, USA). The current was measured from the standard output of the Waters Quanta 4000 by a Kipp and Zonen voltage recorder.

Electron and visible microscopy

All samples were covered with a thin layer of gold in an Edwards 306 metallizer (Edwards High Vacuum, Crawley, UK). The capillaries were then viewed in a Stereoscan 250 scanning electron microscope (Cambridge Scientific Instruments, Cambridge, UK) operated at 20 kV. Photographs were taken with Kodak Tri-X Pan 120 film. The capillaries were also examined under an Orthoplan visible microscope (Leitz, Wetzlar, Germany) at 900× magnification.

RESULTS AND DISCUSSION

As the calibration procedure needs an accurate value of thermal coefficients of buffer electric conductivity, we suggest standardizing for calibration two buffer solutions with relatively high and low electric conductivities.

The linear temperature dependence of the phosphate buffer solution has already been reported [2]. However, the value of α given in Table III in ref. 2 (denoted there by k_1) is 0.046°C^{-1}, whereas the value of α evaluated from Fig. 5 in the same paper, with reference to the temperature $T_0 = 25$°C, is

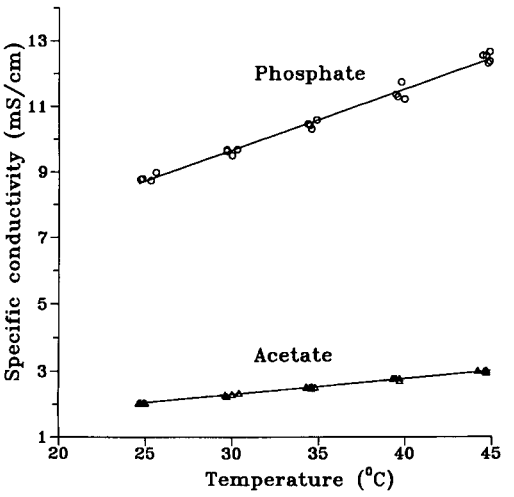

Fig. 1. Temperature dependences of specific conductivities for (○) phosphate and (△) acetate buffers. The measurements were taken at 5°C increments in the range 25–45°C with an Orion Model 101 conductivity meter with a 1-cm path cell. Each measurement was repeated four times. Note the apparent difference in slopes between the two buffers.

TABLE I

CAPILLARY DIAMETERS MEASURED ELECTROCHEMICALLY AND OPTICALLY

Nominal diameter (μm)	Electrochemical calibration (μm)	Optical microscope (μm)	Electron microscope (μm)
50	48.4	47.55	50.3
75	74.3	74.2	78.7
100	104	103.6	109.5

approximately equal to $0.02\ °C^{-1}$. Therefore, we could not use the previously measured data for calibration and measured the temperature dependences of the specific electric conductivities for both buffers.

The temperature dependences of the specific electric conductivity for the phosphate and acetate buffers are shown in Fig. 1. Four runs were performed for each solution and the data were fitted by straight lines by using the least-squares method. It can be seen from Fig. 1 that linear dependences of the electric conductivity of the buffers on temperature in the range 20–50°C are good approximations for both phosphate and acetate buffers. The coefficients for linear representation (eqn. 3) of the electric conductivities of the buffers are found to be

$$\sigma_0 = 8.72 \pm 0.14\ (\text{mS cm}^{-1}),$$

$$\alpha = 0.021 \pm 0.001\ (°C^{-1}) \quad (9a)$$

for phosphate buffer and

$$\sigma_0 = 2.04 \pm 0.03\ (\text{mS cm}^{-1}),$$

$$\alpha = 0.023 \pm 0.001\ (°C^{-1}) \quad (9b)$$

for acetate buffer. The reference temperature T_0 is 25°C.

According to the calibration procedure described above, we measured the current and voltage for capillaries with nominal diameters of 50, 75 and 100 μm filled with either phosphate or acetate buffer. The inner diameters calculated according to eqn. 2 for both buffers agree well with each other and with those measured using the optical microscope. Measurements made by using the electron microscope gave different results, probably owing to

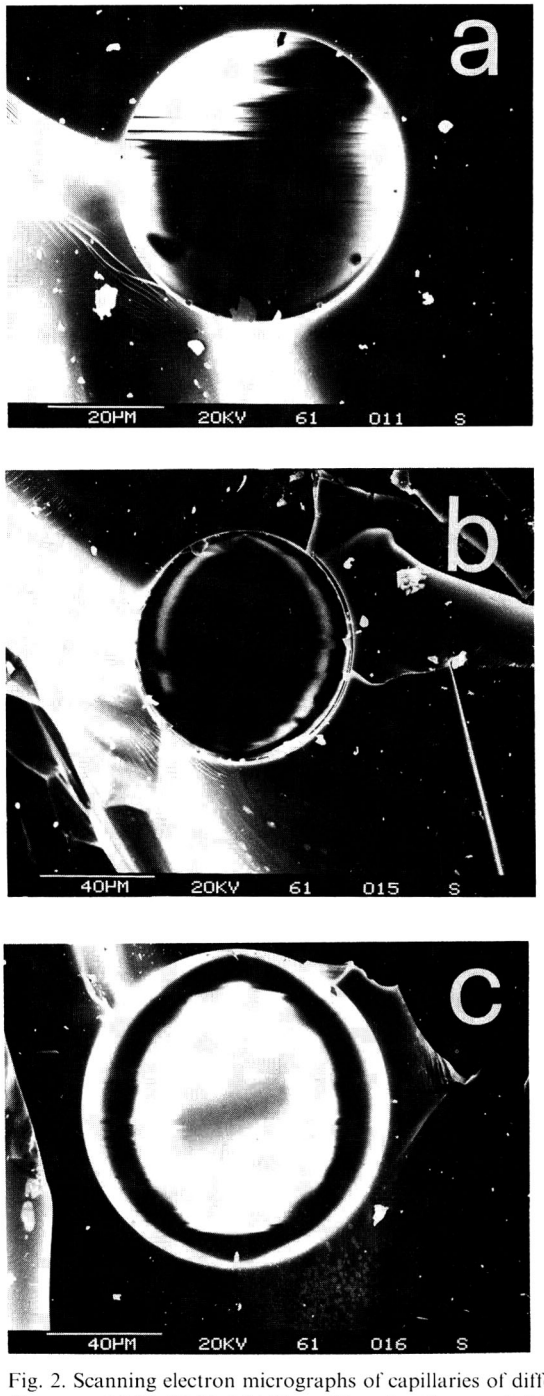

Fig. 2. Scanning electron micrographs of capillaries of different diameters: (a) 50; (b) 75; (c) 100 μm. Note that the round object is the lumen of the capillary. At these magnifications, only a small portion of the fused-silica wall can be seen around the lumen. The white, star-like objects are minute chips of fused-silica as a result of cutting a sharp edge.

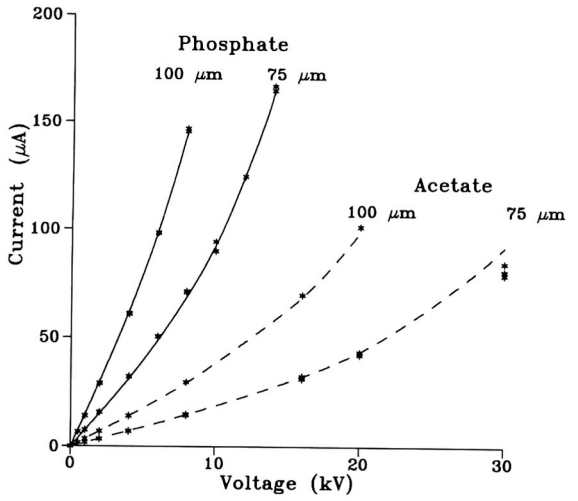

Fig. 3. Current–voltage plots for phosphate (solid lines) and acetate (dashed lines) buffers. The experiments were performed in two sets of capillaries of nominal inner diameter 75 and 100 μm. Note how, owing to the much higher conductivity of phosphate buffer, much lower voltage gradients can be applied as compared with an acetate buffer. Note also the excellent agreement between the experimental points (stars) and the theoretically calculated lines (the latter were calculated from eqn. 7b and do not represent the lines of best fit joining the experimental points!). Note also that each star represents four different experiments (not the average values, the data simply overlap completely on the target, except for a few points!).

the insufficient statistics for electron microscope measurements. Results of the determination of capillary diameters are presented in Table I. Fig. 2 shows a series of photographs of the capillary lumen, made with the electron microscope, for three sizes (50, 75 and 100 μm).

Series of measurements of current at progressively increasing voltage were performed for four combinations of two capillaries and two buffers. The temperature of the air in the CZE unit was also measured and the values of the current were reduced to the reference temperature of 25°C according to eqn. 7a.

The capillary inner diameters found by electrochemical calibration were used for obtaining Biot numbers for the 75- and 100-μm capillaries from measurements for phosphate buffer at voltages of 14 and 8 kV, respectively. The values of the Biot numbers calculated from eqn. 8a are $Bi_{0A}^{75} = 0.0455$ and $Bi_{0A}^{100} = 0.061$ for the 75- and 100-μm diameters, respectively. These values were used to calculate current–voltage dependences over the whole range of voltages for both phosphate and acetate buffers by using eqn. 7b.

The theoretical curves are compared with the experimental points in Fig. 3. It can be seen that there is very good agreement between the theoretical and experimental data. Note that the Biot number obtained with the single value for a relatively high current for a capillary filled with the phosphate buffer was also suitable for the same capillary filled with the acetate buffer.

The Biot numbers were applied to calculate the buffer temperature according to eqn. 5. The dependences of the buffer temperature are shown in Fig. 4. These curves show that our measurements of R_0 were correct in the sense that the voltages used did not produce a significant temperature rise able to affect the capillary resistance. Together with the current–voltage curves the temperature–voltage curves appear to be useful for setting the correct votage for an analysis.

Fig. 4 also illustrates the effect of the buffer electric conductivity on the average temperature of the buffer. It can be seen by comparing curves that higher voltages are applicable for the low-conductivity acetate buffer. As a general rule, buffers of low

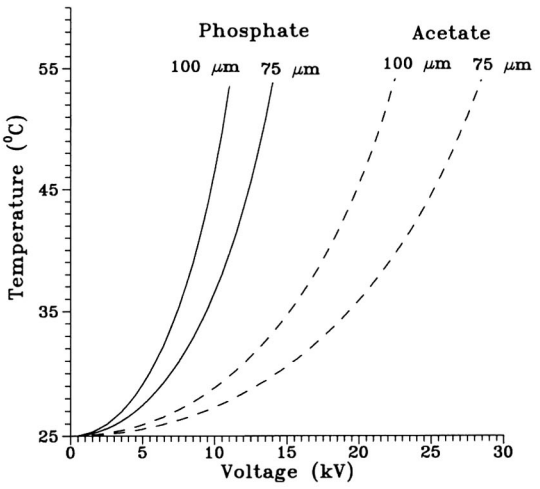

Fig. 4. Temperature–voltage plots for phosphate (solid lines) and acetate (dashed lines) buffers. Note how, owing to the much lower conductivity of the acetate ion, much higher voltage gradients can be applied for a given value of temperature rise as compared with a phosphate buffer.

conductivity should be preferred, as they allow high voltages (and thus rapid separations) with minimum temperature rises inside the capillary. Zwitterionic (such as Good's) buffers should therefore be selected. A recent study [8] has shown that, *e.g.*, a histidine buffer (with a conductivity of only 123 μmho, 0.1 *M*, pH 7.81) is vastly superior to a Tris–phosphate buffer (0.1 *M*, pH 7.74) with a conductivity of 2060 μmho.

An important consequence of our conductivity measurements is discussed further. It is seen from eqn. 9 that the thermal coefficients of both buffers are close to each other. The reason for this is that the ion mobilities and, thus, electric conductivities of different electrolyte solutions depend on the viscosity of the solution in approximately the same way. With dilute solutions the electric conductivity is inversely proportional to the viscosity. We approximated the reciprocal of the water viscosity (taken from ref. 9) by a straight line and plotted it together with the relative conductivities of phosphate and acetate buffers in Fig. 5. It can be seen that these lines are close to each other. It is well known that the electrophoretic mobility of a charged particle and the electroosmotic mobility, which determine the retention time, are inversely proportional to the viscosity of the buffer. Therefore, these mobilities are very likely to depend on temperature just as do the buffer conductivity and the electric current. Thus, electrophoretic and electroosmotic mobilities are supposedly given by

$$U_{ep} = U^0_{ep}[1 + \alpha(T - T_C)] \quad (10a)$$

$$U_{os} = U^0_{os}[1 + \alpha(T - T_C)] \quad (10b)$$

where U^0_{ep} and U^0_{os} are the electrophoretic and electroosmotic mobilities, respectively, at the reference temperature.

Retention time is given by the following expression:

$$t_R = \frac{L^2}{(U_{ep} + U_{os})V} \quad (11)$$

which can be reduced algebraically to

$$t_R = L^2/[(U^0_{ep} + U^0_{os})IR_0] \quad (12)$$

One concludes from eqn. 12 that retention time is inversely proportional to the electric current, as the other variables in eqn. 12 do not depend on temperature and voltage. It is also seen from eqn. 12 that the ratio of the retention times of a substance at different voltages is equal not to the reciprocal of the ratio of voltages but to the reciprocal of the ratio of currents:

$$t_{R1}/t_{R2} = I_2/I_1 \quad (13)$$

whereas at low applied voltage the ratio of voltages or of currents can be used interchangeably (see also ref. 10).

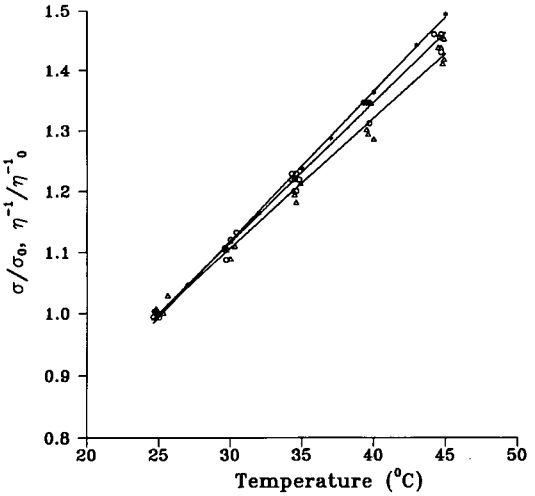

Fig. 5. Plot of relative electric conductivities for (△) phosphate and (○) acetate buffers and (✳) relative reciprocal water viscosity *vs.* temperature. Note how, on such plots, the slopes are the same in the three cases (in contrast to Fig. 1), suggesting that the conductivity increments of the buffers follow closely (in fact are due to) the reciprocal viscosity increments of the solvent.

CONCLUSIONS

Most workers perform a series of measurements at progressively increasing voltage gradients in order to obtain the point of deviation from Ohms' law. In our case, two current–voltage measurements (a first one at low-voltage, in the absence of thermal effects, and a second one at high voltage) allow the derivation of the overall Biot number and easy prediction of electric current and temperature within a capillary. The calibration procedure proposed here appears to be correct and useful for air-cooled CZE data interpretation and for setting parameters of an analytical run.

The present data experimentally justify the approximate thermal theory [5] for air-cooled capillaries in that the theoretical current–voltage curves fit the experimental points well.

We propose eqn. 12, which states that at high voltages the retention time is inversely proportional not to applied voltage but to the electric current. Although this equation has not been directly proved, we believe it to be accurate (see ref. 10).

ACKNOWLEDGEMENTS

We gratefully acknowledge the kind help of and useful consultations with Dr. P. Mussini, University of Milan, and Dr. E. Levin, Ioffe Physicotechnical Institute, Saint Petersburg. M.S.B. thanks the European Space Agency (ESA) for a fellowship enabling him to carry out this work at the University of Milan. P.G.R. thanks ESA, ASI (Agenzia Spaziale Italiana) and Progetto Finalizzato Chimica Fine II (CNR, Rome) for funding these studies.

REFERENCES

1 R. J. Nelson, A. Paulus, A. S. Cohen, A. Guttman and B. L. Karger, *J. Chromatogr.*, 480 (1989) 111–127.
2 W. A. Gobie and C. F. Ivory, *J. Chromatogr.*, 516 (1990) 191–200.
3 H. J. Issaq, I. Z. Atamna, G. M. Muschik and G. M. Janni, *Chromatographia*, 32 (1991) 155–161.
4 M. Bello and P. G. Righetti, *J. Chromatogr.*, 606 (1992) 95–102.
5 M. Bello and P. G. Righetti, *J. Chromatogr.*, 606 (1992) 103–111.
6 J. W. Jorgenson and K. D. Lukacs, *Anal. Chem.*, 53 (1981) 1298–1301.
7 *Gmelins Handbuch der Anorganischen Chemie, Kalium*, Verlag Chemie, Berlin, 1938, p. 440.
8 T. D. Mao, G. M. Satow and K. A. Turner, *4th International Symposium on High-Performance Capillary Electrophoresis, Amsterdam, February 9–13, 1992*, Abstract M-15.
9 R. C. Weast (Editor), *CRC Handbook of Chemistry and Physics*, CRC Press, Boca Raton, FL, 67th ed., 1987, p. F-37.
10 S. Hjertén, *Chromatogr. Rev.*, 9 (1967) 122–219.

Journal of Chromatography, 625 (1992) 331–340
Elsevier Science Publishers B.V., Amsterdam

CHROM. 24 490

Comparative study of capillary zone electrophoresis and high-performance liquid chromatography in the analysis of oligonucleotides and DNA☆

Peter J. Oefner and Günther K. Bonn

Department of Analytical Chemistry, Johannes-Kepler-University, Altenbergerstrasse 69, A-4040 Linz (Austria)

Christian G. Huber and Suraphol Nathakarnkitkool

Institute of Radiochemistry, Leopold-Franzens-University, Innrain 52a, A-6020 Innsbruck (Austria)

(First received February 10th, 1992; revised manuscript received June 29th, 1992)

ABSTRACT

Capillary zone electrophoresis and high-performance liquid chromatography were compared with regard to the separation of oligonucleotides and double-stranded DNA. Both anion-exchange and reversed-phase high-performance liquid chromatography on non-porous particles are considered to be superior to capillary electrophoresis in terms of speed and selectivity in the analysis of oligonucleotides up to 30 bases in length. Moreover, reversed-phase chromatography allows the simultaneous purification of detritylated oligonucleotides with recoveries >90%. Compared with anion-exchange chromatography, there is no need for a subsequent desaltation step because the volatile buffer system can be readily evaporated. With regard to dsDNA, however, the resolving power of capillary electrophoresis cannot be matched by anion-exchange chromatography at present. Moreover, the combined use of hydroxyethylcellulose and ethidium bromide not only yielded a separation efficiency equal to that achieved by means of gel-filled capillaries but also avoids some of their limitations such as the destruction of the gel matrix at high current densities and the bias involved in electrokinetic injection.

INTRODUCTION

The impressive advances made over the past few years in the fields of biotechnology and molecular biology, such as solid-phase DNA synthesis and polymerase chain reaction, have resulted in a growing demand for rapid and automated analytical methods for the separation of single- and double-stranded DNA molecules. Early attempts to replace slab-gel electrophoresis with high-performance liquid chromatography (HPLC) on porous stationary phases have not yielded the expected enhancement in speed and resolution owing to the restricted intraparticle diffusion of biopolymers [1]. Since the introduction of non-porous micropellicular packings, however, chromatographic analyses of biopolymers can be obtained within minutes owing to such properties as fast mass transfer kinetics, maximum surface accessibility and fast column regeneration [2]. Recently, a great challenge to HPLC in the analysis of oligo- and polynucleotides has arisen through the use of capillaries as the migration channel in electrophoresis. This has not only put electrophoresis on the same instrumental footing as HPLC

Correspondence to: Dr. G. K. Bonn, Department of Analytical Chemistry, Johannes Kepler University, Altenbergerstrasse 69, A-4040 Linz, Austria.

☆ Presented at the *4th International Symposium on High-Performance Capillary Electrophoresis, Amsterdam, February 9–13, 1992*. The majority of the papers presented at this symposium were published in *J. Chromatogr.*, Vol. 608 (1992).

0021-9673/92/$05.00

but has also allowed the rapid analysis of sample volumes as small as a few picolitres with unprecedented resolution and sensitivity [3]. As HPLC and capillary electrophoresis have their own advantages and limitations, they may be more or less suited for specific applications. Therefore, we have undertaken the present comparison of the two techniques with regard to their speed and efficiency in separating synthetic oligonucleotides and double-stranded DNA.

EXPERIMENTAL

Chemicals

Non-porous, fused-silica microspheres (particle diameter, $d_p \approx 2$ μm) were obtained from Glycotech (Hamden, CT, USA). Styrene, divinylbenzene (DVB) and polyvinyl alcohol (PVA) were purchased from Riedel-de Haën (Seelze, Germany). Polyethyleneimine (PEI, molecular mass 600) and ethanediol diglycidyl ether were obtained from Polysciences (Warrington, PA, USA). HPLC gradient-grade acetonitrile, dioxane, 2-propanol and methanol were obtained from Merck (Darmstadt, Germany) and triethylammonium acetate (TEAA) from Applied Biosystems (San Jose, CA, USA). Hydroxyethylcellulose (HEC, viscosity of a 2% aqueous solution 0.3 Pa s) was purchased from Serva (Heidelberg, Germany). Tris, sodium dodecyl sulphate (SDS) and boric acid were of electrophoretic purity (Bio-Rad Labs., Richmond, CA, USA). Ammonium sulphate, ethidium bromide, EDTA and alkali metal salts were obtained from Sigma (St. Louis, MO, USA). Mesityl oxide, which served as electroosmotic flow-marker, was purchased from Merck. Buffer solutions were prepared with high-purity water (NANOpure; Barnstead, Newton, MA, USA) and filtered through a 0.2-μm pore size filter (Schleicher & Schuell, Keene, NH, USA).

Oligonucleotides

Standards of dephosphorylated and phosphorylated oligodeoxyadenylic acids [$d(A)_{12-18}$, $pd(A)_{16}$, $pd(A)_{12-18}$] were purchased from Pharmacia (Uppsala, Sweden). Heterooligonucleotides were synthesized on a DNA synthesizer (Model 381-A, Applied Biosystems) using phosphoramidite chemistry. Trityl-on oligonucleotides were purified by means of oligonucleotide purification cartridges (OPC, Applied Biosystems).

DNA size standards

Double-stranded DNA size standards were purchased from Bio-Rad Labs. (pBR322 DNA-*Ava* II/*Eco*R I Digest), Boehringer (Mannheim, Germany, pBR322 DNA-*Hae* III Digest and pBR328 DNA-*Bgl* I/*Hinf* I Digest) and Pharmacia ($\phi x174$ DNA-*Hae* III Digest and λ-*Hind* III Digest). pBR322-*Msp* I was prepared by digesting 6 μg of pBR 322 (Boehringer) with the restriction endonuclease *Msp* I (Promega, Madison, WI, USA) for 60 min at 37°C using the buffer supplied with the enzyme.

Columns

A Progel-TSK DEAE-NPR column was purchased from Supelco (Bellefonte, PA, USA). PEI-silica was prepared according to the method reported by Regnier and co-workers [4,5]. Before packing into a stainless-steel column (30 × 4.6 mm I.D.), 1 g of the modified silica microspheres was suspended in 10 ml of 2-propanol and sonicated for 20 min, then the slurry was packed into the column at a pressure of 70 MPa with the use of an air-driven pump (Maximator MSF 111; Ammann Technik, Kölliken, Switzerland) and methanol as the driving solvent. Thereafter, methanol was replaced with water at the same inlet pressure. The same procedure was employed to pack a 50 × 4.6 mm I.D. column with 1.1 g of the highly cross-linked polystyrene (PS)–DVB particles [60% (v/v) DVB], which had been prepared by a two-step microsuspension method either in the absence or in the presence of 0.1% (w/v) PVA [6]. Instead of 2-propanol, however, 10 ml of dioxane were used to suspend the beads.

Instrumentation

Capillary zone electrophoretic analyses were performed on either an Applied Biosystems Model 270A or a Beckman (Palo Alto, CA, USA) P/ACE System 2100, equipped with a 72 cm × 50 μm I.D. or a 67 cm × 75 μm I.D. fused-silica capillary, respectively. Moreover, a phenylmethyl-deactivated fused-silica capillary (Restek, Bellefonte, PA, USA) of I.D. 100 μm was used for the separation of DNA restriction fragments. Detection was carried out by on-column measurement of UV absorption at 260 nm at 22 cm from the cathode in the case of the Applied Biosystems equipment or at 254 nm at 7 cm from the cathode in the case of the Beckman sys-

tem. Electropherograms were recorded either on a Shimadzu (Kyoto, Japan) Chromatopac C-R6A integrator or on a IBM PS/2 Model 70 with Beckman System Gold v. 6.01 software. Samples were loaded either by applying a vacuum at a pressure of 16.9 kPa (Applied Biosystems system) or by means of pressure injection at 3.45 MPa (Beckman system). The temperature was kept constant at 30 and 25°C, respectively.

The HPLC system consisted of two pumps (Model 114M; Beckman), a dynamic gradient mixer (Model 340; Beckman), a gradient controller (Model 421; Beckman), a sample injection valve (Model 7125; Rheodyne, Cotati, CA, USA) with a 20-μl sample loop, a variable-wavelength UV monitor (Model 484; Waters, Milford, MA, USA), a column oven (Model CTO-2A; Shimadzu) and an integrator (Model C-R6A; Shimadzu).

Polymerase chain reaction

Polymerase chain reaction (PCR) was performed in a 1.5-ml microcentrifuge tube by adding 2 μl of cDNA, which had been obtained by reverse transcription of 1 μg of mRNA isolated from scrotal skin fibroblasts, to a total volume of 100 μl of 10 m*M* Tris–HCl (pH 9.0, 25°C)–50 m*M* KCl–1.5 m*M* $MgCl_2$–0.2 m*M* deoxynucleotide triphosphates (dNTPs)–0.1 mg/ml gelatin–0.1% Triton X-100–0.5 μ*M* of each oligonucleotide primer–2.5 U Taq polymerase (Promega). To prevent evaporation, the reaction mixture was sealed with 50 μl of mineral oil (Sigma). Thirty cycles of amplification were carried out in a thermocycler (BioMed, Theres, Germany) with a 95°C denaturation step for 25 s, a 57°C annealing step for 30 s and a 73°C extension step for 60 s. The first denaturation step was elongated for 2 min and the last synthesis step for 3 min to ensure completion of the final extension step. Beginning at cycle 16, each following DNA synthesis step was elongated for 5 s. Finally, samples were cooled to room temperature.

Purification of PCR products

PCR products were purified by means of size-exclusion chromatography. Briefly, 0.7 ml of Sephadex G-150 (Pharmacia) slurry was filled into a 1-ml syringe and washed twice with tris-EDTA (TE) buffer. Then, 50–70 μl of PCR sample were applied to the top of the gel bed. The column was centrifuged in a swinging bucket at 1100 *g* for 4 min. This procedure was repeated a second time with 75 μl of TE buffer. The eluted DNA was then precipitated with 0.1 volume of 3 *M* sodium acetate (pH 5.0) and 1 volume of 2-propanol, stored at −30°C for 1 h and centrifuged at 16 000 *g* for 30 min. The supernatant was discarded and the pellet was rinsed twice with 75% ethanol, dried under vacuum and usually resuspended in 10 μl of TE buffer prior to analysis.

Capillary conditioning

Every new fused-silica capillary was flushed with 1 *M* NaOH for 1 h followed by 0.001 *M* NaOH for 5 min. Between runs, the capillary was washed first with 1 *M* NaOH for 2 min and then with 0.001 *M* NaOH for 1 min. Finally, it was equilibrated with running buffer until the baseline remained stable. Overnight the capillary was stored in 0.001 *M* NaOH. Phenylmethyl-deactivated fused-silica capillaries were flushed with doubly distilled water only.

Chromatographic conditions

The gradient profiles used for anion-exchange and reversed-phase separations are given on each chromatogram. In order to keep the concentration of TEAA constant and unaffected by volume contraction during mixing of organic solvents with water, the mobile phase used for reversed-phase chromatography of oligonucleotides was prepared as follows: for a 10% solution of acetonitrile in 0.1 *M* TEAA, 50 ml of a 2 *M* TEAA stock solution were added to 100 ml of acetonitrile in a 1000-ml volumetric flask and the final volume was made up to 1000 ml with water.

RESULTS AND DISCUSSION

Fig. 1 shows the capillary zone electrophoretic separation of non-phosphorylated and phosphorylated oligodeoxyadenylic acids, 12–18 bases in length, in a 67-cm fused-silica capillary of I.D. 75 μm with the use of a borate buffer containing 25 m*M* of SDS, which had been found to enhance the selectivity [7]. It is evident that the additional phosphate group at the 5′-end of phosphorylated oligonucleotides allows them to migrate faster against the overwhelming electroosmotic flow, which car-

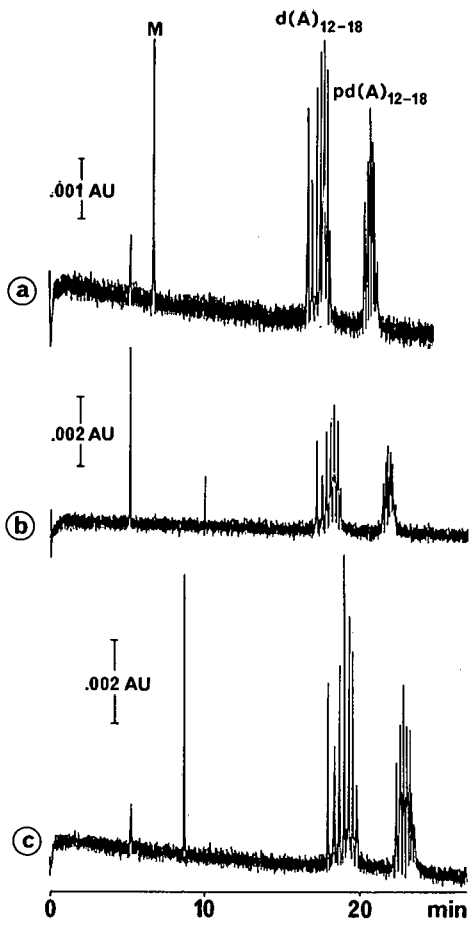

Fig. 1. Capillary zone electrophoretic separations of dephosphorylated and phosphorylated oligodeoxyadenylic acids. Capillary, fused silica, L = 67 cm, l = 60 cm, I.D. = 75 μm; carrier, 300 mM borate (pH 9.0)–(a) 25 mM SDS, (b) 25 mM NaCl and (c) 50 mM SDS; temperature, 25°C; voltage, 30 kV; current, 79, 99 and 89 μA, respectively; injection time, 7.5 s; detection, UV (254 nm); sample, $d(A)_{12-18}$ and $pd(A)_{12-18}$; M = mesityl oxide.

ries them past the detector toward the cathode. When SDS was replaced with an equivalent amount of sodium chloride, no significant change in resolution was observed. This indicates that the micelles are not required in order to obtain good resolution. However, as the sulphate moiety of SDS contributes less than chloride to the overall conductivity of the buffer system, higher concentrations of sodium in the carrier electrolyte can be realized without generating excess Joule heating. This allows a further enhancement in resolution, as can be seen in Fig. 1c.

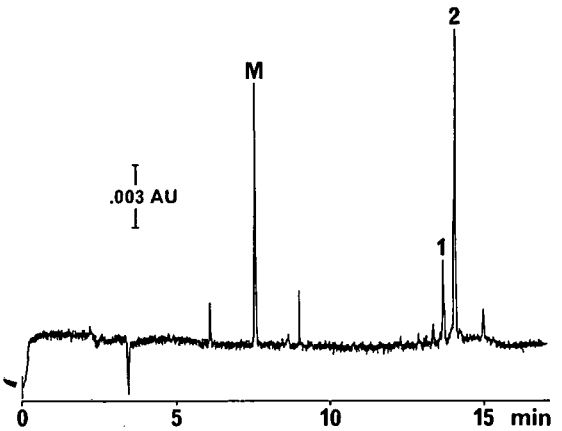

Fig. 2. Electropherogram of a trityl-on crude 21-mer heterooligonucleotide (GTGCTCAGTGTAGCCCAGGAT) and a 20-mer trityl-off sequence failure (M = mesityl oxide). Capillary, fused silica, L = 67 cm, l = 60 cm, I.D. = 75 μm; carrier, 300 mM borate (pH 9.0)–100 mM SDS; temperature, 25°C; voltage, 30 kV; current, 135 μA; injection time, 5 s detection, UV (254 nm).

Fig. 2 depicts the separation of a crude trityl-on

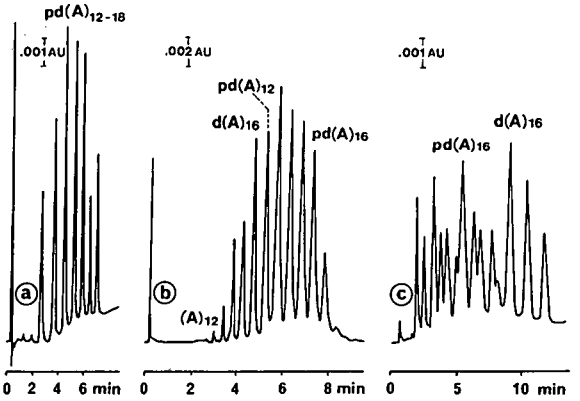

Fig. 3. HPLC separations of oligodeoxyadenylic acids. (a) Column Progel-TSK DEAE-NPR, 2.5 μm, 35 × 4.6 mm I.D.; buffer, 0.020 M Tris–HCl (pH 7.5); gradient, 0.15–0.5 M $(NH_4)_2SO_4$ in 15 min; flow-rate, 1 ml/min; sample, 0.75 μg of $pd(A)_{12-18}$. (b) Column, PEI-silica, 2 μm, 30 × 4.6 mm I.D.; buffer, 0.05 M phosphate (pH 5.9)–30% methanol; gradient, 0–0.5 M $(NH_4)_2SO_4$ in 10 min; flow-rate, 2 ml/min; sample, 1.75 μg pd $(A)_{12-18}$. (c) Column, PS-DVB-PVA, 2.3 μm, 50 × 4.6 mm I.D.; buffer, 0.1 M TEAA (pH 7.0); gradient, 12.5–20% acetonitrile in 20 min; flow-rate, 1 ml/min; sample, 0.5 μg $pd(A)_{12-18}$ and 0.083 μg $pd(A)_{16}$. All chromatograms were obtained by means of UV detection at 254 nm at room temperature.

21-mer heterooligonucleotide from a 20-mer sequence failure. However, with the chosen electrolyte system oligonucleotides cannot be separated according to size, because bases exhibit different electrophoretic mobilities in the order C < T < A. Therefore, this system is of limited value for the rapid characterization of synthetic oligonucleotides in comparison with capillary gel electrophoresis, which allows their strict separation according to size [8,9].

Fig. 3 shows the comparison of three different non-porous packing materials used for the analysis of oligodeoxyadenylic acids by means of anion-exchange and reversed-phase chromatography. The separation depicted in Fig. 3a was performed on a Progel-TSK DEAE-NPR stationary phase which consists of a non-porous hydrophilic resin covalently derivatized with diethylaminoethyl groups. The advantage of the hydrophilic resin is that the totally organic polymer is operable over a wide pH range, typically 1–13, without any damage occurring to the packing. This results in a long column lifetime and allows the regeneration of a deteriorated column with aqueous sodium hydroxide, which is of great advantage in the analysis of biopolymers. The number of functional groups that can be covalently attached, however, is limited by the Van der Waals radius of the molecules used for derivatization. In order to increase the ion-exchange capacity, a durable hydrophilic anion-exchange material was synthesized by the adsorption of polyethylenimine to non-porous silica particles with a diameter of 2 μm. Subsequently, the polyethylenimine layer was cross-linked into a stable layer by ethanediol diglycidyl ether. The resulting pellicular coating is more stable in aqueous media than the underlying silica and can be operated over the pH range 2–9.2 with no change in efficiency [4]. The higher ion-exchange capacity is reflected in the higher concentration of ammonium sulphate required to elute the oligodeoxyadenylic acids (Fig. 3b). However, the charge content has been found not to influence the resolution significantly, which is in accordance with a previous study on the ion-exchange chromatographic separation of double-stranded DNA fragments [10].

As analytes are separated according to charge in ion-exhange chromatography, it is not suprising that non-phosphorylated oligonucleotides are eluted earlier than phosphorylated ones. The presence of dephosphorylated oligodeoxyadenylic acids in a commercial sample of phosphorylated oligodeoxyadenylic acids is due to the incomplete phosphorylation of the oligonucleotides by polynucleotide kinase on completion of solid-phase synthesis. The relative content of dephosphorylated oligonucleotides has been found to vary considerably from batch to batch to batch, as can be seen in Fig. 3.

In order to prevent the corrosive action of halogen-containing eluents on the stainless-steel components of conventional HPLC equipment, an ammonium sulphate gradient was employed instead of the usual sodium chloride gradient. Moreover, ammonium sulphate improved significantly the resolution of oligonucleotides.

For many years anion-exchange chromatography of oligonucleotides has been considered superior to reversed-phase chromatography in terms of resolution and speed. Recently, however, we have succeeded in obtaining a baseline resolution of oligodeoxyadenylic acids up to 30 nucleotides in length on highly cross-linked PS–DVB–PVA particles using a

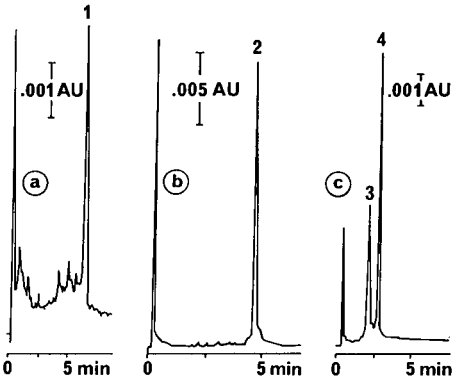

Fig. 4. HPLC analyses of synthetic phosphodiester heterooligonucleotides. (a) Column, Progel-TSK DEAE-NPR, 2.5 μm, 35 × 4.6 mm I.D.; buffer, 0.02 *M* Tris–HCl (pH 8); gradient, 0.4–1.0 *M* $(NH_4)_2SO_4$ in 10 min; flow-rate, 1 ml/min; temperature, ambient; sample, 0.36 μg of GTGCTCAGTGTAGCCCGTGATGCC, crude (1). (b) Column, PEI-silica, 2 μm, 30 × 4.6 mm I.D.; buffer, 0.05 *M* phosphate (pH 5.9)–30% methanol; gradient, 0–0.35 *M* $(NH_4)_2SO_4$ in 10 min; flow-rate, 2 ml/min; temperature, ambient; sample, 0.23 μg of TTGAAGTCACAGGAGACAACCTGGT, OPC-purified (2). (c) Column, PS–DVB–PVA, 2.3 μm, 50 × 4.6 mm I.D.; buffer, 0.1 *M* TEAA (pH 7); gradient, 6.5–8% acetonitrile in 2 min; flow-rate, 1 ml/min; temperature, 40°C; sample, GTGCTCAGTGTAGCCCAGGAT (3) and CTGTTGAACTCTTCTGAGCAA (4), 0.32 μg each. All chromatograms were obtained by means of UV detection at 254 nm.

volatile triethylammonium acetate buffer and a linear gradient of acetonitrile [11]. The particles were synthesized by a two-step microsuspension technique. Improved mass transfer and, hence, high resolution were obtained by adding PVA during polymerization, which yielded a more homogeneous and a less hydrophobic surface in comparison with PVA-free particles. As reversed-phase chromatography separates molecules based on their hydrophobicity, phosporylated oligonucleotides are eluted earlier than their dephosphorylated analogues (Fig. 3c).

Fig. 4a shows the analysis of a crude 24-mer oligonucleotide primer on a DEAE-bonded hydrophilic resin. Almost no failure sequences are detectable in addition to the desired, full-length oligomer. This corroborates the high efficiency of phosphoramidite chemistry [12] in the rapid preparation of oligonucleotides by means of an automated synthesizer, with the average yield per cycle being typically higher than 99%. From the chromatographic conditions chosen it is also evident that in comparison with homooligonucleotides higher concentrations of ammonium sulphate are required to elute heterooligonucleotides. This may be the result of additional hydrophobic interactions of the sample molecules with the stationary phase.

The efficacy of oligonucleotide purification cartridges [13] to purify the desired product from truncated oligomers and various organic salts contained in the crude synthesis mixture is demonstrated by the anion-exchange chromatographic analysis of a purified oligonucleotide on PEI-silica (Fig. 4b).

As illustrated in Fig. 4c, reversed-phase chromatography even permits the separation of isomeric oligonucleotides which differ only with regard to their base composition. The difference between the two oligonucleotides has been the replacement of three guanine residues with one adenine and two thymidine residues in the later eluting oligonucleotide. This retention behaviour is in accordance with our previous findings that the retention times of homooligonucleotides increase in the order C < G < A < T [11]. In addition to base composition, sequence was observed to exert an even greater influence on retention, especially in the presence of clusters of certain bases.

The polymerase chain reaction has revolutionized the identification of disease-associated genes,

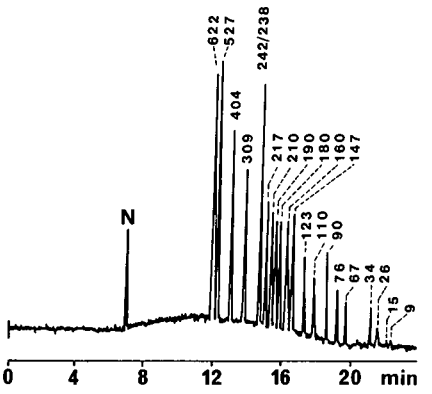

Fig. 5. Electropherogram of a pBR322-*Msp* I digest. Capillary, fused silica, L = 72 cm, l = 50 cm, I.D. = 50 μm; buffer, 0.01 M Tris–borate (pH 8.7)–0.1 mM EDTA–25 mM NaCl–0.5% (w/v) HEC–1.27 μM ethidium bromide; voltage, 15 kV; current, 16 μA; temperature, 35°C; detection, UV (260 nm); injection, vacuum, 5 s; sample concentration, 0.1 μg/μl.

because only a few copies are required to achieve the selective enrichment of DNA sequences of up to 6000 base pairs in length by a factor of 10^6 [14]. Recently, great interest has arisen in the quantification of PCR products to determine, for instance, the methylation of DNA or the rate of expression of certain genes. Quantification has been accomplished by various means such as liquid scintillation counting of excised gel bands, densitometry of photographic negatives of ethidium bromide-stained gels, hydridization with ^{32}P-labelled probes and

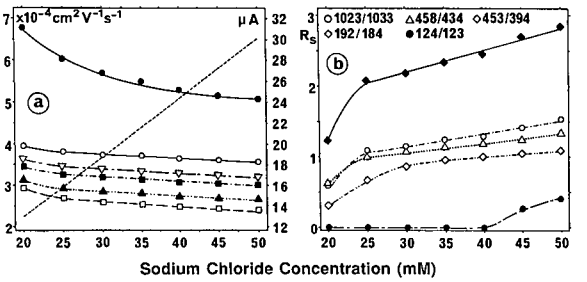

Fig. 6. Effect of sodium chloride concentration on (a) current (- - -), electroosmotic flow (●) and electrophoretic mobilities and (b) resolution (R_s) of DNA restriction fragments: ○ = 154 base pairs; ▽ = 298 base pairs; ■ = 394 base pairs; ▲ = 653 base pairs; □ = 1230 base pairs. Buffer, 0.01 M Tris–borate (pH 8.7)–0.1 mM EDTA–5–50 mM NaCl–0.5% (w/v) HEC; sample, pBR328 DNA-*Bgl* I/*Hinf* I digest, 0.25 μg/μl. Other conditions as in Fig. 5.

autoradiography, or high-performance liquid chromatography. However, these techniques are, for the most part, manually intensive, time consuming and prone to irreproducibility and poor quantitative accuracy.

Recently, we have established a capillary electrophoretic method that allows the rapid quantitative analysis of PCR products with a coefficient of variation as small as 3.4% by determining the molar ratio–peak area ratio of the amplified DNA segment with respect to a restriction fragment of known concentration [15]. Fig. 5 shows the separation of a pBR322 DNA-*Msp* I digest in a fused-silica capillary with an effective length of 50 cm and I.D. 50 μm. Hydroxyethylcellulose was added at a concentration of 0.5% to the running buffer as a sieving agent in order to permit the separation of nucleic acids according to size. Another prerequisite was the addition of sodium chloride, which not only reduced electroosmotic flow by increasing the thickness of the diffusion double layer at the inner capillary wall but also altered the mobility of DNA fragments in a variety of ways which affect charge, shape and size. Fig. 6a depicts the decrease in true electrophoretic mobilities of DNA restriction fragments observed with increasing concentration of sodium ions in the running buffer. The improvement in resolution (Fig. 6b) which can be noted when the sodium chloride concentration is increased from 20 to 25 m*M* is mainly due to the spread in electrophoretic mobilities between the largest and the smallest DNA fragment. Above that, no further increase in selectivity is observed. Hence the slight and linear improvement in resolution seen at even higher concentrations of sodium chloride may be a consequence of the increase in current density which is known to cause a proportional increase in the number of theoretical plates.

The influence of various alkali metal ions, namely lithium, sodium, potassium, rubidium and cesium, on the capillary electrophoretic separation of DNA restriction fragments is depicted in Fig. 7. It is evident that as the cation size increased the migration times increased. This is mainly due to a decrease in ζ potential, which causes a lower electroosmotic flow. The ζ potential is linearly proportional to the charge density, which decreases as the atomic weight of the cation increases. Another observation is that the spread in electrophoretic mobilities between the largest and the smallest fragments increased considerably when lithium or sodium chloride was replaced with potassium chloride. While caesium chloride yielded the best separation of DNA fragments, the migration times were five times longer than when lithium chloride was used. Generally, an increase in resolution of all DNA fragments was achieved with an increase in the size of the cation, but the concomitant increase in migration times might be unacceptable in routine analysis.

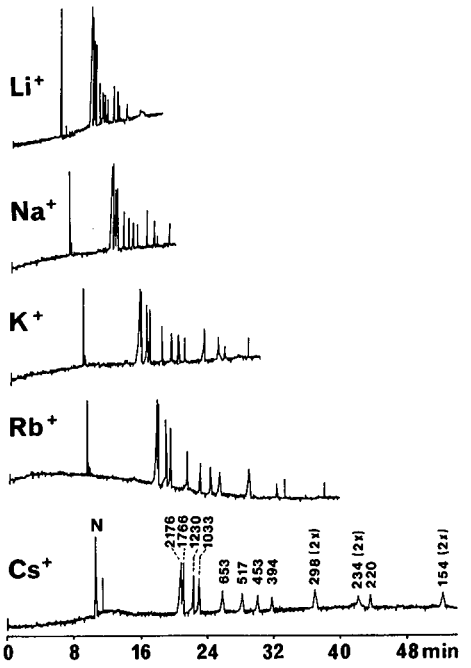

Fig. 7. Effect of various alkali metal cations on the separation of dsDNA. Capillary, fused silica, L = 72 cm, l = 50 cm, I.D. = 50 μm; buffer, 0.01 *M* Tris–borate (pH 8.7)–(0.1 m*M* EDTA–0.5% (w/v) HEC–25 m*M* LiCl, NaCl, KCl, RbCl or CsCl; voltage, 17, 15, 13, 12 and 12 kV, respectively; current, 16 μA; temperature, 35°C; detection, UV (260 nm); injection, vacuum, 8 s; sample, pBR328-*Bgl* I/*Hinf* I digests, 0.25 μg/μl.

A further improvement in resolution was obtained by the addition of ethidium bromide to the running buffer. Ethidium bromide minimizes variations in electrophoretic mobility caused by the metastability of DNA by the way of intercalation between two adjacent GC pairs. Optimum resolution in comparison with a buffer system containing no ethidium bromide (Fig. 8a) was obtained at a

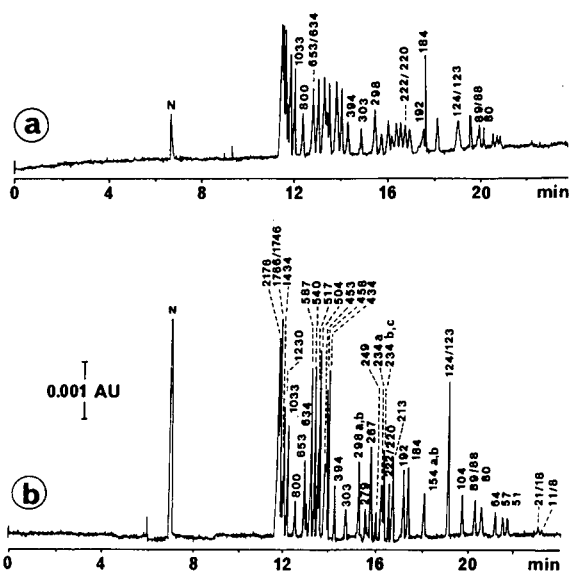

Fig. 8. Effect of ethidium bromide on the capillary electrophoretic separation of DNA restriction fragments. Capillary, fused silica, L = 72 cm, l = 50 cm, I.D. = 50 μm; buffer, 0.01 M Tris–borate (pH 8.7)–0.1 mM EDTA–25 mM NaCl–0.5% (w/v) HEC, (a) without and (b) with 1.27 μM of ethidium bromide; voltage, 15 kV; current, 16 μA; temperature, 35°C; detection, UV (260 nm); injection, vacuum, 8 s; sample, a mixture of pBR322 DNA-*Ava* II/*Eco*R I (0.2 μg/μl), pBR322 DNA-*Hae* III (0.25 μg/μl) and pBR328 DNA-*Bgl* I/*Hinf* I (0.25 μg/μl) digests in a ratio 1:2:2.

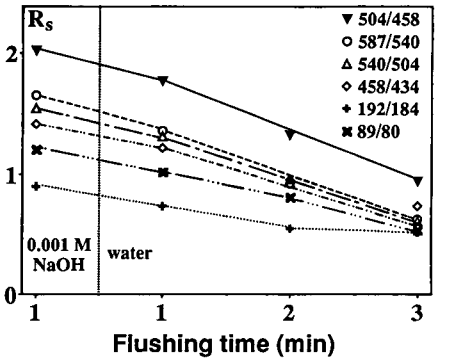

Fig. 9. Effect of flushing fused-silica capillaries with dilute sodium hydroxide or water on resolution of DNA fragments. Capillary, fused silica, L = 72 cm, l = 50 cm, I.D. = 50 μm; buffer, 0.01 M Tris–borate (pH 8.7)–0.1 mM EDTA–25 mM NaCl–0.5% (w/v) HEC; temperature, 35°C; voltage, 12 kV; current, 13 μA; detection, UV (260 nm); injection, vacuum, 5 s.

concentration of 1.27 μM (Fig. 8b). The addition of even more ethidium bromide up to a concentration of 7.6 μM only enhanced the resolution of shorter DNA fragments, whereas the resolution for DNA molecules longer than 400 base pairs started to decline again. The tremendous improvement in efficiency is further endorsed by a fourfold increase in the number of theoretical plates. At 1.27 μM of ethidium bromide up to $2 \cdot 10^6$ plates per metre could be realized for fragments less than 300 base pairs in length. On addition of even more ethidium bromide the number of theoretical plates declined again. Finally, at 7.6 μM the same number of plates per metre was observed as without ethidium bromide, namely $2 \cdot 10^5$–$4 \cdot 10^5$ for DNA restriction fragments ranging from 89 to 1230 base pairs in length.

The physical and the chemical states of the inner capillary surface exert a major impact on the resolution of dsDNA fragments. Hence, capillaries of fused silica must be prepared for use prior to any analytical runs by washing for at least 30 min with 1 M NaOH to remove any adsorbed impurities or traces of old sample and to ensure maximum ionization of silanol groups. Following a flush with 0.001 M NaOH, the capillary has to be equilibrated with the running buffer until the baseline remains stable. This procedure has to be repeated between runs whenever loss of reproducibility and resolution is observed. Otherwise capillaries are flushed first with 1 M NaOH for 2 min, then with 0.001 M NaOH for 1 min. The 2-min rinse with 1 M NaOH yielded optimum resolution, whereas shorter or longer washing periods reduced the separation efficiency. The dilute sodium hydroxide flush was preferred to water, which exerted a deteriorating effect on resolution due to reprotonation of the charged silanols on the inner capillary wall (Fig. 9). Moreover, it is recommended to replace the cathode reservoir during the sodium hydroxide wash in order to avoid a loss of reproducibility and resolution due to a change in buffer composition. Taking these precautions, it suffices to renew the buffer in both reservoirs every 3–4 runs.

Using a phenylmethyl-deactivated fused-silica capillary, theoretical plates in excess of $4 \cdot 10^6$ plates per meter could be realised for restriction fragments ranging from 220 to 1766 base pairs in length when the aforementioned buffer system was replaced with 100 mM Tris–borate (pH 8.7)–0.5% hydroxyethylcellulose–0.653 μM ethidium bromide (Fig. 10). Al-

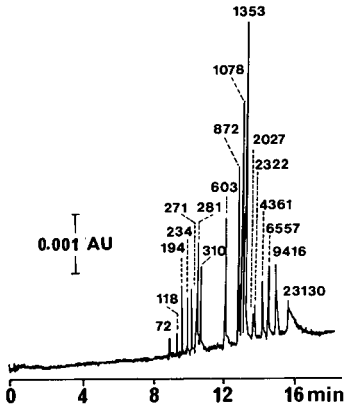

Fig. 10. Electropherogram of a *λ-Hind* III/*ϕ*X174-*Hae* III digest. Capillary, phenylmethyl-deactivated fused silica, L = 72 cm, l = 50 cm, I.D. = 50 μm; buffer, 0.1 *M* Tris–borate (pH 8.7)–1 m*M* EDTA–0.5% (w/v) HEC–0.635 μ*M* ethidium bromide; voltage, −20 kV; current, 26 μA; temperature, 35°C; detection, UV (260 nm); injection, vacuum, 2 s; sample concentration, 0.5 μg/μl.

though separation is achieved basically according to size, minor discrepancies may be observed on addition of ethidium bromide to the buffer system, because its cationic-charged nitrogens interact electrostatically with the phosphate groups of DNA, which slows the migration rate depending on the content of adjacent GC pairs.

Resolution in capillary electrophoresis is also influenced significantly by sample composition. The salts, nucleotides and primers contained in PCR samples have been found to cause considerable band broadening owing to the conductivity difference between the sample zone and the surrounding buffer (Fig. 11a). Hence, purification of PCR products prior to capillary electrophoretic analysis is required. It has been observed that neither ethanol precipitation nor polyacrylamide size exclusion gel chromatography with an exclusion limit of 20 base pairs removes all unincorporated nucleotides and

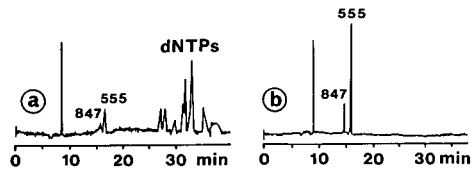

Fig. 11. Electropherograms of two (a) unpurified and (b) Sephadex G-150-purified PCR products. Buffer, 0.01 *M* Tris–borate (pH 8.7)–0.1 m*M* EDTA–0.5% (w/v) HEC–25 m*M* NaCl–1.27 μ*M* ethidium bromide. Other conditions as in Fig. 8.

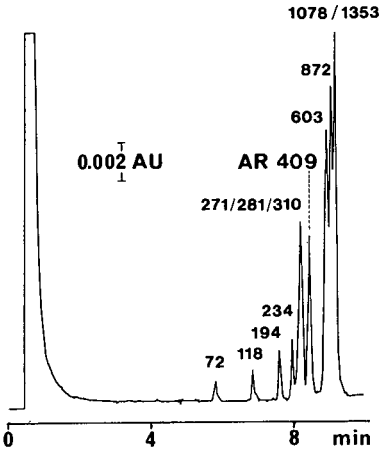

Fig. 12. Anion-exchange chromatographic analysis of a PCR-amplified 409-base pairs fragment of the androgen receptor spiked with a *ϕ*X174-*Hae* III digest. Column, Progel-TSK DEAE-NPR, 2.5 μm (35 × 4.6 mm I.D.); eluents, (A) 0.025 *M* Tris–borate (pH 8.6)–0.25 m*M* EDTA, (B) 1 *M* NaCl in A, linear gradient from 45 to 75% B in 15 min; flow-rate, 1 ml/min; temperature, 25°C; detection, UV (260 nm).

primers. Only Sephadex G-150 retained all nucleotides and primers, hence ensuring optimum resolution of the PCR products (Fig. 11b).

The concentration sensitivity of capillary electrophoresis using on-column UV detection equals that obtained by ethidium bromide-stained gels. However, owing to the lower mass detection limit, which is *ca.* 3 pg for a 72 base pair restriction fragment at a signal-to-noise ratio of 3, only 3–5 nl of sample need to be injected in contrast to the 10 μl required for an agarose slab-gel separation.

Even with the best non-porous packing materials availaible, anion-exchange chromatography fails to provide the same degree of resolution as that obtained by means of capillary electrophoresis (Fig. 12). Moreover, retention times of DNA fragments do not always correlate with their size, because AT pairs interact more strongly than GC pairs with the stationary phase [10]. Therefore, fragments with a relatively high AT content are retarded more than others.

CONCLUSIONS

It is concluded that HPLC on non-porous particles is superior to capillary electrophoresis in terms

of speed and selectivity in the analysis of oligonucleotides up to 30 bases in length. Moreover, reversed-phase chromatography of detritylated oligonucleotides permits their simultaneous purification without the need for subsequent desaltation because the volatile buffer system can be readily evaporated. With regard to dsDNA, however, the resolving power of capillary electrophoresis cannot be matched by anion-exchange chromatography at present. Moreover, the combined use of hydroxyethylcellulose and ethidium bromide not only yields a separation efficiency equal to that achieved by means of gel-filled capillaries but also avoids some of their limitations such as the destruction of the gel matrix at high current densities and the bias involved in electrokinetic injection which does not allow the same amount of each DNA species to be delivered.

ACKNOWLEDGEMENT

This study was supported in part by the Ministry of Science, Vienna, Austria (G.Z. 49.685/3-II/A/4/90).

REFERENCES

1 W. Haupt and A. Pingoud, *J. Chromatogr.*, 260 (1983) 419.
2 G. Jilge, K. K. Unger, U. Esser, H. J. Schäfer, G. Rathgeber and W. Müller, *J. Chromatogr.*, 476 (1989) 37.
3 M. J. Gordon, X. Huang, S. L. Pentoney and R. N. Zare, *Science*, 242 (1988) 224.
4 A. J. Alpert and F. E. Regnier, *J. Chromatogr.*, 185 (1979) 375.
5 K. Kopaciewicz, M. A. Rounds and F. E. Regnier, *J. Chromatogr.*, 318 (1985) 157.
6 S. Wongyai, J. M. Varga and G. K. Bonn, *J. Chromatogr.*, 536 (1991) 155.
7 A. S. Cohen, S. Terabe, J. A. Smith and B. L. Karger, *Anal. Chem.*, 59 (1987) 1021.
8 A. S. Cohen, D. R. Najarian, A. Paulus, A. Guttman, J. A. Smith and B. L. Karger, *Proc. Natl. Acad. Sci. U.S.A.*, 85 (1988) 9660.
9 A. Paulus and J. I. Ohms, *J. Chromatogr.*, 507 (1990) 113.
10 E. Westman, S. Eriksson, T. Låås, P. A. Pernemalm and S. E. Sköld, *Anal. Biochem.*, 166 (1987) 158.
11 C. G. Huber, P. J. Oefner and G. K. Bonn, *J. Chromatogr.*, 599 (1992) 113–118.
12 S. L. Beaucage and M. H. Caruthers, *Tetrahedron Lett.*, 22 (1981) 1859.
13 L. J. McBride, C. McCollum, S. Davidson, J. W. Efcavitch, A. Andrus and S. J. Lombardi, *BioTechniques*, 6 (1988) 362.
14 R. K. Saiki, S. Scharf, F. Faloona, K. B. Mullis, G. T. Horn, H. A. Erlich and N. Arnheim, *Science*, 230 (1985) 1350.
15 S. Nathakarnkitkool, P. J. Oefner, G. Bartsch, M. A. Chin and G. K. Bonn, *Electrophoresis*, 13 (1992) 1.

Journal of Chromatography, 625 (1992) 341–348
Elsevier Science Publishers B.V., Amsterdam

CHROM. 24 537

Optimization of indirect photometric detection of anions in high-performance capillary electrophoresis

Yinfa Ma and Rulin Zhang

Division of Science, Northeast Missouri State University, Kirksville, MO 63501 (USA)

(First received March 3rd, 1992; revised manuscript received June 2nd, 1992)

ABSTRACT

Optimization of the indirect photometric detection in high-performance capillary electrophoresis is demonstrated. The influences of background electrolyte (BGE) concentration, capillary diameters, linear polymers, pH of BGE and types of BGE have been studied and assessed in terms of theoretical predictions. The experimental results fit the theoretical deduction very well. At optimized conditions, sub-femtomoles of simple anions can be detected, offering a 500-fold improvement compared to previous studies, and being close to the predicted limit of detection.

INTRODUCTION

High-performance capillary zone electrophoresis (HPCZE) has been recognized to be a modern separation technique which offers higher resolution with decreased analysis time than high-performance liquid chromatography (HPLC). However, a detection method with wide applicability is urgently needed for the advancement of HPCZE. UV–visible absorbance has been utilized as a detection method for HPCZE and still remains the most popular method of detection [1–5]. This method has several shortcomings: (1) samples separated by HPCZE are required to absorb light in the UV or visible region; (2) the detection limit and linearity are impaired due to the changes in the absorption coefficients (ε) of the analytes in different samples. The ones having lower absorption coefficients could not be detected at lower concentrations (*e.g.* femtomole range). Therefore, this detection method is mainly used for aromatic compounds [6], peptides [7], proteins [8], and nucleotides [9]. Fluorescence is a sensitive and most easily adapted detection method for HPCZE [10–12]. However, it can only be used to detect the samples which fluoresce or can be chemically modified to a fluorescent derivative. Chemical derivatization is an undesirable complication because of possible error in the chemistry and irreproducible operation, which can drastically affect quantitation. Mass spectrometry (MS) has been developed as a detector for HPCZE [13–15]. It is sensitive and can offer structural information of the samples. The high expense of a mass spectrometer, however, limits the widespread use of this technique in practice. Also, the detection of large molecules (MW > 100 000) by MS can be difficult even though some demonstrations have been made [16].

Indirect fluorometric detection has been demonstrated to be a universal, sensitive detector for HPCZE [17–20]. The remarkable aspect of this technique is the potential application to solutes with few other detectable properties. With laser excitation of the background fluorophore, typical detection limits (LOD) are in the attomole range which compares favorably with most other detection techniques. However, the impressive LOD is due to the high intensity of the excitation laser beam, which highly increases the cost of the instrumentation setup.

Correspondence to: Dr. Y. Ma, Division of Science, Northeast Missouri State University, Kirksville, MO 63501, USA.

0021-9673/92/$05.00

Indirect photometric detection is another universal detection technique for HPCZE, which has a similar detection mechanism to that of the indirect fluorometric detection method. Detection of rare earth metals [21], cyclodextrins [22] and anions [23] has been demonstrated. However, the conditions were never optimized. The LOD at present (300–500 femtomoles) has not reached the level that should be attainable. Recently, Nielen [24] has done some quantitative studies on indirect UV absorbance detection in HPCZE. The author used a series of alkylsulphate surfactants as a model system to study the repeatability of the mobilities, response factors and linearity of the detection signal. However, other factors which may influence the separation and detection were not mentioned.

A strategy is presented in this paper for the optimization of indirect photometric detection of anions in HPCZE. Since the detection of trace amount of common anions, such as Cl^-, Br^-, NO_3^-, and SO_4^{2-}, is always of ongoing interest, the development of a rapid and sensitive detection method is very practical. The influence of capillary diameter, buffer pH, linear polymers, concentration of background electrolyte (BGE), and different kinds of BGE is described.

THEORETICAL

In the indirect photometric detection method for HPCZE, the detection limit can be described:

$$C_{lim} = C_{BGE}/(RDr) \quad (1)$$

where C_{lim} is the minimum analyte concentration of detection, C_{BGE} is the concentration of BGE, R is the displacement ratio (which is defined as the number of BGE molecules replaced by one analyte species), and Dr is dynamic reserve (which is defined as the ratio of the background signal to the noise level). Eqn. 1 reveals that the detection limit can be maximized by adjusting C_{BGE} and Dr, R is almost constant for a fixed separation system.

From the Lambert Beer law:

$$A_{BGE} = \log (I_0/I) = \varepsilon_{BGE}\, bC_{BGE} \quad (2)$$

where I_0 is the beam intensity before striking the cell, I is the beam intensity coming out the sample cell, ε_{BGE} is the molar absorption coefficient of BGE, and b is the optical path length of the beam I. Substituting eqn. 2 into eqn. 1:

$$C_{lim} = A_{BGE}\varepsilon_{BGE}bRDr \propto C_{BGE}\varepsilon_{BGE}bRDr \quad (3)$$

The absorbance detectors currently used in HPCZE exhibit a noise level of *ca.* $1 \cdot 10^{-4}$ absorbance units (a.u.). The displacement ratio is usually 1 for anions [25]. If we use 50-μm capillaries for the separation, the b in eqn. 3 will be $5 \cdot 10^{-3}$ cm. The Dr can reach 500 if we stabilize the background absorbance signal. If we choose a BGE with ε = 10 000 l/mol cm, and use the detection limit at signal-to-noise (S/N) = 5 ($A_{BGE} = 5 \cdot 10^{-4}$ a.u.), then the C_{lim} can be estimated:

$$C_{lim} = 5 \cdot 10^{-4}/(10\,000 \cdot 5 \cdot 10^{-3} \cdot 500) = 2 \cdot 10^{-8}\ M$$

If a 5-nl sample is injected, the mole detectability will be 0.1 fmol.

Because of the optical medium, a non-linear response is usually observed for direct absorbance measurement. Higher concentrations of analytes will lead to non-linear calibration plots due to self-absorption, self-quenching and detector saturation. In indirect absorbance detection, the response is not based on the analyte itself and a linear response should be, theoretically, easier to obtain.

EXPERIMENTAL

Equipment

The HPCZE system used was purchased from ISCO (Lincoln, NE, USA; Model 3850). A negative high voltage was applied to the capillary (*i.e.* the injection end was maintained at negative high voltage while the other end was held at ground potential). The data were collected with a Datajet computing integrator (Spectra Physics, Mountain View, CA, USA). The capillary column (Polymicro Technologies, Phoenix, AZ, USA) was 60 cm long. The outer diameter (O.D.) of the columns was always 150 μm, while the inner diameter (I.D.) ranged from 10 to 100 μm. The polymer coating was burned off 25 cm from the anodic end of the capillary to form the detection window.

Reagents

All chemicals were reagent grade unless otherwise noted. Deionized water was obtained using a

Milli-Q system (Millipore, Bedford, MA, USA).

HPLC-grade ethanol, benzoic acid, *o*-benzoyl benzoic acid, 2-sulfobenzoic acid, phthalic acid and hydroxylpropylmethyl cellulose (HMC) (4000 cP at 25°C for 2% solution) were purchased from Aldrich (Milwaukee, WI, USA). Other inorganic chemicals were purchased from Sigma (St. Louis, MO, USA).

RESULTS AND DISCUSSION

Fig. 1 demonstrates the influences of different kinds of BGE on the separation and detection of anions. It is shown that under the same concentration of BGE the detector response of separated anions was different. Even though *o*-benzyl benzoic acid has a much larger absorption coefficient (ε = 19 000 l/molcm) than benzoic acid (ε = 11 900 l/molcm) (at 228 nm), the peak heights of the anions are almost the same. The ε of the 2-sulfobenzoic acid (ε = 40 000 l/molcm) is 3 times larger than that of phthalic acid (ε = 13 000 l/molcm) at 228 nm. However, the detector responses of the anions are also almost the same. It also can be seen that NO_3^- gives a very weak signal when 2-sulfobenzoic acid is used as a BGE. All these phenomena suggest that with indirect photometric detection, the response of the analyte is not totally proportional to the absorption coefficient of the BGE, but also dependent on the displacement ratio (*R*). Also, for different BGEs, the dynamic reserve (*Dr*) is different. This is due to the variation of Joule heating from one BGE

TABLE I

THE ELECTROOSMOTIC VELOCITIES FOR DIFFERENT BGEs

Conditions: 0.02 *M* for each BGE; pH 6.5; other conditions as in Fig. 1.

BGE	μ_{eo} ($10^{-3}cm^2V^{-1}s^{-1}$)[a]
Benzoic acid	0.510 ± 0.13%
Phthalic acid	0.709 ± 0.15%
2-Sulfobenzoic acid	0.532 ± 0.13%
o-Benzylbenzoic acid	0.874 ± 0.14%

[a] The mean values of eight analyses ± relative standard deviation.

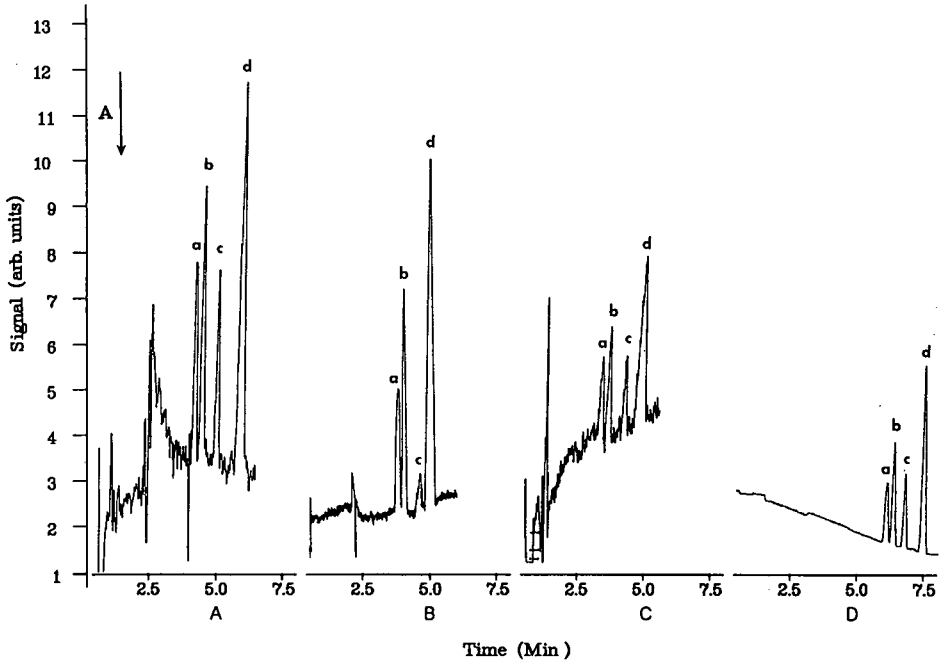

Fig. 1. The influences of different kinds of background electrolytes (BGE) on the separation and detection of anions. BGE used: (A) phthalic acid; (B) 2-sulfobenzoic acid; (C) benzoic acid; (D) *o*-benzyl benzoic acid. BGE concentration: 0.02 *M*. pH of BGEs: 6.5. A 3-s, −20-kV injection of 100 μM of each anion followed by electrophoresis at −20 kV in a 60-cm (75 μm I.D.) capillary column. Detection wavelength: 228 nm. Peak identification: a = bromide; b = chloride; c = nitrate; d = sulfate.

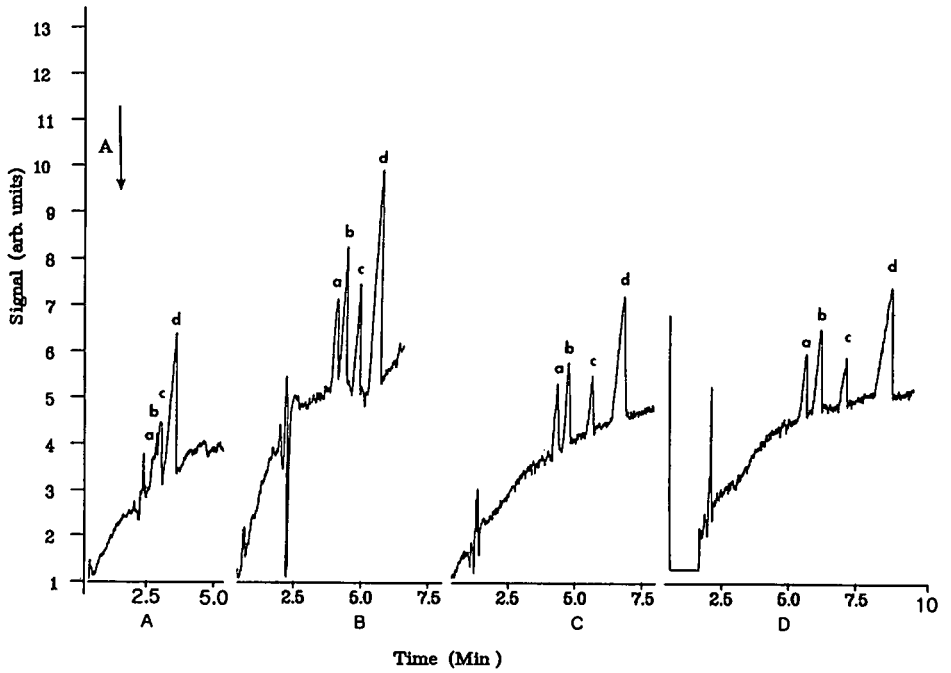

Fig. 2. The influence of the pH of the BGE solution. BGE used: 10 m*M* phthalic acid. The pH tested: (A) pH = 4.3; (B) pH = 6.5; (C) pH = 7.7; (D) pH = 9.2. Injection time: 2 s. The concentration of the anions: 50 μM each. All other conditions and peak identifications are the same as those of Fig. 1.

to another, which causes the variation of baseline drifting. In this case, phthalic acid would be a good choice. We noticed that the migration times of the analytes varies from one BGE to another. This is because of the changes of electroosmotic flow with BGEs, even though the pH values of the BGE were kept same. The μ_{eo} values for different BGEs are tabulated in Table I.

Fig. 2 demonstrates the influence of the pH of the BGE solution (the pH influences are very similar for four different BGEs studied). It is clear that when the pH of the BGE solution is too low, the separation of the anions becomes worse and the signal becomes smaller. The reason is that the BGE molecules are not charged at low pH, the replacement ratio is smaller, and the signal becomes smaller. At lower pH, the electroosmotic flow, migrating oppositely from that of anions, is also smaller, causing the effective mobility and resolution of the analytes to change which also affects the separation. This phenomenon has been described earlier [18]. At higher pH, the separation of the anions becomes better. However, the migration time is longer and the peaks are broader. This is understandable, because the electroosmotic flow at higher pH is much larger.

Fig. 3 shows the influence of the linear polymers. We found that the analyte peaks are sharper and elute faster with the addition of 0.3% hydroxylpropylmethyl cellulose (HMC) in the running buffer, comparing to that containing no HMC. This is due to the decreases of electroosmotic flow by additive HMC. However, addition of 0.5% of HMC in the running buffer causes the analyte peaks to be smaller, more broad and take longer to elute than that of 0.3% HMC. The reason for this is due to: (1) the increases of viscosity of the running buffer solution which decrease the migration rate of analyte ions; (2) the pH change (from pH 6.5 to pH 7.8). These changes will change the separation behavior and displacement ratio. The μ_{eo} values, pH and viscosity for different amount of HMC (in the running buffer) are listed in Table II.

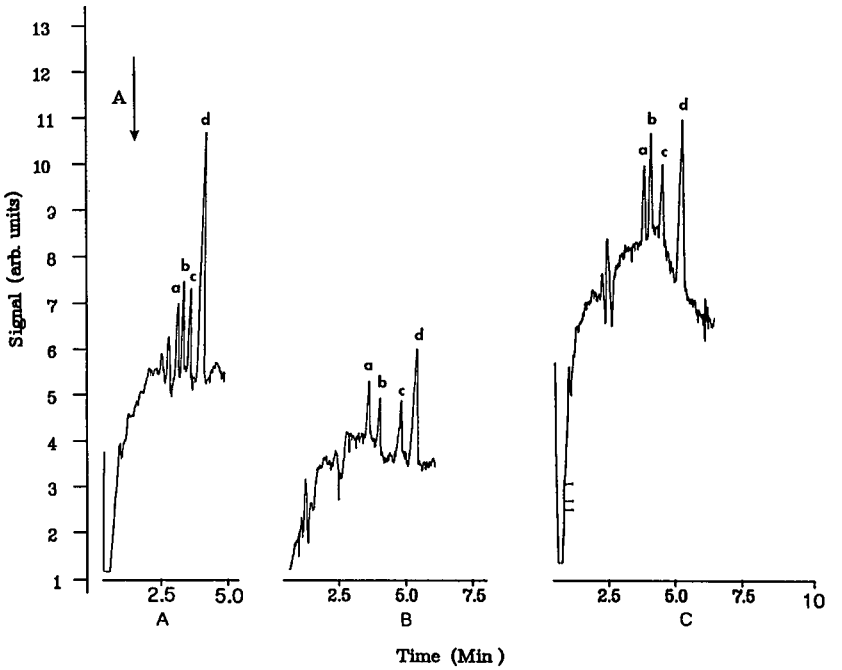

Fig. 3. The influences of the linear polymers (additive). BGE used: 10 m*M* phthalic acid (pH = 6.5). Linear polymer: hydroxylpropyl methyl cellulose (HMC). Polymer concentration: (A) 0.3%; (B) none; (C) 0.5%. Injection time: 2 s. The concentration of the anions: 50 μM each. All other conditions and peak identifications are the same as those of Fig. 1.

The influence of the capillary diameter is shown in Fig. 4. We found that the peak areas of the analytes were smaller and the peaks were sharper in 25 μm I.D. capillary column than those of 75 μm I.D. when the injection time and the other parameters were kept the same. Based on these experiments, the detection limits for both diameters were almost same. This suggests that with a narrow range of column diameters, the column diameter is not the major contribution to the limit of detection. The explanation for this is that when column diameter was changed, Joule heating (increasing with column diameter) [26–28], *Dr*, and velocity of electroosmotic flow would change also. The μ_{eo} values and *Dr* for

TABLE II

THE μ_{eo} VALUES, pH AND VISCOSITY FOR DIFFERENT HMC IN THE RUNNING BUFFER

Conditions: 10 m*M* phthalic acid; the measurements of viscosity were carried out at 25°C and atmospheric pressure; other conditions as in Fig. 1.

% of HMC	μ_{eo} (10^{-3}cm^{2}V^{-1}s^{-1})[a]	pH	viscosity(η)[b] (cP)
0	0.713 ± 0.14%	6.5	0.8940 ± 0.07%
0.3	0.405 ± 0.15%	6.9	1.7391 ± 0.06%
0.5	0.408 ± 0.13%	7.8	2.1739 ± 0.06%

[a] The mean of eight analyses ± relative standard deviation.
[b] The mean of three measurements ± relative standard deviation.

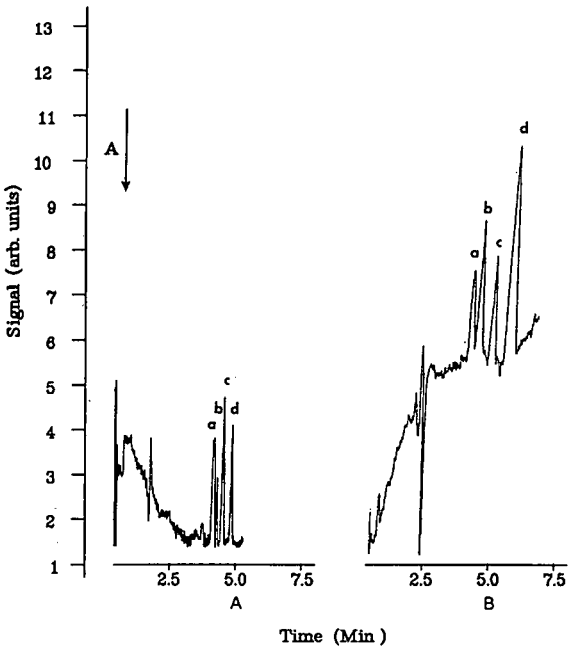

Fig. 4. The influence of the capillary diameters. BGE used: 10 m*M* phthalic acid (pH = 6.5). Capillary diameters: (A) 25 μm; (B) 75 μm. Injection time: 2 s for both. The concentration of the anions: 50 μM each. All other conditions and peak identifications are the same as those of Fig. 1.

different diameter of columns are listed in Table III. However, when a 10 μm-I.D. capillary was used, the LOD worsened dramatically (chromatogram is not included). This was found to be due to the inability to focus all the light onto a 10-μm capillary. When a 100 μm I.D. capillary was used, the large increase of Joule heating caused a serious fluctuation of baseline, which decreased the *Dr* significantly. The Joule heat generated for different diameter of columns (W/cm) is listed in Table IV.

The influence of concentration of the BGE was also investigated. We found that there were no analyte peaks observed when the BGE concentration was smaller than $1.0 \cdot 10^{-5}$ *M*. This was due to the very low background absorbance signal, low dynamic reserve (*Dr*) which was caused by serious baseline shifting and high noise level. Other authors have found the same problem [24,29,30], and the reasons for the baseline problem at very low concentration of BGE have been well explained. All these factors made the replacement signal negligible. When BGE concentration was smaller than ~ 1 m*M*, the broader analyte peaks were observed and the separation was very poor. This can be explained by laminar flow effect [31]. According to the Kohlrausch theory [32], a narrow zone of analytes can be formed when a long plug of low-concentration buffer containing analytes is injected into a column filled with a high-conductivity buffer. However, at low concentration of BGE, since the local electroosmotic flow in the sample plug is smaller than the bulk electroosmotic flow of the running buffer, the pressure difference caused by the mismatch in electroosmotic flow will generate a laminar flow inside the column which will broaden the sharp zone generated by the stacking process and sharply reduce the resolution. The details on this aspect have been reported by Burgi and Chien [33,34]. We also found that 5 to 15 m*M* BGE was the best concentration range to work with. In addition, the BGE concen-

TABLE III

THE μ_{eo} VALUES AND *Dr* FOR DIFFERENT DIAMETERS OF COLUMNS

Conditions: 10 m*M* phthalic acid; pH 6.5; other conditions as in Fig. 1.

Capillary diameter	μ_{eo} (10^{-3}cm^{2}V^{-1}s^{-1})[a]	*Dr*
25 μm	0.705 ± 0.14%	741
50 μm	0.709 ± 0.13%	638
75 μm	0.713 ± 0.14%	474

[a] The mean of eight analysis ± relative standard deviation.

TABLE IV

THE JOULE HEAT GENERATED FOR DIFFERENT DIAMETERS OF COLUMN

Conditions: 10 m*M* phthalic acid; pH 6.5; capillary length: 60 cm; voltage applied: −20 kV; the molar conductivity of phthalic acid: 382 Ω^{-1}cm^{2}mol^{-1}.

Column diameter (μm)	Joule heat generated (V$^2\Omega^{-1}$cm^{-1}) or (Watt/cm)
10	$1.06 \cdot 10^{-4}$
25	$6.63 \cdot 10^{-4}$
50	$2.65 \cdot 10^{-3}$
75	$5.97 \cdot 10^{-3}$
100	$1.06 \cdot 10^{-2}$

TABLE V

THE REPEATABILITY OF MOBILITIES AND DETECTION SIGNALS

Conditions: 10 m*M* phthalic acid; pH 6.5; other conditions as in Fig. 1.

Component	Migration time[a] (min)	Peak area[a] (10^5 counts)
Br^-	4.15 ± 0.69%	3.87 ± 7.3%
Cl^-	4.42 ± 0.82%	4.92 ± 4.9%
NO_3^-	4.86 ± 0.91%	3.99 ± 4.3%
SO_4^-	5.31 ± 0.96%	15.21 ± 6.8%

[a] The mean values of eight analysis ± relative standard deviation.

tration needed to be increased when the analyte concentration was high.

The repeatability of the mobilities and detection signals have been evaluated. The mean values and relative standard deviations based on eight times of analysis are listed in Table V. It can be concluded that the mobilities and detection signals are very constant based on statistic rules (at 90% confidence level).

The detection limit of the anions was demonstrated at optimized conditions. The detection limit for four common anions is shown in Fig. 5 . Sub-femtomoles of each anion were detected, which fits the theoretical prediction very well.

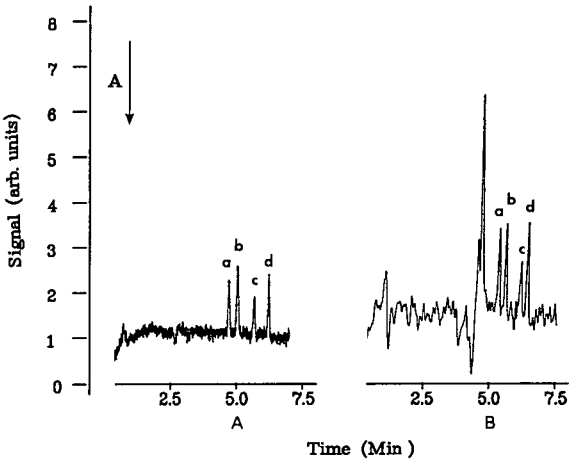

Fig. 5. The detection limits of anions. BGE used: 10 m*M* phthalic acid (pH = 6.5). Capillary diameter: (A) 25 μm; (B) 75 μm. Concentration of anions: $[Br^-] = [NO_3^-] = 2.0 \cdot 10^{-6}$ *M*; $[Cl^-] = 1.0 \cdot 10^{-6}$ *M*; $[SO_4^{2-}] = 2.0 \cdot 10^{-7}$ *M*. Injection time: (A) 5 s; (B) 2 s. Moles injected: 0.3 fmol and 1.1 fmol of Cl^- were injected for (A) and (B) individually. All other conditions and peak identifications are the same as those of Fig. 1.

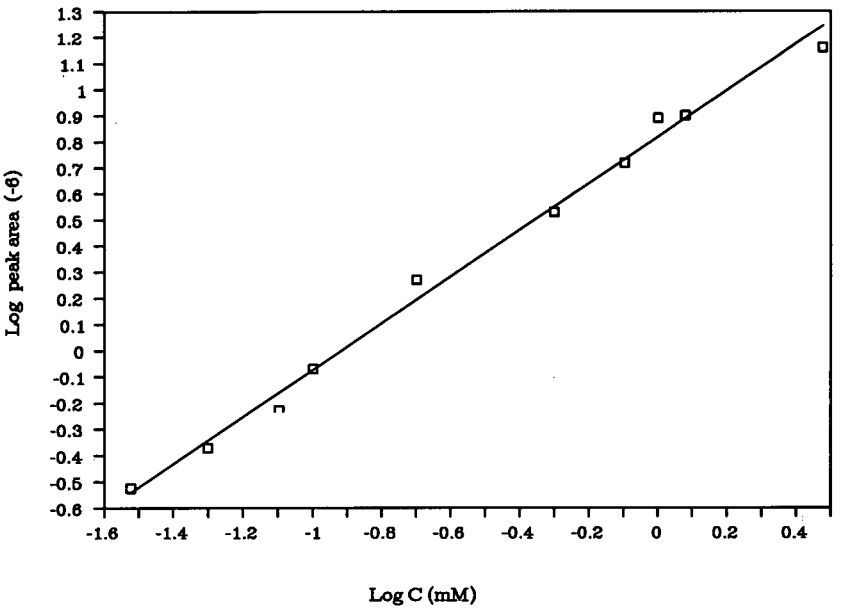

Fig. 6. The linearity for indirect photometric detection based on peak areas. The test anion is chloride.

Finally, the linearity for indirect photometric detection is shown in Fig. 6. A linear response range with two orders of magnitude was obtained for chloride, which would be impossible for direct UV absorption measurement.

CONCLUSION

The theoretical and practical strategies for optimization of indirect photometric detection in HPCZE have been presented in this paper. The influences of background electrolyte (BGE) concentration, capillary diameters, free flow linear polymers, pH of the BGE and type of BGE have been studied with our HPCZE system. The experimental results fit the theoretical deduction very well. Under optimized conditions, sub-femtomoles of simple anions were detected, offering a 500-fold improvement compared to previous studies [23,35], and approaching the predicted limit of detection. In addition, the linearity for indirect photometric detection was studied. Over two orders of magnitude of linearity were observed based on the peak area calculations.

ACKNOWLEDGEMENT

The work was supported by a Faculty Research Grant awarded to Y. M. from Northeast Missouri State University.

REFERENCES

1 S. Hjertén, *J. Chromatogr.*, 347 (1985) 191.
2 Y. Walbroehl and J.W. Jorgenson, *J. Chromatogr.*, 315 (1984) 135.
3 F. Foret and P. Bocek, *Chem: Listy*, 83 (1989) 191.
4 M. Sepaniak, D. Swalle and A. Powell, *J. Chromatogr.*, 480 (1989) 185.
5 T. Wang, R. Hartwick and P. Chaplin, *J. Chromatogr.*, 462 (1989) 147.
6 S. Terabe, K. Otsuks, K. Ichikawa, A. Tsuchiya and T. Ando, *Anal. Chem.*, 56 (1984) 111.
7 Z. Deyl, V. Rohlicek and M. Adam, *J. Chromatogr.*, 480 (1989) 371.
8 K. A. Cobb and M. Novotny, *Anal. Chem.*, 61 (1989) 2226.
9 T. Kaspar, M. Melera, P. Gozel and R. Brownlee, *J. Chromatogr.*, 458 (1988) 303.
10 J. S. Green and J. W. Jorgenson, *J. Chromatogr.*, 352 (1986) 337.
11 D. F. Swaile and M. J. Sepaniak, *J. Microcol. Sep.*, 1 (1989) 155.
12 J. S. Green and J. W. Jorgenson, *J. High Resolut. Chromatogr. Commun.*, 7 (1984) 529.
13 J. A. Olivares, N. T. Nguyen, C. R. Yonker and R. D. Smith, *Anal. Chem.*, 59 (1987) 1230.
14 J. A. Loo, H. R. Udseth and R. D. Smith, *Anal. Chem.*, 179 (1989) 404.
15 J. A. Loo, H. K. Jones, H. R. Udseth and R. D. Smith, *J. Microcol. Sep.*, 1 (1989) 223.
16 R. D. Smith, H. R. Udseth, J. A. Loo, B. W. Wright and G. A. Ross, *Talanta*, 36 (1989) 161.
17 W. G. Kuhr and E. S. Yeung, *Anal. Chem.*, 60 (1988) 1832.
18 W. G. Kuhr and E. S. Yeung, *Anal. Chem.*, 60 (1988) 2642.
19 L. Gross and E. S. Yeung, *J. Chromatogr.*, 480 (1989) 169.
20 T. W. Garner and E. S. Yeung, *J. Chromatogr.*, 515 (1990) 639.
21 F. Foret, S. Fanali, A. Nardi and P. Bocek, *Electrophoresis*, 11 (1990) 780.
22 A. Nardi, S. Fanali and F. Foret, *Electrophoresis*, 11 (1990) 774.
23 F. Foret, S. Fanali, L. Ossicini and P. Bocek, *J. Chromatogr.*; 470 (1989) 299.
24 M. W. F. Nielen, *J. Chromatogr.*, 588 (1991) 321.
25 T. Takeuchi and E.S. Yeung, *J. Chromatogr.*, 366 (1986) 145.
26 J. W. Jorgenson and K. D. Lukacs, *Anal. Chem.*, 53 (1981) 1298.
27 J. W. Jorgenson and K. D. Lukacs, *Science, (Washington, DC)*, 222 (1983) 266.
28 K. D. Lukacs and J. W. Jorgenson, *J. High Resolut. Chromatogr. Chromatogr. Commun.*, 8 (1985) 407.
29 G. J. Bruin, A. C. van Asten, J. C. Kraak and H. Poppe, presented at *the 3rd International Symposium on High-Performance Capillary Electrophoresis, San Diego, CA, February 3–6, 1991*, poster PM57.
30 W. G. Kuhr and E. S. Yeung, *Anal. Chem.*, 60 (1988) 2642.
31 R.-L. Chien and J. C. Helmer, *Anal. Chem.*, 63 (1991) 1354.
32 F. Kohlrausch, *Ann. Phys. Chem.*, 62 (1987) 209.
33 D. S. Burgi and R.-L. Chien, *Anal. Chem.*, 63 (1991) 2042.
34 D. S. Burgi and R.-L. Chien, *Anal. Chem.*, 64 (1992) 1046.
35 P. Gebauer, M. Deml, P. Bocek and J. Janak, *J. Chromatogr.*, 267 (1983) 455.

Journal of Chromatography, 625 (1992) 349–352
Elsevier Science Publishers B.V., Amsterdam

CHROM. 24 550

Short Communication

Improved chiral recognition of some compounds via the simultaneous use of β-cyclodextrin and its permethylated derivative in a reversed-phase high-performance liquid chromatographic system

D. Sybilska, A. Bielejewska, R. Nowakowski and K. Duszczyk

Institute of Physical Chemistry, Polish Academy of Sciences, Kasprzaka 44/52, 01-224 Warsaw (Poland)

J. Jurczak

Institute of Organic Chemistry, Polish Academy of Science, Kasprzaka 44/52, 01-224 Warsaw (Poland)

(Received August 7th, 1992)

ABSTRACT

Two chiral additives, β-cyclodextrin and (2,3,6-tri-O-methyl)-β-cyclodextrin, were applied to improve the enantioselectivity of reversed-phase high-performance liquid chromatography for methylphenobarbital, glutethimide, mephenytoin and morsuximide. It was found that the joint use of these two additives leads to an improved enantioselectivity, except for mephenytoin.

INTRODUCTION

For a long time chiral discrimination has received close attention in organic chemistry, biology, pharmacology and other natural sciences and the problem of how biological chiral receptors operate is still under discussion. In consequence, the development and extension of methods for enantioselective synthesis and chiral separations have become an important issue.

During the last decade, chromatography has proved to be a major technique for the resolution of stereoisomers, including enantiomers [1–7]. The basic rule, which is generally accepted, states that two enantiomeric species can be recognized exclusively by their interactions with a chiral resolving agent, and a variety of optically active separating agents have been applied in this respect. For chromatographic enantioselectivity the "three-point attachment" concept was proposed by Dalgliesh [8] in the early 1950s. Depending on the localization of the discriminating agent in the chromatographic system, chiral stationary, coated and mobile phases could be distinguished.

Unfortunately, the basic thermodynamic differentiation of enantiomers in many chiral systems is

Correspondence to: Dr. D. Sybilska, Institute of Physical Chemistry, Polish Academy of Sciences, Kasprzaka 44/52, 01-224 Warsaw, Poland.

0021-9673/92/$05.00

usually poor, *i.e*, the enantioselectivity (α) reaches values very close to 1.00. Hence, the requirements for column efficiency are severe, frequently making the separation unrealizable because of technical limitations. To enhance enantioselectivity, various approaches have been reported, mainly via derivatization of chiral stationary phases, of chiral additives or of the solute molecules themselves [1–7]. Recently, a new idea for a combined method was proposed, using simultaneously a chiral stationary phase and a chiral additive in the mobile phase solution [9]. This method permitted the enhanced resolution of acidic compounds.

In this paper we report an analogous idea for the simultaneous use of the two chiral selectors, but in a different manner. We propose the use of two chiral additives able to form molecular inclusion compounds in a reversed-phase high-performance liquid chromatographic (RP-HPLC) system. These two selectors are β-cyclodextrin (β-CD) and (2,3,6-tri-O-methyl)-β-cyclodextrin (TM-β-CD).

EXPERIMENTAL

Reagents

β-CD and TM-β-CD were supplied by Chinoin (Budapest, Hungary). All other reagents and solvents were of analytical-reagent grade and were used as received.

The model compounds tested, which included well known therapeutic drugs, were methylphenobarbital, glutethimide, mephenytoin and morsuximide (Fig. 1).

Apparatus and procedures

Chromatographic experiments were performed on a Type 310 HPLC unit (Institute of Physical Chemistry, Polish Academy of Sciences, Warsaw, Poland) equipped with a 0.5-μl injector and a UV detector (254 nm) containing a 1-μl flow cell. The columns (250 × 1 mm I.D.) were packed with 5-μm LiChrosorb RP-18 by the viscosity method. The mobile phases were aqueous ethanolic solutions containing various amounts of the appropriate CD; a pH of 2 was maintained with phosphoric acid solution. Experiments were carried out on the columns equilibrated with the mobile phase solutions at 20 ± 1°C. Experimental data were collected and processed using the Chromblues software package (Insitute of Physical Chemistry, Polish Academy of Sciences).

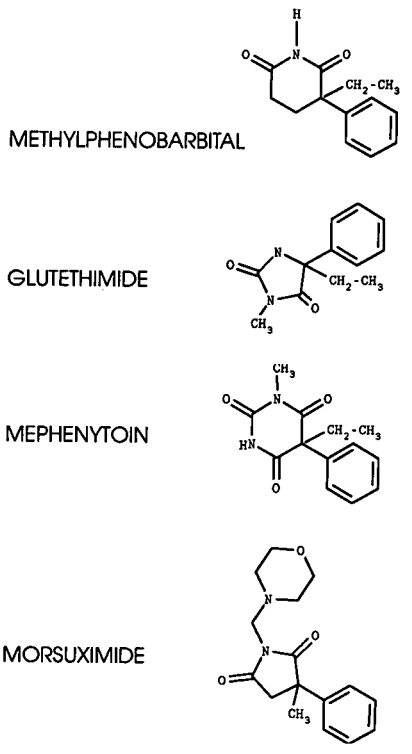

Fig. 1. Structural formulae of the compounds investigated.

RESULTS AND DISCUSSION

Experimental examinations

The values of the capacity factors (k') and enantioselectivity factors (α) for the four compounds investigated are given in Table I; they were determined with β-CD and TM-β-CD used separately and as a mixture.

For all the compounds except mephenytoin an improvement in enantioselectivity followed the joint use of the two chiral additives. These overall effects may be more or less distinct, depending on the solute under investigation and the starting values of the selectivity factor [α] found for the two additives separately. The enantioselectivity of β-CD complexation, undetectable under the conditions of the experiment with glutethimide, really exists and is revealed when β-CD is used together with TM-β-CD.

TABLE I

CAPACITY FACTORS (k') AND SELECTIVITIES (α) AS A FUNCTION OF THE ELUENT COMPOSITION

Compound	$k'_{1,2}$[a]	β-CD[b]			TM-β-CD[c]			TM-β-CD + β-CD[d]		
		k'_1	k'_2	α	k'_1	k'_2	α	k'_1	k'_2	α
Methylphenobarbital	18.0	6.5	7.1	1.09	13.3	16.0	1.20	4.2	5.4	1.30
Glutethimide	23.0	3.4	3.4	1.00	20.7	22.4	1.08	1.8	2.1	1.12
Mephenytoin	16.0	9.1	10.2	1.13	7.4	7.4	1.00	4.5	5.0	1.13
Morsuximide	6.1	2.2	2.2	1.00	4.2	4.6	1.08	1.2	1.4	1.16

[a] 20% ethanol; pH 2.
[b] 20% ethanol; $1.5 \cdot 10^{-2}$ M β-CD; pH 2.
[c] 20% ethanol; $5 \cdot 10^{-4}$ *M* TM-β-CD; pH 2.
[d] 20% ethanol; $1.5 \cdot 10^{-2}$ *M* β-CD, $5 \cdot 10^{-4}$ *M* TM-β-CD; pH 2.

Typical data concerning changes in the resolution (R_s) and the analysis time for methylphenobarbital presented in Table II, and the chromatograms shown in Fig. 2, demonstrate the beneficial role of the use of two chiral additives under appropriate conditions.

It has been found previously [7,10] that additions of β-CD to a solution are always accompanied by a decrease in the efficiency of the column. This phenomenon may explain why the R_s value remains approximately constant for methylphenobarbital (Table II) in spite of the improved enantioselectivity. Generation of enantioselectivity by β-CD always proceeds at the expense of the number of theoretical plates. This problem, which is difficult to follow experimentally when inclusion compounds are involved, has not yet been explored sufficiently. Nevertheless, the present data indicate that by using two additives together one may obtain a suitable resolution in a much shorter time. The latter effect seems to be unachievable using simple organic solvent additions.

The exceptional behaviour of mephenytoin can

TABLE II

RESOLUTION (R_s) AND TIME OF RESOLUTION (t) ACHIEVED FOR METHYLPHENOBARBITAL DEPENDING ON THE ELUENT COMPOSITION

Chiral additive	R_s	t (min)
β-CD[b]	0.9	36.3
TM-β-CD[c]	2.1	76.6
β-CD + TM-β-CD[d]	2.0	28.5

[b,c,d] Conditions as in Table I.

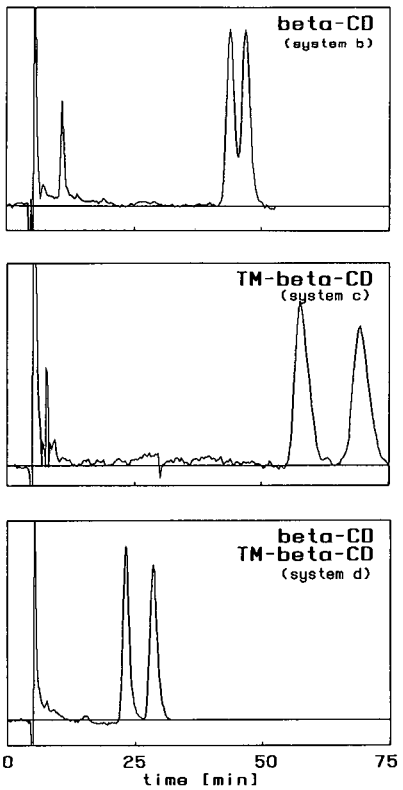

Fig. 2. Chromatograms obtained on a column (250 × 1 mm I.D.) filled with 5-μm LiChrosorb RP-18. Systems b, c and d: for conditions, see footnotes *b*, *c* and *d* in Table I.

be explained by its unusual mechanism of separation that occurs on an ODS column in the presence of β-CD [10]. In such a system two different phenomena may initiate enantioselectivity: a differentiation of stability constants of complexes formed in the bulk mobile phase solution and a differentiation of capacity factors of these complexes on the ODS phase. Most frequently the first phenomenon predominates, but mephenytoin represents a rare example of where the second factor plays the major role and the separation of enantiomeric mephenytoins is due to the difference in adsorption of β-CD diastereoisomeric complexes on the ODS phase.

In conclusion, it has been shown that the simultaneous use of two chiral additives, β-CD and TM-β-CD, may offer under appropriate conditions better enantioselectivity and better resolution in a shorter time of analysis. Moreover, in contrast to the previously described method [9], which is useful for acidic compounds, the present method using CDs should be more universal, *i.e.*, applicable to compounds of various nature, acidic, basic and neutral. The questions of when and why these synergistic effects occur are under study and a theoretical treatment will be presented in the near future [11].

ACKNOWLEDGEMENT

This work was supported by grant 202429101 from the State Committee for Scientific Research.

REFERENCES

1 V. A. Davankov, *Adv. Chromatogr.*, 18 (1980) 139.
2 R. W. Souter, *Chromatographic Separations of Stereoisomers*, CRC Press, Boca Raton, FL, 1985.
3 S. Hara and J. Cazes (Editors), *Optical Resolution by Liquid Chromatography, J. Liq. Chromatogr.*, 9 (1986).
4 D. Stevenson and I. D. Wilson (Editors), *Chiral Separations*, Plenum Press, New York, 1988.
5 S. G. Allenmark, *Chromatographic Enantioseparation: Methods and Applications*, Ellis Horwood, Chichester, 1988.
6 M. Zief and L. J. Crane (Editors), *Chromatographic Chiral Separations*, Marcel Dekker, New York, 1988.
7 A. M. Krstulovic (Editor), *Chiral Separations by HPLC. Applications to Pharmaceutical Compounds*, Ellis Horwood, Chichester, 1989.
8 C. E. Dalgliesh, *J. Chem. Soc.*, (1952) 3940.
9 C. Pettersson and C. Gioeli, *J. Chromatogr.*, 435 (1988) 225.
10 D. Sybilska, J. Zukowski and J. Bojarski, *J. Liq. Chromatogr.*, 9 (1986) 591.
11 R. Nowakowski, D. Sybilska and A. Bielejewska, in preparation.

Journal of Chromatography, 625 (1992) 353–356
Elsevier Science Publishers B.V., Amsterdam

CHROM. 24 585

Short Communication

Optimization of naphthylethylurea multiple-bonded chiral stationary phases for optical resolution of enantiomeric amino acid derivatives

Kazuo Iwaki and Mitsuru Yamazaki

School of Pharmacy, Hokuriku University, Ho-3 Kanagawa-machi, Kanazawa-shi, Ishikawa 920-11 (Japan)

Noriyuki Nimura and Toshio Kinoshita

School of Pharmaceutical Science, Kitasato University, 9-1 Shirokane-5, Minato-ku, Tokyo 108 (Japan)

(First received July 8th, 1992; revised manuscript received July 31st, 1992)

ABSTRACT

The polyethyleneamine spacer length of naphthylethylurea multiple-bonded chiral stationary phases (CSPs) was optimized for optical resolution of *p*-bromophenylcarbamyl (Br-PC) amino acid enantiomers. Four multiple-bonded CSPs having different lengths of polyethyleneamine spacer, diethylenetriamine, triethylenetetramine, tetraethylenepentamine and pentaethylenehexamine, were prepared via an activated carbamate intermediate from aminopropylsilyl silica gel. The resolution data of Br-PC amino acids on these CSPs by elution with an aqueous mobile phase were compared. The CSP with the triethylenetetramine spacer showed the best resolution of the enantiomers in the four CSPs. The other conditions, pH, concentration and temperature, etc., were also investigated using this CSP. They influenced the retention time of Br-PC amino acids, but they hardly affected the enantio recognition of the CSP.

INTRODUCTION

Recently, optical resolution methods using high-performance liquid chromatography (HPLC) have been rapidly advanced. In particular, the chiral stationary phase (CSP) methods have become of interest, and numerous CSPs have been developed [1–3]. We have also reported a versatile method for the preparation of chemically bonded phase-type CSPs via activated carbamate type silica gel [4,5]. In addition, the optical resolution of *p*-bromophenylcarbamyl (Br-PC) derivatives of enantiomeric amino acids by the prepared CSP,the naphthylethylurea multiple-bonded CSP, in reversed-phase mode has been reported [4]. In this case, we have confirmed that when optically active 1-(α-naphthyl) ethylamine (NEA) as a chiral source is introduced into the packing, the use of pentaethylenehexamine as a spacer and a chiral centre-increasing agent gives better resolution of Br-PC amino acids than the naphthylethylurea monolayer CSP [5].

In this study, polyethyleneamine spacer length on

Correspondence to: K. Iwaki, School of Pharmacy, Hokuriku University, Ho-3 Kanagawa-machi, Kanazawa-shi, Ishikawa 920-11 Japan.

0021-9673/92/$05.00

the multiple-bonded CSP was optimized for the Br-PC derivatives of enantiomeric amino acids. Multiple-bonded CSPs having various lengths of polyethyleneamine spacer were prepared. The resolution data of the enantiomeric Br-PC amino acids on these CSPs were compared.

EXPERIMENTAL

Chemicals

Nucleosil 5-NH_2 (aminopropylsilyl silica gel) was obtained from Macherey–Nagel (Düren, Germany). Distilled water was purified by passage through a Milli-Q Labo system (Nihon Millipore, Tokyo, Japan). Optically active NEA and pentaethylenehexamine (n = 4) were obtained from Tokyo Kasei Kogyo (Tokyo, Japan). Tetraethylenepentamine (n = 3), HPLC-grade acetonitrile and methanol were purchased from Kanto Chemical (Tokyo, Japan). Disuccinimido carbonate (DSC) was purchased from Chemiscience (Tokyo, Japan). Diethylenetriamine (n = 1), triethylenetetramine (n = 2) and other reagents were obtained from Wako Pure Chemicals (Osaka, Japan). Succinimido p-bromophenylcarbamate (SIBr-PC) and optically active succinimido 1-(α-naphthyl)ethylcarbamate (SINEC) were prepared as described previously [6,7].

Chromatographic conditions

The HPLC system consisted of an LC-6A high-pressure pump (Shimadzu Seisakusyo, Kyoto, Japan), a Model 7125 loop injector (Rheodyne, Cotati, CA, USA) and a UVIDEC 100-III spectrophotometric detector (Jasco, Tokyo, Japan). The detector wavelength was set at 250 nm. Column temperature was thermostated by Thermo Minder Mini-80 and Coolpipe 150L (Taiyo Scientific, Tokyo, Japan). Mobile phases are shown in the table and figures.

Samples

Br-PC derivatives of amino acid enantiomers were prepared by the reaction of SIBr-PC with amino acids as described previously [6].

Preparation of CSPs

Multiple-bonded CSPs having various lengths of polyethyleneamine spacer were prepared by the successive reaction of Nucleosil 5-NH_2 prepacked into a stainless-steel column (150 × 4.6 mm I.D.) with

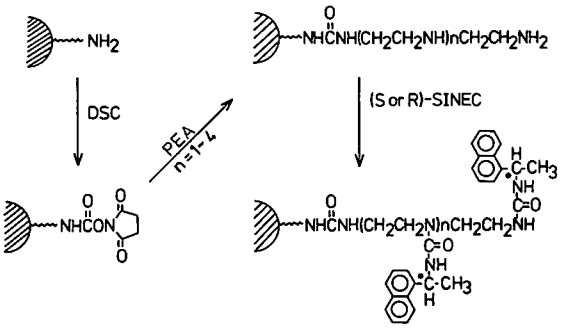

Fig. 1. Reaction scheme for the preparation of naphthylethylurea multiple-bonded CSPs having various lengths of polyethyleneamine spacer. DSC = Disuccinimido carbonate; PEA = polyethyleneamine; SINEC = succinimido 1-(α-naphthyl)ethylcarbamate.

DSC, polyethyleneamine and SINEC as described previously [4]. The reaction scheme is shown in Fig. 1. The CSPs prepared from each polyethyleneamine, n = 1–4, are called columns 1–4, respectively, in the following text.

Elemental analysis for the initial packing was 3.28% C, 0.85% H, 1.08% N; for column 1, 9.04% C, 1.38% H, 3.02% N; for column 2, 13.33% C, 1.73% H, 3.32% N; for column 3, 12.68% C,

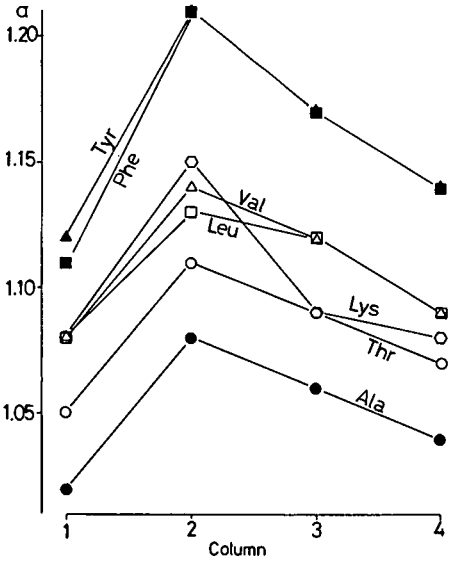

Fig. 2. Effect of the polyethyleneamine length of multiple-bonded CSPs on the separation factor of seven Br-PC amino acids enantiomers.

1.76% H, 3.74% N; for column 4, 15.91% C, 2.07% H, 4.08% N.

RESULTS AND DISCUSSION

Fig. 2 shows the relationship between polyethyleneamine length and the separation factor (α) of Br-PC amino acid enantiomers. The maximum α value was obtained with column 2. The separation data, capacity ratios (k'), α values and resolution values (R_s), are indicated in Table I. Columns 3 and 4 retained the enantiomers longer than column 2, however column 2 exhibited the maximum R_s value. In spite of this, since the R_s values of columns 1 and 2 are easily compared, the retention time of the enantiomers on column 1 was controlled by the mobile phase. Column 2 exhibited a better R_s value than column 1. These results evidently prove that column 2 gave the best resolution of Br-PC amino acids enantiomers on the four CSPs. Chromatograms of Br-PC valine and phenylalanine enantiomers are shown in Figs. 3 and 4, respectively.

This finding can be confirmed by C/N ratios calculated from elemental analysis. The C/N ratios suggest that the amount of naphthylethylurea residue introduced to column 2 was not less than that introduced into the other columns.

In order to optimize other conditions, column 2 was tested under various conditions. Component salts of buffer, acetate, phosphate, tartarate and citrate affected the retention time, but did not affect the separation factor of the enantiomers. Sodium acetate in the concentration range 0.05–0.15 *M* and mobile phase pH in the range 4.0–6.0 produced the same results. The effect of column temperature was investigated in the range 10–50°C in steps of 10°C. The theoretical plate number increased with a rise in temperature, but the separation factor was hardly affected.

TABLE I

SEPARATION OF ENANTIOMERIC Br-PC AMINO ACIDS ON FOUR MULTIPLE-BONDED CSPs

t_0 = 1.5 min; k', α and R_s refer to the capacity ratio, separation factor and resolution value for a pair of enantiomers, respectively. Mobile phase: 0.15 *M* sodium acetate (pH 5.0)–acetonitrile (30:70, v/v).

Sample	Column 4			Column 3			Column 2			Column 1		
	k'	α	R_s	k'	α	R_s	k'	α	R_s	k'	α	R_s
Thr L	9.59	1.07	1.18	7.00	1.09	0.98	7.30[a]	1.11	1.38	10.77[b]	1.05	0.82
D	10.27			7.65			7.80			11.29		
Ala L	10.32	1.04	0.69	8.19	1.06	0.70	9.91[a]	1.07	0.96	13.81[b]	1.02	–
D	10.77			8.68			10.63			14.12		
Val L	9.48	1.09	1.42	8.04	1.12	1.41	5.21	1.14	1.61	6.47[a]	1.08	1.09
D	10.33			8.99			5.97			6.97		
Leu L	9.96	1.09	1.60	8.69	1.12	1.47	5.59	1.13	1.61	7.41[a]	1.08	1.15
D	10.88			9.69			6.37			8.00		
Phe L	11.52	1.14	2.55	10.37	1.17	2.31	6.56	1.21	2.46	9.08[a]	1.11	1.60
D	13.19			12.16			7.91			10.09		
Tyr L	19.49	1.14	2.10	14.77	1.17	2.01	8.63	1.21	2.01	9.28[a]	1.12	1.85
D	22.19			17.35			10.47			10.45		
Lys L	18.23	1.08	1.55	16.01	1.09	1.45	9.83	1.15	1.87	14.11[a]	1.08	0.93
D	19.83			17.84			11.32			15.21		

[a] 0.15 *M* Sodium acetate (pH 5.0)–acetonitrile (50:50, v/v).
[b] 0.15 *M* Sodium acetate (pH 5.0)–acetonitrile (70:30, v/v).

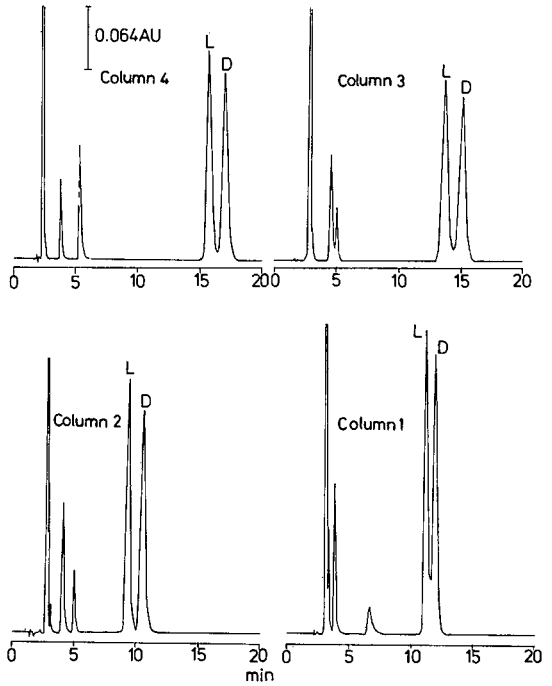

Fig. 3. Separation of enantiomeric Br-PC valine on four multiple-bonded CSPs. Mobile phase: 0.15 *M* sodium acetate (pH 5.0)–acetonitrile (30:70, v/v, for columns 2–4; 50:50, v/v, for column 1). Flow-rate: 1.0 ml/min. Column temperature: room temperature. Each peak corresponds to 500 ng of enantiomeric valine.

Thus, a multiple-bonded CSP with greater enantio recognition (column 2) for Br-PC amino acid enantiomers than the previous type (column 4) is presented. Column 2, in spite of showing high enantio recognition, exhibitis retention behaviour to Br-PC amino acids that is the same as column 4. Therefore column 2 will give superior simultaneous analysis of Br-PC amino acid enantiomers than that previously reported by us [4].

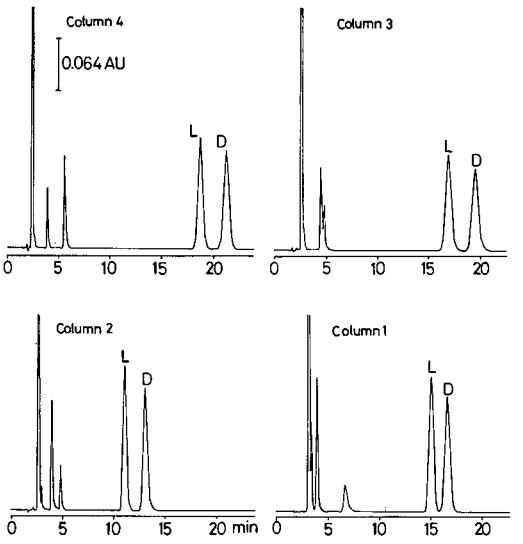

Fig. 4. Separation of enantiomeric Br-PC phenylalanine on four multiple-bonded CSPs. Conditions as in Fig. 3.

REFERENCES

1 W. Lindner and C. Pettersson, in L. W. Wainer (Editor), *Liquid Chromatography in Pharmaceutical Development*, Aster, Springfield, 1985, p. 63.
2 R. Dappen, H. Arm and V. R. Meyer, *J. Chromatogr.*, 373 (1986) 1.
3 A. C. Mehta, *J. Chromatogr.*, 426 (1988) 1.
4 K. Iwaki, S. Yoshida, N. Nimura, T. Kinoshita, K. Takeda and H. Ogura, *J. Chromatogr.*, 404 (1987) 117.
5 K. Iwaki, S. Yoshida, N. Nimura, T. Kinoshita, K. Takeda and H. Ogura, *Chromatographia*, 23 (1987) 727.
6 K. Iwaki, N. Nimura, T. Kinoshita, K. Takeda and H. Ogura, *Anal. Chem.*, 58 (1986) 2372.
7 K. Iwaki, S. Yoshida, N. Nimura, T. Kinoshita, K. Takeda and H. Ogura, *Chromatographia*, 23 (1987) 899.

Journal of Chromatography, 625 (1992) 357–361
Elsevier Science Publishers B.V., Amsterdam

CHROM. 24 559

Short Communication

Resolution of carboxylic acid enantiomers by high-performance liquid chromatography with highly sensitive laser-induced fluorescence detection

Toshimasa Toyo'oka, Mumio Ishibashi and Tadao Terao

Division of Drugs, National Institute of Hygienic Sciences (NIHS), 1–18–1 Kamiyoga, Setagaya-ku, Tokyo 158 (Japan)

(First received June 5th, 1992; revised manuscript received August 11th, 1992)

ABSTRACT

Optical resolution of carboxylic acid enantiomers by high-performance liquid chromatography with laser-induced fluorescence detection after chiral derivatization was investigated. Both laser power and time constants influence the detection limit of the fluorophore. The minimum detectable levels of three derivatives of naproxen [4-(aminosulphonyl)-7-(3-aminopyrrolidin-1-yl)-2,1,3-benzodioxazole, 4-(N,N-dimethylaminosulphonyl)-7-(3-aminopyrrolidin-1-yl)-2,1,3-benzoxadiazole and 4-nitro-7-(3-aminopyrrolidin-1-yl)-2,1,3-benzodiazole derivatives] were in the femtomole–attomole ranges, and the lowest detection limit was obtained with the last derivative.

INTRODUCTION

The enantiomeric separation of racemates of various drugs is one of the most important subjects in pharmacokinetic studies. When the pharmacological activity and side-effects are different for each enantiomer, the enantiomers must be determined for the study of the efficiency and safety of drugs. Therefore, a reliable method for the determination of drug enantiomers at trace levels is a prerequisite. There are several methods for the separation of enantiomers, such as gas chromatography (GC) [1], high-performance liquid chromatography (HPLC) [2] and high-performance capillary electrophoresis (HPCE) [3,4]. Of these, the HPLC method is widely employed owing to the development of many efficient chiral stationary phase (CSPs) and to the progress in derivatization techniques. Although a CSP often provides excellent separations of enantiomers, selection of the column is difficult and it may be applicable to only a limited number of racemates. A method based on diastereomer formation, including a derivatization step with a chiral reagent, is favourable for the determination of enantiomers in biological specimens because high sensitivity and selectivity can be achieved.

In a previous paper [5], we described the syntheses of fluorescent chiral tagging reagents for the carboxylic acid functional group [(+)- and (−)-isomers of 4-nitro-7-(3-aminopyrrolidin-1-yl)-2,1,3-benzoxadiazole (NBD-APy), 4-(N,N-dimethylaminosulphonyl)-7-(3-aminopyrrolidin-1-yl)-2,1,3-

Correspondence to: Dr. T. Toyo'oka, Division of Drugs, National Institute of Hygienic Sciences (NIHS), 1–18–1 Kamiyoga, Setagaya-ku 158, Tokyo, Japan.

0021-9673/92/$05.00

benzoxadiazole (DBD-APy) and 4-(amino sulphonyl)-7-(3-aminopyrrolidin-1-yl)-2,1,3-benzoxadiazole (ABD-APy)] and their application to the resolution of some enantiomeric drugs and N-acetylamino acids by HPLC with conventional fluorescence detection. The reagents react with the carboxylic acid enantiomers at room temperature in the presence of 2,2'-dipyridyl disulphide (DPDS) and triphenylphosphine (TPP) to form fluorescent diastereomers. The diastereomers corresponding to each pair of carboxylic acid enantiomers are separated completely with an ODS column in a single chromatographic run [*e.g.*, R_s = 2.40, *rac*-naproxen derived from (+)-DBD-APy; R_s = 3.45, *rac*-naproxen derived from (+)-NBD-APy]. The resolution by reversed-phase chromatography is advantageous for the determination of carboxylic acid enantiomers in biological samples because complicated pretreatment is not necessary. The detection limits of authentic diastereomers after separation by HPLC is in the 15–45 fmol range (signal-to-noise ratio = 3). Further, all the resulting compounds have relatively long excitation maximum wavelengths (*ca.* 470 nm) and emissions at 570 nm (DBD-APy-naproxen), 580 nm, (ABD-APy-naproxen) and 540 nm (NBD-APy-naproxen) (Fig. 1). As the excitation maximum wavelength is close to the light emission of an argon ion laser (488 nm), the minimum detectable level might be expected to be improved with laser-induced fluorescence (LIF) detection. In this work we evaluated the applicability of the chiral tagging reagents DBD-APy, NBD-APy and ABD-APy to the resolution of carboxylic acid enantiomers when a commercially available LIF detector is used.

EXPERIMENTAL

Materials and reagents

(+)-4-(Aminosulphonyl)-7-(3-aminopyrrolidin-1-yl)-2,1,3-benzoxadiazole [(+)-ABD-APy], (+)-4-nitro-7-(3-aminopyrrolidin-1-yl)-2,1,3-benzoxadiazole [(+)-NBD-APy] and (+)-4-(N,N-dimethylaminosulphonyl)-7-(3-aminopyrrolidin-1-yl)-2,1,3-benzoxadiazole [(+)-DBD-APy] were synthesized as described previously [5]. Racemic 2-(6-methoxy-2-naphthyl)propionic acid (*rac*-naproxen) was donated by Tokyo Tanabe Pharmaceutical (Tokyo, Japan). The derivatives of (+)-naproxen with (+)-ABD-APy, (+)-NBD-APy and (+)-DBD-APy were also synthesized according to the previous paper [5]. TPP (Wako, Osaka, Japan) and DPDS (Tokyo Kasei, Tokyo, Japan) were used as received. Acetonitrile and water were of HPLC grade (Wako). All other chemicals were of analytical-reagent grade and were used as received.

HPLC–LIF detection

The high-performance liquid chromatograph consisted of two LC-9A pumps and an SCL-6B system controller (Shimadzu, Kyoto, Japan). Sample solutions were injected by a SIL-6B autoinjector (Shimadzu). The analytical columns were an Inertsil ODS-2 (150 × 4.6 mm I.D., 5 μm) (GL Sciences, Tokyo, Japan), a TSK-gel ODS-80TM (150 × 4.6 mm I.D., 5 μm) (Tosoh, Tokyo, Japan) and a TSK-gel PTH Pak (250 × 2.0 mm I.D. 5 μm) (Tosoh). The column was maintained at 40°C with a 655A-52 column oven (Hitachi, Tokyo, Japan). A Tosoh LF-8010 monitor equipped with a 5-μl flow cell was employed for detection. The peak areas obtained

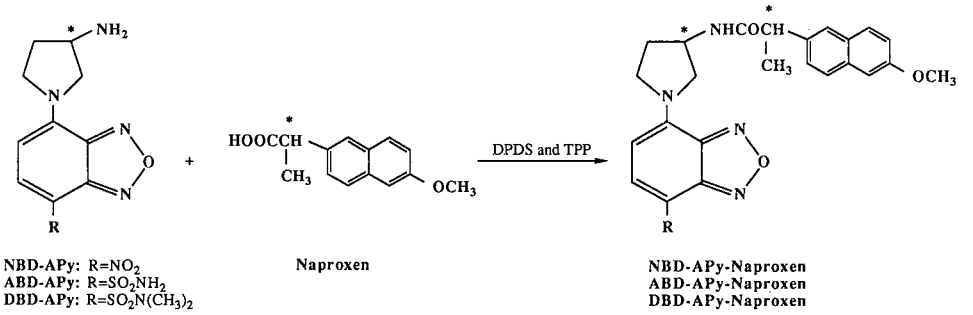

Fig. 1. Reaction of naproxen with chiral tagging reagents in the presence of activation agents.

from the LIF monitor were calculated with a C-R4A Chromatopac (Shimadzu). All mobile phases were degassed with a DGU-3A on-line degasser (Shimadzu).

RESULTS AND DISCUSSION

Table I lists the detection limits (signal-to-noise ratio = 3) of the three authentic derivatives obtained from (+)-naproxen and the (+)-isomers of the chiral tagging reagents under various conditions. Although the peak heights of the derivatives were slightly reduced with increasing time constants, the background noise level was also decreased. As a result, lower detection limits were obtained from longer time constants. In addition, the laser power has the greatest influence on detection. Although the baseline noise levels increased with increasing laser power, the peak heights of the fluorescent derivatives increased considerably. Hence lower detection limits were obtained with higher laser power (Table I). However, the sensitivity of NBD-APy-naproxen was essentially the same at 200 and 500 mW. The ratio of peak heights at 500 and 200 mW was *ca.* 2.4, while that of the background noise was 2.2. Therefore, the difference in detection limits between 200 and 500 mW was not great (0.69 *versus* 0.62 fmol). Greater variation of the baseline noise, based on emission of impurities etc., in the eluent, may be the main reason for the low sensitivity in spite of the use of a high power laser, compared with the use of a low-power laser at 5–15 mW. However, the results in Table I indicate that both a high-power laser and long time constants provide low detection limits.

Another approach to sensitive detection is the use of a microbore column. The chromatogram in Fig. 2 illustrates the separation and detection of a mix-

TABLE I

DETECTION LIMITS OF DIASTEREOMERS BY HPLC WITH LIF DETECTION

Diastereomer	Conditions[a]	Retention time (min)	Detection limit (fmol)[b]	Laser power (mW)	Time constant (s)
ABD-APy-naproxen	A	27.0	265	5	0.5
	D	5.27	42	10	3
	D	5.27	29	15	3
	E	6.64	10	10	3
	E	6.64	6.6	15	3
DBD-APy-naproxen	B	20.8	33	5	0.5
	D	11.4	18	10	3
	D	11.4	11	15	3
	E	11.4	2.7	10	3
	E	11.4	1.7	15	3
NBD-APy-naproxen	C	24.2	14	5	0.5
	C	24.2	7.2	10	0.8
	C	24.2	5.1	10	1.5
	D	7.72	4.4	10	3
	D	7.72	2.9	15	3
	E	9.05	1.0	10	3
	E	9.05	0.66	15	3
	C	24.2	0.69	200	4
	C	24.2	0.62	500	4

[a] Eluent: A, water–acetonirile (65:35); B, 0.1 *M* phosphate buffer (pH 6.8)–acetonitrile (55:45); C, water–acetonitrile (60:40); D, water–acetonitrile (50:50); E, water–acetonitrile (40:60). Column for A, B and C, TSK-gel ODS-80TM (150 × 4.6 mm I.D., 5 μm); column for D, Inertsil ODS-2 (150 × 4.6 mm I.D., 5 μm); column for E, TSK-gel PTH Pak (250 × 2.0 mm I.D., 5 μm). Column temperature, 40°C. Flow-rate for A, B, C and D, 1.0 ml/min; flow-rate for E, 0.2 ml/min. Amount injected, 10 μl. Interference filter for A, B and C, 540 ± 10 nm; Interference filter for D and E, 540 ± 20 nm.

[b] Signal-to-noise ratio = 3.

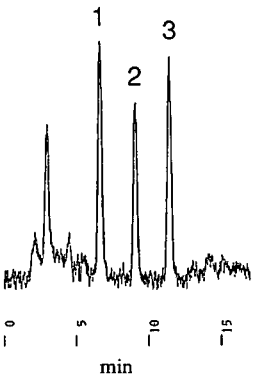

Fig. 2. Chromatogram of diastereomers separated using a microbore column. HPLC conditions: column, TSK-gel PTH Pak (250 × 2.0 mm I.D., 5 μm) at 40°C; eluent, water–acetonitrile (40:60); flow-rate, 0.2 ml/min; detection, argon ion laser at 15mW; interference filter, 540 ± 20 nm. Peaks: 1 = ABD-APy-naproxen (40 fmol); 2 = NBD-APy-naproxen (3 fmol); 3 = DBD-APy-naproxen (10 fmol).

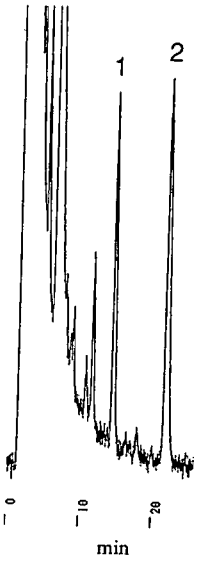

Fig. 3. HPLC separation of *rac*-naproxen labelled with (+)-NBD-APy. Racemic naproxen (1 μ*M* each) and (+)-NBD-APy (1 m*M*) in acetonitrile reacted at room temperature in the presence of DPDS (1 m*M*) and TPP (1 m*M*). After 2 h of reaction, the sample solution was diluted with acetonitrile and injected on to the column. HPLC conditions: column, Inertsil ODS-2 (150 × 4.6 mm I.D., 5 μm) at 40°C; eluent, water–acetonitrile (57:43); flow-rate, 1.0 ml/min; detection, argon ion laser at 15mW; interference filter, 540 ± 20 nm. Peaks: 1 = (+)-naproxen; 2 = (−)-naproxen. Each peak coresponds to 50 fmol.

ture of three derivatives, ABD-APy-naproxen (40 fmol), NDB-APy-naproxen (3 fmol) and DBD-APy-naproxen (10 fmol), using a microbore ODS column with an LIF monitor at 15 mW. Compared with a conventional column, the detection limits were decreased by a factor of 4–7 (Table I). Those of DBD-APy-naproxen (11 fmol) and ABD-APy-naproxen (29 fmol), separated by the conventional column, were in same range as those obtained with a conventional fluorescence detector (DBD-APy-naproxen, 15 fmol; ABD-APy-naproxen, 45 fmol) [5]. Among the fluorophores, NBD-APy-naproxen showed the highest sensitivity with LIF detection. It is well known that the fluorescence intensity depends on the light intensity (I_0), concentration of fluorophore (c), cell length (l), molar absorptivity (ε) and fluorescence quantum yield (ϕ). When I_0, c and l remain the same, the intensity changes according to the ε and ϕ values of the compound. The values of ε at the absorption maximum wavelengths of NBD-APy-naproxen, DBD-APy-naproxen and ABD-APy-naproxen were 22 800 (493 nm), 12 400 (450 nm) and 10 400 (450 nm), respectively, in acetonitrile–water (1:1), whereas the values at 488 nm (light emission of the argon ion laser) were *ca.* 22 400, 5400 and 5000, respectively. As the ε value of NBD-APy-naproxen is about four times larger than those of the other two derivatives, the higher sensitivity of NBD-APy-naproxen may be due to the larger ε value at 488 nm. Further, the interference filter (540 nm) used in the LIF detector fits the emission maximum of NBD-APy-naproxen (543 nm) [5]. The large difference in sensitivity between DBD-APy-naproxen and ABD-APy-naproxen cannot be explained solely by ε, as the values of ε are almost equal and the absorption spectra at 300–700 nm are almost superimposable (data not shown). As described previously [5], the fluorescence intensity of DBD-APy-naproxen was approximately three times stronger than that of ABD-APy-naproxen. The results suggest that the ϕ value of DBD-APy-naproxen is larger than that of ABD-APy-naproxen. Hence the lower detection limit of DBD-APy-naproxen with LIF detection might be mainly caused by ϕ. On the other hand, the interference filter of 540 nm employed in the LIF detector was not suitable for the detection of ABD-APy-naproxen and DBD-APy-naproxen because the derivatives

have emission maxima at *ca.* 585 and 580 nm, respectively [5].

Fig. 3 shows the resolution of *rac*-naproxen using the conventional ODS column after derivatization with (+)-NBD-APy. Excellent separation and high sensitivity were obtained with LIF detection. The detectability is better than that of conventional fluorescence detection using a xenon arc lamp. NBD-APy is a useful reagent for the resolution of carboxylic acid enantiomers with sensitive LIF detection. Although the sensitivity of the DBD-APy derivative is lower than that of the NBD-APy derivative, it might be improved by the use of a high-power laser source and a suitable interference filter at *ca.* 580 nm. Hence the proposed technique should provide an ultratrace analytical method for carboxylic acid enantiomers. Further studies of optical resolution using DBD-APy and NBD-APy with real samples are in progress.

ACKNOWLEDGEMENTS

The authors thank Tosoh (Tokyo, Japan) for the loan of the LF-8010 LIF detector. Thanks are also due to Dr. C. R. Warner, Food and Drug Administration (FDA), USA, for reviewing the manuscript.

REFERENCES

1 D. W. Armstrong, W. Li, C. D. Chang and J. Pitha, *Anal. Chem.*, 62 (1990) 914–923.
2 A. M. Krstulovic (Editor), *Chiral Separation by HPLC*, Ellis Horwood, Chichester, 1989.
3 H. Nishi, T. Fukuyama and S. Terabe, *J. Chromatogr.*, 553 (1991) 503–516.
4 T. Ueda, F. Kitamura, R. Mitchell, T. Metcalf, T. Kuwana and A. Nakamoto, *Anal. Chem.*, 63 (1991) 2979–2981.
5 T. Toyo'oka, M. Ishibashi and T. Terao, *Analyst (London)*, 117 (1992) 727–733.

Journal of Chromatography, 625 (1992) 362–367
Elsevier Science Publishers B.V., Amsterdam

CHROM. 24 615

Short Communication

Determination of benzalkonium chloride in eye care products by high-performance liquid chromatography and solid-phase extraction or on-line column switching

Lee Elrod, Jr., Timothy G. Golich and James A. Morley

PPD Physical Analytical Chemistry Department, Abbott Laboratories, 1401 Sheridan Road, North Chicago, IL 60064 (USA)

(First received July 9th, 1992; revised manuscript received September 9th, 1992)

ABSTRACT

Benzalkonium chloride (BAK) is a mixture of alkylbenzyldimethylammonium chlorides, which is commonly used as a bacteriostat. In this work, the three major homologues of BAK are quantitated in the over-the-counter eye care products Murine and Murine Plus using high-performance liquid chromatography (HPLC). The analytes are separated from various product excipients and concentrated by either solid-phase extraction onto Sep-Pak C_{18} cartridges or by an on-line column-switching technique using 1-cm reversed-phase precolumns. Absolute recoveries of BAK homologues by the solid-phase extraction technique ranged from 97.2 to 98.7% for standards and from 98.0 to 98.4% for samples. Absolute recovery of the BAK homologues by the column-switching technique was 101.3% for standards and ranged from 99.9 to 103.7% for samples. Relative recoveries were quantitative by both techniques. Assay precision (R.S.D. values) were ±2.2% to ±2.6% and ±0.4% to ±0.8% by solid-phase extraction and column-switching techniques, respectively. The method provides advantages of high sample throughput, excellent column life and automation.

INTRODUCTION

Benzalkonium chloride (BAK) is a bacteriostat, which is commonly used in a wide variety of health care and cosmetic preparations. Chemically, BAK is a mixture of alkylbenzyldimethylammonium chlorides consisting of three major homologues having straight chain alkyl substituents of C_{12}, C_{14} and C_{16} at the quaternary ammonium salt (Fig. 1). In order to control the effectiveness of the bacteriostat, reliable quantitation of BAK is necessary. High-performance liquid chromatography (HPLC) has been used extensively for this purpose using bonded phases of C_{18} [1,2] and CN [3–5], or by using ion-exchange phases [6,7].

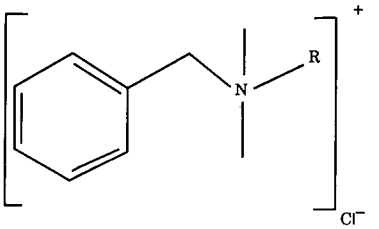

Benzalkonium Chloride ($R=C_{10}H_{21}$ to $C_{16}H_{33}$)

Fig. 1. Structure of BAK.

Correspondence to: L. Elrod, Jr., PPD Physical Analytical Chemistry Department, Abbott Laboratories, 1401 Sheridan Road, North Chicago, IL 60064, USA.

0021-9673/92/$05.00

In this work, BAK is determined in the over-the-counter eye care products Murine and Murine Plus (Abbott Labs., North Chicago, IL, USA) using HPLC and low-wavelength UV detection. Previously reported procedures for determining BAK in ophthalmic preparations [8,9] have used direct injection of the sample. While simple, this approach did not provide enough sensitivity for routine determination of all three major BAK homologues using normal chromatographic equipment. Concentration techniques for BAK have been reported using liquid–liquid extraction [1,10] to improve the quantitation by HPLC. Solid-phase extraction of BAK from cosmetics has been reported using silica gel columns [11], while the C_{12} and C_{14} homologues of BAK have been quantitated in plasma using C_{18} extraction columns in combination with extensive additional sample treatment [12]. To improve the detectability of all three major homologues of BAK, we developed (1) a solid-phase extraction procedure and (2) an automated column-switching technique for use with HPLC. The solid-phase extraction procedure uses C_{18} reversed-phase cartridges, while the column-switching procedure uses 1-cm commercially packed precolumns plumbed into a 10-port high-pressure valve which is electrically actuated. For the chromatographic finish, a cyanopropyl bonded phase (Zorbax SB-CN) was chosen over older, conventional cyano bonded phases, which typically suffer from instability over prolonged use.

EXPERIMENTAL

Apparatus

The HPLC system consisted of a Model SP-8800 ternary pump and a Model Chromjet data handling system (Spectra-Physics, Santa Clara, CA, USA). A Model 757 variable-wavelength UV detector (ABI Analytical Kratos Division, Ramsey, NJ, USA) was used. A Model WISP-710B autosampler and Model 6000 HPLC pump (Waters, Milford, MA, USA) was used. A Model 7940 HPLC column heater (Jones Chromatography, Lakewood, CO, USA) was used. Chromatographic separations described in the method were made using Zorbax Stablebond CN columns (5 μm) measuring 15 cm × 4.6 mm I.D. (Mac-Mod Analytical, Chadds Ford, PA, USA). Precolumns employed in the column-switching system were LiChrosorb RP-8 (5 μm) 1 cm × 4.6 mm I.D. (Alltech, Deerfield, IL, USA; cat. No. 1542). Other precolumns evaluated included Adsorbosphere C_{18}, Hypersil C_{18}, Partisil ODS-2 and LiChrosorb RP-18. These precolumns all measured 1 cm × 4.6 mm I.D. and were also obtained from Alltech. For the column-switching system, a 10-port high-pressure valve and electric actuator was used (Valco, Houston, TX, USA, cat. No. ECIOU). Prior to use, the components of the eluent were filtered through 0.45-μm nylon membranes (Alltech).

Reagents

A commercial USP grade BAK solution containing 169.8 mg/ml of BAK was used as a standard throughout this work. The BAK content is expressed as the sum of the three major homologues characterized *versus* the USP standard. Tetrahydrofuran (THF) was UV grade, distilled in glass, from Fisher Scientific (Fair Lawn, NJ, USA). Triethylamine was reagent grade (99%) from Aldrich (Milwaukee, WI, USA). Phosphoric acid was reagent grade (85%) from J.T. Baker (Phillipsburg, NJ, USA).

The chromatographic eluent used was distilled water–THF–triethylamine (2500:1500:20), which was adjusted to an apparent pH of 3.0 ± 0.1 with phosphoric acid. The solid-phase extraction solution was a mixture of 70% THF and 30% chromatographic eluent (v/v). The column-switching wash solvent was distilled water–THF–phosphoric acid (1600:400:3). Murine and Murine Plus were formulated at Abbott Laboratories.

Chromatographic conditions

The following conditions were used: flow-rate, 2.0 ml/min; pressure, approximately 2600 p.s.i. (1 p.s.i. = 6894.76 Pa); detector, 215 nm at 0.10 a.u.f.s.; attenuation at 128 (solid-phase extraction) or 256 (column switching); and injection volume, 100 μl (solid-phase extraction) or 200 μl (column switching). The analytical column was maintained at 40°C.

Analytical procedure

The BAK standard solution was prepared by serially diluting the 169.8 mg/ml BAK solution in distilled water to a concentration of 51.0 μg/ml total

BAK. Replicate injections of the standard and sample preparations were made to obtained summed integrated areas of the C_{12}, C_{14} and C_{16} homologues with typical agreement of $\leqslant 2\%$. The sample was quantitated using the external standard method by ratioing the total peak areas of sample to standard and multiplying by the BAK concentration (μg/ml).

For the solid-phase extraction procedure Sep-Pak cartridges were pre-conditioned with the extraction solution followed by distilled water. In a batch process, 10 ml of sample, standard or blank (distilled water) were eluted through the cartridge. Each cartridge was washed with distilled water and the BAK was eluted with 3.0 ml of extraction solution followed by a 3.0-ml aliquot of eluent. The two extracts were combined and mixed.

For the column-switching procedure, the arrangement used to preconcentrate the sample and standard is shown in Fig. 2. A 0.20-ml aliquot of the sample or standard preparation was injected into the system with the valve in the load position. The wash pump was pumping the wash solvent at 3.0 ml/min. After 2 min, the valve was switched to the inject position to back-flush the BAK onto the analytical column. After the C_{16} homologue was detected, the valve was switched to the load position and the precolumn was re-equilibrated for 5 min before the next injection.

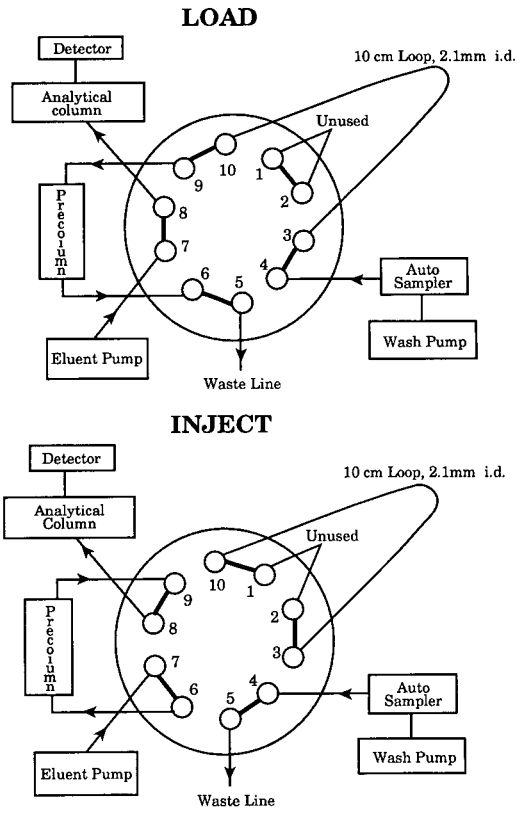

Fig. 2 Schematic diagram of HPLC system for column-switching procedure.

RESULTS AND DISCUSSION

In this work, our goal was to develop a rugged and reliable determination of BAK at a target concentration of 50 μg/ml in Murine and Murine Plus. Initial attempts at routine quantitation of BAK by direct injection using a previously reported method [9] did not provide acceptable sensitivity or precision at the target concentration. This approach failed because the chromatographic separation must resolve the C_{12} BAK homologue from relatively high concentrations of excipients present in the formulations while eluting the C_{16} BAK homologue in a reasonable time and with enough sensitivity to obtain reproducible peak areas. To overcome these difficulties, we originally developed the solid-phase extraction technique to remove the majority of the detectable product excipients and preconcentrate the analytes of interest. Shown in Fig. 3 are typical chromatograms for the BAK determination by solid-phase extraction. Detector linearity of the chromatographic finish was demonstrated by chromatographing standard solutions containing 40.8 to 204% of the analyte present after preconcentration. A plot of concentration (range = 34.0 to 169.9 μg/ml) *versus* total integrated peak area of BAK (range = $2.59 \cdot 10^6$ to $13.0 \cdot 10^6$ counts) gave a linear regression line having correlation coefficient > 0.9999, slope = $7.69 \cdot 10^4$, y-intercept = $-4.06 \cdot 10^4$. Standard errors in slope and y-intercept were $\pm 0.05 \cdot 10^4$ and $\pm 4.96 \cdot 10^4$, respectively.

The routine described in the solid-phase extraction was a compromise of conditions necessary for removing the majority of the formulation excipients while obtaining quantitative recovery of BAK. Absolute recoveries of individual BAK homologues and total BAK were determined from standards

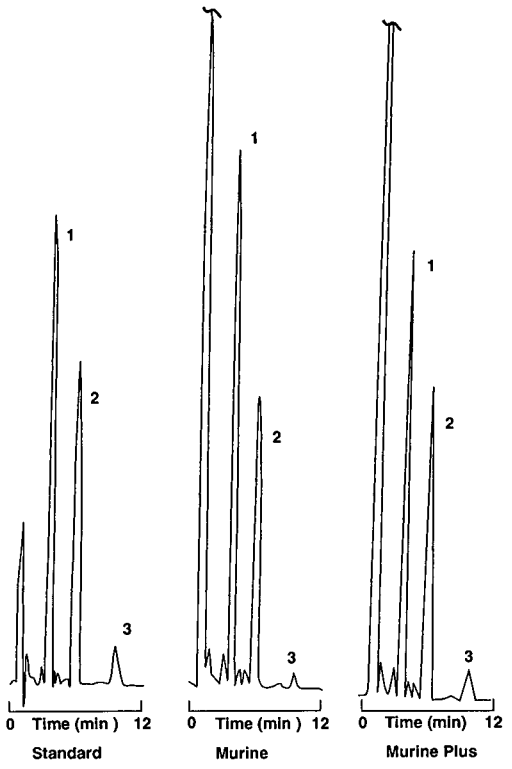

Fig. 3. Typical chromatograms by solid-phase extraction procedure. Peaks: 1 = C_{12} homologue; 2 = C_{14} homologue; 3 = C_{16} homologue.

and placebos using the procedure and a non-preconcentrated standard at appropriate concentrations. The recoveries were comparable between standards and the synthetic preparations containing the formulation excipients (Table I). Total recoveries ranged from 97.2 to 98.7%, with a slight, but consistent, loss of the C_{16} homologue. Also included in Table I are data from standard addition and recovery experiments in which both standard and synthetic mixtures were taken through the assay procedure to give relative recoveries. As shown, relative total recoveries of BAK ranged from 99.2 to 101.7% at 67.9 to 169.8% of the target concentration.

The assay precision for the solid-phase extraction technique was evaluated by determining BAK in Murine and Murine Plus on separate days using different analysts, chromatographic equipment and analytical columns. In Murine, a mean BAK concentration of 47.7 μg/ml was obtained with a relative standard deviation (R.S.D.) of ± 2.6%. In Murine Plus, a mean BAK concentration of 47.4 μg/ml was obtained with a R.S.D. of ± 2.2%.

To fully automate the preconcentration step, the column-switching procedure was designed. We chose to investigate this approach using 1 cm cartridges for the following reasons: (1) these columns are conveniently plumbed directly into the switch-

TABLE I

STANDARD ADDITION AND RECOVERY OF BAK BY SOLID-PHASE EXTRACTION

Homologue	Absolute recovery (%)					
	Standard 1	Standard 2	Standard 3	Average	Murine Plus	Murine
C_{12}	99.8	100.5	102.4	100.9	101.8	100.7
C_{14}	95.5	95.8	96.4	96.0	95.9	97.1
C_{16}	91.3	92.2	91.7	91.7	90.1	93.8
Total	97.2	97.6	98.7	97.8	98.0	98.4

Addition level (%)	Added (μg/ml)	Relative recovery			
		Murine		Murine Plus	
		Recovery (μg/ml)	Recovery (%)	Recovery (μg/ml)	Recovery (%)
67.9	34.0	34.5	101.7	34.2	100.6
101.9	51.0	51.8	101.6	51.2	100.4
169.8	84.9	85.7	100.9	84.2	99.2

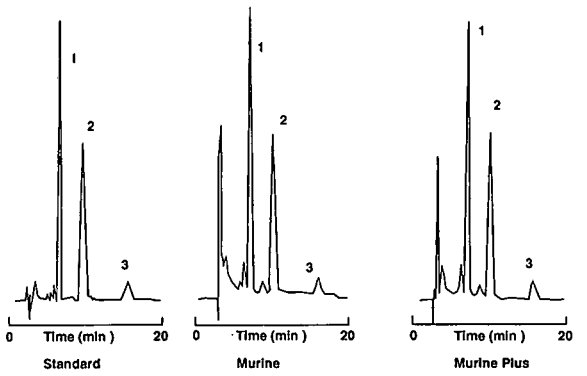

Fig. 4. Typical chromatograms by column-switching procedure. Peaks: 1 = C_{12} homologue; 2 = C_{14} homologue; 3 = C_{16} homologue.

ing valve, minimizing the dead volume of the system, and (2) this format is now commercially available in a variety of different packings. In order to obtain comparable results as shown for the solid-phase extraction, we investigated packings of Partisil ODS-2, Adsorbosphere C_{18}, LiChrosorb RP-18 and RP-8 and Hypersil ODS. The behavior of BAK on the LiChrosorb RP-8 phase was most acceptable in our application. This packing material retained BAK strongly enough to elute the formulation excipients prior to the back-flush while allowing the analytes of interest to be quantitatively removed by the HPLC eluent. Fig. 4 shows typical chromatograms for BAK using the column-switching procedure. Both the LiChrosorb RP-18 and Hypersil ODS materials show extremely strong retention of the analytes and would require eluents containing prohibitively large amounts of organic modifier in the back-flush step.

Detector linearity for the column-switching procedure was demonstrated using aqueous standards with the switching valve functioning as described in the procedure. A plot of BAK concentration (range = 17.0 to 169.8 μg/ml) *versus* total integrated area (range = $2.96 \cdot 10^6$ to $28.2 \cdot 10^6$ counts) gave a linear regression line having correlation coefficient > 0.9999, slope = $1.65 \cdot 10^5$ and *y*-intercept = $1.63 \cdot 10^5$). Standard errors in slope and *y*-intercept were ± $0.003 \cdot 10^5$ and ± $2.87 \cdot 10^5$, respectively.

The absolute recovery of BAK was assessed in a similar manner as described previously for the solid-phase extraction experiment. A standard solution of appropriate concentration was chromatographed directly without precolumn concentration.

TABLE II

STANDARD ADDITION AND RECOVERY OF BAK BY COLUMN SWITCHING

Homologue	Absolute recovery (%)						
	Standards, average (± R.S.D., %; n = 5)	Synthetic mixtures					
		At 68% level		At 102% level		At 170% level	
		Murine Plus	Murine	Murine Plus	Murine	Murine Plus	Murine
C_{12}	100.6 (± 0.98)	100.1	99.5	98.8	99.6	99.4	98.8
C_{14}	103.0 (± 0.66)	104.6	103.9	102.6	104.4	100.1	100.0
C_{16}	95.7 (± 1.2)	118.5	103.3	115.7	123.3	103.8	105.1
Total	101.3 (± 0.55)	103.6	101.8	101.9	103.7	100.0	99.9

Addition level (%)	Added (μg/ml)	Relative recovery (%)			
		Murine		Murine Plus	
		Recovery (μg/ml)	Recovery (%)	Recovery (μg/ml)	Recovery (%)
67.9	34.0	34.2	100.5	34.8	102.2
101.9	51.0	52.1	102.2	51.2	100.4
169.8	84.9	83.7	98.5	83.8	98.7

Absolute recoveries of total BAK from the standard averaged 101.3% (Table II). For the synthetic placebo mixtures, at concentrations of 68, 102 and 170% of the target value, total recoveries ranged from 99.9 to 103.7%. The variability of the recovery for the C_{16} homologue is attributable to the lower relative concentration of this component and to a slight peak broadening in the chromatography. Also shown in Table II are relative recoveries when the stated procedure is performed on the standard preparation and on synthetic mixtures of BAK added to placebos. Relative recoveries ranged from 98.5 to 102.2%.

The assay precision by column-switching was evaluated by determining BAK in Murine and Murine Plus on separate days using different analysts, chromatographic columns and precolumns. In Murine, a mean BAK concentration of 50.1 μg/ml was obtained with R.S.D. of ± 0.4%. In Murine Plus, a mean BAK concentration of 50.9 μg/ml was obtained with R.S.D. of ± 0.8%. The lots used in this study were different than those described previously in the solid-phase extraction experiments.

Throughout this work, the chromatographic finish appeared quite rugged. More than 200 injections of samples were made on columns packed from separate batches of packing with little loss in resolution. This probably results from the choice of the analytical column used and from eliminating the majority of the formulation excipients from the sample preparations. The two methods described provide comparable relative and absolute recoveries of the major BAK homologues and total BAK. Using the column-switching procedure, a slight amount of peak-broadening was observed in the chromatography. Both methods of pretreatment provide advantages of high sample throughput and excellent precision. The column-switching procedure allows total automation of the determination, eliminating the cost of the disposable cartridges and the time expended in manipulating the samples.

ACKNOWLEDGEMENTS

We thank Peggy Machak for her assistance in preparation of the manuscript.

REFERENCES

1 P. Leroy, V. Leyendecker, A. Nicolas and C. Garret, *Ann. Falsif. Expert. Chim. Toxicol.*, 79 (1986) 283.
2 A. Bettero, A. Semenzato and C. A. Benassi, *J. Chromatogr.*, 507 (1990) 403.
3 M. R. Euerby, *J. Clin. Hosp. Pharm.*, 10 (1985) 73.
4 L. J. Cohn, V. J. Greely and D. L. Tibbetts, *J. Chromatogr.*, 321 (1985) 401.
5 R. C. Meyer, *J. Pharm. Sci.*, 69 (1980) 1148.
6 A. Nakae, K. Kunihiro and G. Muto, *J. Chromatogr.*, 134 (1977) 459.
7 S. L. Abidi, *J. Chromatogr.*, 362 (1986) 33.
8 G. Ambrus, L. T. Takahashi and P. A. Marty, *J. Pharm. Sci.*, 76 (1987) 174.
9 A. Gomez-Gomar, M. M. Gonzalez-Aubert, J. Garces-Torrents and J. Costa-Segarra, *J. Pharm. Biomed. Anal.*, 8 (1990) 871.
10 D. F. Marsh and L. T. Takahashi, *J. Pharm. Sci.*, 72 (1983) 521.
11 K. Ikeda, T. Amemiya, K. Ito, T. Kan, H. Nakamura and Y. Watanabe, *Kenkyu Nenpo —Tokyo-toritsu Eisei Kenkyusho*, 38 (1987) 101.
12 G. Bleau and M. Desaulniers, *J. Chromatogr.*, 487 (1989) 221.

Journal of Chromatography, 625 (1992) 368–371
Elsevier Science Publishers B.V., Amsterdam

CHROM. 24 583

Short Communication

High-performance liquid chromatographic separation of intermediate products and potential impurities by the synthesis of roxatidin

N. Dimov and Ch. Ivanov

Chemical Pharmaceutical Research Institute - (NIHFI), 3 Kl. Okhridsky Street, 1156 Sofia (Bulgaria)

(First received December 17th, 1991; revised manuscript received August 25th, 1992)

ABSTRACT

A high-performance liquid chromatographic method is described for routine analytical control of the synthesis of roxatidin —a new β-blocker. Under control are three groups of compounds: starting products, intermediates and final substance. A reversed-phase RP-18 column for the first and last groups and an RP-2 column for the intermediates are preferred, although all three stationary phases are effective. The mobile phases are methanol–water (30:7, v/v) and tetrahydrofuran–acetonitrile–buffer (20:10:70, v/v/v) for the RP-18 column and tetrahydrofuran–acetonitrile–water (25:5:70, v/v/v) for the RP-2 column. The intra-assay precision is about 2% for the principal component in the chromatograms.

INTRODUCTION

Roxatidin, N-{3-[3-(1-piperidylmethyl)phenoxy]propyl}-acetoxyacetamide hydrochloride, is a new H_2 blocker with a marked effect on benign and post-operative ulcer or duodendal ulcer. Its structure is different from the other known β-blockers and its synthesis requires the analysis of a series of compounds as given in Table I.

To the best of our knowledge only one analytical method for the analysis of roxatidin, a thin-layer chromatographic method, exists in the literature [1]. Thus we are faced with the problem of analysing the compounds listed. They have a low vapour pressure and some of them are amides, *e.g.* with a low thermal stability. All of the compounds absorb in UV light. Therefore a liquid chromatographic method with UV detection seems to be the most suitable analytical method. According to the technological scheme a smaller subset of these compounds needs to be separated in one run. Based on our experience in routine analysis in factory laboratories, we prefer isocratic elution and reversed-phase columns.

Correspondence to: N. Dimov, Chemical Pharmaceutical Research Institute (NIHFI), 3 Kl. Okhridsky Street, 1156 Sofia, Bulgaria.

EXPERIMENTAL

Equipment

A Pye Unicam LXD pump equipped with a Model 4025 UV detector and LiChrosorb RP-18, RP-8 and RP-2 columns, 250 × 4.6 mm I.D. and 10 μm particle size, from Merck (Darmstadt, Germany) were used. The integrator was a Waters (Milli-

0021-9673/92/$05.00

TABLE I

STRUCTURES OF COMPOUNDS

No.	Structure	Abbreviation	Compound name
1	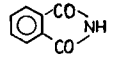	PhI	Phthalimide
2	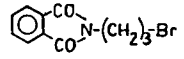	BPrPh	Brompropylphthalimide
3	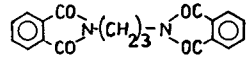	DPhPr	1,3-Diphthalimidopropane
4	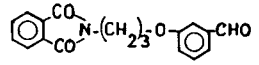	PhPrBA	3-Phthalimidopropoxybenzaldehyde
5	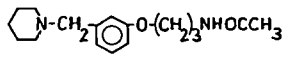	AA	N-{3-[3-(1-Piperidinylmethyl)phenoxy]propyl}acetamide
6	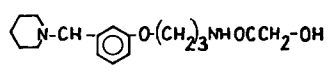	HAA	N-{3-[3-(1-Piperidinylmethyl)phenoxy]propyl}hydroxyacetamide
7	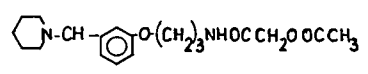	Rx	N-{3-[3-(1-Piperidinylmethyl)phenoxy]propyl}acetoxyacetamide hydrochloride (roxatidin)

pore, Milford, MA, USA) Model 740. The appropriate analytical wavelength is 278 ± 2 nm.

Chemicals

The organic modifiers tetrahydrofuran (THF), acetonitrile and methanol were from Merck and Fluka (Buchs, Switzerland) and were HPLC grade. *o*-Phthalimide (PhI) and *m*-hydroxybenzaldehyde (BA) were from Fluka. Roxatidin was obtained in our laboratory and its properties were compared with roxatidin extracted from existing market formulations. All other compounds were synthesized in NIHFI. After checking the purity, their structure was verified by IR and ^{1}H NMR.

Mobile phases

According to the structure of compounds, (Table I), two different types of mobile phases were tested: "neutral" and "buffered". The buffer consisted of 0.1 *M* orthophosphoric acid, the pH of which was adjusted to 3.0 with triethylamine (TEA). A flow-rate of 1.0 ml/min was set in all cases. The exact compositions are given in the legends to the figures.

RESULTS AND DISCUSSION

Starting products

m-Hydroxybenzaldehyde, although "acidic", emerged as a symmetrical peak from an RP-18 column with methanol–water (30:70, v/v) and was well separated from *o*-phthalimide. Changing the column to RP-8 or RP-2 necessitated only a small change in the mobile phase composition.

Intermediates

The target product from the first stage of the synthesis was brompropylphthalimide (BPrPh). The sample from the second stage consisted of one desired compound, 3-phthalimidopropoxybenzaldehyde (PhPrBA), and as impurities BPrPh and by-products, the majority of which was diphthalimidopropane (DPhPr).

Quantitation of these impurities necessitated a baseline separation. The sequence of the peaks, using acetonitrile as modifier, was DPhPr, BPrPh, PhPrBA, and the resolution (R_s) from the target compound was 1.4; however, neither DPhPr nor BPrPh could be quantified correctly, because of overlapping (R_s < 0.8). The sequence of the peaks

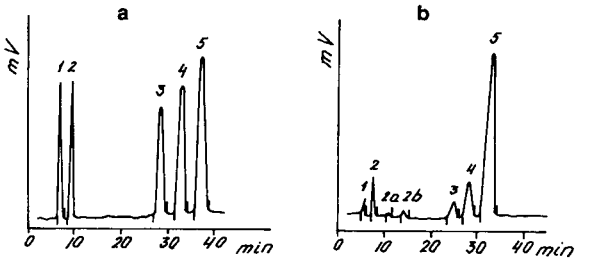

Fig. 1. (a) HPLC profile of a mixture of reference substances (total concentration 2 mg/ml) eluted onto a LiChrosorb RP-2 column. Detection at 280 nm. Mobile phase: tetrahydrofuran–acetonitrile–water (27.0:4.0:69.0, v/v/v). Peaks: 1 = PhI; 2 = BA; 3 = BPrPh; 4 = DPhPr; 5 = PhPrBA. For abbreviations, see Table I. (b) As in (a) but with a real sample of PhPrBA (about 1 mg/ml). Peaks 2a and 2b are unknown.

of DPhPr and BPrPh was reversed when tetrahydrofuran was used as the mobile phase and on RP-2 only their separation could be improved by reducing the content of tetrahydrofuran. The analysis time, however, increased to more than 40 min. An iterative method described in ref. 2 was applied for further optimization. The analysis time (the retention time of the last peak) was accepted to be not more than 30 min and two isoelutropic mobile phases were prepared to meet this demand. Following the optimization steps as given in ref. 2, the mixture tetrahydrofuran–acetonitrile–water (25.0:5.0:70.0, v/v/v) was accepted as adequate for the necessary separation (Fig. 1). All components were resolved to the baseline. The relative retention (RR), given as k'_i/k'_{BPrPh}, and the separation presented by R_s are given in Table II.

TABLE II

RELATIVE RETENTION (RR) AND R_S VALUES ON AN RP-2 COLUMN FOR THE COMPOUNDS UNDER INVESTIGATION

No.	Compound	RR	R_s
1	PhI	0.13	1.1
2	*m*-Hydroxybenzaldehyde	0.16	>2
3	DPhPr	0.85	1.2
4	BPrPh	1.00	1.2
5	PhPrBA	1.15	

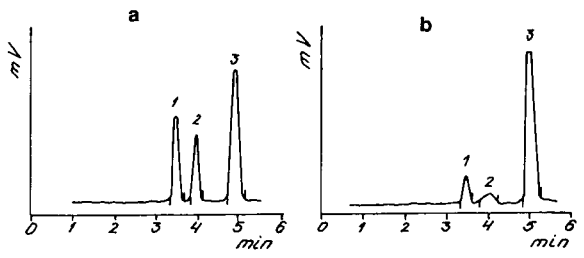

Fig. 2. HPLC profile of a mixture of roxatidin base and HAA eluted onto a LiChrosorb RP-18 column (about 0.3 mg/ml each). Detection at 280 nm. Mobile phase: methanol–acetonitrile–buffer (30:10:60, v/v/v). Buffer: 0.1 *M* phosphoric acid adjusted to pH 3.0 with TEA. Peaks: 1 = HAA; 2 = AA (see text); 3 = Rx. For abbreviations, see Table I. (b) As in (a) but with a real sample of roxatidin (1 mg/ml).

Substance

Roxatidin could be accompanied by the preceding product in its synthesis: N-{3-[3-(1-piperidinylmethyl)phenoxy]propyl}hydroxyacetamide (HAA) (Table I). With an RP-18 column and methanol–acetonitrile–buffer (20:10:70, v/v/v) as the mobile phase a baseline separation was achieved. The impurities emerged before the base peak (Fig. 2). The problem which arose in this stage of the synthesis was the second peak. Neither of the compounds in the Table I gave this peak. It was assumed that it belongs to the compound N-{3-[3-(1-piperidinylmethyl)phenoxy]propyl}acetamide (AA) (see Table I). By synthesizing this compound and employing chromatography under various conditions it was confirmed that the second peak is due to this compound.

Method validation

The amount of tetrahydrofuran is crucial to the resolution of DPhPr and PhPrB, which is why its optimum content should be determined experimentally for every column, after good conditioning. Solutions of BPrPh are unstable and they must be freshly prepared before analysis (storage time not longer than 20 min.)

The linearity of the detector response against roxatidin was verified from 0.05 to 0.5 mg/l. The limit of detection at a signal-to-noise ratio of 5 for AA and HAA was 2 μg/ml.

The intra-assay precision (eight injections) was about 2% for the principal component in the chromatogram and increased to *ca.* 3–4% for components present in a concentration of about 1%. The inter-assay precision (between first and third and third and fifth days) was 2.2% and 5%, respectively.

If the purity of PhPrBA is the problem, the concentration of the sample solution in the mobile phase must be 1 mg/ml. In this case, because of the non-linearity of the response, quantitation of the impurities was made by the external standard method using a dilute solution of PhPrBA.

Whichever approach was used, the principal compound of every stage of the synthesis could be determined accurately: in the first stage the separation of PhI and BA could be performed onto an RP-18 column with methanol–water as the mobile phase; in the next stage, again with an RP-18 column, both DPhPr and BPrPH were eluted together but separately from PhPrBA. We have endeavoured to use a limited range of conditions using an RP-2 column. This approach worked very well with the compounds from this stage that are difficult to chromatograph, and eluted the principal component at last. At the last stage the purity of roxatidin was also determined very well using again an RP-18 column with a ternary mobile phase. Thus, the proposed chromatographic methods allow the qualitative and quantitative control of the whole process of roxatidin synthesis.

ACKNOWLEDGEMENT

The authors acknowledge Miss D. Mondishka from VHTI (Sofia, Bulgaria) for the ^{1}H NMR spectra and their interpretation.

REFERENCES

1 K. Shibata, T. Itaya, N. Yamakoshi, Sh. Kurata and N. Koizumi, *Iyakuhin Kenkyu*, 6 (1985) 485.
2 P. J. Schoenmakers, *Optimization of Chromatographic Selectivity*, Elsevier, Amsterdam, 1986; (Russian version, Mir, Moscow, 1989).

Journal of Chromatography, 625 (1992) 372–376
Elsevier Science Publishers B.V., Amsterdam

CHROM. 24 567

Short Communication

Simultaneous determination of retinol and tocopherols by high-performance liquid chromatography

Yukiko Satomura, Mieko Kimura and Yoshinori Itokawa

Department of Hygiene, Faculty of Medicine, Kyoto University, Kyoto 606 (Japan)

(First received March 16th, 1992; revised manuscript received August 11th, 1992)

ABSTRACT

A high-performance liquid chromatographic (HPLC) method to determine retinol and all four tocopherols (α-, β-, γ- and δ-) simultaneously was established using a reversed-phase column (YMC-PACK A-302 S-5 120A ODS). The HPLC conditions were mobile phase 65% isopropanol, sample solvent 99.5% methanol and temperature 30°C. Retinol and tocopherols were measured in rat liver.

INTRODUCTION

Reports on the simultaneous measurement of retinol and tocopherols by high-performance liquid chromatography (HPLC) using reversed-phase columns have been presented by several groups [1–4]. However, with these methods tocopherols can be separated into only three fractions, *i.e.*, α-, β- + γ- and δ-tocopherols. Vatassery *et al.* [5] reported that the separation of β- and γ-tocopherols using reversed-phase columns is difficult. Although Wahyuni and Jinno [6] succeeded, the separation was inadequate and the elution time was over 2 h.

Using the reversed-phase HPLC procedure described in this paper, the separation of all four tocopherols and retinol was clearly achieved within 1 h. Retinol and tocopherols were measured in rat liver using this method.

Correspondence to: Yukiko Satomura, Department of Hygiene, Faculty of Medicine, Kyoto University, Kyoto 606, Japan.

EXPERIMENTAL

Apparatus

The following instruments (all obtained from Shimadzu, Kyoto, Japan) were used; HPLC pump, Model LC-3A; sample injector, Model LC-1; detector RF-500 spectrofluorometer (for retinol, λ_{ex} 340 nm, λ_{em} 460 nm; for tocopherol, λ_{ex} 298 nm, λ_{em} 325 nm); and recorder and computer, Chromatopac C-R6A.

A YMC-PACK A-302 S-5 120A ODS reversed-phase column (150 mm × 4.6 mm I.D. silica gel particle diameter 5 μm, pore size 120 Å, with residual silane groups end-capped with trimethylsilyl chloride, was kindly donated by YMC (Kyoto, Japan).

Reagents

d-α-, -β-, -γ- and -δ-tocopherols were kindly donated by Eisai (Tokyo, Japan). Retinol was obtained from Fluka (Buchs, Switzerland). Ethanol,

0021-9673/92/$05.00

n-hexane, methanol and 2-propanol were of HPLC grade from Nacalai Tesque (Kyoto, Japan).

As mobile phases, several mixtures of ethanol, methanol, 2-propanol and deionized, distilled water were examined.

Procedure

Standard solutions of the four tocopherols and retinol were prepared in 99.5% methanol, 50.0% methanol, 99.5% ethanol and 99.5% 2-propanol. They were injected directly into the column.

Preparation of sample

Under diethyl ether anaesthesia, blood was drawn from the abdominal aorta of 9-week-old rats. The livers were then collected. Tocopherols and retinol were extracted from the livers by the method of Abe and Katsui [7].

RESULTS

Mobile phase and temperature

First, HPLC was performed at ambient temperature (*ca.* 24°C) and 99.5% methanol was used as the sample solvent.

It was possible to determine retinol and three fractions of tocopherols (α-, β- + γ, δ-) using the mobile phases containing from 5% to 20% of water in methanol. However, β- and γ-tocopherols were not separated using methanol–water mobile phases.

It was found that β- and γ-tocopherols were hardly separated using mobile phases containing from 5% to 13% of water in ethanol. With over 14% of water in ethanol in the mobile phase, β- and γ-tocopherols could be separated, but the separation was insufficient. By further increasing the water content in ethanol, the difference in retention time between β- and γ-tocopherol was increased. With 20% of water in ethanol as the mobile phase, the time delay between β- and γ-tocopherols was 2.7 min. However, as the content of water in the mobile phase was increased, the retention times of the peaks became longer.

With mobile phases containing more than 15% of water in 2-propanol it was possible to separate β- and γ-tocopherols better than with other mobile phases, and a clear separation was obtained with 30% of water. However, it was found that the separation of β- and γ-tocopherols was incomplete when the ambient temperature was over 25°C. Even below 24°C, unstable temperatures resulted in unstable retention times. In order to obtain the optimum retention time, a constant column temperature was found to be necessary, which was controlled by a column oven. From 30 to 40°C, separation was performed using mobile phases containing from 60% to 70% of 2-propanol. When the 2-propanol content was 60% at 35°C, the maximum resolution (R_s) [8] was obtained (Table I). However, it took 74.7 min to elute all the tocopherols. At

TABLE I

PEAK RESOLUTION (R_s) OF β- AND γ-TOCOPHEROLS UNDER DIFFERENT HPLC CONDITIONS

Mobile phase	Sample solvent	Temperature (°C)	Flow-rate (ml/min)	Retention time of α-tocopherol (min)	R_s
80% ethanol	99.5% methanol	Ambient (24)	0.7	102.7	0.89
70% 2-propanol	99.5% methanol	Ambient (24)	0.7	49.8	1.24
70% 2-propanol	99.5% methanol	30	0.7	28.5	0.89
70% 2-propanol	99.5% methanol	35	0.7	25.1	0.86
65% 2-propanol	99.5% methanol	30	0.7	48.9	1.26
65% 2-propanol	99.5% methanol	35	0.7	44.4	1.07
65% 2-propanol	99.5% methanol	40	0.7	41.2	0.89
60% 2-propanol	99.5% methanol	30	0.7	88.8	1.22
60% 2-propanol	99.5% methanol	35	0.7	74.7	1.28
60% 2-propanol	99.5% methanol	40	0.7	67.7	1.13
65% 2-propanol	99.5% ethanol	30	0.7	49.2	0.96
65% 2-propanol	99.5% 2-propanol	30	0.7	48.0	0.60
65% 2-propanol	65.0% 2-propanol	30	0.7	47.5	1.10
65% 2-propanol	50.0% methanol	30	0.7	47.7	1.22

30°C, using 65% of 2-propanol in the mobile phase, the resolution R_s was 1.26, and all the tocopherols were eluted within 50 min (Table I).

Sample solvent

As sample solvents, 99.5% ethanol, 99.5% 2-propanol and 99.5% methanol were compared, while employing a mobile phase containing 65% of 2-propanol at 30°C. The best peak separation was obtained with 99.5% methanol (Table I). Then 99.5% methanol was compared with 50% methanol under the same conditions as described above. No difference was found concerning the separation of β- and γ-tocopherols (Table I). To dissolve the sample easily, 99.5% methanol was adopted as the solvent.

The most suitable conditions for the determination of retinol and all four tocopherols are shown in Table II. An elution profile for a standard solution obtained under these conditions is shown in Fig. 1A.

Sensitivity

The sensitivity of the method was calculated from the differences between duplicates using the method of Brown *et al.* [9]. The detection limits were 10 ng of α-tocopherol, 5 ng of β-, γ- and δ-tocopherols and 60 pg of retinol.

Quantification

There was a linear relationship between peak area and the amount of each compound injected ranging from 0.1 to 2.0 μg. The equations for retinol and α-, β-, γ- and δ-tocopherols were $y = 6.29x$, $y = 1.76x$, $y = 3.14x$, $y = 3.25x$ and $y = 2.84x$, respectively, where y = peak area ($\times 10^4$) and x = amount of compound (μg).

TABLE II

HPLC CONDITIONS FOR SIMULTANEOUS DETERMINATION OF RETINOL AND TOCOPHEROLS AFTER COMPLETE SEPARATION

Column	YMC-PACK A-302 S-5 120A ODS (150 mm × 4.6 mm I.D.)
Mobile phase	65% 2-propanol
Sample solvent	99.5% methanol
Detector	Spectrofluorometer For retinol: λ_{ex} 340 nm, λ_{em} 460 nm For tocopherols: λ_{ex} 298 nm, λ_{em} 325 nm
Flow-rate	0.7 ml/min
Temperature	30°C
Column pressure	140 kg/cm²

Determination of retinol and tocopherols in rat liver

Fig. 1B shows an elution profile of retinol and tocopherols in a rat liver sample. The mean extraction recoveries ± standard error (n = 10) were retinol 100.3 ± 3.1, α-tocopherol 106.1 ± 1.8, β-tocopherol 98.1 ± 2.9, γ-tocopherol 98.2 ± 3.4 and δ-tocopherol 96.3 ± 2.8%.

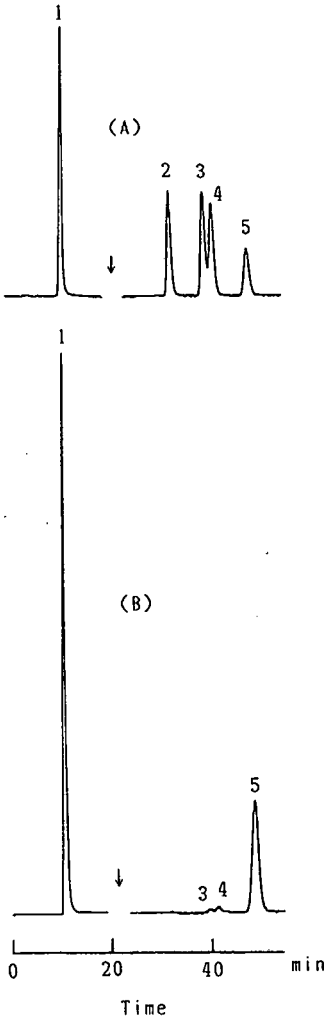

Fig. 1. Chromatograms of retinol and tocopherols. (A) Standard solution; (B) sample of rat liver. Conditions as in Table II. Peaks: 1 = retinol; 2 = δ-tocopherol; 3 = γ-tocopherol; 4 = β-tocopherol; 5 = α-tocopherol. Arrows indicate change of wavelength.

DISCUSSION

The effects of vitamin E on vitamin A metabolism have been reported in a number of papers [10–13]. Many physicians recommend concomitant treatment with vitamin A when patients suffering from abetaliproproteinaemia are treated with vitamin E [14,15]. Clinically, the simultaneous measurement of vitamin A and vitamin E is useful and important not only to clarify the relationship between these vitamins but also to evaluate the effect of supplementary therapy. HPLC has become a common method for measuring vitamins because of its high sensitivity and accuracy. Some methods for the simultaneous measurement of retinol and tocopherols using reversed-phase columns have been reported [1–4], but an improvement is achieved with the present method, namely the simultaneous separation of retinol and all four tocopherol homologues within 1 h. In addition, the peak resolution (R_s) of β- and γ-tocopherol was 1.26. The method satisfied the criterion of 4 σ separation [8]. The effective separation is mainly due to the column used. Another type of C_{18} column was tested under the conditions in Table II, but it did not separate β- and γ-tocopherols. Although YMC-PACK A-302 S-5 120A ODS is a commercially available, common type of ODS column, the slurry packing technique differentiates it from other C_{18} columns. Information about the slurry packing technique is not available from the manufacturer, however.

Using normal-phase columns all four tocopherols can be separated in a short time [7,16–19]. However, there have been no reports of the simultaneous determination of retinol and all four tocopherols using normal-phase columns, as far as we are aware. As Handelman *et al.* [20] reported, reversed-phase columns have some merits compared with normal-phase columns. When reversed-phase columns are used to determine tocopherols, δ-, γ-, β- and α-tocopherols are eluted in that order, whereas when normal-phase columns are used they are eluted in the opposite order. Because earlier peaks are sharper and higher than later peaks, the sensitivity for earlier peaks is higher than that for later peaks. Therefore, β-, γ- and δ-tocopherols can be determined with high-sensitivity using reversed-phase columns. In contrast, the sensitivity for α-tocopherol is low with reversed-phase columns. The sensitivity for α-tocopherol was 5 ng by the method of Russell *et al.* [1] using a reversed-phase column. Even compared with their data, the sensitivity for α-tocopherol was low with our method (10 ng). However, when our method was applied to rat liver, the α-tocopherol level was high enough to be determined.

The biopotency of α-tocopherol is considered to be the strongest among the four tocopherol homologues [21]. The concentration of α-tocopherol in animal tissues was shown to be higher than those of β-, γ- and δ-tocopherols in our previous studies. In contrast, γ-tocopherol is mainly found in the Japanese diet [22]. It is still unclear whether tocopherol homologues are metabolized in the same manner. There are some reports that the metabolism of γ-tocopherol is not the same as that of α-tocopherol [23–25]. This could imply that the effects of each tocopherol on retinol metabolism may be different. Our method can be used as a first step to clarify the relationship between retinol and individual tocopherol homologues.

REFERENCES

1 M. J. Russell, B. S. Thomas and E. Wellock, *J. High Resolut. Chromatogr. Chromatogr. Commun.*, 9 (1986) 281.
2 L. A. Kaplan, J. A. Miller and E. A. Stein, *J. Clin. Lab. Anal.*, 1 (1987) 153.
3 L. J. Hatam and H. J. Kayden, *J. Lipid Res.*, 20 (1979) 639.
4 W. J. Driskell, J. W. Neese, C. C. Bryant and M. M. Bashor, *J. Chromatogr.*, 231 (1982) 439.
5 G. T. Vatassery, V. R. Maynard and D. F. Hagen, *J. Chromatogr.*, 161 (1978) 299.
6 W. T. Wahyuni and K. Jinno, *J. Chromatogr.*, 448 (1988) 398.
7 K. Abe and G. Katsui, *Vitamins*, 50 (1976) 453.
8 J. J. Kirkland (Editor), *Modern Practice of Liquid Chromatography*, Wiley-Interscience, New York, 1972, pp. 8–15.
9 J. B. Brown, R. D. Bulbrook and F. C. Greenwood, *J. Endocrinol.*, 16 (1957) 41.
10 S. R. Ames, *Am. J. Clin. Nutr.*, 22 (1969) 934.
11 E. Søndergaard, *Experientia*, 29 (1972) 773.
12 J. L. Napoli, A. M. McCormick, B. O'Meara and E. A. Dratz, *Arch. Biochem. Biophys.*, 230 (1984) 194.
13 J. A. Kusin, V. Reddy and B. Sivakumar, *Am. J. Clin. Nutr.*, 27 (1974) 774.
14 E. Azizi, J. L. Zaidman, J. Eschar and A. Szeinberg, *Acta Paediatr. Scand.*, 67 (1978) 797.
15 D. P. R. Muller, J. K. Lloyd and A. C. Bird, *Arch. Dis. Child.*, 52 (1977) 209.
16 P. J. Niekerk, *Anal. Biochem.*, 52 (1973) 533.
17 K. Abe, Y. Yuguchi and G. Katsui, *J. Nutr. Sci. Vitaminol.*, 21 (1975) 183.

18 G. T. Vatassery, *J. Chromatogr.*, 161 (1978) 299.
19 A. J. Speek, J. Schrijver and H. P. Schreurs, *J. Food Sci.*, 50 (1985) 121.
20 G. J. Handelman, L. J. Machlin, K. Fitch, J. J. Weiter and E. A. Dratz, *J. Nutr.*, 115 (1985) 807.
21 M. Mino, H. Tamai, K. Yasuda, C. Yamada, O. Igarashi, M. Hayashi, F. Hirahara, G. Katsui and S. Kijima, *Vitamins*, 62 (1988) 241.
22 F. Hirahara, T. Ueda, T. Nishimune, O. Igarashi and M. Mino, *Vitamins*, 65 (1991) 103.
23 I. R. Peake and J. G. Bieri, *J. Nutr.*, 101 (1971) 1615.
24 I. R. Peake, H. G. Windmueller and J. G. Bieri, *Biochim. Biophys. Acta*, 260 (1972) 679.
25 W. A. Behrens and R. Madere, *Nutr. Res.*, 5 (1985) 167.

Journal of Chromatography, 625 (1992) 377–381
Elsevier Science Publishers B.V., Amsterdam

CHROM. 24 535

Short Communication

Determination of nicotinamide and pyridoxine in an elemental diet by column-switching high-performance liquid chromatography with UV detection

Hiroshi Iwase

Ajinomoto Co., Inc., Kawasaki Factory, 1–1 Suzuki-cho, Kawasaki-ku, Kawasaki 210 (Japan)

(First received May 5th, 1992; revised manuscript received July 2nd, 1992)

ABSTRACT

The determination of nicotinamide and pyridoxine in an elemental diet containing 46 compounds was performed by column-switching high-performance liquid chromatography with UV detection at 260 and 290 nm, respectively. The method is simple, rapid, sensitive and reproducible. The calibration graphs for the two vitamins were linear in the ranges 0–0.2 and 0–0.015 μg, respectively. The recoveries of both vitmins by the standard addition method were over 95%. There was good agreement between the concentrations indicated and found for both vitamins.

INTRODUCTION

The routine determination of nicotinamide and pyridoxine in elemental diets such as Elental (Ajinomoto, Kawasaki, Japan), which is a mixture of 46 compounds (*e.g.*, amino acids, vitamins, organic acids, soybean oil, dextrin, minerals) [1], is required for process control, quality control purposes and in clinical chemistry.

Nicotinamide and pyridoxine hydrochloride have been determined by spectrophotometry [2], potentiometric titration [3], a microbiological method [4] and high-performance liquid chromatography (HPLC) [5–10]. Spectrophotometry and potentiometric titration are not suitable for complex sample matrices. In most instances, microbiological methods have generally been used for the routine determination of vitamins. However, this method is tedious and time consuming [4,11]. The Nicotinamide and pyridoxine have been determined by HPLC [5–10]. However, HPLC could not be used for the routine determination of these vitamins in Elental, because the experimental conditions and the removal of interferences caused by the complex sample matrix had not been investigated in detail.

Previous papers [11–13] reported the routine determination of cyanocobalamin, ascorbic acid and folic acid in Elental by HPLC. This paper deals with the routine determination of nicotinamide (27.5 μg/g) and pyridoxine (as hydrochloride salt, 3.34 μg/g) in Elental by column-switching HPLC with UV detection at 260 and 290 nm, respectively. This paper also describes the determination of the above vitamins in two other elemental diets, Elental P for paediatrics and Hepan ED for hepatic failure.

Correspondence to: Dr. H. Iwase, Ajinomoto Co., Inc., Kawasaki Factory, 1–1 Suzuki-cho, Kawasaki-ku, Kawasaki 210, Japan.

0021-9673/92/$05.00

EXPERIMENTAL

Reagents and materials

Elental, Elental P and Hepan ED were obtained from Ajinomoto. Nicotinamide and pyridoxine hydrochloride were of Japanese Pharmacopoeia standard. Sodium 1-heptanesulphonate was obtained from Aldrich (Madison, WI, USA). Acetonitrile (Wako, Osaka, Japan) was of HPLC grade. Other reagents were of analytical-reagent grade.

Sample preparation

To a solution of Elental (20 g) dissolved completely in deionized water (60 ml) on a water-bath at 50°C was added sodium chloride (10 g). After the solution had been allowed to stand at room temperature for 30 min, it was diluted to 100 ml with deionized water in a Volumetric flask and then extracted with hexane (10 ml) for 3 min to remove oils. This aqueous layer was used as the test sample. An aliquot (20 μl) was injected into the chromatograph. Elental P and Hepan ED samples for injection were prepared in the same manner.

Nicotinamide and pyridoxine were stable in aqueous solution at 50°C for 1 h.

Apparatus

Two Model 655 A-11 high-performance liquid chromatographs (Hitachi, Tokyo, Japan) equipped with two Model 655 A variable-wavelength detectors (Hitachi, Tokyo, Japan) set at 260 or 290 nm and a Model HPV 6A column-switching device (Gaskurokogyo, Tokyo, Japan) were used. Capcellpak C_{18} (5 μm) (Shiseido, Tokyo, Japan) (3 × 0.46 cm I.D. and 25 × 0.46 I.D.) were used as the precolumn and analytical column, respectively. The samples were applied with a Rheodyne Model 7125 sample loop injector with an effective volume of 20 μl. A Model UV-2100 variable-wavelength UV spectrophotometer (Shimadzu, Kyoto, Japan) was used for measuring absorption spectra.

Chromatographic conditions

After injection of 20 μl of sample solution on to the precolumn, which has been previously equilibrated with acetonitrile–water (pH 2.1, adjusted with phosphoric acid) (1.5:98.5), the column was washed for 1.33 min (nicotinamide) or 1.66 min (pyridoxine) with the above mobile phase at a flow-rate of 0.8 ml/min. The substances adsorbed on the precolumn were introduced on to the analytical column with acetonitrile–water (pH 2.1, adjusted with phosphoric acid) (9:91) with 1.5 m*M* sodium 1-heptanesulphonate for 0.75 min (both vitamins) at a flow-rate of 0.6 ml/min and a column temperature of 35°C by switching the six-port valve. After introducing the substances on to the analytical column, the six-port valve was returned to the original

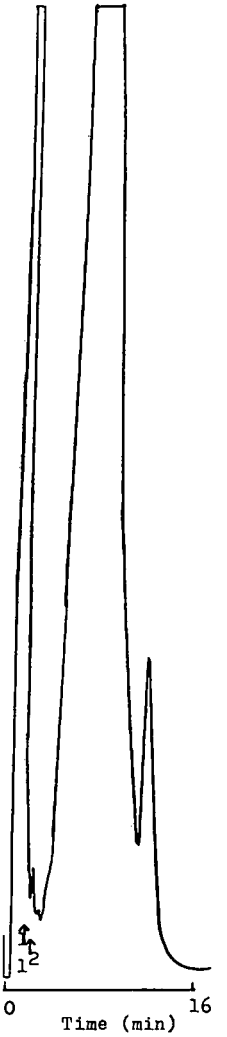

Fig. 1. Elution of nicotinamide and pyridoxine in Elental on the precolumn (3 × 0.46 cm I.D.) with detection at 260 nm. Mobile phase, acetonitrile–water (pH 2.1, adjusted with phosphoric acid) (1.5:98.5) at a flow-rate of 0.8 ml/min. Peaks: 1 = nicotinamide; 2 = pyridoxine.

position. The precolumn was washed with acetonitrile–water (pH 2.1) (1.5:98.5) for the next injection.

RESULTS AND DISCUSSION

Chromatography

The first efforts were focused on the determination of nicotinamide and pyridoxine in Elental using only one analytical column, without the use of the column-switching method, with UV detection at 260 or 290 nm. However, these vitamins could not be identified because many overloading peaks, which might be due to tryptophan, phenylalanine, ascorbic acid, thiamine or riboflavine, with maximum concentrations 10^3 times higher than that of the two vitamins, were observed on the chromatogram.

Subsequent efforts were focused on the determination of the two vitamins in Elental using column-switching HPLC with UV detection at 260 or 290 nm. At the beginning of the work, retention times of standard nicotinamide and pyridoxine and column connection times from the precolumn to the analytical column were examined for the determination of the two vitamins and for the elimination of interferences caused by the complex sample matrix.

A chromatogram of Elental obtained by HPLC with UV detection at 260 nm on the precolumn is shown in Fig. 1. The peaks of nicotinamide and pyridoxin were observed at retention times of *ca.* 1.33 and 1.66 min, respectively. Other compounds were eluted completely within about 16 min (Fig. 1).

After washing for 1.33 or 1.66 min with acetonitrile–water (pH 2.1) (1.5:98.5), the precolumn and analytical column were connected for various periods to examine the connection time. When the connection times were set shorter than 0.75 min, the peaks of the two vitamins were smaller, and when they were set longer than 0.75 min, other many unknown overloading peaks were observed and neither vitamin could be identified. Therefore, the column connection time was set at 0.75 min.

Chromatograms of nicotinamide and pyridoxine in Elental obtained column-switching HPLC with detection at 260 or 290 nm are shown in Figs. 2 and 3. The peaks of these vitamins were separated completely. The detection limits (signal-to-ratio ratio = 2) of the two vitamins were about 5.5 and 0.7 ng, respectively.

It was found that the simultaneous determination

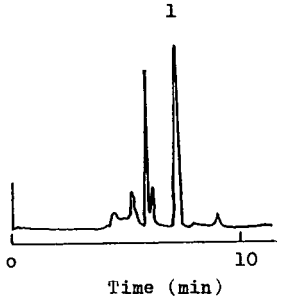

Fig. 2. Chromatogram of nicotinamide (peak 1) in Elental obtained by column-switching HPLC with UV detection at 260 nm Amount of nicotinamide injected, 0.11 μg in 20 μl.

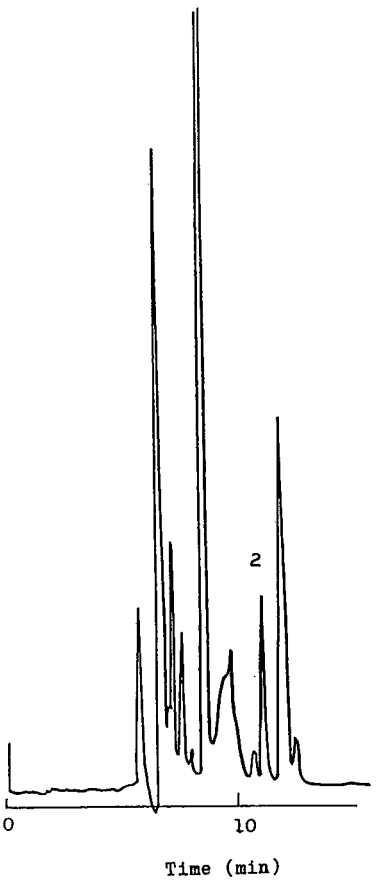

Fig. 3. Chromatogram of pyridoxine (peak 2) in Elental by column-switching HPLC with UV detection at 290 nm. Amount of pyridoxine injected, 13.4 ng in 20 μl.

TABLE I

RECOVERIES OF NICOTINAMIDE AND PYRIDOXINE ADDED TO ELENTAL

According to the label Elental contains 2.75 mg of nicotinamide and 0.334 mg of pyridoxine hydrochloride per 100 g. R.S.D.: nicotinamide 2.2% (n = 5) without addition of nicotinamide, pyridoxine 1.8% (n = 5) without addition of pyridoxine.

	Recovery (μg/100 g)		Recovery (%)
	Added	Found	
Nicotinamide	0	2.66	–
	1.38	3.98	95.7
	2.75	5.28	95.3
	5.50	7.91	95.5
Pyridoxine hydrochloride	0	0.321	–
	0.167	0.481	95.8
	0.334	0.640	95.5
	0.668	0.956	95.1

of the two vitamins was impossible when different wavelengths were used or different washing times of the precolumn.

For the identification of the two vitamins in Elental, a freshly prepared model solution containing the 44 constituent coupounds but with no addition of the two vitamins of interest was examined by the proposed method. No peak of other compounds with the same retention times as the two vitamins was observed on the chromatograms. Hence, the proposed procedure might be considered advantageous for the routine determination of nicotinamide and pyridoxine in complex mixtures.

Determination of nicotinamide and pyridoxine

Calibration graphs for nicotinamide and pyridoxine (as hydrochloride) were constructed by plotting the peak height against the amount of two vitamins, and satisfactory linearity was obtained in the ranges 0–0.2 and 0–0.015 μg, respectively.

A known amount of nicotinamidde or pyridoxine was added to Elental and the overall recovery was determined by the standard addition method. The recoveries of nicotinamide and pyridoxine were over 95% (Table I). The within-day relative standard deviation (R.S.D.) (without addition of nicotinamide and pyridoxine) was 2.2% (n = 5) and 1.8% (n = 5) and the between-day R.S.D. for these two vitamins was 2.5% and 2.2%, respectively.

The analytical data for the two vitamins in Elental, Elental P and Hepan ED (Table II) show that there was good agreement between the nicotinamide and pyridoxine contents found and the values indicated by the manufactures.

In conclusion, this method is satisfactory with respect to selectivity, rapidity and accuracy. It is simple and convenient, and therefore applicable to the routine determination of nicotinamide and pyridoxine in elemental diets such as Elental, Elental P and

TABLE II

ANALYTICAL DATA FOR NICOTINAMIDE AND PYRIDOXINE IN THREE ELEMENTAL DIETS

Elemental diet	Vitamin	Concentration indicated (mg/100 g)	Found (mg/100 g)	Recovery (%)
Elental	Nicotinamide	2.75	2.77	100.7
			2.66	96.7
			2.68	97.4
	Pyridoxine hydrochloride	0.334	0.330	98.8
			0.321	96.1
			0.319	95.5
Elental P	Nicotinamide	4.58	4.38	95.6
	Pyridoxine hydrochloride	0.556	0.533	95.9
Hepan ED	Nicotinamide	4.13	3.98	96.4
	Pyridoxine hydrochloride	0.839	0.805	95.9

Hepan ED. Application of the proposed method to the determination of drugs in biological fluids is also being studied.

REFERENCES

1 S. Ogoshi (Editor), *Elental Diet*, Nankodo, Tokyo, 1983.
2 *The Pharmacopoeia of Japan*, Hirokawa, Tokyo, 12th ed., 1992, p. C-1618.
3 *The Pharmacopoeia of Japan*, Hirokawa, Tokyo, 12th ed., 1992, p. C-633.
4 T. Suzuki and S. Muraoka, *Bitamine Aminosan no Biseibutsuteiryoho*, Nanzando, Tokyo, 1956, p. 101.
5 *The United States Pharmacopeia, XX11 Revision*, US Pharmacopeial Convention, Rockville, MD, 1990, pp. 944 and 1194.
6 R. B. H. Wills, C. G. Shaw and W. R. Day, *J. Chromatogr. Sci.*, 15 (1977) 262.
7 M. Amin and J. Reusch, *Analyst (London)*, 112 (1987) 989.
8 J. X. de Vries, W. Günthert and R. Ding, *J. Chromatogr.*, 221 (1980) 161.
9 G. S. Shephard, L. V. Westhuizen and D. Labadarios, *J. Chromatogr.*, 491 (1989) 226.
10 B. Mc Chrisley, H. M. McNair and J. A. Driskell, *J. Chromatogr.*, 563 (1991) 369.
11 H. Iwase, *J. Chromatogr.*, 590 (1992) 187.
12 H. Iwase, *J. Chromatogr.*, 606 (1992) 277.
13 H. Iwase, *J. Chromatogr.*, 609 (1992) 399.

Journal of Chromatography, 625 (1992) 382–386
Elsevier Science Publishers B.V., Amsterdam

CHROM. 24 564

Short Communication

Determination of mustard gas and related vesicants in rubber and paint by gas chromatography–mass spectrometry

E. R. J. Wils, A. G. Hulst and A. L. de Jong

TNO Prins Maurits Laboratory, P.O. Box 45, 2280 AA Rijswijk (Netherlands)

(First received April 3rd, 1992; revised manuscript received August 17th, 1992)

ABSTRACT

The determination of mustard gas (2,2'-dichlorodiethyl sulphide) and some related vesicants in rubber and paint was investigated. The vesicants were isolated by extraction with methylene chloride or by dynamic headspace analysis at elevated temperatures. The latter procedure had the advantage that high-boiling additives did not interfere during the analysis by capillary column gas chromatography–mass spectrometry. The stability of the vesicants in the materials used proved to be good. No great losses were found after storage for weeks at room temperature.

INTRODUCTION

Since the use of mustard gas (2,2'-dichlorodiethyl sulphide) in the Iran–Iraq conflict [1–3], several reports have appeared describing the determination of this vesicant and its related compounds in various matrices. Attention was focused on the environmental matrices air [4–8], water [9] and soil [10] and on biological samples. Analytical procedures for mustard gas and its degradation products have been established for these last samples [11–18]. So far no procedures have been published for the determination of mustard gas and related vesicants in contaminated materials such as rubber and paint. It is to be expected that in comparison with aqueous samples, degradation in these hydrophobic materials will be limited. Rubber and paint are possible samples to be taken on a battlefield or during an inspection of a facility under a future chemical weapons convention. It is most likely that in both situations, a certain chemical background will also be present against which the possible presence of the sulphur vesicants has to be identified. Therefore, the fate of these vesicants in rubber and paint was not studied with the pure compounds themselves but in combination with diesel fuel and an aromatic white spirit. Unambiguous identification of the presence of mustard gas and its related compounds in such complicated mixtures can only be achieved by a combination of chromatography and spectrometry. Owing to its sensitivity and selectivity, capillary column gas chromatography–mass spectrometry (GC–MS) is at present the most suitable technique for this purpose.

Correspondence to: E. R. J. Wils, TNO Prins Maurits Laboratory, P.O. Box 45, 2280 AA Rijswijk, Netherlands.

0021-9673/92/$05.00

EXPERIMENTAL

Chemicals

The vesicants mustard gas (2,2′-dichlorodiethyl sulphide), mustard disulphide (2,2′-dichlorodiethyl disulphide), mustard sulphone (2,2′-dichlorodiethyl sulphone), sesquimustard [1,2-bis(2-chloroethylthio)ethane] and dimustard ether [bis(2-chloroethylthioethyl) ether] were all prepared at this laboratory.Their identity and purity were controlled by NMR and GC–MS before the preparation of stock solutions. The purity of all compounds was >95% except for sesquimustard (Q), which contained about 7% of 2-chloroethyl 2-chloroethoxyethyl sulphide.

Shellsol AB, an aromatic white spirit with a boiling range of 165–220°C, was obtained from Shell. Diesel fuel was obtained from a commercial petrol station. It consisted of aliphatic hydrocarbons with a boiling range of 150–350°C. Methylene chloride (No. C14500) was purchased from Lamers & Pleuger (Netherlands).

Materials and pretreatment

The rubber sample, which had been used for the sealing of a window of a car, was a common type of black rubber containing soot and a relatively high concentration (*ca.* 30%) of high-boiling hydrocarbons used as plasticizers. An analysis by pyrolysis mass spectrometry pointed to an ethylene–propylene copolymer. The rubber was cut into pieces of *ca.* 8 g, which were spiked as homogeneously as possible with mustard gas and other vesicants, an aromatic solvent mixture (Shellsol AB) with the same volatility as mustard gas and diesel fuel. The spiked amounts of the vesicants were in the ppm (mg/kg) range, whereas the aromatic solvent mixture and the diesel fuel were added at a higher level. A methylene chloride solution was brought on the surface of each piece by means of a syringe. After *ca.* 15 min the rubber was visibly dry. For storage experiments the piece of rubber was wrapped in aluminium foil. Before the extraction the spiked piece of rubber (*ca.* 8 g) was cut into smaller pieces (about twenty) and extracted by sonication using 20 ml of methylene chloride for 30 min. After extraction, the solution was centrifuged for 5 min at 1000 *g* and directly analysed by GC–MS.

Metal plates (2 x 4 cm) covered with a layer of alkyd paint (film thickness 60 μm) were used. This paint is used by the Dutch Army and possesses the characteristic military green colour. The plates were prepared by the TNO Centre for Coatings Research (Delft, Netherlands) and were stored at room temperature for *ca.* 5 months. The painted surface was spiked with vesicants in a Shellsol solution (5 μl). The spiking and storage were performed in the same way as for the rubber samples. The paint (mass *ca.* 50 mg) was scratched off the plates with a scalpel and transferred into a small test tube (1 ml). Extraction was carried out by sonication with 0.5 ml of methylene chloride for 15 min, followed by centrifugation (5 min at 1000 *g*). Extracts were directly analysed by GC–MS.

GC–MS analysis of extracts

A 0.5-μl volume of an extract was injected on to a fused-silica capillary column (50 m × 0.3 mm I.D., film thickness 0.25 μm) coated with CP-Sil 5 CB (Chrompack) by means of a Carlo Erba on-column injector installed on a Hewlett Packard HP 5890A gas chromatograph. The column was directly connected to the ion source of a VG70-250S mass spectrometer. The temperature of the interface was 250°C and the helium flow-rate was 2 ml/min. The oven temperature was 40°C for 1 min, then increased at 8°C/min to a final temperature that depended on the analysis, *viz.* 300°C (25 min) for the rubber extracts and 275°C (5 min) for the paint extracts.

Electron impact (70 eV) mass spectra were continuously scanned over the mass range *m/z* 25–500 every 1 s. The temperature of the ion source block was *ca.* 200°C.

Quantitative analysis was carried out by comparing the peak areas of the analytes with those obtained from standards added to an extract of a blank material.

Thermodesorption

A piece of rubber (*ca.* 10 mg) or paint (*ca.* 1 mg) was transferred into a glass tube (16 × 6 cm O.D.) fitted with a quartz-wool plug. The glass tube was placed in the flow system of a Chrompack thermodesorption cold trap injector installed on an HP 5890A gas chromatograph as part of the above-described GC–MS combination. Volatile compounds were desorbed at various temperatures (100–150°C)

in a helium flow (15 ml/min) for 10 min and trapped in a piece of deactivated fused silica at −120°C. After completion of the thermodesorption step the trap was flash heated to 220°C, this temperature being maintained for 5 min. The same GC–MS conditions were used as described for the analysis of the extracts.

RESULTS AND DISCUSSION

Two approaches for the determination of sulphur mustard gases were investigated. In addition to extraction followed by GC–MS analysis of the extracts, dynamic headspace (thermal extraction or gas stripping) was carried out. Pieces of rubber were extracted by sonication using methylene chloride for 30 min. This relatively long extraction time proved to be necessary in order to obtain a high extraction efficiency of mustard gas (>90%). Using an extraction time of 5 min could reduce the efficiency to below 30%. The high percentage of high-boiling hydrocarbons used as plasticizers in the rubber caused problems during the GC–MS analysis of the extracts after on-column injection. As an example the gas chromatogram of an extract obtained from a piece of rubber (*ca.* 8 g) spiked with 0.38 mg of mustard gas, 0.21 mg of mustard disulphide, 4.45 mg of Shellsol and 7.32 mg of diesel fuel is presented in Figs. 1 and 2. The recorded mass spectra of the vesicants were similar to those described in the literature [10, 19, 20]. Owing to the large amounts of high-boiling hydrocarbons, peak broadening occurred, leading to a severe decrease in GC resolution. Optimum resolution will be a prerequisite for the determination of the studied vesicants in such complicated mixtures. Better results were obtained with the dynamic headspace procedure. In order to prevent unwanted thermal decomposition reactions and also to achieve maximum separation between the vesicants and the plasticizers the lowest possible temperature was evaluated. Heating a small piece of spiked rubber (*ca.* 10 mg) at 120°C in a flow of helium resulted in an almost quantitative release of mustard gas and its disulphide. As the major part of the plasticizer hydrocarbons were not released, no decrease in GC resolution was noticed (see Fig. 3). The temperature of 120°C was too low for a complete release of the higher boiling vesicant sesqui-

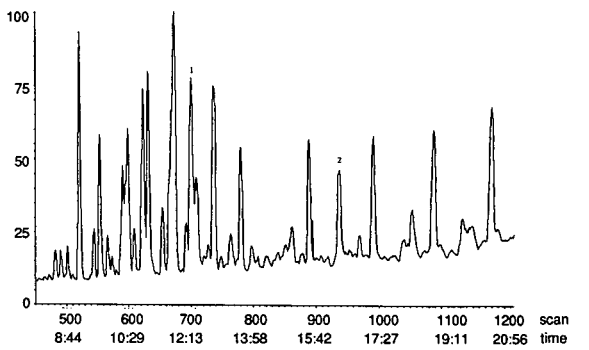

Fig. 2. Gas chromatogram of a methylene chloride extract of the spiked rubber sample shown in Fig. 1 (expanded range). Peaks: 1 = mustard gas; 2 = mustard disulphide.

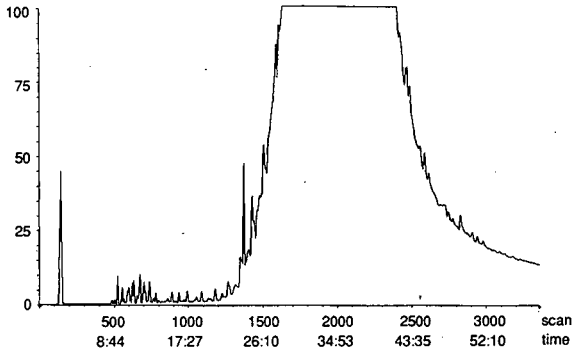

Fig. 1. Gas chromatogram of a methylene chloride extract of a spiked rubber sample. Peaks: 1 = high-boiling hydrocarbons used as plasticizers. Time in min:s.

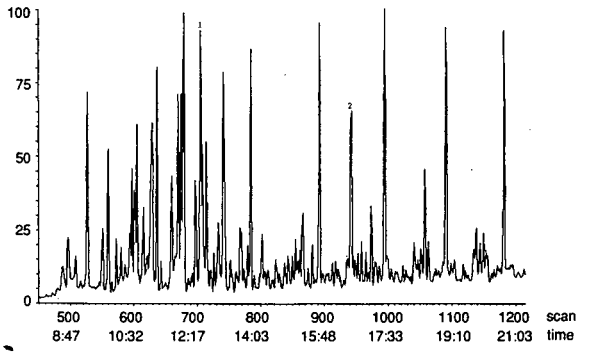

Fig. 3. Gas chromatogram obtained after the thermodesorption of a spiked rubber sample at 120°C (expanded range). Peaks: 1 = mustard gas; 2 = mustard disulphide.

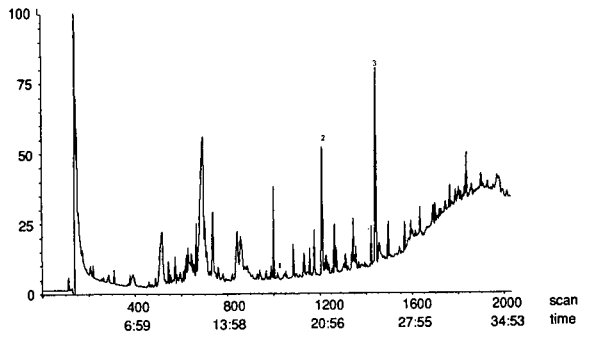

Fig. 4. Gas chromatogram of a methylene chloride extract of a spiked paint sample. Peaks: 1 = 2-chloroethyl 2-chloroethoxyethyl sulphide; 2 = sesquimustard (Q); 3 = dimustard ether (T).

mustard (Q) from the rubber and for this compound the lowest temperature needed proved to be 150°C.

The developed work-up procedure for the plates covered with paint consisted of scratching off the paint followed by extraction using sonication with methylene chloride. As the paint particles were somewhat static, unexpected losses sometimes occurred. None of the tested compounds showed a recovery above 90% even if the samples were worked up immediately after the spiking. Decomposition by the paint components was ruled out as low recoveries were also measured for unreactive hydrocarbons. It was found that compounds with the volatility of mustard gas and the aromatic hydrocarbons present in Shellsol gave very low recoveries. After 15 min the recovery for mustard gas was less than 10%. Evaporation of the added compounds before they were adsorbed by the paint is the most probable explanation. Therefore, experiments were mainly carried out with the higher boiling vesicants sesquimustard (Q) and dimustard ether (T). A characteristic gas chromatogram of an extract obtained from a paint sample spiked with 67 μg of sesquimustard (Q), 98 μg of dimustard ether (T) and 460 μg of diesel fuel is presented in Fig. 4. Despite the fact that a Shellsol solution was used for the spiking of the paint hardly any aromatic compounds could be detected. The relatively large broad peak at the beginning of the chromatogram corresponded to 2-ethylhexanoic acid. In addition to the two vesicants the impurity in the sesquimustard (Q) used, *viz.*, 2-chloroethyl 2-chloroethoxyethyl sulphide, could also be detected. Paint could also be thermally desorbed. For an almost quantitative release of the highest boiling vesicant tested, dimustard ether (T), a temperature of 150°C was necessary. For sesquimustard (Q), 120°C turned out to be sufficient. As the paint did not contain large amounts of additives, hardly any differences between the extraction and the thermodesorption results were found. However, care should be taken that during the removal of the paint from the plates by scratching the paint does not become contaminated with metal particles. These may catalyse unwanted thermal decomposition reactions at elevated temperatures.

TABLE I

RECOVERIES (%) OF SULPHUR MUSTARD GASES IN RUBBER AND PAINT

Compound	Recovery (%)			
	Material	30 min	3 weeks	6 weeks
Mustard gas	Rubber	86	60	57
Mustard disulphide	Rubber	100	92	84
Sesquimustard (Q)	Paint	68	55	43
Dimustard ether (T)	Paint	59	33	25

The stabilities of the vesicants in the investigated materials were determined. The recoveries obtained after storage of the samples at room temperature (*ca.* 22°C) are presented in Table I. Owing to the relatively large spread (up to 20% between duplicate experiments) the values have to be considered more as an indication. Although there was a decrease, after 6 weeks of storage more than 50% of the added mustard gas and its disulphide could still be recovered in the rubber sample. However, the rubber material used was not completely inert as was experienced with mustard sulphone. Although this compound could initially be retrieved with a recovery of *ca.* 85%, it could not longer be detected (recovery $<1\%$) 3 days after the spiking. The recoveries found with the paint samples were lower than those obtained with the rubber. This was mainly due to initial losses during the spiking of the samples, as explained above.

The relatively good stabilities of the sulphur vesicants in hydrophobic materials such as rubber and

paint are in marked contrast with their instabilities in environmental and biological samples. The hydrolysis of mustard gas in water is very fast ($t_{1/2}$ = 10 min at 20°C) [21]. The degradation on soil will depend on the type of soil and its wetness. In a number of soil samples (humic sand, humic loam and clayey peat), mustard gas could not be retrieved with a recovery greater than 1% one day after applying the agent to the soil [22]. Therefore, materials such as rubber and paint may be considered as good samples for the retrospective identification of mustard gas and related vesicants.

REFERENCES

1 *Report S/16433*, United Nations New York, 26 March 1984.
2 *Report S/17911*, United Nations New York, 12 March 1986.
3 *Report S/20134*, United Nations New York, 19 August 1988.
4 J. C. Posner, *Chemosphere*, 22 (1991) 461.
5 J. R. Hancock, J. M. McAndless and R. P. Hicken, *J. Chromatogr. Sci.*, 29 (1991) 40.
6 J. Steinhanses and K. Schoene, *J. Chromatogr.*, 514 (1990) 273.
7 P. A. D'Agostino, L. R. Provost, J. F. Anacleto and P. W. Brooks, *J. Chromatogr.*, 504 (1990) 259.
8 W. K. Fowler and J. E. Smith, Jr., *J. Chromatogr. Sci.*, 28 (1990) 118.
9 P. A. D'Agostino, L. R. Provost, A. S. Hansen and G. A. Luoma, *Biomed. Environ. Mass Spectrom.*, 18 (1989) 484.
10 P. A. D'Agostino and L. R. Provost, *Biomed. Environ. Mass Spectrom.*, 15 (1988) 553.
11 W. Vycudilik, *Forensic Sci. Int.*, 28 (1985) 31.
12 W. Vycudilik, *Forensic Sci. Int.*, 35 (1987) 67.
13 E. R. J. Wils, A. G. Hulst, A. L. de Jong, A. Verweij and H. L. Boter, *J. Anal. Toxicol.*, 9 (1985) 254.
14 E. R. J. Wils, A. G. Hulst and J. van Laar, *J. Anal. Toxicol.*, 12 (1988) 15.
15 G. Drasch, E. Kretschmer, G. Kauert, L. von Meyer, *J. Forensic Sci.*, 32 (1987) 1788.
16 R. M. Black and R. W. Read, *J. Chromatogr.*, 449 (1988) 261.
17 R. M. Black and R. W. Read, *J. Chromatogr.*, 558 (1991) 393.
18 E. M. Jakubowski, C. L. Woodward, M. M. Mershon and T. W. Dolzine, *J. Chromatogr.*, 528 (1990) 184.
19 E. Ali-Mattila, K. Siivinen, H. Kenttämaa and P. Savolahti, *Int. J. Mass Spectrom. Ion. Phys.*, 47 (1983) 371.
20 E. R. J. Wils and A. G. Hulst, *Fresenius Z. Anal. Chem.*, 321 (1985) 471.
21 M. Sartori, The War Gases, Churchill, London, 1940.
22 J. Kaaijk, TNO-Prins Maurits Laboratory, Rijswijk, unpublished results.

Journal of Chromatography, 625 (1992) 387–391
Elsevier Science Publishers B.V., Amsterdam

CHROM. 24 608

Short Communication

Separation of phenylenediamine isomers by capillary zone electrophoresis

M. W. F. Nielen

Analytical and Environmental Chemistry Department, Corporate Research, Akzo Research Laboratories Arnhem, P.O. Box 9300, 6800 SB Arnhem (Netherlands)

(First received August 10th, 1992; revised manuscript received September 8th, 1992)

ABSTRACT

A capillary zone electrophoretic method for the separation of positional isomers of phenylenediamine is presented. The phenylenediamines were baseline resolved using a fused-silica capillary. However, the analysis of samples containing both an excess of *p*-phenylenediamine and minor traces of the *meta* and *ortho* isomers, and also a high salt content, required a non-polar (DB-1) bonded phase in order to reduce the electroosmotic flow. The method can be used for purity testing of *p*-phenylene diamine and for the determination of impurities in hydrolysates of synthetic polymers.

INTRODUCTION

Phenylenediamines are widely used in the chemical industry, *e.g.*, in dye manufacture and as building blocks in synthetic polymers. The separation of the positional isomers of phenylenediamine by chromatographic methods is difficult. Liquid chromatographic methods [1–3] suffer from interferences from related compounds. Gas chromatographic methods are a good alternative from the resolution point of view, but they cannot be applied directly to aqueous samples. In addition, the cationic phenylenediamines have to be converted into their free bases, which are less stable.

Capillary zone electrophoresis (CZE), offering rapid and efficient separations of ionic compounds [4,5], has been successfully applied to the separation of positional isomers of aminobenzoic acid [6,7]. Employing minor differences in the pK_a values of *o*-, *m*- and *p*-phenylenediamine by selecting an appropriate pH of the buffer solution might be adequate for obtaining baseline resolution. However, the resolution of cationic analytes in CZE might be hindered by unintended interactions with the negatively charged surface of fused-silica capillaries. Apart from these interactions, the resolution of cationic analytes will also suffer from the similar directions of the electrophoretic migration and the electroosmotic flow. The resolution equation in CZE [4]:

$$R_s = 0.177\,(\mu_{ep1} - \mu_{ep2})\left[\frac{VL_d}{D(\mu_{epm} + \mu_{osm})L_t}\right]^{1/2} \quad (1)$$

where μ_{ep} is the electrophoretic mobility of the analyte, μ_{epm} the mean of the two electrophoretic mobilities, V the applied voltage, D the diffusion coefficient, L_d and L_t the length of the capillary to

Correspondence to: M. W. F. Nielen, Analytical and Environmental Chemistry Department, Corporate Research, Akzo Research Laboratories Arnhem, P.O. Box 9300, 6800 SB Arnhem, Netherlands.

0021-9673/92/$05.00

the detection window and the total length, respectively, and μ_{osm} the coefficient of electroosmotic flow, predicts that the maximum resolution will be obtained when the electroosmotic flow is low or, even better, in the opposite direction to the electrophoretic migration. Consequently, the separation of cationic analytes in unmodified fused-silica capillaries is theoretically less favourable. Several groups have studied modifications of fused-silica capillaries [8–18] and different types have recently been introduced commercially [19]. In this study, we used both unmodified fused-silica and DB-1 coated fused-silica capillaries for the separation of phenylenediamine isomers, traces of isomeric impurities and for the analysis of aqueous saline samples, this matrix simulating neutralized hydrochloric acid digests of synthetic polymers.

EXPERIMENTAL

Apparatus

An Applied Biosystems (San Jose, CA, USA) Model 270A capillary electrophoresis system [20] was used, equipped with a variable-wavelength UV absorbance detector, operated at 225 or 200 nm with a 0.5-s rise time. CZE was performed in 70 cm (50 cm from injection to detection) × 50 μm I.D. fused-silica capillaries (Applied Biosystems) and fused-silica capillaries coated with 0.05-μm DB-1 methylsilicone (J&W Scientific, Folsom, CA, USA). The voltage was +25 kV (constant-voltage mode) and the oven temperature was 30°C. Samples were introduced using a controlled vacuum system; the injection time was 0.5 or 1.0 s, which corresponds to volumes of *ca.* 1.5 and 3 nl, respectively. The coefficient of electroosmotic flow was calculated using the migration time of the system peak. The electrophoretic mobilities and the plate numbers were calculated using the equations in ref. 7. Data were recorded using a Nelson Analytical Model 4400 integration system.

Chemicals

Tris(hydroxymethyl)aminomethane (Tris) was obtained from Fluka (Buchs, Switzerland) and serine from Sigma (St. Louis, MO, USA). Phenylenediamine isomers were obtained from laboratory stock. All other chemicals were of analytical-reagent grade from J. T. Baker (Deventer, Netherlands). Distilled water was purified in a Milli-Q apparatus (Millipore, Bedford, MA, USA).

Methods

The detection window in the DB-1 capillary was prepared by removing 4 mm of the polyimide outer film using a razor blade. Buffers were filtered through 0.45-μm Spartan 30/B membrane filters (Schleicher & Schuell, Dassel, Germany) prior to use. Stock solutions of the phenylenediamines ($1.0 \cdot 10^{-2}$ *M*) were prepared in water or saline solutions. Sample solutions were prepared by dilution of the stock solutions with the electrophoresis buffer.

RESULTS AND DISCUSSION

Initial experiments were performed using an electrophoresis buffer of 40 m*M* Tris–acetate (pH 4.8). The excess of protonated Tris ions and the weakly acidic pH suppressed adsorption of the cationic phenylenediamines on the fused-silica wall, thus yielding good peak shapes without any tailing. The separation of a mixture consisting of $1.0 \cdot 10^{-4}$ *M* of *p*-phenylenediamine (PPD) and $5.0 \cdot 10^{-5}$ *M* of *m*-phenylenediamine (MPD) and *o*-phenylenediamine (OPD) is shown in Fig. 1. All isomers are easily baseline resolved within 6.5 min and non-ionic or anionic matrix components, if present, will show up at or later than 7.8 min (electroosmotic flow marker) and not interfere. The electrophoretic mobilities and the coefficient of electroosmotic flow were $0.282 \cdot 10^{-3}$, $0.137 \cdot 10^{-3}$, $0.085 \cdot 10^{-3}$ and $0.297 \cdot 10^{-3}$ cm^2 V^{-1} s^{-1}, respectively. The plate numbers ranged from 173 000 for PPD and MPD to 143 000 for OPD.

In order to test the feasibility for purity testing, an excess of PPD ($1.0 \cdot 10^{-2}$ *M*) was mixed with $1.0 \cdot 10^{-4}$ *M* of MPD and OPD. The electropherogram is shown in Fig. 2. It can be seen that, despite the 100-fold excess of PPD, the resolution has been maintained and the migration times are still the same. However, the response of MPD and OPD decreased significantly in comparison with Fig. 1. It can be concluded that the isomeric purity of PPD reagents can be determined in this way semiquantitatively only; the detection limit for the isomeric impurities will be of the order of 0.5%, relative to the main component.

Next, the feasibility of the determination of traces

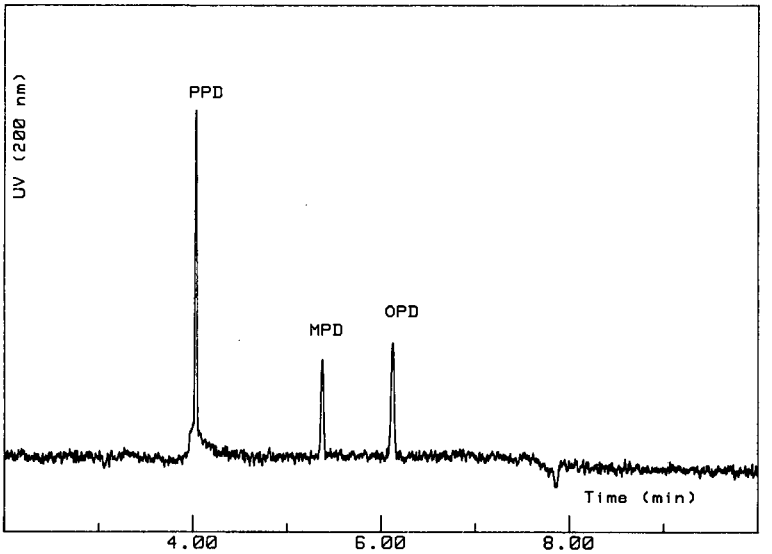

Fig. 1. CZE separation of positional isomers of phenylenediamine using an uncoated fused-silica capillary and 40 m*M* Tris–acetate buffer (pH 4.8). Constant voltage, +25 kV. Detection by UV absorbance at 200 nm. Injection, 1-s vacuum of 10^{-4} *M* PPD and $5 \cdot 10^{-5}$ *M* of both MPD and OPD. System peak (electroosmotic flow marker) at 7.8 min.

of OPD and MPD in an excess of PPD, dissolved in an aqueous saline solution, was investigated. The presence of 0.3 *M* sodium chloride in the sample turned out to be disastrous as OPD and MPD traces could not be detected owing to excessive band broadening. Nevertheless, the presence of high salt concentrations can also be exploited in a positive way [21,22]: the excess of sodium can act as a leading ion and provide a temporarily isotachophoretic stage with inherent peak focusing, provided that the appropriate terminating ion is present. Replacement of Tris– with serine–acetate (pH 4.5) should fulfil

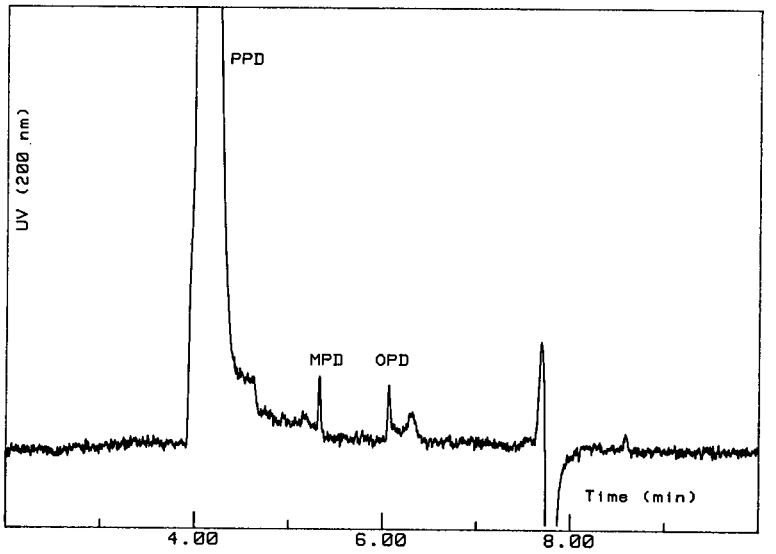

Fig. 2. CZE separation of an excess of PPD (10^{-2} *M*) and traces of MPD and OPD (10^{-4} *M* each). System peak (electroosmotic flow marker) at 7.8 min. Other conditions as in Fig. 1.

this requirement. The mobility of serine is very low as the pH of the buffer is relatively close to the isoelectric point of serine. The serine–acetate buffer showed an increased separation speed and an increase in the electroosmotic flow ($\mu_{osm} = 0.686 \cdot 10^{-3}$ cm^2 V^{-1} s^{-1}) owing to the decreased ionic strength and the lower tendency of serine to interact with the capillary wall. The positional isomers were still baseline separated but the resolution and peak capacity decreased because of the increase in the electroosmotic flow (*cf.*, eqn. 1); moreover, an excess of PPD in a saline matrix overlapped with traces of MPD and OPD. Decreasing the electroosmotic flow while maintaining the new buffer ion would be attractive. Therefore, a hydrophobically (DB-1) modified fused-silica capillary was investigated.

With the modified DB-1 capillary, the electroosmotic flow decreased towards $0.424 \cdot 10^{-3}$ cm^2 V^{-1} s^{-1} (system peak at 5.5 min) using serine–acetate. When the samples were dissolved in a 0.3 *M* sodium chloride sample matrix, the intended focusing occurred: the peak width decreased from 4.0 to 2.0 s while the migration time increased by 1 min (the plate number of OPD increased from 86 000 to 445 000). The electropherograms obtained with a real sample are shown in Fig. 3: (1) the electropherogram of $1.0 \cdot 10^{-2}$ *M* PPD in 0.3 *M* NaCl, where the two arrows indicate traces of isomeric impurities; (2) the same sample spiked with $1.0 \cdot 10^{-4}$ *M* MPD, where the arrow indicates the OPD impurity in the original sample, and (3) the sample spiked with $1.0 \cdot 10^{-4}$ *M* of both OPD and MPD. Note that the system peak has shifted from 5.5 towards 6.5 min because of the focusing step. Consequently, the system peak can no longer be used as an electroosmotic flow marker. A disadvantage of isotachophoretic-like sample introduction techniques is the decreased reproducibility of migration times, which actually become matrix dependent. Consequently, identification and quantification via standard addition techniques is recommended. The isomeric impurities in our PPD reagent were thus found to represent 0.1% of MPD and OPD. The detection limit of OPD relative to an excess of PPD will be lower than 0.05%, which is adequate both for purity testing of PPD reagents and for the detection of impurities in hydrolysates of synthetic polymers.

REFERENCES

1 R. M. Riggin and C. C. Howard, *J. Liq. Chromatogr.*, 6 (1983) 1897.
2 M. W. F. Nielen, R. W. Frei and U. A. Th. Brinkman, *J. Chromatogr.*, 317 (1984) 557.
3 M. W. F. Nielen, U. A. Th. Brinkman and R. W. Frei, *Anal. Chem.*, 57 (1985) 806.
4 J. Jorgenson and K. D. Lukacs, *Anal. Chem.*, 53 (1981) 1298.

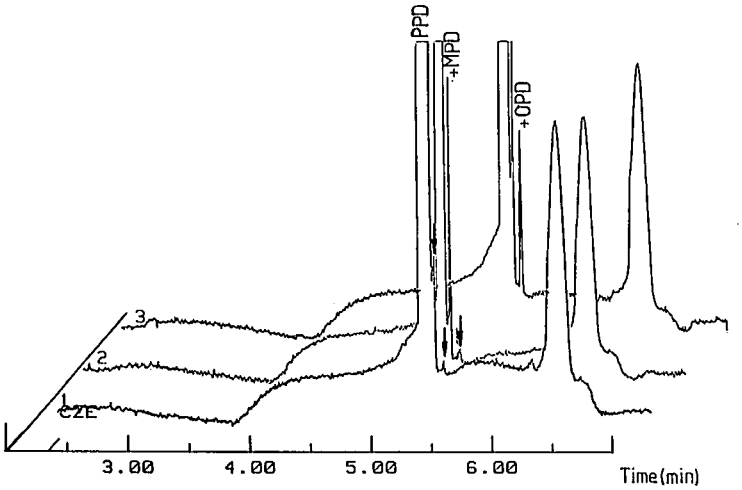

Fig. 3. Electropherograms of (1) 10^{-2} *M* PPD in 0.3 *M* sodium chloride, (2) spiked with 10^{-4} *M* MPD and (3) spiked with 10^{-4} *M* MPD and 10^{-4} *M* OPD. Conditions: DB-1 coated fused-silica capillary and 0.6 *M* serine–acetate buffer (pH 4.5). Injection, 1-s vacuum of a $2 \cdot 10^{-2}$ *M* PPD solution in 0.6 *M* NaCl, diluted 1:1 with buffer, followed by 10-s vacuum injection of the buffer. Detection by UV absorbance at 225 nm. System peak at 6.5 min.

5 R. A. Wallingford and A. G. Ewing, *Adv. Chromatogr.*, 29 (1989) 1.
6 S. Fujiwara and S. Honda, *Anal. Chem.*, 59 (1987) 487.
7 M. W. F. Nielen, *J. Chromatogr.*, 542 (1991) 173.
8 S. Hjertén, *J. Chromatogr.*, 347 (1985) 191.
9 K. A. Cobb, V. Dolnik and M. Novotny, *Anal. Chem.*, 62 (1990) 2478.
10 M. Strege and A. Lagu, *Anal. Chem.*, 63 (1991) 1233.
11 G. Schomburg, M.-H. Kleemiss, J. A. Lux, S. R. Motsch and H. F. Yin, presented at the *4th International Symposium on High-Performance Capillary Electrophoresis, Amsterdam, 1992.*
12 J. K. Towns and F. E. Regnier, *J. Chromatogr.*, 516 (1990) 69.
13 G. J. M. Bruin, R. Huisden, J. C. Kraak and H. Poppe, *J. Chromatogr.*, 480 (1989) 339.
14 G. J. M. Bruin, J. P. Chang, R. H. Kuhlman, K. Zegers, J. C. Kraak and H. Poppe, *J. Chromatogr.*, 471 (1989) 429.
15 W. Nashabeh and Z. El Rassi, *J. Chromatogr.*, 536 (1991) 31.
16 J. A. Lux, H. Yin and G. Schomburg, presented at the *18th International Symposium on Chromatography, Amsterdam, 1990.*
17 S. A. Swedberg, *Anal. Biochem.*, 185 (1990) 51.
18 H. E. Schwartz, K. Ulfelder, F. J. Sunzeri, M. P. Busch and R. G. Brownlee, *J. Chromatogr.*, 559 (1991) 267.
19 A. M. Dougherty, J. D. McCullock, C. T. Silverstein and C. L. Woolley, presented at the *4th International Symposium on High-Performance Capillary Electrophoresis, Amsterdam, 1992.*
20 S. E. Moring, J. C. Colburn, P. D. Grossman and H. H. Lauer, *LC · GC Int.*, 3 (1990) 46.
21 J. L. Beckers and F. M. Everaerts, *J. Chromatogr.*, 508 (1990) 3.
22 J. L. Beckers and F. M. Everaerts, *J. Chromatogr.*, 508 (1990) 19.

Journal of Chromatography, 625 (1992) 392–396
Elsevier Science Publishers B.V., Amsterdam

CHROM. 24 612

Short Communication

Thin-layer chromatographic study of the lipophilicity of triazine herbicides

Influence of different organic modifiers

G. L. Biagi, A. M. Barbaro and A. Sapone

Dipartimento di Farmacologia, Università di Bologna, Via Irnerio 48, 40126 Bologna (Italy)

M. Recanatini

Dipartimento di Scienze Farmaceutiche, Università di Bologna, 40126 Bologna (Italy)

(First received May 20th, 1992; revised manuscript received September 8th, 1992)

ABSTRACT

The R_M values of a series of triazine herbicides were measured using a reversed-phase TLC system with acetone, methanol or acetonitrile as the organic modifier of the mobile phase. The overlapping of the extrapolated R_M values from three different systems shows that they are not dependent on the nature of the organic solvent. However, a more interesting point arises from a comparison of the b values of the TLC equations. The slopes of the straight lines describing the relationship between R_M values and composition of the mobile phase are related to the solvent strength of the solvents.

INTRODUCTION

In a previous paper we considered the study of lipophilicity indices of a series of triazine herbicides [1]. Very good correlations were shown between chromatographic indices and log P data. The usefulness of TLC and HPLC techniques as complements to the classical octanol–water partition coefficients was pointed out.

This paper reports a study of the lipophilicity of triazine herbicides in order to investigate more general aspects of the chromatographic determination of R_M values as lipophilicity indices.

Correspondence to: G. L. Biagi, Dipartimento di Farmacologia, Università di Bologna, Via Irnerio 48, 40126 Bologna, Italy.

EXPERIMENTAL

The R_M values were obtained using a reversed-phase TLC technique, where the non-polar stationary phase was a silica gel G layer impregnated with silicone DC 200 (350 cSt) from Applied Science Labs. (State College, PA, USA), and the mobile phase was an aqueous buffer (sodium acetate–1/7 M Veronal at pH 7.0) alone or mixed with acetonitrile in different proportions. The details of the chromatographic technique for the determination

0021-9673/92/$05.00

TABLE I

STRUCTURES OF TRIAZINE HERBICIDES

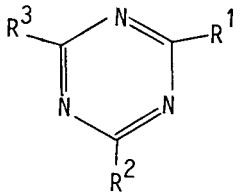

No.	Compound	R^1	R^2	R^3
1	Terbutylazine	$NHC(CH_3)_3$	Cl	$NHCH_2CH_3$
2	Cyanazine	$NHC(CH_3)_2$ CN	Cl	$NHCH_2CH_3$
3	Desisopropylatrazine	Cl	$NHCH_2CH_3$	NH_2
4	Atrazine	Cl	$NHCH_2CH_3$	$NHCH(CH_3)_2$
5	Simazine	Cl	$NHCH_2CH_3$	$NHCH_2CH_3$
6	Secbumeton	$NHCHCH_2CH_3$ CH_3	OCH_3	$NHCH_2CH_3$
7	Terbumeton	$NHC(CH_3)_3$	OCH_3	$NHCH_2CH_3$
8	Terbutryn	$NHC(CH_3)_3$	SCH_3	$NHCH_2CH_3$
9	Trietazine	$NHCH_2CH_3$	$N(CH_2CH_3)_2$	Cl
10	Anilazine	Cl	NHC_6H_4Cl-*o*	Cl
11	Aziprotryne	SCH_3	N_3	$NHCH(CH_3)_2$
12	Propazine	Cl	$NHCH(CH_3)_2$	$NHCH(CH_3)_2$
13	Ametryn	$NHCH_2CH_3$	$NHCH(CH_3)_2$	SCH_3
14	Desmetryn	$NHCH_3$	SCH_3	$NHCH(CH_3)_2$
15	Desethylatrazine	Cl	NH_2	$NHCH(CH_3)_2$
16	Dipropetryn	$NHCH(CH_3)_2$	SCH_2CH_3	$NHCH(CH_3)_2$
17	Atraton	$NHCH_2CH_3$	$NHCH(CH_3)_2$	OCH_3
18	Methoprotryne	$NH(CH_2)_3OCH_3$	SCH_3	$NHCH(CH_3)_2$
19	Prometon	$NHCH(CH_3)_2$	OCH_3	$NHCH(CH_3)_2$
20	Simetryn	$NHCH_2CH_3$	SCH_3	$NHCH_2CH_3$

of the R_M values have been described previously [1–3].

The structures of triazine herbicides are shown in Table I.

RESULTS

In the reversed-phase TLC system, the range of the linear relationship between the R_M values and the organic modifier concentration in the mobile phase allowed the calculation of extrapolated R_M values at 0%. The TLC equations obtained with acetonitrile in the mobile phase and those previously calculated using acetone or methanol systems are reported in Table II.

$$R_{M\ \text{methanol}} = 0.030\ (\pm 0.064) + 1.002\ (\pm 0.046)\ R_{M\ \text{acetone}} \quad (1)$$
$(n = 20;\ r = 0.981;\ s = 0.076;\ F = 467.0;\ P < 0.005)$

$$R_{M\ \text{methanol}} = -0.019\ (\pm 0.065) + 0.999\ (\pm 0.046)\ R_{M\ \text{acetonitrile}} \quad (2)$$
$(n = 20;\ r = 0.982;\ s = 0.075;\ F = 478.5;\ P < 0.005)$

$$R_{M\ \text{acetone}} = -0.013\ (\pm 0.076) + 0.971\ (\pm 0.053)\ R_{M\ \text{acetonitrile}} \quad (3)$$
$n = 20;\ r = 0.974;\ s = 0.087;\ F = 334.7;\ P < 0.005)$

TABLE II

TLC EQUATIONS FOR THE ACETONE, METHANOL AND ACETONITRILE SYSTEMS

$R_M = a + b$ (% organic modifier).

No.	$R_{Mextrap} = a$	b	r	Organic modifier	Concentration range (%)
1	1.588	−0.042	0.993	Acetone	12–60
2	0.970	−0.034	0.991		0–60
3	0.546	−0.071	0.965		0–8
4	1.273	−0.036	0.993		4–60
5	1.035	−0.034	0.979		0–60
6	1.348	−0.036	0.989		4–60
7	1.525	−0.042	0.989		12–60
8	2.003	−0.045	0.993		16–60
9	1.485	−0.040	0.992		12–60
10	1.627	−0.037	0.993		4–60
11	1.223	−0.033	0.979		4–60
12	1.620	−0.040	0.990		12–60
13	1.454	−0.037	0.991		4–60
14	1.117	−0.038	0.991		4–60
15	0.637	−0.062	0.966		0–8
16	1.986	−0.045	0.989		16–60
17	1.101	−0.035	0.991		0–60
18	1.552	−0.038	0.992		12–60
19	1.349	−0.037	0.992		4–60
20	1.252	−0.042	0.995		4–60
1	1.540	−0.028	0.998	Methanol	20–70
2	0.985	−0.026	0.998		0–70
3	0.588	−0.026	0.999		0–8
4	1.252	−0.027	0.995		4–70
5	1.003	−0.026	0.995		0–70
6	1.495	−0.029	0.997		16–70
7	1.491	−0.027	0.998		20–70
8	1.950	−0.027	0.979		20–70
9	1.595	−0.027	0.987		20–70
10	1.623	−0.031	0.987		20–70
11	1.301	−0.023	0.989		12–70
12	1.711	−0.031	0.994		28–70
13	1.465	−0.027	0.994		12–70
14	1.239	−0.026	0.996		12–70
15	0.599	−0.021	0.987		0–70
16	2.100	−0.030	0.996		24–70
17	1.188	−0.025	0.991		0–70
18	1.498	−0.029	0.999		20–70
19	1.522	−0.029	0.996		20–70
20	1.210	−0.026	0.987		4–70
1	1.679	−0.036	0.995	Acetonitrile	20–60
2	1.019	−0.037	0.995		0–55
3	0.568	−0.033	0.998		0–8
4	1.302	−0.033	0.992		4–60
5	1.049	−0.033	0.995		0–55
6	1.521	−0.039	0.994		12–55
7	1.561	−0.037	0.993		16–60
8	1.872	−0.040	0.996		20–60
9	1.542	−0.034	0.995		12–60
10	1.631	−0.038	0.996		16–60

TABLE II *(continued)*

No.	$R_{Mextrap} = a$	b	r	Organic modifier	Concentration range (%)
11	1.416	−0.031	0.997	Acetonitrile	8–60
12	1.553	−0.035	0.995		16–60
13	1.460	−0.035	0.993		12–60
14	1.278	−0.034	0.995		4–60
15	0.655	−0.029	0.995		0–55
16	2.135	−0.044	0.993		20–60
17	1.130	−0.036	0.993		0–60
18	1.640	−0.042	0.998		16–55
19	1.532	−0.040	0.997		12–55
20	1.217	−0.035	0.995		0–55

The slopes and intercepts of eqns. 1, 2 and 3, very close to 0 and 1 respectively, show the overlapping of the R_M values extrapolated from three solvent systems.

In fact, if the extrapolated R_M values represent the partitioning of the compounds between the silicone oil of the stationary phase and a mobile phase constituted only by water, then we expect the same R_M values whether the organic modifier is acetone, methanol or acetonitrile. These findings are in agreement with earlier results for series of dermorphin-related oligopeptides [4], prostaglandins [5] and quinolines and naphthalenes [6]. This shows that the linear relationship between R_M values and mobile phase composition yields extrapolated R_M values that are not dependent on the nature of the organic solvent.

However, a more interesting point arises from the analysis of the b values in Table II. Their mean values in the acetone, acetonitrile and methanol systems are reported in Table III. The low standard deviations are due to the strong parallelism existing in each chemical class among the straight lines describing the relationship between R_M values and composition of the mobile phase. The more negative slopes in the acetone compared with the other systems are related to the higher eluting power of acetone and indicate that the same decrease in R_M value is given by a smaller increase in the acetone concentration. In Table III are also reported previous data obtained with series of dermorphin-related oligopeptides [4], prostaglandins [5], and quinolines and naphthalenes [6], together with the solvent strenght parameters (E_o) of acetone, acetonitrile

TABLE III

RATIOS BETWEEN SLOPES IN DIFFERENT TLC SYSTEMS

Compounds	Slopes in solvent systems			Ratios		
	Acetone	Acetonitrile	Methanol	Acetone/ acetonitrile	Acetone/ methanol	Acetonitrile/ methanol
Triazines	−0.041 (±0.002)	−0.036 (±0.001)	−0.027 (±0.001)	1.14	1.52	1.33
Prostaglandins	−0.071 (±0.002)	–	−0.042 (±0.002)		1.69	
Dermorphin-related oligopeptides	−0.089 (±0.002)	–	−0.055 (±0.002)		1.62	
Quinolines and naphthalenes	−0.046 (±0.002)	–	−0.030 (±0.002)		1.53	
Solvent strenght ($1/E_o$)	1.78	1.54	1.05	1.15	1.70	1.47

and methanol, when considered in a reversed-phase chromatographic system ($1/E_o$) [7,8].

The ratios between the mean slopes in different solvent systems, and the corresponding ratios between the solvent strengths, are also given in Table III. It can be seen that the ratios between the slopes are very close to the ratios between the $1/E_o$ values for the corresponding solvent pairs.

DISCUSSION AND CONCLUSIONS

The results show the reliability of the TLC system for determining the lipophilic character of molecules. As the R_M values extrapolated to 0% organic solvent are not dependent on the nature of the modifier of the mobile phase, they actually measure the partitioning of the compounds between silicone oil and water. As a consequence, the TLC system shows versatility. In fact, one can choose the most convenient solvent for a given series of compounds and obtain extrapolated R_M values measuring the lipophilic character in the same standard system.

In each solvent system the R_M values change with the composition of the mobile phase at a rate that is correlated with the solvent strength of the organic modifier as expressed by its $1/E_o$ value. In fact, the ratios between the slopes in different solvent systems follow the ratios between the corresponding $1/E_o$ values.

REFERENCES

1 G. L. Biagi, M. C. Guerra, A. M. Barbaro, M. Recanatini, P. A. Borea and A. Sapone, *Sci. Total Environ.*, 109/110 (1991) 33.
2 G. L. Biagi, A. M. Barbaro, M. F. Gamba and M. C. Guerra, *J. Chromatogr.*, 41 (1969) 371.
3 G. L. Biagi, M. C. Guerra, A. M. Barbaro, S. Barbieri, M. Recanatini, P. A. Borea and M. C. Pietrogrande, *J. Chromatogr.*, 498 (1970) 179.
4 A. M. Barbaro, M. C. Pietrogrande, M. C. Guerra, G. Cantelli Forti, P. A. Borea and G. L. Biagi, *J. Chromatogr.*, 287 (1984) 259.
5 A. M. Barbaro, M. C. Guerra, G. L. Biagi, M. C. Pietrogrande and P. A. Borea. *J. Chromatogr.*. 347 (1985) 209.
6 G. L. Biagi, M. Recanatini, A. M. Barbaro, M. C. Guerra and A. Sapone, in H. Kalász and L. S. Ettre (Editors), Proceedings of the *Budapest Chromatography Conference, 1991*, Intercongress, Budapest, 1992, pp. 215–234.
7 K. J. Bombaugh, in K. Tsuji and W. Morozowich (Editors), *GLC and HPLC Determination of Therapeutic Agents, Part I*, Marcel Dekker, New York, 1978, p. 83.
8 L. R. Snyder and J. J. Kirkland, *Introduction to Modern Liquid Chromatography*, Wiley, New York, 1978.

Journal of Chromatography, 625 (1992) 397–398
Elsevier Science Publishers B.V., Amsterdam

CHROM. 24 574

Book Review

Introduction to micellar electrokinetic chromatography, by J. Vindevogel and P. Sandra, Hüthig, Heidelberg, 1992, X + 231 pp., price DM 88.00, ISBN 3-7785-0861-X.

To the best of my knowledge, this is the first book on a capillary electrophoretic technique, except for books on isotachophoresis. It is a great personal pleasure that this book on micellar electrokinetic chromatography (MEKC) is the first book on capillary electrophoresis (CE), because MEKC has been mainly developed by the reviewer's group. It is now more than 10 years since the first few papers on CE were published, but so far no book has been published in this rapidly growing area, in spite of strong demands for good textbooks from those who have started work in this field and companies selling CE apparatus and equipment. I would like to congratulate Dr. J. Vindevogel and Professor P. Sandra on the successful publication of this first and excellent book on CE.

The authors state that "This book is primarily devoted to MEKC" and also "As it is intended for those who have a background in chromatography but not in electrophoresis, the basic principles of electrophoresis in general but also, more specifically, of capillary zone electrophoresis (CZE) are included". I think this principle is natural and reasonable, because most readers of this book will be chromatographers considering using CE in their fields and, moreover, MEKC will be more familiar than other CE techniques to those readers. An easily understandable introduction to the fundamental characteristics of CE techniques is provided and this is useful not only for those interested in MEKC but also for those working in CE to review the basic principles. In addition, the size of the book is suitable for a quick overview of CE. However, the book does not intentionally include topics on protein analysis and capillary gel electrophoresis, which are the other important fields of wide interest.

The book consists of four parts, and about half of the book is devoted to the general aspects of CE. Part I contains five chapters on general principles of electrokinetic analysis, factors affecting mobility, CZE, capillary electrochromatography and MEKC. Each chapter is short but well organized and provides a quick survey of the essence of electrokinetic analysis from a practical point of view. The chapter on factors affecting mobility is excellent and very helpful in understanding the basic principles of mobility in CE. The chapter on capillary electrochromatography will be interesting for chromatographers, explaining concisely the essential difference between CE and electrochromatography. The authors try to describe an outline of MEKC with their own data in the last chapter of Part I, and this is successful. A table of methodologies to obtain electrokinetic separations is especially interesting to the reviewer, and the authors' classification is also reasonable, although it is different from the reviewer's view.

Part II on instrumental aspects is also a good introduction to CE practice. The authors may not expect readers to construct CE instruments themselves, although it is not difficult. Various commercial instruments are now available and most users probably do not want to build the instruments themselves. This part of the book is a good guide to fundamentals for the proper operation of the instruments. In particular, the chapters on thermal effects and injection are valuable for recognizing the importance of the effects of joule heating and the injection volume on efficiency.

Part III, on resolution in MEKC, describes fundamentals of MEKC in more detail, especially optimization of the operating parameters. The authors have produced many original chromatograms, mostly by computer simulation, to permit an easy understanding of the effects of various parameters on resolution. This chapter is another excellent one

and highly recommended even to those who are already using the MEKC technique. Although the authors explain efficiency in MEKC primarily based on the reviewer's paper, the reviewer does not think that the band broadening mechanism has been completely clarified, as the authors also suggest other causes.

Part IV treats applications and provides a comprehensive review of the applications of MEKC up to the time of completing the manuscript. As the authors indicate via the tale of Achilles and the tortoise, this field is rapidly growing and it is very difficult to catch up with the most recent results. A comprehensive review is unnecessary for this kind of book and typical examples in different application fields would be satisfactory. From this point of view, the chapters on general applications and enantiomeric separations include every important advance in MEKC.

The one aspect that the reviewer felt personally was slightly unsatisfactory was that the book traces fairly closely the reviewer's views on MEKC. This is, of course, not a weak point of the book. The reviewer appreciates the authors' tremendous efforts to complete this excellent book on MEKC. Other books on CE will soon be published by different authors, but the present book will definitely remain to be recommended as a book on MEKC and as a good textbook on CE.

Hyogo (Japan) Shigeru Terabe

Author Index

Erratum

J. Chromatogr., 600 (1992) 344–351.

Page 348, Table II, heading 2nd column should read: Concentration (mg/ml).

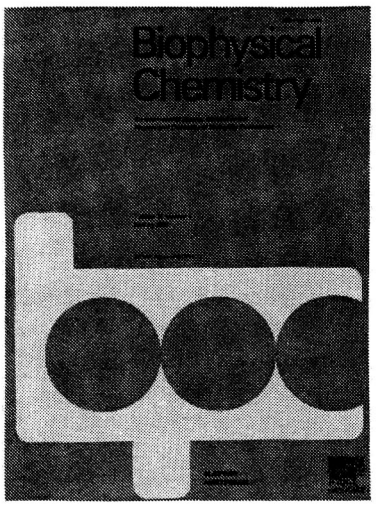

BIOPHYSICAL CHEMISTRY

An International Journal devoted to the Physics and Chemistry of Biological Phenomena

Audience

Chemical physicists, physical chemists, biochemists, biophysicists.

AIMS AND SCOPE

The journal is devoted to the interpretation of biological phenomena in terms of the principles and methods of physics and chemistry. It is receptive to articles which deal with biological molecules and systems, and to papers which treat systems serving as models for these. Treatments, phenomenological as well as molecular, of the interactions, structure and biological functions of individual biological macromolecules and of supramolecular structures are also within the journal's domain.

ABSTRACTED/INDEXED IN: Biological Abstracts, Chemical Abstracts, Current Awareness in Biological Sciences (CABS), Current Contents (Life Sciences), Excerpta Medica (EMBASE).

1993 SUBSCRIPTION INFORMATION

Volumes 45-47 (in 9 issues)

Dfl. 1176.00 / US $ 708.50 (including postage)

ISSN 0301-4622

I would like ☐ a free sample copy of Biophysical Chemistry

☐ Instructions to Authors.

☐ to enter a subscription for 1993. Please send me a Proforma Invoice.

Name _____

Address _____

_____

_____

Elsevier Science Publishers
Attn. Eugene P.M. Wijnhoven
P.O. Box 330, 1000 AH Amsterdam
The Netherlands
Fax: (+31-20) 5862 845

In the USA & Canada
Attn. Judy Weislogel
P.O. Box 945, Madison Square Station
New York, NY 10160-0757, USA
Fax: (212) 633 3880

PUBLICATION SCHEDULE FOR 1993

Journal of Chromatography and *Journal of Chromatography, Biomedical Applications*

MONTH	O 1992	N 1992	D 1992	
Journal of Chromatography	623/1 623/2 624/1+2	625/1 625/2	626/1 626/2 627/1+2	The publication schedule for further issues will be published later.
Cumulative Indexes, Vols. 601–650				
Bibliography Section				
Biomedical Applications				

INFORMATION FOR AUTHORS

(Detailed *Instructions to Authors* were published in Vol. 609, pp. 439–445. A free reprint can be obtained by application to the publisher, Elsevier Science Publishers B.V., P.O. Box 330, 1000 AH Amsterdam, The Netherlands.)

Types of Contributions. The following types of papers are published in the *Journal of Chromatography* and the section on *Biomedical Applications:* Regular research papers (Full-length papers), Review articles, Short Communications and Discussions. Short Communications are usually descriptions of short investigations, or they can report minor technical improvements of previously published procedures; they reflect the same quality of research as Full-length papers, but should preferably not exceed five printed pages. Discussions (one or two pages) should explain, amplify, correct or otherwise comment substantively upon an article recently published in the journal. For Review articles, see inside front cover under Submission of Papers.

Submission. Every paper must be accompanied by a letter from the senior author, stating that he/she is submitting the paper for publication in the *Journal of Chromatography*.

Manuscripts. Manuscripts should be typed in **double spacing** on consecutively numbered pages of uniform size. The manuscript should be preceded by a sheet of manuscript paper carrying the title of the paper and the name and full postal address of the person to whom the proofs are to be sent. As a rule, papers should be divided into sections, headed by a caption (*e.g.*, Abstract, Introduction, Experimental, Results, Discussion, etc.). All illustrations, photographs, tables, etc., should be on separate sheets.

Abstract. All articles should have an abstract of 50–100 words which clearly and briefly indicates what is new, different and significant. No references should be given.

Introduction. Every paper must have a concise introduction mentioning what has been done before on the topic described, and stating clearly what is new in the paper now submitted.

Illustrations. The figures should be submitted in a form suitable for reproduction, drawn in Indian ink on drawing or tracing paper. Each illustration should have a legend, all the *legends* being typed (with double spacing) together on a *separate sheet*. If structures are given in the text, the original drawings should be supplied. Coloured illustrations are reproduced at the author's expense, the cost being determined by the number of pages and by the number of colours needed. The written permission of the author and publisher must be obtained for the use of any figure already published. Its source must be indicated in the legend.

References. References should be numbered in the order in which they are cited in the text, and listed in numerical sequence on a separate sheet at the end of the article. Please check a recent issue for the layout of the reference list. Abbreviations for the titles of journals should follow the system used by *Chemical Abstracts*. Articles not yet published should be given as "in press" (journal should be specified), "submitted for publication" (journal should be specified), "in preparation" or "personal communication".

Dispatch. Before sending the manuscript to the Editor please check that the envelope contains four copies of the paper complete with references, legends and figures. One of the sets of figures must be the originals suitable for direct reproduction. Please also ensure that permission to publish has been obtained from your institute.

Proofs. One set of proofs will be sent to the author to be carefully checked for printer's errors. Corrections must be restricted to instances in which the proof is at variance with the manuscript. "Extra corrections" will be inserted at the author's expense.

Reprints. Fifty reprints will be supplied free of charge. Additional reprints can be ordered by the authors. An order form containing price quotations will be sent to the authors together with the proofs of their article.

CATALOGUE 1993 ON CD-ROM

Elsevier Science Publishers - the world's largest scientific publisher - presents for the first time details of all its publications on CD-ROM

ADVANTAGES

- ➢ Easy to use.
- ➢ Get more comprehensive information than ever before.
- ➢ Make fast and effective searches.
- ➢ Find what you want even with incomplete information.
- ➢ Compile special lists of products without typing.
- ➢ Improve your control of scientific product information.
- ➢ Enhance service to clients.

PRODUCT DESCRIPTION

The CD-ROM contains descriptions of all Elsevier products.

- ➢ All the journals, with complete information about journal editors and editorial boards
- ➢ Listings of recently published papers for many journals
- ➢ Complete descriptions and contents lists of book titles
- ➢ Independent reviews of published books
- ➢ Forthcoming title information
- ➢ Book series
- ➢ All other products, e.g. software, CDs, dictionaries, wallcharts.

In addition, the CD-ROM features easy-to-use search tools, making the information accessible and useful. For example, searches can be made by subject area, by year of publication, by author/editor or title and by "free text" search.

Full book and journal information can be printed to initiate your order.

If you do not find what you need, or wish to know more about Elsevier's publishing programme, the CD-ROM can supply you with the name, address and fax number of the correct person to contact.

AUDIENCE

Librarians, booksellers, researchers, agents and information specialists.

SYSTEM REQUIREMENTS

The CD-ROM has been designed to run under Microsoft® Windows™ 3.0, on IBM PC-ATs and compatibles. The CD-ROM is Microsoft® Windows™ 3.1 compatible.

ELSEVIER
SCIENCE PUBLISHERS

The minimum requirements are:

- ➢ IBM or IBM-compatible PC with a 80286 or higher processor
- ➢ 2 MB or more RAM
- ➢ MS-DOS® 3.3 or higher installed
- ➢ Microsoft® Windows™ 3.0 (or 3.1) installed
- ➢ Microsoft® Windows™ compatible mouse or other pointing device
- ➢ VGA graphics adapter (colour or monochrome)
- ➢ Hard disk with at least 2 MB free disk space
- ➢ CD-ROM drive which is accessible from Microsoft® Windows™
- ➢ For faster operation a 80386SX or higher processor is recommended, as well as a fast CD-ROM drive (access time less than 0.4 seconds).

The CD-ROM can be installed in a local area network.

For further information please contact

ELSEVIER SCIENCE PUBLISHERS
Attn. Vivian Wong Swie San
Marketing Services Department
P.O. Box 211
1000 AE Amsterdam
The Netherlands
FAX: (020) 5862 425

In the USA & Canada
Journal Information Center
P.O. Box 882
Madison Square Station
New York, NY 10159, USA
FAX: (212) 633 3764

711/414\141\0001-00